



***PROCEEDINGS OF THE***

***23rd International Symposium***  
***on Analytical and Environmental Problems***

*October 9-10, 2017*

**University of Szeged, Department of Inorganic and  
Analytical Chemistry**



***Szeged***  
***Hungary***

**Edited by:**  
Tünde Alapi  
István Ilisz

**Publisher:**  
University of Szeged, Department of Inorganic and Analytical  
Chemistry, H-6720 Szeged, Dóm tér 7, Hungary

**ISBN 978-963-306-563-1**

**2017.**  
**Szeged, Hungary**

***The 23<sup>rd</sup> International Symposium  
on Analytical and Environmental Problems***

**Organized by:**

SZAB Kémiai Szakbizottság Analitikai és Környezetvédelmi Munkabizottsága

**Supporting Organizations**

*University of Szeged, Department of Inorganic and Analytical Chemistry  
Hungarian Academy of Sciences*

**Symposium Chairman:**

*István Ilisz, PhD*

**Honorary Chairman:**

*Zoltán Galbács, PhD*

**Organizing Committee:**

*István Ilisz, PhD*

*associate professor*

*University of Szeged Department of Inorganic and Analytical Chemistry  
ilisz@chem.u-szeged.hu*

*Tünde Alapi, PhD*

*assistant professor*

*University of Szeged Department of Inorganic and Analytical Chemistry  
alapi@chem.u-szeged.hu*

## **Lecture Proceedings**



NEW MONONUCLEAR COBALT(III) AND MANGANESE(III) COMPLEXES  
CONTAINING A HEXADENTATE SCHIFF BASE LIGAND

Anamaria Ardelean<sup>1</sup>, Ildiko Buta<sup>1</sup>, Liliana Cseh<sup>1</sup>, Viorel Sasca<sup>1</sup>, Florica Manea<sup>2</sup>,  
Peter Lönnecke<sup>3</sup>, Evamarie Hey-Hawkins<sup>3</sup>, Otilia Costisor<sup>1</sup>

<sup>1</sup> Institute of Chemistry of the Romanian Academy, 24 Mihai Viteazu Bvd. 300223-Timisoara,  
Romania

<sup>2</sup> University Politehnica Timisoara, Faculty of Industrial Chemistry and Environmental  
Engineering, 6 Vasile Parvan Bvd. 300223-Timisoara, Romania

<sup>3</sup> Institute of Inorganic Chemistry, Universität Leipzig, Faculty of Chemistry and Mineralogy,  
Johannisallee 29, 04103-Leipzig, Germany  
e-mail: ana\_maria.ardelean@yahoo.com

**Abstract**

Manganese and cobalt complexes in high oxidation state play an important role in a diverse range of enzymatic and electron-transfer processes in biological systems<sup>1</sup> and as antibacterial or antiviral agents<sup>2</sup>. Here, we report the synthesis and crystal structures of two new mononuclear complexes [MnL](ClO<sub>4</sub>) (**1**) and [CoL](NO<sub>3</sub>)·2CH<sub>3</sub>OH (**2**) containing N,N'-bis[(2-hydroxybenzylideneamino)propyl]-piperazine (H<sub>2</sub>L) (Figure 1). X-ray structure determinations of **1** and **2** revealed that both compounds consist of mononuclear complex cations containing trivalent metal centers, Mn<sup>III</sup> or Co<sup>III</sup>. The metal ions are coordinated in a distorted octahedral fashion by the N<sub>4</sub> donor set of the ligand in basal and the two phenoxo oxygen atoms in apical positions. Spectral properties are consistent with the crystallographic results and the electrochemical properties of the complexes have been investigated by cyclic voltammetry. Furthermore, thermal studies were performed to deduce the stabilities of the ligand and complex **2**.

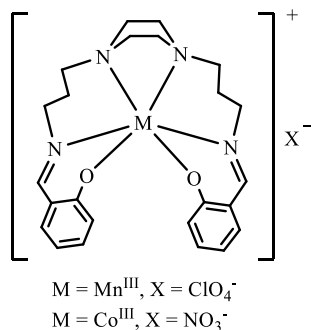


Figure 1. Chemical structure of the complexes **1** and **2**

**Acknowledgements**

We are thankful to the Romanian Academy of Science, (Project 4.1.) for the financial support.

**References**

- [1] K. Wieghardt, *Angew. Chem. Int. Ed. Engl.* 28 (1989) 1153.  
[2] E. L. Chang, C. Simmers, D. A. Knight, *Pharmaceuticals*, 3 (2010), 1711.

## STANDARDIZATION PROCESS BY NAA METHOD FOR PHYTOPHARMACEUTICAL INDUSTRY

**Daniela Haidu<sup>1</sup>, Dénes Párkányi,<sup>2</sup> Diana Antal<sup>3</sup>, Cecilia Savii<sup>1</sup>, Ludovic Kurunczi<sup>1,3</sup>**

<sup>1</sup> *Institute of Chemistry Timișoara of the Romanian Academy, 24 Mihai Viteazul Bvd., 300223  
– Timișoara, Romania*

<sup>2</sup> *Centre for Energy Research, Hungarian Academy of Sciences, 29 – 33 Konkoly Thege  
Miklós út, 1121 – Budapest, Hungary*

<sup>3</sup> *Pharmacy I Department, Faculty of Pharmacy, “Victor Babeș” University of Medicine and  
Pharmacy, 2 Eftimie Murgu Sq., 300041 – Timișoara, Romania  
e-mail: dana\_141@yahoo.com*

### **Abstract**

The ancient therapeutic remedies for modern needs are represented by medicinal crop plants, the raw material for phytopharmaceutical forms. Medicinal plants are generally viewed only in terms of beneficial effects without considering the potentially toxic side [1]. In this context in the present study elemental composition for seven representative medicinal crop plants as: coriander, dill, Echinacea, lavender, chamomile, mint and plantain, cultivated in unpolluted areas in Romania, were analyzed. Among many analytical methods used for determination of plant elemental content, that generally imply the vegetal matrix disintegration, the Neutronic Activation Analysis (NAA) is classified as primary ratio method [2]. By validating the NAA procedure by statistical evaluation of the nominal error  $En \leq 1$  (ISO 13528-2015) [3], NAA proved to be an accurate, specific and multielement analysis technique for medicinal plants with the advantage of eliminating the preliminary step of digestion, in this way certain errors being avoided. This method is differentiated as one with high potential to obtain internal plant standards in the phytopharmaceutical industry. These standards can be vegetable matrix, or plant specific, once achieved can be used a long period of time to verify and validate more routinely accessible analytical techniques, which in turn require a digestion stage.

A critical assessment provided by the results include the essential nutrients (K, Ca, Mg, Na, Fe, K, Mn, Zn), micro- and trace elements (Co, Cr, Cu, Ni, Se, V), as well as the undesirable, potentially toxic elements (Al, As, Ba, Co, Cr, Ni, Sb) together with rare earth elements. The values are comparable with literature. These plants may provide a useful contribution to food intake with essential macronutrients (K, Ca, Mg) and the concerns regarding the toxicity of metals for a person, are removed. Seemingly the Al (4997 ppm) and Fe (3315 ppm) [4] content in lavender is of some worry. In fact, many studies [5] revealed that some plants species, and lavender among them, exhibit metal bioaccumulation properties and are used for phytoremediation of contaminated soils. This dual implication, beneficial for soil depollution, but critical in transmitting the accumulated metals to humans, is to be considered. Choosing an unpolluted area, in order to cultivate medicinal plants, seems to be an efficient strategy from this point of view. Still, another conclusion is that a rigorous analytical control of the raw materials is advisable for some of the elements (among them aluminium) to avoid risks.

### **Acknowledgements**

This project has received funding from the European Union's 7th Framework Programme for research, technological development and demonstration under the NMI3-II Grant number

283883. We want to thank for the financial support of the MTA INFRA infrastructure development grants and to Romanian Academy.

### **References**

- [1] P. Pohl, A. Dzimitrowicz, D. Jedryczko, A. Szymczycha-Madeja, M. Welna, P. Jamroz, J. Pharm. Biomed. Anal. 130 (2016) 326.
- [2] L. Szentmiklósi, D. Párkányi, I. Sziklai-László, J. Radioanal. Nucl. Chem. 309 (2016) 91.
- [3] ISO 13528, 2015. Statistical methods for use in proficiency testing by interlaboratory comparison. Published in Switzerland  
[http://www.iso.org/iso/catalogue\\_detail.htm?csnumber=56125](http://www.iso.org/iso/catalogue_detail.htm?csnumber=56125)
- [4] D. Haidu, D. Párkányi, R.I. Moldovan, C. Savii, I. Pinzaru, C. Dehelean, L. Kurunczi, J Anal Methods Chem. 2017 (2017) 9748413.
- [5] V.R. Angelova, D.F. Grekov, V.K. Kisyov, K.I. Ivanov, Int. J. Biol., Biomol., Agric., Food Biotechnol. Eng. 9 (2015) 522.

## SUPRAMOLECULAR „SOFT“ ASSEMBLIES BASED ON COPPER(I) COORDINATION COMPLEXES

**Elisabeta Ildyko Szerb<sup>1</sup>, Carmen Cretu<sup>1</sup>, Adelina Antonia Andelescu<sup>1</sup>, Liliana Cseh<sup>1</sup>,  
Otilia Costisor<sup>1</sup>**

<sup>1</sup>*Institute of Chemistry Timisoara of Romanian Academy, 24, Mihai Viteazu Blvd.  
300223 – Timisoara, Romania  
e-mail: szella73@gmail.com*

Copper(I) coordination complexes with N<sup>N</sup> chelating oligopyridines are valuable candidates for applications in solar energy conversion<sup>1</sup> or lightning technologies<sup>2</sup> because of their excellent photophysical and photochemical properties and for the low cost and ready availability of the metal. The most attractive systems are based on ligands able to stabilise their tetrahedral geometry (D<sub>2d</sub> symmetry) and to hinder the flattening distortions which facilitates oxidation to Cu(II) species.<sup>3</sup>

Herein we present the synthesis and characterisation of new stable Cu(I) complexes based on functionalised 2,2'-biquinoline ligands (Figure 1) that self-assemble into “soft” supramolecular architectures.

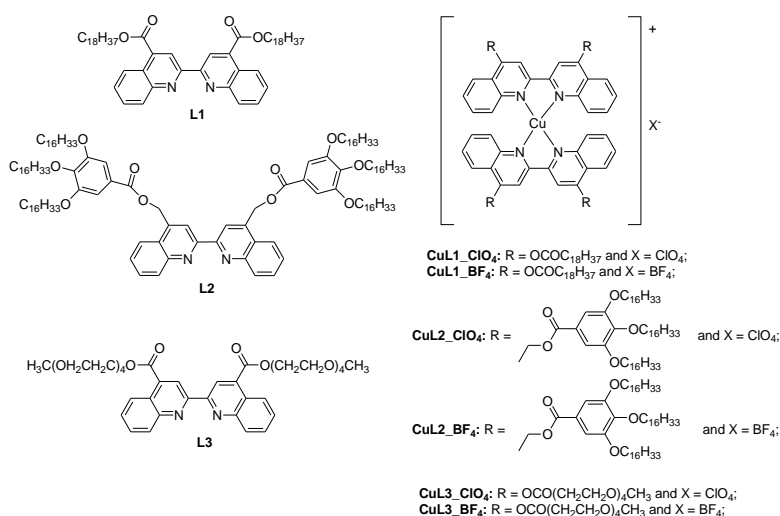


**Figure 1.** Chemical structure of ligands L1-L3 and their Cu(I) complexes CuL<sub>n</sub>\_X, where X = ClO<sub>4</sub> or BF<sub>4</sub>.

The stoichiometry and purity of all compounds were determined using elemental analyses, Atomic Absorption, IR and <sup>1</sup>H NMR spectroscopies. The functionalisation of the biquinoline ligand with long alkyl chains yielded thermotropic liquid crystalline systems (CuL1\_X and CuL2\_X), whereas insertion of hydrophilic groups promoted the assembly in water into supramolecular aggregates (CuL3\_X).

The thermal behaviour of complexes CuL<sub>n</sub>\_X with n = 1 and 2 was investigated by polarized optical microscopy (POM) and differential scanning calorimetry (DSC). UV-Vis studies on CuL3\_X evidenced the presence of supramolecular aggregates in water. Stabilization of Cu(I) systems can be also achieved by building supramolecular assemblies and thus blocking the

fluxional process towards a distorted “Cu(II)-like” geometry in concentrated solution of complexes.

### **Acknowledgements**

Authors are thankful to the Romanian Academy of Science (Project 4.1.).

### **References**

- [1] M. W. Mara, D. N. Bowman, O. Buyukcakir, M. L. Shelby, K. Haldrup, J. Huang, M. R. Harpham, A. B. Stickrath, X. Zhang, J. F. Stoddart, A. Coskun, E. Jakubikova, L. X. Chen, *J. Am. Chem. Soc.*, 137 (2015) 9670.
- [2] N. Armaroli, G. Accorsi, M. Holler, O. Moudam, J.-F. Nierengarten, Z. Zhou, R. T. Wegh, R. Welter, *Adv. Mater.* 18 (2006) 1313.
- [3] A. Crispini, C. Cretu, D. Aparaschivei, A. A. Andelescui, V. Sasca, V. Badea, I. Aiello, E. I. Szerb, O. Costisor, *Inorg. Chim. Acta* (2017) DOI: 10.1016/j.ica.2017.05.064.

## NOBLE METAL COLLOID AND Co-PORPHYRIN HYBRID SENSITIVE TO 4-AMINOSALICYLIC ACID

**Anca Lascu<sup>a\*</sup>, Ionela Fringu<sup>a</sup>, Anca Palade<sup>a</sup>, Mihaela Birdeanu<sup>a,b</sup>, Mirela Vaida<sup>b</sup>**

<sup>a</sup> *Institute of Chemistry Timisoara of Romanian Academy, M. Viteazul Ave. 24, 300223-Timisoara, Romania, Tel: +40256/491818; Fax: +40256/491824*

<sup>b</sup> *National Institute for Research and Development in Electrochemistry and Condensed Matter, 1 Plautius Andronescu Street, 300569 Timisoara, Romania  
email: ancalascu@yahoo.com*

### Abstract

A hybrid organic-inorganic nanomaterial (*Co-3OHPP/n-Au*) composed of Co(II) 5,10,15,20-meso-tetra(3-hydroxyphenyl)porphyrin (*Co-3OHPP*) and gold nanoparticles (*n-Au*) was tested as sensitive material for the optical detection of 4-aminosalicylic acid (*PAS*). This novel nanomaterial is able to detect 4-aminosalicylic acid in a reasonable concentration domain, covering one order of magnitude:  $1.24 \times 10^{-5} - 3.9 \times 10^{-4}$ M. The dependence between the intensity of absorption and the concentration in 4-aminosalicylic acid is linear, with a fair correlation coefficient of 95 %. This hybrid material can be further included in simple devices for the rapid and facile dosage of this antituberculosis drug in body fluids.

### Introduction

Aminosalicylic acid has bacteriostatic activity against *Mycobacterium tuberculosis* but it has seriously debilitating side effects. It is currently used only in the severe cases of multi-drug resistant TB. The controlled release of this drug was attempted by the intercalation of 4-amino salicylic acid (*PAS*) anions into biocompatible zinc layered hydroxide, using zinc oxide as starting material, and the creation of a nanocomposite [1].

The detection of PAS in body fluids is necessary [2], in spite of the fact that the detection of amino acids in general is affected by the continuous change of their ionic form with pH [3].

Among the detecting methods, the chromatographic ones [4] require laborious preparations of the samples. A method that uses samples without pretreatment implies capillary zone electrophoresis [5].

Porphyrins and metalloporphyrins provide recognition sites for amino acids and oligopeptides through their central metal ion and various functional groups at the four meso- and eight  $\beta$ -positions of pyrroles. Immobilized metallo-phenylporphyrins can be used as sensitive and selective sensors for different L-amino acids at pH 7 as they provide two avenues of interaction: the first via the metallic center of porphyrin and the second between the  $\pi$ - $\pi$  electrons of the macrocycles with the analytes [3].

In the present work a hybrid organic-inorganic nanomaterial (*Co-3OHPP/n-Au*) composed of Co(II) 5,10,15,20-meso-tetra(3-hydroxyphenyl)porphyrin (*Co-3OHPP*) and gold nanoparticles (*n-Au*) was tested as sensitive material for the optical detection of 4-aminosalicylic acid (*PAS*) (Figure 1).

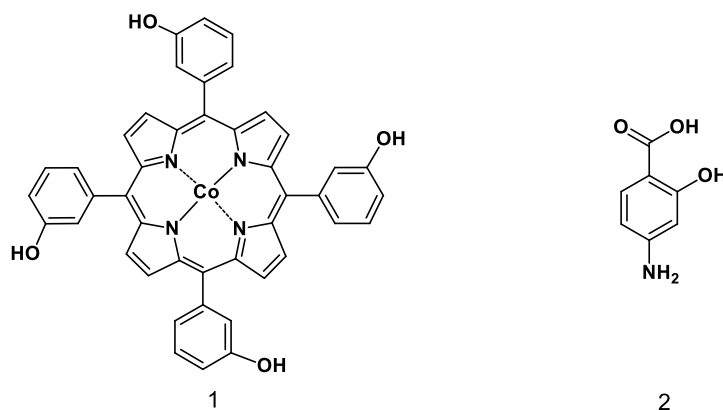


Figure 1. The structure of the investigated compounds

### Materials and methods

A JASCO model V-650 spectrometer was used for the UV-vis measurements in 1 cm quartz cuvettes at room temperature. Atomic force microscopy (AFM) measurements were performed on a Nanosurf®EasyScan 2 Advanced Research AFM (Switzerland) microscope. The samples were deposited onto pure silica plates from solvent mixtures (THF-water). Images were obtained in noncontact mode at room temperature.

Solvents (THF) were acquired from Merck and used without any further purification. The synthesis, optical and morphological characterization of the hybrid material was presented in previous work [6]. The 4-aminosalicylic acid (purchased from Merck) was solved in distilled water to obtain a final solution of  $4.23 \times 10^{-3}$  molar concentration.

The tested organic-inorganic hybrid material was obtained as follows: to 3 mL gold colloid solution ( $c = 4.58 \times 10^{-4}$  M)(Figure 2a) was added 1 mL of Co-porphyrin solution in THF ( $c = 5.15 \times 10^{-5}$  M)(Figure 2b) under intense stirring. The obtained hybrid presents the largest plasmonic band as compared to the initial materials' spectra (Figure 2c) [6].

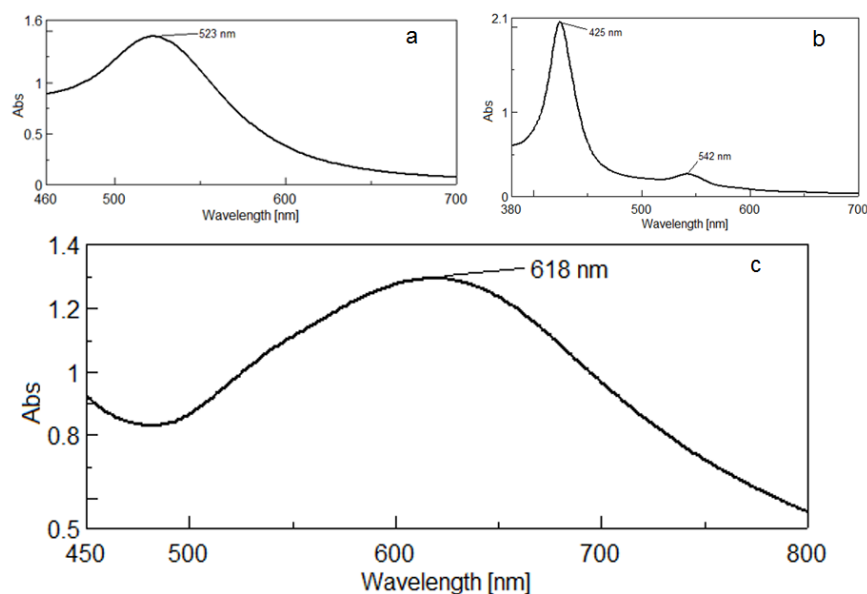


Figure 2. UV-vis spectra of the gold colloid solution ( $c = 4.58 \times 10^{-4}$  M)(a); of the Co-porphyrin ( $c = 5.15 \times 10^{-5}$  M) (b); and of the hybrid material (c)



Figure 3 depicts the AFM images of the obtained hybrid material, in which the triangular platelets of the hybrid form both H and J type aggregates by self-assembly.

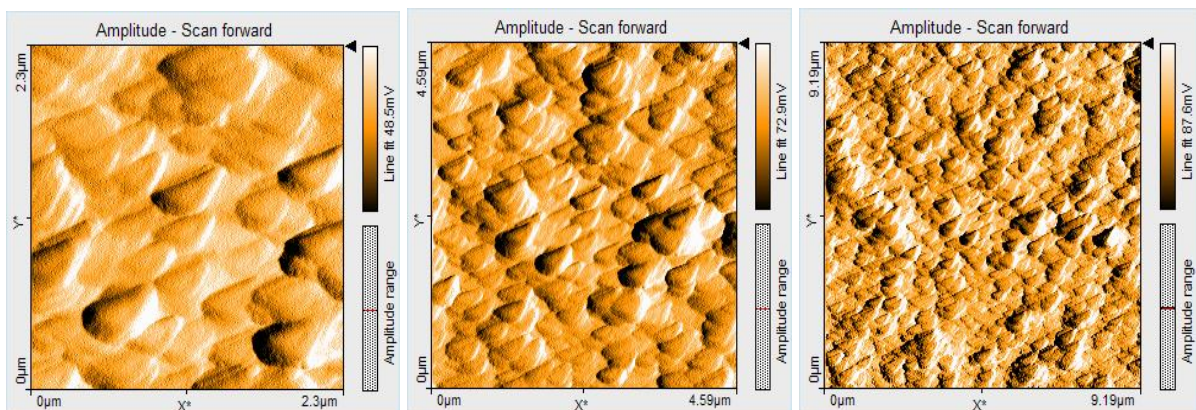


Figure 3. AFM images at 2, 4 and 9 micrometers respectively for the *Co-3OHPP-nAu* hybrid

The sensitivity tests were performed as follows: to 3 mL hybrid solution were added portions of 20  $\mu\text{L}$  of 4-aminosalicylic acid solution, the mixtures were stirred for 30 seconds and the UV-vis spectra were recorded for each step.

### Results and discussions

The optical response of the *Co-3OHPP-nAu* hybrid to the adding of 4-aminosalicylic acid solution was monitored by UV-vis spectroscopy (Figure 4). It can be observed that the plasmonic band presents a red shift and a decreasing intensity with the increase in *PAS* concentration, from 620 nm ( $c = 2.8 \times 10^{-5}\text{M}$ ) to 677 nm ( $c = 1.1 \times 10^{-3}\text{M}$ ). An isosbestic point can also be noticed at 680 nm on the plasmonic band. The detectable concentration domain for which the dependence between the intensity of absorption and the 4-aminosalicylic concentration is linear spans from  $1.24 \times 10^{-5}\text{M}$  to  $3.9 \times 10^{-4}\text{M}$ .

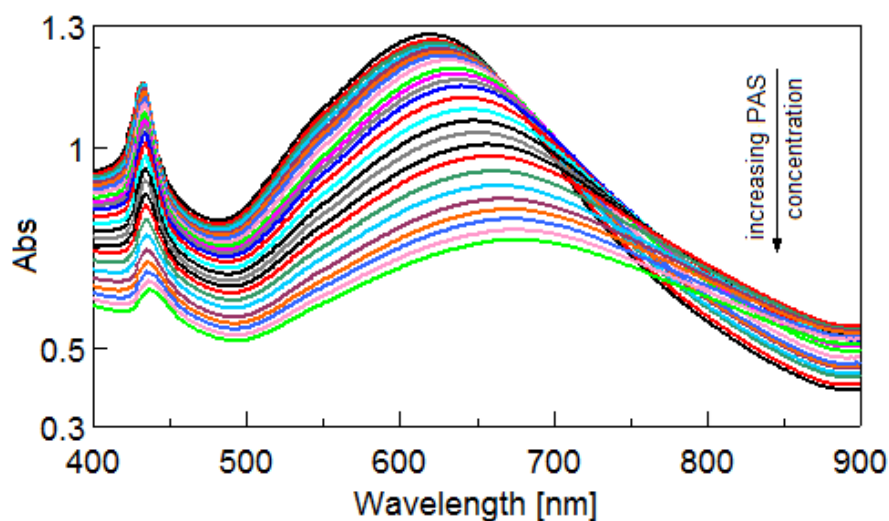


Figure 4. Overlapped UV-vis spectra registered during adding of increasing amounts of *PAS* solution to the *Co-3OHPP/nAu* hybrid material



The dependence between the intensity of absorption and the concentration in 4-aminosalicylic acid is linear, with a good correlation coefficient of 95 %.

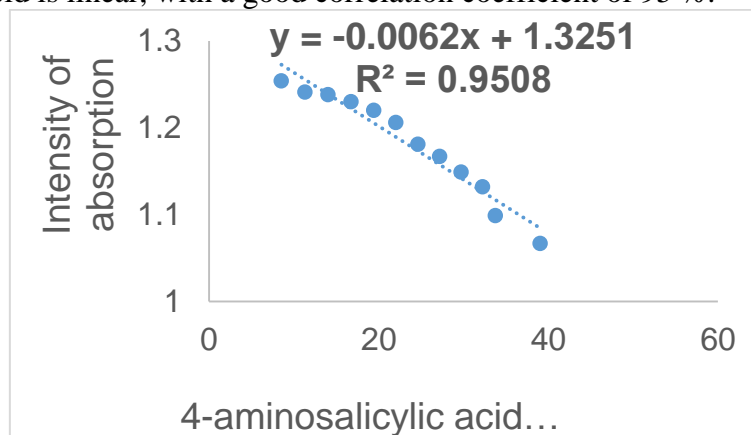


Figure 5. The linear dependence between the intensity of absorption of the hybrid plasmon and the increasing *PAS* concentration

### Conclusion

A hybrid organic-anorganic nanomaterial composed of a Co-metallated symmetrical porphyrin, Co(II) 5,10,15,20-meso-tetra(3-hydroxyphenyl)porphyrin and gold nanoparticles was tested as sensitive material for 4-aminosalicylic acid detection. It can be concluded that this novel optically active nanomaterial is able to detect 4-aminosalicylic acid in a large concentration domain, covering one order of magnitude:  $1.24 \times 10^{-5} - 3.9 \times 10^{-4}$  M. The dependence between the intensity of absorption and the concentration in 4-aminosalicylic acid is linear, with a fair correlation coefficient of 95 %. This hybrid material can be further included in simple devices for the rapid and facile dosage of this antituberculosis drug in body fluids.

### Acknowledgements

The authors from Institute of Chemistry Timisoara of Romanian Academy are kindly acknowledging the support of Romanian Academy, Program 3-Porphyrins/2017

### References

- [1] B. Saifullah, M. Z. Hussein, S. H. Hussein-Al-Ali, P. Arulselvan, S. Fakurazi, Chem. Cent. J. 7:72 (2013) DOI: 10.1186/1752-153X-7-72.
- [2] F. das Neves Almeida, Am. Rev. Respir. Dis. AJRCCM 82(4) (1960) 580.
- [3] M. A. Awawdeh, J. A. Legako, H. J. Harmon, Sens Actuators B 91 (2003) 227–230.
- [4] M. G. H. Laghari, Y. Darwis, A. H. Memon, Trop. J. Pharm. Res. 13(7) (2014) 1133-1139.
- [5] C. L. Cummins, W. M. O'Neil, E. C. Soo, D. K. Lloyd, I. W. Wainer, J. Chromatogr. B. Biomed. Sci. Appl. 697(1-2) (1997) 283-288.
- [6] E. Fagadar-Cosma, I. Sebarchievici, A. Lascu, I. Creanga, A. Palade, M. Birdeanu, B. Taranu, G. Fagadar-Cosma, J. Alloys Compds. 686 (2016) 896-904.

**PROFILING AND STRUCTURAL CHARACTERIZATION BY MASS SPECTROMETRY OF REGION-SPECIFIC GANGLIOSIDES IN BRAIN**

**Mirela Sarbu<sup>1,2</sup>, Željka Vukelić<sup>3</sup>, David E. Clemmer<sup>4</sup>, Alina D. Zamfir<sup>1,2</sup>**  
([mirela.sarbu86@yahoo.co.uk](mailto:mirela.sarbu86@yahoo.co.uk))

<sup>1</sup>National Institute for Research and Development in Electrochemistry and Condensed Matter, Timisoara, Romania; <sup>2</sup>Department of the Analysis and Modeling of Biological Systems, Aurel Vlaicu University of Arad, Romania; <sup>3</sup>Department of Chemistry and Biochemistry, University of Zagreb Medical School, Zagreb, Croatia; <sup>4</sup>Department of Chemistry, Indiana University, Bloomington, Indiana, United States of America  
e-mail: [alina.zamfir@uav.ro](mailto:alina.zamfir@uav.ro)

**Abstract**

Gangliosides (GGs), a particular class of glycosphingolipids ubiquitously found in tissues and body fluids, exhibit the highest expression in the central nervous system, especially in brain. GGs are involved in crucial processes, such as neurogenesis, synaptogenesis, synaptic transmission, cell adhesion, growth and proliferation. For these reasons, efforts are constantly invested into development and refinement of specific methods for GG analysis. We have recently shown that ion mobility separation (IMS) mass spectrometry (MS) has the capability to provide consistent compositional and structural information on GGs at high sensitivity, resolution and mass accuracy. In the present study we have implemented IMS MS for the first time in the study of a highly complex native GG mixture extracted and purified from a normal fetal hippocampus in the 17<sup>th</sup> gestational week (denoted FH17). The combination of electrospray ionization, ion mobility separation and high resolution mass spectrometry in the negative ionization mode enhanced ganglioside separation based not just on the  $m/z$  value, but also on the charge state, the carbohydrate chain length and the degree of sialylation. In the generated driftscope plot (drift time versus  $m/z$ ), 131 distinct gangliosides characterized by high variability of the oligosaccharide core and diversity of the ceramide moiety were identified with an average mass accuracy of 12.3 ppm. As compared to previous studies where no separation techniques prior to MS were applied, IMS MS technique has not just generated valuable novel information on the GG pattern characteristic for hippocampus in early developmental stage, but also provided data related to the GG molecular involvement in the synaptic functions by the discovery of 25 novel structures modified by  $\text{CH}_3\text{COO}^-$ . By applying IMS in conjunction with collision induced dissociation (CID) tandem MS (MS/MS), novel GG species modified by  $\text{CH}_3\text{COO}^-$  attachment, discovered here for the first time, were sequenced and structurally investigated in details. The present findings, based on IMS MS, provide a more reliable insight into the expression and role of gangliosides in human hippocampus, with a particular emphasis on their cholinergic activity at this level.

**Acknowledgements**

This project was supported by the Romanian National Authority for Scientific Research, UEFISCDI, project PN-III-P4-ID-PCE-2016-0073 granted to ADZ.

## THE CHROMATOGRAPHIC ANALYSIS OF CARAWAY ESSENTIAL OIL AS THE POTENTIAL BIOPESTICIDE

Tijana Stojanović<sup>1</sup>, Vele Tešević<sup>2</sup>, Vojislava Bursić<sup>1</sup>, Gorica Vuković<sup>3</sup>, Jovana Šučur<sup>1</sup>, Aleksandra Popović<sup>1</sup>, Miloš Petrović<sup>1</sup>

<sup>1</sup>University of Novi Sad, Faculty of Agriculture, Trg Dositeja Obradovića 8, 21000 Novi Sad, Serbia

<sup>2</sup>University of Belgrade, Faculty of Chemistry, Studentski Trg 16, Beograd, Srbija

<sup>3</sup>Institute of Public Health, Bul. despota Stefana 54a, 11000 Belgrade, Serbia

e-mail: [tijana.stojanovic@polj.edu.rs](mailto:tijana.stojanovic@polj.edu.rs)

### Abstract

The chromatographic analysis of essential oil was carried out by recording the mass spectrums of the detected components by GC-MS. After confirming the components through retention times and Kovats indices, their quantification was done by GC-FID. The main constituents of the caraway essential oil are carvone with 68.22% and limonene with 21.80% in content. Beside carvone and limonene there were 25 constituents which in total make less than 10.00% of the studied essential oil.

### Introduction

In recent years essential oils have drawn attention due to their biological effect as potential agents in pest control [1]. As the by-products of plant metabolism they are regarded as evaporable secondary metabolites of plants which are the mixture of mono and sesquiterpenes. The biological activity of essential oils depends on their chemical composition, the part of the plant they have been extracted from, phenological state of the plant, environmental conditions and the extraction methods [2].

Caraway (*Carum carvi*) is an annual or biannual herbaceous plant with an axial root system from *Apiaceae* family. The name of the genus is derived from the Greek *kara*, which means „head“, due to the appearance of its inflorescence [3]. Most essential oils are active in low concentrations (0.1 g/kg of food). The chemical composition of the essential oil of *C. carvi* collected from various countries has been widely studied and great variations in essential oil content and chemical composition of the essential oil were observed. Many data indicated that the essential oil possessed antimicrobial, antifungal, molluscidal, nematicidal, antioxidant and antiaflatoxic activities, as well as potential as a cancer preventing agent [4].

The content of essential oils, the amount of carvone and limonene in the oil and the ratio of both substances are the main quality criteria determined in caraway production. To determine carvone and limonene contents, mostly the gas chromatography with flame ionisation (GC/FID) or mass spectrometry (GC/MS) detection are used. Highperformance liquid chromatography (HPLC) with polarimetric detection, derivative spectrophotometry and proton magnetic resonance can also be applied [5].

Since the main components of essential oils are considered responsible for their biological activity, the objective was to determine the chemical composition of caraway essential oil by the chromatographic analysis, obtained in the distillation by water vapor.

## Experimental

The caraway essential oil was extracted from the fruit (fructus) by hydrodistillation (HD) with n-hexane as an organic solvent/recipient, collected on a private farm at Mošorin (N 45°17'28.113 E 20°11'43.80936). Thirty grams of caraway were subjected to hydrodistillation for 3 hours using a Clevenger-type apparatus. The essential oil was collected over water, separated, dried over anhydrous sodium sulphate, and stored in the dark at 4 °C.

The chromatographic analysis of essential oil was carried out by recording the mass spectrums of the detected components by gas chromatography with mass spectrometry (GC-MS). After confirming the components through retention times and Kovats indices, their quantification was done by the gas chromatography with flame ionization detector (GC-FID).

**GC/FID analysis** of tested samples of essential oils was carried out on an Agilent Technologies, model 7890A gas chromatograph, equipped with split-splitless injector and automatic liquid sampler (ALS), attached to HP-5MS column (30 m x 0.25 mm, 0.25 µm film thickness) and fitted to flame ionisation detector (FID). Carrier gas flow rate (H<sub>2</sub>) was 1 ml/min, injector temperature was 250 °C, detector temperature 300 °C, while column temperature was linearly programmed from 40-260 °C (at the rate of 4 °C /min), and held isothermally at 260 °C next 5 minutes. Solutions of tested samples in EtOH (~15 ml/ml) were consecutively injected by ALS (2 µl, split mode 1:30). Area percent reports, obtained as result of standard processing of chromatograms, were used as the base for the quantification purposes.

**Gas chromatography/mass spectrometry (GC/MS).** The same chromatographic conditions as those mentioned for GC/FID were employed for GC/MS analysis, using HP G 1800C Series II GCD system [Hewlett-Packard, Palo Alto, CA (USA)]. Instead of hydrogen, helium was used as carrier gas. Transfer line was heated at 260°C. Mass spectra were acquired in EI mode (70 eV), in the range of 40-450 Da. Sample solutions were injected by ALS (2 µl, split mode 1:30).

The constituents were identified by comparison of their mass spectra to those from Wiley275 and NIST/NBS libraries, using different search engines (PBM and NIST). In addition, the experimental values for retention indices were determined by the use of calibrated Automated Mass Spectral Deconvolution and Identification System software (AMDIS ver. 2.64.) [6], compared to those from available literature [7], and used as additional tool to approve MS findings.

## Results and discussion

The chromatogram obtained by the GC-MS analysis is shown (Figure 1), while the constituents of caraway essential oil are shown in Table 1. From the obtained results it can be concluded that the main constituents of the caraway essential oil are carvone with 68.22% and limonene with 21.80% in content (Table 1).

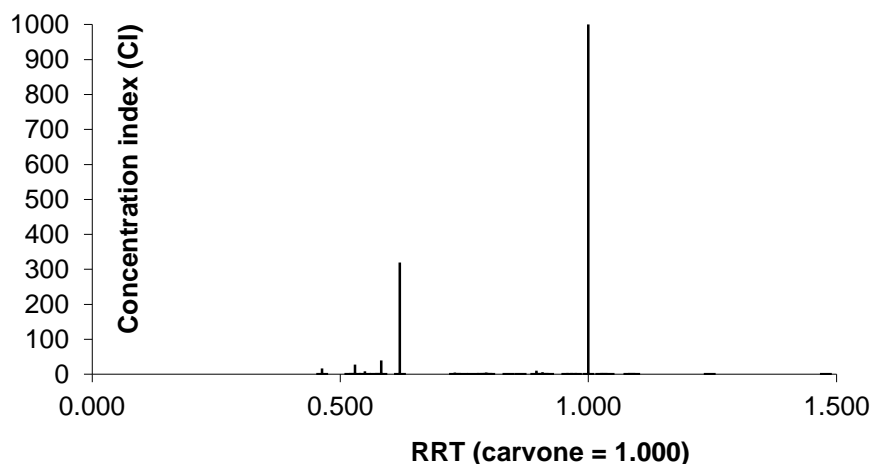


Figure 1. Chromatogram of caraway essential oil

Table 1. Constituents of the caraway essential oil

No	Constituents	KIE	KIL	RT/MS	RT/FID	Area	%, m/m	% ID	RRT	CI
1	$\alpha$ -Pinene	926.6	932	6,57	10,767	841,4	1,12	1,12	0,464	16
2	Verbenene	965.5	961	7,73	12,095	74,4	0,10	0,10	0,521	1
3	$\beta$ -Pinene	969.2	974	7,84	12,304	1411,4	1,88	1,88	0,530	28
4	Myrcene	988.6	988	8,42	12,765	415,9	0,56	0,56	0,550	8
5	$\beta$ -Phellandrene	1000.7	1002	8,79	13,272	59,6	0,08	0,08	0,571	1
6	$\beta$ <sup>3</sup> -Carene	1004.8	1008	8,93	13,533	1995,1	2,66	2,66	0,583	39
7	Limonene	1025.3	1024	9,63	14,405	16323,3	21,80	21,80	0,620	320
8	Linalool	1101.9	1095	12,20	16,981	217,4	0,29	0,29	0,731	4
9	trans-Sabinene hydrate	1108.5	1098	12,47	17,313	10,6	0,01	0,01	0,745	0
10	trans-p-Mentha-2,8-dien-1-ol	1118.9	1119	12,84	17,844	148,1	0,20	0,20	0,768	3
11	cis-Limonene oxide	1128.2	1132	13,16	18,282	164,5	0,22	0,22	0,787	3
12	trans-Limonene oxide	1133.4	1137	13,35	18,446	237,0	0,32	0,32	0,794	5
13	Camphor	1136,5	1141	13,46	18,588	19,2	0,03	0,03	0,800	0
14	Pinocarvone	1157,0	1160	14,17	19,483	70,7	0,09	0,09	0,839	1
15	trans-2-Caren-4-ol	1174,3	1176	14,77	20,046	68,7	0,09	0,09	0,863	1
16	Myrtenal	1190,6	1195	15,39	20,788	532,0	0,71	0,71	0,895	10
17	trans-Dihydro carvone	1199,1	1200	15,63	21,077	292,1	0,39	0,39	0,908	6
18	trans-3-Caren-2-ol*	1203,3	n/a	15,77	21,330	112,4	0,15	0,15	0,918	2
19	cis-Carveol	1223,3	1226	16,45	22,242	202,8	0,27	0,27	0,958	4
20	neoiso-Dihydro carveol	1231,9	1226	16,74	22,640	210,0	0,28	0,28	0,975	4
21	Carvone	1247,3	1239	17,26	23,225	51088,7	68,22	68,22	1,000	1000
22	Perilla aldehyde	1276,6	1269	18,27	23,835	178,1	0,24	0,24	1,026	3
23	n.i.	n/a		n/a	24,165	29,0	0,04		1,040	1
24	n.i.	1312,3		19,44	25,142	69,9	0,09		1,083	1
25	n.i.	1325,1		19,87	25,361	21,3	0,03		1,092	0
26	trans-Caryophyllene	1408,3	1417	22,54	28,904	53,4	0,07	0,07	1,244	1
27	Caryophyllene oxide	1573,0	1582	27,47	34,339	36,8	0,05	0,05	1,479	1
						74883,9	100,00	99,84		

## Conclusion

Based on the chromatographic analysis of caraway essential oil obtained in the distillation by water vapor it can be concluded as follows:

- The main constituents of the caraway essential oil are carvone with 68.22% and limonene with 21.80% in content.
- Beside carvone and limonene there were 25 constituents which in total make less than 10% of the studied essential oil.
- Since the main components affect the biological activity of essential oil the conclusion is that the biological effect of caraway essential oil is affected by monocyclic monoterpenes carvone and limonene.

## Acknowledgements

The authors would like to thank the Ministry of Education, Science and Technological Development for the financial support (Project TR 31027).

## References

- [1] T. Stojanović, A. Popović, X Conference of Agronomy students, 23-25 August, Čačak, Serbia, Proceedings (2017) 134.
- [2] D.A. Ukeh, S.B.A. Umoetok, Crop Protection. 30 (2011) 1351.
- [3] M. Šarović (2012). Kim (*Carum carvi*) i začini i lek, Nutricia.
- [4] R. Fang, C. Jiang, X. Wang, H. Zhang, H. Liu, L. Zhou, S. Du, Z. Deng, Molecules 15 (2010) 9391.
- [5] J. Sedláková, B. Kocourková, L. Lojková, V. Kubáň, Plant Soil Environ. 49(6) (2003) 277.
- [6] Automated Mass Spectral Deconvolution and Identification System software (AMDIS ver. 2.64.), National Institute of Standards and Technology (NIST), Standard Reference Data Program, Gaithersburg, MD (USA).
- [7] R.P. Adams (2007) Identification of Essential Oil Components by Gas Chromatography / Mass Spectrometry, 4th Ed., Allured Publishing Corporation, Carol Stream, Illinois, USA.
- [8] A. Ebadollahi, Ecologia Balkanica 5(1) (2013) 151.

## THE EFFECTS OF ELEVATED SUMMER TEMPERATURES ON CONTENT OF PESTICIDE RESIDUES IN SNR „OBEDSKA BARA“

Martina Mezei<sup>1\*</sup>, Vojislava Bursić<sup>1</sup>, Vuković Gorica<sup>2</sup>, Jasna Grabić<sup>1</sup>, Sonja Gvozdenac<sup>3</sup>, Aleksandra Petrović<sup>1</sup>, Dušan Marinković<sup>1</sup>

<sup>1</sup>University of Novi Sad, Faculty of Agriculture, Trg Dositeja Obradovića 8, Novi Sad, Serbia

<sup>2</sup>Institute of Public Health, Bulevar despota Stefana 54a, 11000 Beograd, Serbia

<sup>3</sup>Institute of Field and Vegetable Crops, Maksima Gorkog 30, 21000 Novi Sad, Serbia

e-mail: [tinica91@gmail.com](mailto:tinica91@gmail.com)

### Abstract

A special nature reserve Obedska Bara is a world famous swamp area which has been, throughout its long history, a true home for plants and animals and a center of attention of many explorers, scientists and nature lovers. It appeared more than several thousand years ago and since then many things have changed. Given that Obedska Bara is surrounded with agricultural land, there is a possibility that the swamp could be polluted with pesticides. The aim of this study was to highlight the influence of elevated summer temperatures on the content of pesticide residues in SNR „Obedska Bara“. Sampling was carried out at the end of July and August 2017. Pesticide analysis of 90 pesticides was performed by using LC/MS-MS detection. The obtained recoveries were from 69.8 – 114.7% with the relative standard deviation of 2.28 – 11.7% for all investigated pesticides. The obtained limits of quantification - LOQs for all twenty-one investigated pesticides were 0.010 µg/L. The results of pesticide analysis in a water sample from Obedska Bara indicate the presence of 8 pesticides. Just one of them was detected at levels exceeding maximum allowable concentrations –MACs.

### Introduction

Once a famous ornithological reserve and today a special nature reserve, Obedska Bara-forest complex is located along the river Sava in southern Srem, Vojvodina, Serbia. In the area of the reserve three-level protection regime is established on the total area of 9820 ha. Obedska Bara has been known around the world since the mid-nineteenth century, since when the stories of it as of "paradise" for birds have been spreading. It was proclaimed the protected area in 1994, however the first data about its protection is "since 1874". Thus, it is the oldest protected area in the country, and also one of the oldest natural resources in the world. "Golden Age" of Obedska swamp lasted throughout the 19th and early decades of the 20th century. Due to its extraordinary natural values, Obedska Bara is on the list of wetlands of the Ramsar Convention from 1977, as the first in our country, and it was declared in 1989 an internationally important bird area (IBA) as well. Obedska Bara is known for the variety of wetland and forest habitats, many species of mammals, fish, amphibians, reptiles, insects and extreme wealth of flora, fish fauna and especially of bird fauna.

The degradation of water quality caused by an anthropogenic influence is a problem which is present even at some SNRs in the Province of Vojvodina, Serbia [1, 2]. The pollution problem of aquatic environments has become the main topic of discussion of many scientists and experts from the field of environmental protection. Unfortunately, this problem was noticed relatively late (at the end of 1980's), after the chemicals in the water caused the disappearance of many aquatic organisms. The special attention is devoted to pesticides which can migrate to surface and groundwater, after the application to plants and soil [3]. Pesticides can get into the



water directly during treatments, by atmospheric precipitation, by desorption from aquatic organisms and sediments, by incorrect use of sprayers, when washing the machines and protective clothing after the pesticides application, and by waste packaging of pesticides [4]. When getting into the water, pesticides can be transformed by physical, chemical and biological processes. A large amount of toxic and persistent compounds can be bound to the solid matter and become an integral part of the sediment. The polluted sediment, due to resuspension, becomes a basic and permanent source of these pollutants and the largest potential source of water quality risks [5, 6].

Keeping in mind all above mentioned, the regular monitoring of pesticides presence in Obedska Bara is required.

### **Material and methods**

**Water sample collection and preservation.** Water samples from Obedska Bara were collected at the end of July and August 2017, from two locations Obrež (N 44° 73' 421" E 19° 99' 061") and Kula (N 44° 73' 811 E 19° 99' 123"). The water sample was taken from the boat, at the central and ultimate positions of the swamp.

The water was collected in amber glass bottles (1 L) by plunging at the depth of 50 cm and closing with the lid under the water surface. The sample was transported to the laboratory in handy cool boxes and kept at 4 °C until the analysis.

**Pesticide analysis.** Pesticide analysis of 90 pesticides was performed with an Agilent 1200 HPLC system equipped with a G1379B degasser, a G1312B binary pump, a G1367D autosampler and a G1316B column oven (Agilent Technologies, Waldbronn, Germany). Chromatographic resolution was achieved with Zorbax XDB C18 analytical column of 50×4.6 mm and 1.8 μm particle size (Agilent Technologies) maintained at 30 °C. The analytical separation was performed using a gradient program starting with 90% mobile phase B and progressing to 5% mobile phase B at 15 min, with methanol as mobile phase A, and water as mobile phase B, both containing 0.1% formic acid. The flow rate was maintained at 0.5 mL min<sup>-1</sup>. The tandem mass spectrometry analysis was carried out with an Agilent 6410 Triple Quadrupole mass spectrometer equipped with an multimode source (Agilent Technologies, Palo Alto, CA, USA). The following ionization conditions were used: electrospray ionization (ESI<sup>+</sup>) positive ion mode, drying gas (nitrogen) temperature 325 °C, drying gas flow rate 5 L/min, nebulizer pressure 40 psi and capillary voltage 3000 V. The dwell time was 100 ms. The data acquisition and quantification was conducted using MassHunter Workstation software B.03.01 (Agilent Technologies 2010). The method was validated according to SANTE/11945/2015 document. The limits of detection (LODs) were determined as the lowest concentration giving a response of three times the average baseline noise. The signal/noise ratio (S/N) in the obtained chromatograms for the LOD estimation was calculated by MassHunter Qualitative Software. LODs were defined as analyte peaks giving the S/N ratio of 3 extracted from the less intense (confirmation) MRM transition, calculated using an extract of Milli-Q water (250 mL) spiked at the 50 ng/L level. The linearity was checked using matrix matched standards (MMS) at concentrations from 10 to 200 ng/mL. The recovery was checked by enriching a blank sample (250 mL of tap water) with the mixture of pesticide standards of 10 μg/mL to get the final mass concentration of 20, 100 and 200 ng/L, with the addition of the internal standards carbofuran-D3, atrazine-D5 and isoproturon-D6 (mass concentration 10 μg/mL).

The sample preparation was performed with Bond ElutPlexa (60 mg, 3 mL) which were conditioned with 3 mL of methanol and 3 mL of HPLC - grade water. After conditioning, 250



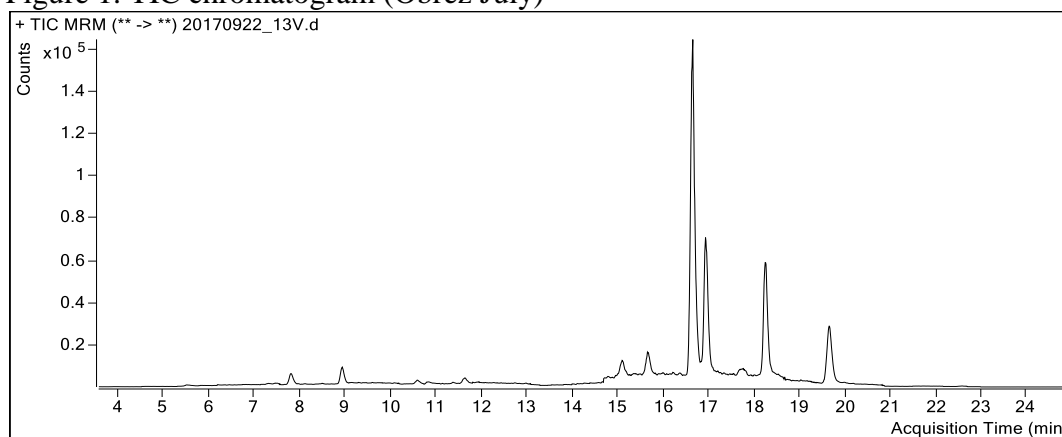
mL volume of water was enriched onto the cartridge with the flow rate settled between 3 and 10 mL/min. The cartridge was then flushed with 5 mL of HPLC - grade water. Pesticides were eluted from the sorbent with 5 mL of methanol and collected in the 10 mL amber glass vial. The solvent was evaporated under a gentle stream of nitrogen in a Techne-Dry block and the residue was dissolved in 0.25 mL of initial mobile phase composition. An extract volume of 10  $\mu$ L was injected into the LC/MS-MS for the detection.

### Results and discussion

The developed LC-MS/MS chromatographic procedure exhibits excellent linearity ( $R^2 > 0.99$ ) in the 10 – 200 ng/mL range with satisfactorily precision ( $RSD < 15\%$ ). Detection limits were defined for a ratio of S/N of 3 from the less intense (confirmation) MRM transition, calculated using a extract of Milli-Q water (250 mL) sample spiked at the 50 ng/L level. The accuracy and precision were determined via recovery experiments, spiking reagent water at 20, 100 and 200 ng/L, at six replicates per level. The obtained recoveries were from 69.8 – 114.7% with the relative standard deviation of 2.28 – 11.7% for all investigated pesticides.

The obtained limits of quantification - LOQs for all twenty-one investigated pesticides were 0.010  $\mu$ g/L.

Figure 1. TIC chromatogram (Obrez July)



In Table 1. the concentration detected of the different pesticides are presented.

Table 1. Detected pesticide in the water samples ( $\mu$ g/L)

Pesticide	Kula (July)	Obrež (July)	Kula (August)	Obrež (August)
metamitron	0.009			
metolachlor	0.017	0.015	0.092	<b>0.134</b>
terbutylazine	0.039	0.006	0.03	0.036
Desethyl-terbutylazine	0.005	0.004		0.005
acetamipride	0.005	0.006	0.087	0.041
imidacloprid	0.038	0.01	0.006	0.008
klothianidin	0.004	0.004	0.001	0.002
thiamethoksam	0.012	0.028	0.003	0.006

Directive 2013/39/EC [8] brings us environmental quality standards (EQS) 21 pesticides. The presence in the environment of the pesticides that are not encompassed in this Directive is regulated by maximum allowable concentration (MAC) of 0.1 µg/L (sum 0.5 µg/L).

The results of pesticide analysis in a water sample from Obedska Bara indicate the presence of 8 pesticides, which are all detected in the sample Kula from July. Just one of them (*Table 1*) was detected at levels exceeding maximum allowable concentrations -MACs (0.1 µg/L) according to the Decision 495/2015/EC and Directive 2008/105/EC [9]. The highest concentration of pesticides (metolahlor 0.134 µg/L) was detected in the sample from Obrež sampled in August.

## Conclusion

Elevated temperatures during summer months are able to increase a degree of degradation and volatilization of pesticides, but based to our findings and results we are not able to confirm that clames.

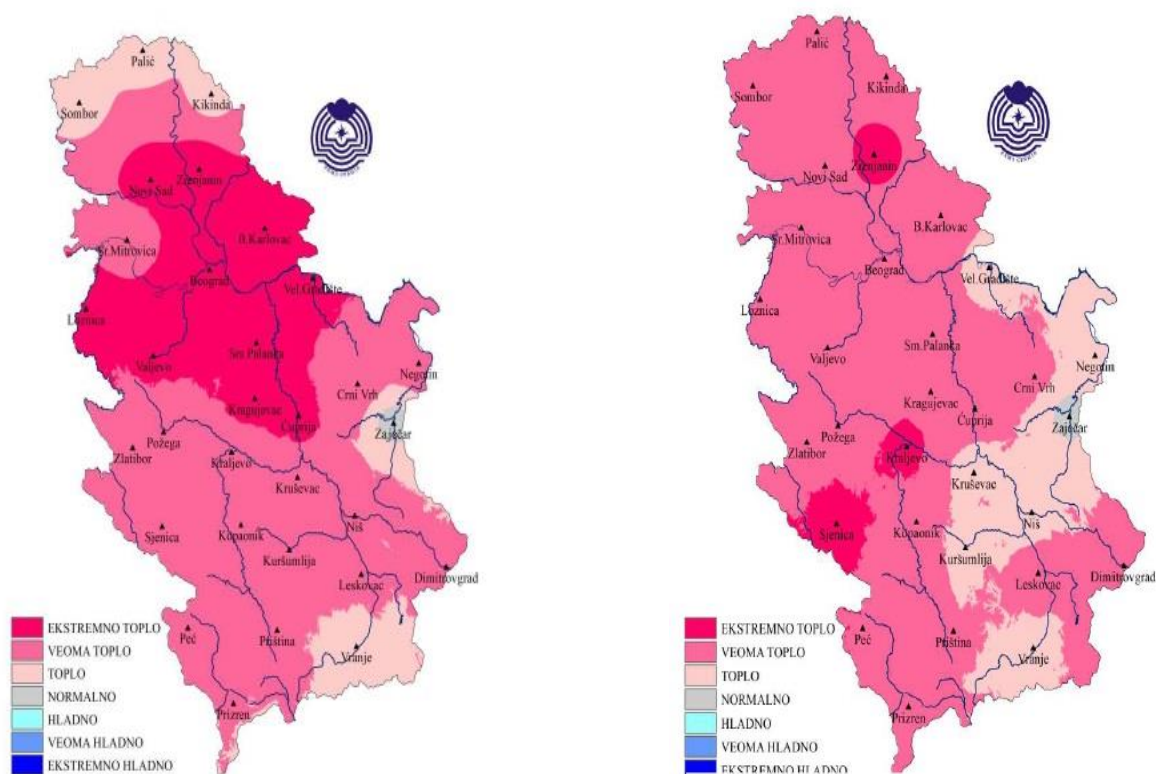


Figure 2. average temperatures during July (left) and August (right)

## Acknowledgement

The authors acknowledge the financial support of the Ministry of Education and Science, Republic of Serbia, Project Ref. III 43005

## Reference

- [1] J. Grabić, V. Ćirić, P. Benka, S. Đurić, University of Novi Sad, Faculty of Agriculture. (2016).
- [2] J. Grabić, V. Ćirić, P. Benka, S. Đurić, A. Bezdan, V. Bursić, L. Pavlović, N. Antičić, R. Zemunac, Univerzitet u Novom Sadu, Poljoprivredni fakultet. (2017).

- [3] R. Đurović, J. Gajić-Umiljendić, T. Đorđević, *Pestic. Phytomed.* 24 (2009) 51.
- [4] V. Bursić, G. Vuković, Z. Stojanović, S. Gvozdenac, T. Zeremski, M. Meseldžija A. Petrović, XXI Savetovanje o biotehnologiji sa međunarodnim učešćem, 11-12. mart, Čačak, Zbornik radova 21 (23) (2016) 359.
- [5] S. Gvozdenac, Univerzitet u Novom Sadu, Poljoprivredni fakultet. Doktorska disertacija (2016).
- [6] S. Gvozdenac, V. Bursić, G. Vuković, S. Đurić, C. Goncalves, D. Jovičić, S. Tanasković, *Environ. Sci. Pollut. Res.* 23 (18) (2016) 18596.
- [7] SANTE/11945/2015. Guidance document on analytical quality control and validation procedures for pesticide residues analysis in food and feed.
- [8] European Union, Directive 2013/39/EC of the European Parliament and of the Council, Official Journal of the European Communities, L226/1.
- [9] European Union, Directive 2015/495/EC of the European Parliament and of the Council, Official Journal of the European Communities, L348.

## PRECURSOR FOR SOFT MATERIALS BASED ON IONIC LIQUID CRYSTALS

**Angela M. Spirache<sup>1</sup>, Carmen Cretu<sup>1</sup>, Viorel Sasca<sup>1</sup>, Liliana Cseh<sup>1</sup>, Otilia Costisor<sup>1</sup>  
Elisabeta I. Szerb<sup>1</sup>**

<sup>1</sup>*Institute of Chemistry Timisoara of Romanian Academy, 24 Mihai Viteazu Bvd., 300223 - Timisoara, Romania, e-mail: spirache@acad-icht.tm.edu.ro*

Ionic liquid crystals (ILCs) are emerging as appealing materials for practical applications since are expected to combine the technological properties of ionic liquids (ILs: such as ionic conductivity) and those of liquid crystals (LCs: order and mobility).[1] The field of ILCs is continuously growing as many recent applications were found: solar cells, membranes, batteries, electrochemical sensors or electroluminescent switches.[2] Different factors are responsible for governing the nature of ILC phases, such as the molecular shape, location and size of ionic groups, intermolecular interactions and microphase segregation [2]. Herein, we report the synthesis and characterization of new ionic liquid crystalline salts of nicotinic acid (Figure 1).

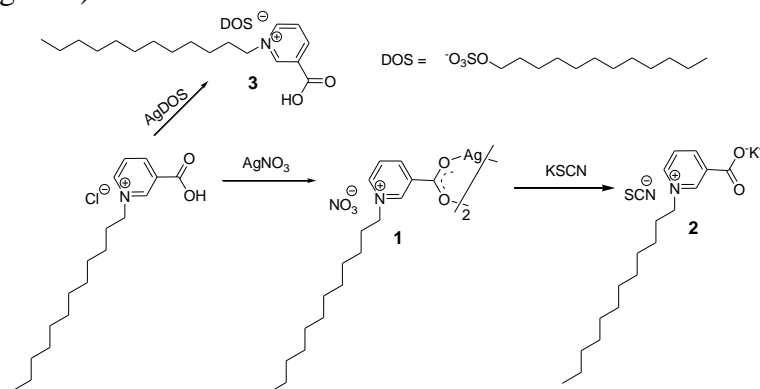


Figure 1. Synthesis and chemical structures of the new ILCs.

These compounds were characterized by spectral (IR, UV-Vis and <sup>1</sup>H NMR) and thermogravimetric methods (TGA). Their mesomorphic behavior was investigated by polarized optical microscopy (POM) and differential thermal analysis (DTA).

The influence of the counterions on the stability and mesomorphic properties of the obtained compounds will be presented.

These compounds will be used as precursors for the synthesis of advanced functional materials for electrooptical devices.

### Acknowledgements

This work was supported by a grant of Ministry of Research and Innovation, CNCS - UEFISCDI, project number PN-III-P4-ID-PCE-20160720, within PNCDI III. The authors are kindly acknowledging also the support from the Romanian Academy (Project 4.1).

### References

- [1] J. W. Goodby, I. M. Saez, J. S. Cowling, V. Görtz, M. Draper, A. W. Hall, S. Sia, G. Cosquer, S. E. Lee, E. P. Raynes, *Angew. Chem. Int. Ed.*, 47 (2008) 2754.
- [2] E. J. R. Sudholter, J. B. F. N. Engberts, W. H. de Jeu, *J. Phys. Chem.*, 86 (1982) 1908.

**ÚJ Fe(II)-KOMPLEXEK ELŐÁLLÍTÁSA  $\alpha$ -DIOXIMOKKAL, BÓRSÁVVAL ÉS ÉSZTEREIVEL, SZEMI- ÉS TIOSZEMIKARBAZONOKKAL, SCHIFF-BÁZISOKKAL, VALAMINT FIZIKAI-KÉMIAI ÉS BIOLÓGIAI VIZSGÁLATUK**

**ifj. Várhelyi Csaba<sup>1</sup>, Kuzmann Ernő<sup>2</sup>, Pokol György<sup>3</sup>, Szalay Roland<sup>2</sup>, Goga Firuța<sup>1</sup>, Papp Judit<sup>4</sup>, Golban Ligia-Mirabela<sup>1</sup>, Várhelyi Melinda<sup>1</sup>, Kovács Ildikó<sup>1</sup>**

<sup>1</sup> *Kémia és Vegyész-mérnöki Kar, „Babeş-Bolyai” Tudományegyetem, RO-400 028 Kolozsvár, Arany János u. 11, Románia*

<sup>2</sup> *Kémiai Intézet, „Eötvös Loránd” Tudományegyetem, H-1117 Budapest, Pázmány Péter sétány 1/a, Magyarország*

<sup>3</sup> *Vegyész-mérnöki és Biomérnöki Kar, Budapesti Műszaki és Gazdaságtudományi Egyetem, H-1111 Budapest, Műegyetem rkp. 3, Magyarország*

<sup>4</sup> *Biológia és Geológia Kar, „Babeş-Bolyai” Tudományegyetem, RO-400 015 Kolozsvár, Gheorghe Bilaşcu u. 44, Románia, e-mail: vcaba@chem.ubbcluj.ro*

**Abstract**

In our research project new iron(II) complexes were synthesized with azomethines, such as [Fe(1,4-dibromo-2,3-butane-GlyoxH)<sub>2</sub>(3-HO-aniline)<sub>2</sub>], [Fe(1,4-dibromo-2,3-butane-GlyoxH)<sub>2</sub>(2-amino-pyrimidine)<sub>2</sub>], [Fe(4-benzyl-2-HO-propiofenone-GlyoxH)<sub>2</sub>], [Fe(5-methyl-2-hexanone)<sub>2</sub>(en)], [Fe(5-methyl-2-hexanone)<sub>2</sub>(1,2-pn)], [Fe(5-methyl-2-hexanone)<sub>2</sub>(1,3-pn)], [Fe(5-methyl-2-hexanone)<sub>2</sub>(o-fen)], [Fe(2,4,5-trimethoxy-acetophenone-SC)<sub>2</sub>], [Fe(2,4,5-trimethoxy-acetophenone-TSC)<sub>2</sub>], [Fe(5-methyl-2-hexanone-SC)<sub>2</sub>], [Fe(5-methyl-2-hexanone-TSC)<sub>2</sub>], [Fe(Me-Pr-Glyox)<sub>3</sub>(BOH)<sub>2</sub>], [Fe(Me-Pr-Glyox)<sub>3</sub>(BOMe)<sub>2</sub>], [Fe(Me-i-Bu-Glyox)<sub>3</sub>(BOH)<sub>2</sub>], [Fe(Me-i-Bu-Glyox)<sub>3</sub>(BOMe)<sub>2</sub>], [Fe(Me-i-Bu-Glyox)<sub>3</sub>(BO-n-propyl)<sub>2</sub>] (en = ethylenediamine, pn = propylenediamine, fen = phenylenediamine, SC = semicarbazone, TSC = thiosemicarbazone), by reacting iron(II)-chloride with different glyoximes, Schiff-bases, semi- or thiosemicarbazones in suitable solvent. The Schiff-bases were obtained with the condensation of 5-methyl-2-hexanone, with diamines. The semi- or thiosemicarbazones were prepared by the condensation of 2,4,5-trimethoxy-acetophenone or 5-methyl-2-hexanone with semicarbazide or thiosemicarbazide. We analyzed their physicochemical properties using mass spectrometry, infrared-, NMR-, UV-VIS-, Mössbauer-spectroscopy, powder-XRD and thermal analysis (TG, DTG and DTA). The biological activity of complexes, especially their antibacterial activity was also explored.

The importance of this class of compounds is gained in biochemistry, since some of them act as antibacterial agents and potential anticancer drugs. Furthermore, some members can play role as catalysts in organic chemistry transformations [1–2].

**Bevezető**

Az azometinek közül első ízben az  $\alpha$ -dioximok Fe(II)-reakcióját Csugaev jelezte a XX. század első éveiben. A vasnak jelentős szerepe van az O<sub>2</sub> különböző szövetekhez való szállításánál (hemoglobinnal), a sejtekben végbemenő oxidatív folyamatokban, valamint a különböző baktériumok és algák által termelt nitrogén megkötésében.

A Schiff-bázisok széles körben elterjedtek, többek között a festékiparban is használatosak fonalszínezékként. Tudjuk róluk, hogy biológiailag aktívak: antibakteriális, antivirális, és gyulladáscsökkentő hatással is rendelkeznek. Egyes ferrocén-származékok rosszindulatú daganatok ellen hatásosak (egereken próbált) [3].

A  $[M(\text{dioximát})_3(\text{BOR})_2]$  típusú komplexeket Schrauzer fedezte fel [4], aki feljegyezte, hogy a klasszikus  $[\text{Ni}(\text{Me}_2\text{GlioxH})_2]$  komplex könnyen reagál  $\text{BF}_3$ -dal és alkil-boránokkal éteres közegben. Voloshin és munkatársai állítottak elő egy sor  $[\text{Fe}(\text{dioximát})_3(\text{BOR})_2]$  típusú komplexet, és jellemezték különböző fizikai-kémiai módszerekkel. Átmenetifémet tartalmazó klatrokelátok HIV fertőzések esetén használatosak.

### Kísérleti rész

**Felhasznált anyagok:**  $\text{FeSO}_4 \cdot 7 \text{H}_2\text{O}$ , 1,4-dibróm-2,3-butándion, 4-benzil-2-HO-propiofenon, 5-metil-2-hexanon, 2,4,5-trimetoxi-acetofenon, 2,3-hexándion, hidroxilamin-klórhidrát, etil-nitrit, etilén-diamin, 1,2-propilén-diamin, 1,3-propilén-diamin, o-fenilén-diamin, bórsav, bórax, 3-hidroxi-anilin, 2-amino-pirimidín, Et-OH, Me-OH, n-propil-OH.

**Eljárás:** -  $[\text{Fe}(1,4\text{-dibróm-2,3-bután-GlioxH})_2(\text{amin})_2]$  és  $[\text{Fe}(4\text{-benzil-2-HO-propiofenon-GlioxH})_2]$  típusú komplexek előállítása

Először előállítjuk az 1,4-dibróm-2,3-bután-GlioxH<sub>2</sub>-ot 1,4-dibróm-2,3-butándionból hidroxilammal kondenzálva, Na-acetát jelenlétében, etil-alkoholos, vizes közegben, majd a kapott oldatot  $\text{FeSO}_4$  vizes oldatával reagáltatjuk. A 4-benzil-2-HO-propiofenon-GlioxH<sub>2</sub>-ot 4-benzil-2-HO-propiofenonból kiindulva állítjuk elő etil-nitrittel való izonitrozálással (kis mennyiségű sósav jelenlétében gáz alakú etil-nitritet buborékolatunk a folyékony ketonba) a megfelelő monoximot, majd hidroxilamin-klórhidráttal kondenzálva a karbonil-csoportot, Na-acetát jelenlétében, alakul ki a glioxim. Az oldatot hasonlóan  $\text{FeSO}_4$  vizes oldatával reagáltatjuk. Mindkét esetben a kapott vas-glioxim oldatokat a molaránynak megfelelően, különböző aminokkal reagáltatjuk, vízfürdőn melegítve 1 – 2 órán keresztül. A keletkezett termékeket lehűtjük, vákuum alatt szűrjük, víz-alkohol (1:1) eleggyel mossuk, és levegőn szárítjuk.

-  $[\text{Fe}(5\text{-metil-2-hexanon})_2(A)]$ , A: en, 1,2-pn, 1,3-pn, o-fen, típusú komplexek előállítása

A Schiff-bázisokat 5-metil-2-hexanonból kiindulva, etil-alkoholban oldva, állítjuk elő, a megfelelő diamin (en, 1,2-pn, 1,3-pn, o-fen) etil-alkoholos oldatának elegyítésével és keverésével enyhe melegítéssel (molarány 2:1). A keletkezett Schiff-bázis oldatát használjuk, amit  $\text{Fe}_2\text{SO}_4$  vizes oldatával elegyítünk (molarány 1:1), hozzáadunk egy késhegyi C-vitamint (aszorbinsavat) a vas(II) oxidációjának elkerüléséért, majd 1 – 2 órán keresztül forraljuk inert atmoszférában ( $\text{CO}_2$ ). A keletkezett terméket lehűtjük, vákuum alatt szűrjük, víz-alkohol (1:1) eleggyel, majd dietil-éterrel mossuk, és levegőn szárítjuk.

-  $[\text{Fe}(2,4,5\text{-trimetoxi-acetofenon-SC})_2]$ ,  $[\text{Fe}(2,4,5\text{-trimetoxi-acetofenon-TSC})_2]$ ,  $[\text{Fe}(5\text{-metil-2-hexanon-SC})_2]$ ,  $[\text{Fe}(5\text{-metil-2-hexanon-TSC})_2]$  komplexek előállítása

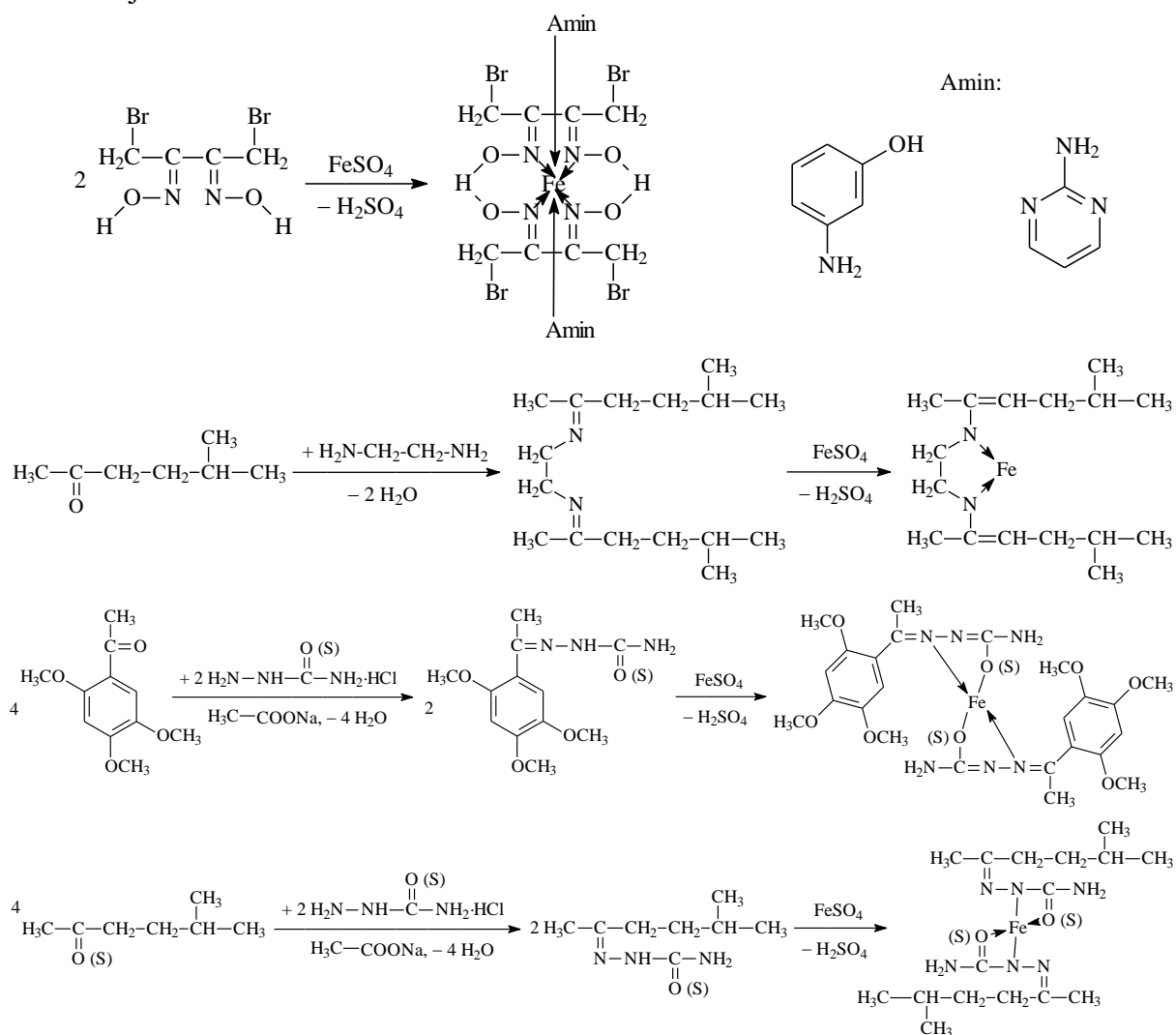
A 2,4,5-trimetoxi-acetofenon, illetve az 5-metil-2-hexanon etil-alkoholos oldatát szemikarbazid-klórhidrát etil-alkoholos oldatával reagáltatjuk, melybe még nátrium-acetát vizes oldatot teszünk, a molaránynak megfelelően, a sósav semlegesítése érdekében. Az elegyet 2 – 3 órán keresztül keverjük, és melegítjük 60 – 70 °C körül. A kapott szemikarbazon oldatokat elegyítjük  $\text{Fe}_2\text{SO}_4$  vizes oldatával (molarány 2:1), hozzáadunk egy késhegyi C-vitamint (aszorbinsavat) a vas(II) oxidációjának elkerüléséért, majd 1 – 2 órán keresztül forraljuk inert atmoszférában ( $\text{CO}_2$ ). A keletkezett terméket lehűtjük, vákuum alatt szűrjük, víz-alkohol (1:1) eleggyel, majd dietil-éterrel mossuk, és levegőn szárítjuk. A tioszemikarbazonok előállításánál hasonlóan járunk el, azzal a különbséggel, hogy nem szükséges a Na-acetát hozzáadása a tioszemikarbazid oldatához, mert nem sósavas só formájában van jelen.

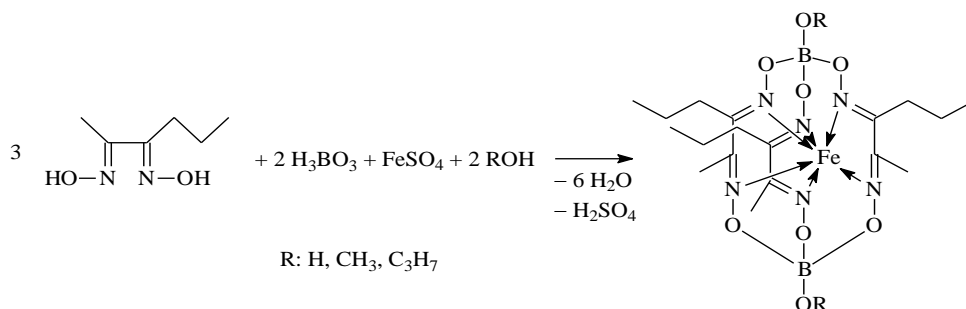
-  $[\text{Fe}(\text{Me-Pr-Gliox})_3(\text{BOR})_2]$ ,  $[\text{Fe}(\text{Me-i-Bu-Gliox})_3(\text{BOR})_2]$ , R = H, Me, n-propil, típusú komplexek előállítása



A Me-Pr-GlioxH<sub>2</sub>-ot 2,3-hexándionból, a Me-i-Bu-GlioxH<sub>2</sub>-ot pedig 5-Me-2-hexanonból kiindulva, a fennebb leírt módon állítjuk elő. A vas-komplekek előállításához a FeSO<sub>4</sub>-ot és a megfelelő dioximot oldjuk vízben vagy alkoholban az *R* csoporttól függően (*R*: H, Me, n-Pr), mólarány 1:3. A [Fe(dioximát)<sub>3</sub>(BOH)<sub>2</sub>] típusú komplexek esetében, ha nem oldódik vízben a glioxim, akkor etil-alkoholban oldjuk, de ne haladja meg a 10 %-ot a víz mennyiségéhez képest. Az így kapott elegyhez bórsavat adunk, a glioxim móljaival egyenlő mennyiségben, és egy késhegynyi C-vitamint (aszkorbinsavat). Az elegyet refluxáljuk 15 percen keresztül inert atmoszférában, majd hozzáadunk bóraxot a megfelelő oldószerben oldva, fele annyi mól-mennyiségben, mint a glioxim. Tovább folytatjuk a refluxálást 2 – 3 órán keresztül inert atmoszférában. A keletkezett terméket lehűtjük, vákuum alatt szűrjük, majd dietil-éterrel mossuk, és levegőn szárítjuk.

Lejátszódó reakciók:





### Eredmények és kiértékelés

Az előállított komplexek mikroszkópos jellemzése és előállítási hozama az 1. táblázatban látható.

1. táblázat. Az előállított komplexek mikroszkópos jellemzése, hozama és móltömege.

Sz.	Vegyület	Számít. móltöm.	Hozam (%)	Mikroszkópos jellemzés
1.	[Fe(1,4-dibróm-2,3-bután-DioxH) <sub>2</sub> (3-HO-anilin) <sub>2</sub> ]	819,91	15	Sötét barna színű, apró, háromszög alapú hasábok
2.	[Fe(1,4-dibróm-2,3-bután-DioxH) <sub>2</sub> (2-am.-pirimidin) <sub>2</sub> ]	791,86	51	Sötét barna színű, apró, háromszög alapú hasábok
3.	[Fe(4-benzil-2-HO-propiofenon-DioxH) <sub>2</sub> ]	622,46	95	Sötét barna színű, háromszög alapú hasábok
4.	[Fe(5-metil-2-hexanon) <sub>2</sub> en]	306,27	67	Sötét barna színű, háromszög alapú hasábok
5.	[Fe(5-metil-2-hexanon) <sub>2</sub> (1,2-pn)]	320,30	25	Fekete színű, lemezekbe tömörült háromsz. al. has.
6.	[Fe(5-metil-2-hexanon) <sub>2</sub> (1,3-pn)]	320,30	24	Fekete színű, lemezekbe háromszög alapú hasábok
7.	[Fe(5-metil-2-hexanon) <sub>2</sub> (o-fen)]	354,31	95	Vöröses-barna színű, szabálytalan mikrokristályok
8.	[Fe(2,4,5-trimetoxi-acetofenon-SC) <sub>2</sub> ]	588,40	78	Barna színű, apró, háromszög alapú hasábok
9.	[Fe(2,4,5-trimetoxi-acetofenon-TSC) <sub>2</sub> ]	620,52	95	Sötét barna színű, háromszög alapú hasábok
10.	[Fe(5-metil-2-hexanon-SC) <sub>2</sub> ]	396,31	32	Sárgás-zöld színű, háromszög alapú hasábok
11.	[Fe(5-metil-2-hexanon-TSC) <sub>2</sub> ]	428,43	10	Vöröses-barna színű, háromszög alapú hasábok
12.	[Fe(Me-Pr-Diox) <sub>3</sub> (BOH) <sub>2</sub> ]	537,95	39	Vöröses-barna színű, háromszög alapú hasábok
13.	[Fe(Me-Pr-Diox) <sub>3</sub> (BOMe) <sub>2</sub> ]	566,00	44	Vöröses-barna színű, háromszög alapú hasábok
14.	[Fe(Me-i-Bu-Diox) <sub>3</sub> (BOH) <sub>2</sub> ]	580,03	55	Vöröses-barna színű, háromszög alapú hasábok
15.	[Fe(Me-i-Bu-Diox) <sub>3</sub> (BOMe) <sub>2</sub> ]	608,08	52	Vöröses-narancssárga sz., háromszög alapú hasábok
16.	[Fe(Me-i-Bu-Diox) <sub>3</sub> (BO-n-propil) <sub>2</sub> ]	664,19	31	Barnás-zöld színű, háromszög alapú hasábok



### Tömegspektrometria

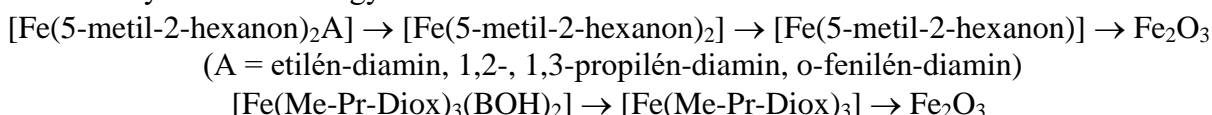
A tömegspektrumokat Agilent/Technologies 6320 Mass Spectrometer készülékkel rögzítették. A spektrumokban benne van a várt anyagok molekulatömege és bizonyos bomlási fragmenseket is sikerült azonosítani.

### Hőbontás (TG, DTG, DTA)

A hőbontást egy 951 TG és 910 DSC kaloriméter (DuPont Instruments) készülékkel végeztük Ar vagy N<sub>2</sub> atmoszférában, 10 K/min fűtési sebességgel (mintatömeg: 4 – 10 mg).

A Schiff-bázisos komplexek esetében első lépésben a diaminos rész távozik 150 °C körül, majd fokozatosan válik le a két ketonból származó rész a nitrogénnel együtt, végül Fe<sub>2</sub>O<sub>3</sub> marad vissza 700 °C körül. A bórsavas komplexeknél első lépésben leválik a két bóros rész 150 °C körül, majd egy robbanásszerű exoterm folyamat révén (a molekulában jelen levő sok oxigén miatt) leválik a három dioximos rész. Ezután a vashoz kötött nitrogének távoznak fokozatosan, végül visszamarad a Fe<sub>2</sub>O<sub>3</sub>.

A nyert adatokból egy általános bomlási mechanizmust állíthatunk fel:



### Por-Röntgen diffrakciós mérések

A por-röntgen diffrakciós méréseket egy PANalytical X'pert Pro MPD X-ray diffraktométerrel végeztük. A röntgen diffrakciós mérésekkel a komplexeink kristályosságát vizsgáltuk. Mivel új anyagok, nem találhatóak meg a diffraktogramjai a Cambridge-i adatbázisban.

### Infravörös spektroszkópai vizsgálatok

Az infravörös spektrumokat Varian 2000 FTIR spectrométerrel (Scimitar series) vettük fel, szobahőmérsékleten, 4000–400 cm<sup>-1</sup> hullámszám tartományban. A mintákat szilárd halmazállapotban, elporítva mértük. A főbb IR adatokat a négy típusú komplex egy-egy képviselőjéről a 2. táblázat tartalmazza.

2. táblázat. Az előállított Fe-komplexek IR adatai.

Vegyület	cm <sup>-1</sup>	$\nu_{\text{O-H}}$	$\nu_{\text{C-H}}$	$\nu_{\text{C=N}}$	$\delta_{\text{CH}_2}$	$\nu_{\text{N-O}}$	$\nu_{\text{B-O}}$	$\gamma_{\text{C-H}}$	$\nu_{\text{Fe-N}}$
[Fe(1,4-diBr-2,3-bután-DioxH) <sub>2</sub> (3-HO-anilin) <sub>2</sub> ]		3296 e	2934 gy	1612 ie	1356 k	1312 e	-	696 gy	602 ie
[Fe(5-Me-2-hexanon) <sub>2</sub> en]		-	2941 k	1638 e	1348 k	-	-	727 k	594 k
[Fe(5-Me-2-hexanon-SC) <sub>2</sub> ]		3393 k	2953 k	1661 e	1362 k	-	-	731 k	557 ie
[Fe(Me-Pr-Diox) <sub>3</sub> (BOH) <sub>2</sub> ]		3409 e	2963 e	1636 k	1385 e	1331 k	977 e	721 gy	597 k

(ie = igen erős, e = erős, k = közepes, gy = gyenge)

### NMR spektroszkópia

A spektrumokat (<sup>1</sup>H és <sup>13</sup>C NMR) egy Bruker AVANCE spectrométerrel vettük fel 250 MHz (<sup>13</sup>C: 63 MHz) frekvenciával. Csak a ligandumokra vettük fel, mellyel igazoltuk a ligandumok képződését.

### UV-VIS spektroszkópia

Felvettük komplexeink UV spektrumait 10%-os etil-alkoholos oldatban, valamint pH függvényében, Britton-Robinson puffer-oldatokat használva, és meghatároztuk savassági

állandóikat. Példaként két komplexnél a tiszta oldatokra kapott hullámhossz értékek, [Fe(5-metil-2-hexanon-SC)<sub>2</sub>]: 191, 226, 357 nm, [Fe(Me-Pr-Diox)<sub>3</sub>(BOH)<sub>2</sub>]: 192, 225, 447 nm.

### KÖVETKEZTETÉSEK

Munkánk során három típusú Fe(II)-komplexeket állítottunk elő, melyek várhatóan biológiai szempontból lesznek jelentősek, mint pl. antibakteriális és antitumor hatás.

### KÖSZÖNETNYILVÁNÍTÁS

A szerzők közül ifj. Várhelyi Csaba köszöni a „Domus Hungarica“ alapítványnak, hogy a számára megítélt évi egy hónapos ösztöndíjakkal lehetővé tette a jelen dolgozat létrejöttét.

### IRODALOM

- [1] M.H. Soliman, A.M.M. Hindy, G.G. Mohamed, *J. Therm. Anal. Calorim.* 115 (2014) 987
- [2] E.M. Zayed, M.A. Zayed, A.M.M. Hindy, *J. Therm. Anal. Calorim.* 116 (2014) 391
- [3] F.U. Shah, M. Jamil, J. Aslam, A. Gul, Z. Akhter, B. Mirza, *J. Chem. Soc. Pak.*, 38(06) (2016) 1112
- [4] G.N. Schrauzer, *Chem. Ber.* 95(6) (1962) 1438

## BASIC LEVEL OF ENVIRONMENTAL KNOWLEDGE AMONG HIGHER EDUCATION STUDENTS

László Berényi<sup>1</sup>

<sup>1</sup>*Institute of Management Science, University of Miskolc, H-3515 Miskolc-Egyetemváros, Hungary  
e-mail: szyblaci@uni-miskolc.hu*

### Abstract

Moving towards a sustainable World requires many efforts in various fields including technological development, financing, management and even education. People as consumers and employees are both the beneficiaries and the responsible for the sustainable development. Especially young people play an important role since they are expected to become the corporate decision makers. Improving corporate environmental performance contributes significantly to sustainable development. Accordingly, the level of environmental knowledge is a fundamental influencing factor. The paper summarizes the results of a survey about basic knowledge related to environmental issues. The analysis explores the characteristics of Hungarian higher education business students (n=104). The results show a lack of the average knowledge level based on the learning material of the elementary school.

### Introduction

There was an enhancing interest in solving the global environmental and social problems over the past decades. However, the break-through fails due to the conflict of interests, especially economic ones [1]. Notwithstanding that involving economic aspect can explain both personal and corporate behavior, other viewpoints should not be ignored.

The United Nations set up a comprehensive framework model of sustainable development goals. It covers environmental, social and economic aspects (Figure 1). The varied scope of the goals seems to be wordy and diffuse but it denotes the aspects to consider in the related decisions.



Figure 1. Sustainable development goals [2]

Even if economic interest and financial possibilities do not inhibit the sustainable actions, the lack of knowledge may have a negative impact. I believe that professional and environmental knowledge is a key factor in understanding the related competencies both on individual and corporate level towards a sustainable living. If the basic knowledge in the topics is missing,

reliable and effective decisions are hard to expect; people as consumer can be either influenced or abused by profit-seeking companies.

Models of environmental conscious behavior usually use the factors of knowledge. The theory of reasoned action [3] is a base model that deduces behavior from knowledge and values (norms) through intention to behavior. Other researchers refine and enhance the concept (see [4][5][6]).

A recent survey about the perception of the content of corporate social responsibility (CSR) analyzes the attitudes and presupposition of business students [7]. The results show the CSR is a popular topic and achievable but they doubt the usefulness of the initiations in solving the global problems. Other results of the research also show contradictions and uncertainty in the opinions. This experience suggests the special importance of developing the knowledge.

### Experimental

I started a survey first in 2008 to explore the attitudes and knowledge level related to environmental issues as a part of the OTKA PD71685 research entitled ‘Factors and Measurement of Environmental-Consciousness’ [8]. The target group was the public education and the research also involved higher education business students as a control group. A repeating survey was conducted in the higher education with the same questionnaire in 2016.

The questionnaire is a single-choice test including 22 questions about physics and chemistry, biology, geography and living. All questions come from the official training material of the elementary schools and a 10-year-old child can answer about the half of the questions. The questions are presented in the results and discussion section.

The research sample of 2016 includes 104 answers of business education students from various Hungarian universities. All of the respondents were born between 1990 and 1997. 42.3% of them are female.

The conclusion of the former survey said that the general level of environmental knowledge is quite poor, though the results depend on the scientific area [8]. The research aims to explore the state and characteristics in 2016.

### Results and discussion

Based on the ratio of correct answers it can be stated that the knowledge about physics, chemistry and biology has deficiencies that are more serious in 2016 than in 2008.

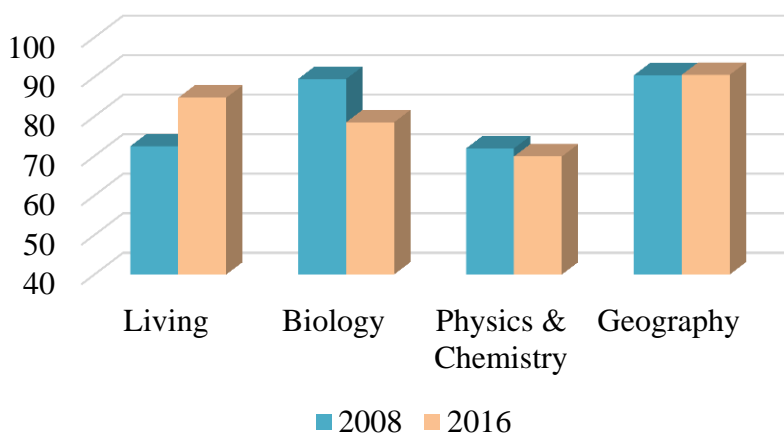


Figure 2: Survey results by knowledge are (average ratio of correct answers)

Comparing the data between 2008 [8] and 2016 there is a notable improvement in the fields of living issues and a relapse in biology (Figure 2). The independent samples T-test confirms that these differences are statistically significant (living:  $t=-6.051$ ,  $d_f=156$ ,  $sig=.000$ ; biology  $t=2.861$   $d_f=156$   $sig=.005$ ).

Table 1 summarizes shows the test questions and the ratio of correct answers in % of the samples for the total sample and by gender in 2016.

Category	Question	Total sample	Female	Male
Biology	Which animal does NOT take a quiescence?	87.5	90.9	85.0
	Which type of tree is typical in Hungary?	82.7	90.9	76.7
	Which organ is for the balance of the body?	69.2	54.5	80.0
Geography	If North is in front of me, on the left is...	93.3	93.2	93.3
	Which direction is shown by the compass?	97.1	97.7	96.7
	What is the reason for flood?	96.2	95.5	96.7
	The sea level is increased by...	98.1	97.7	98.3
	The altitude of snow line in temperate areas is...	64.4	52.3	73.3
	The color of mountains in the atlas is...	94.2	90.9	96.7
Living	How often should We have meal in a day?	72.1	81.8	65.0
	Which vitamin aids the health of bones?	71.2	68.2	73.3
	Paprika contains much of...	95.2	93.2	96.7
	Which is NOT an element of healthy living?	97.1	93.2	100.0
	Man can run in 12 minutes...	87.5	81.8	91.7
	Which makes us bronzed?	79.8	84.1	76.7
	What is the substance of selective waste collection?	90.4	97.7	85.0
Physics & Chemistry	The highest temperature on the Earth was...	65.4	61.4	68.3
	Which accelerates the melting of the arctic ice?	96.2	95.5	96.7
	Which is an important greenhouse-gas?	82.7	79.5	85.0
	Which gas effects acid rain?	90.4	90.9	90.0
	The air contains mainly...	55.8	38.6	68.3
	The pH of acid rain is...	28.8	25.0	31.7

Table 1: Survey results (ratio of correct answers in % of the samples)

Since the ratios of the correct answers shows the upper fifth in almost all questions, it is worth to focus on the weak points:

- Only 69.2% of the respondents did know that the ear is for the balance of the body. 24% think the brain.
- The snow line in our area is ca. 1,000-15,000 by 23.1% of the respondents.
- 25.9% of the respondents believe that three meals a day is ideal instead of five.
- 19% marked vitamin A as necessary for the bones.
- 7.7% is suntanned by infra and 11.5% by VHF radiation.

- There is an uncertain average opinion about the highest ever temperature. 22.1% think 80 °C and 7.7 % 45 °C.
- 55.8% of the respondents did know that the air contains mainly nitrogen, 41.3% marked oxygen.
- pH of the acid rain shows the worse result of the test. 33.7% marked pH 5-7, 28.8% pH 7-9 and 8.7% is ratio who do not know.

The bivariate correlation analysis point out that the ratio of correct answers by categories do not depend from each other. A significant correlation can be found only between living and physics & chemistry but this connection is weak (Pearson correlation=.228 N=104 sig=.020). The distribution of the knowledge level is presented in Figure 3. 13.5% of the respondents completed the test under the two-thirds of the available points; only one person performed under a 50% level. However, 71 respondents completed the test over 80%; the number of respondent under 90% is twice as above this performance.

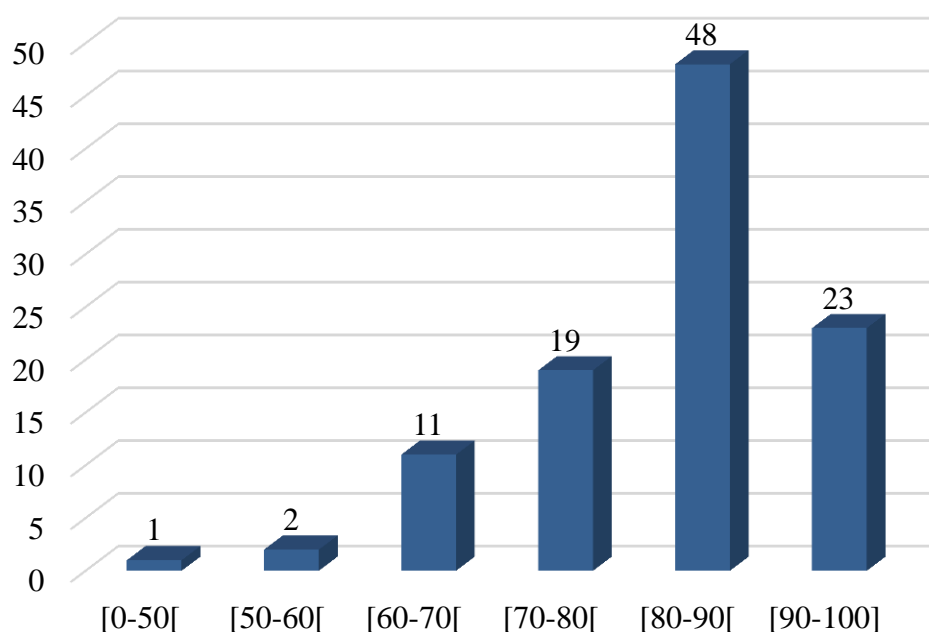


Figure 3: Distribution of individual knowledge level (in persons)

The research sample allowed comparing the knowledge level also by gender. Former research experiences in the field point out that the female respondents usually gave higher ratings, the overall picture shows a more definite and more sensitive approach of them to environmental and social problems and they have trust more in the usefulness of CSR [9].

The question comes whether there is a significant pattern in case of the knowledge level. Since the data set is different, a direct test is not feasible but comparing the tendencies may help to designate the further research activities and necessary interventions.

Females are usually better in biology, “sun-bathing”, eating issues, and selective waste collection. The independent-samples T test (Levene’s Test for equality of variances is passed) show that there is not significant difference between females and male in case of living ( $t=.632$   $d_f=102$   $sig=.529$ ) and biology ( $t=.885$   $d_f=102$   $sig=.378$ ) issues. Males’ knowledge level is

significantly higher in geography ( $t=-2.360$   $d_f=102$   $sig=.020$ ) and physics & chemistry ( $t=2.090$   $d_f=102$   $sig=.039$ ) issues in the sample.

### **Conclusion**

The main conclusion of the survey can be formulated as adults are not smarter than a primary school student in general issues linked to the sustainable development. A simple test can show that basic knowledge of may be out of the memory, while everyday decision would need those. The results do not draw a disastrous picture but development is expected.

Moreover, further investigation is required in order to explore the reasons of the weaker performances that must include testing the knowledge at various study levels and faculties. Nevertheless, the low level of knowledge in this topic has a risk that important decisions will be made without the adequate basics.

The difference between the responsiveness of females and males gives the question whether education requires two different strategies for them or a common solution is available. I believe that common way is viable.

### **References**

- [1] T. Laudal. Drivers and barriers of CSR and the size and internationalization of firms. *Social Responsibility Journal* 7(2) (2011) 234–256.
- [2] UNITED NATIONS. *Transforming our World: The 2030 Agenda for Sustainable Development* (2015)
- [3] I. Ajzen, M. Fishbein. *Understanding attitudes and predicting social behaviour*. Prentice-Hall. Englewood Cliffs. 1980. pp. 278.
- [4] R. G. Disposito. Interrelationships Among Measures of Environmental Activity, Emotionality and Knowledge. *Educational and Psychological Measurement* 37(Summer) (1977) 451–459.
- [5] J. M. Hines, H. M. Hungerford, A. N. Tomera. Analysis and Synthesis of Research on Responsible Pro-environmental Behavior: a meta-analysis. *The Journal of Environmental Education* 18(2) (1986) 1–8.
- [6] R. Y. K. Chan. Environmental Attitudes and Behavior of Consumers in China: Survey Findings and Implications. *Journal of International Consumer Marketing* 11(4) (1998) 25–52.
- [7] L. Berényi., N. Deutsch. Perception of the Content of Corporate Social Responsibility by Hungarian Business Students *WSEAS Transactions on Advances in Engineering Education* 14 (2017) 81–89.
- [8] L. Berényi. Level of Environmental Knowledge and Attitudes. *Proceedings of the 16th International Symposium on Analytical and Environmental Problems* (2010) 337–340.
- [9] L. Berényi, N. Deutsch, É. Pintér. Business students' preferences about social responsibility in Hungary. *WSEAS Transactions on Business and Economics* 13 (2016) 662–674.



## DEVELOPMENT OF REDOXPROTEIN-BASED BIOHYBRID SENSOR DEVICE

**Richárd Csekő, Bence Kecskés, Tibor Szabó, László Nagy, Kata Hajdu,**

*Institute of Medical Physics and Informatics, University of Szeged, H-6720, Szeged,  
Rerrich B. tér 1. Hungary  
e-mail: Richárd Csekő<csekorichard@gmail.com>*

### **Abstract**

We have successfully developed an enzyme electrode based on photosynthetic reaction centre (RC) protein of *Rhodobacter sphaeroides* purple bacteria. We bound the protein chemically to the electrode surface through a layer of multi-walled carbon nanotubes (MWCNTs). The surface was borosilicate glass covered with indium-tin-oxide (ITO) for its transparency and well-known qualities as an electric semiconductor. We achieved a bio-nanocomposite with good features to support the protein's photosynthetic activity. To test it, we used the nanocomposite as a working electrode in a traditional electrochemical cell with electrolytes containing only mediators or mediators and inhibitors (herbicides that block the protein's activity specifically). Our measurements provided great results in terms of electric current ("photocurrent") generated by the photon-excited RC, regeneration of the electrode surface and stability of the composite. For further optimization of the system, we decided to replace the RC/MWCNT part with a two-component protein complex of chemically bound RC and cytochrome c, which is a natural electron donor of the RC protein. We have successfully prepared the complex and made several measurements to determine the quantity and quality of the product, with good results.

### **Introduction**

The unique attributes of the RC protein [1] offers a great number of possible applications in photoelectric devices [2-4]. It also has to be emphasized that in the presence of mediator molecules and light, the RC completes its photosynthetic cycle even *in vitro*. In an electrochemical cell as a working electrode it produces an easily measureable amount of electric current [5]. It has been proven that the RC protein, bound to a gold electrode in a photoelectrochemical cell produces notable activity under various conditions [6]. This photocurrent can be blocked by several herbicides or quinone-side inhibitors [7]. There are numerous "triazine-type", RC specific, environmentally hazardous herbicides long forbidden in the EU but still used in USA, China, etc. Monitoring their concentration in the soil is an important goal of environmental protection.

The RC has a natural electron donor protein, c type cytochrome. There are many experiments noted in the literature [8-10] to bind cytochrome and RC together in a complex formula. This would open ways to control the orientation of the RC bound on the surface. A nanocomposite with an oriented dual protein complex layer immobilized chemically and used as a working electrode of an electrochemical cell would give further opportunities to examine and apply the RC's photosynthetic activity in the future.

### **Experimental**

Preparation of the electrodes We created thiol groups on the ITO surface by a functionalization procedure with (3-mercaptopropyl)trimethoxy-silane, and used these groups to bind MWCNTs through their amine groups, which we previously activated with sulfo-



SMCC. After 2 hours of reaction time the excess nanotubes were washed down from the surface. As crosslink agents we used NHS and EDC, solved in distilled water, to immobilize the RCs deposited on the surface for 2 hours at 4°C. After the fixation of the proteins, we washed the electrode surface intensively with 0.1M pH 7 phosphate buffer.

Electrochemistry We used the prepared nanocomposite as a working electrode in an electrochemical cell with three electrodes. The counter and the reference electrode was Pt and Ag\AgCl, respectively. As an electrolyte, we used UQ-0 and ferrocene solved in 20 mM TRIS buffer, pH 8.00. The measurements were carried out using a Metrohm PGSTAT204 type potentiostat/galvanostat at ambient temperature. The light source was a 150W halogen lamp. The light intensity was 78 mW·cm<sup>-2</sup>.

Sensory measurements We used orto-phenantroline (o-Phe) and terbutryn as inhibitors of the protein activity. Both are herbicides that bind specifically to the RC's secondary quinone binding site, thus preventing it from binding its electron acceptors and completing its charge separation cycle. In the absence of the herbicides, we measured current densities of a few μA cm<sup>-2</sup> after 100 s dark incubation. The measured photocurrent was successfully inhibited with o-Phe gradually increased from zero to 600 μM. The same experiment was completed with terbutryn as well (data not shown). We have determined the fitted inhibitor constants of both terbutryn and o-Phe from the figure of the photocurrent inhibition as a function of herbicide concentration. We stored the prepared composites in dark environment and 4°C, and gained evidence that the RCs bound to the electrode surface stayed active (produced measurable photocurrent) even after weeks. Dipping the electrode into the solution of the RC's substrate ubiquinone-0 caused the herbicides to dissociate from the protein thus led to the regeneration of the electrode surface. The speed and efficiency of the regeneration increased with greater substrate concentrations from 100 μM UQ-0 to 1 mM.

Preparation of the RC/cytochrome protein complex We have prepared protein complexes from RC and horse heart cytochrome c by chemically binding them together in their natural state of redox interaction. We followed the steps described by Drepper et al. [10] and Rosen et al. [9] for the preparation of the complex. The proportion of cytochrome to RC was 3:1, and both proteins were in a solution of 10 mM pH 7.5 HEPES buffer in the presence of 0.025% LDAO to prevent the RC from aggregation. The proper redox environment for the reaction was granted by 1 mM of ascorbate and 60 μM of 1,4-naphtoquinone. After the addition of 12 mM NHS and 6 mM EDC crosslinking agents, the reaction was carried out in 3 hours of dark incubation at room temperature. We stopped the reaction with the addition of 50 mM ammonium acetate. After 10 minutes, we dialyzed the solution at 4°C overnight against 10 mM TRIS-HCl, pH 8 with 0,025% LDAO.

Purification and measuring of the complex The dialyzed sample was eluted through a Sephadex G-75 column (1x15 cm) with pH 8.00 TRIS-HCl buffer to separate the complex from the excess RC and cytochrome molecules. We took 12 fractions of 0.5 cm<sup>3</sup> and measured them one by one with UV-Vis spectroscopy. The fractions providing the best results of RC and cytochrome presence were passed through a Sephadex G-50 column again for better resolution. The second set of 0.5 cm<sup>3</sup> fractions was measured with UV-Vis spectroscopy as well, and 3 fractions (4th, 5th and 6th) contained the full amount of the product. They were put together in a filtered Falcon tube and concentrated by centrifuge at 5000 RPM. We studied the concentrated sample with absorption kinetics spectroscopy at 860 nm wavelength to search for the characteristic absorption change of the light excitation and charge separation in the RC.

## Results and discussion

**Electrochemistry** Figure 1 shows the unmodified photocurrent generated by the RC/MWCNT/ITO electrode in the electrochemical cell, and the steps of increasing inhibition by the successive addition of *o*-Phe up to a concentration of 600  $\mu\text{M}$ . The electrolyte contained 100 mM UQ-0, 20  $\mu\text{M}$  ferrocene as electron donor and 20 mM TRIS-HCl buffer. The results clearly show the capability of sensory application of the system.

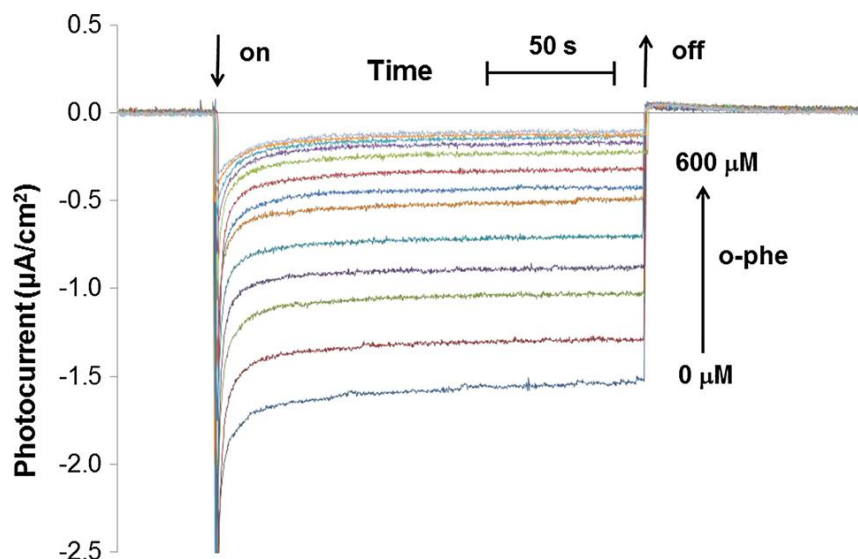


Figure 1. Generated photocurrent in the absence and in the presence of herbicide.

Based on this measurement we fitted a logistic function (Figure 2) to determine the  $K_I$ , the fitted inhibitor constant (the concentration that causes half of the maximum inhibition). The fitting was done with the function: 
$$Y = \frac{Y_{max} - Y_{min}}{1 + \frac{[K_I]}{[I]}}$$

$Y_{Max}$  and  $Y_{Min}$  are the signals in the absence and presence of the inhibitor, respectively;  $K_I$  is the fitted inhibitor constant,  $[I]$  is the actual inhibitor concentration.

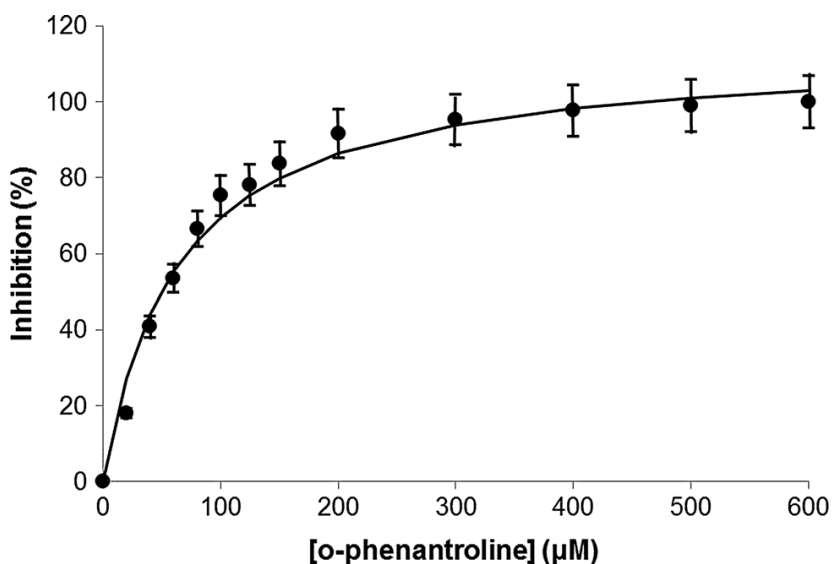


Figure 2. Fitted logistic function of the photocurrent inhibition.

Measuring the RC/cytochrome complex After cleaning the complex from the excess RC and cytochrome we took measurements with an UNICAM UV4 type spectroscope. We collected data through the 325-900 nm wavelength interval, but figures show only the part of the spectra that has information value. Figure 3 shows the spectra of the fractions containing the protein complex, with two samples from the start and end of the set as references.

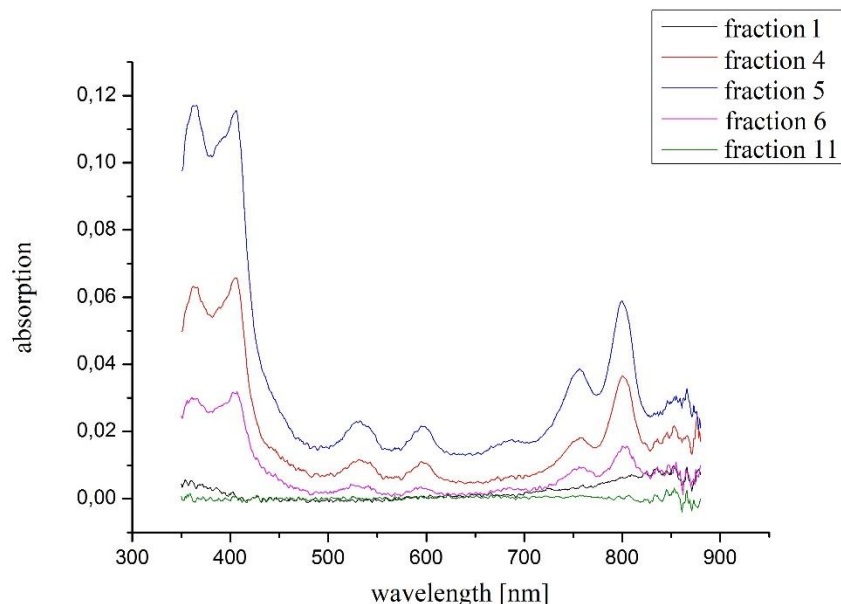


Figure 3. Only three of the 12 fractions contained the product.

After we concentrated these fractions with a centrifuge, we tested the complex to see if the cytochrome was still intact and active. We measured the sample in both oxidized and reduced state to see the characteristic reduced double peak at 530 nm. Figure 4 shows the result of the measurement.

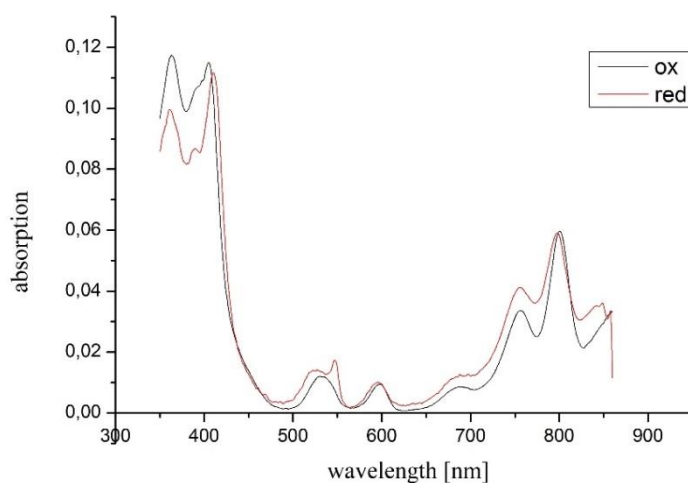


Figure 4. The spectroscopy proved we had an intact and working cytochrome bound to the RC

This was followed by a measurement of absorption kinetics for real time monitoring of the redox activity of the complex. Background signal was complemented using offset voltage to set the base line to zero, then flash kinetics were measured on 860 nm where the P\*/P+ shift can be seen upon the light excitation and charge separation of the RC protein. Figure 5 shows the result of the absorption kinetics experiment.

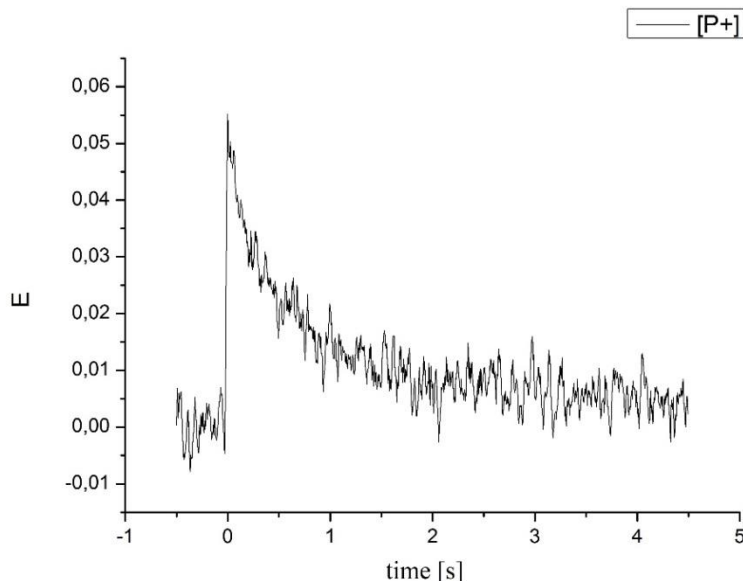


Figure 5. Flash absorption kinetics of the protein complex at 860 nm.

### Conclusion

It is clear that the RC/MWCNT/ITO nanocomposite produced good results of photoelectric activity and as a sensor for herbicides. The system can be further optimized by utilizing a RC/cytochrome complex to control the orientation of the RC protein. Preparation of this complex has been successfully done at our lab. Results of the RC/cytochrome complex measurements indicate good chances for its application in the electrochemical biosensor.

### Acknowledgements

This work was supported by the Hungarian National Scientific Research Fund OTKA (PD 116739) and by the New National Excellence Program of The Ministry of Human capacities, UNKP-17-1.

### References

- [1] L. Nagy, K. Hajdu, B. Fisher, K. Hernádi, K. Nagy, J. Vincze, *Notulae Scientia Biologica* (2) (2010) 7–13.
- [2] AO Govorov, I Carmeli, *Nano Letters*, 7(3) (2006) 620–625.
- [3] VM Friebe, JD Delgado, DJK Swainsbury, JM Gruber, A Chanaewa, R van Grondelle, E von Hauff, D Millo, MR Jones, RN Frese, *Adv. Funct. Mater.*, 26(2) (2016) 285-292.
- [4] C Nakamura, M Hasegawa, N Nakamura, J Miyake, *Biosensors and Bioelectronics* 18 (2003) 599-603.
- [5] T Szabó, E Nyerki, T Tóth, R Csekő, M Magyar, E Horváth, K Hernádi, B Endrődi, Cs Visy, L Forró, L Nagy, *Phys Status Solidi B*, 252 (2015) 2614–2619.

- [6] M den Hollander, JG Magis, P Fuchsenberger, TJ Aartsma, MR Jones, NR Frese, *Langmuir*, 27 (2011) 10282–10294.
- [7] DJK Swainsbury, VM Friebe, RN Frese, MR Jones *Biosensors and Bioelectronics*, 58 (2014) 172–178.
- [8] T. Uneo, Y. Hirata, M. Hara, T. Arai, A. Sato, J. Miyake, T. Fujii, *Materials Science and Engineering: C* 3 (1995) 1-6.
- [9] D. Rosen, M. Y. Okamura, E. C. Abresch, G. E. Valkirs, és G. Feher, *Biochemistry*, 22 (1983) 335-341.
- [10] F. Drepper, P. Dorlet, P. Mathis, *Biochemistry*, 36 (1997) 1418-1427.

## **STREFOWA - STRATEGIES TO REDUCE AND MANAGE FOOD WASTE IN HUNGARY**

**Sandra Stojanović, Renata Bodnárné Sándor**

*Department of Logistic Systems, Bay Zoltán Nonprofit Ltd. for Applied Research  
Division of Intelligent Systems (BAY-SMART), H-3519 Miskolc, Iglói út 2.  
e-mail: sandra.stojanovic@bayzoltan.hu*

### **Abstract**

Food waste and the food wastage are nowadays a major problem mainly in the developed countries because of numerous environmental impacts such as exploitation of the croplands, surplus production, carbon-dioxide emissions, waste problems etc. Food waste also represents the economic problems: it has a financial loading, which is mainly at the population, who purchase products and later they generate the waste from that. In addition to the environmental and economic issues, there is also social problem: hundreds of thousands of people live in extreme poverty and hunger, not only in Europe.

Within the STREFOWA project – which is supported by the European Union – the action has been undertaken in order to reduce the amount of food waste by implementing different innovative pilots in some countries of Central Europe.

In Hungary, the main actor of the pilot is the retail sector, which has the possibility to affect the population to reduce the amount of the food waste, influencing them to change wrong habits and consider the possibility of food donation for needy people.

### **1. Introduction**

With continuous growth of population, the issue of the worldwide food loss and waste is classified as a highly important, since it has countless negative social, environmental and economic impacts. Global demand for food leads to overexploitation of resources used for the excessive food production and can also affect the increase in the effects of global climate change due to improper food waste disposal. Economically, wasted food directly represents an unnecessary cost for both farmers and consumers. But above all, food waste is primarily an ethical problem since many people live on the margins of hunger and food insecurity [1, 2, 3]. “Food loss” can be related to the reduction of edible food material predetermined for human consumption which can occur at any stage of the food supply chain as a result of agricultural process, technical limitations or marketing. On the other hand, food losses of good quality food which arise at the end of food supply chain are mainly defined as a “food waste” since the food suitable for consumption gets discharged. This phenomenon is related to behavioural issues such as negligence or conscious decision of consumers and retailers to throw food away [1, 2, 4].

The overall food losses and waste, according to The Food and Agriculture Organization of the United Nations (FAO), are estimated at nearly 1.3 billion tons/year, which represents 1/3 of the food produced in the world [1, 2]. The European Union generates about 88 million tons of food waste yearly which values around 143 billion EUR – according to the data derived from the Fusion EU project. As shown at figure 1, consumption stage generates the most of European food waste. The amount of food waste in Hungary is estimated to approximately 1.8 million tonnes per year with calculation of 400 000 tons annually from consumers, which is actually 40 kg per person.

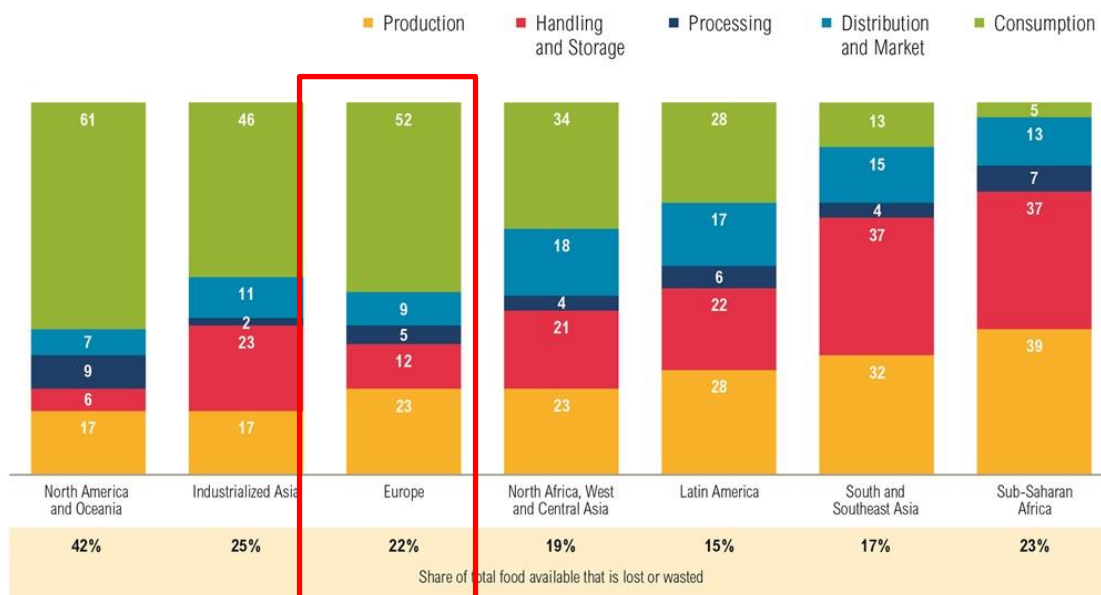


**Figure 1: Share of total food wasted or lost**

STREFOWA - Strategies to Reduce and Manage Food Waste in Central Europe (CE), is the Interreg CE project on natural and cultural resources for sustainable growth. The project’s main objective is improvement in food waste management in selected CE functional urban areas by encouraging food waste prevention and treatment which is triggering reduction of environmental impacts. Achieved results of the project are contributing to raise the level of knowledge and improve implementation capacity on food waste management throughout whole food supply. Different pilot and demonstration actions are implemented in order to enable true reduction of food waste and optimisation in food waste treatment. Within the STREFOWA project, the aim of the Hungarian pilot actions is to raise the knowledge and consciousness of people while simultaneously working on the reduction of food waste arisen at the customers. Regularly repeated pilot actions should result in raised awareness and change of wrong habits.

## 2. Experimental

### 2.1 Data collection

The main aim of the research was to determine food waste amounts generated in small shops such as butchery, fruit/vegetable grocery stores and bakeries; to identify the root causes of food waste generation at retailers and to highlight some potential possibilities and good practices in terms of food waste prevention and management. This work focuses on two different types of retailers (hypermarkets and small shops) together with consumer sector.

For the purpose of research, short survey has been used as the main form of data collection and it was conducted in small shops by Bay Zoltán Nonprofit Ltd. for Applied Research. The inquiry took place in the area of Miskolc city (except Görömböly, Helyőcsaba, Majláth) and some of its surrounding settlements (Felsőzsolca and Onga). Altogether, 34 interviews had been filled out in shops – 16 in fruit/vegetable stores, 10 in bakeries and 8 in butchers. There were 6 different questions in each questionnaire and most of the personnel were willing to cooperate. The questionnaire covered following key elements:

- Qualitative and quantitative waste data – concerning type of waste, volumes and percentages
- Seasonal fluctuations in waste volume



- Food waste prevention measures and management – including good practices and ideas for further measures

Due to the sensitivity of waste data information the survey does not contain covering details about the company.

### 2.2 Data analysis

For the analysis and data comparison, also food waste data generated in hypermarkets and households were observed. The TESCO Co. published the data of their food surplus and waste, which was used in this work [5]. For the information about lost food in the households, data from the research conducted by NÉBIH (The National Food Chain Safety Agency) in 100 households during 1 week were used [6].

### 3. Results and discussion

The results are presented according to 2 key elements. First step includes overall comparison of food waste amount which is followed by the main food waste prevention measures and management plans.

Inquiry conducted in small retailers shows that the average amount of food waste is estimated between 0-10%. The lowest percentage can be found in meat shops, never exceeding 5%. As for qualitative properties of the waste, in fruit/vegetable stores, the percentage distribution is equal: 50% fruit and 50% vegetable; in bakery the most dominant are bakers' ware and bread while in butchers shop the main source of food waste are processing remains (bones, fat, etc.). Seasonal fluctuations are not recorded in bakery, while in butchers as well as in fruit/vegetable shops production of food waste is higher during the summer.

According to the data published by TESCO (2017) and as shown at Figure 2, the surplus food material generated in this company is estimated to be about 2% of the all sold products (in tons). Important share in those 2 percent belongs to edible part of food surplus – approximately 54.74% while inedible part makes 45.26%.

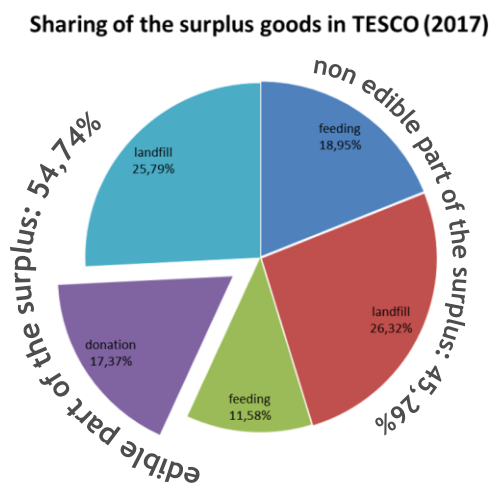


**Figure 2: Distribution of the food surplus and waste in TESCO (2017) [5]**

The amount of food lost in households estimates at 68.04 kg/capita/year which is equal to 30 000 Ft. As shown at Figure 3, the highest percentage of this amount makes avoidable food waste (48.7%), immediately followed by non-avoidable (47.13%) and at the end, only small share, 4.17% is estimated to be potentially avoidable food waste.

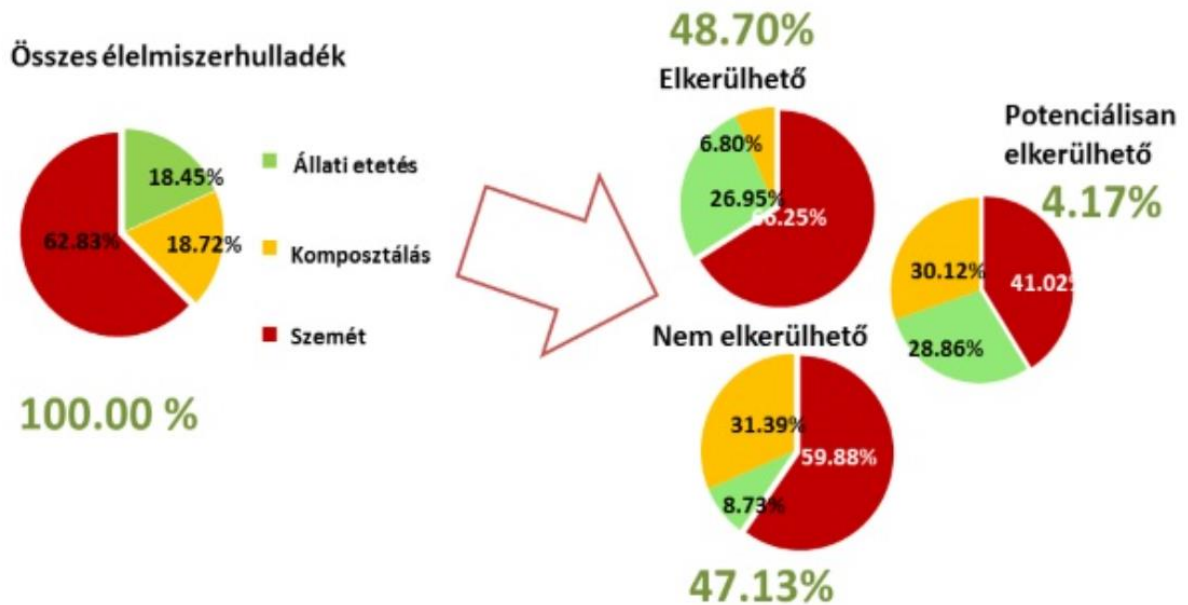


**Figure 3: Share of total food waste generated in Hungarian households [6]**

According to the survey conducted in small retail shops, the main practices for food waste prevention are the price reduction and quantitative/qualitative modification in the future orders. The most preferred waste treatment is communal waste, followed by donation for animal feeding and others. Same as in small shops, data published by TESCO shows that the biggest part of food waste end up at landfills (approximately 52%) while feeding and donation are less represented with nearly 31% and 17%, respectively. On this issue households don't differ from retail sector since food waste is primarily being landfilled (almost 63%). The rest of the food waste generated in households is either composted or donated for animal feeding (both approx. 18%).

#### 4. Conclusion

This study was aimed to identify and compare food waste data from small shops, hypermarkets and households. The results revealed that main management practices in each observed category is similar, meaning that landfill is the leading practice. Even though donations, either for humans or for animals, are present in retail sector as a waste prevention measure, they are not enough to change the behavior and conscious of consumers. Therefore, one of the main roles in household food waste prevention belongs exactly to retailers. Due to closely connected relationship between retailers and customers, it is highly recommended that retailers influence their customers to prevent and decrease food waste in their households. These measures can be implemented in many different ways, such as pilot actions, promotions, educational material etc.

#### Acknowledgements

This research was conducted as a part of STREFOWA Interreg CE project funded by European Union.

#### References

1. Lipinski, B., Hanson, C., Lomax, J., Kitinoja, L., Waite, R., & Searchinger, T. (2013). Reducing Food Loss and Waste. *World Resource Institute*, (June), 1–40.

2. FAO. (2011). *Global food losses and food waste - Extent, causes and prevention. SAVE FOOD: An initiative on Food Loss and Waste Reduction*. Rome.
3. Godfray, C., Beddington, J., Crute, I., Haddad, L., Lawrence, D., Muir, J. F., ... Toulmin, C. (2010). Food Security : The Challenge of Feeding 9 Billion People. *Science*, 327(February), 812–818.
4. Parfitt, J., Barthel, M., & Macnaughton, S. (2010). Food waste within food supply chains: quantification and potential for change to 2050. *Philosophical Transactions of the Royal Society B: Biological Sciences*, 365(1554), 3065–3081.
5. Index - Gazdaság - A felesleges kaja fele a kerül kukába, és ez nagyon jó eredménynek számít. (n.d.). Retrieved September 21, 2017, from [http://index.hu/gazdasag/2017/09/21/elemiszerhulladek\\_tesco\\_jelentes\\_kidobott\\_adoman\\_yozott\\_etel/](http://index.hu/gazdasag/2017/09/21/elemiszerhulladek_tesco_jelentes_kidobott_adoman_yozott_etel/)
6. Igazgatóság, É. K. (2017). NÉBIH – Maradék nélkül program Kutatási eredmények összefoglalása.

## FEASIBILITY STUDY OF spICP-MS FOR THE DETERMINATION OF THE STRUCTURE AND COMPOSITION OF BIMETALLIC NANOPARTICLES

Albert Kéri<sup>1</sup>, Ildikó Kálmista<sup>1</sup>, Ditta Ungor<sup>2</sup>, Ádám Bélteki<sup>1</sup>, Edit Csapó<sup>3,4</sup>,  
Imre Dékány<sup>3</sup>, Thomas Prohaska<sup>5</sup>, Gábor Galbács<sup>1</sup>

<sup>1</sup>*Dept. of Inorg. and Anal. Chem., University of Szeged,  
6720 Szeged, Dóm sq. 7, Hungary, e-mail: galbx@chem.u-szeged.hu*

<sup>2</sup>*Dept. of Med. Chem., University of Szeged,  
6720 Szeged, Dóm square 8, Hungary*

<sup>3</sup>*Dept. of Phys. Chem. and Mat. Sci., University of Szeged,  
6720 Szeged, Aradi V. square 1, Hungary*

<sup>4</sup>*MTA-SZTE Biomim. Sys. Res. Gr., Dept. of Med. Chem., University of Szeged,  
6720 Szeged, Dóm square 8, Hungary*

<sup>5</sup>*Div. of Anal. Chem., University of Natural Resources and Life Sciences,  
1180 Vienna, Gregor-Mendel-Straße 33, Austria*

### Abstract

Our present work is focused on the spICP-MS measurement of bimetallic (gold-silver core-shell and alloy) nanoparticles. We found that suitable measurement conditions and data evaluation approaches actually allow the determination of not only the elemental composition (Au:Ag molar ratio) of such particles, but we can gain information about their structure too. Our paper will present data obtained by using both regular (millisecond-range) and high (microsecond-range) time resolution spICP-MS experiments.

### Introduction

Nanoscience is a rapidly developing field in science and technology. Nanomaterials (nanoparticles, nanocomposites, nanostructures, etc.) are nowadays widely used in a broad range of application fields including medicine, catalysis, energetics, sensorics, etc. Certain bimetallic nanoparticles (BNPs) have tunable magnetic, catalytic and optical properties, therefore they have been designed and synthesized in great numbers for novel application areas in recent years. The morphological and compositional characterization of zero dimensional nanocomposites or BNPs are traditionally done by a combination of methods including electron microscopy (TEM, SEM-EDS), X-ray diffraction (XRD), UV-Vis spectroscopy, X-ray photoelectron spectroscopy (XPS), or atomic spectroscopy following dissolution [1].

Single particle, or particle-mode, inductively coupled plasma mass spectrometry (spICP-MS) is a novel technique where ICP-MS spectrometers are used in the time-resolved mode for the measurement of dilute nanodispersions. Each detected NP produces a narrow signal peak (a few hundred  $\mu$ s in duration) with a height (count) that is proportional to the mass of the analyte in the NP. The dwell time (or integration time) is typically in the 5-10 ms range in order to minimize the occurrence of NP signal peak overlaps. After the statistical evaluation of the signal time profile, information can be obtained about not only the elemental (isotopic) composition of the NPs, but also their size distribution, as well as the particle concentration. The measurement is fast (takes only a couple of minutes) and the required sample volume is also small (a few mL). For monometallic NPs, typical size detection limits range from 10 to 30 nm [2].

Recently, quadrupole ICP-MS instruments with 100 microsecond or less dwell times („high resolution”) became available commercially (e.g. Perkin Elmer NexION). The introduction of high resolution spICP-MS (HR-spICP-MS) provides new possibilities and advantages, such as offering dual-element detection capability, lowered spectral backgrounds and resolution of particle peak profiles, but it also seems to generate new drawbacks, e.g. increased split-particle events and decreased sensitivity [3]. In this study, the information that can be obtained by combining normal and high resolution single particle ICP-MS (spICP-MS) measurements for spherical bimetallic nanoparticles (BNPs) was assessed.

### **Experimental**

Two ICP-MS instruments were used in the experiments. Normal resolution spICP-MS (dwell time was set to 6 ms) and solution-mode ICP-MS measurements were performed on an Agilent 7700x type instrument, while HR-spICP-MS measurements (dwell time was set to 20  $\mu$ s) were carried out on a Perkin Elmer NexION 350 instrument. NP data was always collected in the time-resolved analysis (TRA) mode. On the NexION 350, the Syngistix Nano Application Module was used. Pre-processing of the collected data was necessary prior to the statistical evaluation of HR-spICP-MS measurements. For this purpose, we developed and used a macro-based program, written in Visual Basic for Applications (Microsoft, USA). This program counted individual particle events in the dataset and calculated the transit time of their ion cloud. Particle discrimination was based on the condition that a particle peak should be preceded and followed by at least three datapoints with zero signal. The transit time was then calculated as the product of the number of data points in that event and the dwell time. The total particle signal for a given NP detection event was obtained as the sum of time-resolved signals in that event.

A series of standard PELCO NanoXact nano-dispersions containing tannic acid capped gold and silver NPs obtained from Ted Pella (Redding, California, USA) were used for spICP-MS size calibration. The certified size of the gold NPs used were 28.8, 39.3, 61.3 and 75.4 nm, whereas the diameter of the silver NPs were 43.4, 59.0, 82.1 and 95.7 nm. Sodium citrate stabilized, silver-shelled gold nanospheres with 79.0 nm diameter (51.0 nm core diameter and 14.0 nm shell thickness) were obtained from NanoComposix (San Diego, USA). Gold-silver alloy nanoparticles - with 40:60, 60:40 and 80:20 molar ratios – have been synthesized with the combination of co-reduction of gold and silver salts and seeded growth methodology [4].

For sample preparation purposes of solution-mode ICP-MS measurements ultratrace quality HCl and HNO<sub>3</sub> acids (VWR Chemicals, Pennsylvania, USA) were used. The duration of dissolution of the composite NPs, which was carried out by heating the sample at 170 °C in aqua regia, was one hour. Calibration in solution-mode was performed using the Agilent Multi-Element Calibration Standard-3 (for gold) and Inorganic Ventures IV-ICPMS-71A (for silver).

### **Results and discussion**

The single particle ICP-MS (Method A) has the potential to become a practical alternative technique for the determination of the concentration of the component elements in composite NPs. Therefore, we carried out comparative measurements to assess its accuracy and precision in the case of Au-Ag alloy BNPs. We tested the performance of spICP-MS with normal time resolution (6 ms) against two solution-mode ICP-MS approaches: i) direct NP nebulization (Method B) and ii) conversion of the nanodispersion to a real solution by acid digestion of the NPs (Method C). As can be seen in **Table 1.**, there is a good agreement between the nominal

molar ratio and the results of solution mode ICP-MS after acidic digestion and spICP-MS. The advantage of spICP-MS is that the measurements are largely free from the influence of dissolved contaminants in the nanodispersion and the analysis is fast, as sample preparation is reduced to a simple dilution. At the same time, results of solution mode ICP-MS with direct NP nebulization can not be considered as accurate. The precision (RSD%) value is also poorer in the latter case.

Particle	Method A			Method B		Method C	
	Nominal Au/Ag molar ratio	Found Au/Ag molar ratio	Precision	Found Au/Ag molar ratio	Precision	Found Au/Ag molar ratio	Precision
Au-Ag core-shell	0.7500	0.6895	0.0058	0.3579	0.0269	0.7234	0.0211
Au-Ag alloy (40:60)	0.6667	0.7444	0.0111	1.639	0.0880	0.7560	0.0254
Au-Ag alloy (60:40)	1.500	1.585	0.0358	3.207	0.1988	1.586	0.0531
Au-Ag alloy (80:20)	4.000	3.934	0.0838	10.11	0.7976	4.320	0.1650

Table 1. A comparison of the analytical performance of three approaches used for the determination of the composition of Au-Ag bimetallic NPs.

Method A: spICP-MS analysis; Method B: Solution-mode ICP-MS analysis with direct particle nebulization; Method C: Solution-mode ICP-MS analysis after particle dissolution.

As a step towards the investigation of the structure of spherical BNPs, we studied the high resolution signal time profile for monoelemental gold and silver spherical nanoparticles, with the central interest of the transit time of the ion cloud through the instrument and the shape of the signal time profile.

We found that the transit time of the ion cloud correlates fairly linearly with the particle diameter (Figure 1.), as it can be more or less expected. A further observation can also be made, namely that the transit time for the same particle diameter is longer for gold than for silver.

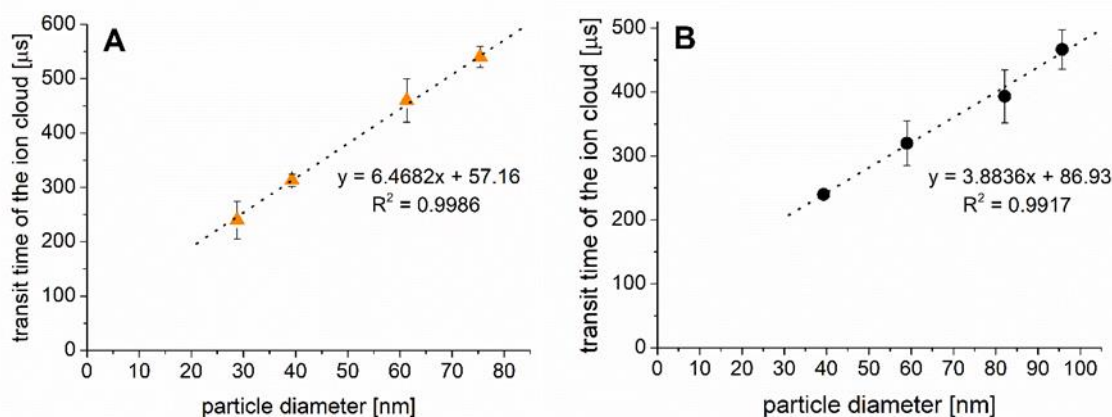


Figure 1. Correlation of transit time with the diameter for gold (A) and silver (B) spherical nanoparticles. Error bars indicate standard deviation from three repeated measurements

In order to obtain reliable, characteristic data about the structure of the investigated BNPs, we



applied filtering according to the total NP signal (the integrated signal for one NP detection event in the HR-spICP-MS) and the transit time. This was executed by only retaining those time profiles from the collected dataset which produced a total NP signal equal to, within a  $\pm 10\%$  tolerance range, the mode (maximum) of the lognormal function fitted to the signal histogram, and the same transit time within a  $\pm 10\%$  tolerance range. As an example, **Figure 2.** shows the average signal time profile for an 80 nm Ag NP. The shape of the profile is fairly Gaussian. The presented signal profile was calculated by averaging, after executing the filtering.

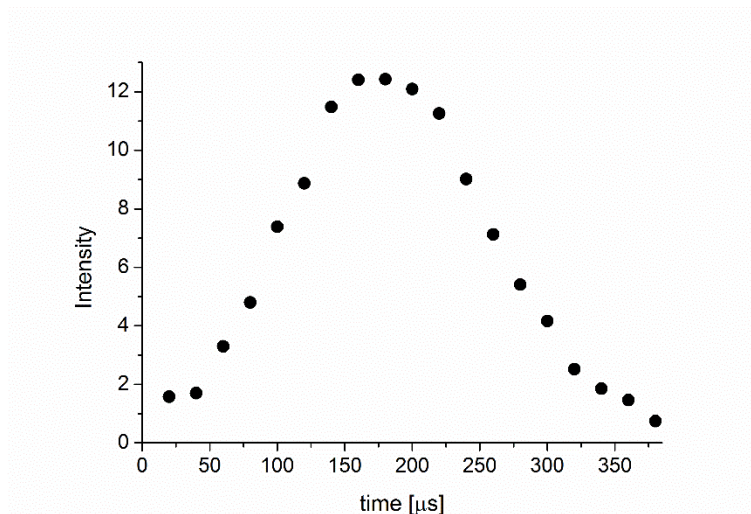


Figure 2. Average signal time profile for an 80 nm nominal diameter spherical Ag nanoparticle.

Applying the data evaluation method presented above we can obtain beneficial information about the structure of BNPs. Component elements in homogeneous alloy particles results in signal profiles that have comparable shape and duration, whereas, it is distinctly different for the ion cloud of the core and the shell of a core-shell BNP. Detailed experimental data on this matter will be disseminated in our presentation.

## References

- [1] A. Sápi, A. Kéri, I. Kálomista, D.G. Dobó, Á. Szamosvölgyi, K.L. Juhász, Á. Kukovecz, Z. Kónya, G. Galbács, *Anal. At. Spectrom.* 32 (2017) 996.
- [2] S. Lee, X. Bi, R.B. Reed, J.F. Ranville, P. Herckes, P. Westerhoff, *Environ. Sci. Technol.* 48 (2014) 10291.
- [3] M.T. Montano, H.R. Badiei, S. Bazargan, J.F. Ranville, *Environ. Sci.: Nano* 1 338 (2014) 338.
- [4] D. Rioux, M. Meunier, *J. Phys. Chem. C* 119 (2015) 13160.



## TRANSFORMATION OF ATRAZIN BY DIFFERENT ADVANCED OXIDATION PROCESSES

**Georgina Rózsa<sup>1,2</sup>, Ákos Fazekas<sup>1</sup>, Tünde Alapi<sup>1</sup>, Krisztina Schrantz<sup>1</sup>, Thomas Oppeländer<sup>2</sup>, Erzsébet Takács<sup>3</sup>, László Wojnárovits<sup>3</sup>**

<sup>1</sup>*Department of Inorganic and Analytical Chemistry, University of Szeged, H-6720 Szeged, Dóm tér 7, Hungary*

<sup>2</sup>*Physical Chemistry and Environmental Technology Department, Faculty of Medical and Life Sciences, Furtwangen University Jakob Kienzle-Str.17, 78054 VS-Schwenningen, Germany*

<sup>3</sup>*Radiation Chemistry Department, Centre for Energy Research, Hungarian Academy of Sciences, H-1121 Budapest, Konkoly-Thege Miklós út 29-33, Hungary  
e-mail: rozsa.georgina@chem.u-szeged.hu*

### Abstract

In this work ultraviolet photolysis (UV) and three advanced oxidation processes (AOPs), vacuum ultraviolet (VUV) photolysis, ultraviolet photolysis combined with vacuum ultraviolet photolysis (UV/VUV) and gamma ( $\gamma$ ) radiolysis were used for the generation of reactive primary free radicals (hydroxyl radical ( $\cdot\text{OH}$ ), hydrated electron ( $e_{\text{aq}}^-$ ), hydrogen radical ( $\cdot\text{H}$ )) to induce the transformation of atrazine in aqueous solution. We examined different reaction conditions (solutions of atrazine saturated with dissolved oxygen or nitrogen). The aim of this work is the comparison of the oxidative transformation of atrazine during UV (254 nm), UV/VUV (254/185 nm) and VUV (172 nm) photolysis, as well as  $\gamma$  radiolysis. The efficiency of the photolytic methods increased in the following order: UV < VUV < UV/VUV photolysis. The economic efficiency of the used processes was compared based on Electric Energy per Order ( $E_{\text{EO}}$ ).  $\gamma$  radiolysis was found to be the economically most feasible method compared to UV/VUV, VUV and UV photolysis.

### Introduction

Atrazine (2-chloro-4-ethylamino-6-isopropylamino-1,3,5-triazine) (Figure 1.) is an s-triazine derivative and belongs to the group of Endocrine Disruptor Chemicals (EDCs). It is a widely used herbicide in crop production to control broadleaf and annual grasses. It is commonly detected in groundwater and soil in many countries, due to its high mobility and moderate solubility in water ( $34.7 \text{ mg L}^{-1}$  at  $26^\circ\text{C}$ ) [1]. S-triazine derivatives are characterized by strong aromaticity and high stability against biological degradation [2]. Chemical degradation of atrazine is environmentally more important than biodegradation. Its elimination using AOPs, based on generation of reactive radicals ( $\cdot\text{OH}$ ,  $e_{\text{aq}}^-$ , and  $\cdot\text{H}$ ), is widely investigated.

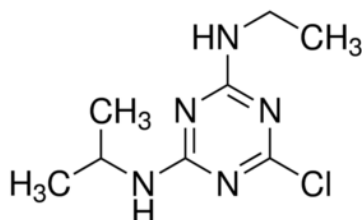
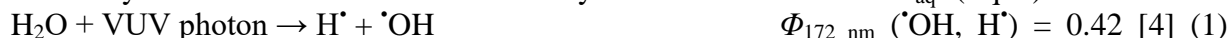


**Figure 1.** Chemical structure of atrazine

VUV radiation induces homolytic dissociation of water molecules, resulting in the formation of  $\cdot\text{OH}$  and  $\text{H}^\bullet$  (Eq. 1, 2) [3, 4]. With low yield, ionization also takes place. The so-called dry electron released in ionization may stabilize in the form of  $e_{\text{aq}}^-$  (Eq. 3):

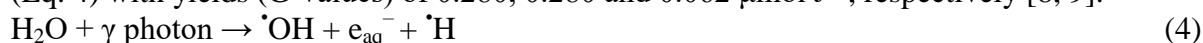


$$\Phi_{185 \text{ nm}}(\cdot\text{OH}, \text{H}^\bullet) = 0.33 \text{ [4] (2)}$$



The efficiency of VUV photolysis can be increased, in some cases, *e.g.* by the combination of this method with other techniques, like UV photolysis. The synergistic effect reported during some of the combinations underlines the relevancy of the combined techniques [6].

During  $\gamma$  radiolysis of aqueous solutions, the decomposition of water molecules results in  $\cdot\text{OH}$ ,  $e_{\text{aq}}^-$  and, in lower yield,  $\cdot\text{H}$  as primary species. These reactive species are surrounded by water molecules in a small volume part, called Spur [7]. The primary radicals are generated (Eq. 4) with yields (G-values) of 0.280, 0.280 and 0.062  $\mu\text{mol J}^{-1}$ , respectively [8, 9].



Using various dissolved gasses the radical set formed in solutions can be affected and therefore the effect of different species on the transformation of atrazine can be investigated.

In the presence of dissolved oxygen (DO) the reductive primary species ( $\cdot\text{H}/e_{\text{aq}}^-$ ) transform to less reactive  $\text{HO}_2^\bullet/\text{O}_2^{\cdot-}$  [10]. The reaction of atrazine with  $e_{\text{aq}}^-$  can be examined in the presence of nitrogen ( $\text{N}_2$ ).

## Experimental

### Materials and equipment

During all photolytic methods 250 mL and during  $\gamma$  radiolysis 5 mL atrazine (Sigma-Aldrich, 99.9%) solutions ( $c_0 = 1.0 \times 10^{-4} \text{ mol L}^{-1}$ ) were irradiated. For UV (254 nm) and UV/VUV (254/185 nm) degradation a 15 W low pressure mercury vapour lamp (LightTech) was applied. A Radium Xeradex<sup>TM</sup> 20 W  $\text{Xe}_2^*$  excimer lamp emitting at  $172 \pm 14 \text{ nm}$  was used for VUV photolysis. Atrazine solutions were circulated by a peristaltic pump between the reactor and reservoir tanks (both thermostated at  $25 \pm 0.5 \text{ }^\circ\text{C}$ ) at  $375 \text{ ml min}^{-1}$  flow rate. To investigate the influence of DO,  $\text{O}_2$  or  $\text{N}_2$  gas (Messer, > 99.5% purity) were bubbled through the solutions, starting 15 or 30 minutes before the measurement and continued until the end of the irradiation.

In  $\gamma$  radiolysis experiments the 5 mL ampoules with atrazine solution were placed to equal distance from the  $^{60}\text{Co}$ - $\gamma$  source of an SSL-01 panoramic type irradiator, to have a dose rate of  $0.7 \text{ kGy h}^{-1}$  ( $700 \text{ J kg}^{-1} \text{ h}^{-1}$ ). The solutions were irradiated in open ampoules or in sealed ampoules saturated with  $\text{N}_2$ .

### Analytical methods

The concentration of atrazine was followed by high performance liquid chromatography (Agilent 1100 HPLC equipment using a LiChroCART<sup>®</sup> C18 reverse-phase column) with diode array detector (DAD). Mixture of methanol (70%) and water (30%) was used as eluent, at a flow rate of  $1.0 \text{ ml min}^{-1}$ .

## 3. Results and discussion

The kinetic curves of atrazine ( $c_0 = 1.0 \times 10^{-4} \text{ mol L}^{-1}$ ) were compared in presence and absence of DO during UV photolysis, VUV photolysis, UV/VUV photolysis and  $\gamma$  radiolysis. The results show that both in presence (Fig.2a) and absence (Fig.2b) of DO the degradation of

atrazine was faster with VUV and UV/VUV photolysis, than using only UV photolysis. This suggests that both  $\cdot\text{OH}$  and  $e_{\text{aq}}^-$  can have a significant role in the degradation of atrazine. The important role of the  $e_{\text{aq}}^-$  is also supported by the results observed during  $\gamma$  radiolysis (1 kGy), where again no significant effect of the DO (Fig.2c) on the transformation rates of atrazine could be observed. During the combined UV/VUV photolysis, atrazine and water molecules are excited by the UV and VUV photons, respectively. Although the 185 nm photons induce the generation of  $\cdot\text{OH}$  less effectively, than 172 nm light, used by VUV photolysis, the combined photolysis is more efficient than the simple UV or VUV photolysis, due to the presence of both radical and photoionization degradation mechanisms. The UV transformation of the target molecule was faster (30 min) in presence, than in the absence of DO (40 min). In this case the target molecule absorbs the UV light, and the presence of DO inhibits the recombination of the species formed by photoionization, increasing slightly the transformation rate.

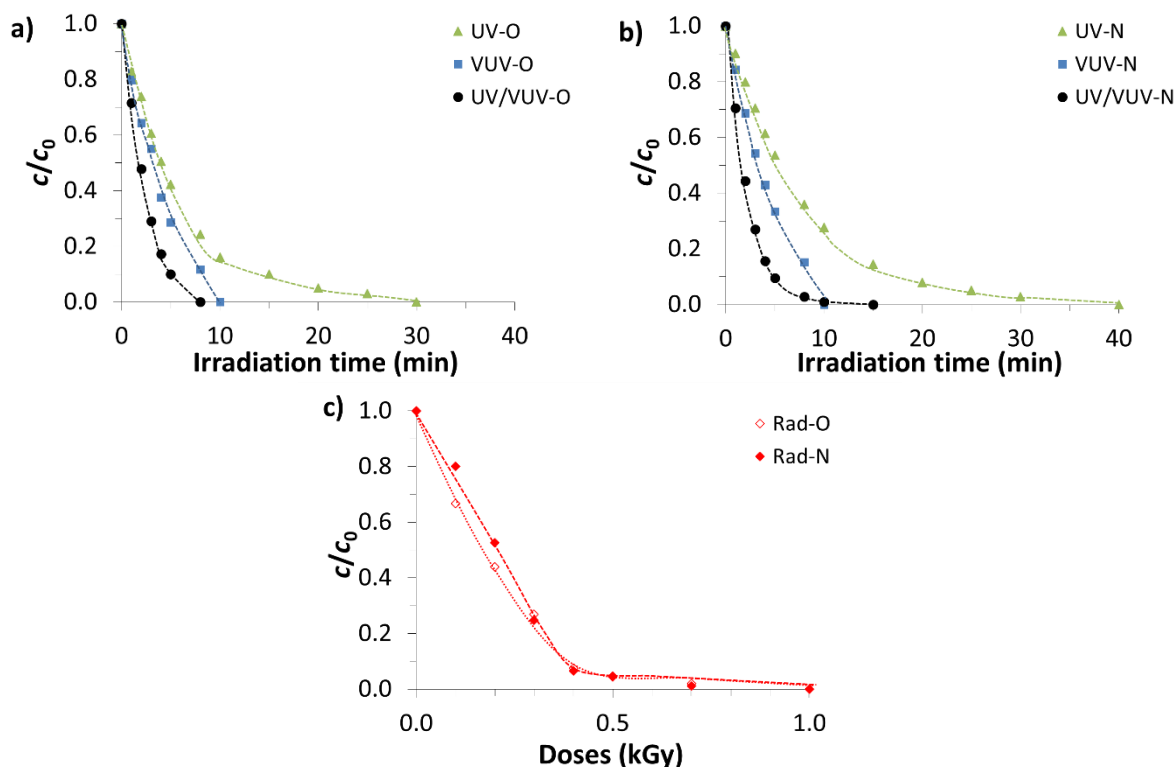


**Figure 2.** Kinetic curves of atrazine ( $c_0 = 1.0 \times 10^{-4} \text{ mol L}^{-1}$ ) degradation during UV photolysis, VUV photolysis, UV/VUV photolysis and  $\gamma$  radiolysis in the presence (a, c) and absence (b, c) of dissolved  $\text{O}_2$

The complete transformation of atrazine was reached by 30 and 40 min of UV, 15 and 15 min of VUV, 8 and 15 min of UV/VUV photolysis, and by 1.0 and 1.0 kGy of  $\gamma$  radiolysis for the initial concentration in the presence and absence of DO, respectively, showing that all investigated methods are suitable for the elimination of atrazine from aqueous solution.

**Table 1.** The electric energy per order ( $E_{EO}$ ) calculated in case of various initial atrazine concentrations and methods

	UV photolysis	VUV photolysis $\gamma$ radiolysis	UV/VUV photolysis	
	$E_{EO}$ (kW m <sup>-3</sup> order <sup>-1</sup> )			
$E_{EO1}$ ( $10^{-4}$ - $10^{-5}$ )	<b>50.0</b>	<b>40.0</b>	<b>15.0</b>	<b>0.13</b>
$E_{EO2}$ ( $10^{-5}$ - $10^{-6}$ )	40.0	5.33	3.00	0.03
$E_{EO2}/E_{EO1}$	1.25	7.50	5.00	4.33

Calculated  $E_{EO}$  data are presented in Table 1 and show that  $\gamma$  radiolysis is the economically most feasible method, followed by UV/VUV, VUV and UV photolysis. Another observation can be made from the ratio of the  $E_{EO}$  calculated at different initial concentrations, namely, that in case of all methods it decreases strongly with the decrease of the initial concentration. This shows that the economic feasibility can be tuned with the initial concentration of the treated solution.

### Conclusion

- Hydroxyl radicals and hydrated electrons both play vital role in the transformation of atrazine.
- The results showed that atrazine can be eliminated by all photolytic methods and  $\gamma$  radiolysis, as well.
- The combination of 185 nm VUV and 254 nm UV irradiation is the most effective method for the fast transformation of atrazine.
- Based on  $E_{EO}$  values  $\gamma$  radiolysis was the economically most feasible method for atrazine degradation.

### References

- [1] R. Reh, T. Licha, T. Geyer, K. Nodler, M. Sauter, Occurrence and spatial distribution of organic micro-pollutants in a complex hydrogeological karst system during low flow and high flow periods, results of a two-year study, *Sci. Total Environ.*, 443 (2013) 438-445.
- [2] A.M. Cook, R. Huetter, s-Triazines as nitrogen sources for bacteria, *J. Agric. Food. Chem.*, 29 (1981) 1135-1143.
- [3] N. Getoff, G.O. Schenck, Primary Products of Liquid Water Photolysis at 1236 Å, 1470 Å and 1849 Å, 1968.
- [4] A.N. Gernot Heit, Pierre-Yves Saugy, and André M. Braun, Vacuum-UV (172 nm) Actinometry. The Quantum Yield of the Photolysis of Water, *The Journal of Physical Chemistry A*, 102 (1998) 5551-5561.
- [5] E.J. Hart, M. Anbar, *The hydrated electron*, Wiley-Interscience, New York, 1970.
- [6] M. Bagheri, M. Mohseni, A study of enhanced performance of VUV/UV process for the degradation of micropollutants from contaminated water, *J. Hazard. Mater.*, 294 (2015) 1-8.
- [7] L. Wojnárovits, *Sugárkémia, Akadémiai Kiadó, Budapest*, 2007.
- [8] G.V. Buxton, *The radiation chemistry of liquid water: Principles and applications.*, in: A. Mozumder, Y. Hatano (Eds.) *Charged particle and photon interaction with matter*, Marcel Dekker, New York, 2004, pp. 331-365.
- [9] J.W.T. Spinks, R.J. Woods, *An introduction to radiation chemistry* 3rd edition, Wiley-Interscience, New-York, 1990.

[10] G.V. Buxton, C.L. Greenstock, W.P. Helman, B.A. Ross, Critical review of rate constants for reactions of hydrated electrons, hydrogen atoms and hydroxyl radicals ( $\cdot\text{OH}/\text{O}^\cdot$ ) in aqueous solution, *J. Am. Chem. Soc.*, 110 (1988) 513-886.

**Acknowledgement:** The work was done in the frame of the DAAD 151955 bilateral project.

UV- AND VISIBLE LIGHT ACTIVE PHOTOCATALYSTS IN SOLAR  
HETEROGENEOUS PHOTOCATALYSIS

UV ÉS LÁTHATÓ FÉNNYEL GERJESZTHETŐ FOTOKATALIZÁTOROK A  
NAPFÉNYT HASZNOSÍTÓ HETEROGÉN FOTOKATALÍZISBEN

**Gábor Veréb<sup>a, b, \*</sup>, Tamás Gyulavári<sup>b, c</sup>, Orsolya Virág<sup>b</sup>, Krisztina Vajda<sup>b</sup>, Zsolt Pap<sup>b, d</sup>,  
Tünde Alapi<sup>e</sup>, Zsuzsanna László<sup>a</sup>, András Dombi<sup>b</sup>, Klára Hernádi<sup>b, c</sup>**

<sup>a</sup> Department of Process Engineering; Faculty of Engineering, University of Szeged; H-6725,  
Moszkvai krt. 9, Szeged, Hungary

<sup>b</sup> Research Group of Environmental Chemistry, University of Szeged; H-6720, Tisza Lajos krt.  
103, Szeged, Hungary

<sup>c</sup> Department of Applied and Environmental Chemistry, University of Szeged;  
H-6720, Rerrich Béla tér 1, Szeged, Hungary

<sup>d</sup> Institute for Interdisciplinary Research on Bio-Nano-Sciences; RO-400271, Treboniu  
Laurian 42, Cluj-Napoca, Romania

<sup>e</sup> Department of Inorganic and Analytical Chemistry, Institute of Chemistry, University of  
Szeged; H-6720, Dóm tér 7, Szeged, Hungary  
\*e-mail address: verebg@mk.u-szeged.hu

### Abstract

In the present study, the photocatalytic efficiencies of 2 doped and 4 non-doped TiO<sub>2</sub> photocatalysts were investigated in detail, applying solar- and different artificial irradiations. On one hand, in case of visible light irradiation, doped TiO<sub>2</sub>-s and rutile TiO<sub>2</sub> showed much higher activity compared to Aeroxide P25. On the other hand, non-doped TiO<sub>2</sub>-s' activity was much higher in the UV range than the investigated doped TiO<sub>2</sub>-s'. Since the calculated apparent quantum yields were 1-2 order of magnitudes lower in the visible range, than in the UV range, therefore non-doped titanium-dioxides had higher performance in case of solar light utilization despite the 1 order of magnitude lower quantity of UV photons in the solar light.

Consequently, higher visible light activity not necessarily leads to higher performance in case of solar light irradiation. If higher solar light utilization efficiency is the aim during the development of a novel photocatalyst, UV excitability is also a crucial property, and needs to be investigated besides the red-shifted light absorbance and the high visible light activity.

**Keywords:** TiO<sub>2</sub>; visible light; UV light; solar irradiation; quantum yield

### 1. Bevezetés

A heterogén fotokatalízis ígéretes innovatív vízkezelési módszer, mely félvezető nanorészecskéket alkalmaz, melyeket megfelelő energiájú fényel gerjesztve (töltésszeparáció indukálta összetett gyökös folyamatokon keresztül) a szerves szennyező anyagok széles köre lebontható. A titán-dioxid (TiO<sub>2</sub>) az egyik legszéleskörűbben vizsgált fotokatalizátor, mely számos előnyös tulajdonsága ellenére azzal a nem kívánatos tulajdonsággal rendelkezik, hogy hagyományosan csak UV fényel gerjeszthető hatékonyan. Ugyanakkor a módszer gazdaságos üzemeltetéséhez célszerű a katalizátorok napfényel történő gerjesztése. A napfény intenzitása azonban egy nagyságrenddel nagyobb a látható fény hullámhossztartományában (45%), mint az UV tartományban (3-6%). Ebből adódóan számtalan kutató igyekszik lecsökkenteni a



félvezető nanorészecskék gerjesztési küszöbértékét, vagyis kifejleszteni olyan  $\text{TiO}_2$  alapú fotokatalizátorokat, melyek a (kisebb energiájú) látható fény hullámhossztartományába eső fotonokkal is hatékonyan gerjeszthetők, így elérve a hatékonyabb napfényhasznosítást.

A szakirodalomban számtalan tanulmány található, melyekben sikerrel állítottak elő látható fényvel gerjeszthető fotokatalizátorokat, ugyanakkor a tanulmányok többségében nem vizsgálták a katalizátorok hatékonyságát napfényvel történő gerjesztés esetében. Sőt, Wang és munkatársai [1] arról publikáltak, hogy a referenciaként hagyományosan elismert Aeroxide P25 fotokatalizátorhoz viszonyítva, az általuk előállított látható fényre aktív fotokatalizátor kisebb hatékonysággal bírt napfényvel történő gerjesztéskor.

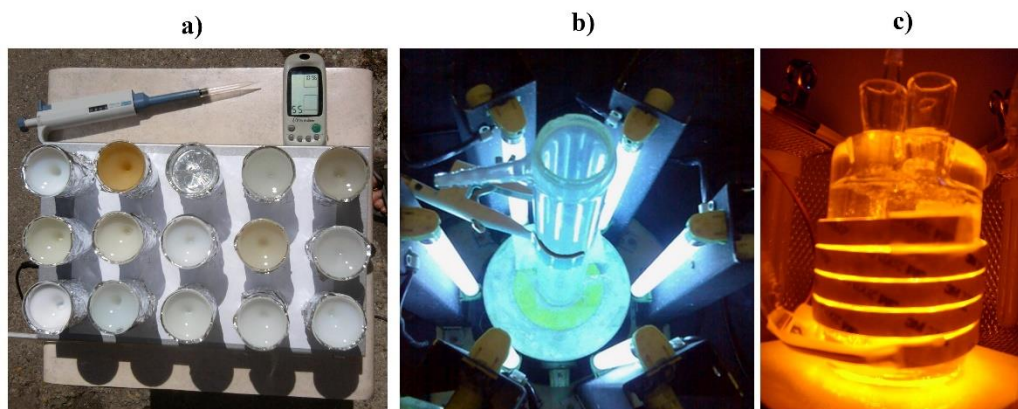
Korábbi tanulmányunkban [2] 10 különböző  $\text{TiO}_2$  alapú fotokatalizátor látható fényvel történő gerjeszthetőségét hasonlítottuk össze, melyek közül a 3 leghatékonyabbat kiválasztva jelen tanulmányban összehasonlítottuk azok aktivitását nem adalékolt (nagy részben anatóz kristályfázisú) titán-dioxidok (Aeroxide P25, Aldrich anatóz és egy saját fejlesztésű  $\text{TiO}_2$ ) aktivitásával, napfényvel történő gerjesztés esetén (fenolt alkalmazva modellszennyezőként). A nem várt eredmények magyarázatára részletesen vizsgáltuk valamennyi fotokatalizátor aktivitásának hullámhossz szerinti függését többféle megvilágítás alkalmazásával. A vizsgálatok során 6 különböző hullámhossztartományra határoztuk meg a látszólagos kvantumhasznosítási tényezőket fenol fotokatalitikus bontása során.

## 2. Alkalmazott anyagok és módszerek

A vizsgált fotokatalizátorok: Aeroxide P25 ( $\text{TiO}_2$ -P25; *Evonik Industries*) Aldrich anatóz ( $\text{TiO}_2$ -AA), Aldrich rutil ( $\text{TiO}_2$ -AR), ugyancsak kereskedelmi forgalomban kapható, adalékolt (látható fényvel gerjeszthető) titán-dioxid ( $\text{TiO}_2$ -VLP7000; *Kronos Titan GmbH*), saját készítésű nitrogénnel adalékolt (látható fényvel gerjeszthető) titán-dioxid ( $\text{TiO}_2$ -N [3]), illetve ugyancsak saját készítésű (lánghidrolízissel előállított) nem adalékolt (UV megvilágítás esetén nagy aktivitással rendelkező) titán-dioxid ( $\text{TiO}_2$ -FH [4]). Valamennyi vizsgált fotokatalizátor részletesen jellemzésre került korábbi tanulmányainkban [2-5].

A fotokatalitikus kísérletek során 0,1 mM-os fenololdat (*Spektrum 3D*) fotokatalitikus oxidációját vizsgáltuk 1 g/L  $\text{TiO}_2$  szuszpenziótöménységet alkalmazva ( $V=100\text{mL}$ ). A kísérletek során vett minták fenolkoncentrációját nagyhatékonyságú folyadékkromatográfiával (*Agilent 1100*) mértük, és a bomlásgörbék kezdeti ( $t=0$ ) meredekségéből (empirikus függvényvel [5]) számítottuk a fenol kezdeti ( $r_0$ ) bomlási sebességét [ $\text{mol}/(\text{dm}^3 \cdot \text{s})$ ].

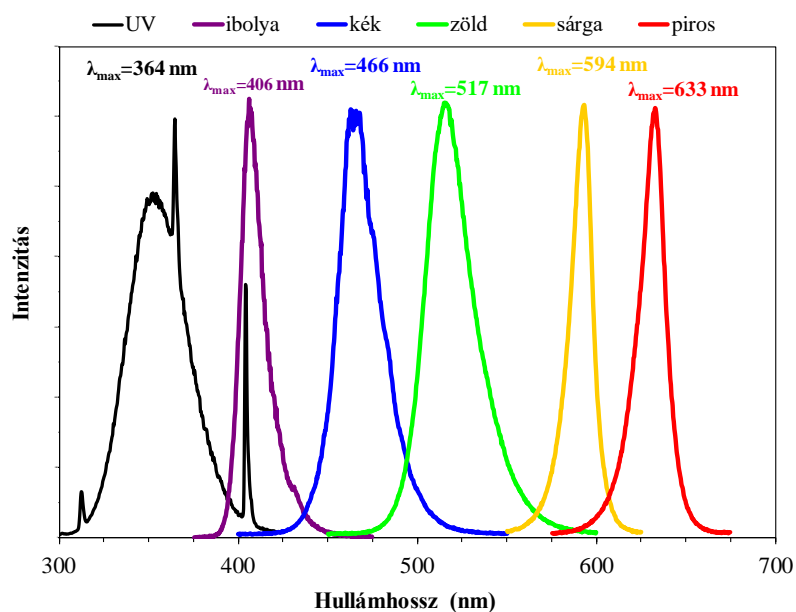
A napfényvel történő gerjesztés az **1/a ábrán** látható kísérletelrendezés szerint történt.



**1. ábra** Fotokatalitikus kísérletekhez használt elrendezések, reaktorok: (a) napfényvel történő gerjesztés; (b) UV fotoreaktor; (c) látható fényvel végzett kísérletekhez használt reaktor.



A fotokatalizátort tartalmazó szuszpenziókat ( $V=100\text{mL}$ ) főzőpoharakban helyeztük el, melyeket kívülről alufóliával borítottuk annak biztosítására, hogy valamennyi főzőpoharat kizárólag felülről érje napfény, így biztosítva az egyforma fényintenzitást. Az UV fényvel történő gerjesztéshez az **1/b ábrán** látható duplafalú Pyrex reaktort alkalmaztuk, melyet 6 db UV fluoreszcens fénycsővel sugároztunk be (*Vilber-Lourmat T-6L UV-A*, 6W,  $\lambda_{\text{max}} = 365\text{ nm}$ ). A látható fényvel történő gerjesztéshez szintén egy duplafalú (üveg)reaktort használtunk. A reaktor körül 4db hagyományos energiatakarékos kompakt fluoreszcens fénycső került elhelyezésre (*DÜWI 25920/R7S-24W*; további részletek és emissziós spektrum megtalálható korábbi közleményünkben [2]). Más kísérletek során (szűkebb hullámhossztartományok vizsgálatok) különböző színű (ibolya, kék, zöld, sárga, piros) LED szalagokat (14.4 W; típus: *5050 SMD*; 60 db LED;  $l=1\text{ m}$ ) tekertünk a reaktor köré (**1/c ábra**). A fényforrások emissziós spektrumát (**2. ábra**) egy *AvaSpec-ULS 2048* típusú spektrométerrel jellemeztük.



**2. ábra** A katalizátorok gerjesztésére használt UV fluoreszcens fénycső illetve a különböző színű LED szalagok emissziós spektrumai.

A különböző megvilágítások esetén a reaktortérbe érkező fotonok számát (a fotonfluxust) vas-oxalát aktinometriával (*Fischer* [6]) határoztuk meg. A vizsgálatokhoz vas-szulfátot (Reanal; analitikai tisztaság), o-phenanthrolint (Reanal; analitikai tisztaság) kálium-oxalátot (Spektrum 3D; 99.5%), nátrium-acetátot (Spektrum 3D; > 99%) és kénsavat (Spektrum 3D; 95-97%) használtunk.

Az 550 nm-nél nagyobb hullámhosszúságú fény esetén a vas-oxalát aktinometria nem alkalmazható a fotonfluxus meghatározására, így a zöld, a sárga és a piros színű LED-ek esetében egy „*Apogee MQ-200*” típusú intenzitásmérőt („*PPF meter*” – *photosynthetic photon flux* – fotoszintetikus foton fluxus) alkalmaztunk, mely  $\mu\text{mol}/(\text{m}^2 \cdot \text{s})$  egységben méri a fotonfluxust. A műszer érzékenysége a látható hullámhossztartományban közel konstans, ebből adódóan a mért intenzitásértékekből, illetve a kék színű LED szalagra (a vas-oxalát aktinometriával) mért fotonfluxusból aránypárokkal kiszámolható a zöld, a sárga, illetve a piros megvilágítás esetében is a reaktortérbe jutó fotonfluxus.

### 3. Eredmények és értékelésük

A fotokatalitikus kísérletek elvégzése előtt ellenőriztük a fenol adszorpcióját sötétben a különböző fotokatalizátorokon, és az minden esetben 1% alatt maradt. A fenol fotokatalizátor nélküli (fotolitikus) bomlása pedig UV megvilágítás esetében sem haladta meg a 2%-ot (120 perc alatt), míg a többi megvilágítás esetén 1% alatti volt a koncentráció csökkenése.

#### 3.1. Energiatakarékos (látható fényt sugárzó) fénycsövekkel végzett kísérletek

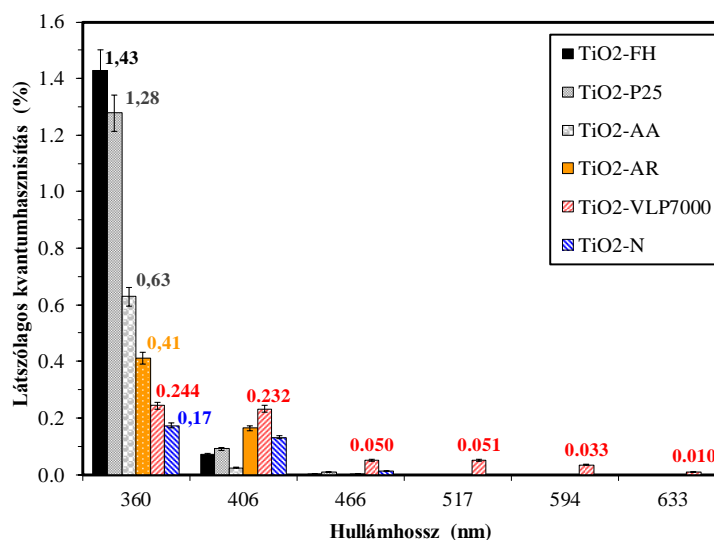
Az Aldrich anatáz ( $\text{TiO}_2$ -AA) igen csekély <5%-os, az Aeroxide P25 ( $\text{TiO}_2$ -P25) 17%-os, a saját készítésű  $\text{TiO}_2$ -N fotokatalizátor 26%-os, Az Aldrich rutil ( $\text{TiO}_2$ -AR) 37%-os, míg a  $\text{TiO}_2$ -VLP7000 fotokatalizátor kiemelkedő 94%-os csökkenést eredményezett a fenol koncentrációjában (a 4 órás megvilágítások végére). Figyelembe véve, hogy a napfény intenzitása 1 nagyságrenddel nagyobb a látható fény hullámhossztartományában, mint az UV tartományban, az várható, hogy a látható fényvel hatékonyan gerjeszthető fotokatalizátorok nagyobb bomlási sebességet fognak eredményezni napfényvel történő gerjesztéskor.

#### 3.2. Napfényvel történő gerjesztéssel végzett kísérletek

Nem várt módon a nem adalékolt, nagyrészt anatáz fázisú titán-dioxidok ( $\text{TiO}_2$ -AA,  $\text{TiO}_2$ -FH,  $\text{TiO}_2$ -P25) jelentősen nagyobb hatékonysággal bontották a fenolt (87-89%-os bomlás a 90 perces kísérletek végére), mint a látható fényben leghatékonyabb  $\text{TiO}_2$ -VLP7000 fotokatalizátor (44%-os csökkenés). Ezen felül a látható fényben kisebb aktivitást mutató Aldrich rutil esetén is kissé nagyobb (55%-os) koncentrációcsökkenést mértünk, míg a  $\text{TiO}_2$ -N fotokatalizátoron a fenolnak mindösszesen 19%-a bomlott le.

#### 3.3. UV fénycsövekkel és különböző színű LED megvilágításokkal végzett kísérletek

A nem várt eredmények magyarázatára részletesen vizsgáltuk az egyes katalizátorok hatékonyságának hullámhossz szerinti függését, és a fenol kezdeti bomlási sebességeinek [M/s], illetve az egyes megvilágításokra meghatározott fotonfluxusoknak [M/s] az ismeretében (azok hányadosaként) kiszámítottuk a látszólagos kvantumhasznosítási tényezőket valamennyi megvilágítás és valamennyi fotokatalizátor esetében (3. ábra).



2. ábra A fenol kezdeti bomlási sebességeinek, illetve a fotonfluxusoknak a hányadosaként számított látszólagos kvantumhasznosítási tényezők különböző hullámhossztartományokban.

UV megvilágítás esetében a nem adalékolt, nagyrészt anatóz fázisú titán-dioxidok ( $\text{TiO}_2$ -AA,  $\text{TiO}_2$ -P25,  $\text{TiO}_2$ -FH) jelentősen nagyobb hatékonyságot mutattak, mint a  $\text{TiO}_2$ -AR illetve az adalékolt titán-dioxidok ( $\text{TiO}_2$ -VLP7000 és  $\text{TiO}_2$ -N).

A  $\text{TiO}_2$ -FH fotokatalizátor esetén mértük a legnagyobb látszólagos kvantumhasznosítást (1.43%) UV megvilágítás esetén, illetve hasonló értéket mértünk az Aeroxide P25 fotokatalizátor esetében is (1.28%). Egyrészt a **3. ábra** alapján egyértelmű, hogy a nem adalékolt (nagyrészt anatóz kristályfázist tartalmazó) titán-dioxidok (Aeroxide P25, Aldrich anatóz illetve a  $\text{TiO}_2$ -FH) sokkal nagyobb hatékonysággal hasznosítják az UV fotonokat, mint az adalékolt titán-dioxidok ( $\text{TiO}_2$ -VLP7000 és  $\text{TiO}_2$ -N). Ugyanakkor már a lila fény hullámhossztartományától jelentősen kisebb értékeket mértünk az előbbi fotokatalizátorok esetében (0.02-0.09%), mint a  $\text{TiO}_2$ -VLP7000 (0.23%), a  $\text{TiO}_2$ -N (0.13%) és az Aldrich rutil (0.16%) esetében. A nagyobb hullámhosszúságú megvilágítások vonatkozásában kiemelendő, hogy csak a  $\text{TiO}_2$ -VLP7000 mutatott számottevő fotokatalitikus aktivitást, mely katalizátor a teljes vizsgált hullámhossztartományban gerjeszhető volt.

Összességében az a következtetés vonható le, hogy a nem adalékolt, nagyrészt anatóz fázisú titán-dioxidok 1-2 nagyságrenddel nagyobb látszólagos kvantumhasznosítást eredményeznek az UV tartományban, mint a vizsgált adalékolt fotokatalizátorok a látható fény hullámhossztartományában. Ez azt eredményezte, hogy a kisebb gerjesztési küszöb (a látható fényel történő hatékonyabb gerjesztés) ellenére a jelentősen kisebb UV aktivitás túlkompenzálta előbbieket előnyét, és napfényel történő gerjesztés esetén kisebb hatékonyságot eredményezett annak ellenére, hogy az UV fény intenzitása 1 nagyságrenddel kisebb a napfényben, mint a látható fény intenzitása

#### 4. Következtetések

Látható fényel történő gerjesztés esetében természetesen nagyobb hatékonysággal alkalmazhatók a sikeresen adalékolt (illetve a rutil fázisú) titán-dioxidok, mint az anatóz fázisú, nem adalékolt titán-dioxidok, de a látható fényel történő hatékony gerjesztés nem feltétlenül eredményez nagyobb fotokatalitikus aktivitást a napfényel történő megvilágítás során. A  $\text{TiO}_2$ -VLP7000 a teljes vizsgált UV-Vis hullámhossztartományban gerjeszhető volt, de a számított látszólagos kvantumhasznosítási értékek 1-2 nagyságrenddel kisebbek voltak, mint a nem adalékolt  $\text{TiO}_2$ -ok UV fényel történő gerjesztése során mért értékek. Ennek következménye, hogy a nagy UV aktivitású fotokatalizátorok nagyobb hatékonyságot mutattak a napfényel történő gerjesztés során annak ellenére, hogy az UV fotonok száma 1 nagyságrenddel kisebb, mint a látható fény hullámhossztartományába eső fotonok száma.

Vagyis ha egy látható fényel is hatékonyan gerjeszhető fotokatalizátor fejlesztésének célja a hatékonyabb napfényhasznosítás, akkor az UV fényel történő gerjesztés hatékonyságának vizsgálata is szükségszerű, és nem elegendő a hatékonyabb látható fényel történő gerjesztés igazolása. Természetesen a fotokatalizátorok beltéri alkalmazás esetén (az UV fotonok hiányában) kizárólag a látható fényel való gerjeszhetőség a jelentős tulajdonság.

#### Köszönetnyilvánítás

A munka a Bolyai János Kutatási Ösztöndíj támogatásával készült. A szerzők hálásak a Nemzeti Kutatási, Fejlesztési és Innovációs Hivatal által biztosított anyagi támogatásért (NKFI témaszám: K112096). A kutatáshoz szükséges infrastruktúra beszerzését részben a Svájci Alap (SH/7/2/20) biztosította.

**Irodalomjegyzék**

- [1] Z. Wang, W. Cai, X. Hong, X. Zhao, F. Xu, C. Cai, *Appl. Catal.*, B 57 (2005) 223-231.
- [2] G. Veréb, L. Manczinger, G. Bozsó, A. Sienkiewicz, L. Forró, K. Mogyorósi, K. Hernádi, A. Dombi, *Appl. Catal.*, B 129 (2013) 566-574.
- [3] Z. Pap, L. Baia, K. Mogyorósi, A. Dombi, A. Oszko, V. Danciu, *Catal. Comm.* 17 (2011) 1-7.
- [4] N. Balázs, D. F. Srankó, A. Dombi, P. Sipos, K. Mogyorósi, *Appl. Catal.*, B 96 (2010) 569-576.
- [5] G. Veréb, Z. Ambrus, Z. Pap, Á. Kmetykó, A. Dombi, V. Danciu, A. Cheesman, K. Mogyorósi, *Appl. Catal.*, A 417-418 (2012) 26-36.
- [6] E. Fischer, *Newsletters* 21 (1984) 33-34.

## DETERMINATION OF SURFACTANTS USED IN AGROCHEMICALS

**Mária Mörtl, András Székács**

<sup>1</sup> *Agro-Environmental Research Institute, National Agricultural Research and Innovation Centre, H-1022, Budapest, Herman O. u. 15, Hungary  
e-mail: mortl.maria@akk.naik.hu*

### **Abstract**

Examples for determination of surfactants used in agrochemicals will be presented by using different instrumental analytical methods. Liquid chromatography coupled to mass spectrometry (LC-MS) is more convenient for characterization of these mixtures compared to gas chromatographic (GC) methods. However, due to better separation of GC it allows more detailed information about the composition of the mixtures analysed, but usually prior to GC derivatisation is required. Two chemical modifications for GC-MS measurements were investigated in detail: conversion of sulfonates to trifluoroacyl esters as well as silylation of hydroxy compounds.

### **Introduction**

Surfactants are often used in formulated pesticides to improve water solubility or as spray adjuvants to improve spreading and penetration abilities of pesticide active ingredients in tank mixture. These formulation additives are had widely been regarded as inert components, but have been proven in many cases to exert detrimental side-effects or modify the toxicity of the active ingredient(s). Thus, authorisation and use of these agricultural additives should be regulated more strictly.

Environmental assessment, i.e. identification of toxic hazards, as well as determination of maximum residue levels require reliable analytical methods. Analysis is often challenging as surfactants are usually complex mixtures, their composition is not exactly known or not well defined, and reliable information and certified reference materials are not available. In addition, they represent a wide range of chemicals in a broad range of polarity, which should be monitored in the environment as pollutants. Surfactants are determined mainly by liquid chromatography coupled to mass spectrometry (LC-MS) [1], as gas chromatography (GC) can be applied only to smaller groups and often rely on derivatisation. An advantage of the GC method is that due to better separation it allows more detailed information about the composition of the mixtures analysed.

To facilitate our ecotoxicology studies of the components in formulated pesticides containing neonicotinoid insecticides (clothianidin, CLO; acetamiprid, ACE) and herbicide glyphosate (GLY) as active ingredients, methods for analytical determination of these ingredients and their surfactant additives were assessed. We have developed an LC-MS method for characterisation of sulfonic acid surfactants in CLO-based insecticide formulation, found to be 46.5 times more toxic than CLO itself on the great water flea *Daphnia magna* Straus [2]. Similarly, linear alkylbenzene sulfonate (LAS) surfactants in an ACE-based insecticide were analysed, and their decomposition in surface water was determined. Thus, the dissipation of LASs was determined alone and in the presence of ACE by using an HPLC-UV instrumental method.

In the present work we focussed on investigation of derivatisation reactions of different sulfonates, as well as silylation of a trisiloxane surfactant and similar surfactants.

Measurements were carried out by using GC coupled to MS (GC-MS), and the results were compared to those obtained by GC with electron capture detection mode or by HPLC-UV.

## Experimental

Liquid chromatographic analyses using UV detection mode were performed on a Younglin YL9100 HPLC system equipped with a YL9150 autosampler. LASs were separated on an Acclaim Surfactant Plus column (150 mm × 4.6 mm i.d., 5 μm) at 30°C, and UV detector signals were recorded at λ=225 nm. Quantitative analysis was performed by external calibration. The eluent flow rate was 0.6 mL/min with isocratic elution for 8 minutes (25:75 = A:B eluents, A = 100 mM ammonium acetate in water, B= acetonitrile. Limit of detection (LOD), determined with standard solutions, was at 1.0 μg/mL for dodecylbenzene sulfonate. Analysis of sulfonates in CLO-based formulation was carried out by LC-MS according to the method described in [2].

For GC measurements conversion of LASs and alkylsulfonates (e.g. Nonit, dioctyl sulfosuccinate salt) were investigated. Derivatisation reactions with potassium iodide and trifluoroacetic acid were studied in detail (See Figure 1.). Procedures were carried out according to the method published by Cohen et al. [3].

For chemical modification of Silvet Star, a silylcarbamate derivatising reagent was used [4] (See Figure 2.). This silylating agent was also applied to other surfactants (Triton X, Genamin and Sapogenat).

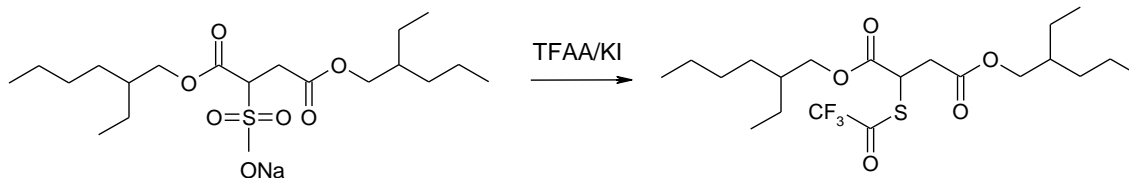


Figure 1. Derivatisation of sulfonates (e.g. Nonit)

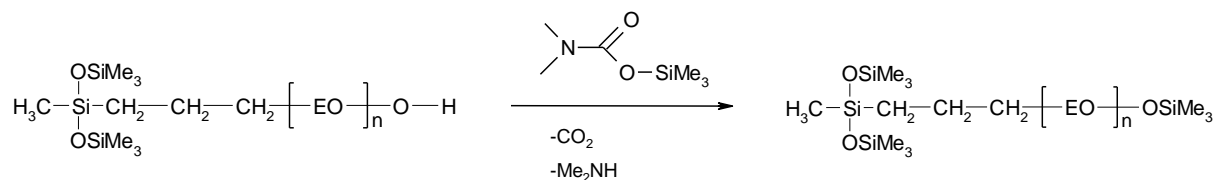


Figure 2. Silylation of Silvet Star

### Typical procedures

**A.** Nonit 0,24 g, 0,42 g KI, 1 mL DMSO, 100 μL trifluoroacetic anhydride (TFAA), heated to 60°C for 60 min, stopped (quench) by Na<sub>2</sub>S<sub>2</sub>O<sub>3</sub> solution

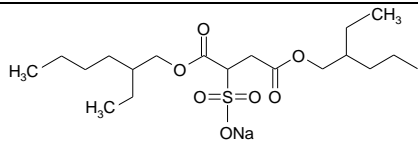
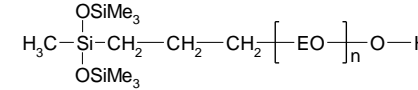
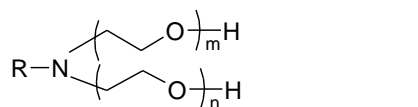
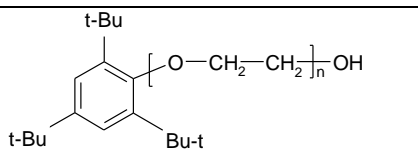
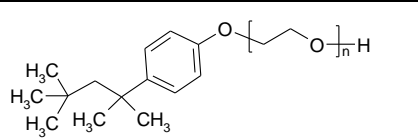
**B.** Silvet Star (Trisil) 20 μL, 100 μL *N,N*-dimethyl-*O*-trimethylsilyl carbamate (Me<sub>2</sub>SiC), 1 mL hexane, room temperature, 30 min

## Results and discussion

Several types of surfactants used for formulation of pesticides were studied (Table 1). In case of CLO-based formulation, components of a long-chain sulphonate mixture were detected by using liquid chromatography coupled with mass spectrometry [2]. Homologues were eluted separately from the Acclaim surfactant column, but only partial separation of isomers was achieved. In the extracted ion chromatograms appeared double, triple or even more peaks belonging to the different (groups of) isomers. Isomers containing a sulfonate group in an

internal position of the linear alkyl chain eluted earlier compared to the isomer where the sulfonate group was connected to the second carbon atom (external). As no standards were available for each homologue, we used a practical assumption that every homologue gives equal instrument responses. For quantitative determination of sulfonates, we used the linear calibration obtained for linear hexadecane-1-sulfonic acid that was not present in sample. Concentrations of homologues were calculated by their extracted ion intensities ( $[M-H]^-$ ) related to that of linear hexadecane-1-sulfonic acid. The amounts of surfactants were underestimated, but probably more precise results are obtained if internal standard or standard addition methods are applied.

Table 1. Surfactant substances investigated in the present study

Trade name	Chemical name	Chemical formula	Structure
Nonit	Diocetyl sulfosuccinate sodium salt	$C_{20}H_{37}NaO_7S$	
Silvet Star	Trisiloxane (7.5 EO units on average)	$(C_2H_4O)_n$ $C_{10}H_{28}Si_3O_3$	
Genamin O 080	Cetyl(C16)/oleyl(C18)-amine ethoxylate (8 EO unit on average)	$(C_2H_4O)_m$ $(C_2H_4O)_n-N-C_{16}H_{35}$	
Sapogenat T 080	tributylphenyl ethoxylate (8 EO units on average)	$(C_2H_4O)_n C_{18}H_{30}OH$	
Triton X100	polyoxyethylene-octyl-phenyl ether, (9-10 EO units on average)	$C_{14}H_{22}O-(C_2H_4O)_n$	

Linear alkylbenzene sulfonates (LASs) were determined in an ACE-based insecticide, and the decomposition of these substances was characterised in distilled water and surface water. Dissipation of LASs was determined alone and in the presence of ACE by using an HPLC-UV method.  $DT_{50}$  values were found to be  $67 \pm 9$  hrs and  $21.7 \pm 4.5$  days for LAS alone and in formulation in surface water, respectively. No significant differences were determined between the corresponding  $DT_{50}$  values in distilled water.

Reactions of sulfonates with potassium iodide and trifluoroacetic acid progressed into completeness in 1 hr (Figure 3.), but the stability of these derivatives is poor. As responses recorded by ECD are high, LODs are low for these trifluoroacyl derivatives. Decomposition was observed after one day of incubation, thus, long-term storage of the derivative is not possible. Therefore, application of other reagents (e.g., in port derivatisation with tetrabutylammonium hydrogensulfate) resulting in more stable derivatives should be more suitable.



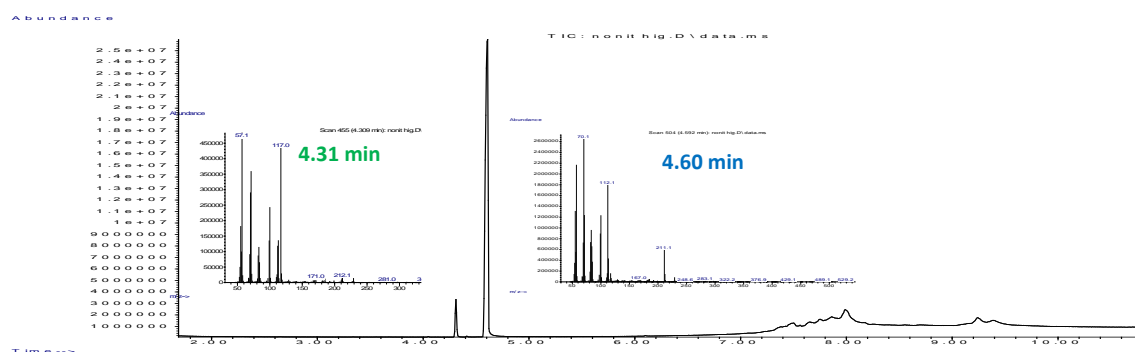


Figure 3. GC-MS chromatogram and mass spectra of Nonit derivative

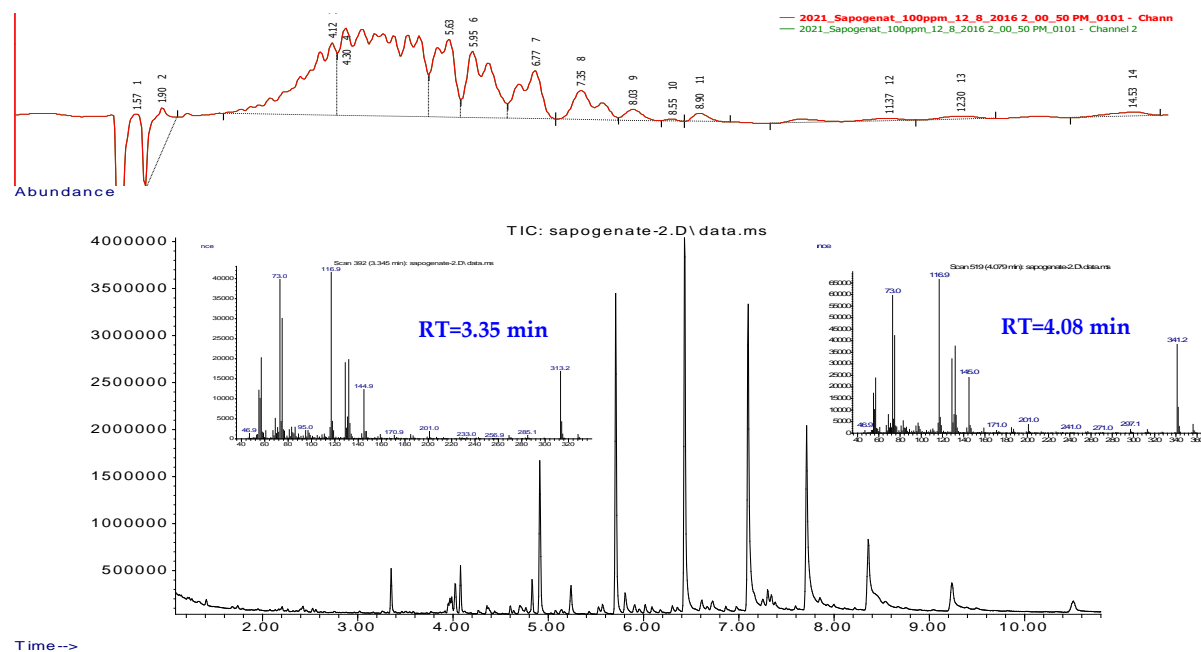


Figure 4. HPLC-UV chromatogram of Sapogenat (upper) and GC-MS chromatogram of silylated Sapogenat and mass spectra of two derivatives (lower)

Silvet Star (Trisil, heptamethyl-trisiloxane modified with polyalkene oxide) together with related surfactants (Triton X, Genamin and Sapogenat) were silylated by using silylcarbmates that were used earlier [4]. GC-MS chromatogram provides more detailed information compared to HPLC-UV chromatogram (See Figure 4.). Based on their mass spectra and chromatographic properties, oligomers of Silvet Star and other investigated surfactants were identified, and their distribution pattern was determined. Stability of the silyl derivatives was ensured by using the appropriate reagent excess or can be further improved by formation of corresponding tert-butyl-dimethylsilyl esters.

### Conclusion

Usually liquid chromatography with UV detection or coupled to mass spectrometry (LC-MS) is more convenient for characterization of surfactant mixtures than gas chromatography. However, composition of the mixtures can be characterized in details by using derivatization

and GC separation. Conversion of sulfonates to trifluoroacyl esters and silylation of hydroxy functional group are suitable procedures for chemical modification of surfactants prior to GC measurements.

### **Acknowledgements**

The work was funded by the Hungarian Scientific Research Fund (OTKA K109865 and K112978).

### **References**

- [1] E. Olkowska, *Talanta* 88 (2012) 1.
- [2] E. Takács, Sz. Klátyik, M. Mörtl, G. Rácz, K. Kovács, B. Darvas, A. Székács, *Intern. J. Environ. Anal. Chem.* 97(9) (2017) 885.
- [3] L. Cohen, F. Soto, M.S. Luna, C.R. Pratesi, G. Cassani, L. Faccetti, *J. Surfact. Deterg.* 6(2) (2003) S1298.
- [4] E. Maloschik, M. Mörtl, A. Székács, *Anal. Bioanal. Chem.*, 397 (2010) 537

## ENANTIOSEPARATION OF CYCLIC $\beta$ -AMINO ACIDS ON ION-EXCHANGER-BASED CHIRAL STATIONARY PHASES

**Tímea Orosz<sup>1</sup>, Enikő Forró<sup>2</sup>, Ferenc Fülöp<sup>2</sup>, Wolfgang Lindner<sup>3</sup>, Gyula Lajkó<sup>1,2</sup>, Attila Bajtai<sup>1</sup>, Antal Péter<sup>1</sup>, István Ilisz<sup>1</sup>**

<sup>1</sup>*Department of Inorganic and Analytical Chemistry, University of Szeged, H-6720 Szeged, Dóm tér 7, Hungary*

<sup>2</sup>*Institute of Pharmaceutical Chemistry, University of Szeged, H-6720 Szeged, Eötvös u. 6, Hungary*

<sup>3</sup>*Department of Analytical Chemistry, University of Vienna, Währinger Strasse 83, 1090 Vienna, Austria*

*e-mail: orosz.ti@chem.u-szeged.hu*

### Abstract

In the present work a direct HPLC method is described for the separation of the stereoisomers of the ampholytic non-methylated, *N*-methyl-, *N*-dimethyl- and *N*-amidino protected cyclic  $\beta$ -amino acids through the application of novel *Cinchona* alkaloid and sulfonic acid-based zwitterionic chiral stationary phases Chiralpak ZWIX(+)<sup>TM</sup> and ZWIX(-)<sup>TM</sup>. The enantioseparations were carried out in polar-ionic mobile phase mode in the temperature range 5–40 °C. The effects of the composition of the bulk solvent, the acid and base additive, the temperature, the structures of the ampholytic analytes on the separations were investigated.

### Introduction

Nowadays, one of the most interesting challenges of the modern analytical chemistry is the separation of chiral compounds. Chirality is momentous for the modern pharmaceutical industry since many drug compounds are chiral whose stereoisomers usually dispose of variant pharmacological and toxicological properties. One of the enantiomers (eutomer) have the desired pharmacological activity, while the other isomer (distomer) is inactive or in worst cases some undesirable effects or even toxic effect can also be produced. Consequently, it is important that the enantiomerically pure form become available, preeminently in the pharmaceutical field. For the separations of the enantiomers chiral high performance liquid chromatography (HPLC) is one of the most frequently applied techniques.

In recent years, cyclic  $\beta$ -amino acids have been intensively investigated due to their potential biological activity and their benefits in synthetic chemistry. The simplest carbocyclic  $\beta$ -amino acid - (1*R*,2*S*)-2-aminocyclopentanecarboxylic acid (cispentacin) - is an antifungal antibiotic [1], while its methylene derivative (icofungipen, PLD-118) is active *in vitro* against *Candida species* [2]. Cyclic  $\beta$ -amino acids can also serve as building blocks for the synthesis of modified peptides.

### Experimental

An 1100 Series HPLC system equipped with a solvent degasser, a pump, an autosampler, a column thermostat, a multiwavelength UV–Vis detector and ChemStation chromatographic data software (Agilent Technologies, Waldbronn, Germany), and a corona-charged aerosol detector from ESA Biosciences Inc. (Chelmsford, MA, USA) was applied for chromatographic measurements. Analyses were also performed on a Waters chromatographic system consisted of a M600 pump, a 2996 PDA detector (Waters Chromatography, Milford,

MA, USA) and connected with a Jasco 2031 Plus refractive index (RI) detector (Jasco Tokyo, Japan) and Empower 2 data manager software (Waters Chromatography). The HPLC columns used were Chiralpak ZWIX(+)<sup>TM</sup> and ZWIX(-)<sup>TM</sup> (150 x 3.0 mm I.D., 3- $\mu$ m particle size for both columns). Chromatography was performed in isocratic mode at a flow rate of 0.6 mL min<sup>-1</sup> and a column temperature of 25 °C. The dead-time ( $t_0$ ) of the column was determined via the injection of acetonitrile solution of methanol.

## Results and discussion

### Influence of mobile phase composition on chromatographic parameters

Cyclic  $\beta$ -amino acids investigated in this study were chromatographed on Chiralpak ZWIX(+)<sup>TM</sup> and ZWIX(-)<sup>TM</sup> columns. In polar-ionic mobile phase mode, a mixture of MeOH as a protic solvent and MeCN as aprotic solvent in combination with acid and base additives provides the best enantioseparation of zwitterionic chiral CSPs. The increased retention observed for the investigated analytes at higher MeCN content were accompanied with increased selectivity and resolution in most cases. The observed chromatographic behavior can likely be explained on the basis of decreased solvation of the ionizable compounds. The values of selectivity increased monotonously in most cases, when the MeCN content in mobile phase changed from 20 to 60 v% due to enhanced electrostatic and H-bonding interactions. The best separation performances were achieved applying mobile phase composition of MeOH/MeCN (60/40 v/v) containing 25 mM TEA and 50 mM FA, thus most of the measurements were performed by using the above mentioned mobile phase system.

The applied *Chincona*-based selectors are diastereoisomers, but they often behave as pseudo-enantiomers. This extraordinarily useful property makes these chiral columns greatly effective in enantiomeric excess determination. Hence, the sequence of elution of the enantiomers can be reversal on change from the quinine-, to the quinidine-based CSP. The elution sequence was determined in all cases (when enantioseparation was achieved) and was found to be reversal in every case on switching from ZWIX(+)<sup>TM</sup> to ZWIX(-)<sup>TM</sup>. It should be mentioned that for Fmoc-substituted analytes no separation could be achieved on these stationary phases.

### Effects of structures of N-substitution

The structure (substituent position and size) have a strong influence on the chiral recognition. In order to study the structure - retention (selectivity) relationships the same mobile phase system (MeOH/MeCN (60/40 v/v) containing 25 mM TEA and 50 mM FA) was applied. It was observed that with increase of the degree of substitution of the amino group and the size of the substituent the retention decreased appreciably. The values of  $k_I$  were smaller for *N*-methylated, *N*-dimethylated and *N*-amidino substituted cyclic  $\beta$ -amino acids compared to the non-substituted ones for both CSPs. The lowest  $k_I$  values were observed in the case of Fmoc-protected analytes. The Fmoc protection of the amino group results in decreased basicity with the consequence that the double ion pairing interaction mechanism is not possible anymore. Investigated the free amino acids it can be presumed that steric effects have a great influence on the selector-analyte interactions. The obtained results show that selectivity changed in different ways. The highest  $\alpha$  values were observed for *N*-amidino substituted analytes. In addition, the values of selectivity was higher in the case of *N*-methylated compounds compared to *N*-dimethylated and non-methylated ones. Comparing the analytes containing cyclopentane- or cyclohexane skeleton the same trend was observed considering  $k_I$  and  $\alpha$  values. The *cis-trans* configuration and the degree of substitution possess marked influence on

the retention and selectivity. In the case of compounds with *trans* configuration  $k_1$  values were higher for the studied analytes on both CSPs. This observation can be explained by more tight interactions between the cationic- and anionic-sight of the selector and the *trans*-isomers. Comparing the two CSPs, in most cases ZWIX(-)<sup>TM</sup> CSP was more suitable for the enantioseparation of the studied analytes. However, ZWIX(+)<sup>TM</sup> exhibited more effective separation for the *N*-amidino protected analytes.

### Effects of temperature and thermodynamic parameters

In order to investigate the effects of temperature on the chromatographic parameters, a variable-temperature study was carried out on ZWIX(+)<sup>TM</sup> and ZWIX(-)<sup>TM</sup> over the temperature range 5–40 °C. The retention factors and selectivities generally decreased with increasing temperature in most cases. The changes observed in the selectivity with increasing temperature were not consistent. Resolution usually decreased with the increase of temperature on both ZWIX(+)<sup>TM</sup> and ZWIX(-)<sup>TM</sup> CSPs. On the other hand, an increasing tendency was also registered on ZWIX(-)<sup>TM</sup>. All of the van't Hoff plots ( $\ln \alpha$  vs.  $1/T$  curves) were linear. Under the conditions when  $\Delta(\Delta H^\circ)$  was negative,  $\Delta(\Delta S^\circ)$  was also negative, and positive  $\Delta(\Delta H^\circ)$  was accompanied by positive  $\Delta(\Delta S^\circ)$ . The obtained results revealed that enantioselective separations were in most cases enthalpically-driven, but entropically-driven separation was also observed.

### Conclusion

The chromatographic retention behavior and resolution proved to depend the composition of the bulk solvent, the acid and base additive, the temperature and the positions of the substituents. The retention behavior and resolution proved to dependent on the mobile phase compositions and the temperature. The studied CSPs, ZWIX(+)<sup>TM</sup> and ZWIX(-)<sup>TM</sup> exhibited complementary behavior in the direct enantioseparation of the non-methylated, *N*-methyl, *N*-dimethyl and *N*-amidino substituted analytes, while separation for the enantiomers of *N*-Fmoc protected cyclic  $\beta$ -amino acids could not be achieved on these CSPs. The values of thermodynamic parameters such as the changes in  $\Delta(\Delta H^\circ)$ ,  $\Delta(\Delta S^\circ)$  and  $\Delta(\Delta G^\circ)$  proved to depend on the structures of the analytes and on the chiral selector used.

### Acknowledgements

This work was supported by Hungarian National Science Foundation grant OTKA K 108847. The support of Pilar Franco (Chiral Technologies Europe) in providing the Chiralpak columns is gratefully acknowledged.

### References

- [1] F. Fülöp, The chemistry of 2-aminocycloalkanecarboxylic acids, Chem. Rev. 101 (2001) 2181–2204.
- [2] R. Petraitiene, V. Petraitis, A. M. Kelaher, A. A. Sarafandi, D. Mickiene, A. H. Groll, T. Sein, J. Bacher, T. J. Walsh, Efficacy, plasma pharmacokinetics, and safety of icofungipen, an inhibitor of *Candida* isoleucyl-tRNA synthetase, in treatment of experimental disseminated candidiasis in persistently neutropenic rabbits, Antimicrob. Agents Chemother. 49 (2005) 2084–2092.

## REMOVAL OF COLD TRUB FROM HOPPED WORT BY CROSSFLOW MICROFILTRATION: ANALYTICAL ASPECTS

Áron Varga<sup>1</sup>, Richard Bertok<sup>1,2</sup>, Beáta Hegyesné-Vecseri<sup>2</sup>, Edit Márki<sup>1</sup>

<sup>1</sup>*Department of Food Engineering, Szent István University, H-1118 Budapest, Ménesi út 44., Hungary*

<sup>2</sup>*Department of Brewing and Distilling, Szent István University, H-1118 Budapest, Ménesi út 45., Hungary*  
*e-mail: mr.aron.varga@gmail.com*

### Abstract

Removing cold trub (cold break) from hopped wort is important, because of yeast viability, beer quality and less fouling during fermentation in a Membrane Bioreactor (MBR). Cold trub can be removed from hopped wort by several methods, but Crossflow Microfiltration (CFMF) would be an alternative technology. For the membrane filtration experiment a pale wort was made in pilot scale. The membrane filtration was performed with the following operating parameters: temperature ( $10\pm 1^\circ\text{C}$ ), Transmembrane Pressure (0.4 bar) and Retentate Flow Rate (50 l/h). The size of particles in cold trub is about  $0.5\ \mu\text{m}$ , the nominal pore size of the used membrane was  $0.2\ \mu\text{m}$ . The Initial Flux and Steady State Flux of the membrane filtration were calculated. Chemical and physical properties ( $\beta$ -glucan content, bitterness, colour, dynamic viscosity, extract content, free amino nitrogen content, pH, turbidity, particle size distribution) of original wort and permeate samples were measured and retentions of different components ( $\beta$ -glucan, iso-alpha acids, extract, free amino nitrogen) were calculated. The Initial Flux and Steady State Flux of the membrane filtration were  $16.75\ \text{L}/(\text{m}^2\text{h})$  and  $4.89\ \text{L}/(\text{m}^2\text{h})$ , respectively. Changing of the analytical parameters are appropriate, for example, retention of  $\beta$ -glucan was 40.17 % and free amino nitrogen content of original wort and permeate were same. According to the particle size distribution measurement cold trub can be completely removed by CFMF. CFMF is an alternative method for removing cold trub from hopped wort based on the results, but the optimization of the technology is needed for purposes of increasing Flux values and improve analytical parameters.

### Introduction

The scope of this study is to investigate the analytical aspects of removal of cold trub (cold break) from hopped wort by Crossflow Microfiltration (CFMF).

Hopped wort is an intermediate product of brewing. It is the liquid extracted from the mashing process and boiled with hops [1]. Wort cooling before fermentation leads to the formation of cold trub (composed of proteins, protein-polyphenol complexes and carbohydrates). The size of particles in cold trub is about  $0.5\ \mu\text{m}$  and it settles only with great difficulty [2], [3]. Removing at least some cold trub can improve yeast viability and the quality of finished beer [4]. Furthermore, if primary fermentation is performed in a Membrane Bioreactor (MBR), cold trub causes membrane fouling [5]. Centrifugation, diatomaceous earth filtration, flotation and sedimentation are some methods used to promote the removal of cold trub [2], but CFMF would be an alternative technology [6]. In CFMF, the fluid (wort in this case) to be filtered flows parallel to the membrane surface and permeates through the membrane by Transmembrane Pressure [7].



The goals of the present investigation are to determine Flux values of the CFMF with given operating parameters, chemical and physical properties of feed (original wort) and permeate.

## **Experimental**

### *Wort production*

Pale wort was made with multi step mashing in pilot scale at the Department of Brewing and Distilling, Szent István University. Pilsner Malt from Boortmalt, Hungary and Hallertauer Tradition pellet hops from HVG, Germany were used at the brewhouse.

### *Membrane filtration*

The membrane filtration experiment was carried out with bench scale in-house developed CFMF equipment. Membralox T1-70 tubular ceramic membrane (Pall, USA), with active layer of aluminium oxide, 0.2  $\mu\text{m}$  nominal pore size, 7 mm channel diameter, 250 mm length and 0.005  $\text{m}^2$  active surface was used for filtration purpose. During the membrane filtration process temperature, Transmembrane Pressure and Retentate Flow Rate were maintained  $10\pm 1^\circ\text{C}$ , 0.4 bar and 50 l/h, respectively. Permeate samples were collected with a constant volume and Flux values were calculated.

After membrane filtration experiment, the membrane was cleaned thoroughly by deionized water for 5 minutes at  $25^\circ\text{C}$  and then by 1 % (w/w) Sodium hydroxide for 60 minutes at  $60^\circ\text{C}$ . After cleaning by alkali the membrane was rinsed again by deionized water for 10 minutes at  $25^\circ\text{C}$  followed by cleaning with 1 % (w/w) Hydrogen peroxide for 60 minutes at  $25^\circ\text{C}$  temperature. Finally the membrane was cleaned thoroughly by deionized water for 10 minutes at  $25^\circ\text{C}$ . In all cases Transmembrane Pressure and Retentate Flow Rate were maintained 0.4 bar and 50 l/h, respectively. Sodium hydroxide were purchased from Reanal, Hungary and Hydrogen peroxide from Hungaro Chemicals, Hungary.

### *Chemical and physical measurements*

The  $\beta$ -glucan content of the samples were determined by “Analytica EBC 8.13.2 High Molecular Weight  $\beta$ -Glucan Content of Wort: Fluorimetric Method”, 2008. The bitterness (concentrations of iso-alpha acids in ppm) and colour of the samples were measured according to “Analytica EBC 8.8 Bitterness of Wort”, 2004 and “Analytica EBC 8.5 Colour of Wort: Spectrophotometric Method (IM)”, 2000. Dynamic viscosity of original wort and permeate samples were measured with Physica MCR 51 Rheometer (Anton-Paar Hungary Ltd., Hungary) with DG27 double gap concentric cylinder measurement system. Data were acquired and analysed using Rheoplus/32 v.3.40 software. Flow curve of samples were measured by increasing the shear rate from 500 to 1000 1/s at temperature of  $20^\circ\text{C}$ . Dynamic viscosity of samples were calculated based on Herschel Bulkley model [8] fitted to measured data of flow curve (shear stress in function of shear rate). Extract contents of samples were measured with Alcolyzer Plus (Anton-Paar, Austria). The free amino nitrogen (FAN) content of samples were determined by the “Analytica EBC 8.10.1 Free Amino Nitrogen in Wort by Spectrophotometry – Manual method (IM)”, 2017. All of the absorbances were measured with DR 6000 spectrophotometer (Hach, USA). The pH of samples were determined with 1100 H pH meter (VWR, USA). Turbidity of samples were measured at  $20^\circ\text{C}$  with 2100P Turbidimeter (Hach, USA) in NTU and converted to EBC. Retentions of  $\beta$ -glucan, iso-alpha acids, extract and FAN were calculated. Particle size distribution was measured with Malvern Zetasizer Nano-ZS. Data were acquired and analysed using Zetasizer 6.32 software.



## Results and discussion

### Membrane filtration

The Initial Flux and Steady State Flux of the membrane filtration were 16.75 L/(m<sup>2</sup>h) and 4.89 L/(m<sup>2</sup>h), respectively. These values are quite low, because of fouling mechanism.

### Chemical and physical measurements

Analytical parameters of original wort and permeate are shown in Table 1.

**Table 1.** Analytical parameters of original wort and permeate

Parameter	Original wort	Permeate
β-glucan content (mg/L)	117	70
Bitterness (IBU)	49	44
Colour (EBC)	12.98	8.98
Dynamic viscosity at 20°C (mPas)	5.43	4.95
Extract content % (w/w)	11.16	10.34
FAN content (mg/L)	159	159
pH	6.02	6.42
Turbidity at 20°C (EBC)	106.75	7.88

β-glucan content decreased dramatically that leads to less fouling during fermentation in a MBR. Furthermore, the lower β-glucan content can improve clarification of rough beer (higher filtration throughput and less haze problems in the final product). The bitterness decreased by 5 unit, but this difference can't be evaluated with sensory analysis. Colour became paler, supposedly due to notable retention of polyphenols, carbohydrates and Maillard reaction products. The dynamic viscosity decreased, this is mainly because of the lower β-glucan content. The extract decreased by reason of retention of different compounds (e.g. carbohydrates). FAN content wasn't changed that is essential, because adequate level of FAN (150 - 200 mg/L [9]) in wort ensures efficient yeast cell growth and desirable fermentation performance. The pH increased that negatively affects the microbiological stability of the permeate. The turbidity was decreased by two orders of magnitude, because of removal of cold break. This results in less haze problems in the final product.

Retentions of different components are shown in Table 2.

**Table 2.** Retentions of different components

Component	Retention (%)
β-glucan	40.17
Iso-alpha acids (bitterness)	10.20
Extract	7.65
FAN	0

From a technological point of view, the retention values of β-glucan and FAN are suitable. The retention values of iso-alpha acids and extract are acceptable.

Original wort sample was too polydisperse for particle size distribution analysis and the average particle size of this sample was larger than upper size analysis limit (10 μm).

Particle size distribution of permeate is shown in Figure 1.

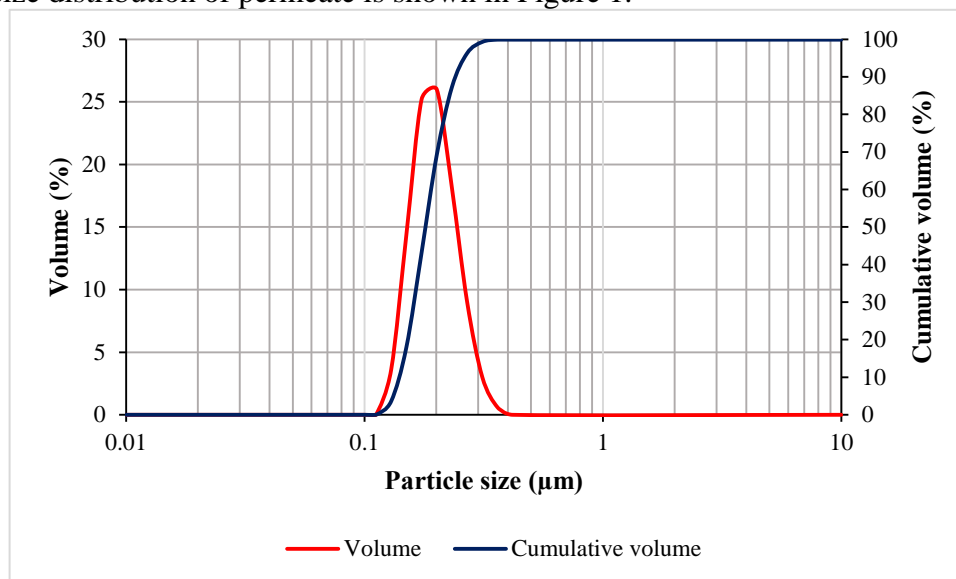



**Figure 1.** Particle size distribution of permeate

As it can be seen in Figure 1, cold trub (particles about 0.5 µm in diameter) was completely removed by microfiltration. The average particle size of the permeate is around 0.2 µm that corresponds to the nominal pore size of the membrane.

### Conclusion

Flux values of the membrane filtration experiment were quite low, but these values could be increased by the optimization of operating parameters (e.g. Transmembrane Pressure and Retentate Flow Rate). It has been proven that the changing of the analytical parameters are appropriate and cold trub can be completely removed by CFMF.

### Acknowledgements

This work was  supported by the ÚNKP-17-3 the New National Excellence Program of the Ministry of Human Capacities; the Szent István University, Doctoral School of Food Sciences; the European Union and co-financed by the European Social Fund (grant agreement no. EFOP-3.6.3-VEKOP-16-2017-00005). We would like to say thanks to Szent István University, Faculty of Food Science, Department of Brewing and Distilling and Szent István University, Faculty of Food Science, Department of Food Preservation for supporting the measurements.

### References

- [1] J. Csanádi, 'Sörlékészítés', in *Élelmiszer-technológia mérnököknek*, Szeged, Hungary: Szegedi Tudományegyetem Mérnöki Kar, 2010, pp. 451–454.
- [2] R. Barchet, 'Cold Trub: Implications for Finished Beer, and Methods of Removal', *Brewing Techniques*, 1994. [Online]. Available: <http://www.morebeer.com/brewingtechniques/library/backissues/issue2.2/barchet.html>. [Accessed: 22-Sep-2017].

- [3] W. Kunze, 'Formation and optimal remove of cold break', in *Technology Brewing and Malting*, 3rd ed., Berlin, Germany: VLB, 2004, p. 347.
- [4] L. Narziß and W. Back, 'Abtrennung des Kühltrubs', in *Die Bierbrauerei - Die Technologie der Würzebereitung*, Weinheim, Germany: WILEY-VCH Verlag GmbH & Co. KGaA, 2009, pp. 700–701.
- [5] S. Schildbach and L. Stumpf, 'Enhancing Main Fermentation Velocities in Beer by the Use of a Membrane Bioreactor – Approach and First Results', presented at the BiosysFoodEng 2016, Budapest, 08-Dec-2016.
- [6] A. Ambrosi, N. S. M. Cardozo, and I. C. Tessaro, 'Membrane Separation Processes for the Beer Industry: A Review and State of the Art', *Food Bioprocess Technol.*, vol. 7, no. 4, pp. 921–936, 2014.
- [7] R. El *et al.*, 'Cross-flow microfiltration applied to oenology: A review', *J. Membr. Sci.*, vol. 382, no. 1–2, pp. 1–19, 2011.
- [8] T. G. Mezger, 'Model functions for flow curves including a yield point', in *The Rheology Handbook*, 2nd ed., Hannover, Germany: Vincentz Network, 2006, p. 57.
- [9] I. Hornsey, 'Nitrogen Metabolism', in *Brewing*, 2nd ed., Cambridge, United Kingdom: RSC Publishing, p. 153.

## PHOTOCATALYTIC OZONATION OF MONURON - EFFECT OF REACTION PARAMETERS ON THE HYDROXYL RADICAL FORMATION AND MONURON TRANSFORMATION

**Máté Náfrádi<sup>1</sup>, Milán Molnár<sup>1</sup>, Krisztina Schrantz<sup>1</sup>, Klára Hernádi<sup>2</sup>, Tünde Alapi<sup>1</sup>**

<sup>1</sup>*Department of Inorganic and Analytical Chemistry, University of Szeged, H-6720 Szeged, Dóm tér 7, Hungary*

<sup>1</sup>*Department of Applied and Environmental Chemistry, University of Szeged, H-6720 Szeged, Rerrich Béla tér 1.*

*e-mail: nafradim@chem.u-szeged.hu*

### Abstract

The combination of ozonation and heterogeneous photocatalysis (photocatalytic ozonation) can enhance the efficiency of the transformation of target pollutant and sometime results in synergistic effect, which is generally explained by the higher rate of formation of hydroxyl radical due to the presence of ozone. The transformation of organic pollutants on the surface of the photocatalyst is very complex, mainly in the presence of ozone. In the case of the heterogeneous photocatalysis the efficiency highly depends on the chemical structure of the target pollutant which determines its rate of reaction with molecular ozone and/or hydroxyl radical, and the adsorbed amount of pollutants on the surface of the photocatalyst, which is crucial in the case of the transformation by direct charge transfer. Moreover the properties of the solutions such as pH and ionic strength, affect the way and efficiency of the transformation through the modification of the surface properties of the photocatalyst (surface charge and potential, adsorption properties).

In the present work, the ozonation, heterogeneous photocatalysis and photocatalytic ozonation of monuron and coumarin were investigated. Monuron, one of the phenyl urea pesticide and suspected endocrine disruptor was used as target substance, while the rate of formation of hydroxylated byproduct of coumarin (umbelliferone) was used to compare the formation rate of hydroxyl radical under various circumstances.

Both ozonation and photocatalysis were found to be effective in the transformation of coumarin and monuron. Efficiency was enhanced using photocatalytic ozonation, but synergism was not observed. pH had significant effect neither in the case of monuron nor coumarin. The formation rate of umbelliferone formed from coumarin due to its reaction with hydroxyl radical was much higher during photocatalysis compared to ozonation, verifying the importance of the HO•, which was confirmed by the negative effect of methanol as HO• scavenger. Addition of NaF proved the importance of catalyst surface properties during photocatalytic ozonation.

### Introduction

The advanced oxidation processes (AOPs) give us possibility to solve one of the most important problems of water treatment: elimination of those organic pollutants which can be treated hardly by conventional water treatment methods. Using AOPs the transformation of the contaminants takes place in reactions with different reactive radicals. The most important radical is HO• due to its high reactivity and low selectivity. The combination of AOPs can result in synergism, which is generally explained by the increased HO• formation rate. [1]

Addition of ozone to a photocatalytic system can have several positive effects. The ozone can react directly with the organic substrate. Moreover adsorption of ozone is preferred comparing to oxygen and behaves as an excellent electron scavenger, successfully inhibiting the recombination of photogenerated electron and hole pairs.



The adsorbed  $H_2O_2$  can react with photogenerated electron and hole and results in the formation of  $HO\bullet$  and  $HO_2^{\bullet}$ :



While formation of one  $HO\bullet$  from oxygen requires three electrons, that needs only one electron from adsorbed ozone. [2,3]



Planning efficient and economically feasible water purification systems based on photocatalytic ozonation, several parameters must be taken into account. The pH of the solution is critical, because it affects the aggregation of catalyst particles, surface properties and consequently the reactions taking place on the surface. The surface charge of  $TiO_2$  depends on the pH, which influences the absorption of substrates. pH also affects the concentration of dissolved ozone in the solution. [4,5]

In this work the effect of pH, methanol and NaF on the efficiency of ozonation, heterogeneous photocatalysis and photocatalytic ozonation was investigated. The model pollutant monuron was a phenyl-urea pesticide, which may generate several environmental and health problems due to its persistence, toxicity, and possible endocrine effects.

Methanol was used as  $HO\bullet$  scavenger for investigation the role and importance of this radical in the transformation of monuron. NaF was used as surface modifying agent to study the effect of adsorption. Coumarine can be used in photocatalytic systems to measure the formation rate of  $HO\bullet$ . The formation rate of umbelliferon, which is the hydroxylated byproduct of coumarin is directly proportional to the formation rate of  $HO\bullet$ . [6]

## Experimental

500  $cm^3$  monuron solution ( $5.0 \times 10^{-4}$  mol  $dm^{-3}$ ) and coumarine solution ( $1.0 \times 10^{-4}$  mol  $dm^{-3}$ ) were irradiated in a reactor equipped with a fluorescent mercury-vapor lamp, which emits in the region 300 - 400 nm UV light. The solution was circulated using a peristaltic pump with 375  $cm^3$   $min^{-1}$  flow rate, thermostated at  $25 \pm 1^\circ C$  and saturated with oxygen. The oxygen/ozone mixture was generated using an ozonator based on silent electric discharge. The concentration range was adjustable between 5-20  $mg$   $dm^{-3}$ . The concentration of ozone in oxygen/ozone mixture, which was bubbled through the solution or suspension was 10  $mg$   $dm^{-3}$  in each case. The  $TiO_2$  photocatalyst (Aeroxide P25<sup>®</sup>) was added in 1.0  $g$   $dm^{-3}$  concentration, and the suspension was centrifuged and filtered before analysis. NaOH and HCl solutions (0.1

mol dm<sup>-3</sup>) were used to set the pH. Ionic strength was constant and adjusted with addition of NaCl (5.0×10<sup>-3</sup> mol dm<sup>-3</sup>). Concentration of methanol or NaF was 2.5×10<sup>-2</sup> mol dm<sup>-3</sup>.

The concentration of monuron was determined by high performance liquid chromatography equipped with DAD detector (Merck-Hitachi L-7100 pump, RP-18 column, water-methanol 40:60 eluent, L-4250 UV-Vis detector, wavelength of detection: 210 nm ). The degradation of coumarine was followed using spectrophotometry at 277 nm, while the formation of umbelliferone by fluorimetry at 456 nm, wavelength of the excitation light was 332 nm.

### Results and discussion

At first the effect of pH on the concentration of dissolved ozone was investigated. There was found no significant effect between pH 3 - 9, while above pH 10 it was significantly reduced because of the OH<sup>-</sup> initiated degradation of ozone. Consequently, the effect of pH was investigated between pH 3 and 9 in the further experiments.

Table I. Effect of pH, methanol and NaF on the initial transformation rate of monuron ( $r_0^{mon}$ )

pH		O <sub>3</sub>	TiO <sub>2</sub> /UV	TiO <sub>2</sub> /UV/O <sub>3</sub>
		$r_0^{mon} (\times 10^{-8} \text{ moldm}^{-3}\text{s}^{-1})$	$r_0^{mon} (\times 10^{-8} \text{ moldm}^{-3}\text{s}^{-1})$	$r_0^{mon} (\times 10^{-8} \text{ moldm}^{-3}\text{s}^{-1})$
3.0	-	8.67	8.92	12.9
	NaF	-	9.08	18.7
	Methanol	-	3.58	2.0
5.5	-	9.50	13.0	14.8
	NaF	-	19.8	29.3
	Methanol	4.75	2.70	3.33
9.0	-	9.42	13.0	12.9
	NaF	-	20.0	23.6
	Methanol	4.25	4.08	2.33

In the case of ozonation the pH has no significant effect on the transformation rate of monuron (Table I.) similar to the concentration of dissolved ozone. Consequently, the transformation of monuron is probably caused by the reaction with molecular ozone. However methanol decreased significantly the rate of transformation (Table I.), proving that the relative contribution of the HO• initiated transformation is not negligible. Using heterogeneous photocatalysis the rate of transformation at pH 3 was found to be significantly lower than that under neutral or basic pH. Methanol strongly inhibited the transformation at each adjusted pH, while the positive effect of NaF depended on pH. That was observed only at pH 5.5 and pH 9.0 and significantly enhanced the transformation rate of monuron (Table I.). The effect of NaF can be explained by the better hydrophobicity of the TiO<sub>2</sub> favoring the adsorption of monuron.

The negative effect of methanol as radical scavenger and positive effect of NaF suggest that, monuron does not adsorbed well on the surface of TiO<sub>2</sub> under neutral and basic pH and

mainly the formed HO• is responsible for the its transformation. At pH 3.0 NaF has no effect and the initial transformation rate decreased comparing that to the pH = 5.5 (Table I.). Regarding that, the point of zero charge (where the net surface charge is zero) of TiO<sub>2</sub> is at pH = 5.6 in the 5.0×10<sup>-3</sup> NaCl solution, the positive net surface charge is probably favors, while the zero or negative net surface charge hinders the adsorption of monuron and favours the formation of HO•.

Table II. Effect of pH on the initial transformation rate of coumarin ( $r_0^{kum}$ ), the slope ( $m_0^{umb}$ ) of the initial part of the curve fluorescent light intensity versus treatment time (linear fitting) and the maximum value of the fluorescence light, emitted by umbelliferon ( $I_{max}$ )

		$r_0^{kum}$ ( $\times 10^{-8}$ mol dm <sup>-3</sup> s <sup>-1</sup> )	$r_0^{kum}/r_0^{kum}(ref)$	$m_0^{umb}$	$m_0^{umb}/m_0^{umb}(ref)$	$I_{max}$
<b>O<sub>3</sub></b>	pH = 5.5 without NaCl	32.3	1.04	0.17	1.21	85
	pH = 3.0	30.9	0.99	0.18	1.30	83
	pH = 5.5	31.1	-	0.14	-	76
	pH = 9.0	31.6	0.78	0.15	1.07	74
<b>TiO<sub>2</sub>/UV</b>	pH = 5.5 without NaCl	60.1	1.31	8.95	0.91	3725
	pH = 3.0	33.8	0.74	6.42	0.65	2034
	pH = 5.5	45.7	-	9.85	-	4298
	pH = 9.0	51.7	1.13	9.64	0.98	3540
<b>TiO<sub>2</sub>/UV/O<sub>3</sub></b>	pH = 3.0	57.6	1.04	4.56	1.82	1224
	pH = 5.5	59.8	-	2.50	-	738
	pH = 9.0	66.1	1.10	0.46	0.184	192

Behavior of coumarin was found to be very similar to that of monuron. pH has no effect in the case of ozonation and the rate of transformation slightly increased with increase pH in the presence of TiO<sub>2</sub>. Using photocatalytic ozonation, the transformation of coumarin was faster than using ozonation or photocatalysis, but synergism was not observed. (Table II.)

Using ozonation the rate of formation of umbelliferone ( $m_0^{umb}$ ) and the maxima of its concentration was almost negligible (two order of magnitude lower) comparing that to the values determined in the case of heterogeneous photocatalysis (Table II.). This confirmed that during ozonation mainly the reaction with molecular ozone is responsible for the transformation of coumarin and this reaction does not results in the formation of umbelliferon. However the pH effect is not countable on the rate of transformation of coumarin, the formation rate of umbelliferon was two times higher at pH 5.5 and 9.0 than under acidic pH in the case of heterogeneous photocatalysis (Table II.). This result is in accordance with the observation of Tunesi and Anderson [7] and shows that, the formation rate of HO• on the surface of the TiO<sub>2</sub> is strongly depend on pH and favored under neutral and basic conditions.

The enhanced efficiency of the combination of ozonation with heterogeneous photocatalysis is generally explained by the higher rate of HO• formation. The effect of ozone



in on the formation rate of umbelliferon was out of accord with our expectation, since significantly decreased the formation rate of umbelliferon. This suggests that the addition of ozone not enhances but inhibits the formation of HO•. But the effect of methanol, as HO• scavenger is contradicts of this, since the inhibition effect is well magnifested and the transformation rated of monuron was decreased with more than 80% (Table I).

Comparing the reaction rate constants of the coumarin, ozone and oxygen with electron, each value is in the same order (Table III). Regarding that, the concentration of oxygen is much higher than that of coumarin or ozone, the photogenerated electrons reacts mainly with oxygen. But adsorption has to be taken into account, because affects importantly the concentration of the compounds on the surface of the TiO<sub>2</sub>. Thus there is a possibility for the competition between ozone and coumarin for the photogenerated electrons and both this competition and the direct reaction of coumarin and ozone in the solution can be responsible for the fact that, ozone decreased the formation rate of the hydroxylated byproduct of coumarin.

Table III. The concentration and reaction rate constants (data from the NIST Standard Reference Database 40) of the compounds with electron

	c (mol dm <sup>-3</sup> )	k(e <sup>-</sup> ) (mol dm <sup>-3</sup> s <sup>-1</sup> )	c×k(e <sup>-</sup> ) (s <sup>-1</sup> )	k(HO•) (mol dm <sup>-3</sup> s <sup>-1</sup> )	c×k(HO•) (s <sup>-1</sup> )
O <sub>3</sub>	6×10 <sup>-5</sup>	3.6×10 <sup>10</sup>	2.2×10 <sup>6</sup>	2×10 <sup>8</sup>	1.2×10 <sup>4</sup>
O <sub>2</sub>	1.25×10 <sup>-3</sup>	1.7×10 <sup>10</sup>	2.1×10 <sup>7</sup>	-	-
coumarin	1.0×10 <sup>-4</sup>	1.6×10 <sup>10</sup>	1.6×10 <sup>6</sup>	2×10 <sup>9</sup>	2.0×10 <sup>5</sup>

## Conclusion

- Combination of ozonation and heterogeneous photocatalysis enhances the efficiency of the transformation of monuron and coumarin, but synergism was not observed
- pH has no significant effect on the transformation rates
- methanol strongly decreased while NaF enhances the transformation rate of monuron. The degree of effect depends on pH.
- Ozone significantly inhibits the formation rate of umbelliferone, probably because of the competition for the photogenerated electrons.

## Acknowledgements

The work was done in the frame of the DAAD 151955 bilateral and TÉT\_15\_IN-1-2016-0013 project.

## References

- [1] R. Bolton. K.G. Bircher. W. Tumas. C.A. Tolman. (IUPAC Technical Report). *Pure Appl. Chem.* 73 (2001)
- [2] F. Parrinoa. G.Camera-Rodab.,V. Loddoo. V.Augugliaroa. L.Palmisanoa (2015) *Appl. Catal. B: Env.* 178 37–43
- [3] F.J. Beltran. A. Aguinaco. A. Rey. J.F. Garcia-Araya (2012) *Ind. Eng. Chem. Res.* 51 4533–4544.
- [4] Bhatkhande. D.S.. Pangarkar. V.G.. Beenackers. A.A.. (2002) *J. Chem. Technol. Biotechnol.* 77. 102–116.
- [5] H. Czili. A. Horváth (2008) *Appl. Catal. B: Environ.* 81 295–302

**Poster Proceedings**

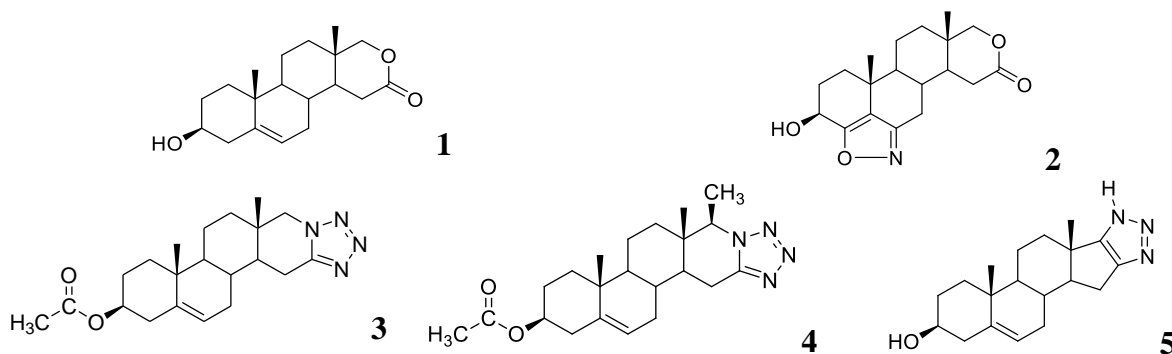
ENVIRONMENTALLY FRIENDLY SYNTHESIS OF PHARMACOLOGICALLY ACTIVE HETEROCYCLIC ANDROSTANE DERIVATIVES

Aleksandar Oklješa<sup>1</sup>, Andrea Nikolić<sup>1</sup>, Marina Savić<sup>1</sup>, Marija Sakač<sup>1</sup>, Suzana Jovanović-Šanta<sup>1</sup>, Bianka Edina Herman<sup>2</sup>, János Gardi<sup>2</sup>, Katarina Penov Gaši<sup>1</sup>, Ksenija Pavlović<sup>1</sup>, Mihály Szécsi<sup>2</sup>

<sup>1</sup> University of Novi Sad Faculty of Sciences, Department of Chemistry, Biochemistry and Environmental protection, Trg Dositeja Obradovića 3, 21000 Novi Sad, Serbia,

<sup>2</sup> First Department of Medicine, University of Szeged, Korányi fasor 8-10 H-6720 Szeged, Hungary  
aleksandar.oklješa@dh.uns.ac.rs

Environmentally friendly synthetic approach of new potential drugs is of great importance in today's medicinal chemistry. Recent trends in organic synthesis utilize non-conventional green techniques such as ultrasound, microwave irradiation or using ionic liquids. In this work microwave (MW) assisted reactions were performed as rapid and eco-friendly procedures for the synthesis of androstane compounds possessing D-homo lactone or D-ring fused azole moieties (**1–5**). Effect of the synthesized compounds exerted on a key enzyme of the steroid hormone biosynthesis was investigated *in vitro* [1]. Compound **5** bearing 3-hydroxyl function and triazole moiety fused to D-ring inhibited the 17 $\alpha$ -hydroxylase-C<sub>17,20</sub>-lyase enzyme considerably (IC<sub>50</sub> = 27 $\pm$ 7  $\mu$ M). Our results may be applied in the development of pharmacones to be used potentially in the pharmacotherapy of tumors of male and female reproductive tissues.



### Acknowledgements

The authors thank the Ministry of Education, Science and Technological Development of the Republic of Serbia (grant No.172021)

[1]. N. Szabó, J. Ajduković, E. Djurendić, M. Sakač, I. Ignáth, J. Gardi, G. Mahmoud, O. Klisurić, S. Jovanović-Šanta, K. Penov Gaši, M. Szécsi, Acta Biol Hung 66 (2015) 41.

## THE INFLUENCE OF ELECTRODE COMBINATIONS ON THE KINETICS REMOVAL OF ORGANIC SUBSTANCES FROM THE PRINTING EFFLUENT

Savka Adamović<sup>1</sup>, Miljana Prica<sup>1</sup>, Dragan Adamović<sup>1</sup>, Aleksandra Mihailović<sup>1</sup>,  
Božo Dalmacija<sup>2</sup>, Snežana Maletić<sup>2</sup>, Jelena Spasojević<sup>2</sup>

<sup>1</sup>University of Novi Sad, Faculty of Technical Sciences, Department of Graphic Engineering  
and Design, Trg Dositeja Obradovića 6, 21000 Novi Sad, Serbia

<sup>2</sup>University of Novi Sad, Faculty of Sciences, Trg Dositeja Obradovića 3, 21000 Novi Sad,  
Serbia

e-mail: miljana@uns.ac.rs

### Abstract

In this research, the electrocoagulation/flotation (ECF) reaction kinetics of organic substances removal from the waste fountain solution was investigated. The ECF reaction kinetics of the organic substances removal from the printing effluent can be described by a pseudo-second rate equation. Obtained results have shown that the trend of decrease in pseudo-second order constant for organic substances removal follows the trend of decrease in the efficiency of electrode combinations (Fe(-)/Al(+) > Al(-)/Fe(+) > Al(-)/Al(+) > Fe(-)/Fe(+)) and current density ( $8 > 4 > 2 \text{ mA cm}^{-2}$ ) of the ECF treatment.

**Key words:** Electrocoagulation/flotation, waste fountain solution, kinetics

### Introduction

The environment is, due to the technological development of the offset printing production, being faced with an extensive amount of printing waste and later with the problem of their disposal. The offset printing wastes may contain various inorganic and organic pollutants, potentially dangerous to the environment, which comes from dyes and pigments, fillers, stabilizers, varnishes, adhesives, etc. [1].

Sheet-fed offset printing process is based on the interaction of printing ink and fountain solution with the process materials. The fountain solution usually contains plate preservative agents, wetting agents, isopropyl alcohol or glycol-based surfactants, buffer substances, and antimicrobial additives [2]. After the printing process, the fountain solution changes its chemical composition due to direct contact with different printing materials (plates, inks, paper, etc.) and becomes enriched by metals, dust consisting of paper fibers and fillers, and organic compounds from printing inks and surface coated offset plates. Following current ecology standards, the offset printing effluents must be adequately treated before they are flushed into the sewage system or a natural recipient.

ECF technique has many advantages when compared to the conventional methods: easier operation, simpler equipment, lower retention time, better safety, selectivity, flexibility, cost effectiveness, and lower sludge production [3]. Also, ECF treatment has been an environmentally friendly process implemented to remove different types of pollutants (dyes, heavy metals, organic substances, etc.). The ECF process involves three successive stages [4]:

1. Production of coagulants in “in situ” by electrolytic oxidation of the sacrificial electrodes;

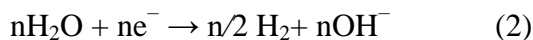
2. Destabilization of the contaminants or particulates suspension and breaking of emulsions by insoluble hydroxides;
3. Aggregation of destabilized phase and formation of flocs.

As well, the ECF process can be described as equations (1) - (3)[5, 6]:

At the anode:

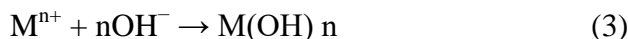


At the cathode:



Where M is the anode of aluminum or iron and n is the stoichiometric number of electrons within the oxidation or reduction reaction.

Soluble metal (Fe or Al) ions (produced at the anode) react with the hydroxide ions (formed at the cathode) and generated insoluble hydroxides (equation (3)) that adsorb the pollutants and eliminate them from the solution.



The literature shows that the kinetic studies of the ECF treated different types of wastewaters have been conducted in order to study the rate of removal of organic pollutants as well as the impact of the ECF operational variables (current density, interelectrode distance, etc.) on reaction rate constant [6, 7, 8, 9, 10].

In this paper, a kinetic study of the ECF treatment was performed to define the rate of removal of organic substances from the waste fountain solution. Also, the correlations between the reaction rate constant and electrode combinations were examined.

## Experimental

### *ECF treatment of waste fountain solution*

Four sets of the ECF experiments have been performed with different electrode combinations: (1) four iron electrodes (Fe(-)/Fe(+)), (2) four aluminum electrodes (Al(-)/Al(+)), (3) two aluminum (one was anode) and two iron electrodes (Al(-)/Fe(+)), and (4) two iron (one was anode) and two aluminum electrodes (Fe(-)/Al(+)). The electrodes were prepared appropriately to ensure electrode surface reproducibility. Before each run, the electrode surface has: (i) mechanically polished with abrasive paper, (ii) rinsed with deionized water, (iii) immersed for 10 min in a 5M solution of hydrochloric acid (35%), (iv) washed again with deionized water, (v) and dried [3].

The total area of electrodes is 100 cm<sup>2</sup> (the effective area being 40 cm<sup>2</sup>) and the gap between the electrodes is 0.5 cm. Electrodes are connected in a bipolar mode to a digital DC power supply (DF 1730LCD) equipped with potentiostatic or galvanostatic operational options. The ECF process was carried out at a current density of 2, 4 and 8 mA/cm<sup>2</sup>. The ECF unit is made of borsilicate glass with the volume of 250 cm<sup>3</sup>. 220 cm<sup>3</sup> of waste fountain solution has been stirred at 150 rpm by a magnetic stirrer (IKA color squid). 15 cm<sup>3</sup> of electrolyte samples have been taken at a particular operating time (1, 5, 10, 20, 40 and 60 minutes). All collected samples have been centrifuged for 10 minutes at 2000 rpm. Supernatant has then been used for

the analyses of organic substances quantities. The content of organic substances present in waste fountain solution is determined by measurement of UV<sub>326</sub> absorbance.

The UV<sub>326</sub> absorbance measurements of organic substances have been performed before and after the ECF treatment in accordance with standard methods [11] by UV-1800 SHIMADZU spectrophotometer at a wavelength of 326 nm with a 1 cm quartz cell.

*The kinetic study of the ECF treatment*

The reaction rate of organic substances removal from the waste printing effluent by applying the ECF treatment can be presented as an equation of the *n*-order rate (1) [6, 7]:

$$\frac{dC}{dt} = -k \cdot C^n \quad (1)$$

Where: *C* – content of organic substances, *n* - reaction order, *k* – reaction rate constant, and *t* – operational time of the ECF treatment. For the reactions of the pseudo-first and pseudo-second order of organic substances removal from the waste fountain solution by the ECF treatment, the equation (1) turns into equations (2) and (3), respectively, by integration:

$$\ln\left(\frac{C_t}{C_o}\right) = -k_1 \cdot t \quad (2)$$

$$\frac{1}{C_t} - \frac{1}{C_o} = k_2 \cdot t \quad (3)$$

Where: *C<sub>o</sub>* – the initial content (the absorbance at λ = 326 nm) of organic substances in the waste fountain solution before the ECF treatment, *C<sub>t</sub>* – content of organic substances in the waste fountain solution at a particular ECF time *t* (min), *k<sub>1</sub>* – reaction speed constant of the pseudo first-order rate (min<sup>-1</sup>), and *k<sub>2</sub>* – the pseudo second-order rate constant (min<sup>-1</sup>). The value of the constant *k<sub>1</sub>* is calculated from the slope of the plot of dependence *ln(C<sub>t</sub>/C<sub>o</sub>) = f(t)*. The slope of the plot of dependence *1/C<sub>t</sub> = f(t)* determines the constant *k<sub>2</sub>*.

**Results and discussion**

The rate of organic substances removal from the ECF treated waste fountain solution can be expressed by a pseudo-second order equation [9, 10]. The results obtained in the kinetic study point out that the pseudo-second order rate constants for organic substances removal with tested electrode combinations decrease as the efficiency of electrode combinations decreases: *k<sub>2</sub>* for Fe(-)/Al(+) > *k<sub>2</sub>* for Al(-)/Fe(+) > *k<sub>2</sub>* for Al(-)/Al(+) > *k<sub>2</sub>* for Fe(-)/Fe(+). It can also be seen that kinetic constants of pseudo-second order for organic substances removal follow the trend of decrease in organic substances removal efficiency with current density (8 > 4 > 2 mA cm<sup>-2</sup>) (Figure 1). According to the literature, [12, 13] data *k<sub>2</sub>* increases together with the increase in current density because by increasing the current density coagulant forming reaction rate is also increased, as well as the rate constant. Thus for the most efficient Fe(-)/Al(+) electrode combination, interelectrode distance of 0.5 cm and increase in current density from 2 to 8 mA cm<sup>-2</sup>, *k<sub>2</sub>* value for the removal of organic substances from the ECF-treated waste fountain solution are in the interval from 1,42 10<sup>-3</sup> to 1,53 10<sup>-3</sup> min<sup>-1</sup>. The dependences of the plot *ln(C<sub>t</sub>/C<sub>o</sub>) = f(t)* are linear with correlation coefficients R<sup>2</sup> at intervals:

from 0.95 to 0.98 for Fe(-)/Al(+), from 0.93 to 0.97 for Al(-)/Fe(+), from 0.94 to 0.97 for Al(-)/Al(+), and from 0.93 to 0.95 for Fe(-)/Fe(+) combinations of electrodes.

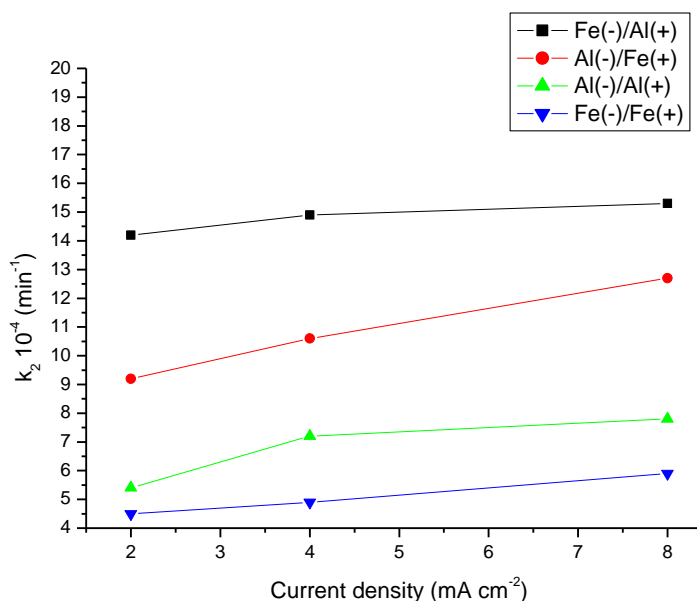


Figure 1. The pseudo second-order rate constant at current densities of 2, 4 and 8 mA cm<sup>-2</sup> (four electrode combinations and interelectrode distances of 0.5 cm)

## Conclusion

The rate of organic substances removal from the ECF-treated waste fountain solution can be expressed by a pseudo-second order equation. Also, the results obtained have shown that the trend of decrease in pseudo-second order rate constant for organic substances removal follows the trend of decrease in the efficiency of electrode combinations and current of the ECF treatment. Thus, for the highest ECF efficiency of the organic substances removal from the waste fountain solution under the best operational conditions (Fe(-)/Al(+), 8 mA cm<sup>-2</sup> and 0.5 cm) the highest ECF reaction pseudo-second order rate constant is also obtained.

## Acknowledgements

The authors acknowledge the financial support of the Ministry of Education, Science and Technological Development, Republic of Serbia (Grant No. III43005).

## References

- [1] S. Adamović, M. Prica, J. Radonić, M. Turk Sekulić, S. Pap, *Journal of Graphic Engineering and Design* 5 (2014) 9.
- [2] H. Kipphan, *Handbook of Print Media-Technologies and Production Methods*. Springer-Verlag, Berlin, Germany, 2001.
- [3] M. Prica, S. Adamovic, B. Dalmacija, Lj. Rajic, J. Trickovic, S. Rapajic, M. Becelic-Tomin, *Process Saf. Environ. Prot.* 94 (2015) 262.
- [4] A.S. Naje, S.A. Abbas, *Civil and Environmental Research* 3 (2013) 29.
- [5] A.S. Naje, S. Chelliapan, Z. Zakaria, S.A. Abbas, *Int. J. Electrochem. Sci.* 10 (2015) 5924.
- [6] A.K. Chopra, A.K. Sharma, *Appl. Water Sci.* 3 (2013) 125.
- [7] S. Kara, *Environ. Prog. Sustain. Energy* 32 (2012) 249.



- [8] I. Arslan-Alaton, I. Kabdaşlı, D., Hanbaba, E., Kuybu, J. Hazard. Mater. 150 (2008) 166.
- [9] Y. Ait Ouaisa, M., Chabani, A., Amrane, A., Bensmaili, J. Environ. Chem. Eng. 2 (2014) 177.
- [10] A.R. Yazdanbakhsh, M.R., Massoudinegad, S., Eliasi, A.S., Mohammadi, Journal of Water Process Engineering 6 (2015) 51.
- [11] AWWA–APHA–WEF, 1998. Standard Methods for the Examination of Water and Wastewater, 20th ed. American Public Health Association/American Water Works Association/Water Environment Federation, Washington, DC.
- [12] M. Al-Shannag, Z. Al-Qodah, K. Bani-Melhem, M. Rasool Qtaishat, M. Alkasrawi, Chem. Eng. J. 260 (2015) 749.
- [13] N. Balasubramanian, T., Kojima, C., Srinivasakannan, Chem. Eng. J. 155 (2009) 76.

## CHEESE – FACTS BETWEEN NUTRITION, HEALTH AND TRADITION

**Mirela Ahmadi<sup>1</sup>, Isabella Ciabrun<sup>2</sup>, Camelia Tulcan<sup>1</sup>, Oana Boldura<sup>1</sup>, Cornelia Milovanov<sup>3</sup> Dorel Dronca<sup>4</sup>, Florin Ciobanu<sup>2</sup>**

<sup>1</sup>Department of Biochemistry, Faculty of Veterinary Medicine, Banat's University of Agricultural Sciences and Veterinary Medicine „King Michael I of Romania“ from Timisoara (USAMVB), Calea Aradului 119, Timisoara – 300645, Romania

<sup>2</sup>S.C. Lactitalia S.R.L., Izvin, DN 6, Jud. Timis, Romania

<sup>3</sup>Department of Animal Husbandry, Faculty of Veterinary Medicine, USAMVB, Calea Aradului 119, Timisoara – 300645, Romania

<sup>4</sup>Department of Animal Genetic Improvement, Faculty of Animal Sciences and Biotechnology, USAMVB, Calea Aradului 119, Timisoara – 300645, Romania

e-mail: ddronca@animalsci-tm.ro

### Abstract

Nowadays, people are more and more interested by their health status, about their diet and are looking for healthy products, less processed, and with moderate content of lipids and salt. Thus, cheese is a traditional, healthy, and varied product - that can be produced from cow, ewe, goat, or buffalo milk, fresh or matured dairy product. The water, dry matter and lipid content are very important for maturation degree of cheese and for preservation time. Lipid and salt content is important for the taste, and for flavor – lipids being responsible for creamy sensorial characteristics. Thus, we analyzed some physico-chemical characteristics (water, dry matter, lipid, salt content, and also the ratio between lipids and dry matter) and some microbiological characteristics for four types of Italian cheese: Pecorino, Basky, Magra and Ricotta. Pecorino presented the lowest water content (32.53%) and highest salt content (5.14%), being a matured cheese (60-70 maturation days). Basky presented low water content (39.06%) and low salt content (2.36%), but 24.3% lipids, and 39.84 lipid / dry matter ratio. Magra is a non-matured cheese, with 50.19% water, with very low content of lipids (1.47%), with low lipid/dry matter ratio (2.67) and no salt, being indicated in different diets. Ricotta is a cheese with highest water content (67.22%), with moderate lipid content (13.9%), with very low salt content (0.91%), and high lipid/dry matter ratio (42.43). Microbiologic tests were performed for all four Italian cheese and the *E. coli*, and *Staphylococcus* were under the maximum limits (<10 *E. coli*; <100 *Staphylococcus*), while the *Listeria monocytogenes* was absent. This study tries to demonstrate that if we know very well the cheese products and our health status we can choose the best product, depending on the water, lipid and salt content of the cheese.

### Introduction

The tradition and nutritional facts of food are two very important challenge issues of the producers, consumers, and also of the government – considering the health status of people. Thus, cheese is a prehistoric technology to preserving the solid components from milk, being wide spread food product with great nutritive properties, made for consumption in all seasons. It can be salted or not, it can be soft pasta or hard, it can be short or long matured product, depending on the cheese technology specific for every cheese type (Hickey, 2017).

Cheese is a product rich in mature milk proteins, lipids, minerals (especially calcium), lipid-soluble vitamins; with low content of carbohydrates (mostly lactose) and hydro-soluble

vitamins. It has specific flavor, depending on milk type and technology – intended for all age. Cheese could be used as a base of probiotic and nutraceutical products. For example, Pecorino cheese was produced with ewe milk and encapsulated *Lactobacillus acidophilus*, and with a mix of *Bifidobacterium longum*, and *Bifidobacterium lactis*. The results presented a good correlation between enzymatic activity and water soluble nitrogen; and of enzymatic activity and protease-peptone. Also, there was recorded a higher content of conjugated linoleic acid in Pecorino cheese with encapsulated *Lactobacillus acidophilus* compared to Pecorino classic cheese and Pecorino cheese with encapsulated mix of *Bifidobacterium longum* and *B. lactis* (Santilo et al., 2012).

Cheese consumption is also depended of brand and caloric information from cheese label. Kevin and his collaborators tested the food consumption related with brand and also caloric information on favor perception and the results proved that low caloric cheese can easily lead to a “halo effect” with could lead to over-consumption in restrained eaters (Kevin et al., 2014). Also, a similar study was performed having in consideration the United States Food and Drug Administration aspects regarding the serving size. The results suggest that serving size could be increased due to Nutrition Facts written on the cheese label, which is reflected in higher consumption compared to the needs, and finally lead to health problems and even obesity (Dallas et al., 2015).

### **Experimental**

We comparative analyzed some physic-chemical parameters (water, lipid, dry matter, lipid/dry matter ration, salt content), and some microbiological test (*Escherichia coli*, *Staphylococcus*, *Listeria*, yeast and molds, for different cheese types. The cheese samples were collected from a milk plant from Timis County – West of Romania. We tested 10 different cheese samples of Pecorino, Baski, Magra, and Ricotta. The samples were collected in sterile containers and the analyses were performed in the laboratory of the milk plant. The humidity (water content) was tested using the analytic Sartorius thermo-balance, the lipid content was performed using Gerber method, titrimetric method for salt content and specific microbiologic culture medium were used for identification and quantification of mentioned microorganism. The results were statistically presented as average and standard deviation.

### **Results and discussion**

The results of our analysis are graphically presented in the figure 1. The physico-chemical characteristics presented for four types of Italian cheese are minimum analysis that any produces have to perform before comercial process. Humidity, dry matter and lipid content are parameters that define the maturation degree of cheese, and also is a quality index of commercial cheese.

The water and salt content are very important for preservation process. Usually hard cheese are perserved for a very long time, and there are some cheese products that have higher qualities if they are older (have long maturation). The salt content helps also in maturation and perservation process, but too much salt it is not healthy for human nutrition.

Water content varies very much due to the type of cheese. Thus, Picorino cheese is matured 60-70 days, so it is a hard cheese with long perservation time, while the Rocotta cheese is not matured cheese, is a soft cheese with a short perservation time. Lipid content is higher in Picorino cheese, and lowest in Magra cheese. So, Magra, Baski and Ricotta (from cow milk) cheese are products destined for low lipid diet. And also if we take in consideration the salt

content, we can say that these three cheese products are low caloric and low salt cheese good for children, athletes, and people with lipid and salt restriction.

Pecorino is a hard pasta cheese, matured, salted, and produced from ewe milk. It contains significant lipid quantities, and also cholesterol. It contains conjugated linoleic acid, known as  $\omega$ -6 polyunsaturated fatty acid. It contains valuable proteins, retinols, riboflavin, niacin, vitamin B12, calciferols, calcium, zinc and phosphorus (Santillo et al., 2014).

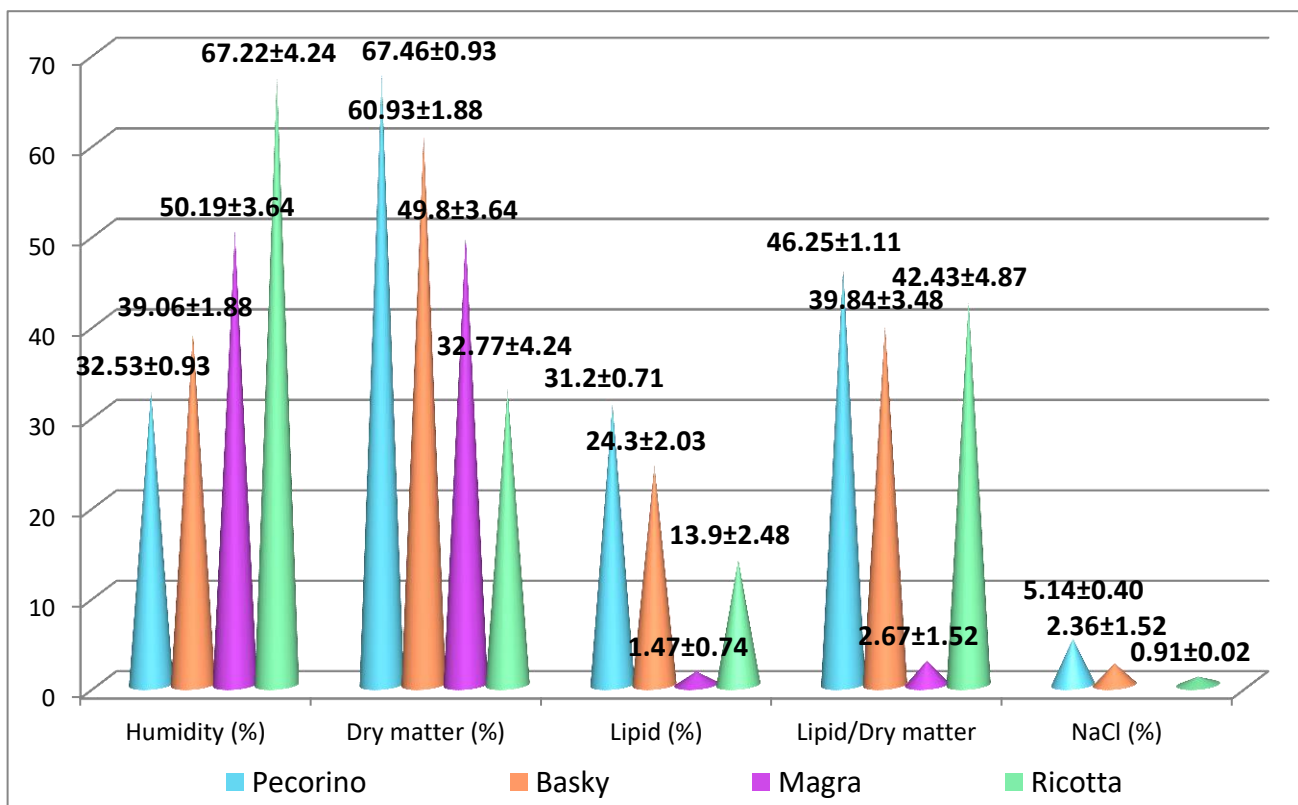


Figure 1. Physico-chemical characteristics of some Italian cheese

Ricotta is a soft pasta cheese, non-matured, low in lipids (contain also cholesterol), salt and calories. It is a very common product preferred by peoples with low caloric and salt restriction. It is low in carbohydrates, but rich in calcium, phosphorus, zinc, riboflavin, vitamin B12, and retinols (Carota et al., 2017).

Generally cheese is a valuable source of proteins, one slice of common cheese (approximate 25g) contain a similar quantity of protein from a glass of milk. The main protein from cheese is casein proteins, and the rest of proteic content is represented by valuable amino acids – with very good digestibility. The  $\alpha$ -casein – the main casein from milk and cheese, is known as promoter of lowering the blood pressure, increasing the absorption process of minerals in the digestive tract. The lipid content is varied very much being depending of the cheese type, brand, maturation process, and stage of maturation. Thus, the main carbohydrate from milk is lactose, but during the preparation or maturation process the lactose (disaccharide) can be broken down forming glucose and galactose (monosaccharides). Cheese is usually rich in minerals such as: calcium, sodium, phosphorus, selenium, zinc, and also rich in vitamins such

as: vitamin B12, riboflavin, retinols and calciferols (Cashman, 2002; Lancet, 2006; King, 2011; Rayman, 2012; Beulens et al., 2012; Calvo and Uribarri, 2013).

Due to its nutritional benefits and its composition, cheese is good for bone health, osteoporosis prevention, and heart health. However, because its lipid and salt content, but also due to lactose, cheese can be a food product hard tolerated or not recommended in some health situations or some population categories.

### **Conclusion**

Cheese are food products found in different types, matured stages, and brands – being characterized by varied nutritional composition and health benefits. Usually, hard pasta cheese, matured, like Pecorino, has low water, moderate lipid, and high salt content. Basky, Magra and Ricotta are cheese with soft pasta, moderate in lipids and salt, with exception of Basky for lipids.

Cheese consumption is a very good diet product, and if the consumers respect the normal size for consumption, the benefits of proteins and amino acids, lipids and fatty acids, minerals, and vitamins can be an alternative in diet and can be helpful for a better health status.

### **References**

- [1] J.W. Beulens, S.L. Booth, E.G. van den Heuvel, E. Stoecklin, A. Baka, C. Vermeer, *Br. J. Nutr.*, 110(8) (2013) 1357-68.
- [2] E. Carota, S. Crohnale, A. D'Annibale, A.M. Gallo, S.R. Stazi, M. Petruccioli, *Science of The Total Environment*, 584-585 (2017) 554-560.
- [3] M.S. Calvo, J. Uribarri, *Am. J. Clin. Nutr.* 98(1) (2013) 6-15.
- [4] K.D. Cashman, *Br. J. Nutr.* 87(Suppl 2) (2002) S169-77.
- [5] S.K. Dallas, J. Peggy, P. Liu, A. Ubel, *Appetite*, 95 (2015) 577-584.
- [6] M. Hickey, Chapter 30: Legislation in Relation to Cheese, in *Cheese – Chemistry, Physics and Microbiology* (P. McSweeney, P. Fox, P. Cotter, D. Everett – Editors), 4th edition, Academic Press, 2017, 757-778.
- [7] V. Kevin, B. Cavanagh, C. Kruja., A. Forestell, *Appetite*, 82 (2014) 1-7.
- [8] J.C. King, *Am. J. Clin. Nutr.* 94(2) (2011) 679S-84S.
- [9] M.P. Rayman, *The Lancet*, 379(9822) (2012) 1256-1268.
- [10] E. Reynolds *Lancet Neurol.*, 5(11) (2006) 949-60.
- [11] A. Santillo, M. Albenzio, A. Bevilacqua, M.R. Corbo, A. Sevi, *Journal of Dairy Science*, 95(7) (2012), 3489-3500.
- [12] A. Santillo, A.B. Bevilacqua, M.R. Corbo, A. Sevi, M. Sinigaglia, M. Albenzio, *Innovative Food Science and Emerging Technologies*, 26 (2014) 389-396.

## HYDROTHERMAL SYNTHESIS OF HYDROXYAPATITE WITH TARTARIC ACID

**Alexandra Ioana Bucur, Raul Alin Bucur, Zoltan Szabadai, Cristina Mosoarca, Petrica  
Andrei Linul, Corina Orha**

*National Institute for Research-Development in Electrochemistry and Condensed Matter  
Timișoara, No. 144 Dr A. Păunescu Podeanu Str, Timișoara 300569, Romania  
e-mail: alexandra.i.bucur@gmail.com*

### **Abstract**

The hydrothermal synthesis of hydroxyapatite (HA) with addition of tartaric acid (TA) is presented in the paper. The role of tartaric acid is to form a complex with the Ca ions and to help in tailoring the crystallization behavior of hydroxyapatite. A comparison is made between two situations: one is characterized by the addition of tartaric acid after the precipitation of hydroxyapatite, and the other is defined by tartaric acid being added to the Ca precursor, followed by the addition of the P precursor. The crystalline particles resulted were studied by means of XRD, FTIR, SEM and TEM, and it was concluded that they consist in hexagonal lamellar crystals with lengths < 200 nm and widths < 50 nm. The difference between the two cases is that the crystallinity degree, the uniformity in crystal dimensions and the aspect ratio are higher when TA was added before the precipitation rather than to the precipitated HA. The dimensions of the achieved crystals are similar to the mineral grains found in the hard tissues of the human body.

### **Introduction**

Synthetic hydroxyapatite represents a widely used biocompatible and bioactive material for human implants [1], due to its similarity with the natural hydroxyapatite (HA,  $\text{Ca}_{10}(\text{PO}_4)_6(\text{OH})_2$ ), which is present in a high amount in the hard tissues of the human body. HA has been synthesized by a variety of methods like precipitation, hydrolysis, sol-gel, solid state reactions, etc [2]; among these methods, in recent years, the hydrothermal method has gained an increasingly important role due to a series of advantages, one of them being the fact that the properties of the final product, such as: crystallinity degree, morphology and size of particles [3], can be tailored.

A different approach in modeling the properties of HA ceramic powders is the addition of some conditioners, such as organic acids. It has been reported that the addition of organic acids, like citric acid, ascorbic acid, tartaric acid, etc, will have an inhibitory effect on the crystallization of HA [4,5], probably due to the attachment of the organic ions to the active growing sites of the newly-formed nuclei. The presumed chemical mechanism (described by us in [6] ) implies the complexation of the metallic ions by the organic ions and lowering the number of active Ca sites onto the crystal seeds; as a result of this inhibition, particles with higher aspect ratio are expected to form.

The purpose of the present work was the use of a small concentration of tartaric acid in order to study its influence on the hydrothermal synthesis of hydroxyapatite, when it is added in different stages of the synthesis process, in a neutral environment. In our knowledge, no studies of hydrothermal synthesis of HA with organic acids have been presented in the literature.



## Experimental

The chemicals used for the synthesis are  $\text{Ca}(\text{NO}_3)_2 \cdot 4\text{H}_2\text{O}$  (Sigma-Aldrich) as Ca precursor,  $(\text{NH}_4)_2\text{HPO}_4$  (Merck) as P precursor and racemic tartaric acid (TA)  $\text{C}_4\text{H}_6\text{O}_6$  (Merck), all brought to 0.05M solutions. Aliquots were used so as to maintain the molar ratio of 1.66 between the Ca and P (because this is the stoichiometric ratio of hydroxyapatite), while the tartaric acid molar ratio is 1.25 in relationship to phosphorus.

In order to establish what is the best stage to add the tartaric acid, this was added either after the HA precipitation, or between the mixing of the two precursors. For the first sample (named HA\_T\_1), the P precursor was added to the Ca precursor and then the tartaric acid was mixed with the solution, while for the second sample (named HA\_T\_2), the tartaric acid was mixed with Ca, then the P precursor was added. The pH value was maintained around 7 by ammonia addition.

After the admixture of the reactants and HA precipitation, the solution + precipitate were closed in Teflon liners are heated at  $220^\circ\text{C}$  for 24 h. After cooling to room temperature, the samples were extracted and washed about 6 times with double distilled water, then dried in the oven at  $60^\circ\text{C}$  for 4 h.

The physico-chemical characterization of the synthesized samples was achieved using the equipments:

- XRD – PANalytical X'Pert Pro MPD Diffractometer equipped with a Cu anode and PixCEL detector, powder samples supported on zero background silicone holders, working parameters: 45 kV, 30 mA
- FT-IR: Vertex 70 Spectrometer from Bruker, within the range  $4000\text{--}400\text{ cm}^{-1}$  with a  $4\text{ cm}^{-1}$  resolution, using transmission technique. For sample preparation, the KBr pressed disc technique was used, mixing approx. 1 mg of each sample with 200 mg KBr. The discs were introduced in the spectrometer immediately, in order to minimize the amount of absorbed water
- SEM: Inspect S (FEI Company); powder samples were supported on carbon tape
- TEM: Titan G2 80–200 (FEI Company), accelerating voltage: 200 kV. Samples were prepared by depositing a droplet of suspension (ethylic alcohol) on 200 mesh copper grids covered with lacey carbon film.

## Results and discussion

The XRD patterns for the two samples are presented in Figure 1:

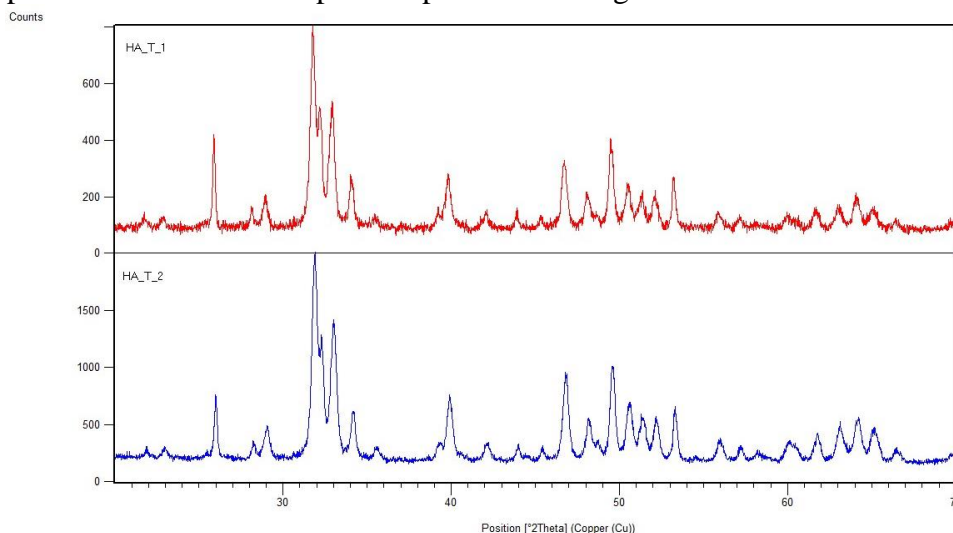




Fig 1 The XRD patterns of the samples HA\_T\_1 and HA\_T\_2

The patterns present the regular lines of crystalline hydroxyapatite, confirming the identity of the synthesized samples. No other crystalline phase is present in the synthesis products. By comparing the intensity of the peaks, it can be noticed that when TA was added after the HA precipitation, the final product is less crystalline than the sample achieved by adding TA to the Ca precursor. Preferential orientation in respect to the *c* crystallographic direction can be observed for the sample HA\_T\_1.

The FT-IR patterns are presented in Figure 2 and confirm the formation of hydroxyapatite, without other calcium phosphates being present. The characteristic vibrational domains are [7]:  $\nu_1$  (around  $950\text{ cm}^{-1}$ ),  $\nu_2$  ( $400\text{--}470\text{ cm}^{-1}$ ),  $\nu_3$  ( $1000\text{--}1150\text{ cm}^{-1}$ ) and  $\nu_4$  ( $500\text{--}620\text{ cm}^{-1}$ ). The broad absorption band at around  $3400\text{ cm}^{-1}$  and the band at  $1630\text{ cm}^{-1}$  are characteristic for the adsorbed water molecules, and the sharp band at  $3570\text{ cm}^{-1}$  represent the free OH anions present in the crystalline lattice. The sharp band in the region  $1379\text{--}1384\text{ cm}^{-1}$  does not belong to HA and is assigned to the deformation vibration of the C-O bond [8], suggesting the adhesion of the tartrate ion to the HA crystals. This adhesion phenomenon is present in both studied cases and is in agreement with the results of other research groups, as mentioned before.

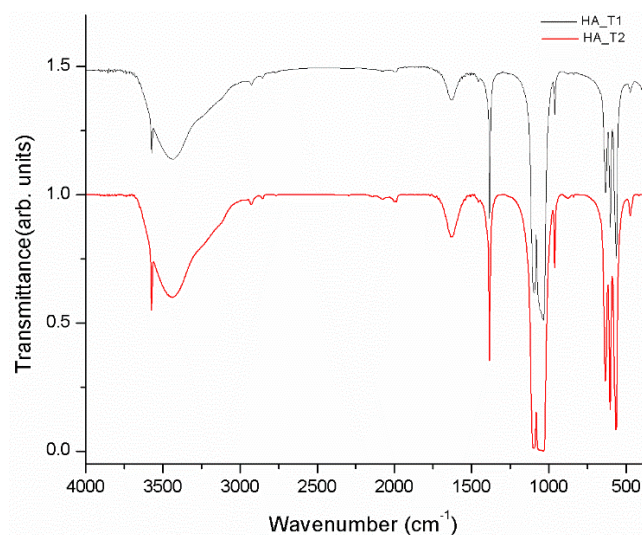


Fig 2 FT-IR patterns of the two HA samples

The morphology of the prepared HA samples was studied by SEM, the images being presented in Figure 3. The both samples present a high degree of compactness; not much information is available due to this agglomeration, so samples were analyzed by TEM (Figure 4). It can be observed in the TEM images that the crystalline particles are lamellar in shape, but the lamellas are not rectangle-shaped. Instead, a deformed hexagonal shape can be observed, with unequal sides. Regarding the size of the crystals, the two samples have similar dimensions, namely lengths of less than 200 nm and widths of less than 50 nm. The sample HA\_T\_2 seem to be more uniform regarding the shape and dimensions of the crystals, compared to the sample HA\_T\_1, and the aspect ratio appears to be better for the sample prepared with TA added to the Ca precursor.

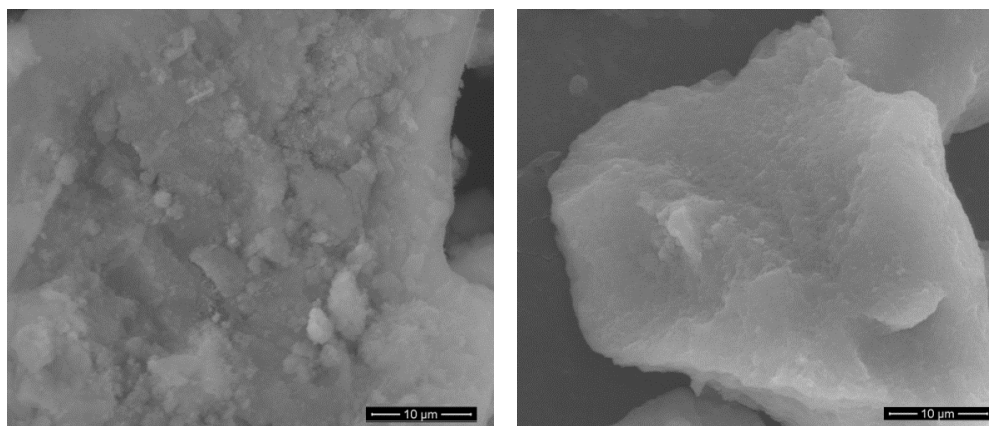


Fig 3 SEM images of the samples: left – HA\_T\_1; right – HA\_T\_2

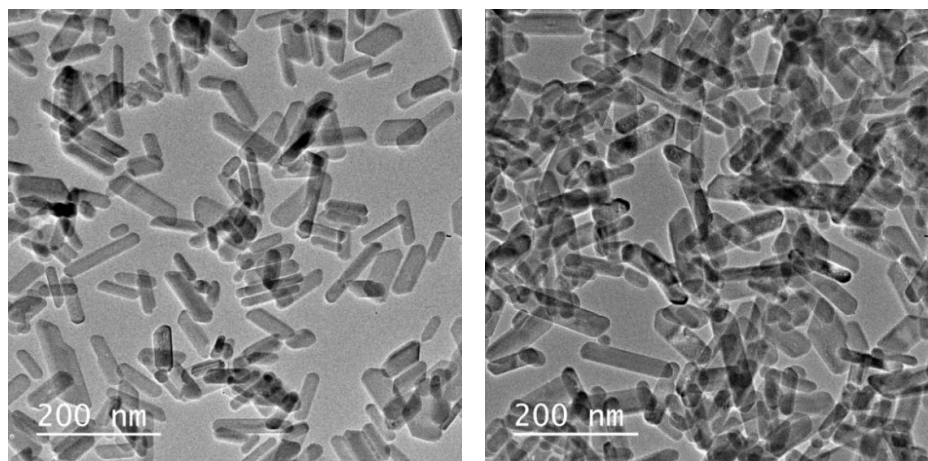


Fig 4 TEM images of the samples: left – HA\_T\_1; right – HA\_T\_2

## Conclusion

Hexagonal lamellas of crystalline hydroxyapatite were synthesized by aqueous precipitation in neutral environment and crystallization by hydrothermal method at 220°C for 24h. Tartaric acid was added either after the HA precipitation or between the mixing of the Ca and P precursors. The formation of a complex between the tartrate ions and the Ca ions has resulted in a more crystalline hydroxyapatite, with more uniform particles shape and dimensions, compared with the crystalline particles achieved when tartaric acid was added after the precipitation of the HA. The dimensions of the achieved crystals are similar to the mineral grains found in the hard tissues of the human body.

## References

- [1]N. Puvvada, P.K. Panigrahi, A. Pathak, *Nanoscale*. 2 (2010) 2631–8
- [2]S. Koutsopoulos, *J. Biomed. Mater. Res.* 62 (2002) 600–12
- [3]H.S. Gupta, F. Guitia, *Cryst. Growth Des.* 9 (2009) 466–474.
- [4]William P. Inskeep, Jeffrey C. Silvertooth, *Soil Sci. Soc. Am. J.* 52941-946. 52 (1988) 941–946.
- [5]J.A.M. Van Der Houwen, E. Valsami-Jones, *Environ. Technol.* 22 (2001) 1325–1335
- [6]R.A.B. Alexandra Ioana Bucur, , Zoltan Szabadai, Cristina Mosoarca, Petrica Andrei Linul, *Mater. Charact.* 132 (2017) 76–82.

- [7]C. Rey, C. Combes, C. Drouet, H. Sfihi, A. Barroug, Mater. Sci. Eng. C. 27 (2007) 198–205
- [8]B. Fu, Q. Shen, W. Qian, Y. Zeng, X. Sun, M. Hannig, J. Mater. Sci. Mater. Med. 16 (2005) 827–831

**ANTIOXIDANT ACTIVITY AND PHOTOCHROMIC PROPERTIES OF 2,6-BIS(2,4-DIHYDROXYBENZYLIDENE)CYCLOHEXANONE**

**Livia Deveseleanu-Corici<sup>1</sup>, Daniela Haidu<sup>1</sup>, Elisabeta I. Szerb<sup>1</sup>, Ramona Tudose, Otilia Costisor<sup>1</sup>, Liliana Cseh<sup>1</sup>**

<sup>1</sup>*Institute of Chemistry Timisoara of Romanian Academy, 24 Mihai Viteazul Bvd., 300223 Timisoara, Romania  
e-mail: lili\_cseh@yahoo.com*

**Abstract**

Xanthylium derivatives have attracted considerable interest due to their potential health effects and replacement of synthetic pigments. Moreover, these type of compounds exhibit versatile photochromic properties by switching from a variety of colors when submitted to external stimuli (light, temperature, pH). Generally, all these compounds hold the same xanthylium core and follow the same pH-dependent network of reversible chemical reactions as structurally related families such as flavylium [1-4].

In the present study we focused the attention on the isolation and characterisation of of the species involved in the network of chemical reactions of 2,6-bis(2,4-dihydroxybenzylidene)cyclohexanone. The pH-dependent photochromic behavior of the xanthylium derivative has been investigated. In order to identify the species, the NMR spectra were recorded in acidic and basic media. The antioxidant activity was also determined using DPPH assay [5]. The IC<sub>50</sub> values of radical scavenging activity for DPPH were found to be 133.68 µg/mL.

**Acknowledgements**

The authors acknowledge the support of the Romanian Academy, Project 4.1.

**References**

- [1]. F. Pina, M. J. Melo, C.A.T. Laia, A.J. Parola, J.C. Lima, Chem. Soc. Rev. 41 (2012) 869.
- [2]. A.M. Diniz, C. Pinheiro, V. Petrov, A.J. Parola, F. Pina, Chem. Eur. J. 17 (2011) 6359.
- [3]. A.M. Pana, V. Badea, R. Banica, A. Bora, Z. Dudas, L. Cseh, O. Costisor, Photochem. Photobiol. A: Chem. 283 (2014) 22.
- [4]. L.N. Corici, S. Shova, V. Badea, D. Aparaschivei, O. Costisor, L. Cseh, Photochem. Photobiol. Sci. 16 (2017) 946.
- [5]. P. Gurumoorthy, A.K. Rahiman, Med. Chem. Res. 24 (2015) 2441.

## OBTAINING IRON OXIDES BY FeII-Na<sub>4</sub>EDTA DECOMPOSITION

Marius Chirita<sup>1,\*</sup>, Liviu Mocanu<sup>1</sup>

<sup>1</sup>National Institute for Research and Development in Electrochemistry and Condensed Matter, Timisoara, Plautius Andronescu Str. No. 1, RO-300224, Timisoara, Romania

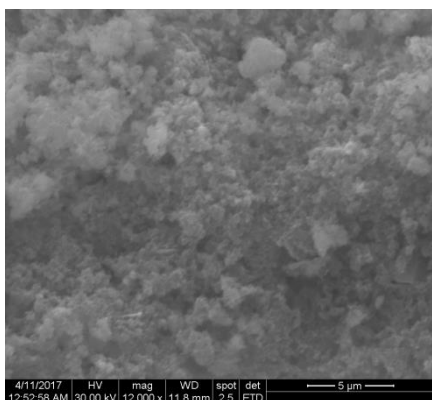
\*Corresponding author: chirifz@gmail.com

Topic: Condensed Matter Physics

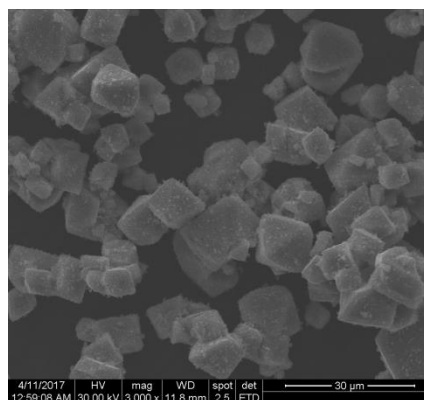
Type of contribution: Poster presentation

Continuing our previous studies [1,2] about hydrothermal decomposition of the Fe(III)-EDTA complex, the present experimental procedure is focused on the hydrothermal decomposition of the Fe(II)-EDTA complex in the presence of urea. Maintaining unchanged the concentration for the precursors at 230°C, we investigated the kinetics of phase transitions between 1,5 hours and 84 hours of high pressure-temperature treatment time.

Nanometric and micrometric magnetite were obtained between 1,5 and 48 hours of high pressure-temperature treatment time. Between 48 and 84 hours of high pressure-temperature treatment time, a mixture of micrometric magnetite and iron carbonate were obtained.



(a)



(b)

Figure 1: SEM Images of nanometric. (a) and micrometric(b) magnetite

**Keywords:** crystal structure, surface structure, nanomaterials, micromaterials.

### References:

- [1] M. Chirita, R. Banica, A. Ieta, A. Bucur, P. Sfirloaga, D. H. Ursu, and I. Grozescu, "Highly Crystalline FeCO<sub>3</sub> Microparticle Synthesis by Hydrothermal Decomposition of Fe-EDTA Complex." American Institute of Physics Conf Proceedings, vol. 1262/2010: 124.
- [2] M. Chirita, R. Banica, P. Sfarloaga, A. Ieta, I. Grozescu, "A short route of micrometric magnetite synthesis via Fe-EDTA thermal decomposition." IEEE Conf Proc 11-13 Oct. 2010, ISBN 978-1-4244-5781-6, pp. 391-394.

ECO-FRIENDLY MICROWAVE-ASSISTED SYNTHESIS OF  
BIOLOGICALLY ACTIVE NAPHTHENIC ACID *N*-CYCLOHEXYL AMIDES

**Bojana Vasiljević<sup>1</sup>, Ljubica Grbović<sup>1</sup>, Ksenija Pavlović<sup>1</sup>, Mirjana Popsavin<sup>1</sup>, Slavko Kevrešan<sup>2</sup>, Vera Ćirin-Novta<sup>1</sup>**

<sup>1</sup>University of Novi Sad, Faculty of Sciences, Department of Chemistry, Biochemistry and Environmental Protection, Trg Dositeja Obradovića 3, 21 000 Novi Sad, Serbia

<sup>2</sup>University of Novi Sad, Faculty of Agriculture, Trg Dositeja Obradovića 8, 21 000 Novi Sad, Serbia

e-mail: bojana.vasiljevic@dh.uns.ac.rs

### Abstract

Inside the framework of green chemistry, a noticeable results were obtained in microwave-assisted solvent-free synthesis of biologically active *N*-cyclohexyl amides of naphthenic acids (NAs). Naphthenic acid amides were synthesized directly from free carboxylic acids in the absence of solvent and catalyst. Synthesized *N*-cyclohexyl amides of naphthenic acid were evaluated for their auxin activity.

### Introduction

The stable and polar amide functionality is an important unit among the organic molecules present in natural-occurring materials (e.g., peptides and proteins). It is also found in many synthetic substances as intermediates or as active pharmaceutical products or prodrugs [1]. Due to its interest in organic synthesis, the preparation of amides from the corresponding amines is an important and well-known transformation, but the main drawbacks of these reactions are long reaction time, low yield, use of organic solvents and expensive or toxic reagents [2,3,4].

Over the last years, a large number of publications have clearly shown that many types of chemical transformations can be carried out successfully under microwave irradiation [5]. Most importantly, microwave processing frequently leads to dramatically reduced reaction times, higher yields, easier work-up matching with the goal of green chemistry, atom economy, and selectivity of reactions. In addition to their wide application, utilization of microwave technology in the amide solvent-free synthesis is not frequently described in the literature [6,7,8].

Napthenic acids (NAs) represent a complex mixture of alkyl-substituted aliphatic and cyclic monocarboxylic acids of the general formula  $C_nH_{2n-z}O_2$ , where  $n$  is the number of carbon atoms and  $z$  the hydrogen deficiency due to ring formation, obtained from oil and oil derivatives by alkaline extraction. In addition to a wide application in the chemical industry, these compounds exhibit biological activity. Low concentrations (up to 0.5 mg/L) of NAs and their salts have been studied for a long time as substances exhibiting biological activity, such as plant growth hormones [9,10] but at high concentrations (above 50 mg/L), NAs are corrosive and toxic substances [11] and for these reasons they represent serious contaminants of refinery wastewaters and act as environmental pollutants.

Having in mind the nature of naphthenic acids and amide group as an important functionality due to its presence in great number of biomolecules, the aim of the present work was to designed simple, eco-friendly method of forming biologically active amide derivatives of naphthenic acids by using microwave irradiation.



## Experimental

The Velebit naphthenic acids (VNA) were extracted from the atmospheric gas oil fraction (distillation interval 168-290 °C) of Vojvodina crude oil [10].

All reagents and solvents were obtained from commercial suppliers and used without further purification, as well as Aldrich naphthenic acids (ANA). Microwave-assisted reactions were carried out in CEM Discover BenchMate single-mode microwave reactor. Reactions were monitored by thin layer chromatography (TLC) on silica gel plates (Silica gel 60 F<sub>254</sub>). Purification of products was carried out by flash column chromatography using Kieselgel 60 (0.040–0.063, Merck). NMR spectra were recorded on a Bruker AC 250 E instrument.

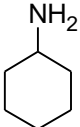
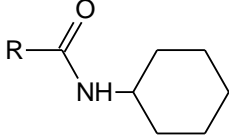
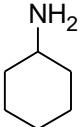
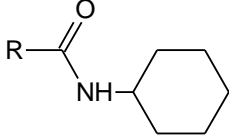
Microwave-assisted synthesis of naphthenic acid *N*-cyclohexyl amides were carried in a 10 mL Pyrex reaction vial. A mixture of NAs (5 mmol) and amine (5 mmol) was heated at 270 °C for 2 min of microwave irradiation with stirring. Upon cooling to 45 °C the reaction mixture was dissolved in CH<sub>2</sub>Cl<sub>2</sub> and washed with 1 M HCl, 5% NaHCO<sub>3</sub> and H<sub>2</sub>O. After removing the solvent with rotavapor, the residue was purified by flash column chromatography on silica gel (dichloromethane:ethyl acetate=9.5:0.5) to afford the pure product **1** (1.40 g, 78%) and **2** (1.27 g, 78%) as a yellow oil.

The auxin activity of the amides was determined by the test of inhibition of white mustard (*Sinapis alba*) germination based on counting the germinated seeds after treatment with VNK, ANK and naphthenic acid *N*-cyclohexyl amides solution (**1** and **2**, 10<sup>-5</sup>-10<sup>-7</sup> M) and the corresponding concentrations of 3-indoleacetic acid (IAA, 10<sup>-5</sup>-10<sup>-7</sup> M). The experiments were repeated two times. Germination was performed in dark, under the temperature of 25 °C for 24h. The results are presented as mean value ± standard deviation.

## Results and discussion

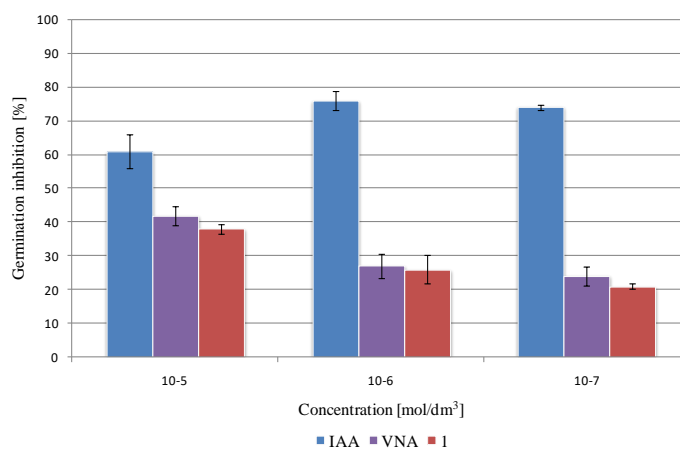
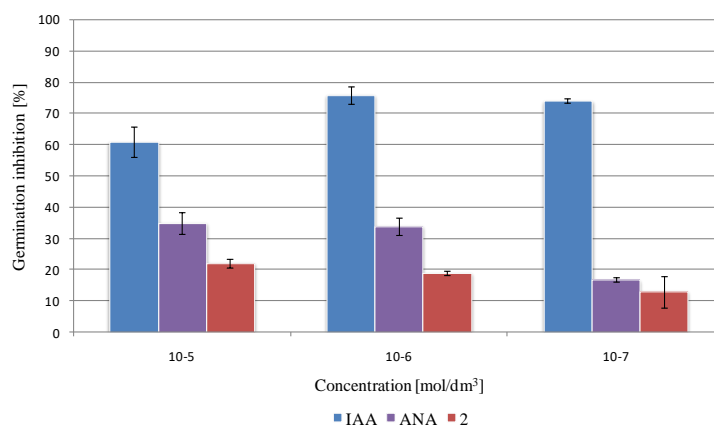
Napthenic acids (NAs), complex mixture of carboxylic acids isolated from middle and higher fractions of the Vojvodina crude oil Velebit and commercial Aldrich naphthenic acids, reacted efficiently with cyclohexylamine under high-temperature heating in closed-vessel system of microwave reactor. The maximal operative temperature for these reaction systems was 270 °C. Microwave-assisted synthesis of NA amides was completed in 2 minutes of microwave irradiation leading to a 78% of isolated yield (Table 1).

**Table 1.** Microwave-assisted synthesis of Velebit (VNA) and Aldrich (ANA) naphthenic acid *N*-cyclohexyl amides

Entry	NAs	Amine	Product ( <b>1/2</b> )	Yield (%)
1	VNA			78
2	ANA			78

The study of biological activity of the type of the plant hormones auxin are presented in Figure 1 and 2. Since the rooting occurs in the presence of plant hormones as it is indol-3-acetic acid, a natural auxin, it has been used as control.



Figure 1. Auxin activity of VNA and their *N*-cyclohexyl amidesFigure 2. Auxin activity of ANA and their *N*-cyclohexyl amides

Based on the test of inhibition of germination (higher inhibition - higher auxin activity) of white mustard it is obvious that NAs Velebit and Aldrich showed somewhat lower auxin activity which corresponds to an IAA concentration of  $10^{-5}$  M. The lowest auxin activity was exhibited by the concentration of  $10^{-7}$  M.

As is evident from Figure 1 and 2, the treatment of white mustard seeds with NA *N*-cyclohexyl amides (**1** and **2**) caused lower inhibition of germination, which may be a result of an activity similar to that of plant hormones of the auxin-type.

### Conclusion

In conclusion, directly from non-activated carboxylic acids and amines and in the absence of coupling reagents and solvents, NA *N*-cyclohexyl amides were successfully synthesized under microwave irradiation. Starting from the equimolar mixture (atom-economical synthesis) of amine and complex mixture of NAs, high yields of NA *N*-cyclohexyl amides were obtained. Biological activity studies of NAs and synthesized amide derivatives as stimulators of plant growth revealed their auxin activity but the chemical transformation of carboxylic functional group didn't lead to increasing of germination inhibition.

### **Acknowledgements**

This study was supported by the Ministry of Science and Technological Development of the Republic of Serbia, Project No. 172006.

### **References**

1. E. Valeur, M. Bradley, *Chem. Soc. Reviews*, 38 (2009) 606-631.
2. L. Perreux, A. Loupy, *Tetrahedron* 57 (2001) 9199.
3. L. Perreux, A. Loupy, M. Delmotte, *Tetrahedron* 59 (2003) 2185.
4. J. Vaughan, R. L. Osato, *J. Am. Chem. Soc.* 73 (1951) 5553.
5. P. Lidstrom, J. P. Tierney, *Microwave-Assisted Organic Synthesis*, Blackwell Publishing, Oxford, 2005.
6. L. J. Gooßen, D. M. Ohlmann, P. P. Lange, *Synthesis* 1 (2009) 160.
7. L. Perreux,; A. Loupy, F. Volatron, *Tetrahedron* 58 (2002) 2155.
8. E. Gelens, L. Smeets, L. A. J. M. Sliedregt, B. J. van Steen, C. G. Kruse, R. Leurs, R. V. A. Orru, *Tetrahedron Lett.* 46 (2005) 3751.
9. J. Severson, *Phytochemistry* 11 (1972) 71.
10. Lj. Grbović, K. Pavlović, B. Prekodravac, K. Kuhajda, S. Kevrešan, M. Popsavin, J. Milić, V. Ćirin-Novta, *J. Serb. Chem. Soc.* 77 (2012) 147.
11. J.A. Brient, P.J. Wessner, M.N. Doyle, *Kirk-Othmer Encyclopedia of Chemical Technology Naphthenic acids*, John Wiley and Sons, New York, 1995.

***Bacillus* spp. AS POTENTIAL BIOCONTROL AGENTS OF BACTERIAL SPOT ON PEPPER CAUSED BY *Xanthomonas euvesicatoria***

**Dragana Bjelić<sup>1</sup>, Maja Ignjatov<sup>1</sup>, Maja Karaman<sup>2</sup>, Suzana Jovanović-Šanta<sup>3</sup>, Jelena Marinković<sup>1</sup>, Dunja Rakić<sup>2</sup>, , Zorica Nikolić<sup>1</sup>**

<sup>1</sup>*Institute of Field and Vegetable Crops, 21000 Novi Sad, Maksima Gorkog 30, Serbia*

<sup>2</sup>*University of Novi Sad Faculty of Sciences, Department of Biology and Ecology, Trg Dositeja Obradovića 2, 21000 Novi Sad Serbia*

<sup>3</sup>*University of Novi Sad Faculty of Sciences, Department of Chemistry, Biochemistry and Environmental protection, Trg Dositeja Obradovića 3, 21000 Novi Sad, Serbia*  
*e-mail: dragana.bjelic@nsseme.com*

**Abstract**

The objective of this research was to identify bacterial spot-causing pathogen and bacterial antagonists for management of the disease using biocontrol agents as environmentally friendly alternatives. Isolates of *Bacillus* spp. were obtained from the soil samples collected at different localities in Serbia. Antibacterial activity of natural antagonists toward the pathogen isolated from infected pepper leaves was examined using a modified well-diffusion assay and standard germination test. Our results confirmed the presence of *Xanthomonas euvesicatoria* as the causal agent of bacterial spot of pepper. Screening of 32 *Bacillus* spp. isolates for antibacterial activity showed that 8 isolates inhibit growth of examined *X. euvesicatoria* isolates. Four isolates identified as *Bacillus subtilis* exhibited the highest antibacterial activity by *in vitro* test (from 5 to 14 mm inhibition zone of bacterial growth). The isolates positively influenced germination of pepper seeds, causing up to 16% and 70% increase in germination and germination viability compared to control seeds infected with pathogen. The most effective isolates of *Bacillus subtilis* could be used as potential biocontrol agents of bacterial spot of pepper.

**Introduction**

Bacterial spot of pepper (*Capsicum annuum* L.) caused by *Xanthomonas* is one of the most damaging diseases resulting in direct economic loss [1]. The symptoms of bacterial spot infection are characterized by smaller lesions with yellow haloes which coalesce into larger ones and occur on leaves, stems, and fruits. Infection leads to germination decrease, leaf necrosis, complete defoliation and destruction of the crop. Bacterial spot-causing xanthomonads were reclassified into 4 species: *X. euvesicatoria*, *X. vesicatoria*, *X. perforans*, and *X. gardneri* [2]. The most common causative pathogen of bacterial spot on pepper plants listed in Serbia is *X. euvesicatoria*, while intensity of the infection depends on environmental conditions [3].

Chemical measures applied in order to prevent the recurrence of bacterial infection do not often provide satisfactory results in maintaining a low level of bacterial flora. Intensive application of synthetic pesticides became an increasing concern, primarily due to toxic chemical residues in food products, frequent environmental pollution and the development of resistant strains of pathogens [4]. Environmentally-friendly alternatives to pesticide such as application of beneficial microorganisms which inhibit the growth of pathogens and prevent the disease they cause, have been developed as a new strategy for biological control of soil-borne diseases [5].

*Bacillus* spp. are frequently found in soils and exert antagonistic activities against several fungal and bacterial pathogens [6]. The ability of forming endospores allows them to survive in different environmental conditions and facilitates the formulation of biocontrol preparations [7]. *Bacillus*-based biopesticides contain strains which have the ability to colonize rhizosphere, promote plant growth and inhibit pathogen growth through various mechanisms [8]. Among these, *Bacillus subtilis*, *B. licheniformis*, *B. pumilus* and *B. amyloliquefaciens* are the most effective species in controlling plant diseases.

The objective of this research was to identify antagonistic *Bacillus* spp. strains for management of the bacterial spot of pepper.

## Experimental

### Isolation of antagonist

Different soil samples were randomly collected from various parts of Serbia. Soil sample collection included the rhizosphere of plants, agricultural and non-agricultural soils. Isolation of bacteria from the soil was done using the serial dilution and streak-plate techniques. Soil dilutions were prepared with 1 g of each soil sample suspended in 9 mL of 0.85% NaCl in sterile test tubes. A 0.1 ml aliquot of each dilution ( $10^{-3}$ - $10^{-6}$ ) was spread aseptically on nutrient agar (NA) (HiMedia Lab. Pvt. Ltd., Mumbai, India) and incubated at 30°C for 24 h. Round colonies, with entire or wavy margins, cream to light yellow and medium size, were recultivated five times to obtain pure cultures of *Bacillus* spp.

### Isolation of pathogen

Isolation of the pathogen was made from infected pepper leaves showing typical bacterial spot lesions. Symptomatic leaves were rinsed with sterile water three times and then dried on a sterile filter paper under aseptic conditions. Small pieces of infected leaf tissues were macerated in sterile water, and the resulting suspension was streak-plated on nutrient agar (NA). After incubation at 27°C for 3–5 days, round, small, yellow and slimy colonies, with entire margins were purified by subculturing. For the evaluation of pathogenicity of isolates, bacterial suspensions ( $10^6$ /ml) were sprayed on pepper seedlings and bacterial spot symptoms were observed 3 weeks post-inoculation.

### Molecular species identification

*Bacillus* and *Xanthomonas* isolates for DNA extraction were grown on NA plates for 24 h. DNA was extracted using a DNeasy Mini Kit (QIAGEN Inc., Hilden, Germany), according to the manufacturer's recommendations. For the amplification of 16S rDNA gene fragments of *Bacillus* isolates, universal primers fd1 (27F) (AGAGTTTGATCMTGGCTCAG) and rP3 (1492R) (TACGGYTACCTTGTTACGACTT) were used [9]. The target DNA gene fragments of *Xanthomonas* isolates, were amplified using primers xeF (CATGAAGAACTCGGCGTATCG) and xeR (GTCCGACATAGTGGACACATAC) [10]. The polymerase chain reaction (PCR) was done in 25- $\mu$ l aliquots using S-thermal cycler (Eppendorf, Germany). Amplicons were electrophoresed in 1.5% agarose gel (Invitrogen) with ethidium bromide. Purification and sequencing of the PCR-amplified DNA fragments was done in the company MACROGEN, Seoul, South Korea (<http://dna.macrogen.com>). FinchTV Version 1.4.0. was used for sequence analysis, and nucleotide sequences were compared with the GenBank Database at the National Center for Biotechnology Information (NCBI).

### **Antibacterial activity assay**

Antibacterial activity of *Bacillus* spp. against *Xanthomonas* was determined by modified well-diffusion assay [11]. *Bacillus* and *Xanthomonas* isolates were cultured for 24 h in nutrient broth (NB), at optimal temperature of 28°C. Petri dishes with NA solid medium were poured with 6 ml of soft NA<sub>7</sub> medium (the same medium, but with half amount of agar), previously inoculated with 60 µL of the pathogen culture (10<sup>6</sup>/ml). The wells (R = 5 mm) were made in the medium using sterile bottom parts of the 200 µL pipette tips. Well-diffusion assay was completed by adding tested culture of *Bacillus* spp. (10<sup>8</sup>/ml) into the well in the volume of 50 µL. Assay was done in three repetitions for each bacterial isolate. The plates were incubated overnight at 28°C. Antibacterial activity was detected by measuring the zone of inhibition from the edge of the well and expressed in mm.

### **Germination test**

The effect of antagonistic bacteria *Bacillus* spp. on germination of pepper seeds infected by *Xanthomonas* was examined using a standard germination test [12]. Seed of pepper cultivar “Amfora” developed at the Institute of Field and Vegetable Crops in Novi Sad was used for test. Seeds were surface disinfested in 2% sodium hypochlorite (NaOCl, Sigma) for 2 to 3 min, rinsed with sterile distilled water four times, and then dried on sterile filter paper under aseptic conditions. Inoculation of seeds was performed with 5 mL of pathogen suspension (10<sup>6</sup>/ml) and 5 mL of antagonist suspension (10<sup>8</sup>/ml). Control seeds were inoculated with 10 mL of pathogen suspension. Treated seeds were placed in Petri dishes (R = 140 mm), while moisturized filter paper was used as the medium. Germination was tested in a germination chamber at alternating temperature of 20- 30°C. Four replicates × 100 seeds were tested. Seed germination and germination viability were determined after 7 and 14 days.

### **Statistical analysis**

Data was subjected to analysis of variance (ANOVA) using software STATISTICA 12.6 (Statsoft, Tulsa, Oklahoma, USA). Means were separated using Tukey’s HSD (honest significant difference) test at the  $P < 0.05$  level.

### **Results and discussion**

This study confirmed that 8 out of the 32 isolates of *Bacillus* spp. from the soil were found positive for antibacterial activity against two isolates of *Xanthomonas* (X6, X18) by *in vitro* test (Table 1).

Table 1. Antibacterial activity of *Bacillus* spp. against *Xanthomonas*

Pathogen vs. Antagonist	X6	X18
	Inhibition (mm)	
B2	1.67 e	2.33 ef
B3	2.33 de	3.00 e
B5	11.33 a	14.33 a
B7	9.00 ab	10.67 b
B11	0.00 e	0.67 f
B13	5.00 cd	6.00 d
B23	2.00 e	4.33 de
B32	7.67 bc	8.33 c
Average	4.87 B	6.21 A

Values with different lowercase/capital letters within the same column/row differ significantly ( $P < 0.05$ ). Values are the means of 3 replicates.

On average, *Bacillus* spp. isolates exhibited higher antibacterial activity against X18. The highest antagonistic activity was exhibited by isolates B5 and B7, followed by isolates B13 and B32. Isolates B2, B3, B11 and B23 had the least antagonistic effect on tested pathogens. Four of the best performing isolates (B5, B7, B13, B32) were selected for further assessment of their effect on germination of pepper seeds infected with pathogen (Table 2). *Bacillus* isolates positively influenced the germination of pepper seeds treated with *Xanthomonas*, and the effect varied depending on the examined isolate of antagonist and pathogen. The highest antibacterial activity against the pathogen X6 was observed using B5 isolate (16% and 34% increase in germination and germination viability), while B32 exhibited the highest antagonistic effect on X18 (14% and 70% increase in germination and germination viability). Isolate B7 also had good antagonistic potential, while the least effect was obtained by B13. Higher antagonistic effect on germination parameters was exhibited by pepper seeds treated with Xe18. These results are in agreement with *in vitro* testing of antibacterial activity.

Table 2. Effect of *Bacillus* on germination of pepper seeds infected with *Xanthomonas*

Pathogen vs. Antagonist	X6	X18	X6	X18
	Germination viability (%)		Germination (%)	
Control (Pathogen)	39.00 c	35.25 c	79.00 d	83.25 d
B5	52.25 a	58.00 a	91.25 a	93.00 b
B7	49.50 a	59.25 a	89.25 b	92.00 b
B13	43.50 b	49.00 b	88.00 bc	87.25 c
B32	45.75 b	59.75 a	87.00 c	95.25 a
Average	47.75 B	56.50 A	88.87 B	91.87 A

Values with different lowercase/capital letters within the same column/row differ significantly ( $P < 0.05$ ). Values are the means of 4 replicates.

By comparing the sequences with the Genbank Database at NCBI, antagonistic isolates were identified as *Bacillus safensis* (B2), *Bacillus pumilus* (B3, B11, B23), and *Bacillus subtilis* (B5, B7, B13, B32) (Table 3), while pathogen isolates were identified as *Xanthomonas euvesicatoria* (X6, X18) (Table 4).

Table 3. Isolates of *Bacillus* spp. from soil

Isolate code	Isolation source	<i>Bacillus</i> species	NCBI
B2	Non-agricultural soil	<i>Bacillus safensis</i>	KU953932
B3	Rhizosphere (wheat)	<i>Bacillus pumilus</i>	KU953923
B5	Rhizosphere (sunflower)	<i>Bacillus subtilis</i>	KU953925
B7	Rhizosphere (maize)	<i>Bacillus subtilis</i>	KU953927
B11	Non-agricultural soil	<i>Bacillus pumilus</i>	KU953931
B13	Rhizosphere (maize)	<i>Bacillus subtilis</i>	KX444639
B23	Rhizosphere (wheat)	<i>Bacillus pumilus</i>	KX444649
B32	Non-agricultural soil	<i>Bacillus subtilis</i>	KX766373

Table 4. Isolates of *Xanthomonas euvesicatoria* from infected pepper leaves

Isolate code	Isolation source	<i>Xanthomonas</i> species	NCBI
X6	Pepper cv. Slonovo uvo	<i>Xanthomonas euvesicatoria</i>	KX512832
X18	Pepper cv. Palanačka bela	<i>Xanthomonas euvesicatoria</i>	KX512834

In general, the highest antagonistic activity toward this important bacterial plant pathogen was observed in *Bacillus subtilis* isolates, while B5, B7 and B32 were the best natural antagonists among them. The mechanisms of this antibacterial effect are uncertain, although it is known that *B. subtilis* can produce a variety of antimicrobial agents, including a broad spectrum of lipopeptides, such as surfactins, iturins and fengycins [13]. Similarly, Dimkić et al. [14] showed very strong inhibition of *Xanthomonas arboricola* by *Bacillus*, while Berić et al. [15] found that 104 out of 203 *Bacillus* isolates exhibit an antagonistic effect on *Xanthomonas oryzae* pv. *oryzae*. Since there is insufficient experimental confirmation on using *Bacillus* in biocontrol of *Xanthomonas*, especially against *X. euvesicatoria*, further research will be of great importance.

### Conclusion

Based on our results, indigenous *Bacillus subtilis* isolates from soil generally had good antagonistic potential for biological control of bacterial spot of pepper caused by *Xanthomonas euvesicatoria*. Further selection of these isolates through *in planta* antagonistic testing will be necessary in order to determine their efficacy in inhibition of pathogen growth and suppression of disease under greenhouse and field conditions.

### Acknowledgements

This research was supported by the Ministry of Education, Science and Technological Development of the Republic of Serbia, projects: TR31030 and TR31072.

### References

- [1] M.S. Kyeon, S.H. Son, Y.H. Noh, Y.E. Kim, H.I. Lee, J.S. Cha, Plant Pathol. J. 32 (2016) 431.
- [2] J.B. Jones, G.H. Lacy, H. Bouzar, R.E. Stall, N.W. Schaad, Syst. Appl. Microbiol. 27 (2004) 755.



- [3] M. Ignjatov, K. Gašić, M. Ivanović, M. Šević, A. Obradović, M. Milošević, *Pestic. Phytomed.* 25 (2010) 139.
- [4] M.W. Aktar, D. Sengupta, A. Chowdhury, *Interdiscip. Toxicol.* 2 (2009) 1.
- [5] G. Berg, *Appl. Microbiol. Biotechnol.* 84 (2009) 11.
- [6] R. Borriss, in: D.K. Maheshwari (Ed.), *Bacteria in Agrobiolology: Plant Growth Responses*, Springer, Berlin, 2011, pp. 41.
- [7] A. Pérez-García, D. Romero, A. de Vicente, *Curr Opin Biotechnol.* 22 (2011) 187.
- [8] I. Francis, M. Holsters, D. Vereecke, *Environ Microbiol.* 1 (2010) 1.
- [9] W.G. Weisburg, S.M. Barns, D.A. Pelletier, D.J. Lane, *J. Bacteriol.* 173 (1991) 697.
- [10] H. Koenraad, B. van Betteray, R. Germain, G. Hiddink, J.B. Jones, J. Oosterhof, *Acta Hortic.* 808 (2009) 99.
- [11] L. Harris, A. Daeshemi, M.E. Stiles, T.R. Klaenhammer, *J. Food Protect.* 52 (1989) 384.
- [12] ISTA, *International Rules for Seed Testing*, International Seed Testing Association, Switzerland, 2016.
- [13] H.P. Bais, R. Fall, J.M. Vivanco, *Plant Physiol.* 134 (2004) 307.
- [14] I. Dimkić, S. Živković, T. Berić, Ž. Ivanović, V. Gavrilović, S. Stanković, Đ. Fira, *Biol. Control.* 65 (2013) 312.
- [15] T. Berić, M. Kojić, S. Stanković, Lj. Topisirović, G. Degrassi, M. Myers, V. Venturi, Đ. Fira, *Food Technol. Biotechnol.* 50 (2012) 25.

## HYDROXYAPATITE COATINGS ON TI SUBSTRATES BY SIMULTANEOUS PRECIPITATION AND ELECTRODEPOSITION

**Bogdan-Ovidiu Taranu, Alexandra Ioana Bucur, Paula Svera,  
Corina Orha, Andrei Racu**

*National Institute for Research and Development in Electrochemistry and Condensed Matter,  
Dr. A. Paunescu Podeanu Street, No. 144, 300569, Timisoara, Romania  
e-mail: b.taranu84@gmail.com*

### **Abstract**

This paper presents the results obtained by analyzing hydroxyapatite (HA) coatings electrodeposited onto titanium plates. Instead of using a solution containing both calcium and phosphorus ions, the present approach starts with just one precursor in the electrolysis cell, and the other precursor is being added while an electrochemical potential of -1500 mV is simultaneously applied. By alternating the order of precursor addition, the Ti substrate surface was modified and the differences were evidenced using XRD, SEM, Raman and AFM. For all samples, needle-like crystals of HA grouped as hemispheres on the substrate surface. There is no significant difference, regarding morphology and hemisphere size, between the samples prepared at 1h deposition time, regardless of the precursor addition order; by contrast, the sample deposited for 4h presented a higher density.

### **Introduction**

The properties of HA, such as its chemical composition and crystal structure, bearing close similarity to the mineral component in human bones and teeth, together with its excellent biocompatibility, make it one of the most suitable implant materials used in orthopedics and dentistry. However, in terms of mechanical properties HA has low strength and high brittleness, which make it unsuitable for use as load bearing implant [1]. Because of this, HA is being used as coating material for metallic implants, such as titanium [2]. Many methods have been developed for depositing HA coatings on metal substrates, including the electrochemical deposition method, having several advantages such as a good stoichiometric ratio [3]. When using this method, the regular approach is to prepare the electrolyte solution so that it contains both calcium and phosphorus ions [4]. In the present work, the electrochemical deposition of HA on Ti substrates started with just one precursor in the electrolysis cell, while the second was added gradually with the simultaneous application of a -1500 mV electrochemical potential.

### **Experimental**

Analytical grade calcium nitrate tetrahydrate  $\text{Ca}(\text{NO}_3)_2 \cdot 4\text{H}_2\text{O}$  (Sigma Aldrich) as 1.75 mM solution and diammonium phosphate  $(\text{NH}_4)_2\text{HPO}_4$  (Merck) as 1.05 mM solution were used as Ca and P precursors, respectively. The Ca:P molar ratio between the solutions was 1.67, corresponding to stoichiometric HA. Bidistilled water was used for all experiments.

Titanium discs of 1 cm in diameter were cut from an as-received pure titanium plate. The discs were polished using SiC sandpaper of different grit sizes and a felt with alumina paste, washed with industrial soap solution and bidistilled water and placed in ethanol/acetone mixture 50:50 for 30 minutes in an ultrasonic bath. Before the experiments the discs were rinsed with bidistilled water and dried.

The electrochemical setup consisted in a PGZ 301 potentiostat, 3 electrodes and a glass cell with heating mantle connected to a thermostat set at 80°C. The titanium discs were used as cathode, after being inserted in a Teflon support (active surface = 0.28 cm<sup>2</sup>). The anode was a Pt plate (active surface = 0.8 cm<sup>2</sup>) and the reference electrode was the Ag/AgCl (sat. KCl) electrode.

50 mL of one precursor was placed inside the glass cell, then, the dropwise addition of the second precursor started simultaneously with the chronopotentiometric experiment. The parameters used for the electrodeposition of HA on the Ti discs and the nature of the added precursor are presented in Table 1.

Table 1. Synthesis parameters for HA samples obtained through electrochemical deposition

Sample name	Temperature (°C)	Time (h)	E (mV)	Added precursor
HAe1	80	1	-1500	P
HAe2	80	4	-1500	P
HAe3	80	1	-1500	Ca

The HA modified Ti discs were studied using various characterization techniques. X-ray diffraction patterns were recorded using a PANalytical X'Pert Pro MPD Diffractometer with Cu anode, working parameters 45 kV and 30 mA.

Images of the samples were obtained using a Phillips Inspect S scanning electron microscope. The discs were fixed with double adhesive tape on the SEM holders.

Atomic force microscopy was performed on a MultiView 2000 scanner from Nanonics Imaging Ltd., in intermittent mode, using 20 nm radius tip. The same platform was used in combination with the proper module for recording Raman spectra (excitation wavelength was 514 nm).

### Results and discussion

The XRD patterns of the three samples are presented in Figure 1. In all three cases, the formation of crystalline HA is confirmed, the standard reflections being evidenced in comparison to the 00-009-0432 JCPDS file. The crystallinity degree improves as the deposition time increases (A and B spectra). By adding the Ca precursor to the P precursor (C spectrum), the crystallinity degree improves even more. A strong preferential orientation along the c crystallographic axis can be observed, an effect which is more obvious for the samples deposited within 1h. In case of the sample deposited within 4h, the crystallographic plane (211) presents a higher intensity.

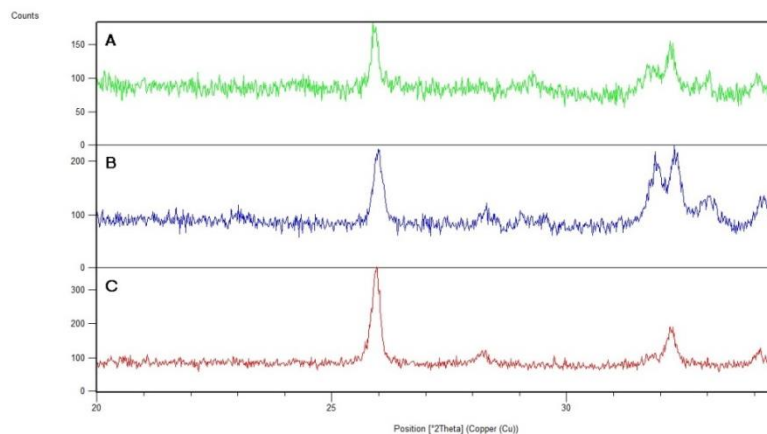


Figure 1. XRD patterns of the samples: A = HAe1, B = HAe2 and C = HAe3

The Raman shift spectra of the HAe3 sample is presented in Figure 2. The very strong peak corresponding to the  $\text{PO}_4$   $\nu_1$  vibration at  $961\text{ cm}^{-1}$ , characteristic for HA [5], can be observed in this case as well. Other indications that the electrodeposited material is HA are the weakly defined peaks observed in the areas  $430\text{--}450\text{ cm}^{-1}$  and  $580\text{--}600\text{ cm}^{-1}$ , characteristic for HA doubly and triply degenerated bending modes of the  $\text{PO}_4$  group.

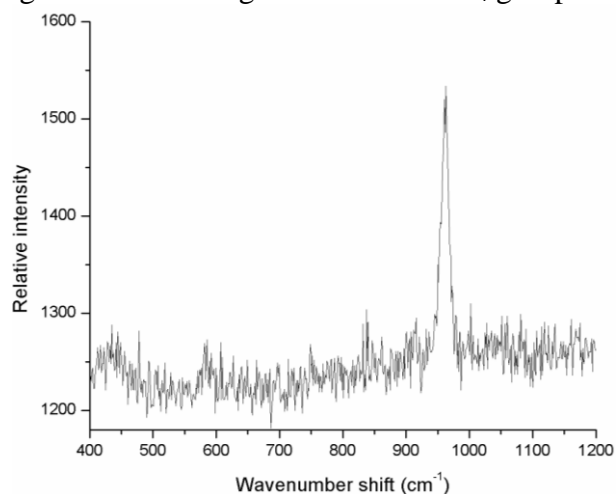


Figure 2. Raman shift spectra of the HAe3 sample

SEM images recorded for the three samples are presented in Figure 3. Sample HAe1 consists of micrometric needle-like crystals with spherical arrangement, displaying lengths of less than  $5\text{ }\mu\text{m}$ .

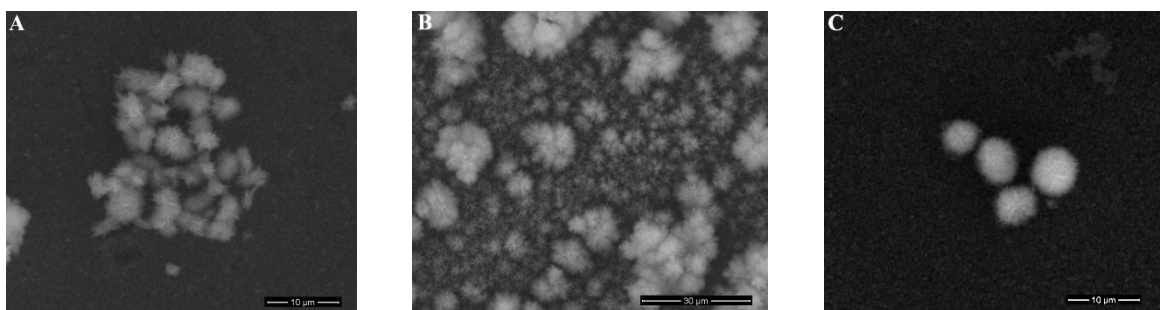


Figure 3. SEM images of the samples: A = HAe1, B = HAe2, C = HAe3

By comparison, sample HAe2 shows the same structure and arrangement of the crystals, the difference being that the number of crystals forming the spherical arrangements is higher in this case. Furthermore, due to the increased deposition time, the amount of deposited HA is larger and its distribution more uniform.

The image of the HAe3 sample shows structures similar to the ones of the HAe1 sample, but the spherical arrangements are slightly larger and better defined. The crystal dimensions of the third sample are similar to the crystal dimensions of the first one, but the crystallinity degree is higher. Because of this, it can be presumed that adding the Ca precursor to the P precursor leads to more satisfactory results.

The AFM images of the three samples are presented in Figure 4. The maps of the HAe1 and HAe3 samples are 10x10  $\mu\text{m}^2$ , while the map of the HAe2 sample is 50x50  $\mu\text{m}^2$  because in this case the deposited material was much thicker and attempts to acquire maps with higher resolution failed. As expected from deposition time and SEM observations, maps A and C are similar, displaying likewise characteristics, with hemispheres as large as 2  $\mu\text{m}$ . The same morphological characteristics can be seen in image B, but the structures are more densely packed, as a result of prolonged deposition time. Completing these information with the SEM data, it can be concluded that the electrochemically-controlled crystalline growth of the HA particles led to the formation of hemispheres attached to the Ti substrate.

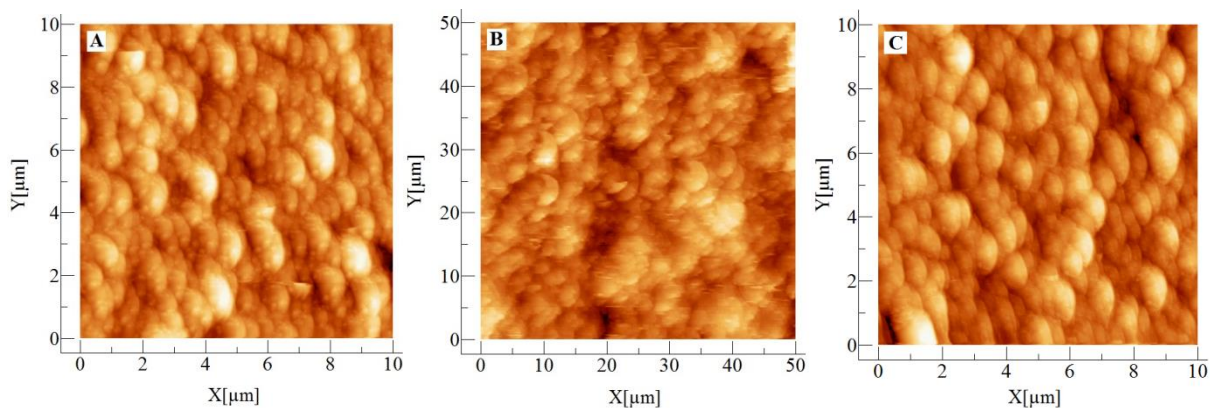


Figure 4. AFM images of the samples: A = HAe1, B = HAe2, C = HAe3

Table 2 shows the values calculated from AFM data. The presented values are: average roughness (Sa), root mean square roughness (Sq), maximum peak height (Sp), maximum valley depth (Sv), maximum peak to valley height (Sy), surface kurtosis (Sku), surface skewness (Ssk).

Table 2. Values obtained from AFM analysis

Sample name	Sa (nm)	Sq (nm)	Sp (nm)	Sv (nm)	Sy (nm)	Sku	Ssk
HAe1	51.88	65.81	252.56	-233.47	486.03	3.29	0.37
HAe2	282.30	355.20	1605	-1277.8	2882.8	3.08	0.10
HAe3	51.58	65.58	269.76	-219.26	489.02	3.3	0.35

The parameters values are similar for the HAe1 and HAe3 samples, which is to be expected, considering the observations previously presented (SEM and AFM). The values for the HAe2

sample cannot be compared to the values of the other two samples because the image had to be recorded on a larger surface.

### **Conclusion**

Electrochemical deposition of HA on Ti substrates was successfully achieved in a novel manner, by adding just one precursor in the electrolysis cell, while the second precursor was added simultaneously with an applied electrochemical potential.

The samples prepared by reversing the order of precursor addition (HAe1 and HAe3 from Table 1) were analyzed using various physico-chemical methods, which revealed no significant morphological differences, but an increase in the crystallinity degree in case of the HAe3 sample. Both samples consist in hemispherical formations composed of needle-like crystals of HA, attached to the Ti surface.

The same methods were employed for the HAe2 sample, prepared the same way as HAe1, but with longer deposition time (4h, compared to 1h), and they indicated a denser deposition layer with similar morphology.

Future research will be directed towards improving the characteristics of the deposited material, aiming at higher degrees of uniformity, homogeneity and crystallinity, suitable for medical applications.

### **References**

- [1] W. Suchanek, M. Yoshimura, J. Mater. Res. 13 (1998) 94.
- [2] A.T. Rad, M. Solati-Hashjin, N.A.A. Osman, S. Faghihi, Ceram. Int. 40 (2014) 12681.
- [3] P. Ducheyne, S. Radin, M. Henghebaert, J.C. Henghebaert, Biomaterials 11 (1990) 244.
- [4] W. Ye, X.-X. Wang, Key Eng. Mater. 330-332 (2007) 601.
- [5] S. Koutsopoulos, J Biomed Mater Res. 62 (2002) 600.



## PRELIMINARY TLC STUDIES ON POSIDONIA OCEANICA SEAGRASS

**Loreta-Andrea Bozin<sup>1</sup>, Mihai-Cosmin Pascariu<sup>2,3</sup>, Alina Georgescu<sup>1</sup>, Georgeta Simu<sup>1†</sup>,  
Anca Dragomirescu<sup>1</sup>, Eugen Sisu<sup>1\*</sup>**

<sup>1</sup>“Victor Babeş” University of Medicine and Pharmacy of Timișoara, 2 Eftimie Murgu Sq.,  
RO-300041 Timișoara, Romania

<sup>2</sup>National Institute of Research & Development for Electrochemistry and Condensed Matter –  
INCEMC Timișoara, 144 Dr. Aurel Păunescu-Podeanu, RO-300569 Timișoara, Romania

<sup>3</sup>“Vasile Goldiș” Western University of Arad, 86 Liviu Rebreanu, RO-310414 Arad, Romania

<sup>†</sup>Deceased in 2017

e-mail: sisueugen@umft.ro

### Abstract

Several photosynthetic pigments, i.e. chlorophylls and carotenoids, belonging to *Posidonia oceanica* seagrass, were separated by thin-layer chromatography (TLC) using a hexane/acetone solvent mixture. Additionally, densitometric measurements and spectral scanning of the TLC plates were performed using the Camag TLC Scanner 3 together with the WinCATS software.

### Introduction

The use of several species of marine magnoliophytes, with the purpose of monitoring and managing the coastal ecosystems, was frequently discussed during recent years. Because of their wide geographical distribution, their longevity, the permanence of their populations during the seasons, the ease of sampling, their abundance, and their ability to concentrate a wide range of xenobiotics, marine magnoliophytes appear as very interesting organisms in the context of environmental monitoring. Among the many studies of magnoliophytes, *Posidonia oceanica* (Fam. *Posidoniaceae*) appears of particular interest.



Figure 1. *Posidonia oceanica* on the Tunisian coast



In the Mediterranean Sea, the *Posidonia oceanica* meadow is a powerful integrator of the overall quality of marine waters [1-3]. Very widely distributed throughout the coastline, which is particularly “receptive” to pollution, and connected to the sea bottom, it indicates by its presence and vitality (or its regression materialized by dead ecosystems) the quality of the water that drifts above it.

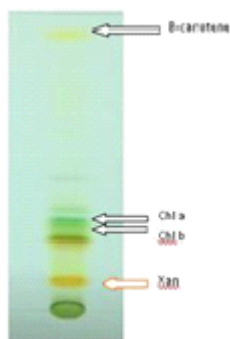
This paper represents a preliminary study regarding the chemical composition of *Posidonia oceanica* leaves. We first determine the optimal thin-layer chromatography (TLC) eluent which allows the separation of a maximum number of components, i.e. photosynthetic pigments [4-6]. In the second step, an identification of the isolated pigments was attempted by using UV/Vis densitometry directly on the TLC plate.

### Experimental

The sample was collected from the Tunisian coast during May 2017. After harvesting, the sample was washed with tap water for several times, was dried and preserved on ice (-28 °C) for further processing. 50 g of seagrass were processed using a blender and extracted in methanol for 24 h using a Soxhlet. Next, the sample was filtered and the solvent was removed using a rotary evaporator. The evaporated sample was redissolved in methanol by stirring for a couple of minutes, and then placed on the TLC plate (10 by 10 cm TLC Silica gel 60F<sub>254</sub> from Merck). The plate was eluted in a developing chamber with a mobile phase composed of a hexane/acetone mixture (70:30 v/v). After drying in an oven, the densitometric evaluation of the TLC plate was performed using the CAMAG TLC Scanner 3.

### Results and discussion

The TLC plate (Fig. 2) was scanned in the 200–700 nm spectral region. Most peaks were revealed at 250 nm (11 peaks) and only a few were found at 700 nm (4 peaks). Fig. 3a shows the overlaid chromatograms obtained at various wavelengths, while the densitogram at 450 nm is illustrated in Fig. 3b. The major photosynthetic pigments identified in *Posidonia oceanica* with the  $R_f$  and the corresponding maximum absorbance are shown in table 1.



Substance	$R_f$	Spectral data (nm)
Chlorophyll a	0.42	426, 662
Chlorophyll b	0.32	453, 643
β-carotene	0.81	451, 478
Xanthophyll	0.31	421, 667

Figure 2. TLC plate with Table 1. The major photosynthetic pigments identified in *Posidonia the identified pigments oceanica* extract

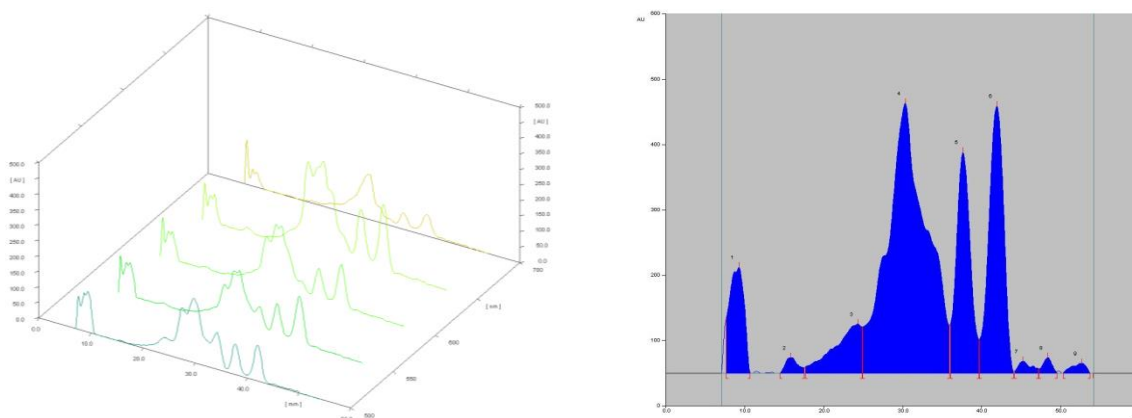


Figure 3. (a) Overlaid densitograms at various wavelengths of photosynthetic pigments, and (b) densitogram of detected peaks at 450 nm

Chlorophylls *a* and *b* (green photosynthetic pigments) are characterized by two absorption bands, located in the blue-violet and, respectively, red region of the visible domain (UV domain not shown here). Carotenoids are revealed as yellow or orange pigments. The migration of photosynthetic pigments was compared with standard samples under the same experimental conditions.

### Conclusion

The densitometric analysis at different wavelengths, which reveals the presence of several peaks corresponding to various photosynthetic pigments, represents a starting point towards a more thorough chemical analysis of components found in *Posidonia oceanica*.

### References

- [1] H. Augier, *Vie marine* 7 (1985) 85.
- [2] H. Augier, G. Gilles, G. Ramonda, in: *International Workshop on Posidonia Oceanica beds*. C.F. Boudouresque, A. Jeudy de Grissac, J. Olivier (eds.), GIS Posidonie publ., France, 1, 1984, p. 399-406.
- [3] L. Tunesi, C.F. Boudouresque, in: *Préservation et conservation des herbiers à Posidonia Oceanica*. C.F. Boudouresque, G. Bernard, P. Bonhomme, E. Charbonnel, G. Diviaco, A. Meinez, G. Pergent, C. Pergent-Martini, S. Ruitton, L. Tunesi (eds.), RAMOGE pub., France, 32-47.
- [4] S.W. Jeffrey, R.F.C. Mantoura, S.W. Wright (eds.), *Phytoplankton pigments in oceanography: guidelines to modern methods*, Paris: Unesco Publishing, 1997.
- [5] R.G. Barlow, D.G. Cummings, S.W. Gibb, *Mar. Ecol. Prog. Ser.* 161 (1997) 303.
- [6] M. Hegazi, A. Perez-Ruzafa, L. Almela, M.-E. Candela, *J. Chromatogr. A*, 829 (1998) 153.

## PHASE TRANSITIONS IN LEAD FREE PIEZOELECTRIC MATERIALS

**Bucur Raul Alin, Farkas Iuliana, Bucur Alexandra Ioana**

*National Institute for Research and Development in Electrochemistry and Condensed Matter,  
Condensed Matter Department, No. 1 Plautius Andronescu, 300224 Timisoara, Romania.  
e-mail: raul\_alin\_bucur@yahoo.com*

### **Abstract**

(K<sub>0.5</sub>Na<sub>0.5</sub>)NbO<sub>3</sub> doped with 1 mol% SmBO<sub>3</sub> (where B= Al, Co, Cr, Fe, Mn) ceramics were obtained through solid state method in air. The refinement of the unit cell reveals a shift from orthorhombic to tetragonal crystalline structure at room temperature, for KNN-SmMnO<sub>3</sub>, KNN-SmFeO<sub>3</sub> and KNN-SmCrO<sub>3</sub>. The variation of the dielectric constant at different frequencies shows an increase of almost one order of magnitude for KNN-SmCoO<sub>3</sub> and KNN-SmMnO<sub>3</sub>, compared to the reference KNN.

### **Introduction**

A major impediment of the currently widely used piezoelectric ceramic, namely Pb(Zr,Ti)O<sub>3</sub>, is the high toxicity of Pb compounds [1, 2]. Hence, the latest trends in research are oriented toward “environmentally friendly” piezoelectric materials, such as (K, Na)NbO<sub>3</sub>.

(Na<sub>x</sub>K<sub>1-x</sub>)NbO<sub>3</sub> is a solid solution of orthorhombic ferroelectric KNbO<sub>3</sub> and anti-ferroelectric orthorhombic NaNbO<sub>3</sub> [3]. A morphologic phase boundary at 50% KNbO<sub>3</sub>, or (K<sub>0.5</sub>Na<sub>0.5</sub>)NbO<sub>3</sub> (noted KNN), was observed to enhanced piezoelectric and ferroelectric properties [4]. At room temperature, KNN is a ferroelectric perovskite, with orthorhombic crystalline structure. As previous authors pointed out [5], the improvement of the piezoelectric properties can be achieved by the shifting of orthorhombic to tetragonal polymorphic phase transitions (PPT) to room temperature, or preparation of improved composition closed to an morphologic phase boundary (MPB) through chemical additions or doping.

The purpose of this work is to investigate the crystallographic phase transitions that may occur during doping with Samarium based perovskite, at a morphologic phase boundary of 50% KNbO<sub>3</sub>. Also, the dielectric behavior of the piezoelectric ceramics will be evaluated in terms of frequencies.

### **Experimental**

(K<sub>0.5</sub>Na<sub>0.5</sub>)NbO<sub>3</sub> (noted KNN) and (K<sub>0.5</sub>Na<sub>0.5</sub>)NbO<sub>3</sub> doped with 1 mol% SmBO<sub>3</sub> (where B= Al, Co, Cr, Fe, Mn) (noted KNN-SmBO<sub>3</sub>) ceramics were obtained using the solid state method in air. The starting materials were K<sub>2</sub>CO<sub>3</sub> ( 99%; Scharlau, Sentmenat, Spain), Na<sub>2</sub>CO<sub>3</sub> ( 99%; Scharlau), Nb<sub>2</sub>O<sub>5</sub> (99%, Merck, Darmstadt, Spain), Gd<sub>2</sub>O<sub>3</sub> ( 99%; Fluka, Buchs, Switzerland). SmBO<sub>3</sub> powders were prepared in air at 1100°C using the following reagents: Mn<sub>2</sub>O<sub>3</sub> ( ), AlN<sub>3</sub>O<sub>9</sub>•9H<sub>2</sub>O ( 99%, Fluka, Buchs, Switzerland), Co(NO<sub>3</sub>)<sub>2</sub>•6H<sub>2</sub>O (99%; Scharlau), Co(NO<sub>3</sub>)<sub>3</sub>•9H<sub>2</sub>O (99%; Scharlau), Co(NO<sub>3</sub>)<sub>3</sub>•9H<sub>2</sub>O (99%, Fluka, Buchs, Switzerland). KNN-SmBO<sub>3</sub> were calcined at 850°C for 6h, with a heating rate of 5 °/min. After calcinations and x-ray purity check, the powders obtained were grinded and mixed with a 5 mass% polyvinyl alcohol binder solution. Disk samples of 6 mm in diameter and approximately 1 mm thick were cold pressed at 200Mpa. The disks were sintered at 1050°C for 6h. After grinding, the crystalline structure of the sintered samples was examined by x-ray

diffraction using a PanAnalytical X'Pert Pro MPD diffractometer. The refinement of the unit cell was performed using Treor algorithm in X'Pert HighScore Plus software. The variation of the dielectric constant at different frequencies was obtained using an Impedance/LRC meter TEGAM model 3550 (Geneva, OH, USA).

## Results and discussion

Figure 1 shows the x-ray diffraction patterns of the obtained  $\text{SmBO}_3$  (B= Al, Co, Cr, Fe, Mn) powders. All compositions obtained possess an orthorhombic crystalline structure at room temperature.

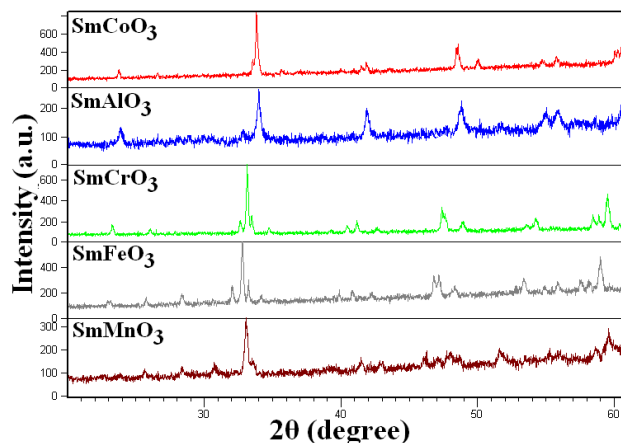
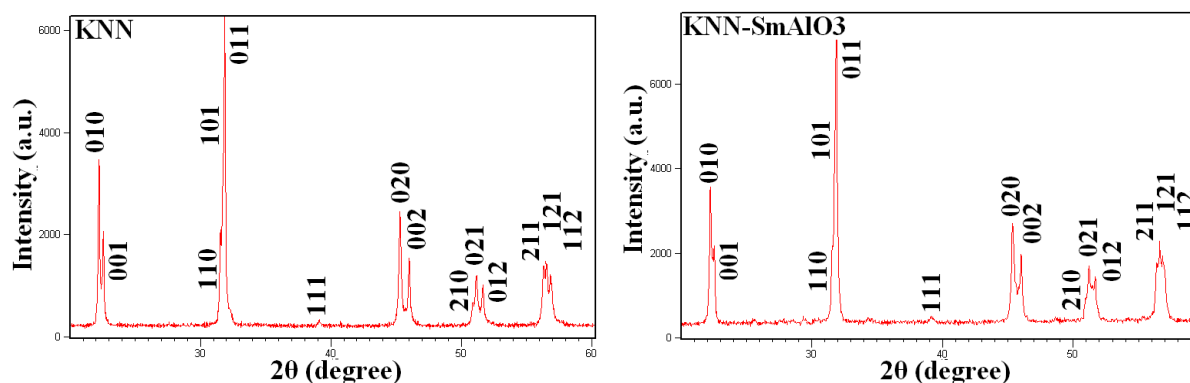


Figure 1. X-ray diffraction patterns of  $\text{SmBO}_3$  (B= Al, Co, Cr, Fe, Mn) ceramics.

Figure 2 shows the X-ray diffraction pattern of the reference sample  $(\text{K}_{0.5}\text{Na}_{0.5})\text{NbO}_3$ , along with the X-ray diffractions patterns of KNN-Sm $\text{BO}_3$  ceramic powders. The reference sample was indexed as pure perovskite using the JCPDS-ICDD file number 01-071-2171. The refinement of the unit cell revealed an orthorhombic crystalline structure (space group  $\text{P2mm}(25)$ ) at room temperature, easily identified from the difference in peak intensity of the crystallographic plane splitting at  $[010]$ - $[001]$ , respectively  $[020]$ - $[002]$ . Similar diffractions patterns were observed for KNN-Sm $\text{AlO}_3$  and Sm $\text{CoO}_3$ . However, for the rest of the combination differences in the above mentioned crystallographic reflections were observed. The explanations of such observations are intimately related to the alteration of the unit cell parameters, as we can see below.



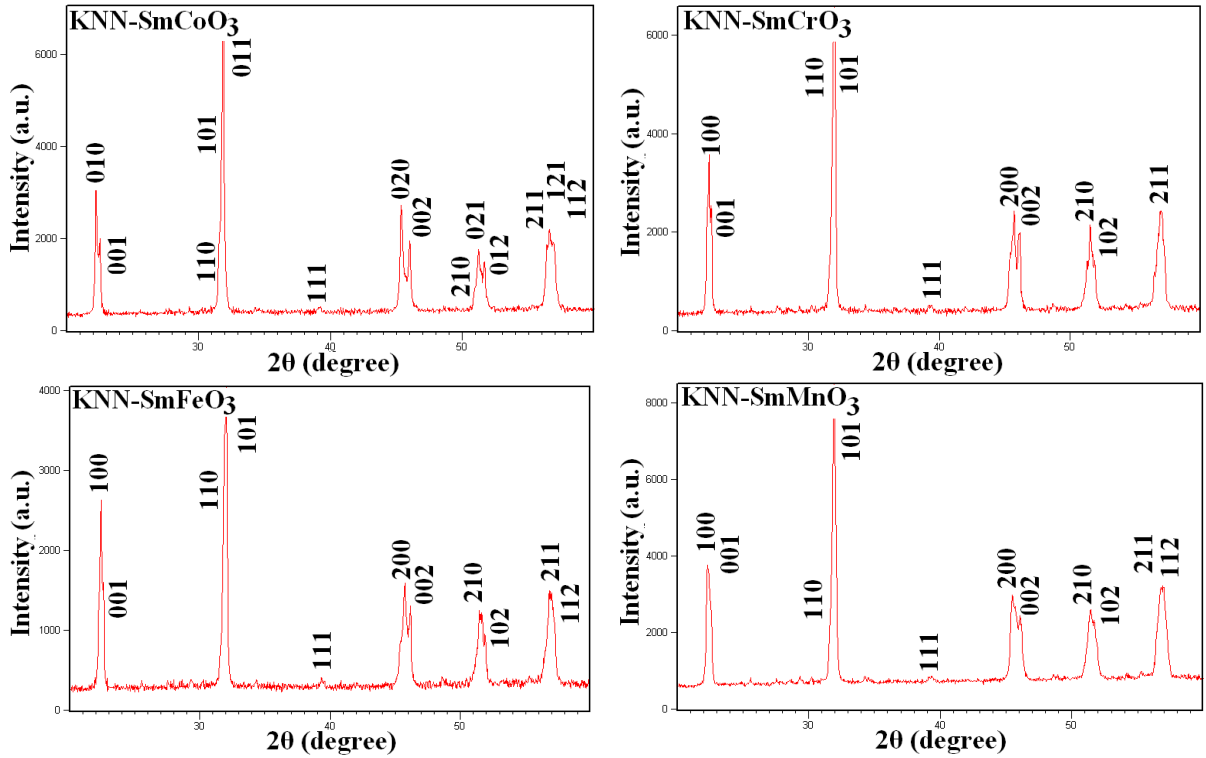


Figure 2. X-Ray diffractions of KNN, respectively KNN-SmBO<sub>3</sub> (B= Al, Co, Cr, Fe, Mn) sintered piezoelectric ceramics.

The results of the unit cell refinement are presented in figure 3. As a general observation, all dopants used decrease the values of a and b, and slightly alters the value of c. As a direct consequence, the unit cell volume decrease for all compositions studied, compared to the reference sample KNN. The refinement of the unit cell also revealed a shift from orthorhombic P2mm(25) crystalline structure for KNN-SmAlO<sub>3</sub> and KNN-SmCoO<sub>3</sub>, to tetragonal P4mm(99) for the rest of the compositions, where a=b≠c.

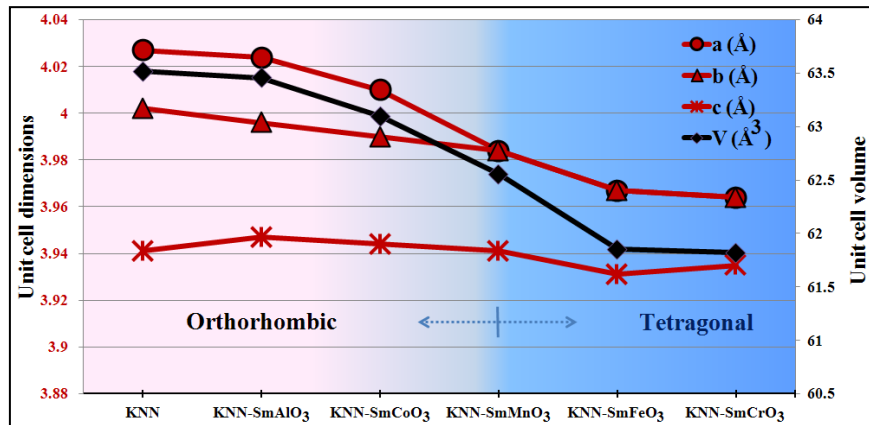


Figure 3. Unit cell dimensions of KNN and KNN-SmBO<sub>3</sub> (B= Al, Co, Cr, Fe, Mn) ceramics.

The dielectric constant of the studied materials was measured at six different frequencies and is presented in figure 4. Starting from a low dielectric constant at room temperature, of 213 (100 Hz) for the reference sample KNN, all composition studied improve

the real part of the electric permittivity significantly. At low frequency, the dielectric constant is higher, but as the frequency increases, all ceramics are affected by the dielectric relaxation, where epsilon tends to decrease. An outstanding increase of the dielectric constant was achieved for KNN-SmCoO<sub>3</sub> (1067 at 100 Hz) and KNN-SmMnO<sub>3</sub> (1115 at 100 Hz). Since the dielectric constant is intimately related to the charge that can be stored in a piezoelectric capacitor, significant improvements of the piezoelectric materials are expected for these materials.

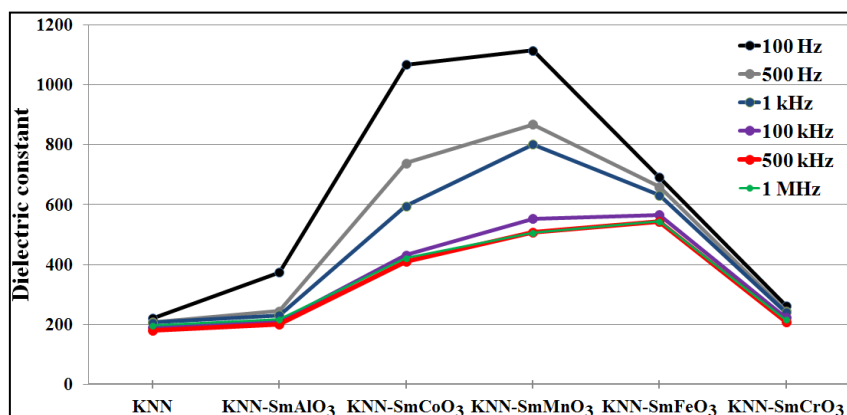


Figure 4. Variations of the dielectric constant at different frequencies for KNN and KNN-SmBO<sub>3</sub> (B= Al, Co, Cr, Fe, Mn) ceramics.

## Conclusion

KNN and KNN-SmBO<sub>3</sub> (B= Al, Co, Cr, Fe, Mn) ceramics were successfully obtained by solid state method. The crystalline structure remain orthorhombic P2mm(25) for KNN-SmAlO<sub>3</sub> and KNN-SmCoO<sub>3</sub>, and is shifted to tetragonal P4mm(99) for KNN-SmMnO<sub>3</sub>, KNN-SmFeO<sub>3</sub> and KNN-SmCrO<sub>3</sub>. For all compositions studied the unit cell volume decrease compared to the reference KNN. The variation of the dielectric constant at different frequencies revealed a significant increase of almost one order of magnitude for KNN-SmCoO<sub>3</sub> and KNN-SmMnO<sub>3</sub>, suggesting these materials as candidates for improved lead-free piezoelectric application.

## Acknowledgements

This research was supported by the national project PN 16 14 01 03.

## References

- [1] M.D. Maeder, D. Damjanovic, N. Setter, J. Electroceram. 13 (2004) 385.
- [2] Restriction of Hazardous Substances in Electrical and Electronic Equipment (RoHS 2), Directive 2011/65/EU.
- [3] S. Wada, K. Muraoka, H. Kakemoto, T. Tsurumi, and H. Kumagai, Jpn. J. Appl. Phys. 43, 6692 (2004).
- [4] R.E. Jaeger and L. Egerton, J. Am. Ceram. Soc. 45, 209 (1962).
- [5] J. Rodel, W. Jo, K.T.P. Seifert, E.M. Anton, T. Granzow, D. Damjanovic, J. Am. Ceram. Soc. 92, 1153 (2009).

**AGRICULTURAL IMPACT ON BROWN HARE: LC-MS/MS KIDNEY  
MULTIRESIDUAL PESTICIDES ANALYSES**

**Vojislava Bursić<sup>1</sup>, Gorica Vuković<sup>2</sup>, Miloš Beuković<sup>1</sup>, Martina Mezei<sup>1</sup>, Bojana Špitović-Trifunović<sup>3</sup>, Aleksandra Petrović<sup>1</sup>, Ivana Ivanović<sup>1</sup>**

<sup>1</sup>*University of Novi Sad, Faculty of Agriculture, Trg Dositeja Obradovića 8, 21000 Novi Sad, Serbia*

<sup>2</sup>*Institute of Public Health, Bul. despota Stefana 54a, 11000 Belgrade, Serbia*

<sup>3</sup>*University of Belgrade, Faculty of Agriculture, Nemanjina 6, 11000 Belgrade, Serbia*  
*e-mail: bursicv@polj.uns.ac.rs*

**Abstract**

By the dramatic increase in the areas under the agricultural crops in Serbia with the intensive use of pesticides and the decrease in areas under fodder crops the possibility of qualitative nutrition for hares is decreased parallel with the change of their typical habitats. Hares feed on grass, weeds, various agricultural crops, vegetable plants, buds, fresh trees bark and grains. They provide the sufficient amount of water through succulent plants so that they almost need no water. That is why the aim of our study was to determine the 30 pesticides content by validated multiresidual LC-MS/MS method. Based on the LC-MS/MS analysis of brown hare kidney samples eight pesticides out of 30 were detected. The detections were very low, except one sample, which contained oxamil, carbendazim and cymoxanil residues in the concentrations above EU MRLs, namely 0.446, 0.071 and 0.711 mg/kg, respectively. In the other sample oxamil residue was over the EU MRLs.

**Introduction**

According to the Food and Agriculture Organization's article [1], 11.0% of Earth's 13.4 billion hectares of land are used for crop cultivation. The plant agriculture leaves one of humanity's biggest ecological footprints and hence has major implications for wild-animal suffering. The crop cultivation plausibly reduces populations of large number of animals [2]. The increasing human populations are associated with greater conversion and fragmentation of wild habitats, and more intense hunting pressure on remaining wildlife stocks. Animals are a part of many agricultural systems. Wild animals can help to manage pest populations and contribute to biodiversity [3]. FAO's concern is that wildlife species are increasingly at risk from the expansion and intensification of agricultural production. The agricultural impact could lead to habitat loss and environmental damage due to pesticides being dispersed into the environment [4]. By the dramatic increase in the areas under the agricultural crops in Serbia with the intensive use of pesticides and the decrease in areas under fodder crops the possibility of qualitative nutrition for hares is decreased parallel with the change of their typical habitats [5-7]. Hares feed on grass, weeds, various agricultural crops, vegetable plants, buds, fresh trees bark and grains. They provide the sufficient amount of water through succulent plants so that they almost need no water [5].

That is why the aim of our study was to determine the 30 pesticides content by validated multiresidual method liquid chromatography coupled with tandem mass spectrometry (LC-MS/MS).



## Experimental

### Chemicals

The analytical fungicide standards were manufactured by Dr. Ehrenstorfer GmbH, Germany. As an internal standard carbofuran-D3 (99.7%) was purchased from Pestanal, Fluka (Germany) and was used in the concentration of 1.0 mg/mL of the basic standard in acetonitrile with the dilution up to 10.0 µg/mL. The stock standard solutions were prepared by dissolving an analytical standard in acetonitrile while the working solution i.e. the mixture of the studied pesticides was obtained by mixing and diluting the stock standards with acetonitrile resulting in the final mass concentration of 10.0 µg/mL.

### Aparature

For LC analysis, an Agilent 1200 (Agilent Technologies, USA) HPLC system th a binary pump was used. This was equipped with a reversed-phase C18 analytical column of 50×4.6mm and 1,8 µm particle size (Agilent Zorbax Eclipse XDB). The mobile phase was methanol and Milli-Q water with 0.1% formic acid in gradient mode, with the flow rate 0.4 mL/min. For the mass spectrometric analysis, an Agilent 6410 Triple-Quad LC/MS system was applied. Agilent Mass Hunter Data Acquisition, Qualitative Analysis and Quantitative Analysis software were used for method development and data acquisition.

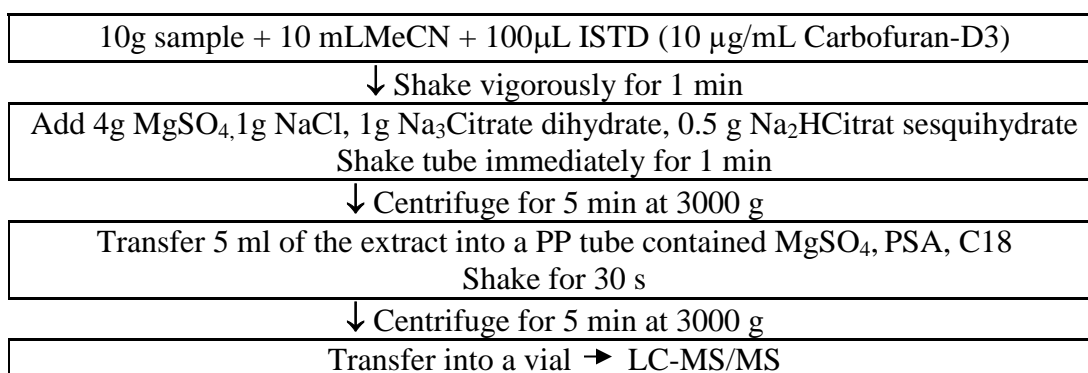
### Validation

Within the validation the recoveries of extraction, detection limits (LOD), quantification limits (LOQ) and linearity with carbofuran-D3 addition as an internal standard (IS) were determined according to SANTE/11945/2015 [8]. The LOD was determined as the lowest concentration giving a response of five times the average baseline. The ratio signal/noise in the obtained chromatograms for the LOD was calculated by MassHunter Qualitative Software. The linearity was checked using matrix matched calibration (MMC) at the concentrations of 5.0, 10.0, 25.0, 50.0 and 100.0 ng/mL. The recovery was checked by enriching 10 g of a blank sample with the mixture of pesticide standard of 10 µg/mL in the amount of 100 and 50 µL (final mass concentration 0.10 and 0.05 mg/kg) and with the mixture of pesticide standard of 1 µg/mL in the amount of 100 µL (final mass concentration 0.01 mg/kg) with the addition of the internal standard carbofuran-D3.

### Samples and fungicide extraction

Brown hare were collected from the agricultural areas from Vojvodina region. The kidneys of ten animals were immediately collected and put in dark plastic bags. All the samples were put in the freezer until they were analyzed by QuEChERS method (Fig. 1).

Figure 1. QuEChERS extraction of fungicide residues



## Results and discussion

The obtained LC-MS/MS TIC chromatogram of pesticide standards (Figure 1) and LC-MS/MS chromatogram of sample number six chromatogram (Figure 2) are shown below.

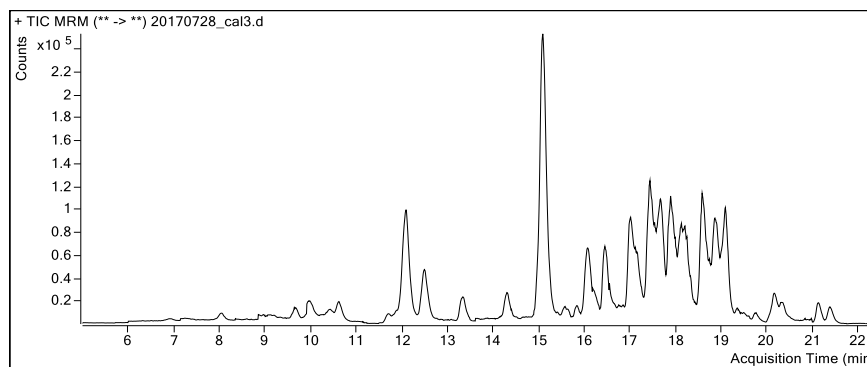


Figure 1. TIC chromatogram of pesticide standards

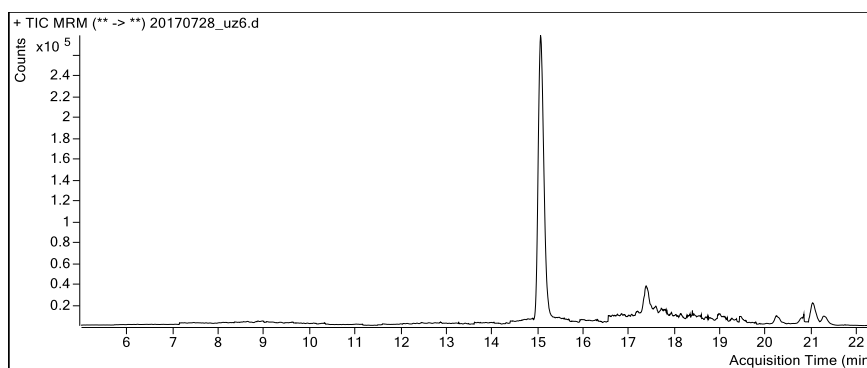


Figure 2. TIC chromatogram of sample number six

According to the obtained LC-MS/MS results, some pesticides were detected (mg/kg) in analysed brown hare kidney samples (Table 1).

N o	Ometho ate	Oxam yl	Carbendaz im	Thiamethox am	Cymox anil	Thiaclop rid	Phos met	Dimethomo rph
1	<LOQ	0.003	<LOQ	0.004	0.006	0.005	<LOQ	<LOQ
2	<LOQ	<b>0.446</b>	<b>0.071</b>	0.061	<b>0.711</b>	0.008	<LOQ	0.005
3	<LOQ	0.006	0.005	0.004	0.005	<LOQ	0.007	<LOQ
4	<LOQ	0.006	<LOQ	<LOQ	0.002	<LOQ	0.007	<LOQ
5	0.003	<b>0.012</b>	0.005	0.004	0.024	<LOQ	0.007	<LOQ
6	0.003	0.007	<LOQ	<LOQ	0.013	0.005	<LOQ	0.003
7	0.003	0.004	0.004	<LOQ	0.011	<LOQ	<LOQ	<LOQ
8	0.003	0.003	<LOQ	<LOQ	0.004	0.005	<LOQ	<LOQ
9	0.003	0.008	0.005	<LOQ	0.012	<LOQ	<LOQ	<LOQ
10	0.003	0.003	<LOQ	0.004	0.009	0.005	0.007	0.003

## **Conclusion**

Based on the LC-MS/MS analysis of brown hare kidney samples eight pesticides out of 30 were detected. The detections were very low, except in sample number 2, which contained oxamil, carbendazim and cymoxanil residues in the concentrations above EU MRLs [9], namely 0.446, 0.071 and 0.711 mg/kg, respectively. In sample number 5 oxamyl residue was over the EU MRLs [9].

## **Acknowledgements**

The authors acknowledge the financial support of the AP Vojvodina, the Republic of Serbia, Project Ref. 104-401-4794/2016.

## **References**

- [1] FAO Corporate document repository, Crop production and natural resource use (2015).
- [2] B. Tomasik, Crop Cultivation and Wild Animals (2017)
- [3] FAO, Food and Agriculture Organization of the United Nations, Animal production and health (2017).
- [4] D. Rondeau, E. Bulte, Amer. J. Agr. Econ. 89(2) (2007) 490.
- [5] M. Beuković, Z. Đorđević, N. Popović, D. Beuković, M. Đurđević, Savremena poljoprivreda 60 (3-4) (2011) 403.
- [6] M. Beuković, Z. Popović Univerzitet u Novom Sadu, Poljoprivredni fakultet Novi Sad, Lovstvo (2014).
- [7] V. Bursić, G. Vuković, D. Beuković, A. Petrović, A. Popović, I. Ivanović, M. Beuković International Symposium of Veterinary Medicine –ISVM, 22-24 June, Belgrade, Serbia, Proceedings (2016) 244.
- [8] SANTE 11945/2015. Guidance document on analytical quality control and validation procedures for pesticide residues analysis in food and feed.
- [9] Regulation (EC) No 396/2005 of the European Parliament and of the Council (2005) on maximum residue levels of pesticides in or on food and feed of plant and animal origin and amending Council Directive 91/414/EEC.

## PHYSICO-CHEMICAL CHARACTERIZATION FOR DIFFERENT TYPES OF FOOD OILS

Cozma Antoanela<sup>1</sup>, Velciov Ariana<sup>1</sup>, Petcu Mihaela<sup>1</sup>, Stoin Daniela<sup>1</sup>, Popescu Sofia<sup>1</sup>,  
Mircov D. Vlad<sup>1</sup>, Gogoasa Ionel<sup>1</sup>

<sup>1</sup> Banat's University of Agricultural Sciences and Veterinary Medicine „King Michael I of Romania” from Timisoara 119 Calea Aradului, 300 645, Romania,  
e-mail: [antoanelacozma@yahoo.com](mailto:antoanelacozma@yahoo.com)

### Abstract

Lipids are indispensable food components, which in large measure determine the energy value as well the nutritional, biological and sensory qualities. The aim of this paper was to evaluate some of the physicochemical characteristics (total soluble solids (TSS), relative density, viscosity and acidity index) in case of three alimentary oils. The analyzed oil assortments, in these works are soybean, rape and corn oil purchased from the commercial market having different origins. Oils density varies from species to species and at the same oil with the conservation conditions (conservation period, climatic conditions in which the plant has developed). Viscosity gives relevant indication of the degree of oil fluidity. The experimental results showed that the highest value for viscosity was registered in rapeseed oil (38,7088cP) and the smallest in soybean oil (34,0174cP). Rape oil from improved varieties is very good cooking oil for human consumption while soybean oil has a neutral taste and is recommended for the preparation of various types of salad.

### Introduction

Vegetable and animal oils and fats play an important role in nutrition because of their high energy potential and as raw materials used to obtain technical products. Due to their nutritional principles (vitamins A, B1, B2, B6 C, E, D, carotenes, minerals: selenium, zinc, potassium) are used mainly in the food and cosmetics industry [2]. Vegetable oils are found in nature in plant tissues, inside fruit kernels, in tubers, or in germs. In our country the main raw material is seed oil plants. Most plants contain oils to a greater or lesser extent, especially in seeds, fruits, kernels, germs. The oil plants in which the oil is concentrated in the seeds are: soybean, rape, sunflower, and plants producing oil fruits: olive, palm, coconut. In Romania, raw materials are used as plant seed oil and corn germs. [1]. Corn germ oil is obtained by pressing or extracting. It is a yellow or reddish oil, being refined in food. Soybean oil obtained is dried in about nine days and forms a dry and non-polluting substance [1]. Rape oil is the highest Omega 3 oil and is recommended in the hypertensive diet [2]. Vegetable oil is often used for cooking, but is also used for industrial, medical and fuel purposes. Moderate intake of unsaturated fats helps to reduce inflammatory processes, regulate blood cholesterol levels, and promotes metabolism in slimming or body modeling [3].

Rape (*Brassica napus oleifera* and *Brassica rapa oleifera*) is a plant of the Brassicaceae cruciferous family with yellow flowers and long, branched stem. Rapeseed is grown for seeds and the oil is used in food and industry (biofuel). Due to its high erucic acid content (up to 30%) rapeseed oil has been considered to be toxic to the human body. Animal experiments have led to the conclusion that the consumption of rapeseed oil with high erucic acid content does not cause negative effects if the proportion in the diet does not exceed 5%. Its introduction into food was possible after world war II when new genetically modified

varieties were created, degraded to erucic acid (less than 2%) and very low glucose (less than 30  $\mu\text{mol}$  / gram) known as "canola". The oil is dark green, has no specific taste and smell and is used in refined form in food.

Soybean (*Glicina hispida Max*) is part of the Glycin family of Oriental Asian legumes. The soy is very rich in protein - 40% (while the meat has only 15-25%), carbohydrates (10-15%), minerals (calcium, iron, magnesium, phosphorus, sulfur), vitamins (A, B1, B2 , D, F, E), lecithin (as well as egg yolk), waxes, resins, cellulose. Essential and non-essential amino acid content is a percentage double of meat. From this content come the general properties for which soy oil is highly recommended in food, representing a completely constructive (muscle, bones, nerves) and easily digestible food, is an energetic, remineralizing and balanced cell nutrition, preventing fattening [4]. The oil obtained from the corn germ, *Zea mays*, is light yellow or orange, if unrefined and almost tasteless. Corn oil is a mono and polyunsaturated oil. Percentage contains 54.7% polyunsaturated fatty acids, 27.6% monounsaturated fatty acids and 13% saturated fatty acids. Of saturated fatty acids, 80% are palmitic acid, 14% stearic acid and 3% arachidic acid [5]. Of the monounsaturated fatty acids, 99% are oleic acid. 98% of the polyunsaturated fatty acids are linoleic acid, an omega-6 and 2% linoleic acid, an omega-3.

### Experimental

In the experimental part, have been analyzed in terms of physicochemical and nutritional characteristics three types of food oils commonly used in the food industry to prepare dishes and culinary products. The oil assortments analyzed in these works are soybean, rapeseed and corn oil purchased from the supermarket. These are used and appreciated due to the nutritional principles in the preparation of various sauces, salads, dressings especially in the cold kitchen as they also highlight the characteristics of the other ingredients.

The purpose of the study was to analyze and compare some physico-chemical characteristics as total soluble solids content (TSS), relative density ( $\rho_r$ ) the dynamic viscosity ( $\eta$ ) and also acidity index in case of the three vegetable food oils. The total soluble solids (TSS) and the refractive index were obtained using the refractometry method, with the Abbe refractometer corrected to the equivalent reading at 20°C (AOAC, 1995). Relative density determination was made using the pycnometer by weighing the analytical balance and for the dynamic viscosity was used the Ostwald type viscometer. The free oils acidity is an important indicator due to the free fatty acids present in the product. The acidity index represents the amount of potassium hydroxide, in mg, required to neutralize free fatty acids from one gram of product.

### Results and discussion

From the determinations of the physico-chemical analyzed parameters, for the oils used it was observed that their values differ from one category to another. The values of the main physico-chemical characteristics are presented in table 1.

**Table 1.** The physico-chemical characteristics of the three types of analyzed oil

Nr.crt	Oil	n	$\eta$ (cp)	$\rho_{rel}$	$\rho$ (g/cm <sup>3</sup> )	Acidity % acid oleic
1	S <sub>1</sub> rapeseed	1.4714	38,7088	0,9134	0,91024	0.24
2	S <sub>2</sub> corn	1.4724	37,2518.	0,9145	0,91134	0.18
3	S <sub>3</sub> soybean	1.4733	34,0174	0,9161	0,91293	0.11

The variable composition of the different oils and fats allows their characterization also by measuring the refractive index. The refractive index of animal and vegetable fats and oils is a qualitative parameter, easily identified in a short time. Refractive index values for oil samples at 27 ° C is in the range 1.4714 -1.4733 .

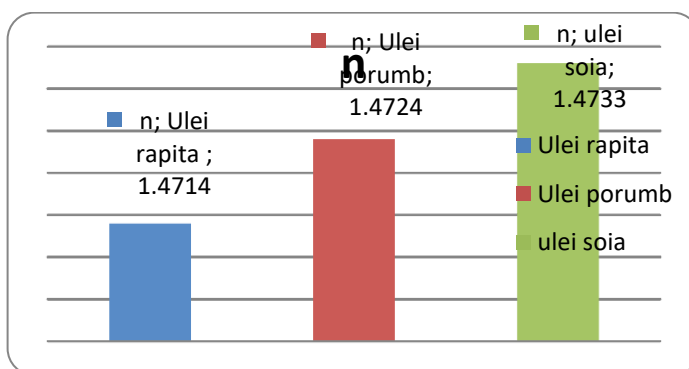


**Figure 1.** Refractive index value for rapeseed, corn and soybean oils

Density of oils varies from one species to another, and in the same type of oil with conservation conditions (storage life and climatic conditions in which the plant is developed). The oils density varies according to each type of oil and the temperature [6]. The value of the relative density of the investigated oils at 27 °C varies between 0.9134 and 0.9161. Compared to water, which has a density of 1.00 g / ml, oils are less dense.

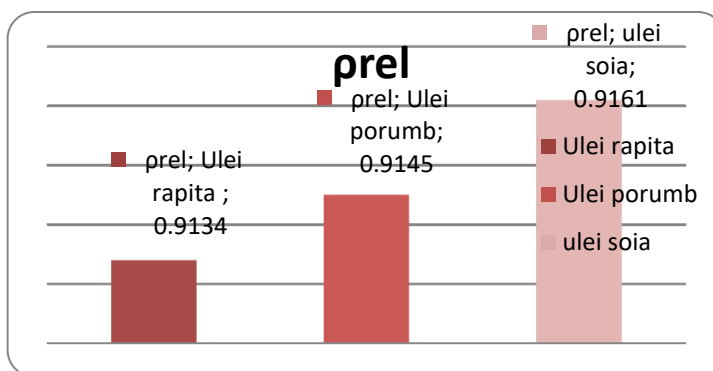


**Figure 2.** Relative density values for rapeseed, corn and soybean oils

Viscosity is considered an important physical property for the quality of liquid foods. The investigated oil samples generally have a Newtonian fluid behavior, the saturated fatty acid content playing a major role in the viscosity size. All edible oils consist of triglycerides with a variety of fatty acids that differ depending on chain length, saturation degree and position, as well as the geometry of the double bond in the carbon chain [3]. The viscosity provides mainly indications of the degree of the oils fluidity.

The viscosity of edible vegetable oils increases with the chain length of triglyceride fatty acids and decreases with unsaturation. Distinctive behavior of the oils subjected to the same thermal stress is due to the composition of saturated, monounsaturated and polyunsaturated fatty acids together with the concentration of minor compounds, mainly phenols and tocopherols[4].

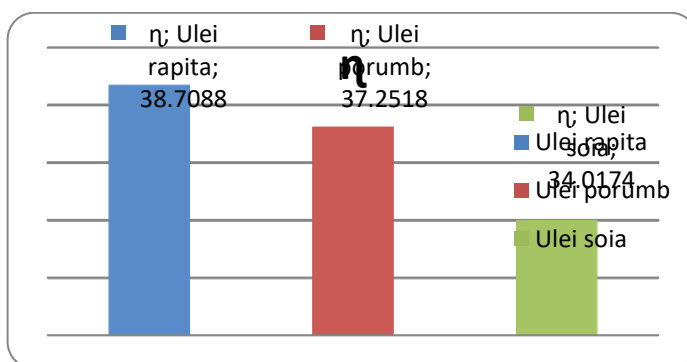


**Figure 3.** Viscosity coefficient values for the analyzed food oils

The free acidity oils studied was determined according to STAS 145-67. Free acidity is the percentage of free fatty acids found in the analyzed oil are conventionally expressed in the most representative fatty acid [7]. For ordinary soybean oils, sunflower, peanut, pumpkin is expressed in oleic acid; for coconut and palm oil in lauric acid; for palm oil in palmitic acid for rapeseed oil in erucic acid. The free acidity values for the analyzed oils correspond to the standards in force, the values being between 0.11 - 0.24% oleic acid [8].

## Conclusion

Refractive index values for oil samples at 27°C are in the range of 1.4714-1.4733. The recorded values are comparable with the literature values. Viscosity is considered an important physical property for the quality of liquid food, indicating the degree of fluidity of the oil in this case. Rapeseed oil has a higher viscosity than corn and soybean oils. This can be directly related to the content of saturated fatty acid. The viscosity of refined rapeseed oil is higher than that of soybeans. Increased viscosity may be the result of the presence of saturated fatty acids in the chemical composition of vegetable oil, higher molecular weight acids than unsaturated ones. The density of oils varies from one species to another, and in the same type of oil with conservation conditions (storage and climatic conditions in which the plant is developed). The value of the relative density of the investigated oils at 27 °C varies between 0.9134 and 0.9161. These are in the range of values presented in the literature. The oils density varies according to each type of oil and the temperature.



The free acidity of the analyzed oils corresponds to the standards in force, but the rapeseed oil still has a higher value.

### **References**

- [1] Boeru, G. 1988, Vegetable oils and animal fats, Editura Ceres, București
- [2] Mucete Daniela, 2005, Chemistry of agro-food products, Eurobit, Timisoara
- [3] Frank D.Gunstone, 2000, Vegetable Oils in Food Technology Composition, Properties and Uses, Second Edition,
- [4] Ramon Aparicio, Garcia-Gonzalez, 2009, Chemical Analysis of Food: Techniques and Applications, First Edition, USA
- [5] TabărăV., 2005, Phytotechnics, Vol. I, Technical-oil plants and textiles, Brumar, Timișoara
- [6] Cozma Antoanela, 2016, Physics and Biophysics, Practical Work, Fizica si Biofizica,
- [7] Mariana-Atena Poiană, 2005 – Vegetable food technologies. Methods of analysis, applications and technological calculations. Eurobit, Timisoara
- [8] Paula Ioana Dorobanțu, Chemical analysis of mixed type of commercial oils and their importance in the diet - USAMVB , Iasi

PHOTOCATALYTIC ACTIVITY OF Mo-DOPED LiInO<sub>2</sub> IN DEGRADATION OF AMITRIPTYLINE FROM WASTEWATERS

**Ljubica Đaćanin Far<sup>1</sup>, Tamara Ivetić<sup>1</sup>, Svetlana Lukić-Petrović<sup>1</sup>, Nina Finčur<sup>2</sup>, Biljana Abramović<sup>2</sup>**

<sup>1</sup>University of Novi Sad, Faculty of Sciences, Department of Physics, Trg Dositeja Obradovica 4, 21000 Novi Sad, Serbia

<sup>2</sup>University of Novi Sad, Faculty of Sciences, Department of Chemistry, Biochemistry and Environmental Protection, Trg Dositeja Obradovica 3, 21000 Novi Sad, Serbia  
e-mail: ljubica@df.uns.ac.rs

**Abstract**

Lithium-indium oxide is a high density, wide band-gap semiconductor with promising applications for scintillating detection of solar neutrinos as well as for efficient phosphorescence when doped with different rare earth ions. Previously, we have examined the photocatalytic efficiency of LiInO<sub>2</sub> powder, synthesized using a simple solid-state method, and it has proved to be a promising photocatalyst in alprazolam photodegradation under UV irradiation [1]. Recently, it was found that doping LiInO<sub>2</sub> with Mo<sup>6+</sup> ions can greatly enhance the degradation of methylene blue under visible light irradiation by tailoring the band-gap of LiInO<sub>2</sub> and extending its light absorption into the visible spectral range [2].

In this research we prepared LiInO<sub>2</sub> powders with 0, 3, and 6at% of Mo<sup>6+</sup> using a two-step mechanochemical procedure followed by annealing. X-ray diffraction measurements confirmed materials tetragonal structural form (with space group: I4<sub>1</sub>/amd), while the microstructure of obtained powders was observed using scanning electron microscopy. Preliminary results of the efficiency of the Mo-doped LiInO<sub>2</sub> powders were obtained in the photocatalytic degradation of amitriptyline under simulated solar irradiation.

Namely, amitriptyline, a widely consumed psychiatric pharmaceutical from the tricyclic antidepressant class [3], is used for the relief of mental depression, including clinical/endogenous depression [4]. Pharmaceuticals like this are lagging behind in treated waters even after their purification and it is necessary to find efficient method for their complete removal, whereas the use of the advanced oxidation processes proved to be the most effective way.

**References**

- [1] Lj. Đaćanin Far, T. Ivetić, S. Lukić-Petrović, D. Štrbac, N. Finčur, B. Abramović, Proceedings of the 22nd International Symposium on Analytical and Environmental Problems, Szeged, Hungary (2016), p. 115
- [2] X. Zhang, D. Xu, D. Huang, F. Liu, K. Xu, H. Wang, S. Zhang, J. Am. Ceram. Soc. 100 (2017), 2781-2789.
- [3] H. Li, M.W. Sumarah, E. Topp, Environ. Toxicol. Chem. 32 (2013), 509-516.
- [4] J.C. Abbar, S.D. Lamani, S.T. Nandibewoor, J. Solution Chem. 40 (2011), 502-520.

**H<sub>2</sub>Ti<sub>2</sub>O<sub>5</sub> · H<sub>2</sub>O NANOWIRE AS AN INTERMEDIARY PHASE OF TiO<sub>2</sub> ANODE FOR DYE SENSITIZED SOLAR CELL**

**Daniel Ursu<sup>1</sup>, Melinda Vajda<sup>1</sup>, Dabici AnaMaria<sup>1</sup>, Miclau Marinela<sup>1\*</sup>**

<sup>1</sup>*National Institute for Research and Development in Electrochemistry and Condensed Matter,  
1 Plautius Andronescu Street, 300224 Timisoara, Romania  
e-mail: marinela.miclau@gmail.com*

**Abstract**

In the last years, nanostructures have been widely used in energy harvesting devices, such as dye-sensitized solar cells (DSSCs), nanogenerators, and fuel cells, due to their high efficiency and light weight [1-4]. Therefore, nanostructure based DSSCs are likely to be low-cost, high efficiency, and simple in preparation, which is promising as a renewable energy resource for sustainable development of the future. Besides DSSC applications, nanostructures have been used in energy storage fields, such as lithium ion batteries (LIBs), due to their high energy density and long cycle life [5, 6]. A great challenge is to combine solar energy conversion and storage into one device. Using (Ti) sheet as substrate for TiO<sub>2</sub> nanorods grown as intermediary, the integrated power pack can be flexible and directly harvest and store energy by the electron conduction of the substrate. Thereby, using double-sided TiO<sub>2</sub> nanorods not only provide larger electrode area for DSSCs and LIBs but also can improve the electron transport properties of DSSCs and avoid irregular expansion when the insertion/removal of lithium along a specific orientation in anode material [7]. Compared with other integrated solar power supplies, double-sided TiO<sub>2</sub> nanorods with large area can be prepared by a simple, cost-effective, and controllable electrochemical process.

Moreover, such H<sub>2</sub>Ti<sub>2</sub>O<sub>5</sub> · H<sub>2</sub>O material are good precursor of titania and metal titanate, and have well-controlled shapes such as nanotubes and nanosheets [8,9]. H<sub>2</sub>Ti<sub>2</sub>O<sub>5</sub> are usually synthesized by solvothermal treatment of titania or by ion-exchange of alkaline metal titanates. Until now, the synthesis of H<sub>2</sub>Ti<sub>2</sub>O<sub>5</sub> have been less frequently reported than those of other hydrogen titanates, such as H<sub>2</sub>Ti<sub>3</sub>O<sub>7</sub> and H<sub>2</sub>T<sub>4</sub>O<sub>9</sub>, and it is formed as sheet-like particles [10,11]. The structure of H<sub>2</sub>Ti<sub>2</sub>O<sub>5</sub> has not been well established, it is reported to be a layered compound which is an isostructure to K<sub>2</sub>Ti<sub>2</sub>O<sub>5</sub> [12].

In this paper, we report the successful hydrothermal synthesis of H<sub>2</sub>Ti<sub>2</sub>O<sub>5</sub> · H<sub>2</sub>O nanowire as an intermediary phase of TiO<sub>2</sub> anode for dye sensitized solar cell. The structure of products was determined by powder X-ray diffraction (XRD) PW 3040/60 X'Pert PRO using Cu-K $\alpha$  radiation with ( $\lambda=1.5418\text{\AA}$ ), in the range  $2\theta = 10-80^\circ$ , at room temperature. A Scanning Electron Microscope InspectS (SEM) was used to observe the morphology of synthesized nanocrystals. The diffuse reflectance spectra (DSR) was obtained using a Lambda 950 UV-Vis-NIR Spectrophotometer with 150 mm integrating sphere in the wavelength range of 300–800 nm.

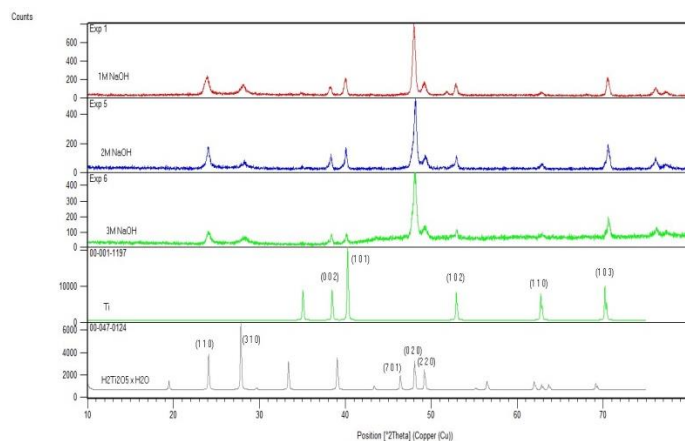


Figure 1. (a) X-ray diffraction patterns of  $\text{H}_2\text{Ti}_2\text{O}_5 \cdot \text{H}_2\text{O}$  obtained at  $220^\circ\text{C}$  for 24 hours at various concentrations of NaOH, a) 1M, b) 2M, c) 3M

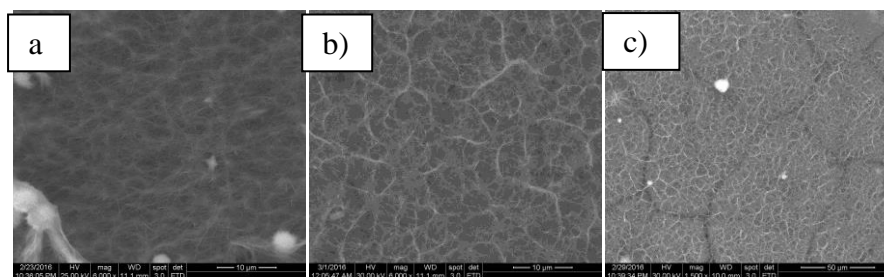


Figure 2. SEM images of  $\text{H}_2\text{Ti}_2\text{O}_5 \cdot \text{H}_2\text{O}$  obtained at  $220^\circ\text{C}$  for 24 hours at various concentrations of NaOH, a) 1M, b) 2M, c) 3M

### Acknowledgements

This paper is supported by the Romanian Government under the project 16-14 01 01.

### References

- (1) B. Oregan, M. Gratzel Nature 1991, 353 (6346), 737–740.
- (2) B.Z.Tian, X.L. Zheng, T.J. Kempa, Y. Fang, N.F. Yu, G.H. Yu, J.L. Huang, C.M. Lieber, Nature 2007, 449 (7164), 885–U8.
- (3) Z.L. Wang, J.H. Song, Science 2006, 312 (5771), 242–246.
- (4) J. Zhu, Y. Cui, Nat. Mater. 2010, 9 (3), 183–184
- (5) C.K. Chan, H.L. Peng, G. Liu, K. McIlwrath, X.F. Zhang, R.A. Huggins, Y. Cui, Nat. Nanotechnol. 2008, 3 (1), 31–35.
- (6) Y. Idota, T. Kubota, A. Matsufuji, Y. Maekawa, T. Miyasaka, Science 1997, 276 (5317), 1395–1397.
- (7) Jiang, J. A.; Li, Y. Y.; Liu, J. P.; Huang, X. T. Nanoscale 2011, 3(1), 45–58.
- (8) T. Kasuga, M. Hiramatsu, A. Hoson, T. Sekino, and K. Niihara: Formation of titanium oxide nanotube. Langmuir 14(12), 3160 (1998).
- (9) T. Kasuga, M. Hiramatsu, A. Hoson, T. Sekino, and K. Niihara: Titania nanotubes prepared by chemical processing. Adv. Mater. 11(15), (1999) 1307.

- (10) V. Etacheri, Y. Kuo, A. Van der Ven, and B.M. Bartlett. *J. Mater. Chem. A* 1(39), (2013), 12028
- (11) N. Sutradhar, S.K. Pahari, M. Jayachandran, A.M. Stephan, J.R. Nair, B. Subramanian, H.C. Bajaj, H.M. Mody, and A.B. Panda: *J. Mater. Chem. A* 1(32), (2013) 9122.
- (12) M. Sugita, M. Tsuji, and M. Abe *Bull. Chem. Soc. Jpn.* 63(7), (1990) 1978.

**DETERMINATION OF PCP IN GROUND/RIVER WATER SAMPLES BY STIR BAR SORPTIVE EXTRACTION–THERMAL DESORPTION–GAS CHROMATOGRAPHY-TRIPLE QUADRUPOLE MASS SPECTROMETRY**

**Ivana Deršek Timotić<sup>1</sup>, Mirjana Balać<sup>1</sup>, Katarina Nedeljković<sup>1</sup>, Daliborka Popadić<sup>1</sup>, Zoran Stojanović<sup>1</sup>, Vojislava Bursić<sup>2</sup>, Dušan Marinković<sup>2</sup>**

<sup>1</sup>*Serbian Environmental Protection Agency, Kneza Višeslava 66, 11000 Belgrade, Serbia*

<sup>2</sup>*University of Novi Sad, Faculty of Agriculture, 21000 Novi Sad, Trg Dositeja Obradovica 8, Serbia*

*e-mail: ivana.dersek@sepa.gov.rs*

**Abstract**

Pentachlorophenol (PCP) use to be in wide usage as insecticide, fungicide and contact-herbicide, but primarily as wood preservative and for industrial purposes. PCP is classified as extremely toxic substance for humans and environment. Systematic investigation of trace amounts PCP in surface water in Serbia has initiated in 2009. For analysis of surface water samples, described in this paper, method using stir bar sorptive extraction (SBSE) after derivatization with acetic acid anhydride followed by thermal desorption (TD) – triple quadrupole gas chromatography mass spectrometer with negative chemical ionization (GC/MS/MS-NCI) analysis was applied. Obtained LOQ of PCP –  $6.25 \times 10^{-4}$  µg/L is much lower than environmental quality standard (EQS) provided by the Water Frame Directive 2013/31/EU (WFD) for this compound – 0,4 µg/L, what makes this method appropriate for determination of PCP in water samples. Recovery and corresponding RSD of PCP is 82.47%, and 8.7%, respectively. Method showed good linearity over the concentration range of 0.6 - 50 pg/L PCP with coefficient of correlation  $R^2$  of 0.999. PCP was detected in all samples and measured amounts were bellow the set EQS values. Minimum ammount of PCP in samples was  $5.55 \times 10^{-3}$  µg/L, maximum ammount was  $111.74 \times 10^{-3}$  µg/L and the average was  $11.62 \times 10^{-3}$  µg/L.

**Introduction**

PCP use to be in wide usage as insecticide, fungicide and contact-herbicide, but primarily as wood preservative. After PCP was recognized as extremely toxic substance for humans and environment its usage was reduced and now PCP is permitted only for industrial purposes. Agricultural and domestic uses are prohibited.

PCP is classified as a highly hazardous pesticide, considered to be a carcinogen and a tumor promoter. The persistence of PCP in soil and water and apparent widespread use has resulted in significant exposure to animals. Studies on relation of exposure to PCP and cancer (on both humans and animals) led to EPAs classification of PCP as a Group B2, probable human carcinogen. Also, a significant amount of hexachlorobenzene is metabolized in animal tissues to PCP [1, 2].

Emission of PCP in water bodies was detected on locations with facilities for water purification or drop-off of dangerous waste. Therefore, PCP was put on a list of priority substances in DIRECTIVE 2013/39/EU as pollutant which presence in environment needs to be monitored. Serbian Water Laws were first are harmonized with Water Framework Directive (2000/60/EC) requirements in 2012, and since than surface water status monitoring in Serbia follows the EUs legislative.

Many analytical methods for the determination of PCP have been reported in literature including derivatization and SBSE followed by gas chromatography (GC) with mass spectrometry (MS).

M. Kawaguchi et al. (2004) investigated trace analysis of phenolic xenoestrogens such as 2,4-dichlorophenol (2,4-DCP), 4-*tert*-butylphenol (BP), 4-*tert*-octylphenol (OP), 4-nonylphenol (NP), pentachlorophenol (PCP) and bisphenol A (BPA) in water samples [3]. L. Montero et al. (2005) assessed presence of phenols and selected chlorophenols in lake and ground water samples [4]. Same approach was applied by J. Llorca-Porcel et al. (2009) on analysis of chlorophenols, bisphenol-A, 4-*tert*-octylphenol and 4-nonylphenols in soil, etc [5].

## Experimental

### *Water samples.*

Surface water samples were collected and analyzed on presence of PCP. Samples were collected in glass containers (approximately 3L), refrigerated at 4°C and stored in the dark from the time of collection until extraction. Samples were extracted within 7 days of collection and completely analyzed within 40 days of extraction [7].

### *Sample extraction.*

A 100 ml of sample was weighed into 250 ml erlenmeyer flask, 1g potassium bicarbonate was added and well mixed. After that, solution was spiked with certain amount of internal standard (2, 3, 5, 6-tetrachlorophenol) and 1 ml acetic anhydride was added as the derivatization reagent. After derivatization (15 minutes), 80ml of that solution was transferred in 100 ml erlenmeyer flask containing 20g of sodium chloride and one stirbar "Twister" was added. Stir bar "Twister" (polydimethylsiloxane-PDMS coated stir bar, 1cm length/1 mm film thickness) must be preconditioned. Then erlenmeyer flask was put on magnetic stirrer and extraction was performed at room temperature for 2 hours while stirring at 1100 rpm. Stir bar was easily removed from erlenmeyer flask with magnetic stick, rinsed with deionized water, dried with lint-free tissue and placed in a special TDU tube for GERSTEL Twister® stir bar.

### *Sample analyses.*

Prepared special TDU tube is put on TDU tray of GERSTEL MultiPurpose Sampler, (MPS2) with Thermal Desorption Unit (TDU2) which through fully automated procedure inserts tube with stir bar in TDU for thermal desorption.

The temperature of TDS 2 was programmed to increase from 30 °C (held for 0.5 min) to 295 °C (held for 10 min) at a rate of 720 °C/min.

After desorption, for chromatography separation, an Agilent 7890B GC with analytical column HP-5MSI 30 m, 0.25 mm, 0.25 µm was used. Applied temperature program is described in Table 1. Helium was used as the carrier gas at a flow rate of 1.5 ml/min.

Table 1. Temperature program of the GC oven

	Rate °C/min	Value °C	Hold Time min	Run Time min
(Initial)		70	0.1	0.1
Ramp 1	600	270	5	23.667
*				

For the mass spectrometric analysis, an Agilent 7000C Triple-Quad MS system was used. The mass spectrometer operated in the multiple reaction monitoring (MRM) mode. Three



transitions were monitored: 307.7→265.0  $m/z$  as transition for quantification and 307.7→230.8  $m/z$  and 264.7→228.7  $m/z$  for qualification.

MassHunter Workstation Software version B.04. was applied for the method acquisition and data processing.

#### *Validation.*

The method was validated according to regulations [8]. The limit of detection-LOD was determined as the lowest concentration of PCP in spiked real sample where ratio of PCP signal and noise is three ( $S/N=3$ ). Limit of quantification-LOQ was determined as the lowest concentration of PCP in spiked real sample where ratio of PCP signal and noise is larger than ten ( $S/N>10$ ). The ratio signal/noise in the obtained chromatograms for the LOD and LOQ was calculated by MassHunter Qualitative Analysis B 07.00 Software.

The recovery and precision of the method were determined by replicate analysis ( $n=6$ ) of different samples spiked with surrogate standards at 2.5 and  $10.0 \times 10^{-3}$  pg/L. The non-spiked and spiked samples were analyzed using the same procedure as for calibration standards and samples. The recovery was calculated by subtracting the results for the non-spiked samples from those for the spiked samples. The results were calculated by using calibration curves obtained from standard solutions with surrogate standards.

#### **Results and discussion**

Assessment of obtained results for validation and analysis showed that applied method is appropriate for trace analysis of PCP in surface water samples, because all relevant parameters are within established performance criteria for the application of this method.

Obtained LOQ of PCP- $6.25 \times 10^{-4}$  pg/L is much lower than environmental quality standard (EQS) provided by the Water Frame Directive 2013/31/EU (WFD) for this compound-0.4 μg/L. Method showed good linearity over the concentration range of 0.6/2.5/5.0/10.0/17.5/25.0/37.5 and  $50.0 \times 10^{-3}$  pg/L PCP with coefficient of correlation higher than  $R^2$  of 0.999. Recovery and corresponding RSD of PCP is 82.47%, and 8.7%, respectively.

The presence of PCP was detected in all samples and measured amounts were below the set EQS values. Minimum amount of PCP in samples was  $5.55 \times 10^{-3}$  μg/L, maximum amount was  $111.74 \times 10^{-3}$  μg/L and the average was  $11.62 \times 10^{-3}$  μg/L (Table 2).

Typical MRM chromatogram of river water samples are shown in Figure 1.

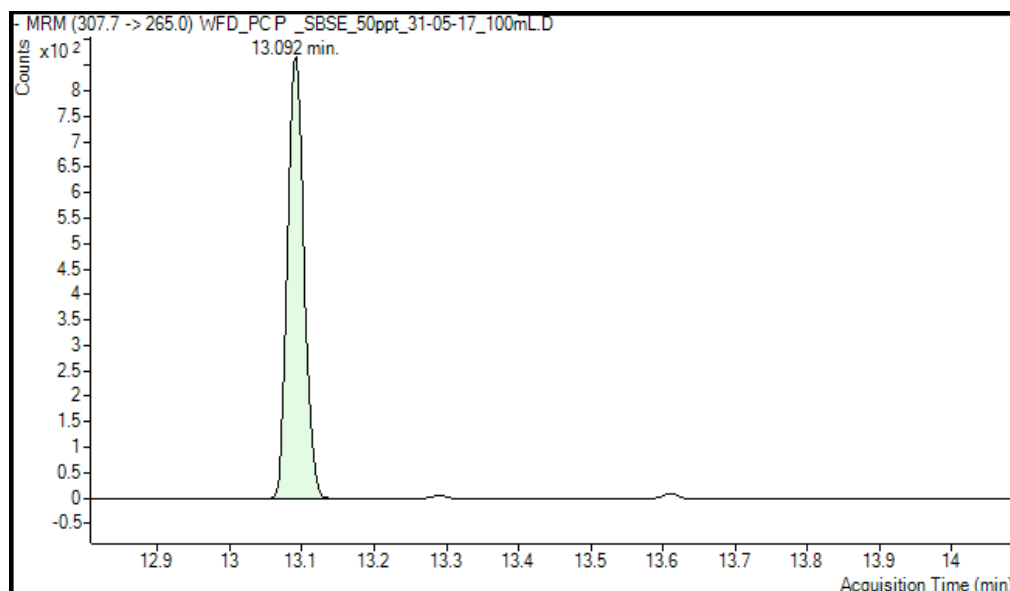


Figure 1. Chromatogram of river water sample

Table 2. PCP residue detected in analyzed samples of surface water samples

Compound	AA EQS ( $\mu\text{g/L}$ ), WFD2013/39/EU	Min conc ( $\mu\text{g/L}$ ), real samples National lab-SEPA	Max conc ( $\mu\text{g/L}$ ), real samples National lab-SEPA	Number of positive results, real samples National lab-SEPA
Pentachlorophenol	0.400	0.005	0.100	101

### Conclusion

Method used for determination of trace amounts PCP in surface water with derivatization followed by SBSE and triple quadrupole gas chromatography mass spectrometer with negative chemical ionization (GC/MS/MS-NCI) analysis is simple and accurate. The method has been validated with good sensitivity and selectivity for PCP and is applied for routine analysis of PCP. It has a potential for application on different types of water samples. We detected presence of PCP in different types of surface water in concentration ranges from  $5.55 \times 10^{-3} \mu\text{g/L}$  to  $111.74 \times 10^{-3} \mu\text{g/L}$ .

PCP was found in all samples and detected amounts were significantly lower the set EQS values.

### Acknowledgements

This work was founded and a part of the project IPA 2012 Establishment of an integrated environmental monitoring system for Air and Water Quality capacity of air and water monitoring in Serbia.

### References

[1] U.S. Department of Health and Human Services Agency for Toxic Substances and Disease Registry (ATSDR), Toxicological Profile for Pentachlorophenol, (1999) str

- [2] U.S. Environmental Protection Agency, Integrated Risk Information System (IRIS) on Pentachlorophenol, (1999) 163.
- [3] M. Kawaguchi, K. Inoue, M. Yoshimura, N. Sakui, N. Okanouchi, R. Ito, Y. Yoshimura, H. Nakazawa, Trace analysis of phenolic xenoestrogens in water samples by stir bar sorptive extraction with in situ derivatization and thermal desorption–gas chromatography–mass spectrometry, (2004) 19.
- [4] L. Montero, S. Conradi, H. Weiss, P. Popp, Determination of phenols in lake and ground water samples by stir bar sorptive extraction–thermal desorption–gas chromatography–mass spectrometry (2005).
- [5] J. Llorca-Pórcel, M. Martínez-Parreno, E. Martínez-Soriano, I. Valor, Analysis of chlorophenols, bisphenol-A, 4-tert-octylphenol and 4-nonylphenols in soil by means of ultrasonic solvent extraction and stir bar sorptive extraction with in situ derivatisation, Spain, (2009) 5955.
- [7] U.S. Environmental Protection Agency, Federal Register, Vol. 49, No. 209, (1984) 61.
- [8] Guidance document on analytical quality control and method validation procedures for pesticides residues analysis in food and feed - SANTE/11945/2015.

## COMPARATIVE ANALYSIS OF DIFFERENT ANIMAL AND HUMAN BLOOD SAMPLES BY UV-VIS SPECTROMETRY AND TESTING OF MAIN BIOCHEMICAL PARAMETERS

**Thomas Dippong<sup>1</sup>, Pauliuc Ivan<sup>2</sup>, Cristina Mihali<sup>1</sup>, Zoita Berinde<sup>1</sup>, Anca Sofronici<sup>1</sup>**

<sup>1</sup> *Technical University of Cluj-Napoca, North University Center of Baia Mare, Department of Chemistry and Biology, 76 Victoriei Street, 430122 Baia Mare, Romania*

<sup>2</sup> *University of Agricultural Sciences and Veterinary Medicine of Banat, 300081, Timisoara  
e-mail: dippong.thomas@yahoo.ro*

### **Abstract**

The paper presents a comparative evaluation of the UV-VIZ spectra for different blood types, with the identification of maximum absorption characteristic of oxyhemoglobin, respectively, a comparative analysis regarding some of the chemical analytical and clinical properties between animal and human blood types. The tests performed are the content of serum amylase, bilirubin, cholesterol (total, HDL, LDL), triglycerides, alanine aminotransferase, aspartate aminotransferase and uric acid.

### **Introduction**

Blood is a vital fluid in the human or animal body that nourishes all body organs and tissues and eliminates unnecessary or residual substances in the body. A human adult has between 5 and 6 liters of blood, which represents 7-8% of the total body weight. During dehydration, for example in a marathon, the current blood volume decreases. [1-5]. Red cells are red-orange in color and make up about 45% of the blood. They are produced continuously in the hematogenous marrow from stem cells. [4-6]. The red blood cells play an important role in the transport of oxygen from lungs to tissue level and in taking up the carbon dioxide, which will be transported to the lung, where it will be eliminated. The red blood cells do not have a nucleus; their membranes are flexible and can stretch in several directions without breaking. Their number may change, it may increase or decrease and may be of a physiological or pathological nature. [6-9]. The color of the blood is conditioned by the amount of hemoglobin found in the blood cells and which, following centrifugation of the blood, separates as erythrocyte concentrate in a 33 ÷ 37% yield. Generally, erythrocyte concentrate contains 65% water, 33% protein (hemoglobin) and 1% mineral salts. [10-14].

### **Experimental**

Horse blood (HB) was sampled from the carotid vein, lamb's (LB) was sampled from the jugular vein. Cow's blood (CB) was sampled from the mammary gland. Pig blood (PB) was sampled from the veins in the ears. Chicken blood (ChB) was sampled from the radial vein after poultry slaughter. Dog blood (DB) was sampled from the animal's cephalic vein. Human blood (HB1-HB7) was sampled intravenously and capillary from the finger pulp from 7 patients of various blood groups. After sampling, the blood was allowed to coagulate completely at room temperature, followed by the removal of serum and clot. Determination of serum amylase, bilirubin, cholesterol (total, HDL, LDL), triglycerides, alanine aminotransferase, aspartate aminotransferase and uric acid involves firstly to prepare the patient, then intravenous sampling and separation in an anticoagulant vacutainer using a separating gel, then centrifuging the analyzed sample to separate the serum. The diluted serum

(about 0.5 mL) separated in this way was analyzed. UV-VIZ analysis was performed with a Perkin Elmer, Lambda 25 spectrophotometer. The blood sample was diluted in a ratio of 1:1000 and then the spectra were recorded in the visible range of 400-700nm.



Figure 1. Stages of blood analysis: A) sampling; B) centrifugation; C) analysis

### Results and discussion

Figure 2 presents the UV-VIZ spectra of animal blood assortments: horse (HoB), lamb (LB), cow (CB), pig (PB), chicken (ChB), dog (DB) and human blood (HB). In the literature [13], the maxima at 542 nm and 576 nm are attributed to oxyhemoglobin. It is observed that the first peak of dog blood and horse blood (548 nm and 546 nm) respectively shows a slight bathochromic shift characterized by a darkening of color. In the cow blood (541 nm), pig blood (539 nm) and human blood (541 nm) there is a hypsochromic shift. The second maximum, the horse blood (590 nm), lamb blood (584 nm), cow blood (579 nm), pig blood (582 nm), cow blood (578 nm) shows a bathochromic shift compared to literature [13]. The composition of oxyhemoglobin in human and animal blood is similar, with a small difference of up to 6 nm.

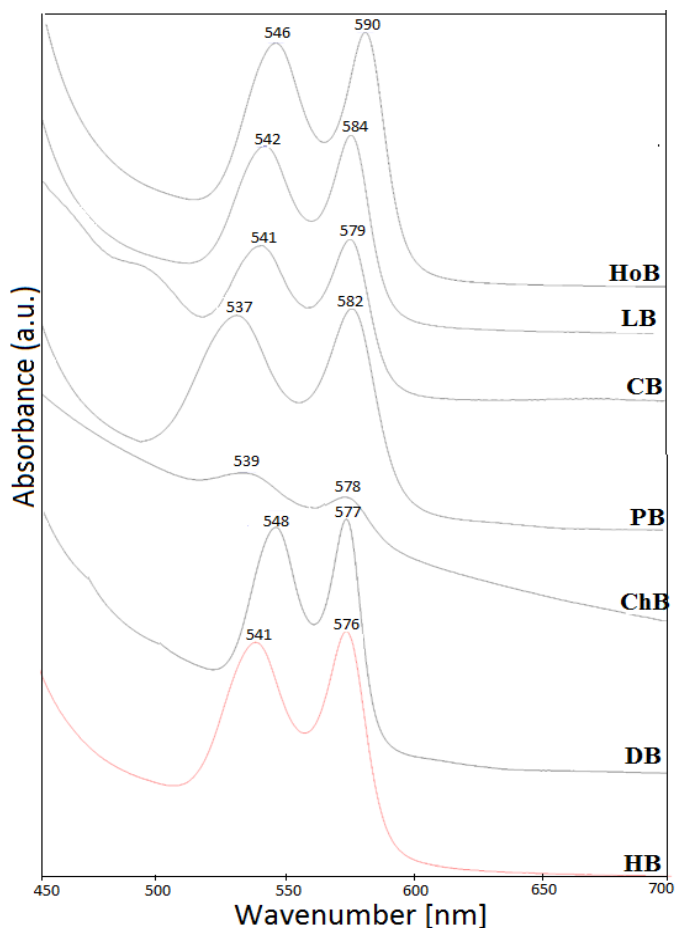


Figure 2. UV-VIS spectra of animal and human blood samples

Serum amylase belongs to the category of hydrolases, enzymes that catalyze the hydrolytic degradation of starch, glycogen, poly- and oligosaccharides.

Figure 3 (left) shows the values obtained for the 6 animal species and an arithmetic mean for the seven human patients. Values in humans are very close and relatively small in the normal range of 15 - 100 U / l. Pig blood was found to have a very high amylase value (14-fold than the upper normal limit). Large amounts of amylase can cause dysfunction in the body (pancreatitis, perforated peptic ulcer, pancreatic cancer) [15-17]. Bilirubin is produced by the catabolism of hemoglobin, is insoluble in water, and in the blood plasma circulates linked to the albumin serum. The oxidation of heme generates biliverdin that metabolizes bilirubin [1].

In the case of lamb and cow blood (Fig. 3 right), bilirubin do not reach the minimum value (0.25 mg / dL). Low levels of bilirubin in human blood generate dysfunctions in the body, leading to jaundice. There are no traces of bilirubin in the chicken blood. Conjugated bilirubin, water-soluble, reacts with diazotized sulfanilic acid in acidic or neutral media to form a red colored complex.

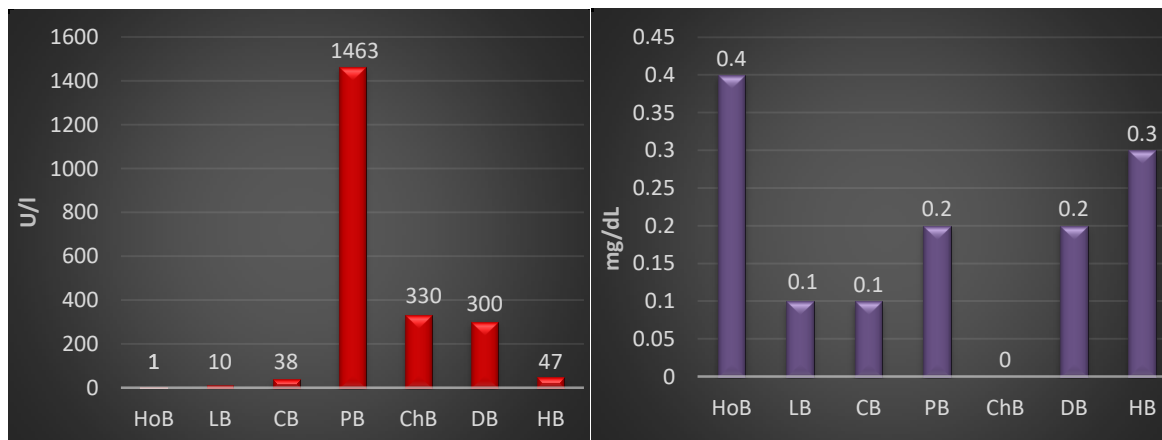


Figure 3. Variation of serum amylase (left) and bilirubin amylase (right) depending on blood type

Cholesterol ( $C_{27}H_{46}O$ ) is a sterol-based alcohol identified in the cell membrane and body tissues and transported in the blood. Total cholesterol should be between 110-220mg / dL. HDL (high density lipoprotein) ranging from 35 to 60 mg / dL. LDL (low density lipoprotein) the so-called "bad" cholesterol should be between 0-130mg / dL.

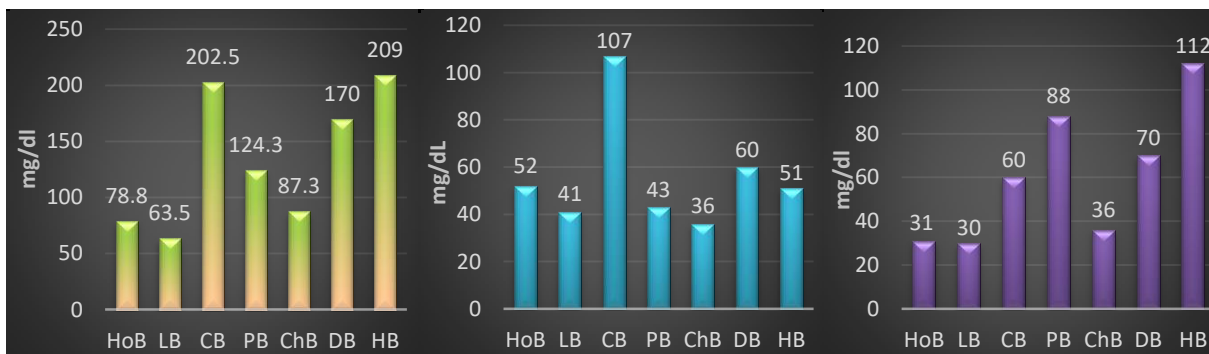


Figure 4 Variation of total cholesterol (left), HLD-cholesterol (middle) and LDL-cholesterol (right) depending on the type of animal blood and human blood

Total cholesterol in humans (Fig. 4) slightly exceeds the upper limit, which can cause cardiovascular disease: risk of arteriosclerosis, coronary stenosis, myocardial infarction. Values below the minimum total cholesterol level found in horse, lamb and chicken's blood may cause malnutrition, hyperthyroidism, infections. The highest HDL-cholesterol value was found in cow's blood, and the lowest value was found in chicken's blood. The lowest amount of HDL-cholesterol results in hyporalphalipoproteinemia, chronic hepatopathy, anorexia, and at high levels cause hyperalphaproteinemia, arteriosclerosis. All blood types fall within the allowable limits for LDL-cholesterol. Excessive hypertension may cause hypercholesterolaemia, hyperlipoproteinemia, hypothyroidism, diabetes mellitus, cholestasis,

chronic renal failure, anorexia and low values cause hypolipoproteinemia, hyperthyroidism, chronic anemia, severe hepatocellular disease, acute stress, pulmonary diseases [15 - 17].

Triglycerides in adipose tissue and other tissues are the most important storage of energy reserves in the body. Normal values range between 40-140 mg / dL. Cow blood is below the minimum, and human, chicken and dog blood above the permissible limit (Fig. 5). Variations in human blood samples were also found, shown separately in Figure 5.

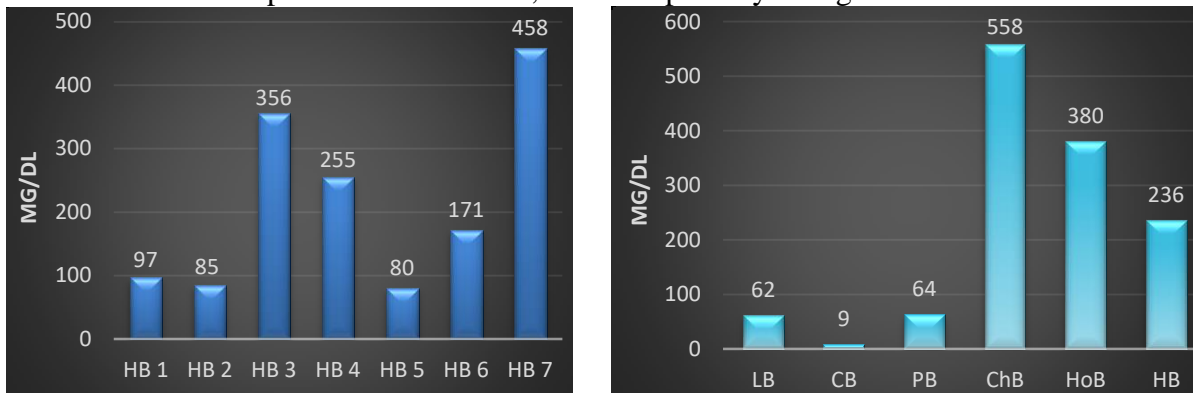


Figure 5 Triglyceride variation depending on human blood samples (left) and animal blood samples depending on human blood mean HB (right)

Alanine aminotransferase or glutamyl transaminase is an enzyme that is part of the transferase class and catalyzes the reversible transfer of the amino (NH<sub>2</sub>) group from an α-ketoglutarate amino acid (alanine) resulting in the formation of pyruvic acid and glutamate. It is found in the liver, kidney, myocardium, pancreas. Normal values are considered between 0-40 U / l, only pig blood exceeds this limit (Fig. 6). Exceeding the maximum values can cause acute hepatitis, cirrhosis and alcoholism [15-17].

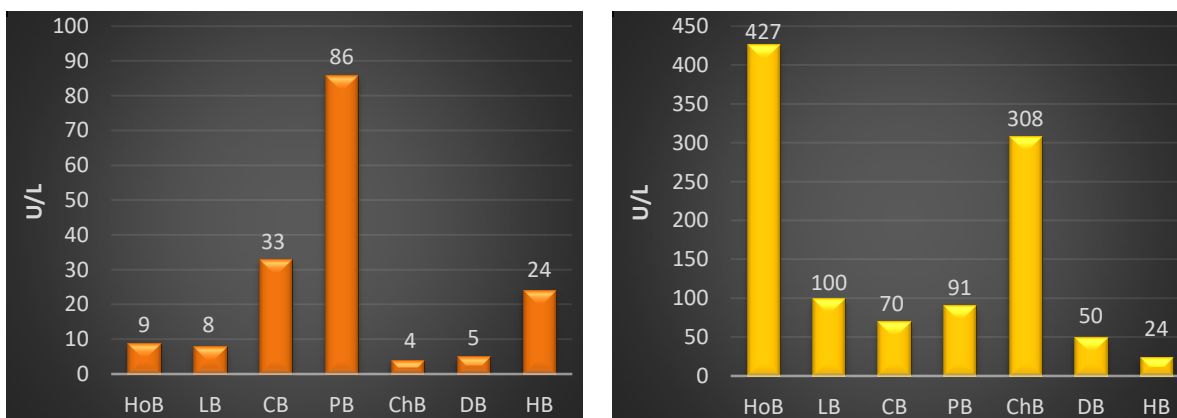


Figure 6. Variation of alanine aminotransferase (left) and aspartaminotransferase (right) depending on the type of animal blood and the mean value of human blood.

Aspartate aminotransferase is an enzyme that is part of the transaminase class and catalyzes the transfer of the amino group from aspartate to the ketone ketoglutarate group, with the formation of oxalocetic acid [10,11]. Limit values are between 0-35 U / L, only human blood falls within this limit (Fig. 6 right), the highest values being observed in horse blood and then in chicken. Values above the maximum may result in hepatic necrosis, CHCl<sub>3</sub> intoxication, and low values lead to chronic kidney dialysis [15-17].



Uric acid results from the degradation of nucleic acids, the ultimate product of purine metabolism. From the liver, it is transported by plasma to the kidneys, where it is filtered and excreted on about 70%. The uric acid residue is eliminated and degraded in the gastrointestinal tract. Normal uric acid values are between 2.5-7.0 mg / dL. All animal blood samples analyzed, apart from human blood and chicken, contain an amount of uric acid less than the admissible limit (Fig. 7 right). There is a rather large variation between the blood from different individuals (Fig. 7 left). Very high uric acid levels lead to kidney failure, gout, asymptomatic hyperuricemia; very low values lead to Wilson's disease [15-17].

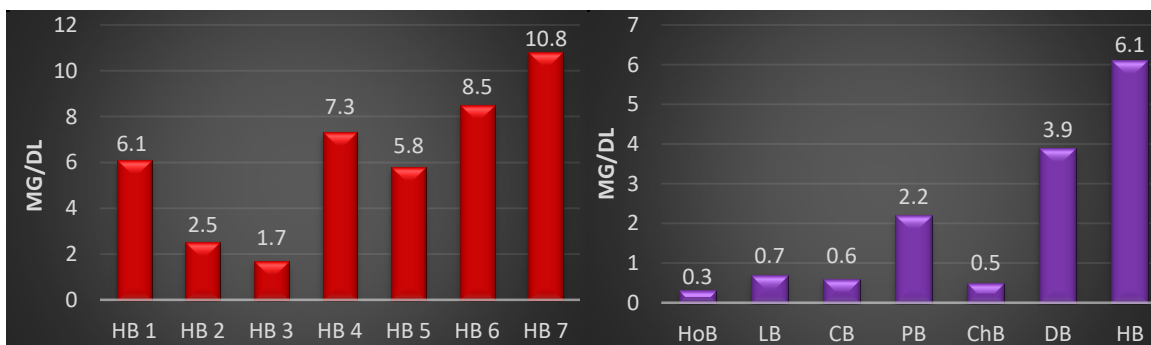


Figure 7 Variation of uric acid depending on human blood samples (left) and animal blood samples depending on the mean of human blood SO (right)

## Conclusion

UV-VIZ spectrophotometric analysis showed that oxyhemoglobin has two maxima in the 539-548 and 576-590 nm ranges, very close at all blood samples studied for both animal and human blood samples. The serum amylase in pig blood is very high. Bilirubin in the blood of the human samples is normal, while in lamb and cow blood is very small. Total cholesterol is within the normal range in human samples. Low concentrations of total cholesterol were found in the horse, lamb and chicken blood. In the chicken blood sample was found a high triglyceride concentration. The highest value of alanine aminotransferase was found in pig blood and the lowest in the chicken and dog blood. High concentrations of aspartat-aminotransferase were found in animal blood samples above the admissible limit for human blood. The highest concentration was found in horse blood while the lowest was in human blood followed by dog blood. Uric acid in all animal blood types except human and chicken blood has a very low concentration.

## References

- [1] D. Bedeleanu, I. Manta, Medical and pharmaceutical biochemistry, Cluj-Napoca, 1985.
- [2] G. Daniels, Human Blood Groups, 3<sup>rd</sup> edition, Wiley-Blackwell, 2013
- [3] F. Fischbach, Blood Studies, Lippincott Williams & Wilkins, USA, 8 ed. 2009, 179.
- [4] P. Jitariu, Animal and human physiology, Ed. didactică și pedagogică, București, 1970
- [5] K.M. Van De Graaf, S.I. Fox, Concepts of Human Anatomy and Physiology, Wm. C. Brown Publishers, Dubuque, USA, 1995.
- [6] I.C. Petricu, I.C. Voiculescu, Human anatomy and physiology, Ed Med București, 1967.
- [7] G.T. Dornescu, O.C. Necrasov, Comparative anatomy of vertebrates, vol. I, București, Ed. didactică și pedagogică, 1968.
- [8] E. Chenzbraun, C.A. Picoș, Course on human anatomy and physiology, vol. I, București, Litografia Universității, 1969.

- [9] G. Benetato, Elements of normal and pathological physiology, vol I-II, București, 1960.
- [10] F. Fischbach, In A Manual of Laboratory and Diagnostic Tests. Lippincott Williams & Wilkins, USA, 8ed., 2009, 412, 1225, 420, 1255, 457.
- [11] T. Dippong, C. Mihali C, Instrumental analysis techniques used in the food, chemical and environmental industries, Risoprint, Cluj-Napoca, 2017.
- [12] I. Motrescu, S. Oancea, A. Rapa, A. Airinei, Spectrophotometric analysis of the blood plasma for different mammals, Romanian J. BIophys., 16(3), (2006) p 215.
- [13] Stryer, Lubert Biochemistry, 4th Ed. W H Freeman & Co, New York, NY, 1995.
- [14] W.Gzjlstra, Spectrophotometry of Hemoglobin (1997)743.
- [15] J. Wallach, Blood analyzes,. Editura Științelor Medicale, România, 7 Edition, (2001) 5.
- [16] J. Wallach, Hepatological and pancreatic disorders.Științelor Medicale, 7 (2001) 49, 273.
- [17] Synevo Laboratory, References specific to the working technology used 2010.

## OBTAINING AND CHARACTERIZATION OF VANILLA ESSENCE FROM MADAGASCAR'S BOURBON PODS

**Thomas Dippong<sup>1</sup>, Pauliuc Ivan<sup>2</sup>, Cristina Mihali<sup>1</sup>, Bianca Tintas<sup>1</sup>**

<sup>1</sup> Technical University of Cluj-Napoca, North University Center of Baia Mare, Department of Chemistry and Biology, 76 Victoriei Street, 430122 Baia Mare, Romania

<sup>2</sup> University of Agricultural Sciences and Veterinary Medicine of Banat, 300081, Timisoara  
e-mail: dippong.thomas@yahoo.ro

### **Abstract**

The paper presents the steps of extracting vanillin from pods of the Bourbon vanilla species in Madagascar. Subsequently, the obtained vanilla extract containing vanillin was characterized in terms of chemical and spectrophotometric properties. The methods of analysis used were UV-VIS spectrophotometry, FT-IR spectrophotometry, mass spectrometry and nuclear magnetic resonance by <sup>13</sup>C-NMR and <sup>1</sup>H-NMR techniques. In the last part of the paper some applications of the obtained vanilla essence are presented.

### **Introduction**

*Vanilla planifolia* is part of the Orchidaceae family, being a hanging and perennial plant, specific and native to tropical rainforest in Mexico but it grows also in Madagascar, Tahiti, Indonesia, Seychelles and the Philippines [1-3]. *Vanilla planifolia* is the main orchid species used to produce vanilla [4]. Vanilla is a tropical perennial plant with very long leaves and stalks, with a height of 10-15 m. It blooms 2-3 years after planting, many years in a row, and from yellow-green flowers, with a diameter of 5 cm, which lasts only one day and must be manually pollinated. After pollination, vanilla pods are formed [5-8]. The vanillin concentration of the fruit is between 1.3-3%. "Bourbon" vanilla produced in Madagascar, contains beside vanilline, cinnamic acid and esters; p-cresol and methyl ethyl; guaiacol; benzoyl benzoate and caprylate capronate [2]. Vanillin can be synthesized using as raw material eugenol or coniferin. Eugenol is a source of cheaper raw material for vanillin synthesis that is found to be 70-90% in the ethereal oil obtained by the water-vapor distillation of *Eugenia caryophyllata* as a matter much more accessible than coniferin [9-11]. The use of vanillin in the perfumer and food industries was a natural consequence of its discovery in vanilla seeds, much used in the flavoring of various foods. Vanilla is one of the most popular flavors, the most precious spice in the world, not only because it is expensive but also because it offers a special flavor [12-14]. Commercial vanilla extracts are obtained by macerating a portion of vanilla seeds in ten parts of 40-50% ethyl alcohol. Although vanillin is the active principle of vanilla seeds, the total vanilla extract flavor is not only due to the presence of vanillin, but also to other ingredients, especially some little known residual materials, which have a significant contribution to the quality of vanilla flavor [15]. Incorporating the vanillin into ethyl cellulose plastics ensures their stability at exposure to the atmosphere [6, 16].

### **Experimental**

The vanilla pods are ripped and then cut into 4-5 cm pieces. This operation is important because the pods must be perfectly covered with alcohol and the bottle should be shaken daily in the first month. The vanilla pods thus prepared are placed in a glass container, over which alcohol is added, then the bottle is hermetically sealed and stored in a dark place. In the first

month, you need to shake the bottle well, at least once a day. After the first month, the bottle can be shaken just once a week. After 2 months, the essence can be used, but the final flavor develops only 9 weeks after the start of the extraction. With the passage of time the essence turns dark until it becomes almost black. To remove any vegetal residue in the essence, it is filtered through a paper filter. The essence doesn't alter its properties through time, it can be used indefinitely. Figure 1 shows the transformation of vanilla extract during 9 weeks.

On the first day, only a transparent solution with pods and a strong odor of alcohol is noticed. After the first week after the daily shake of the extract a slight coloration is observed, the pods begin to decompose into small black particles, the smell being similar with the one from the first day. After two weeks, a slight color appeared, the pods begin to decompose into small black particles, the odor remaining the same. Only after 4 weeks the vanilla smell appears, and the color darkens. After six weeks, the color darkens even more and the vanilla smell intensifies. After 9 weeks, the final coloring is formed and the vanilla essence is obtained. The solution is filtered and it can undergo characterization.



Figure 1. Steps of obtaining vanillin essences

The UV spectra of the synthesized acetylsalicylic acid samples were recorded on Lambda 25 Perkin Elmer spectrophotometer after dissolving of sample in 0.1 N NaOH. The FTIR spectra of the synthesized acetylsalicylic acid were acquired using a Spectrum BX II (Perkin Elmer) spectrometer on 1% KBr pellets. Mass spectra were recorded on a R.F. Quadrupolar Mass Spectrometer. NMR spectra were recorded on a Bruker Fourier 300 FT-NMR apparatus against the line of the solvent ( $\text{CDCl}_3$ ). Chemical shifts are expressed in ppm.

## Results and discussion

After obtaining the vanilla essence it was subjected to spectrophotometric analyzes. The vanilla essence was diluted with distilled water in a ratio of 1: 10000, then the spectra was recorded using the UV-VIZ molecular UV spectrophotometer in the ultraviolet range between 200-400 nm. In the UV-VIS spectrum (Fig. 2 left), the maximum of absorbance was observed at 348 nm, characteristic of vanillin [17].

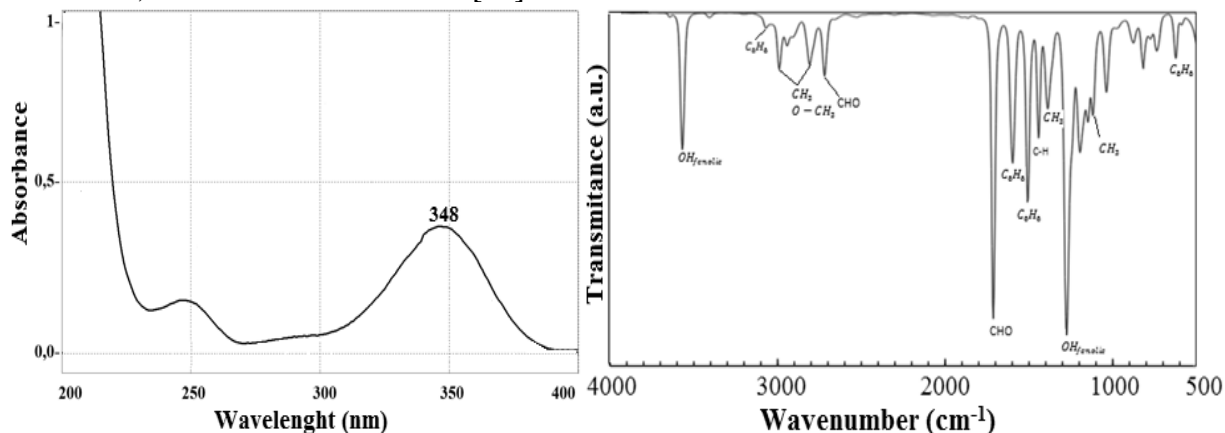


Fig. 2. The UV spectrum (left) and the FT-IR spectrum (right) of the obtained vanillin

In Figure 2 (right), the FT-IR spectrum of vanilla essence is shown. The presence of functional groups in the vanillin structure is attributed to the frequency bands of the C = O bond in the aldehyde group at  $1720\text{ cm}^{-1}$  and  $2720\text{ cm}^{-1}$  respectively [18]. The hydroxy-phenolic group shows a sharp frequency band at  $3620\text{ cm}^{-1}$  and intense deformation band at  $1260\text{ cm}^{-1}$  [18]. The methoxy group ( $\text{OCH}_3$ ) can be identified by the asymmetric vibration band C-H at  $2980\text{ cm}^{-1}$  and symmetrical from  $2870\text{ cm}^{-1}$ , vibration band of valence bond at  $1380\text{ cm}^{-1}$  of the C-O, and less intense at  $1045\text{ cm}^{-1}$  attributed to the vibration band of the C-H bond [18]. The aromatic nucleus is visible in the FT-IR spectrum by the vibration band C-H of the aromatic nucleus at  $3010\text{ cm}^{-1}$ ,  $1600\text{ cm}^{-1}$ , at  $1506\text{ cm}^{-1}$  more intense; and the broad and weak in intensity bands at  $950\text{ cm}^{-1}$  and  $700\text{ cm}^{-1}$  [18]. Substitution 1,2,4 characteristic to vanillin is attributed to deformation vibration out-of-plane of the C-H bond from the ortho-disubstituted benzene nucleus at  $860\text{-}900\text{ cm}^{-1}$  [18].

Figure 3 shows the MS spectrum of vanilla essence. It is observed that the molecular peak overlaps the base peak, and the molecular weight 155, which corresponds to vanillin, can also be deduced from the spectrum.

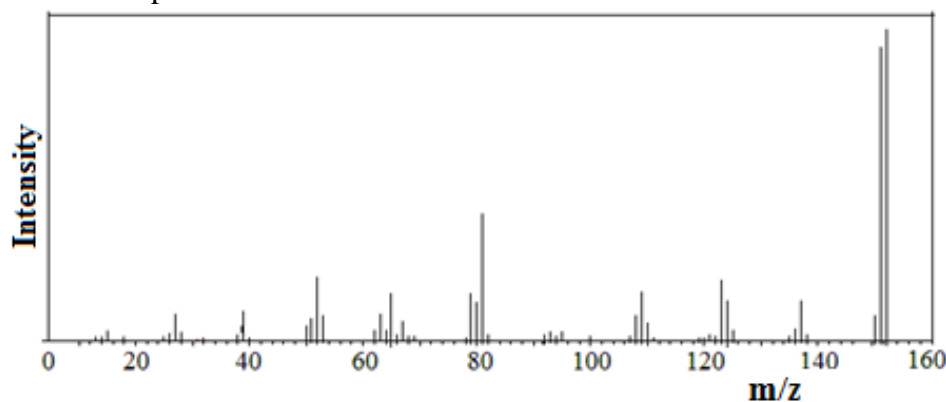


Figure 3. MS spectrum of vanilla essence.



Figure 4 shows the  $^1\text{H}$ -NMR spectrum for the vanillin essence, the hydrogen line in the CHO group of the H singlet is assigned at 9.8 ppm, the very strong singlet of the hydrogen in the methoxy group (ether) is at 3.9 ppm. From a qualitative point of view,  $\text{OCH}_3$  contains three H atoms for which the  $\text{OCH}_3$  singlet line is three times larger than the CHO and OH singlets. The  $\text{H}_3$  singlet line of the hydroxy group would normally be in the range of 0.7-5.5 ppm; but since it binds to the aromatic nucleus it moves to 6.6 ppm. On the aromatic nucleus, we have three unsaturated hydrogen atoms (one singlet and two doublets). The doublets have two electronegative groups in the neighborhood. Although the two groups (substance of order I and substance of order II) are different in the H-NMR spectrum, only one signal is observed which includes both doublets. The hydrogen singlet on the aromatic nucleus located between two active functional groups has a greater chemical shift than the other two doublets on the aromatic nucleus [18].

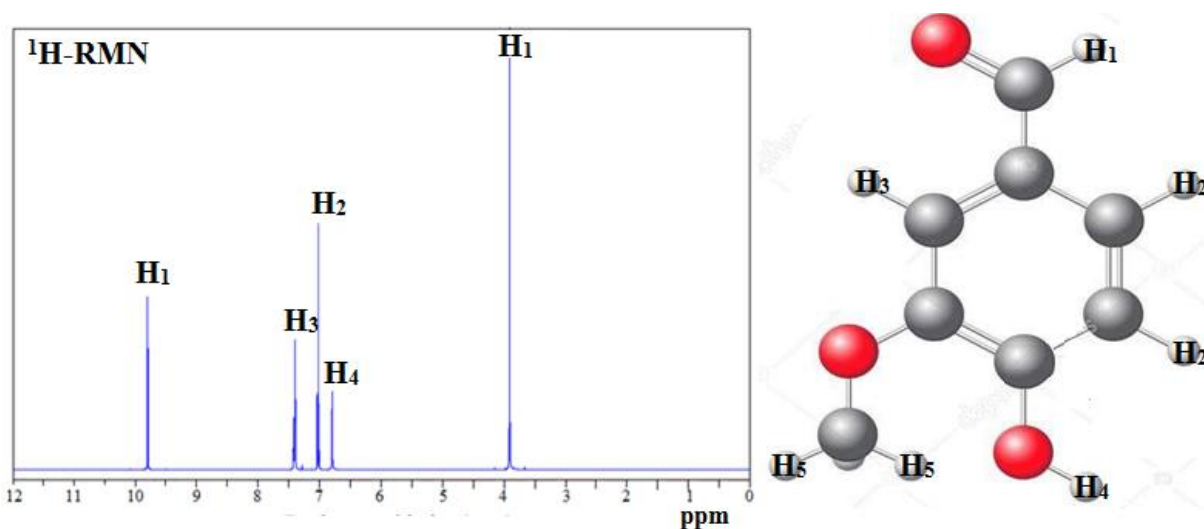


Figure 4.  $^1\text{H}$ -NMR spectrum of vanillin essence

Figure 5 shows the  $^{13}\text{C}$ -NMR spectrum of vanillin essence. The largest chemical shift is due to the carbon atom of the carbonyl group at 192 ppm, and the lowest chemical shift of 55 ppm is attributed to the carbon of the methoxy group. Carbon atoms appear in descending order of their reactivity in pair with the decreasing chemical shifts. The  $\text{C}_5$  and  $\text{C}_2$  carbon atoms bond to reactive groups and have greater chemical displacement than  $\text{C}_7$  and  $\text{C}_6$  carbon atoms which are further away from the reactive groups but are larger than  $\text{C}_3$  and  $\text{C}_4$  [18].

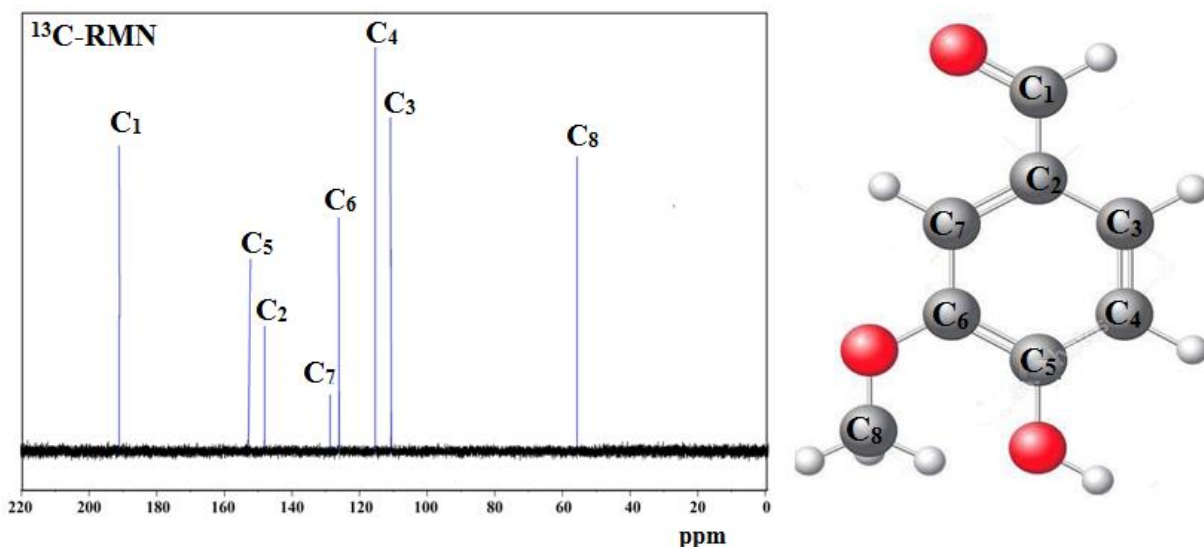


Figure 5.  $^{13}\text{C}$ -NMR spectrum of vanillin essence

Vanilla extract can be used as an aromatic ingredient for food, alcoholic beverages (liqueurs, creams) and soft drinks, dairy products (ice cream and yoghurt), sweets, pastries and confectionery (cakes, puddings, creams).

### Conclusion

House made vanilla was obtained by extraction after 9 weeks, during which, differences in the color of extracts were found. The vanillin in the vanilla extract (vanilla essence) was identified by UV-VIZ spectroscopy by the maximum absorption band at 348 nm and by FT-IR by the presence of the benzyl, carbonyl, hydroxy and methoxy-specific bands.

Also, mass spectra overlap with those of pure vanillin, identifying the molecular weight of vanillin of 155. In the vanilla essence obtained, more intense H-NMR lines are found compared with the pure vanillin. The C-NMR lines of pure vanillin essence are overlapping in most cases with the vanilla essence lines.

### References

- [1] E. Pooper, L. Roman, R. Crăciuneanu, *Chimie analitică cantitativă*, Editura Didactică și Pedagogică București, 1965.
- [2] V. E. Ceausescu, G. Radoias, T. Cadariu, *Odorante și aromatizante-Chimie tehnologie și aplicații*, Editura Tehnică, București, 1988.
- [3] L. Cao, K. Hu, *Detarminarea vanilinei din extractul de vanilie sintetică*, Institutul Pharmacol, Academia Chemică, Shanghai, R.P. Chineza, 1983, 38.
- [4] L. Savici, *Aparate de analiză fizico-chimică*, Editura Tehnică, București, 1980.
- [5] W. Brockel, I. Gatfield, *Vanillin*, Contact, 4, 1997, 16.
- [6] T. Dippong, *Obținerea, caracterizarea și utilizările aditivilor alimentari*, Editura Risoprint, Cluj-Napoca, 2016.
- [7] R. Kumar, P. K. Sharma, P. S. Mishra, *A Review on the Vanillin derivatives showing various Biological activities*, International Journal of PharmTech Research, 4 (2012) 266.
- [8] Z. Wong, K. Chen, J. Li, *Formation of vanillin and syringaldehyde in an oxygen delignification process*, BioResources 5(3) (2010) 1509.



- [9] J. Kerler, R. Verpoorte, Vanilla Production: Technological, Chemical, and Biosynthetic Aspects, *Food Reviews International*, 17 (2) (2001) 119.
- [10] K.J. Edgar, S.N. Falling, Synthesis of vanillin. *J.Org.Chem*, 55 (1990) 5287.
- [11] T. Li, J. P. N. Rosazza, Biocatalytic Synthesis of Vanillin, *Appl Environ Microbial*, 66(2) (2000) 684.
- [12] M. Mitrescu, *Chimie analitică cantitativă*, Editura Institutului Politehnic Timișoara, 1955
- [13] P Suppakul, T. Jinkarn, Antimicrobial effects of vanillin coated solution for coating paperboard intended for packaging bakery products, *J. Food Ag-Ind.* 2 (2009) 138.
- [14] A.I. Badea ,Aplicații ale spectrometriei UV-VIS în chimia analitică, Ed.Didactică și Pedagogică R.A., București, 2006.
- [15] S. Oprea, *Tehnologie Chimică Organică - Îndrumar de laborator*, I.P.I, Iași, 1986.
- [16] B. Toulemande, I. Horman, H. Egli, Diferențierea între vanilina sintetică și cea naturală, doar folosind deuteriu NMR. *Hel. Chem. Acta*, 66(7) (1983) 2342.
- [17] T. Dippong, C. Mihali, *Tehnici avansate de analiză instrumentală utilizate în industria alimentară chimie și mediu*, Editura Risoprint, Cluj-Napoca, 2017
- [18] A.T.Balaban, M. Banciu, I Pogany, *Aplicații ale metodelor fizice în chimia organică*, Editura științifică și enciclopedică, București, 1983

## ANALYSIS OF ASIMILATING PIGMENTS BY MONO AND BIDIMENSIONAL THIN LAYER CHROMATOGRAPHY TECHNIQUE

Cristina Mihali<sup>1</sup>, Thomas Dippong<sup>1</sup>, Pauliuc Ivan<sup>2</sup>, Angelica Berindan<sup>1</sup>

<sup>1</sup> Technical University of Cluj-Napoca, North University Center of Baia Mare, Department of Chemistry and Biology, 76 Victoriei Street, 430122 Baia Mare, Romania

<sup>2</sup> University of Agricultural Sciences and Veterinary Medicine of Banat, 300081, Timisoara  
e-mail: dippong.thomas@yahoo.ro

### Abstract

Considering the major importance of chlorophyll, it was chosen as the subject of this study, the extraction, separation and identification by chromatographic methods of chlorophyll types, assimilating pigments that accompany chlorophyll and chlorophyll degradation products from extracts of selected plants. The paper presents the chromatographic method for the separation of the chlorophyll pigments, focusing on the two-dimensional chromatographic technique, extraction and separation of the components of the vegetal extract and interpretation of results.

### Introduction

Two-dimensional chromatography is a method applied for qualitative analysis, using a square plate on which a single spot is applied in the lower right corner, eluted with the first solvent or mixture of solvents, obtaining a first separation, and after drying, the plate rotates at an angle of 90 ° and a new elution is started with another solvent, after which the plate is compared to a standard plate on which we have a known mixture [1-4]. By two-dimensional chromatographic technique, the separation of chlorophyll (a and b) as well as other assimilating pigments extract from green leaves can be highly improved. Extracts of plants rich in chlorophyll (spinach, dill and nettle) were obtained and analyzed by thin layer chromatography using mono and two dimensional techniques. Also, chlorophyll c that is found in inferior plants was separated by monidimensional thin chromatography. Spinach (*Spinacia oleracea*) is grown for the leaves which besides the high content of chlorophyll are a source of folic acid, vitamins (B1, B2, B6, C, E, K, and PP) iron, carotene, carbohydrates and lutein. Dill (*Anethum graveolens*) has a rich content of volatile oils, mineral salts (Ca, Fe, Mg, P, K, Na, Zn, Cu, Mn). Common nettle (*Urtica dioica*) is beneficial due to detoxification and regeneration of the body [5-6]. The therapeutic properties are due to an abundance of bioactive substances with a high content of mineral salts (iron, magnesium, calcium, potassium and silicon). Spirulina (*Arthrospira platensis*) is a green-bluish microscopic alga that grows in tropical lakes [7]. Its color is due to the blue pigment that together with the chlorophyll form this color. Spirulina is an extremely rich antioxidant food containing 26 times more calcium than milk, protein, amino acids. It is a polyvitamin, contains liposoluble and water-soluble vitamins such as beta-carotene, vitamins B1, B2, B12, C, E, folic acid, nicotinic acid, vitamin H-biotin [6-10].

### Experimental

Vegetal material of spinach, dry dill and dry nettle were used for extraction. 5 large leaves of plant material are triturated with 1 g of quartz sand and 0.5 g of calcium carbonate to neutralize its acidity (Fig. 1). The ground vegetable material is placed in a Berzelius beaker

and is supposed to extraction with 10 mL solvent prepared by mixing benzene: methanol in a ratio of 6: 4. Then, the mixture of vegetable matter and solvent is heated on the water bath for 5 minutes and filtered. In the case of other green plants, the volume of extraction solvent can be doubled, maintaining the proportion of components. If the filtrate is not sufficiently separate, it is centrifuged, then heated on the water bath for 5 minutes and filtered (Fig. 1).

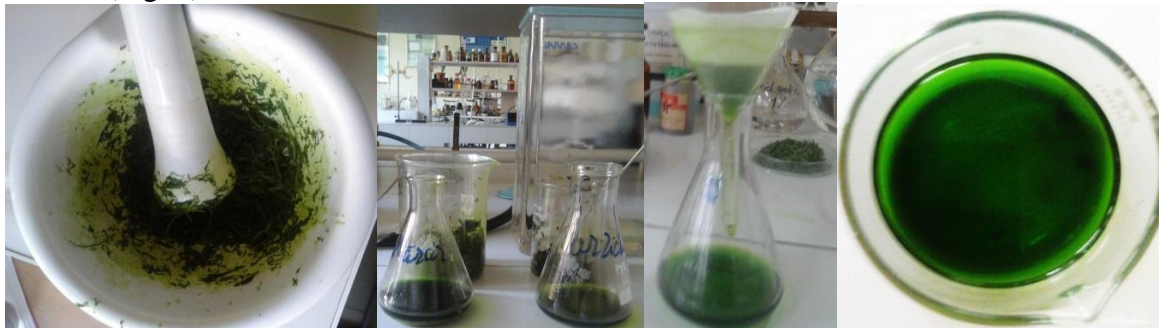


Figure 1 Extraction stages for obtaining extracts of spinach, dill, nettle and spirulina

For the chromatographic separation of the chlorophylls and assimilating pigments, a spot is applied on the chromatographic paper using a Pasteur pipette. In two dimensional-thin layer chromatography technique, the spot must be applied at the starting line in a corner of the chromatographic plate. This is achieved by joining two lines at an angle of  $90^\circ$  in the lower left corner at a distance of 2.5 cm from the edge of the chromatographic plate. Plates will be introduced into a separation chamber that is a glass parallelepiped-shaped container, covered with a lid, ensuring a saturated atmosphere in the vapor of liquid phase (eluent solvent). The mobile phase has to be introduced in the separation chamber 30 minutes prior to the introduction of the chromatographic plate. The development system 1 consists of a mixture of gasoline: petroleum ether: acetone in a volume ratio of 50: 12.5: 2. In the first direction, the separation will take place of chlorophyll a (blue bluish stain), chlorophyll b (greenish yellow), xanthophyll (yellow spots), degradation products of chlorophyll (gray spots) and beta-carotene at the highest point (Fig 2 left). Development is considered to be completed when the solvent front has reached 1 cm from the top edge of the chromatographic paper. After development, the plate is air dried, marked the center of the pigment point, measured the distance traveled by the solvent front ( $X_D$ ) and the distance traveled by each pigment ( $X_s$ ) (Fig. 2). The Retardation factors ( $R_f$ s) are then calculated. In the next step, the plate is rotated at a  $90^\circ$  angle and develop the solution 2, which is a mixture of 4 components: gasoline: petroleum ether: acetone: methanol in a volume ratio of : 50: 12.5: 5: 2.5 gasoline: separating chlorophyll a (bluish green) of chlorophyll b (greenish yellow) and xanthophyll (yellow).

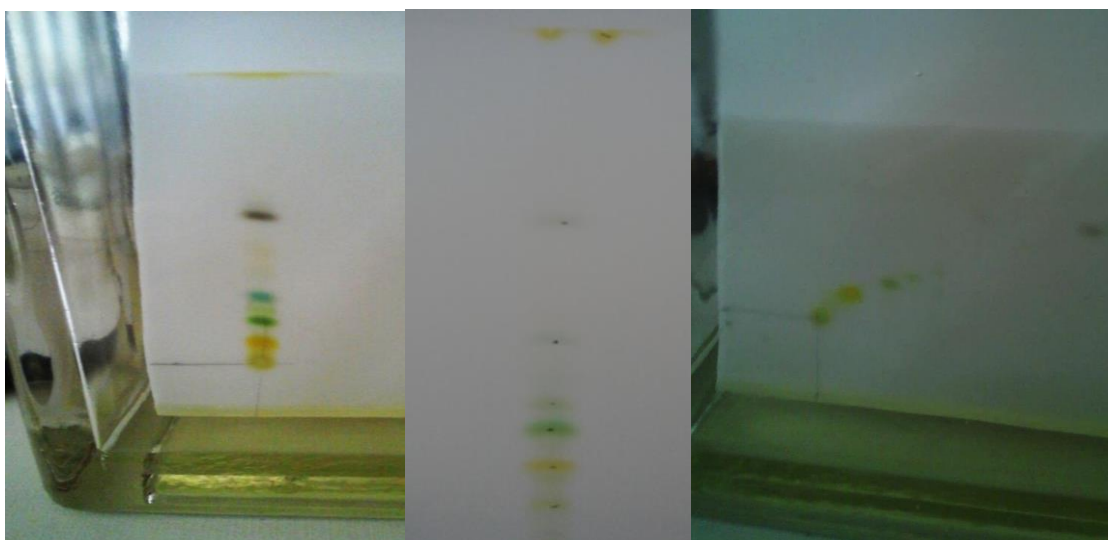


Figure 2. Developing, marking the spots, measuring  $X_d$  and  $X_s$ , developing in solution 2  
In spirulina extract, besides chlorophylls a blue-green spot that was separated. It can be attributed to phycocyanin belonging to the group of phycobilin assimilating pigments. Thus, a comparative separation was performed, an extract of a higher plant and spirulina extract (obtained of spirulina powder), which is part of the group of algae. One gram of spirulina is mixed with 80% acetone, left in the dark overnight at  $4^\circ\text{C}$  for complete extraction. The extract obtained by centrifugation for 5 minutes is subjected to separation by one-dimensional chromatography on a silica gel plate. The chromatographic plate was developed with a solvent composed of petrol: petroleum ether: acetone in the same ratio as solvent 1. After development, the corresponding pigments are identified by the color and position of the obtained points. It was marked the center of the point of each pigment and calculated the value of the  $R_f$ s.

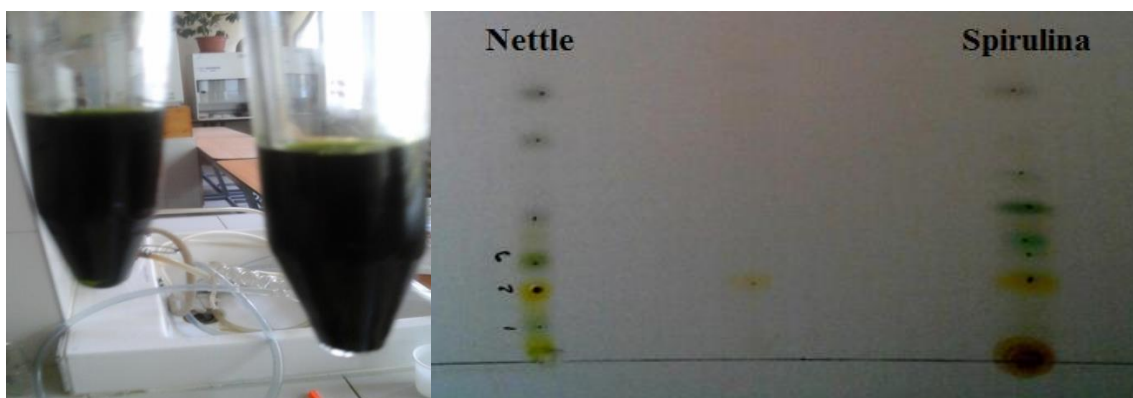


Figure 3. Spirulina extract and the chromatogram of spirulina compared to nettle extracts

### Results and discussions

Chromatogram must be read immediately after the chromatographic paper has dried of, as it discolors immediately if it is exposed to light.  $R_f$ s are calculated. The maximum  $R_f$  value was obtained for carotene, with the highest yellow spot. For the other spots, the center of the pigment and the solvent front will be marked.  $R_f$ s are calculated using formula 1. Vegetable extracts have been used with different degrees of freshness: spinach, nettle and dill. Following development with solvent 1, composed of: petrol: petroleum

ether: acetone for 30 min, the following values of retardation factors (Rf) were obtained, shown in Table 1. By applying a spot of the extracted material from the vegetal mass on the chromatographic paper, it was identified by two-dimensional chromatography, chlorophyll a, chlorophyll b, carotene, xanthophyll and phytol resulting by the degradation of chlorophyll.

$$Rf = \frac{\text{Distance from Baseline travelled by Solute}}{\text{Distance from Baseline travelled by Solvent (Solvent Front)}} = \frac{X_S}{X_D} \quad (1)$$

Table 1. Rf values on TLC separation on silica gel plates of spinach, nettle, dill extracts - bidimensional method, (development with solvent 1; time: 30 minutes)

<b>Rf values for different vegetal materials</b>			
<b>Identified component as spot/ Rf value</b>	Spinach, fresh X <sub>D</sub> =12cm	Nettle ,dehydrated X <sub>D</sub> =15cm	Dill, dried X <sub>D</sub> =13,5 cm
<b>Beta-carotene</b>	0.93	0.83	0.85
<b>Chlorophyll degraded</b>	0.61	0.43	0.49
<b>Chlorophyll a</b>	0.28	0.20	0.25
<b>Chlorophyll b</b>	0.26	0.13	0.16
<b>Xantophile</b>	0.17	0.07	0.07

By rotating on a 90° angle the line after which the decomposition of chlorophyll into the component elements is achieved, it will become a starting line for of a new development. Another solvent, named solvent 2 with the following composition: benzene, petroleum ether, acetone and methanol was used to as mobile phase during 30 minutes. The Rf values for spinach, nettle and dill are shown in Table 2.

Table 2. Rf values at separating on silica gel plates of spinach, nettle, dill extracts by two-dimensional method with solvent 2 (development time: 30 minute)

<b>Rf values for different vegetal materials</b>			
<b>Identified component as spot/ Rf value</b>	Spinach, fresh (X <sub>D</sub> =11,8 cm)	Nettle ,dehydrated (X <sub>D</sub> =13 cm)	Dill, dried (X <sub>D</sub> =13,5 cm)
<b>Beta-carotene</b>	0.95	0.85	0.80
<b>Chlorophyll degraded</b>	0.86	0.60	0.53
<b>Chlorophyll a</b>	0.81	0.46	0.63
<b>Chlorophyll b</b>	0.67	0.35	0.42
<b>Xantophile</b>	0.51	0.24	0.19

By comparing the results of the two developments for the two solvents and the three plant species, the same types of pigments were identified for the three plant species. Beta carotene has the orange color with the highest Rf value for the three studied species. Chlorophyll a, bluish green has values close to elution 1, compared to solvent 2 with different but close values, the lowest values of Rfs being obtained at dehydrated nettle and the highest in fresh spinach. Chlorophyll b, greenish yellow in elution 1 has close Rf values. Elution 2 conducted to different values, the highest Rf in spinach, the lowest in the dehydrated nettle. Xanthophyll, a yellow spot has values close to solvent 1 and very different for solvent 2, the highest for fresh spinach and lowest for dehydrated nettle. Thus, using two-dimensional TLC chromatography, a better separation of the assimilating pigments was realized. In the second separation with solvent 2 the spots were purified removing the impurities. However, the



greatest drawback of two-dimensional TLC chromatography, when compared to other planar techniques, is its limitation to one sample per plate [11]. Unlike superior plants, spirulina contains beside chlorophyll a, b also chlorophyll c as well as phycocyanin pigments. By monodimensional chromatography, based on the color and position of the separated pigments, yellow-green chlorophyll, blue-green chlorophyll and carotenoid pigments were identified in the nettle (Fig. 3). In the same time, an extract of spirulina was analyzed where carotenoid pigments were identified as the highest orange color, gray degraded chlorophyll, blue-green chlorophyll, intense yellow xanthophyll. The Rf values of the spots are shown in Table 3. It was assumed that the dark blue and blue spots that are not present in the nettle extract, are given by phycocyanin and chlorophyll c present in the composition of the spirulina extract [12-14].

Table 3 Rf values for separation on silica gel plates, the monodimensional thin layer chromatography method of nettle and spirulina powder extracts

Identified component as spot/ Rf value	Rf values of vegetal extracts	
	Fresh nettle ( $X_D$ 10.2 cm)	Spirulina ( $X_D$ =10.2 cm)
<b>Carotenoids</b>	0.72	1.00
<b>Chlorophyll degraded</b>	0.67	0.69
<b>Phycocyanin</b>		0.37
<b>Chlorophyll a</b>	0.14	0.26
<b>Chlorophyll b</b>	0.09	
<b>Chlorophyll c</b>		0.31
<b>Xanthophile</b>	0.04	0.22

## Conclusions

In the paper, it was aimed the identification and extraction by chromatographic methods of assimilating pigments existing in the superior green plants – spinach, dill, nettle and algae - spirulina. By separating the extract, it has been observed that in green plants besides the two types of chlorophyll a and b there are significant amounts of carotene, xanthophyll, phycobilin, which play an important role in the functioning of living organisms. Another observation is that by thermal processing and under the action of extraction solvents, a significant portion of the chlorophyll is converted into degradation products. This was observed following the separation process of the components from plant extracts on the chromatographic plate. Chlorophyll type c and phycocyanin present in algae have also been identified separately. The method used for all plant species was that of mono and two-dimensional thin layer chromatography. The presence of a significant amount of beta-carotene in all green plant species studied has been highlighted. These compounds, in the body are converted into vitamin A or retinol. For this reason, it is recommended to consume green plants, which will help maintain the health of the eyes, skin, mucous membranes, maintain the level of collagen within normal limits and contribute to the normal functioning of the immune system.

## References

- 1] T. Dippong, C. Mihali, Tehnici avansate de analiză instrumentală utilizate în industria alimentară chimie și mediu, Editura Risoprint, Cluj-Napoca, 2017.
- [2] I. Jianu, E. Alexa, Cromatografia pe strat subțire în analiza și controlul produselor agroalimentare, Ed. Eurobit, Timișoara, 1998.

- [3] R. W. Scott, Principles and practice of chromatography, Library for science, 2003.
- [4] E. Lundanes, L. Reubsæet, T. Greibrokk, Chromatography: Basic Principles, Sample Preparations and Related Methods, Wiley VCH, 2016.
- [5] C.I. Milică, I. Bărbat, N. Dorobanțu, P. Nedelcu, V. Baia, Fiziologie vegetală, Editura didactică și pedagogică, București 1977.
- [6] C. Bodea, Tratat de biochimie vegetală, Partea I, Fitochimie, Editura Academiei Republicii Populare Române, 1964.
- [7] H. Albu, C. Simion, A. Simion, Determinări Fizico-Chimice în controlul calității alimentelor - Îndrumar de laborator, Universitatea Politehnică București, 2006.
- [8] T. Hao, L. R. Steeper, G.W. Griffin, A Green Approach To Separate Spinach Pigments by Column Chromatography Bunker Hill Community College, Boston, MA 02129, J.Chem. Educ.2004.
- [9] P. Walstra, Physical Chemistry of Foods, Marcel Dekker, Inc., New York, 2003.
- [10] R. Owen, Food chemistry, Ed. Marcel Dekker, New York, 1985.
- [11] C. Lukasz, M. Waksmundzka-Hajnos, Two-dimensional thin-layer chromatography in the analysis of secondary plant metabolites, Journal of Chromatography A, 1216(2009), 1035.
- [12] C. C. Moraes, L. Sala, G. P. Cerveira, S. J. Kalil, C-phycoyanin extraction from *Spirulina platensis* wet biomass, Brazilian Journal of Chemical Engineering, 28(2011), 45.
- [13] V. Cruz de Jesús, G. Alfonso Gutiérrez-Rebolledo, M. Hernández-Ortega, L. Valadez-Carmona, A. Mojica-Villegas, G. Gutiérrez-Salmeán, G. Chamorro-Cevallos, Methods for extraction, isolation and purification of C-phycoyanin. Review., International Journal of Food and Nutritional Science, 3(2016), 1.
- [14] R. Bermejo, M.A. Felipe, E.M. Talavera, et al., Expanded bed adsorption chromatography for recovery of phycoyanins from the microalga *Spirulina Platensis*, Chromatographia 63(2006), 59.



## ANALYSIS OF POLYPHENOLS IN WINE AND JUICES SAMPLES BY UV-VIS SPECTROPHOTOMETRY

Cristina Mihali<sup>1</sup>, Zoita Berinde<sup>1</sup>, Thomas Dippong<sup>1</sup>, Pauliuc Ivan<sup>2</sup>, Mircea Rednic<sup>1</sup>

<sup>1</sup> Technical University of Cluj-Napoca, North University Center of Baia Mare, Department of Chemistry and Biology, 76 Victoriei Street, 430122 Baia Mare, Romania

<sup>2</sup> University of Agricultural Sciences and Veterinary Medicine of Banat, 300081, Timisoara  
e-mail: dippong.thomas@yahoo.ro

### Abstract

Polyphenols are secondary metabolites of plants being involved in the protection against the solar ultraviolet radiation or pathogens aggression and are considered to possess beneficial effects on human health. The paper aims to determine the total concentration of polyphenolic compounds and anthocyanins in various samples such as wine, nectar, coffee and Noni juice, by UV-VIS spectrometry. The analysis of these compounds involves more aspects: determination of polyphenolic substances by the Folin-Ciocalteu method, determination of anthocyanins by the sodium bisulfite method for wine samples.

### Introduction

Polyphenols are natural compounds containing phenol groups playing different roles in the vegetals and animal organisms such as antiviral, antiallergic, antiinflammatory, antitumor and antioxidant agents [1]. Polyphenols are found in fruits, vegetables, cereals and beverages. Fresh fruits, such as grapes, apples, pears, cherries and berries, contain up to 200-300 mg of polyphenols in 100 grams of fresh product [1-3].

Anthocyanins are water-soluble pigments responsible for blue, purple and red colors in many fruits such as blackberries, grapes, cherries, pomegranates, plums, apples, and some citrus and tropical fruit [4-5]. The Folin-Ciocalteu Reagent is also known as "Folin's phenolic reagent" or "gallic acid equivalent" (GEA). It is a mixture of phosphomolybdate and phosphotungstic used in the colorimetric and spectral analysis of phenolic and polyphenolic antioxidants. The GEA reagent has the advantage of the ability to reduce phenolic compounds in samples of different concentrations of polyphenols [6-11]. The method for determining anthocyanins consists in the property of anthocyanins and compounds containing flavil groups to be discolored by sulfur dioxide. The determination of the potassium permanganate index consisted in the cold titration of polyphenolic substances and other oxidizable substances contained in wine against a tartaric and alcoholic solution in the presence of carmine indigo as an indicator of oxidoreduction with potassium permanganate [12-18].

### Experimental

In the experiment, table red wine, blackcurrant nectar from the market made with blackcurrant juice concentrate (minimum 50%), coffee, Noni juice (a Tahitian drink appreciated for its antioxidant qualities) were used in the experiment to analyse their polyphenol concentrations.

The blank solution and the standard solutions were prepared. The blank solution was prepared using 1 mL of distilled water, 20 mL of anhydrous 20% Na<sub>2</sub>CO<sub>3</sub>, 5 mL of Folin-Ciocalteu reagent, and finally the flask is filled to the volume of 100 mL with distilled water. The 5 standard solution was prepared using 1 mL of gallic acid of various known concentrations (50, 100, 150, 250, 500 mg / L), 20 mL 20% anhydrous NaCO<sub>3</sub>, 5 mL Folin-Ciocalteu reagent in a

flask of 100 mL. A complex of blue color is formed and their absorbance is measured after 30 minutes. The standards were analysed measuring their absorbance in 1 cm cuvettes at 760 nm. UV-VIZ analysis was performed with a Perkin Elmer, Lambda 25 spectrophotometer. The samples were diluted in an appropriate ratio of 1:20 or 1:10 volume and then they were treated as the standard solution of galic acid with  $\text{Na}_2\text{CO}_3$  20% solution and Folin-Ciocalteu reagent and by measuring their absorbance at 760 nm after 30 minutes. Samples of red wine, blackcurrant nectar, coffee and Noni juice were thus analyzed to find their polyphenol content. The anthocyanins content analysis in wine based on their decoloration with sodium bisulfite solution was performed for some wine samples. The method of determining the anthocyanins was to add 1 mL of ethanol with 1% HCl, 1 mL of wine and 20 mL of 2% hydrochloric acid to a flask. After homogenizing the mixture, 10 mL of the prepared mixture and 4 mL of distilled water are pipetted into the tube A, and 10 mL of the prepared mixture and 4 mL of 15% sodium bisulfite are pipetted into tube B. After homogenization and 15 minutes rest, sample extinctions at 520 nm were determined in a 10 mm cuvette. The results obtained were recorded with e1 (extinction of the sample with distilled water), respectively with e2 (extinction of the sample with sodium bisulfite). The difference between these values was multiplied by 875, which is a set point from the calibration right obtained with purified anthocyanins from wine. For this experiment, table wines, semi-sweet, semi-sweet and sweet wines were used in 2016.

## **Results and discussion**

After calibration, the calibration curve of Figure 1 was plotted. The determination coefficient  $R^2$  of 0.9919 suggests a very good correlation of the data.



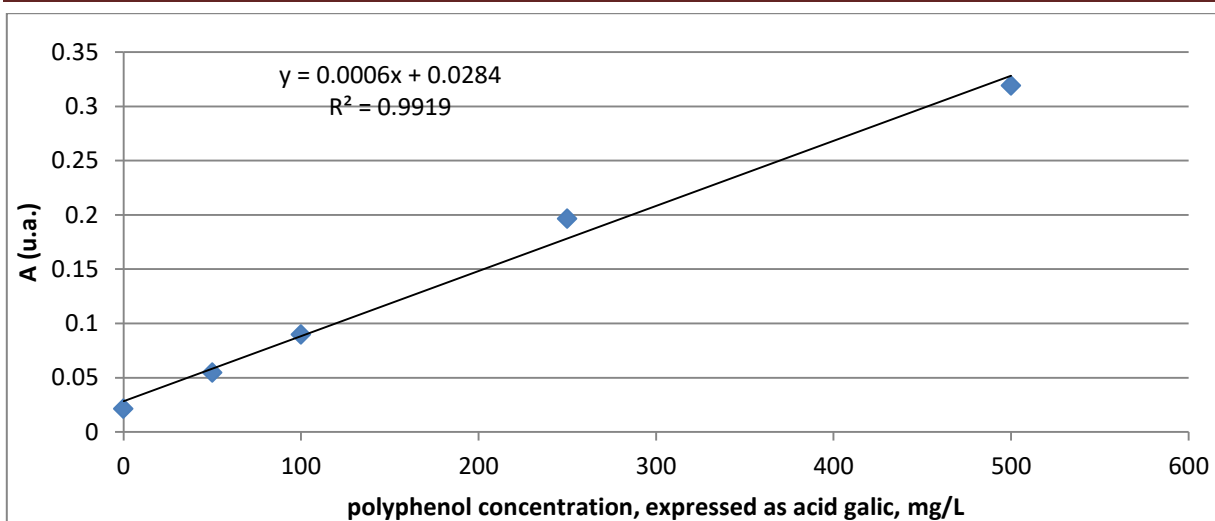


Figure 1. The etalons of galic acid for polyphenol analysis based on Folin-Ciocalteu reagent

The samples thus prepared were analyzed spectrophotometrically at the wavelength of 760 nm, yielding the results presented in Table 1.

Table 1. Polyphenol content of the analysed samples

Sample	Polyphenol content, mg/L
Red wine	419±23.63 <sup>a</sup>
Black currant juice	1368.33±64.85
Coffee (as drink)	4513.33±76.70
Noni juice	2747±51.28

<sup>a</sup> standard deviation

It can be seen from the table that both wine and nectar from black currants, but especially coffee and Noni juice, contain high concentration of antioxidant substances of the polyphenol nature. The very high concentration of polyphenols in coffee samples is explained by the fact that it was prepared a few hours before the experiment and was prepared in a concentrated manner.

The concentration of anthocyanins in wine samples by the spectrophotometric method is shown in Table 2. Table wine has the same provenance as the wine used in the first experiment (the total amount of polyphenols determined was 419 mg / L).

Table 2. The anthocyanin concentration in different wine assortments

Type of sample	Anthocyanins concentration (mg/L)
Table wine	9.58±0.88
Demidry wine	82.75±5.68
Demisweet wine	145±4.41
Sweet wine	167.82±4.78

The weight of anthocyanins in total polyphenols for the first type of wine is 2.28%. The highest concentration of anthocyanins was found for the sweet wine sample followed by the demiwseet wine while table wine sample was poorer in polyphenols.

### **Conclusion**

Polyphenolic compounds are particularly important in the living world, found in all plants, being responsible for the physiological processes inside the organisms that contain them. The structure of anthocyanins plays a determining role in the color formation of fruits, producing shades from red-orange (pelargonidine) to blue-violet (delphinidin). Hydroxylation induces a turning effect of the visible maximum to higher wavelengths, respectively turning to blue. On the other hand, methylation of hydroxyl groups has a counter-effect, producing red-intense colors. Due to their particular spectral properties it is possible to determine their presence, concentration and evolution in the substances that contain them by means of the UV-VIS molecular absorption method. The studies undertaken in the paper provide information and give us the certainty that a greater variety of determinations can be made with this method.

### **References**

- [1] S. Kumar, A. K. Pandey, Chemistry and Biological Activities of Flavonoids: An Overview, *The ScientificWorld Journal*, 2013, <http://dx.doi.org/10.1155/2013/162750>.
- [2] V. Goulas, A. R. Vicente, G. A. Manganaris, Structural diversity of anthocyanins in fruits, 2012, New York Nova Science Publishers, 225.
- [3] I. Burnea, I. Popescu, G. Neamțu, E. Stancu, *Chimie și biochimie vegetală*, Ed. Didactică și Pedagogică din București, 1977, 325
- [4] T. Dippong, C. Mihali, *Tehnici avansate de analiză intrumentală utilizate în industria alimentară, chimie și mediu*, Editura Risoprint, Cluj-Napoca, 2017
- [5] A. C. Ana, *Manual de lucrări practice în oenologie*, Ed. Fundației Universitare „Dunărea de Jos”, Galați, 2002
- [6] D. L. Pavia, G. M. Lampman, G. S. Kriz., J. R. Vyvyan, *Introduction in spectroscopy*, Cengage Learning, 2015
- [7] T. Rong, *Chemestry and biochemestry of dietary polyphenols*, Canada, 2010
- [8] M. Taskeen, Q. Ping Dou, *Black tea polyohenols inhibit tumor proteasome activity*, 2012, U.S.A.
- [9] A. Duda-Chodak, T. Tarko, M. Statek, *The effect of antioxidants on Lactobacillus casei cultures*, Krakov, 2008.
- [10] R. A. Meyers, *Encyclopedia of Analytical Chemistry: Applications, Theory and Instrumentation*, John Wiley and Sons Ltd, Chichester, UK, 2007.
- [11] S. Nielsen et al., *Food analysis*, Fourth Edition, Springer, New York, 2010.
- [12] G. Gauglitz, T. Vo-Dinh, *Handbook of Spectroscopy*, Wiley Press, 2003.
- [13] C. Dumitru *Metode și tehnici de control ale produselor alimentare și de alimentație publică*, Ed. Ceres, 1985.
- [14] W. Kemp, *Organic Spectroscopy*, 3<sup>rd</sup> edition, Freeman and Company, New York, 1991.
- [15] A. F. Dăneț, *Metode instrumentale de analiză*, Ed Științifică, București, 1995/
- [16] A.I. Badea, *Aplicații ale spectrometriei UV-VIS în chimia analitică*, Ed. Didactică și Pedagogică R.A., București, 2006.
- [18] *\*\*\*Enciclopedia of food science, food technology and nutrition*, Academic Press, London, 1993.

ANTIMONY FILM ELECTRODE FOR CHRONOPOTENTIOMETRIC  
DETERMINATION OF INSECTICIDE IMIDACLOPRID

Ana Đurović<sup>1</sup>, Zorica Stojanović<sup>1</sup>, Snežana Kravić<sup>1</sup>, Zvonimir Suturović<sup>1</sup>, Nada  
Grahovac<sup>2</sup>

<sup>1</sup>University of Novi Sad, Faculty of Technology, Department of Applied and Engineering  
Chemistry, Bulevar cara Lazara 1, 21000 Novi Sad, Serbia

<sup>2</sup>Institute of Field and Vegetable Crops, Maksima Gorkog 30, 21000 Novi Sad, Serbia  
e-mail: djurovic.ana@tf.uns.ac.rs

**Abstract**

The most important experimental parameters were investigated for chronopotentiometric determination of imidacloprid using thin film antimony electrode as a working electrode. The film of antimony was *ex-situ* plated on the glassy carbon electrode. Britton-Robinson buffer pH 10 was used as an optimal supporting electrolyte, where imidacloprid provided a well define and reproductive reduction signal at the potential of -1100 mV (vs. Ag/AgCl, 3.5 mol/dm<sup>3</sup> KCl). Based on the height and reproducibility of the analytical signal, initial potential of -0.51 V was accepted as optimal, while selected optimal ranges of reduction current were from -5 μA to -14.4 μA, and from -4.6 μA to -18.2 μA, for concentrations of 2 mg/dm<sup>3</sup> and 10 mg/dm<sup>3</sup>, respectively. It was determined that analytical signal of imidacloprid decreased exponentially with more negative values of reduction current. Before application of this method to environmental samples, additional experiments related to method validation are necessary.

**Introduction**

Agricultural production is an important sector of the worldwide economy. As the human population is growing every day, in order to increase food production, the use of pesticides is inevitable. An estimation is that millions tons of these chemicals are applied in agriculture annually worldwide, but less than 1% of the total applied pesticides reaches the target pests, while the rest remains in the environment, where they can be toxic to humans and other non-target animals [1]. The persistence and mobility of the pesticides in the environment is influenced and controlled by many processes and numerous biological, physical and chemical reactions [2]. Furthermore, the physical and chemical properties of the molecule determine its soil and water mobility and volatility.

Imidacloprid (IM) is the most frequently used neonicotinoid group of insecticide. According to the mode of action, IM is acting as a systematic neurotoxin. It interferes with the synaptic transmission of stimuli in the central nervous system, that is more abundant in insects than in mammals [3]. Despite much lower toxicity of this insecticide to mammals than to vertebrates, many studies shown that IM causes hazards to other non-target organisms such as beneficial insects [4], birds [5], and many aquatic species [6, 7]. Owing to its chemical properties: high water solubility and long half-life in soil and water, IM exhibits a high runoff and releasing potential to surface and groundwater [6]. The highest reported concentration of this insecticides were reported in Netherland 0,32 mg/l [8]. Therefore, development a simple, sensitive and fast analytical method for IM determination in environmental water samples is necessary in analytical chemistry. Principally, IM is analysed by chromatographic techniques that are expensive and time-consuming. On the other hand, electrochemical methods can serve

as an alternative technique for determination of this insecticide, owing to their simplicity, high sensitivity, and simple instrumentation.

For the long time mercury-based electrodes have been extensively used in electrochemistry for determination of many different compounds, due to their reproducibility and wide cathodic potential window [9], but the toxicity of mercury triggered the search for other environment friendly electrode materials. Antimony film electrodes (SbFEs) were introduced in 2007, and revealed interesting characteristics: wide potential window, and favourable performance in very acid media [10]. In most cases the antimony film is plated on a carbon substrate via *in-situ* or *ex-situ* procedure, and the most frequently used substrate electrodes are glassy carbon electrodes [11]. Since the introduction, SbFEs, combined with *in-situ* procedure, were mostly used for determination of heavy metals. On the other hand, a small number of studies describing the use of these electrodes for determination of organic substances: drugs [12], food dyes [13] and pesticides [11].

The main objective of the present study was to investigate the optimal experimental: chemical and instrumental parameters for determination of IM. Chronopotentiometry was used as an electrochemical technique to demonstrate applicability of *ex-situ* prepared SbFE. Developed method can be used as a fast and economical method for quantification of IM in different environmental samples.

## Experimental

### *Chemicals and instrumentation*

Standard stock solution of IM ( $0.4 \text{ g/dm}^3$ ) was prepared by dissolution of solid standard (Dr. Ehrenstorfer, Augsburg, Germany) in double distilled water. Britton-Robinson (BR) buffer was prepared from equimolar  $0.04 \text{ mol/dm}^3$  stock solutions of orthophosphoric, boric, and acetic acids (Lach-Ner, Brno, Czech Republic). Required pH value of the BR buffer was adjusted by addition of  $0.20 \text{ mol/dm}^3$  sodium hydroxide solution (Lach-Ner, Brno, Czech Republic). Saturated solution of sodium sulphite (Centrohem, Stara Pazova, Serbia) was prepared by dissolution of the appropriate amount of the substance in double distilled water. Double distilled water was used throughout the experiments.

Chronopotentiometric measurements were carried out using an automatic stripping analyser, of domestic construction. A three-electrode configuration was used with the working SbFE, Ag/AgCl ( $3.5 \text{ mol/dm}^3$  KCl) reference electrode and a platinum wire as counter electrode. A glassy carbon disc electrode of a total surface area of  $7.07 \text{ mm}^2$  was used as an inert support for the SbFE. All values of the potential were shown versus Ag/AgCl,  $3.5 \text{ mol/dm}^3$  KCl, reference electrode.

Before the deposition of the antimony film, glassy carbon electrode was polished with aqueous slurry of an aluminium oxide ( $0.5 \mu\text{m}$ , Merck, Darmstadt, Germany) on a polishing pad until a mirror-like surface was obtained, and then rinsed with doubly distilled water. The electrode was transferred into the plating solution with  $40 \text{ mg/dm}^3$   $\text{Sb}^{3+}$  in  $0.005 \text{ mol/dm}^3$  HCl. A specific potential of  $-0.8 \text{ V}$  was then applied to the electrode for 240 s in stirred solution. Thin film of antimony was mechanically removed with filter paper wetted with acetone, and then with double distilled water.

For performing chronopotentiometric measurements, SbFE was placed in the electrochemical cell filled with  $20 \text{ cm}^3$  of the analysed solution. Dissolved oxygen was removed from the solution by adding  $1 \text{ cm}^3$  of the saturated solution of sodium sulphite, and stirring the solution for 30 s. After a 10-s quiescence time, chronopotentiogram was recorded by applying a



negative potential scan from -0.51 V to -1.2 V. All experiments were performed using three replicates at the ambient temperature (23–25°C).

### Results and discussion

Preliminary experiments performed in this study were performed by recording chronopotentiograms of IM standard solution (2 mg/dm<sup>3</sup>) in potential range from: -0.70 V to -1.2 V, with applied reduction current of -5.8 μA. The performed experiments included the choice of the optimal chemical (supporting electrolyte and its pH value), and instrumental parameters (initial potential and reduction current) of the chronopotentiometric analysis of IM. Experiments included different supporting electrolytes: 0.04 mol/dm<sup>3</sup> BR buffer, 0.1 mol/dm<sup>3</sup> acetate, citrate, phosphate buffer, and 4.5 g/dm<sup>3</sup> sodium sulphite. In BR buffer and 4.5 g/dm<sup>3</sup> sodium sulphite solution IM provided a single well-defined reduction wave. In reversible potential scan no corresponding signal was recorded indicating that the electrode process can be regarded as electrochemically irreversible. Since BR buffer showed better performances in terms of sensitivity, reproducibility and sharpness of the analytical signal, this buffer was accepted as optimal in further experiments.

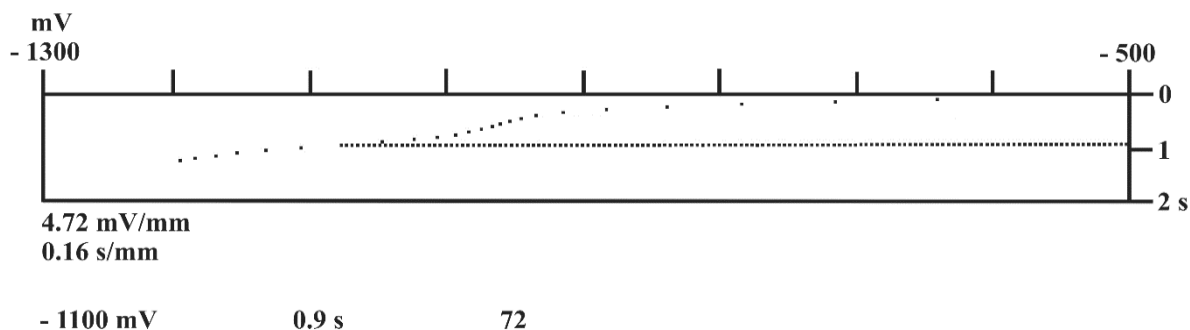
In order to choose optimal pH value of the BR buffer, chronopotentiograms of fixed concentrations of imidacloprid (2 mg/dm<sup>3</sup>), with varying pH value of the buffer in the range from 2 to 12, were recorded, while other parameters of the analysis were kept constant. The signal of the insecticide was obtained in pH range from 9 to 12 (Table 1), while in acid and neutral media the peak totally disappeared. It was also noticed that peaks shifted to more negative potentials by increasing the pH, from -950 mV to -1150 mV. The highest peak intensities were recorded at pH 10 (Table 1), and this value was consequently selected for further analytical studies (Figure 1).

Table 1 Influence of pH of Britton-Robinson buffer on the analytical signal of imidacloprid concentration of 2 mg/dm<sup>3</sup>

pH of Britton-Robinson buffer	Reduction time (s) ± SD*	RSD (%)
9	0.93 ± 0.03	3.33
10	1.05 ± 0.02	2.10
11	0.89 ± 0.03	5.31
12	0.96 ± 0.03	2.63

\*X<sub>mean</sub> ± SD, n = 3.

Figure 1. Chronopotentiogram of imidacloprid on antimony film electrode in Britton-Robinson buffer pH 10, C<sub>im</sub> = 2 mg/dm<sup>3</sup>, E<sub>initial</sub> = -0.51 V, I = -5.8 μA.



Influence of the initial potential on the reduction time of IM was investigated in the range from +0.20 V to -0.75 V, in solution containing 2 mg/dm<sup>3</sup> IM. Applied reduction current was -5.8  $\mu$ A, and the value of the final potential was -1.2 V. It was observed that initial potentials higher than -0.416 V produced a protracted chronopotentiograms, while at values lower than -0.695 V the response of IM was not observed. Considering the height and reproducibility of IM signal ( $\tau_{\text{red}} = 0.85$  s, RSD = 1.67%, Table 2), initial potential of -0.51 V was chosen as a suitable.

Table 2 Influence of the initial potential on the analytical signal of imidacloprid concentration of 2 mg/dm<sup>3</sup>

Initial potential (V)	Reduction time (s) $\pm$ SD*	RSD (%)
-0.695	0.84 $\pm$ 0.04	4.45
-0.649	0.87 $\pm$ 0.04	4.33
-0.602	0.83 $\pm$ 0.03	3.43
-0.556	0.84 $\pm$ 0.04	5.04
-0.510	0.85 $\pm$ 0.01	1.67
-0.464	0.84 $\pm$ 0.02	2.94
-0.416	0.84 $\pm$ 0.03	3.36

\* $\bar{X}_{\text{mean}} \pm \text{SD}$ , n = 3.

Reduction current represents one of the most important experimental parameters in chronopotentiometric analysis, due to its significant influence on height and sharpness of the analytical signal. Influence of the reduction current on IM analytical signal was investigated in model solutions containing 2 mg/dm<sup>3</sup> and 10 mg/dm<sup>3</sup> of IM. Investigated ranges of the reduction current were from -5  $\mu$ A to -14.4  $\mu$ A for solution containing 2 mg/dm<sup>3</sup> of IM, and from -4.6  $\mu$ A to -18.2  $\mu$ A for solution containing 10 mg/dm<sup>3</sup> of IM. IM reduction time exponentially decreased with more negative value of the reduction current, for both lower ( $\tau_{\text{red}} = 2.6238 e^{0.1891 I}$ , r = 0.9943) and higher ( $\tau_{\text{red}} = 11.228 e^{0.215 I}$ , r = 0.9969) concentrations of IM.

### Conclusion

In this study optimization of basic experimental and instrumental parameters was performed using SbFE as a working electrode, and insecticide IM as the tested compound. Thin film of antimony was *ex-situ* plated on the glassy carbon electrode. By using chronopotentiometry, BR buffer of pH 10 was selected as an optimal supporting electrolyte. Optimal instrumental parameters of chronopotentiometric analysis, included the choice of the optimal value of the initial potential, and the ranges of reduction current. Chronopotentiometry in combination with SbFE can be used as a simple and fast method for determination of IM in different environmental samples, still before application further experiments are necessary.

### Acknowledgements

This investigation is financially supported by the Ministry of Education and Science of the Republic of Serbia (Grant III 46009).

### References

- [1] J. Zhang, W. Lan, C. Qiao, H. Jiang, *Biotechnol. Prog.* 20 (2004) 1567.
- [2] M. Gavrilescu, *Eng. Life Sci.* 5 (2005) 497.

- [3] M. Tomizawa, J.E. Casida, *Annu. Rev. Pharmacol. Toxicol.* 45 (2005) 247.
- [4] P.R. Whitehorn, S. O`Connor, F.L. Wackers, D. Goulson, *Science* 336 (2012) 351.
- [5] A. Lopez-Antia, M. E. Ortiz-Santaliestra, F. Mougeot, and R. Mateo, *Environ. Res.* 136 (2015) 97.
- [6] C.A. Morrissey, P. Mineau, J.H. Devries et al., *Environ. Int.* 74 (2015) 291.
- [7] T. Tišler, A. Jemec, B. Mozetič, P. Trebše, *Chemosphere* 76 (2009) 907.
- [8] T. C. Van Dijk, M. A. Van Staaldin, and J. P. Van der Sluijs, *PLoS ONE* 8 (2013) 547.
- [9] J. Barek, A.G. Fogg, A. Muck, J. Zima, *Polarography and voltammetry at mercury electrodes*, *Crit. Rev. Anal. Chem.* 31 (2001) 291.
- [10] S.B. Hočevár, I. Švancara, B. Ogorevc, K. Vytřas, *Anal. Chem.* 79 (2007) 8639.
- [11] J. Gajdár, J. Barek, J. Fischer, *J. Electroanal. Chem.* 778 (2016) 1.
- [12] B. Nigović, S.B. Hočevár, *Electrochim. Acta* 109 (2013) 818.
- [13] J.A. Rodriguez, M.G. Juarez, C.A. Galan-Vidal, J.M. Miranda, E. Barrado, *Electroanal.* 27 (2015) 2329.

## NEW APPROACHES TO DESIGN OF BLENDS BASED ON QUATERNIZED POLYSULFONES WITH OPTIMIZED CONDUCTIVE PROPERTIES

Anca Filimon<sup>1</sup>, Adriana Popa<sup>2</sup>

<sup>1</sup>*Department of Physical Chemistry of Polymers, „Petru Poni“ Institute of Macromolecular Chemistry, Grigore Ghica Voda Alley 41A, 700487, Iassy, Romania*

<sup>2</sup>*Institute of Chemistry Timisoara of Romanian Academy, 24 Mihai Viteazul Blv., 300223, Timisoara, Romania  
e-mail: capataanca@yahoo.com*

### Abstract

New blends based on quaternized polysulfones, namely quaternized polysulfone/polyvinyl alcohol and quaternized polysulfone/cellulose acetate phthalate, were investigated in terms of their electrical properties. The dielectric constants have low values for the studied blends, being dependent on the chemical characteristics of blends compounds, in relation with the charge transfer complex and free volume and, consequently, with packing of the polymer chains and of the polarizable groups per volume units. Moreover, the electrical conductivity of studied blends can be explained in terms of band conduction mechanisms, through band gap representation.

This study analyzes the possibility of using blends based on quaternized polysulfones as possible candidates in electrotechnical industry. Additionally, the outcomes highlight the importance of new polymer blends for better electrical performances.

### Introduction

Conductive polymers - novel type of electroactive biomaterial - allow excellent control of the electrical stimulus, possess good electrical and optical properties, have a high conductivity/weight ratio and can be made biocompatible, biodegradable and porous [1,2]. Therefore, development of the conductive polymer blends with tailor properties for various applications, from photovoltaic devices to nerve regeneration, promises to become an important goal of the scientific community. In this context, polysulfone (PSF) a transparent engineering thermoplastic, characterized by excellent properties, such as flexibility, high mechanical strength, high glass transition temperature, and thermal stability [1,3,4], as well as good film formation property [1,5], is recommended as proper candidate for a variety of applications in medical [4,6,7], food processing equipment, electrical, and electronics components [8,9]. There are also drawbacks in using those polymers in some applications, the main disadvantage being the relative hydrophobic character of them. Thus, the latest researches are focusing on the modification of PSFs that allows a compromise between hydrophobicity and hydrophilicity, and in this way, becomes suitable for the desired applications. Chemical modification of PSF through chloromethylation [10,11] and quaternization with the ammonium groups of the chloromethylated polysulfones (CMPSF) has caused considerable interest from theoretical and practical points of view, leading to improve the properties of these materials. On the other hand, the addition of another polymer to PSF matrix, it is desirable to get a conductive polymer blends with specific properties, which can be used as multifunctional materials for different electronics applications.

Particularly, functionalized polysulfone with quaternary ammonium groups (PSFQ) was combined with cellulose acetate phthalate (CAP) and polyvinyl alcohol (PVA), yielding

flexible, biocompatible, and biodegradable blends with improved conductivity compared to the PSFQ. Thus, CAP and PVA were chosen as additives, knowing that their presence in a system significantly improves besides the hydrophilicity, flexibility, biocompatibility, and tensile strength, the transparency features, as well as electrical conductivity. Therefore, the main objective of this research is to investigate the influence of effects induced by structural and compositional characteristics of polymer blends on the electrical properties. Also, the study realized on PSFQ/CAP and PSFQ/PVA blends provides a new insight into to analyze and understand the polarization and conductivity mechanisms by designing desired conditions of transparency and improved electron interactions and conductivity, for better electrical performances. It is assumed that the quaternization effect and choosing of an appropriate additive significantly improve the ionic conductivity and also, could optimize dielectric properties required by ionic exchange membrane.

### Experimental

Commercial aromatic polysulfone (PSF, UDEL-3500) was used in the synthesis of chloromethylated polysulfones (CMPSF) and subsequently, of ionic polysulfones containing quaternary ammonium side groups (PSFQ) [12,13]. Detailed procedure of reactions was presented in previous study [14]. Celvol polyvinyl alcohol (PVA, Celanese Corporation) has a hydrolysis degree around 98.8% and an average weight molecular weight of 23,000 g/mol. According to manufacturer specification the cellulose acetate phthalate (CAP) has a degree of substitution for acetyl and phthaloyl groups of 1.07 and 0.77, respectively, and a number-average molecular weight of 2,534 g/mol.

The characteristics of the synthesized polysulfones are presented in Table 1. Quaternization reaction of CMPSF occurs at a transformation degree close to 98%, implicitly, can be considered that almost all chloromethylene groups were quaternized.

**Table 1.** Substitution degree, DS, chlorine, ionic chlorine, and nitrogen contents, molecular weights of structural units,  $m_0$ , and number-average molecular weights,  $\bar{M}_n$ , of polysulfone and functionalized polysulfones

Sample/ Properties	DS	Cl (%)	Cl <sub>i</sub> (%)	N (%)	$m_0$	$\bar{M}_n$ (g/mol)
PSF	-	-	-	-	443	39,000
CMPSF	1.03	7.42	-	-	492	29,000
PSFQ	-	-	5.44	2.48	582	28,000

Dielectric spectroscopy measurements were achieved using a Novocontrol Concept 40 broadband dielectric spectrometer, by sweeping the frequency between  $10^0 \div 10^6$  Hz, at fixed temperatures, of 4°C intervals, when temperature varies between -120 and +120°C, and increasing temperature rate is 2°C·min<sup>-1</sup>. Temperature was controlled with a 0.1°C device by the Novocontrol Quatro Cryosystem, in dry nitrogen atmosphere to avoid water absorption.

Films used for these measurements, with a thickness of around 50 µm, were prepared by solution-casting method. Homogeneous solutions of PSFQ and CAP or PVA, with known concentration of 20 g/dL, were dissolved in N-methyl-2-pyrrolidone (NMP) in a water bath with a constant temperature of 70°C under continuous stirring for 2 h. PSFQ/CAP and PSFQ/PVA blends were prepared by mixing the two solutions in different ratios and subsequently were cast on a glass plate and solidified, initially by slow drying in saturated atmosphere of the used solvents, and finally under vacuum for 2 days at 50°C. The

70/30 wt./wt. composition of PSFQ/CAP and PSFQ/PVA blends was chosen as a consequence of the structural peculiarity of polymers in the blend, as well as type of interactions, evidencing the orientation or mobility of chain segments in solution.

### Results and discussion

Dielectric behavior of PSFQ, CAP, PVA, and their blends over wide frequency, 1-10<sup>6</sup> Hz, and temperature, -120°C ÷ +120°C was investigated according to chemical structure and compositional aspects (Figure 1).

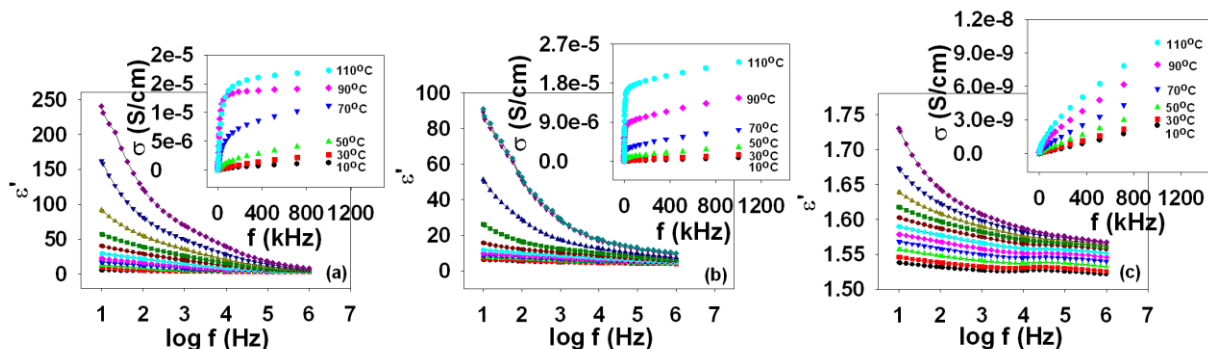


Figure 1. Variation of dielectric constant ( $\epsilon'$ ) vs. frequency ( $f$ ) at different temperatures for: (a) PSFQ, (b) PVA, and (c) CAP samples. Inserted plot represent variation of electrical conductivity vs. frequency at different temperatures.

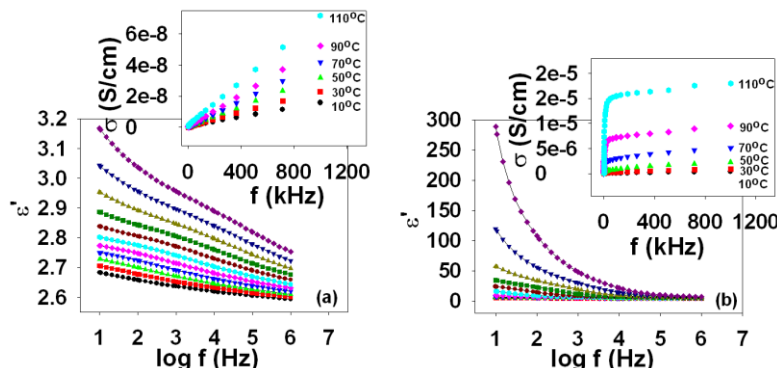


Figure 2. Variation of dielectric constant ( $\epsilon'$ ) vs. frequency at different temperatures for: (a) PSFQ/PVA and (b) PSFQ/CAP blends. Inserted plot represent variation of electrical conductivity vs. frequency at different temperatures.

Increasing of the dielectric constant with temperature represents a consequence of enhanced polarization and a more intense oscillation of the molecules present in the films, while the dielectric constant decreases with increasing of frequency is due to dielectric dispersion, as a result of the molecules lagging behind the alternation of the electric field, at higher frequency [15]. Moreover, rapid decrease of  $\epsilon'$  at higher temperatures is generated by the increase in chaotic thermal oscillations of the molecules and to the degree of dipoles orientation. According to Figure 1, the  $\epsilon'$  value for PSFQ, is higher than for PVA and CAP. Thus, the electronic conjugations from the side chains of PSFQ contribute to the enhancement of  $\epsilon'$  values. Instead, the decrease in  $\epsilon'$  values for PVA and CAP may be attributed on the one hand,



to the ability of macromolecules dipoles to orient themselves in the direction of the applied field in the low frequency range and, on the other hand, the inability of the dipoles to orient themselves in the direction of the applied field, in the high frequency range.

Over the  $1-10^6$  Hz frequency domain, the dielectric constant values of the pure components is reflected in those of the blends. Thus,  $\epsilon'$  takes values in the 2.73-3.20 range for PSFQ/PVA blend (Figure 2a) and in 2.85-285.1 range for PSFQ/CAP blend (Figure 2b). In agreement with these remarks, influence of the composition of polymer blends and competition between the contributions the main chain and the pendant groups are reflected in the  $\epsilon'$  values.

Also, the variation of electrical conductivity,  $\sigma$ , with temperature and frequency is dependent on the structural parameters of the samples. Conductivity presents a linear increase for a limited temperature domain (0.34 - 50.44°C) (see small graphs of Figures 1 and 2). This conduction takes place via localized hopping of carriers between randomly distributed trapping centers [16]. Generally, increasing temperature leads to an increase in electrical conductivity, with lower slope at high frequencies. Moreover, at higher frequencies, it is observed a deviation from linearity, which can be due to the dispersion of charge carriers produced by dipolar relaxation. On the other hand, electrical conductivity, besides electronic conduction is accompanied by an ionic conduction – generated by dimethylbutylammonium group from the PSFQ.

The results obtained from conduction studies showed that the conduction mechanism in the studied blends based on quaternized polysulfones was generated by the electronic hopping process, which can be explained in terms of band conduction mechanisms, through band gap representation.

## Conclusion

The study realized on new blends of quaternized polysulfone/polyvinyl alcohol and quaternized polysulfone/cellulose acetate phthalate provides an insight into future approaches in industrial applications, due to the dielectric properties and conductivity and implicitly, electron interactions which represent fundamental features to enhance their electrical performance. The results obtained showed that the changes in the chemical structure and blends composition correlated to the dielectric behavior effect can provide information on the electronic and ionic conduction mechanisms and the molecular processes involving different relaxations. Consequently, the findings of this study demonstrate that the studied polymer blends may offer important advantages for membrane applications (*e.g.*, ionic exchange membranes).

## References

- [1] M. Barikani, S. Mehdipour-Ataei, J. Polym. Sci. A Polym. Chem. 38 (2000) 1487.
- [2] L.D. Landau, E.M. Lifshitz, Fluid Mechanics, Pergamon, London, 1959.
- [3] P. Väisänen, M. Nyström, Acta Polytech. Scand. 247 (1997), 25.
- [4] A. Filimon, E. Avram, I. Stoica, Polym. Int. 63 (2014) 1856.
- [5] F. Ran, S. Nie, W. Zhao, J. Li, B. Su, S. Sun, Acta Biomater. 7 (2011) 3370.
- [6] B. Zornoza, S. Irusta, C. Tellez, J. Coronas, Langmuir 25 (2009) 5903.
- [7] A.I. Silva, M. Mateus, J. Biotechnol. 139 (2009) 236.
- [8] P. Saxena, M.S. Gaur, P. Shukla, P.K. Khare, J. Electrostat. 66, (2008) 584.
- [9] L. Nayak, D. Khastgir, T.K. Chaki, Polym. Compos. 33 (2012) 85.
- [10] A. Higuchi, K. Shirano, M. Harashima, B.O. Yoon, M. Hara, M. Hattori, Biomaterials 23 (2002) 2659.

- [11] M. Tomaszewska, A. Jarosiewicz, K. Karakulski, *Desalination* 146 (2002) 319.
- [12] E. Avram, E. Butuc, C. Luca, *J. Macromol. Sci. Part A Pure Appl. Chem.* 34 (1997) 1701.
- [13] C. Luca, E. Avram, I. Petrariu, *J Macromol. Sci. Part A* 25 (1988) 345.
- [14] A. Filimon, R.M. Albu, I. Stoica, E. Avram, *Composites Part B* 93 (2016) 1.
- [15] A.M.A. Nada, M. Dawy, A.H. Salama, *Mater. Chem. Phys.* 84 (2004) 205.
- [16] S. Kulanthaisami, D. Mangalaraj, S.K. Narayandass, *Eur. Polym. J.* 31 (1995) 969.

## THERMODYNAMIC PROPERTIES IN QUATERNIZED POLYSULFONES/NEUTRAL POLYMER/SOLVENT COMPLEX SYSTEMS

Adina Maria Dobos<sup>1</sup>, Adriana Popa<sup>2</sup>, Anca Filimon<sup>1</sup>

<sup>1</sup>"Petru Poni" Institute of Macromolecular Chemistry, Grigore Ghica Voda Alley, 41 A, Iasi, Romania

<sup>2</sup>Institute of Chemistry Timisoara of Romanian Academy, 24 Mihai Viteazul Blv., 300223, Timisoara, Romania  
e-mail: capataanca@yahoo.com

### Abstract

Theoretical and experimental aspects concerning the interactions generated via electrostatic interactions and hydrogen-bonding in quaternized polysulfones/neutral polymer/solvent complex ternary systems are investigated. The experimental results related to the intrinsic viscosity and hydrodynamic parameters have been obtained by viscometric measurements, using new Wolf model, and discussed in terms of the chemical structure of compounds, density of charged groups, solution concentrations, and mixing ratio of the two polymers. The conformational changes of the polymer chains in dilute solution as well as the effect of electrostatic interactions, hydrogen bonding or association phenomena are reflected in variations of viscosity function on polysulfone content. Moreover, through the perspective of the new theories approached, this work analyzes the thermodynamic and hydrodynamic functions, making possible choosing of the suitable polymer blends for obtaining membranes with certain applications.

### Introduction

Analysis of polyelectrolyte solution dynamics is of great interest in many technological processes implying a good control of the flow properties of the fluids [1]. Due to the variety of specific physicochemical properties, the ionic polymers have started to be studied, especially in terms of their viscometric behavior in dilute solution. One of these polymers, having polyelectrolyte characteristics, is polysulfone containing quaternary ammonium side groups (PSFQ). Good solubility [2], hydrophilicity [3], biocompatibility [4], and water permeability [5] make them proper for applications from various fields. Moreover, these properties can be improved and tailored by blending with other compounds for further applications in biotechnology as membrane for separation or ultrafiltration [6]. In this context, neutral polymers, as polyvinyl alcohol (PVA) and cellulose acetate phthalate (CAP), were used in blends with PSFQ. Their selection is based on excellent physical properties (*i.e.*, hydrophilicity, flexibility, tensile strength), and on the emulsifying capacity, dispersing power and ability to form films [7].

Knowledge of the thermodynamics and kinetics of the ternary systems in solution is necessary for understand the membrane formation mechanisms, changing of the preparation conditions, and for prediction of the membranes final structure [8]. The presence of the specific interactions in the multicomponent polymer systems namely, nanostructures, polyelectrolytes, polymers in the presence of surfactants, complicates the structural and thermodynamic assessments. Therefore, is necessary to specify all possible interactions between the components system that can lead to the formation of multicomponent complexes in accord with different processes of equilibrium characterized by association/interaction constants. The

specific intermolecular interactions established between the polar groups are also, important in the formation of the hydrogen bonding that must be taken into account in interpreting of the thermodynamic properties.

In this context, the quaternized polysulfones/neutral polymer/solvent multicomponent systems were investigated by viscometric studies to establish the specific interactions developed by electrostatic interactions, hydrogen bonding, and association phenomenon that occur in system. Also, specific interactions of the studied multicomponent systems were theoretical evaluated by means of a theory based on multiple association equilibria. Consequently, the results of this study represent the basis for future researches concerning the good compatibilization of polymers from blends in order to design membranes for bioapplications.

### Experimental

Quaternized polysulfone, with average molecular weight of about  $\bar{M}_w = 28,000$  g/mol, degree of substitution  $DS \cong 1$ , and ionic chloride content of 5.44%, was synthesized starting from commercial polysulfone in powder form (PSF) (UDEL-3500) following the synthesis reactions previously mentioned [9]. Polyvinyl alcohol (PVA) having average molecular weight of  $\bar{M}_w = 23,000$  g/mol and hydrolysis degree of about 98.8% was purchased from Celanese Corporation (Texas). Cellulose acetate phthalate (CAP) with number average molecular weight  $\bar{M}_n = 2,534$  g/mol, a substitution degree for acetyl and phthaloyl groups of 1.07 and 0.77 was purchased from Sigma-Aldrich.

Viscosity measurements were carried out with a Schott AVS 350 computerized apparatus provided with an Ubbelohde suspended-level viscometer at  $25 \pm 0.01^\circ\text{C}$ . The flow volume of the viscometer was higher than 5mL and flow times were obtained with an accuracy of 0.035%, for different measurements. The homogeneous solutions of PSFQ, PVA, CAP, prepared by dissolution in N-methyl-2-pyrrolidone (NMP), and their blends (PSFQ/PVA and PSFQ/CAP in different mixing ratios) whose obtaining protocol was presented in previous studies [9] have concentrations between  $0.01 \div 0.99$  g/dL. For determination of intrinsic viscosities, the Huggins equation was used (Equation 1) [10]:

$$\eta_{sp} / c = [\eta]_{\text{Huggins}} + k_H [\eta]_{\text{Huggins}}^2 c \quad (1)$$

where:  $\eta_{sp}$  - specific viscosity,  $k_H$  - Huggins constant,  $c$  - polymer solution concentration,  $[\eta]$  - intrinsic viscosity.

In addition, due to polyelectrolyte complicated behavior in dilute and semi-dilute domains, as a result of the combined action of electrostatic and hydrodynamic interactions, the new Wolf method (Equation 2) was used [11]:

$$\ln \eta_{rel} = \frac{c[\eta]_{\text{Wolf}} + Bc^2[\eta]_{\text{Wolf}}[\eta]^*}{1 + Bc[\eta]_{\text{Wolf}}} \quad (2)$$

The new parameters included in this equation are the hydrodynamic interaction parameter, (B) and specific hydrodynamic volume  $[\eta]^*$ .

Additionally, in order to evaluate all specific interactions for studied systems, the knowledge of the Gibbs free energy (Equation 3) [12] is necessary. The association constants (

$\sigma_{11}, \sigma_{12}, \eta_{12}, \sigma_{13}, \eta_{13}$ ) - evaluated by the mathematical simulations - correct the binary interaction parameters,  $g'_{ij}$ .

$$\left(\frac{\Delta G}{RT}\right)_{Ter} = \phi_1 \ln \left( \frac{Y + X - [X^2 + 2XY]^{1/2}}{\phi_1 [2\sigma_{11} + 1 - (1 + 4\sigma_{11})^{1/2}]} \right) + s\phi_2 \ln \left( \phi_2 \frac{1 - \sigma_{12}P_1}{1 - (\sigma_{12} - \eta_{12})P_1} \right) + \quad (3)$$

$$r\phi_3 \ln \left( \phi_3 \frac{1 - \sigma_{13}P_1}{1 - (\sigma_{13} - \eta_{13})P_1} \right)^m - \frac{P_1}{1 - \sigma_{11}P_1} +$$

$$\phi_1 \left( \frac{2\sigma_{11} + 1 - (1 + 4\sigma_{11})^{1/2}}{\sigma_{11}(1 + 4\sigma_{11})^{1/2} - \sigma_{11}} \right) + \phi_1\phi_2g'_{12} + \phi_1\phi_3g'_{13} + \phi_2\phi_3g'_{23}$$

### Results and discussion

The obtained results from the dilute solution study (intrinsic viscosity,  $[\eta]$ , listed in Table 1) for the polyelectrolyte/neutral polymer/solvent multicomponent systems (PSFQ/PVA/NMP and PSFQ/CAP/NMP) indicate the balance between the forces acting in these polymeric complex systems, as well as the cumulative effects of the thermodynamic and/or hydrodynamic interactions between the polymers.

**Table 1.** Viscometer parameters evaluated for the multicomponent systems PSFQ/CAP/NMP and PSFQ/PVA/NMP at 25 °C

System	$\phi_1$	$[\eta]$ (dL/g)	$[\eta]^*$ (dL/g)	B
PSFQ/CAP/NMP	1	6.496	0.671	1.490
	0.75	2.473	0.204	0.655
	0.5	1.720	0.192	-1.049
	0.25	1.418	0.140	-0.138
	0	0.715	0	0.225
PSFQ/PVA/NMP	1	6.496	0.671	1.490
	0.75	1.758	0.141	0.774
	0.5	1.205	0	0.658
	0.25	0.961	0	0.611
	0	0.653	0	0.236

Higher values of the viscosity appear as results of the electrostatic repulsion between charge groups and/or intermolecular associations, while small values are determined by the intramolecular associations. Moreover, the structural characteristics of each of the polymer, their mixing ratio, as well as the nature of the used solvent have a major role in generating new type of interactions with impact on the viscometric behavior. Therefore, it can be concluded that the characteristics of the polymers are those that limit the range of solubility and therefore, the viscometric behavior.

Typically, the occurrence of any type of interaction involving hydrogen-bonding, ion-ion pairing, electron-donor, donor-acceptor, dipole-dipole etc., determines a suitable enthalpy which implies a good blending of the constituents. Particularly, the conformational aspects of the mixtures are determined by the hydrogen-bonding and electrostatic interactions presence in the system, and evaluated by the hydrodynamic interaction parameter, B. Thus, it is

observed from Table 1 that, value of B parameter attains a maximum for PSFQ and decrease with at addition of uncharged polymers, CAP and PVA. A poor interaction between the polymer coils and the solvent appears for 50/50 and 25/75 (v/v) PSFQ/CAP mixtures, where B corresponds to negative values. This condition suggests an aggregation tendency as a result of hydrogen bonding formation.

For complete description of the possible specific interactions established in ternary systems, *i.e.*, the electrostatic interactions induced by the ionic groups of the PSFQ structure, disperse interaction, and hydrogen bonding that can generate the association phenomena - CAP or/and PVA, evaluation of the Gibbs free energy (Equation 3) is imposed. Based on the association constants, calculated function of system composition by mathematical simulation (Figure 1), the excess functions, corrected binary interaction parameters and implicitly, the Gibbs free energy were determined.

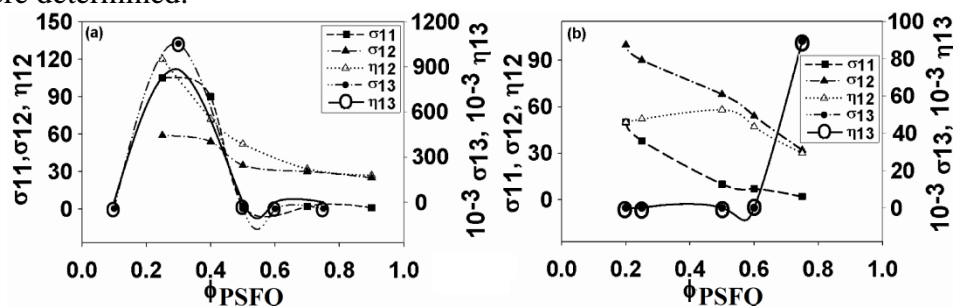


Figure 1. Interaction constants evaluated by mathematical simulations for: (a) PSFQ/CAP/NMP and (b) PSFQ/PVA/NMP multicomponents systems

The polyelectrolyte effect is due to the polyion chain expansion which leads to an progressive intensification of the ionizable groups dissociation. From this reason, the repulsive intermolecular interactions between the ionized groups (*i.e.* ammonium groups attached to the polymer chain) are enhanced. This effect, a result of electrostatic interactions and steric hindrance leads to an increase in long-distance interactions.

## Conclusion

Thermodynamic and hydrodynamic properties of polysulfone/neutral polymer/solvent complex ternary systems have been discussed in terms of the chemical structure of compounds, charged groups density, and polymer mixtures composition, by viscometric measurements and Wolf method ( $[\eta]$ , B). Also, for a good understanding of the specific interactions from the systems, the Gibbs free energy with corresponding association constants specific to each equilibrium ( $\sigma_{11}, \sigma_{12}, \eta_{12}, \sigma_{13}, \eta_{13}$ ) were evaluated. Consequently, this investigation represents a new contribution to understanding the behavior of polyelectrolyte solutions, which is needed in order to obtain membranes for different applications.

## References

- [1] J. Barzin, S. S. Madaeni, H. Mirzadeh, M. Mehrabzadeh, J. Appl. Polym. Sci. 92 (2004) 3804.
- [2] A. Filimon, E. Avram, S. Ioan, J. Macromol. Sci.: Part B – Phys. 46 (2007) 503.
- [3] R. Guan, H. Zou, D. Lu, C. Gong, Y. Liu, Eur. Polym. J. 41 (2005) 1554.
- [4] A. Filimon, E. Avram, S. Dunca, I. Stoica, S. Ioan, J. Appl. Polym. Sci. 112 (2009) 1808.
- [5] H. Yu, Y. Huang, H. Ying, C. Xiao, Carbohydr. Polym. 69 (2007) 29.



- [6] S. Cheng, F. L. Beyer, B. D. Mather, R. B. Moore, T. E. Long, *Macromolecules* 44 (2011) 6509.
- [7] A. Sabetghadam, T. Mohammadi, *Polym. Eng. Sci.* 50 (2010) 2392.
- [8] M.Ö. Arsalan, *Measurements and Modeling of Thermodynamic and Kinetic Data of Membrane-Forming Systems*, Master Thesis, Izmir, 2007.
- [9] A. Filimon, A.M. Dobos, E. Avram, S. Ioan, *Pure Appl. Chem.* 86 (2014) 1871.
- [10] M.L. Huggins, *J. Am. Chem. Soc.* 64 (1942) 2716.
- [11] B.A. Wolf, *Macromol. Rapid Commun.* 28 (2007) 164.
- [12] R. Garcia-Lopera, I.S. Monzo, C. Abad, A. Campos, *Eur. Polym. J.* 43 (2007) 23.

## NOVEL (K,Na)NbO<sub>3</sub> BASED PIEZOELECTRIC CERAMIC

**Farkas Iuliana, Bucur Alexandra Ioana, Bucur Raul Alin**

*National Institute for Research and Development in Electrochemistry and Condensed Matter,  
Condensed Matter Department, No.1 Plautius Andronescu, 300224 Timisoara Romania.  
e-mail: iulia\_b24@yahoo.com*

### **Abstract**

Novel (1-x)(K<sub>0,5</sub>Na<sub>0,5</sub>)NbO<sub>3</sub> – xGdAlO<sub>3</sub> piezoelectric ceramics were obtained using solid state method. The phase purity was confirmed by X-ray diffraction. The unit cell parameters were refined. The results show the presence of a phase transition from orthorhombic to tetragonal.

### **Introduction**

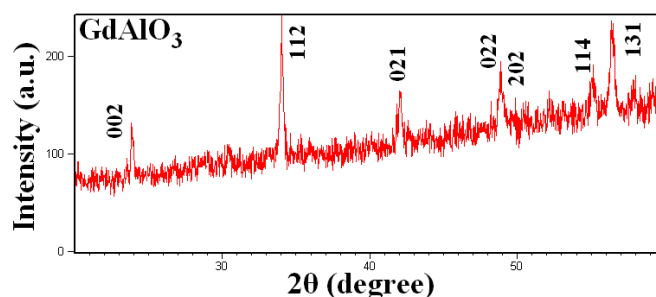
(K<sub>0,5</sub>Na<sub>0,5</sub>)NbO<sub>3</sub> ferroelectric ceramics constitute an environmental friendly substitute to Pb(Zr, Ti)O<sub>3</sub> (1). The applications of such materials are capacitors, sensors, transducers or piezoelectric actuators (2, 3). As shown previously, the improvement of the piezoelectric properties of (K<sub>0,5</sub>Na<sub>0,5</sub>)NbO<sub>3</sub> based ceramics can be accomplished through chemical substitution [4], structural material modification [5] or phase transitions manipulation [6]. In this paper we are considering the use of a new dopant, namely GdAlO<sub>3</sub>, in order to change the crystalline structure from orthorhombic to tetragonal, since the presence of such phase transition can lead to serious improvements of the piezoelectric properties [7].

### **Experimental**

(1-x)(K<sub>0,5</sub>Na<sub>0,5</sub>)NbO<sub>3</sub> – xGdAlO<sub>3</sub> (noted KNN – xGAl), with x= 0 mol%, 0,25mol%, 0,75mol%, 1 mol%, 2,5 mol% and 5 mol% were obtained using the solid state method in air. The raw materials were K<sub>2</sub>CO<sub>3</sub> (99%; Scharlau, Sentmenat, Spain), Na<sub>2</sub>CO<sub>3</sub> (99%; Scharlau), Nb<sub>2</sub>O<sub>5</sub> (99%, Merck, Darmstadt, Spain), Gd<sub>2</sub>O<sub>3</sub> (99%; Fluka, Buchs, Switzerland) and AlN<sub>3</sub>O<sub>9</sub>•9H<sub>2</sub>O (99%, Fluka, Buchs, Switzerland). First the dopant material was prepared in air at 1100°C. Then the piezoelectric powders were heated at 850°C for 6h, with a heating rate of 5 °/min. After calcinations, the powders obtained were grinded and mixed with a 5 mass% polyvinyl alcohol binder solution. Disk samples of 6 mm in diameter and approximately 1 mm thick were cold pressed at 200Mpa. The disks were sintered at 1050°C for 6h. After grinding, the crystalline structure of the sintered samples was examined by x-ray diffraction using a PanAnalytical X'Pert Pro MPD diffractometer. The refinement of the unit cell was performed using Treor algorithm in X'Pert HighScore Plus software,

### **Results and discussion**

The experimental conditions used were sufficient to obtain pure GdAlO<sub>3</sub> powders, as we can observe in figure 1. The pattern was identified using the JCPDS-ICDD file number 00-009-0085: crystal system: orthorhombic, space group Pbnm (62), a= 5.2470 Å, b= 5.3043 Å, c= 7.4470 Å; α,β,γ= 90°; volume of unit cell: 207.25 Å<sup>3</sup>.

Figure 1. X-ray diffraction pattern of  $\text{GdAlO}_3$ .

The X-ray diffraction pattern presented in figure 2 confirmed that the reference sample KNN is indexed as perovskite with an orthorhombic crystalline structure (space group  $P2mm(25)$ ). The key feature of the orthorhombic KNN is represented by the variations in intensity of the peaks splitting at  $2\theta \approx 22^\circ$  and  $45^\circ$ , respectively (010)-(001) and (020)-(002) crystalline planes.

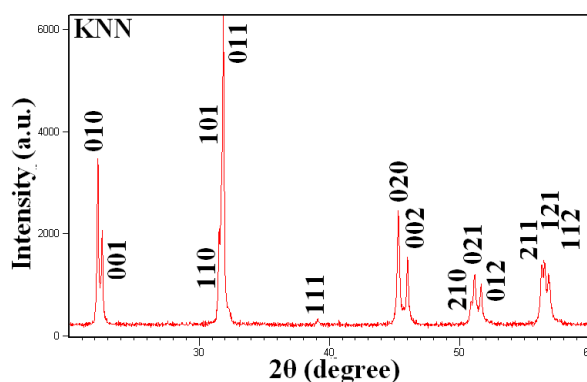
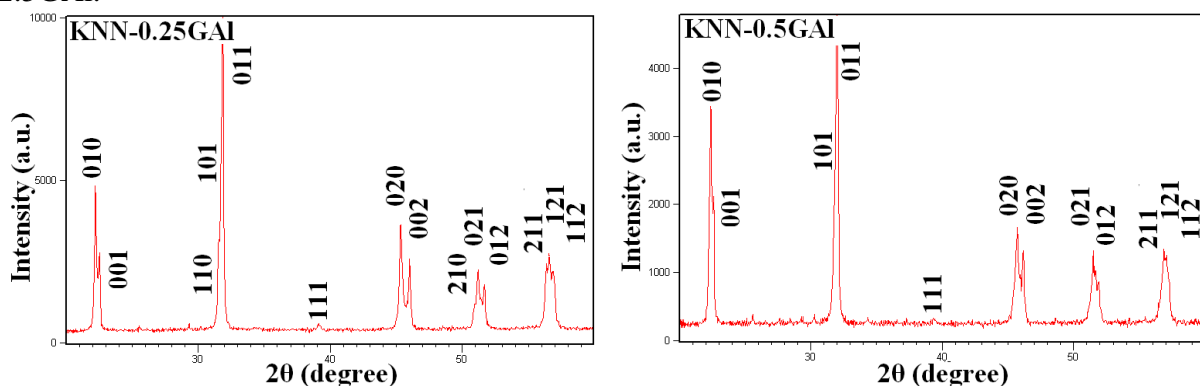


Figure 2. X-ray diffraction pattern of reference sample KNN.

In figure 3, all x-ray diffractions of KNN-GAl are presented. As previously discussed, we can observe a shifting in the peaks at  $2\theta \approx 22^\circ$  and  $45^\circ$ , suggesting a shift in crystalline structure, from orthorhombic to tetragonal. Indeed, the refinement of the unit cell parameters show a shifting from  $P2mm(25)$  orthorhombic to  $P4mm(99)$  tetragonal starting from KNN-2.5GAl.



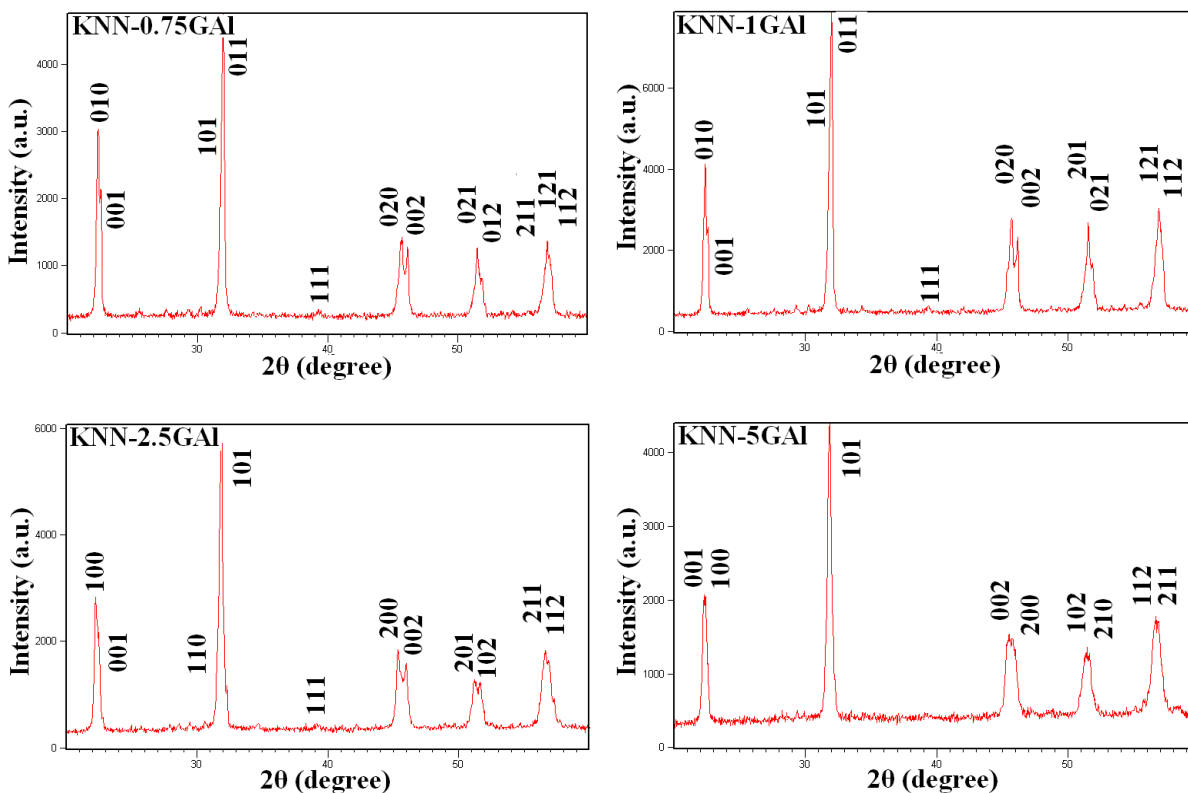


Figure 3. X-ray diffraction patterns of KNN-xGAl

The results of the unit cell refinement are presented in figure 4 and 5. As shown in figure 4, starting from the reference sample KNN, all cell parameters decrease. Above 2.5 mol% GdAlO<sub>3</sub>, a=b since the unit cell is tetragonal.

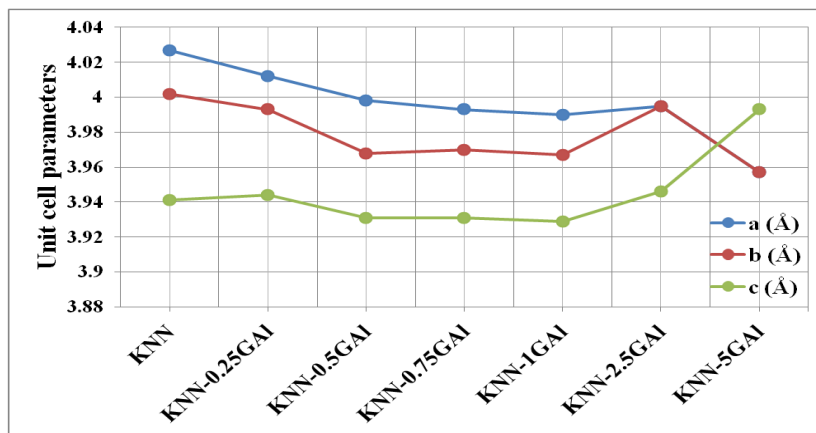


Figure 4. Unit cell parameters of KNN-xGAl

The unit cell volume variation depicted in figure 5 clearly shows the decrease of the unit cell in the orthorhombic phase, followed by a slight increase of the volume in the tetragonal phase. The abnormal variation at KNN-2.5GAl is to be attributed to the presence of a mixture of tetragonal and orthorhombic phases for this compound.

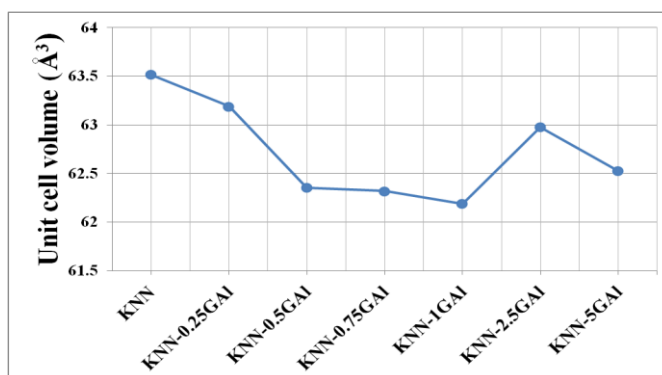


Figure 5. Unit cell volume of KNN-xGAl

### Conclusion

$(1-x)(K_{0.5}Na_{0.5})NbO_3 - xGdAlO_3$  ceramics were obtained by solid state method. The addition of  $GdAlO_3$  induce a phase transition, from orthorhombic to tetragonal at 2.5 mol  $GdAlO_3$ . Also the addition of  $GdAlO_3$  tends to decrease the unit cell parameter, except for the tetragonal phases (KNN-2.5GAl and KNN-5GAl), where the unit cell parameters increase. The presence of a mixture of phases (orthorhombic and tetragonal) at 2.5 mol  $GdAlO_3$ , can be an indicator of the improvement of the piezoelectric properties.

### Acknowledgements

This research was supported by the national project PN 16 14 01 03.

### References

- [1] Li, J.F.; Wang, K.; Zhu, F.Y.; Cheng, L.Q.; Yao, F.Z., *J. Am. Ceram. Soc.* 2013, 96, 3677–3696.
- [2] Lee, T.; Kwok, K.W.; Li, H.L.; Chan, H.L.W, *Sens. Actuators A Phys.* 2009, 150, 267–271.
- [3] Shen, Z.Y.; Li, J.F.; Chen, R.M.; Zhou, Q.F.; Shung, K.K. *J. Am. Ceram. Soc.* 2011, 94, 1346–1349.
- [4] Lu, L.; Gong, Y.Q.; Gong, L.J.; Dong, H.D.; Dong, H.; Yi, X.F.; Zheng, X.J., *Mater. Des.* 2012, 33, 362–366.
- [5] Fu, J.; Zuo, R.Z.; Wang, X.H.; Li, L.T., *J. Alloys Compd.* 2009, 486, 790–794.
- [6] Toshio, K.; Yuan, Y.; Fumito, *Materials* 2010, 3, 4965–4978.
- [7] J. Rodel, W. Jo, K.T.P. Seifert, E.M. Anton, T. Granzow D. Damjanovic, *J. Am. Ceram. Soc.* 92 (2009), 1153.

## ENZYMATIC MODIFICATION OF LIGNIN AND LIGNIN FRACTIONS OBTAINED FROM PRETREATED BIOMASS

**Firuta Ionita Fitigau<sup>1</sup>, Cristian George Vaszilcsin<sup>1</sup>, Zoltan Urmosi<sup>1</sup>.**

<sup>1</sup>*National Institute of Research-Development for Electrochemistry and Condensed Matter, A. P. Podeanu 144, 300569 Timișoara, Romania  
e-mail: fitigau\_firuta@yahoo.com*

### **Abstract**

The potential for using *Trametes versicolor* laccase to graft the polysaccharide chitosan onto chemically fractionated lignin was examined to enhance the solubility of lignin and to obtain products with special properties. Due to the complexity of lignin molecule the reaction was first performed on lignin model compound with small molecular weight. The efficiency of the enzyme was investigated in the oxidative reactions of coniferyl alcohol with glucosamine. Alcell Lignin was previously fractionated by acetone/water 50:50 (v/v) and the enzymatic modification of the soluble fraction with chitosan was carried out in the same solvent system. The modified lignin was isolated and the product was characterized by means of size exclusion chromatography and FT-IR in order to evidence the main lignin modifications after laccase coupling reactions. An important increase of the molecular weight and significant structural modifications were observed for the product obtained after the coupling reactions of Alcell Lignin with chitosane demonstrating the achievement of the modification reactions.

### **Introduction**

Lignin, like cellulose and hemicelluloses, is a major component of plant materials and the most abundant form of aromatic carbon in the biosphere. From the chemical point of view, lignin is a heterogeneous, optically inactive polymer consisting of phenylpropanoid interunits, which are linked by several covalent bonds (e.g. aryl-ether, arylaryl, carbon-carbon bonds) [1]. Despite lignin's natural recalcitrance, a number of microorganisms are known to degrade lignin. [2]. Enzyme systems for the degradation of macromolecular lignin face several challenges. The substrate is a large heterogeneous polymer that necessitates attack by extracellular enzymes or agents. Lignin does not contain hydrolysable linkages, which means that the enzymes must be oxidative. Laccases (EC 1.10.3.2) are copper containing enzymes that can oxidize a variety of phenolic compounds including those typically found in lignin [3]. They provide an attractive means to modify the physical and chemical properties of lignin, e.g. by altering solubility, surface properties, and hydrophobicity of the polymer via oxidation. Potential options to increase the value of isolated lignin include addition of key functionalities or molecules directly to the lignin, thereby increasing its versatility. The activity of laccases on small lignin model compounds has been reported in several publications [4]. It has been proved that lignin fractions can also have a number of useful properties, like antioxidant character, and by grafting of various molecules can induce new functions and properties. The aim of our studies was to obtain modified lignin fractions with potential utilization as biomaterials



## Experimental

### Chemicals, enzyme and lignin.

Glucosamine hydrochloride (98%), laccase from *Trametes versicolor* (30.6 U mg<sup>-1</sup> of solid), lignin peroxidase (LiP, 0.18 U mg<sup>-1</sup> of solid), coniferyl alcohol (98%), veratryl alcohol, chitosan (Flonac C, M=100000) and the substrate syringaldazine were purchased from Sigma-Aldrich (Taufkirchen, Germany). Organosolv lignin from mixed hardwoods (Alcell) was obtained from Repap Technologies Inc. (Valley Forge, PA, USA). Horseradish peroxidase II (HRP, 181 Purpurogallin units/mg) was purchased from Sigma Chemical St. Louis, MO.

### Enzyme assay

*Laccase* activity was determined spectrophotometrically using syringaldazine as substrate in different acetone-water mixtures. The reaction mixture (1 ml) contained 0.027 mM syringaldazine dissolved in acetone-water 50 % (v/v) and 0.5 µg ml<sup>-1</sup> laccase. The formation of the syringaldazine radical ( $\epsilon_{530} = 65 \text{ mM}^{-1}\text{cm}^{-1}$ ) was followed in time at 530 nm and 25°C [5].

*Lignin peroxidase (LiP)* and *Horseradish peroxidase (HRP)* activities were assayed spectrophotometrically using veratryl alcohol (for LiP) and coniferyl alcohol (for HRP) as substrates in 0.1M sodium citrate-phosphate pH=3 (for veratryl alcohol) and 0.1M sodium acetate trihydrate pH=5 (for coniferyl alcohol), respectively. The reaction mixture (1 ml) contained veratryl alcohol/coniferyl alcohol dissolved in buffer and 10 µg LiP/ 0.25 µg HRP solubilized in buffer. The oxidation of the veratryl alcohol was followed in time at 310 nm using  $\epsilon_{310} = 9.3 \text{ mM}^{-1}\text{cm}^{-1}$ , respectively at 262 nm for coniferyl alcohol consumption using  $\epsilon_{262} = 14000 \text{ M}^{-1}\text{cm}^{-1}$ . The increase in absorbance is followed at 310 nm and 25°C, to determine the LiP activity in international units meanwhile for coniferyl alcohol the decrease in absorbance was followed at 262 nm and 25°C, to determine the HRP activity.

### Enzymatic modification of coniferyl alcohol with glucosamine using laccase as catalyst.

The covalent coupling of coniferyl alcohol with glucosamine was studied using laccase as catalyst in 50:50 (v/v) acetone/air-saturated water. The typical experimental conditions were as follows: 100 mg coniferyl alcohol; 200 mg glucosamine hydrochloride ( molar ratio coniferyl alcohol to co-substrate 1:2), 0.24 mg ml<sup>-1</sup> laccase dissolved in air-saturated water, reaction volume 10 ml. The reaction was started by the addition of laccase solution and the reaction mixture was stirred at 20 °C for 24 hours. Two control reactions without enzyme and without the co-substrate, respectively, were carried out at the same conditions. The coniferyl alcohol consumption was monitored by HPLC analysis.

### Enzymatic modification of Alcell lignin using laccase.

The covalent coupling of a low molecular weight Alcell lignin sample with chitosane was studied using laccase as catalyst in 50:50 (v/v) acetone/air-saturated water. The isolated lignin fraction soluble in acetone/water 50:50 (v/v) were used as the starting substrates for laccase modification reactions. The typical experimental conditions were as follows: 100 mg Alcell lignin fraction, 200 mg chitosan Flonac C, 0.24 mg ml<sup>-1</sup> laccase dissolved in air-saturated water, reaction volume 10 ml. Since the chitosan is not soluble in acetone-water mixture it was suspended in the reaction mixture and stirred at room temperature for 24 hours. The solid was filtrated and washed with acetone for several times to remove the adsorbed lignin, dried and analyzed. Two control reactions were carried out at the same conditions. Reactions were stopped by adding 50 ml deionized water and lignin precipitation by lowering the pH to 1.0 with 1M HCl. The reaction products were separated on a glass filter (G4), washed two times with acetone to remove the soluble unreacted substrates and dried overnight in a vacuum oven at 60°C. All experiments were carried out at least in duplicate.

### **Fourier transform infrared spectroscopy (FT-IR).**

Fourier Transform Infrared (FT-IR) spectra of the lignin samples were obtained in attenuated total reflectance (ATR) mode on a Varian Scimitar 1000 FT-IR spectrometer equipped with a DTSG-detector PIKE MIRacle ATR equipped with a diamond w/ZnSe lens single reflection plate. Spectra were collected in the range 4000-650  $\text{cm}^{-1}$  with a resolution of 4  $\text{cm}^{-1}$  and with 128 co-added scans. The spectra were baseline corrected and normalized to 1510  $\text{cm}^{-1}$ . Shoulders and complex bands were deconvoluted for a good assessment. The assignment of peaks was performed as described by Faix (1991) and Boeriu et al. (2004) [6,7].

### **Size exclusion chromatography (SEC).**

The molar mass distribution of lignins was analyzed by alkaline SEC using a TSK gel Toyopearl HW-55F column, 0.5 M NaOH as eluent, UV detection at 280 nm and calibration with sodium-polystyrene sulfonates, according to the procedure described elsewhere [8]. Mw (weight-average molecular weight), Mn (number average molecular weight) and polydispersity (PD, Mw/Mn) were calculated.

### **High Performance Liquid Chromatography (HPLC)**

The HPLC analysis was performed using a HPLC equipped with UV detector (Waters 2487 Dual 1 absorbance detector) operating at 260 nm. A reversed phase column was used (Inersil ODS-2 5mm, 4.6  $\times$  250 mm GL Sciences Inc. Tokyo, Japan). Mobile phase was water and acetonitrile supplemented with phosphoric acid (0.01 % v/v) at the ratio of 80:20 (isocratic). Analysis was performed at 30°C and mobile phase flow rate of 0.8 mL/min. Retention time of coniferyl alcohol was 12.1 min.

## **Results and discussion**

### **1. Selection of biocatalyst**

Laccase and peroxidase oxidize phenolic substrates, including lignin, to phenoxy radicals with concomitant reduction of oxygen or hydrogen peroxide, respectively. The phenoxy radicals generated in situ are unstable, and reactions involving polymerization as well as depolymerization of lignin can take place. Many phenols are enzymatically oxidized into homopolymers, but in the presence of lignin coupling between lignin and the phenols occurs. The influence of acetone on the laccase, lignin peroxidase and horseradish peroxidase catalytic activity was studied.

#### *1.1. Kinetic study of syringaldazine enzymatic oxidation*

Enzymes speed up the rate of a reaction by a definite amount, proportional to quantity of enzyme present. To measure reaction rate, some property difference between reactant and product must be identified. Rate can be measured as disappearance of reactant or accumulation of product [9]. To better understand the organic solvent effect on the kinetic mechanism in the laccase oxidation reaction several experiments were conducted with different syringaldazine concentrations. In previous study we have shown that laccase from *Trametes versicolor* showed good stability in high acetone concentrations (50% vol) and the oxidative polymerization reactions were efficient using the acetone: water 50: 50 (v/v) soluble lignin fractions with low molecular weights (Mw < 4000 g/mol) and dispersities [10]. The kinetic studies were conducted in 50:50 (v/v) acetone/air-saturated water, at 25 °C and different syringaldazine concentrations (10 - 90  $\mu\text{M}$ ) the enzyme concentration being maintained constant (0.5  $\mu\text{g mL}^{-1}$ ).

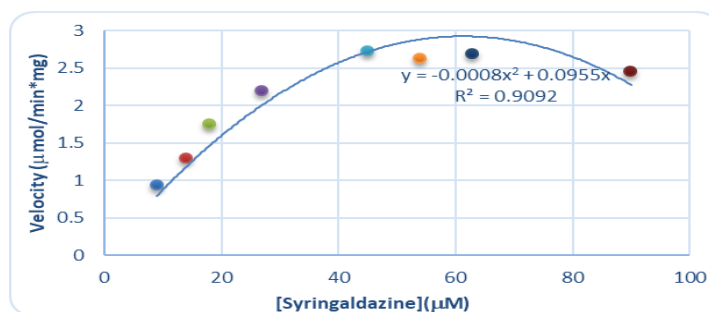


Figure 2. Michaelis-Menten kinetic curve in the oxidation reaction of syringaldazine using laccase as catalyst

From Figure 2 could be observed a hyperbolic behaviour of the substrate saturation curve, confirming the enzyme follows Michaelis-Menten behaviour. The  $K_m$  value can be understood as enzyme's affinity for the substrate and was found to be  $29,1 \mu\text{M}$  meanwhile the velocity  $V_{\text{max}}$  is  $4,1 \mu\text{mol min}^{-1} \text{mg}^{-1}$ .

1.2. *The influence of the reaction media on the catalytic efficiency of lignin peroxidase and horseradish peroxidase.*

The catalytic activity of lignin peroxidase and horseradish peroxidase was assayed spectrophotometrically using coniferyl alcohol and veratryl alcohol as substrate. The HRP and LiP activity decreased dramatically when acetone was introduced in the reaction media. Because of enzyme inhibition by the reaction solvent HRP and LiP could not be used in the coupling reaction of lignin with different compounds.

## 2. Covalent coupling of coniferyl alcohol with glucosamine

Due to the complexity of lignin macromolecule first we attempted to enzymatically modify model compounds with lower molecular weight. Laccase modification of coniferyl alcohol with glucosamine in 50 % vol. acetone-water mixture was monitored by HPLC analysis. Coniferyl alcohol consumption during the enzymatic reaction with glucosamine was compared with two control reactions without enzyme and without the co-substrate, respectively (Figure 3).

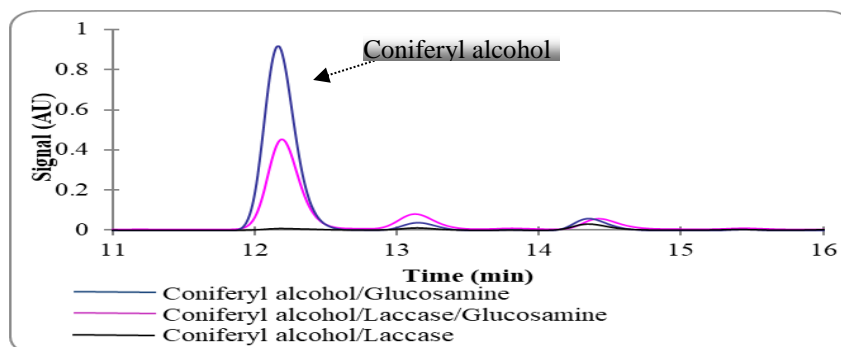


Figure 3. The HPLC chromatogram of the coniferyl alcohol modification reactions with glucosamine using laccase as catalyst

By comparing the obtained chromatograms, it can be observed that reactions take place different. In the reaction control without laccase were not observed any changes of the coniferyl alcohol meanwhile in the reaction of coniferyl alcohol with enzyme the substrate was entirely consumed (Figure 3- black line). In the case of the glucosamine coupling reaction, the reaction is different, only a certain amount of alcohol has been transformed

demonstrating that the coupling reaction take place. The reaction product could not be separated by means of HPLC analysis due to the substrate polymerization the resulting products having high molecular weights.

### Covalent coupling of Alcell lignin with chitosan

The production lignin-chitosan conjugates using laccase as catalyst is challenging having a great impact on chitosan applications. The lignin-chitosan conjugates can improve the properties of chitosan such as enhanced antimicrobial properties with use in antimicrobial hydrogels or in packaging as well they can improve the optical response having a potential use as pigmenting materials and fillers in paints and coatings. Since the chitosan is not soluble in acetone-water mixture having great solubility in acid media, the chitosan was suspended in the reaction mixture and stirred at room temperature for 24 hours. The solid was filtrated and washed with acetone for several times to remove the adsorbed lignin, dried and analysed. Both the supernatant and the obtained solid phase were analysed by means of FT-IR (Figure 4) and SEC (Table 1) analysis.

Table 1. Molecular weight distribution of Alcell lignin before and after enzymatic coupling reactions with chitosan

	Mw	Mn	Mw/Mn
Alcell-50	2346	264	8.9
Alcell-50/Chitosan	2330	282	8.3
Alcell-50/Laccase	5708	714	8.0
Alcell-50/Laccase/Chitosan	10091	858	11.8

During the reaction coupling of Alcell lignin with chitosan the suspended chitosan changed from white in slightly brown. The SEC analysis of liquid phase (supernatant) revealed a significant increase of the molecular weight and polydispersity subsequent to the reaction as compared with the control reactions, that could be concluded by the coupling of chitosan residues to the lignin backbone. Unfortunately, we encountered solubilization problems and thus the characterization of the obtained product became difficile. FT-IR spectroscopy provided evidence that chitosan was grafted onto oxidized lignin by the apparition of a new absorption band at  $1122\text{ cm}^{-1}$  and an increase in the intensity of the absorption band from  $1500\text{ cm}^{-1}$  as compared with the control product and starting material. Follow up studies will be performed to optimize the reaction conditions and to isolate and characterize the formed products.

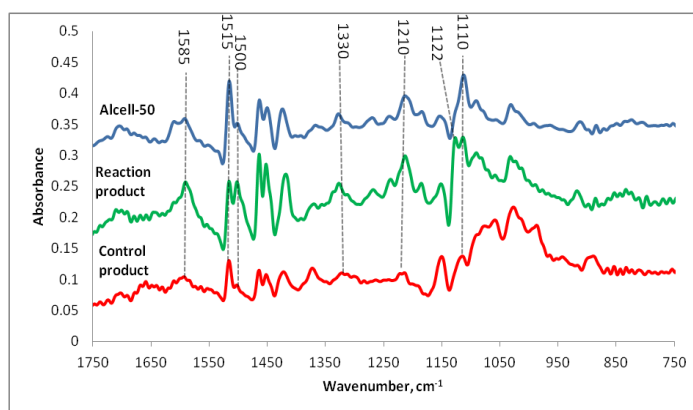


Figure 4. Comparison between the FT-IR deconvoluted spectra of the reaction product obtained in the enzymatic coupling of Alcell lignin with chitosan, the starting material and reaction control without laccase

### Conclusion

Utilization of 50% concentration of acetone in the reaction mixture doesn't affect the activity of laccase in modification reactions. This finding opens up further possibilities for the utilization of laccases in areas where the solubility of the reactants or products is limited. Enzymatic modification of Alcell lignin with chitosan using laccase as catalyst looks promising. The exact mechanisms and chemical factors that contribute to the enzymatic modification of lignin with chitosan still require additional research. This study demonstrated the occurrence of structural changes of the lignin generated by the treatment with chitosan in a medium containing an organic co-solvent, employing laccase as catalyst.

### References

- [1] M. Hofrichter, *Enzyme and Microbial Technology* 30(4) (2002), 454-466.
- [2] M. Ahmad, C. R. Taylor, D. Pink, K. Burton, D. Eastwood, G.D. Bending, T.D. Bugg, *Molecular Biosystems* 6(5) (2010), 815-821.
- [3] S. Rodríguez Couto, J.L. Toca Herrera, *Biotechnology Advances* 24 (2006), 500–513.
- [4] E. Uzan, P. Nousiainen, V. Balland, J. Sipila, F. Piumi, D. Navarro, M. Asther, E. Record, A. Lomascolo, *J. Appl. Microbiol.* 108 (2010), 2199–2213.
- [5] J. Sealey, A. Ragauskas, *Enzyme Microb. Technol.*, 23 (1998), 422-426.
- [6] G. Boeriu, D. Bravo, R. J. A. Gosselink, J. E. G. van Dam, *Ind. Crops Prod.*, 20(2) (2004), 205-218.
- [7] O. Faix, *Holzforschung*, 45 (Suppl.) (1991), 21–27.
- [8] R. J. A. Gosselink, J. E. G. van Dam, E. de Jong, E.L. Scott, J. P. M. Sanders, J. Li, G. Gellerstedt, *Holzforschung*, 64 (2010), 193-200.
- [9] D.L. Nelson, M.M. Cox, *Lehninger: Principles of Biochemistry*, 2004.
- [10] F. I. Fițigău, F. Peter, C. G. Boeriu, *ActaBiochim. Pol.*, 60 (2013), 817-822.

## OPTICAL PROPERTIES OF SnO<sub>2</sub> FILM

Stefania Florina Rus<sup>1\*</sup>, Andreas Herklotz<sup>2</sup>, Iuliana Sebarchievici<sup>1</sup>, Mirela Iorga<sup>1</sup>

<sup>1</sup>National Institute for Research and Development in Electrochemistry and Condensed Matter, Timisoara, Romania

<sup>2</sup>Materials Science and Technology Division, Oak Ridge National Laboratory, Oak Ridge, TN, 37831, USA

e-mail: rusflorinastefania@gmail.com

### Abstract

A SnO<sub>2</sub> epitaxial thin film with thickness of 25 nm is grown by the PLD technique on a (111) orientated SrTiO<sub>3</sub> (STO) substrate. The effects of epitaxial growth on the lattice structure, microstructure and optical properties of oxide thin film has been studied. The film is out-of-plane epitaxial oriented to the substrate. The XRD diffractograms show only tin dioxide peaks which can be assigned to the (002) and (004) reflexes of the tin dioxide phase. The thickness of the film is calculated from the distance of X-ray reflectivity oscillations. The observation of clear thickness fringes is an indication for a low surface roughness of the film. Atomic force microscopy (AFM) was also used to investigate the surface of the films. AFM images reveal a film surface that shows a flat film surface. Variable angle spectroscopic ellipsometry (VASE) has been used to determine the optical properties of the SnO<sub>2</sub> film.

### Introduction

The aim of the present project is to extend the knowledge acquired to date to study the main parameters for obtaining epitaxial films by various methods, determine optimum conditions necessary and analyze the phenomena involved during deposition, so that the structural and optical properties of the films they have finally qualify for applications in the energy and environmental industries.

In the literature, metal oxides such as SnO<sub>2</sub> are of major interest in solar and environmental applications, and it is necessary to deepen the studies in this field.

Tin oxide in its pure form is an n-type semiconductor [Chowdhury, 2011]. Its results in terms of electrical conductivity are due to the existence of punctual defects (native and foreign atoms) acting as donors or acceptors. Some unique properties make this material extremely useful for many applications. Thus, increased attention is paid to studies on tin oxide, particularly with regard to the preparation methods, its electrical and optical properties.

### Experimental

The tin dioxide thin film was deposited on commercial (111) oriented SrTiO<sub>3</sub> (STO) substrate using the pulsed laser deposition (PLD) technique. The substrate was ultrasonically washed using acetone and methanol before deposition. The PLD technique includes a relatively simple concept of ablation using laser pulses on the target material. With each pulse, an amount of material is removed and transported in the direction of the substrate via the plasma. Stoichiometric transfer of the target material to the substrate, mass propagation time comparable to crystallization and growth processes, atomic scale growth control of the film,



allow the formation of well-defined, layered structures. One of the most fascinating features of PLD, is a nearly stoichiometric transfer from the SnO<sub>2</sub> target through the ablation process [Díaz, 2012]. During the laser ablation process, photons penetrate into the surface layers of the target material in accordance with the optical absorption depth and, first, by removing some of the atoms' valence electrons (in the PS duration). These surface-valent electrons oscillate in the electromagnetic field of the laser and collide with atoms and ions by neighbors, transferring some of their energy to the crystal lattice. Once the particles have reached the surface of the substrate, diffusion occurs until the atoms reach low energy levels. Since each pulse emits less than one layer of deposited material, sequential ablation from multiple lenses can be used to increase the material. PLD is considered to be one of the most widely used flexible research techniques for filming large-scale films. A KrF excimer laser (248 nm wavelength and 23 ns pulse width, Lambda Physics) was used for ablating the tin dioxide target with an energy density of about 2 J/cm<sup>2</sup> and a repetition rate of 3 Hz. The films were deposited at a substrate temperature of 700 °C using an oxygen pressure of 50mTorr. After growth the films were annealed for 20 min and cooled down to room temperature at an oxygen pressure of about 0.5 atm O<sub>2</sub>. Film quality and structural properties were investigated by X-ray diffraction (XRD) using a high resolution thin film diffractometer. Different measurements were made: (1). Reflection in order to estimate the thickness of the films, (2) Normal Bragg-Brentano geometry to obtain information about the phase and structural order of the films. Before every XRD analysis, the sample alignment was performed on STO (111) peaks of the substrate in order to avoid the peak shift due to the sample misalignment. Atomic force microscopy (AFM) has been employed to investigate the surface of the films. A *DI Nanoscope III* AFM in tapping mode was used for this purpose. In order to study the optical properties of thin films the ellipsometry technique will be employed. Ellipsometry is a non-destructive optical technique used in this paper for optical characterization of thin film, in which the sample to be characterized is illuminated with a beam of polarized light.

## Results and discussion

### 1. XRD results of the SnO<sub>2</sub> film

The SnO<sub>2</sub> film was grown by on-axis pulsed laser deposition from the SnO<sub>2</sub> target on STO (111). In figure 1a) the reflectivity curve of the film grown on STO (111) substrate is shown. The thickness of the films is calculated from the distance of the oscillations. The observation of clear thickness fringes is an indication for a good surface roughness of the films. We calculate the thickness to be 25 nm.



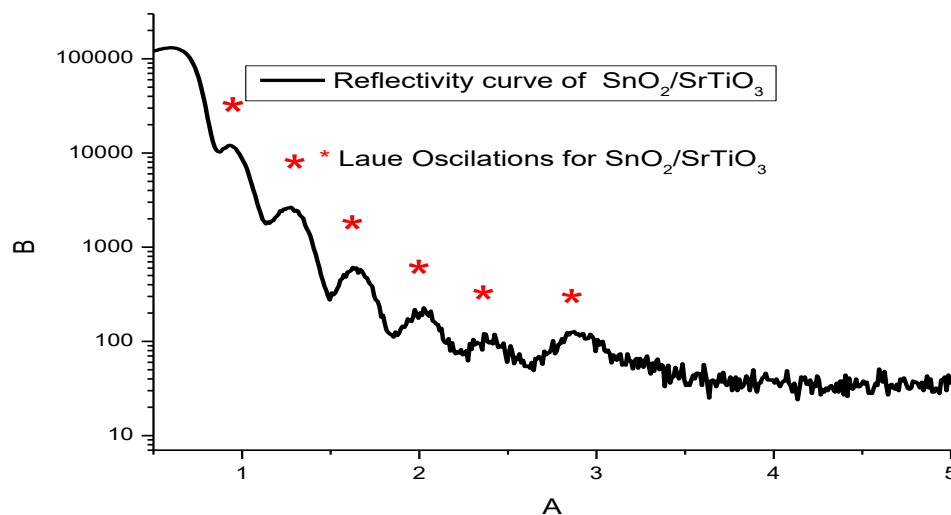


**Figure 1.** The reflectivity curve of the film grown on STO (111) substrate.

Laue oscillations remain observable for SnO<sub>2</sub> thin film which indicate that the structural quality of the film is not deteriorated.

Wide angle  $\theta$ - $2\theta$  XRD scans of the film grown on STO (111) has been recorded to investigate the phase-purity and epitaxial nature of the films and are plotted in figure 2a). The scans show only (111) substrate peaks and peaks that can be assigned to the (00l) reflexes of SnO<sub>2</sub>. The films are out-of-plane epitaxial oriented to the substrate. There are no peaks corresponding to other phases or impurities of films.

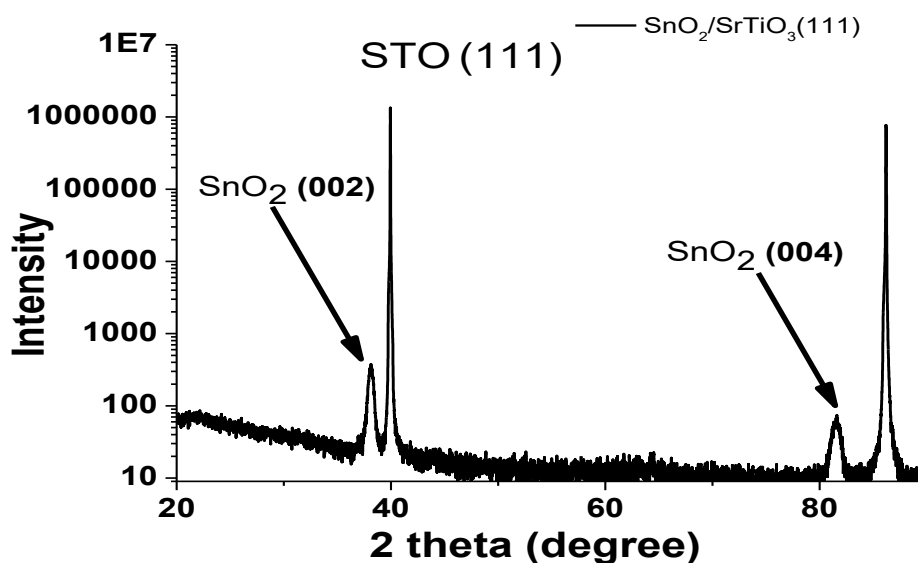


**Figure 2.a)** X-ray diffraction patterns (Bragg-Brentano  $\theta$ - $2\theta$ ) of the 25 nm film grown on STO (111).

**Figure 2.b)** shows X-ray diffraction (XRD)  $\omega$ - $2\theta$  Bragg scans along the 002 reflection of the as-grown film. We determined the out of plane lattice parameter to be 4.716 Å, which is close to that of bulk SnO<sub>2</sub> ( $c = 4.73$  Å)

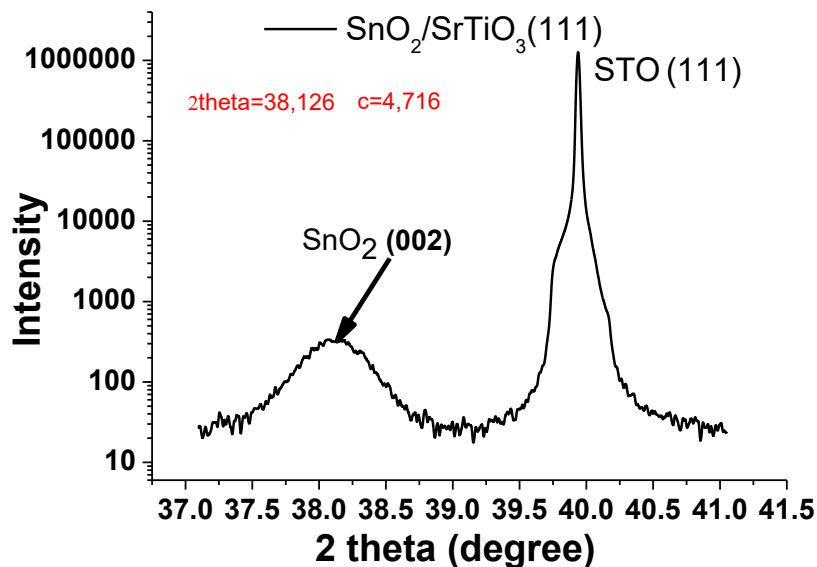


**Figure 2.** X-ray diffraction (XRD)  $\omega$ - $2\theta$  Bragg scan around the 002 reflections of the SnO<sub>2</sub> film and the STO (111) substrate.

### 2. Topography of the SnO<sub>2</sub> film

Atomic force microscopy (AFM) was used to investigate the surface of the films. AFM images reveal a film surface that shows a flat film surface and with no visual droplets or defects.

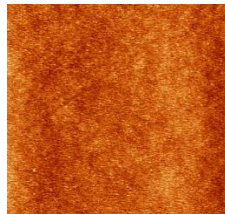


**Figure 3.** Surface morphology images of 25 nm films of SnO<sub>2</sub> deposited on STO (111).

### 3. Optical properties of the film

Ellipsometry measures the change in polarization state of the measurement beam induced by reflection from (or transmission through) the sample. The change in polarization state is commonly characterized by the ellipsometric Psi ( $\Psi$ ) and Delta ( $\Delta$ ) parameters. In Spectroscopic Ellipsometry (SE),  $\Psi$  and  $\Delta$  values are acquired as a function of wavelength. However, to extract sample parameters such as film thickness and optical constants from the measured SE data set, an optical model must be built to fit the data. The CompleteEASE software provides a graphical user interface for building models and displaying measured data and model fits. It also provides a simple interface to the SE hardware, making acquisition of accurate SE data fast and easy.

The optical constants of the STO substrate have been determined by a VASE measurement on the bare substrate and have been fixed in the two-layer model system. The SnO<sub>2</sub> layer was fitted by a Kramers-Kronig consistent B-spline model. In figure 4a) we show the Tauc-plot of the optical absorption spectrum for 25 nm thin film. This plot allows for the determination of direct optical band gap by extrapolating the linear parts of the curves to zero.

The inset presents ellipsometric  $\Psi$  parameter function of wavelength recorded for 3 different angles (65, 70 and 75 degree) together with the fitting calculated curves. The band gap energy of the 25 nm thin  $\text{SnO}_2$  film deposited by on-axis pulsed laser on STO (111) substrate is 4.18 eV.

It is observed that the band gap energy can be tunable to be bigger than the values observed by other researchers [Mishra, 2009]

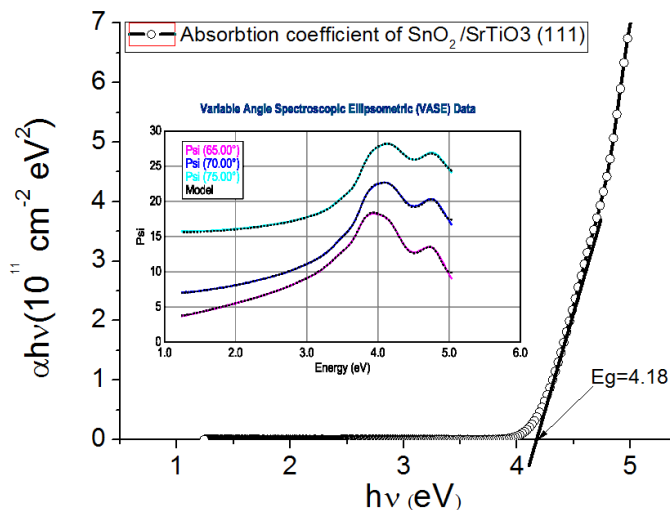


**Figure 4.a)** Tauc-plot of the optical absorption spectrum for 25 nm thin  $\text{SnO}_2$  film. In the inset ellipsometric Psi ( $\Psi$ ) and Delta ( $\Delta$ ) parameters function of wavelength were recorded for 3 different angles.

The refractive index ( $n$ ) and extinction coefficient ( $k$ ) for the 25 nm  $\text{SnO}_2$  film calculated with Complete EASE software are presented in figure 4b). The inset presents the average values for  $n$  and  $k$  parameters of the film.

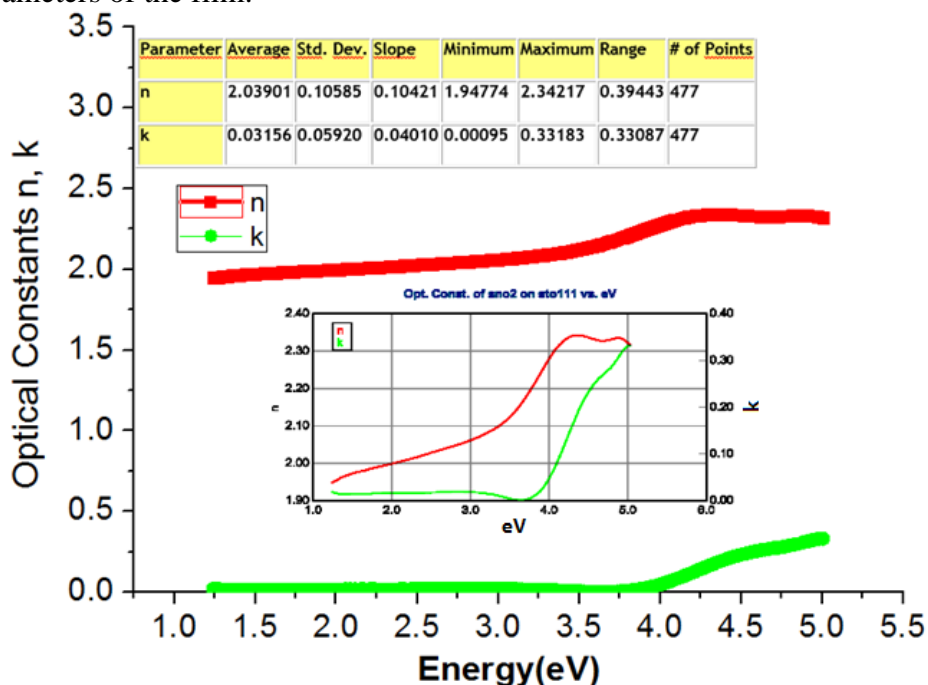


**Figure 4. b)** Optical constants ( $n$ ,  $k$ ) of 25 nm  $\text{SnO}_2$  film. The results are in accordance with

the findings of Baco et al. [Baco, 2012]

### **Conclusion**

Epitaxial films of SnO<sub>2</sub> have been grown by on-axis pulsed laser deposition from the SnO<sub>2</sub> target on (111) oriented crystalline SrTiO<sub>3</sub> substrate with a band gap energy of 4.18 eV. The results demonstrate that epitaxial strain can be deployed to change optical properties of oxide films. This could potentially be used to produce films with properties designed for specific application.

### **Acknowledgements**

This work was supported by a grant of the Romanian Ministry of National Education, project number PN 16 14 02 04.

### **References**

- F.R. Chowdhury, S. Choudhury, F. Hasan, T. Begum, Optical properties of undoped and indium-doped tin oxide thin films, *Journal of Bangladesh Academy of Sciences*, Vol. 35, No. 1, 99-111, 2011
- E.C. Díaz, A. Duarte-Moller, J.M. Camacho, R. Castro-Rodríguez, *SnO<sub>2</sub> thin films grown by pulsed Nd:YAG laser deposition*, *Applied Physics A*, Volume 106, Issue 3, 619–624, 2012
- R.L. Mishra, S.K. Mishra, S.G. Prakash, Optical and gas sensing characteristics of tin oxide nano-crystalline thin film, *Journal of Ovonic Research*, Vol. 5, No. 4, 77 – 85, 2009
- S. Baco, A. Chik , F.M. Yassin, Study on Optical Properties of Tin Oxide Thin Film at Different Annealing Temperature *Journal of Science and Technology*, Vol 4, No 1, 61-71, 2012.

**ANALYTICAL INVESTIGATION OF ADDUCTS FORMED BY  
DEOXYRIBONUCLEIC ACID WITH CHEMICAL XENOBIOTICS  
OF FOOD INTEREST**

**Zeno Gârban<sup>1,2</sup>, Hortensia Ioniță<sup>3</sup>, Gabriela Gârban<sup>4</sup>, Florin Muselin<sup>5</sup>  
Robert Ujhelyi<sup>2,6</sup>, Sorin Marinescu<sup>7</sup>**

*1)Department of Biochemistry and Molecular Biology (former), Faculty of Food Products Technology, University of Agricultural Sciences and Veterinary Medicine of Banat "King Michael I of Romania" Timișoara, Calea Aradului No. 119, 300 645 Timișoara, Romania; 2) Working Group for Xenobiochemistry, Romanian Academy-Branch Timișoara, Bd. M.Viteazu Nr.24, Timișoara, Romania; 3) Clinic of Hematology-Oncology, Faculty of Medicine, „Dr. Victor Babeș” University of Medicine and Pharmacy, Timișoara, Romania; 4) Laboratory of Environment and Nutrition, National Institute of Public Health - Branch Timișoara, Romania; 5)Faculty of Veterinary Medicine, University of Agricultural Sciences and Veterinary Medicine of Banat "King Michael I of Romania", Calea Aradului No. 119, Timișoara, Romania; 6) Medical Department, S.C. CaliVita International, Timișoara, Romania; 7)Institute of Chemistry of the Romanian Academy, Bd. M.Viteazu Nr.24, Timișoara, Romania  
e-mail.: zeno.garban@yahoo.com*

**Abstract**

Investigation of chemical xenobiotics of food interest is of major importance for food safety and for public health. In this context classes of substances, specific reactions of biotransformation (with the xenobiodegradation and xenobiosynthesis phases) and the harmful effects of xenobiotics on the organism are presented.

With reference to the analytical methods applied in the investigation of the deoxyribonucleic acid (DNA)-food xenobiotics adducts, the physico-chemical methods used, the facilities offered by them and the applicability in the genomic technologies are discussed succinctly. Also, the predictive character of data for pathological risk assessment is highlighted.

**Keywords:** chemical xenobiotics of food interest, DNA-xenobiotics adducts

**Introduction**

Chemical xenobiotics of food interest reach the organism together with nutrients and undergo biotransformation reactions. Among those, a particular interest show the reactions of xenobiosynthesis which generate adducts of type DNA-xenobiotic

To emphasize the importance of the above mentioned issue there are discussed the physico-chemical methods used in the investigation of adducts with applications in genomic technologies and the importance for nutrition and prophylactic medicine.

**1. Specificity of the chemical xenobiotics biotransformation.**

In food science it is important to know the specific aspects related to metabolization of nutrients - the field of biochemistry and the biotransformation of chemical xenobiotics - a field of xenobiochemistry.

A general assessment of chemical xenobiotics of food interest leads to the observation that they can be grouped in two classes: a) compounds of deliberate provenance (additives), e.g.: food colouring matters (synthetic), preservatives, sweeteners, antioxidants, etc.;

b) compounds of accidental/illicit provenance (pollutants), e.g.: pesticides, polycyclic aromatic hydrocarbons, mycotoxins, steroid hormones, nitrates, nitrites, metals of toxicogenic potential.

It is known that in xenobiochemistry there are specific biotransformation reactions in the phase of xenobiodegradation (i.e. oxidation-reduction reactions; hydrolysis reaction) and in the phase of xenobiosynthesis (i.e. various conjugation reactions and adduction reactions). Following the adduction reactions various adducts may form, among which those of DNA are of interest in pathobiochemistry with possible consequences in genomics and proteomics.

Biomarkers which are formed following the biotransformation processes are suitable for use in monitoring the physiological / physiopathological status of the organism (at certain time intervals), which can be determined and applied individually or within a population group.

Between biomarkers, various metabolites, particularly proteins, such as enzymes, metalloproteins, nucleoproteins, are noted. Among nucleoproteins deoxyribonucleic acid (DNA) is of particular interest because its adducts with various xenobiotics can be accurately investigated by physico-chemical means.

Among the possibilities to approach the problems of xenobiochemistry in relation to food safety / security, the biomarkers keep the attention due to the fact that they offer a real guide to the measures that are required. The use of biomarkers allows risk prediction and predictive assessment of possible pathobiochemical effects due to xenobiotics (Schulte, 1989; Schugart et al., 1992; Ehrenberg et al., 2000; Gil and Pla, 2001; Gârban, 2016).

Monitoring of biomarkers in biochemistry/xenobiochemistry is also important for the reason that it provides preliminary information on the occurrence of some clinical manifestations. It is, in fact, the stage of the occurrence and expansion of the „molecular injuries”.

The used biomarkers according to their attributes can be classified as: a) exposure biomarkers; b) effect biomarkers; c) susceptibility biomarkers.

## **2. Biogenesis of DNA-xenobiotics adducts and the pathological risk assessment**

Once the xenobiotics and xenobioderivatives entered in the organism they interact with the bioconstituents and / or metabolites. Among them, from the point of view of pathobiochemistry, a particular importance are the xenobiosynthesis reactions with the formation of DNA adducts.

The more known adducts of DNA are formed with polycyclic aromatic hydrocarbons, mycotoxins (e.g. aflatoxins), steroid hormones, some pesticides, nitrosamines (derived from nitrates and nitrites), ions of potential toxicogenic metals ( $M^{n+}$ ). Those macromolecular adducts are noted by abbreviations of type such as: DNA-HPA; DNA-AFB; DNA-  $M^{n+}$

The mechanisms incriminated in the pathobiochemistry of chemical xenobiotics are mainly their interaction with cellular bioconstituents or cellular metabolites. The manifestation of pathobiochemical effects follows the passage of xenobiotics through biochemical barriers.

Chemical xenobiotics of food interest as well as the xenobioderivatives originated from them are at the origin of „molecular injuries”, specific to pathobiochemistry. Afterwards those evolve to „cellular lesions”, important in the pathophysiology.

In xenobiochemistry but also in the field of food chemistry, clinical chemistry, pharmacology, toxicology, etc. a correlation can be made between the nature of the xenobiotics and the appropriate biomarker. Under these circumstances, the possible changes in

protein, lipid, enzyme metabolites, etc., are taken as a reference. The biomarker-xenobiotic relationship has been studied by Walker et al. (1996).

Among biomarkers of major interest for molecular biology-specific investigations are also adducts of deoxyribonucleic acid (DNA) with various xenobiotics (Alford and Caskey, 1994; Dipple, 1995; Gârban and Drăgan, 2004).

### 3. Analytical detection of DNA-xenobiotic adducts

Biogenesis of DNA adducts is of particular importance for the consideration that these compounds can be analytically detected to provide information on the consequences of „molecular injury”. Detection of DNA adducts is important especially in the diagnosis of neoplastic disease, but also in the biomonitoring of evolution during oncotherapy.

For the detection of DNA adducts there are currently various physico-chemical methods (Perera et al., 1995; Phillips and Arlt, 2009 a.o.). Between these are mentioned: <sup>32</sup>P postlabelling; high-performance liquid chromatography (HPLC); enzyme-linked immunosorbent assay (ELISA); chemoluminescence immunoassay (CIA); immunohistochemistry (IHC); synchronous fluorescence spectroscopy (SFS), mass spectrometry (MS); accelerator mass spectrometry (AMS) a.o. Systematized data on the main detection methods of DNA adducts are presented in Table 1.

**Table 1.** Detection methods for DNA adducts applicable for biomonitoring in humans (according to Phillips and Arlt, 2009)

Methods	Variations	Amount of DNA required (µg)	Approximate detection limit
<sup>32</sup> P-postlabelling	Nuclease digestion, P21 Butanol extraction, HPLC	1-10	1 adduct per 10 <sup>9</sup> -10 <sup>10</sup> nucleotides
Immunoassay	ELISA, DELFIA, CIA, IHC	20	1.5 adducts per 10 <sup>9</sup> nucleotides
Fluorescence	HPLC fluorescence; SFS	100-1000	1 adduct per 10 <sup>9</sup> nucleotides
Mass spectrometry	MS	Up to 100	1 adduct per 10 <sup>8</sup> nucleotides
Accelerator mass spectrometry	AMS	Up to 100	1 adduct per 10 <sup>11</sup> -10 <sup>12</sup> nucleotides

For the purpose of applying methods for detection of DNA adducts in human exposure are considered important: 1) the sensitivity of the method for detecting low levels of adducts; 2) the need for quantification only in micrograms of DNA; 3) providing quantifiable quantitative results for exposure; 4) the ability to detect, quantify and identify adducts.

The methods used for the determination of DNA adducts can be classified into two categories: detection methods applicable to the identification of most DNA adduct types and detection methods with limited applicability to certain types of DNA adducts (Hemminiki, 1998). With reference to these methods, the important advantages and disadvantages are presented both bio-analytically and cost-effectively (Table 2).



**Table 2.** Avantages and disadvantages of the main detection methods of DNA adducts used as exposure biomarkers (according to Hemminiki - 1998)

General methods	Advantages and	Disadvantages
A. For most adducts		
<sup>32</sup> P post-labelling	Very sensitive; Small amounts of DNA	Laborious, radiation
Immunoassay	Sensitive, easy to prepare columns	Raising antibodies, specificity
GC-MS	Specific, quantitative	Cost, derivatization, volatile adducts
Accelerator MS	Very sensitive, quantitative	Cost, radioactivity
B. For certain adducts		
Electrochemical	Easy, sensitive, cheap	Specificity, contaminants
Fluorescence	Easy, specific	Large amounts of DNA, contaminants
Alkyltransferase	Specific class of adducts, cheap, easy	Specific O6-alkylguanines?
Atomic absorption	Specific, sensitive	Specific metals, platinum

Determination of exposure biomarkers is the basis of the biomonitoring concept, a concept in which DNA adducts are increasingly applicable with the advancement of their detection techniques.

In biomonitoring, DNA adducts can generally be used to evaluate exposure to certain chemical xenobiotics of food, pharmaceutical or toxicological origin. Thus, in food chemistry - viewed from the point of view of xenobiochemistry - biomonitoring based on DNA adducts can highlight exposure to certain xenobiotics, such as carcinogenic substances occurring in food after processing (e.g. polycyclic aromatic hydrocarbons, heterocyclic amines a.o). In pharmacology, DNA adducts can be used to determine the efficacy of chemotherapeutic cytostatics (e.g. cisplatin, tamoxifen, etc.). From the point of view of xenobiochemistry, the use of DNA biomarkers in biomonitoring is important for determining the exposure especially to some environmental xenobiotics (heavy metals, pesticides, nitrates etc.).

#### 4. Contribution of genomics to the investigation of DNA-chemical xenobiotic adducts

In molecular biology, the issue of chemical xenobiotics - of food, pharmaceuticals, cosmetics, and biocides - is of application interest of „molecular injury” at the level of genes and also its effects on genomic level (Irendale and Longley, 1997; Heijne et al., 2005).

Genomics is a branch of biotechnology in which molecular biology and genetics methods for genome studies are applied to all genes in an organism. In humans, for example, the genome includes about 30,000 genes.

With the help of genomics one can study the structure of an individualized gene, the interactions between genes and interactions of the genes with the environment etc. The appearance and evolution of genomics was favored by the possibilities of sequencing the genome with the development of knowledge about DNA fragmentation and computer applications in the analysis of multiple variables.

In genomics, it is mainly intended: i) knowledge of the molecular mechanisms of adverse biological processes (caused by xenobiotics); ii) identifying changes in homeostasis status; iii) the use of screening means in order to detect harmful effects.

Interestingly, the comparison between genetics and genomics. Classical genetics aimed to locate a gene's locus on the chromosome, then cloning the gene and sequencing DNA from it. Genomics follows DNA sequencing of chromosomes, then identifying all genes. This is followed by the mapping of the genes (going up to the definition of places) of the chromosomes.

Applications of genomics also involve the evaluation of some biomarkers. In relation to xenobiochemistry, exposure biomarkers are of particular importance. They can provide predictive information (Groten et al., 2000; Paustenbach and Galbraith, 2006; Gârban, 2016).

In the genomics investigation, two important groups of so-called „genomic technologies” are distinguished from the applicative point of view: structural genomics and functional genomics. In fig.1 there are presented, after Karahalil (2010), the interrelations between genomic technologies.

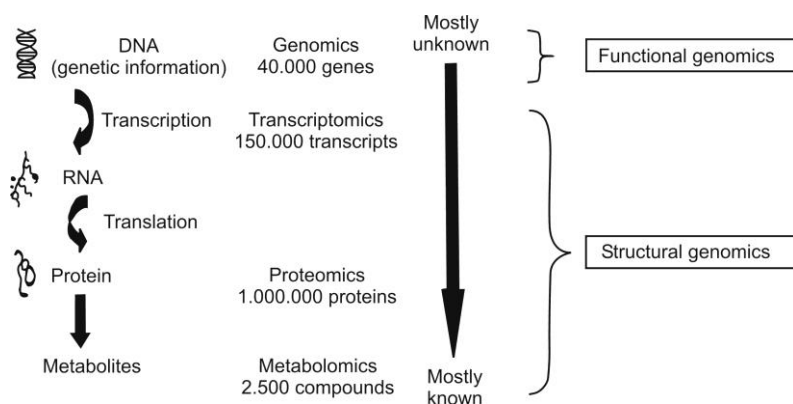


Fig.1. Interrelation between structural and functional genomics (according to Karahalil, 2010)

Structural genomics include genomic mapping, sequencing, genome and genome organization, manipulation of the genome, three-dimensional determination of structures of all proteins, study of networks (of genes, proteins). In this way, following nutrigenomics, one can study the effects of food xenobiotics starting from the DNA macromolecule.

Functional genomics include three distinct investigation directions: a) transcriptomics - evaluating a number of 150.000 transcripts; b) proteomics – considering that there are about one million proteins; c) metabolomics – appreciating that there are around 2600 compounds (Heijne et al., 2005; Fratamico and Luchansky, 2007).

Investigation of the effects of nutrients / chemical xenobiotics in food on organism is important in nutrigenomics. The study of adducts DNA-chemical xenobiotics of food interest are of particular significance because such compounds could be at the origin of teratogenic, mutagenic and oncogenic processes. Detection of the presence of adducts DNA-xenobiotics has a predictive, therapeutic and metaphylactic importance.

### Concluding remarks

Approaching the general problems of adducts and of the specific adducts of DNA-xenobiotics was influenced by the progresses in molecular biology. Thus, some issues of

pathobiochemistry based on the applications of genomics were investigated with modern physico-chemical methods.

The information obtained is suitable for use in food xenobiochemistry with applications in nutrivi-gilance.

#### References (selective)

1. Alford, R.L., Caskey, C.T. - DNA analysis in forensics, disease and animal/plant identification, *Curr. Opin. Biotechnol.*, 1994, 5(1), 29-33.
2. Dipple A. - DNA adducts of chemical carcinogens, *Carcinogenesis*, 1995, 16, 437-441.
3. Gârban Z., Drăgan P. (Eds.) - *Metal Elements in Environment, Medicine and Biology, Tome VI*, Publishing House Eurobit, Timișoara, 2004
4. Gârban Z. - *Quo vadis food xenobiochemistry* (in romanian) ediția 2-a Editura Academiei Române, București și Editura Politehnica, Timișoara, 2016
5. Gil F., Pla A. - Biomarkers as Biological Indicators of Xenobiotic Exposure, *Journal of Applied Toxicology*, 2001, 21, 245-255.
6. Groten J.P., Butler W., Feron V.J., Kozianowski G., Renwick A.G., Walke R. - An analysis of the possibility for health implications of joint actions and interactions between food additives, *Regulat. Toxicol. Pharmacol.*, 2000, 31, 77-91.
7. Hemminiki K., Byhov V., Yang K., Rajaniemi H. - Use of DNA adducts in Biomonitoring, pp. 133-135, în *Biomarkers: Medical and Workplace Applications* (Mendelson L., Mohr L.C., Peeters J.P., Eds.), Joseph Henry Press, Washington DC, 1998.
8. Karahalil B. - Pharmacogenomics and toxicogenomics in food chemicals, pp.477-496, în *Advances in food biochemistry* (Fatih Yldiz, Ed.), CRC Press, Taylor and Francis Group, Boca Raton – London - New York, 2010.
9. Phillips D.H., Arlt M.V. - Genotoxicity: damage to DNA and its consequences, pp. 87-110, in *Molecular, Clinical and Environmental Toxicology, Vol. 1, Molecular Toxicology* (Luch A., Ed.), Birkhäuser Verlag AG Basel, Switzerland, 2009.
10. Walker C.H., Hopkin S.P., Sibly R.M., Peakall D.B. (Eds) - *Principles of Ecotoxicology*, Taylor and Francis, London, 1996.

LABORATORY SIMULATED DISSIPATION OF RIMSULFURON,  
PROSULFURON AND OXASULFURON IN SOIL

Nada Grahovac\*<sup>1</sup>, Ankica Kondić-Špika<sup>1</sup>, Zorica Stojanović<sup>2</sup>, Snežana Kravić<sup>2</sup>, Ana Đurović<sup>2</sup>, Snežana Jakšić<sup>1</sup>

<sup>1</sup>*Institute of Field and Vegetable Crops, Maksima Gorkog 30, 21000 Novi Sad, Serbia,*

<sup>2</sup>*University of Novi Sad, Faculty of Technology, Department of Applied and Engineering Chemistry, Bulevar cara Lazara 1, 21000 Novi Sad, Serbia*

*e-mail:nada.grahovac@ifvcns.ns.ac.rs*

**Abstract**

Rimsulfuron, prosulfuron and oxasulfuron are a group of sulfonylurea herbicides that have been widely used for controlling weeds in a variety of vegetables and other crops. Because of the high herbicidal activity of this sulfonylureas, they are beneficial at low application rates which are approximately 1000 times less than other of conventional herbicides. Hence the using of this herbicides is increasing constantly worldwide.

The fate of rimsulfuron, prosulfuron and oxasulfuron in soil type Calcic Chernozem Clayic, Pachic (according to the FAO-WRB classification) were investigated using ultra-performance liquid chromatography with diode array detection for herbicide detection. Their dissipation behaviour in soil were evaluated under laboratory incubated condition at 70% water holding capacity of soil and two temperature (25°C and 30°C) were maintained in thermostat. In order to investigate dissipation selected sulfonylureas were used as aqueous solution of commercial formulation herbicides. The recommended dosage of rimsulfuron, prosulfuron and oxasulfuron were 50, 20 and 80 g active ingredient (a.i.) per hectare, respectively. Representative soil samples were collected after 2 hours, and then after 2, 6, 15, 30 and 50 days after the application of herbicides. Initial residues of all investigated herbicides were higher at temperature 25°C than 30°C. The residues of rimsulfuron on both analysed temperature for tested dose were less than LOQ (3.04 µg kg<sup>-1</sup>) after 2 days and 6 days for prosulfuron (2.97 µg kg<sup>-1</sup>) and oxasulfuron (3.40 µg kg<sup>-1</sup>). The dissipation of this three sulfonylureas in studied soil was described by using the Mittag-Leffler function  $c E_a (-bt)$ . Model coefficients a, b, c were received from the experimental data by using a fitting procedure. Rimsulfuron and prosulfuron showed faster degradation in tested soil with half lives of 0.49 and 0.03 days at temperature 30°C, respectively. The degradation rate of oxasulfuron appeared something slower with half lives of 0.64 day at temperature 25°C.

These results indicate how herbicides belonging to the identical chemical class can behave in various way concerning dissipation in soil.

## GERMINATION ENERGY AND SEED GERMINATION OF CULTIVATED PLANTS AS INDICATORS OF WATER CONTAMINATION WITH NICKEL

**Sonja Gvozdenac<sup>1</sup>, Vojislava Bursić<sup>2</sup>, Martina Mezei<sup>2</sup>, Jelena Ovuka<sup>1</sup>, Mladen Tatić<sup>1</sup>,  
Dejan Prvulović<sup>2</sup>**

<sup>1</sup>*Institute of Field and Vegetable Crops, Maksima Gorkog 30, Novi Sad, Serbia*

<sup>2</sup>*University of Novi Sad, Faculty of Agriculture, Trg Dositeja Obradovića 8, Novi Sad, Serbia  
sonja.gvozdenac@ifvcns.ns.ac.rs*

### Abstract

Heavy metal pollution of water ecosystems is currently one of the major environmental problems. Nickel ( $\text{Ni}^{+2}$ ) is a metal that usually occurs in the environment at very low levels. However, its presence in water at higher concentrations is becoming more frequent, as a result of antropogenic activity. The majority of cultivated plants do not tolerate high concentrations of nickel in the environment. Therefore, its detection in water is of great importance for irrigation water risk assessment. The aim of this study was to evaluate the tolerance of sunflower, maize, buckwheat, cabbage and white mustard seeds to different levels of nickel in water and assess their potential as bioindicators of water contamination with this heavy metal. Bioassay was carried out according to a standard filter paper method, and the results were processed with statistical software SPSS 17, using Duncan's multiple range test. The effect of nickel on GE and G differed depending on plant species and the applied concentration. GE and G of sunflower seeds were significantly inhibited by  $\text{Ni}^{+2}$  when applied at MAC rate for irrigation water ( $100\mu\text{g/l}$ ), while maize and buckwheat seeds were tolerant to MAC rates of this metal.  $\text{Ni}^{+2}$  stimulated GE and G of cabbage seeds at MAC for irrigation water ( $100\mu\text{g/l}$ ) and G of white mustard seeds at MAC rate for II class of water (ICPDR -  $50\mu\text{g/l}$ ).

**Key words:** nickel, seed, germination, phytotoxicity, bioindicators

### Introduction

Water pollution with heavy metals is one of the major environmental problems, because their uncontrolled release has led to accumulation in aquatic systems [1,2]. Nickel ( $\text{Ni}^{+2}$ ) is a metal that occurs in the environment at very low levels. Maximal allowable amount (MAC-EQS) in surface waters according to ICPDR (The Danube River Basin District Document IC/084) is  $50\mu\text{g/l}$  for II class of water and according to Regulation on allowable amounts of dangerous and harmful substances in soil and irrigation water and methods of analysis (Off. Gazette 23/94) is  $100\mu\text{g/l}$ . However, due to antropogenic activities, it is more often present at higher concentrations in water bodies and often exceeds the abovementioned limits. Although  $\text{Ni}^{+2}$  is essential element in plants, the higher levels can cause phytotoxic symptoms to sensitive species. There are more than 300 taxa of  $\text{Ni}^{+2}$  hyperaccumulators, i.e. plants which accumulate more than  $1000\text{ mg Ni kg}^{-1}$  of dry weight in their shoots. There are also plants called hypernickelophores, which accumulate  $>10,000\text{ mg N kg}^{-1}$  (*Psychotria douarrei*, *Geissois pruinosa*, *Alyssum murale*) and can be developed as a commercial crop for phytoremediation/phytomining of  $\text{Ni}^{+2}$  from metal-enriched soils [3,4]. However, the majority of cultivated plants do not tolerate high concentrations of  $\text{Ni}^{+2}$  in the environment. Thus, its detection in water is of great importance for irrigation water risk assessment. Certain plant species are highly sensitive and react with physiological and morphological changes and are successfully used as test organisms in bioassays for contamination detection [5].

The aim of this study was to evaluate the tolerance of sunflower, maize, buckwheat, cabbage and white mustard seeds, to different levels of  $\text{Ni}^{+2}$  in water and determine their potential as bioindicators of water contamination with this heavy metal.

### Material and methods

Bioassay was carried out according to a standard filter paper method recommended by [6] and [7]. The toxic effects of nickel, applied at rates: 25, 50, 100, 250, 500, 750 and 1000 $\mu\text{g/l}$ , was assessed according to changes in germination energy - GE (%) and seed germination - G (%) of sunflower, maize, buckwheat, cabbage and white mustard.

For germination assessment, 50 sunflower and maize and 100 cabbage seeds were placed in plastic boxes on pleated filter paper, previously moistened with 25 mL of  $\text{Ni}^{+2}$  solution, while 100 seeds of buckwheat and white mustard were placed in Petri dishes, also on filter paper, but moistened with 10 mL of  $\text{Ni}^{+2}$  solution. Distilled water was the control. Seeds were incubated in dark at  $25 \pm 2$  °C and after three (white mustard) or four days (sunflower, maize, cabbage, buckwheat) GE was recorded. After seven (maize, buckwheat and white mustard) and ten (sunflower and cabbage) days G was recorded. The experiment was set in four replicates.

The values for GE and G were transformed in  $\arcsin\sqrt{\%}$  prior to statistical analysis. The results were processed with statistical software SPSS 17, using Duncan's multiple range test (F value) for confidence interval 95%.

### Results

The effect of nickel on GE and G differed depending on plant species and the applied concentration. The results are presented in Table 1.

GE and G of sunflower seeds were statistically significantly inhibited by  $\text{Ni}^{+2}$  when applied at MAC rate for irrigation water (100 $\mu\text{g/l}$ ) and at higher concentrations ( $F=10.51^{**}$ ;  $10.51^{**}$ ,  $p<0.01$ , respectively). However,  $\text{Ni}^{+2}$  did not affect GE and G of maize, regardless on the applied rate and all values were on the same level of significance with the control ( $F=1.85\text{ns}$ ;  $1.85\text{ns}$ ,  $p>0.05$ , respectively). Mentioned parameters of buckwheat seeds were significantly inhibited by  $\text{Ni}^{+2}$  at 750-1000 $\mu\text{g/l}$  ( $F=12.96^{**}$ ;  $13.44^{**}$ ,  $p<0.01$ , respectively), but when applied at MAC rate, did not express effect on GE and G.  $\text{Ni}^{+2}$  stimulated GE and G of cabbage seeds at MAC for irrigation water (100  $\mu\text{g/l}$ ), and the difference between treatments were statistically highly significant ( $F=19.12^{**}$ ,  $19.12^{**}$ ,  $p<0.01$ , respectively). G of white mustard seeds was also significantly stimulated by  $\text{Ni}^{+2}$  applied at MAC rate for irrigation water (100 $\mu\text{g/l}$ ), while at other rates, the values of GE and G were on the same level with the control ( $F=5.38^{**}$ ,  $p<0.01$ , respectively).

A number of standardized phytotoxicity tests point out germination, as a parameter that reliably indicates at changes in water quality [8, 9, 10,]. Also, according to [11] germination is fast indicative parameter for phytotoxicity, which was proven in this work for seeds of sunflower, buckwheat, cabbage and white mustard, because G of mentioned seeds was influenced by  $\text{Ni}^{+2}$ . Nickel is toxic to most plant species, because it is affecting amylase, protease and ribonuclease activity, causing the inhibition of seed germination and growth of many crops [12]. It has been reported to affect the digestion and mobilization of food reserves like proteins and carbohydrates in germinating seeds. [13] confirmed that high concentrations of this metal can cause changes in seed metabolic activity and inhibit germination, which was proven in the case of sunflower and buckwheat seeds in this work. According to [14],  $\text{Ni}^{+2}$  in amount of 60 mg/l reduces the physiological parameters and the inhibition is stronger with the increase of concentration.  $\text{Ni}^{+2}$  toxic effects on seeds are a result of disturbed activity of



amylase, protease and ribonuclease, which is manifested as a delaying of seed germination [15]. According to [16], low concentration (10 and 20 mg L<sup>-1</sup>) of nickel significantly promoted seed germination and improved early seedling growth, while higher levels (40, 20 and 60 mg L<sup>-1</sup>) caused a significant inhibition in germination and resulted in a considerable delay to achieve 50% germination.

Table 1. The effect of Ni<sup>+2</sup> on germination energy and seed germination of cultivated plants

Plant species	Ni (µg/l)	Germination energy (%)		Germination (%)	
		%	arcsin√%	%	arcsin√%
Sunflower	1000	92.0	73.6±0.30 c	92.0	73.6±0.30 c
	750	90.0	71.6±2.00 c	90.0	71.6±2.00 c
	500	96.0	78.6±2.00 ab	96.0	78.6±2.00 ab
	250	96.0	78.5±0.00 ab	96.0	78.5±0.00 ab
	100 <sup>2</sup>	93.0	74.7±0.70 bc	93.0	74.7±0.70 bc
	50 <sup>1</sup>	98.0	82.0±1.00 a	98.0	82.0±1.00 a
	25	98.0	82.0±0.00 a	98.0	82.0±0.00 a
	control	96.0	78.5±0.00 ab	96.0	78.5±0.00 ab
	<b>F value</b>		<b>10.51**</b>		<b>10.51**</b>
Maize	1000	100	90.0±0.00 a	100	90.0±0.00 a
	750	100	90.0±0.00 a	100	90.0±0.00 a
	500	99.5	88.0±1.00 a	99.5	88.0±1.00 a
	250	99.5	88.0±1.00 a	99.5	88.0±1.00 a
	100 <sup>2</sup>	100	90.0±0.00 a	100	90.0±0.00 a
	50 <sup>1</sup>	99.5	88.0±1.00 a	99.5	88.0±1.00 a
	25	99.5	88.0±1.00 a	99.5	88.0±1.00 a
	control	98.0	83.1±1.00 a	98.0	83.1±1.00 a
	<b>F value</b>		<b>1.85ns</b>		<b>1.85ns</b>
Buckwheat	1000	86	68.1±0.00 b	86.0	68.1±0.00 b
	750	88.5	70.7±1.50 b	88.5	70.7±1.50 b
	500	94	75.9±0.00 ab	95.0	77.1±0.00 ab
	250	98	82.0±0.00 a	98.0	82.0±0.00 a
	100 <sup>2</sup>	98.5	83.1±0.50 a	98.5	83.1±0.50 a
	50 <sup>1</sup>	98	82.0±1.00 a	98.0	82.0±1.00 a
	25	98.5	83.1±0.50 a	98.5	83.1±0.50 a
	control	98.5	83.1±0.00 a	99.0	85.9±0.00 a
	<b>F value</b>		<b>12.96**</b>		<b>13.44**</b>
Cabbage	1000	78.0	62.0±1.00 c	78.0	62.0±1.00 c
	750	98.7	84.5±0.70 a	98.7	84.5±0.70 a
	500	98.0	82.0±0.00 a	98.0	82.0±0.00 a
	250	98.7	84.5±1.60 a	98.7	84.5±1.70 a
	100 <sup>2</sup>	98.0	82.0±0.00 a	98.0	82.0±0.00 a
	50 <sup>1</sup>	94.0	75.9±0.00 b	94.0	75.9±0.00 b
	25	93.5	75.4±0.50 b	93.5	75.4±0.50 b
	control	94.5	76.4±0.50 b	94.5	76.4±0.50 b
	<b>F value</b>		<b>19.12**</b>		<b>19.12**</b>
White mustard	1000	71.0	57.4±3.00 a	75.0	60.0±2.00 b
	750	73.0	58.7±2.20 a	76.7	61.3±2.10 b
	500	75.0	60.0±1.30 a	76.7	61.3±2.30 b
	250	74.0	59.3±1.70 a	79.0	62.7±0.70 b
	100 <sup>2</sup>	80.0	63.4±1.50 a	84.0	66.4±1.00 a
	50 <sup>1</sup>	72.0	58.0±2.50 a	77.7	61.4±2.50 b
	25	72.0	58.0±4.00 a	75.0	60.0±1.20 b
	control	73.0	58.7±2.70 a	76.7	61.3±1.60 b
	<b>F value</b>		<b>2.34ns</b>		<b>5.38**</b>



F test  $\pm$ SD; values with the same letter in the column are on the same level of significance for the confidence interval 95%; \*\* $p < 0.01$ ; \*  $p < 0.05$ ; ns  $p > 0.05$ , <sup>1</sup>-MAC for II class of water (ICPDR, 2004); <sup>2</sup>-MAC in irrigation water (Regulation, Off. Gazette RS 23/94)

The stimulating effect that Ni<sup>+2</sup> expressed on cabbage and sunflower seeds is in accordance with [16, 17]. These authors report that, when applied at 10 and 20 mg/l, Ni<sup>+2</sup> significantly stimulated germination of different seeds.

However, the results of [2] indicate that the seed germination is a physiological parameter that is rarely affected by heavy metals, including Ni<sup>+2</sup>. This was proven for maize seeds in this work.

## Conclusion

Germination energy and germination of sunflower seeds were significantly inhibited by Ni<sup>+2</sup> at maximum allowable rate, stipulated by several Regulations, which indicates at good potential of this plant species and mentioned parameters in detection of water pollution with Ni<sup>+2</sup>. Maize was very tolerant to high levels of in Ni<sup>+2</sup> in water and does not have potential to be used as an indicator of water pollution with this heavy metal.

## Acknowledgement

This work is a part of project III43005, financed by the Ministry of Education and Science of the Republic of Serbia.

## References

- [1] M. Prica, B. Dalmacija, M. Dalmacija, J. Agbaba, D. Krčmar, J. Tricković, E. Karlovic (2010): Changes in metal availability during sediment oxidation and the correlation with immobilization potential. *Ecotoxicology and Environmental Safety*, 73(6): 1370-1377.
- [2] M. Aycicek, M. Ince, M. Yaman (2008): Effects of cadmium on germination, early seedling growth and metal content of cotton (*Gossypium hirsutum* L.), *International Journal of Science and Thechnology*, 3(1): 1-11.
- [3] R. Tappero, E. Peltier, M. Grafe, K. Heidel, M. Ginder-Vogel, K. Livi, M. Rivers, M. Marcus, R. Chaney, D. Sparks (2007): Hyperaccumulator *Alyssum murale* relies on a different metal storage mechanism for cobalt than for nickel. *New Phytologist*, 175(4): 641-654.
- [4] C. Grison, V. Escande, E. Petit, L. Garoux, C. Boulanger, C. Grison (2013): *Psychotria douarrei* and *Geissois pruinosa*, novel resources for the plant-based catalytic chemistry. *RSC Adv.*, 4(3): 22340-22345.
- [5] G.T. Ankley, D.A. Benoit, R.A. Hoke, E.N. Leonard, C.W. West (1993): Development and evaluation of test methods for benthic invertebrates and sediments: Effects of flow rate and feeding on water quality and exposure conditions, *Archives of Environmental Contamination and Toxicology*, 25(1): 12-19.
- [6] ISTA (International Seed Testing Association): *International Rules for Seed Testing* (2013).
- [7] Regulations on the quality of seed of agricultural plants (Official gazette, RS 34/2013).
- [8] OECD Guideline for Testing of Chemicals 208 (1984): *Terrestrial Plants, Growth Test*
- [9] US EPA, OPPTS Ecological Effect Guideline, 850 Series, (1996).
- [10] AFNOR X31-203/ISO 11269-1 (1993): *Determination des effets des polluants sur la flore du sol: Méthode de mesurage de l'inhibition de la croissance des racines.*

- [11] X. Wang, C. Sun, Sh.Gao, L. Wang, H. Shokui (2001): Validation of germination rate and root elongation as indicator to assess phytotoxicity with *Cucumis sativus*. Chemosphere, 44, 1711-1721.
- [12] M. Smiri (2011): Effect of cadmium on germination, growth, redox and oxidative properties in *Pisum sativum* seeds, Journal of Environmental Chemistry and Ecotoxicology, 3(3): 52-59.
- [13] R.M. Khan, M.M. Khan (2010): Effect of varying concentration of nickel and cobalt on the plant growth and yield chickpea. Australian Journal of Basic and Applied Science, 4(6): 1036-1046.
- [14] M.Y. Ashraf, R. Sadiq, M. Hussain, M. Ashraf, M.S.A. Ahmad (2011): Toxic effect of nickel (Ni) on growth and metabolism in germinating seeds of sunflower (*Helianthus annuus* L.). Biol. Trace Elem. Res., 143: 1695-1703.
- [15] S.K. Sethy, S. Ghosh (2013): Effect of heavy metals on germination of seeds. J. Nat. Sc. Biol. Med. 4: 272-275.
- [16] S.A. Ahmad, M. Hussain, M. Ashraf, R.I. Ahmad, M.A. Ashraf (2009): Effect of nickel on seed germinability of some elite sunflower (*Helianthus annuus* L.) cultivars. Muhammad Pak. J. Bot., 41(4): 1871-1882.
- [17] M.S. Ahmad, M. Ashraf, M., Hussain (2010): Phytotoxic effects of nickel on yield and concentration of macro-and micro-nutrients in sunflower (*Helianthus annuus* L.). Achenes. J. Hazard. Mater., 10: 234-240.

## ADSORPTION STUDY OF CARBENDAZIM PESTICIDE BY BENTONITE CLAY

**Ali. Mohammed. Hgeig<sup>1\*</sup>, Mladenka Novaković<sup>1</sup>, Veselin Bežanović<sup>1</sup>, Ivana Mihajlović<sup>1</sup>**

<sup>1</sup>University of Novi Sad, Faculty of Technical Sciences, Novi Sad, Serbia

\* e mail: alihagaig2017@yahoo.com

### **Abstract**

Bentonite clay (BC) was used for the adsorption of carbendazim pesticide from aqueous solution. Adsorption with BC was investigated because of its large surface area and high cation exchange capacity. Influence of pH, dose of adsorbent, contact time and initial concentration of carbendazim were studied in adsorption processes by BC. Adsorption experiments were conducted in a batch system and found to be with maximum effectiveness at pH 3. The maximum recoveries of adsorption processes were 0.44mg/g and 0.25mg/g with 0.5 g and 1.0 g of BC, respectively. Contact time was 10 min and initial concentration of carbendazim was 5 mg/L for both experiments.

### **Introduction**

The use of clay minerals as solid components in sorption of pesticide formulations is based on their adsorption properties or on formation of particular types of aggregates. The clay mineral often has to be modified by ion exchange with organic cations when used as adsorbent for a pesticide [1]. However, certain bentonite can be directly used in slow-release pesticides formulations. Adsorption is used especially in the water treatment field and the investigation has to be made to determine inexpensive and good adsorbent. Clay minerals such as kaolin, bentonite are the most wide-spread minerals of the earth crust which are known to be good adsorbents/sorbents of various metal ions, inorganic anions and organic ligands [2]. BC is widely used in pesticide formulations as adsorbents or particulate fillers.

Acidic pesticides, which are often in their anionic form at the pH of soil and water environments, display a particularly high risk of ground and surface water contamination, because they are weakly retained by the most of soil types and sediment components [3]. For this reason, the development of pesticide adsorbents to prevent and remediate environmental contamination by anionic pesticides has become an important research goal [4]. Carbendazim is in a priority list for preventing the contamination of ground and drinking waters by pesticides in Europe, which considers pesticides used in quantities over 50 tons per annum and their capacities as portable or transient leachable substances [5].

The aim of this paper was to investigate the adsorption processes of carbendazim pesticide by BC. Adsorption experiments were conducted in a batch system and influence of pH, mass of adsorbent, contact time and initial concentration of carbendazim were studied.

### **Experimental**

All chemicals used were of analytical grade. The Stock solution of carbendazim (200 mg/l) was prepared by dissolving 5 mg of standard in 25 mL of methanol. The experimental solutions of desired concentration were prepared by diluting the stock solution with distilled water. The residual concentration of carbendazim was determined by HPLC. pH of solutions were adjusted using 0.1M HCl and 1M NH<sub>4</sub>OH.

The clay material used in the present study was commercial bentonite obtained from Republic of Serbia. The sample was washed with boiling distilled water and dried in oven at 80 °C for

12 h and crushed. BC was then sieved in order to get fractions < 160 µm. Then, it was kept in hermetically closed bottle for further uses.

Carbendazim adsorptions were evaluated at room temperature  $25^{\circ}\text{C} \pm 2^{\circ}\text{C}$  (298 K) in a 150 mL Erlenmeyer flask. Equilibrium experiments were carried out by contacting different mass (0.50, 0.75, 1.00, 1.50 and 2.00 g) of BC with 50mL of 5 mg/L carbendazim solution. The flasks were shaken on a shaker under 140 rpm and the pH value of the reaction solution was maintained at 3.0, and contact time was 30 min. to know the optimal mass. Then, at pH value 7.95 (without modification), and different pH values (3.0, 5.0, 7.0, 9.0) the experiments were initiated with the addition of 0.50 g and 1.00 g of BC.

In the following experiments, the influences of solution at pH value 3.0 were evaluated. Samples were withdrawn from the flask at pre-determined time intervals (10, 20, 30, 40, 60, 80 min) and immediately filtered by membrane filters prior to further analysis. The uptake per mg of adsorbent,  $q_e$  was calculated using Eqs. (1) as follows:

$$q = \frac{(C_0 - C_f)}{C_0} * V \quad 1$$

Where  $q_e$  is the adsorption capacity (mg/g),  $C_0$  and  $C_f$  are the initial and final carbendazim concentrations, respectively (expressed in mg/L),  $V$  is the solution volume (mL) and  $m$  is the adsorbent dosage (g).

Adsorption at different concentrations (2,4,5,6,8 and 10 mg/L) of carbendazim assays were carried out in 50-mL flask containing 50 mL of reaction solutions and 0.50 g and 1.00 g of adsorbents. The flasks were shaken on the shaker at 140 rpm.

The target pesticide carbendazim was analyzed by HPLC-DAD. Separation was performed with a reversed phase column Eclipse XDB-C18 (3 x 150, particle size 3.5µm). The operating conditions were: flow of 0.4 mlmin<sup>-1</sup>, the temperature of the column was 30°C and injection volume of 10µL. The mobile phase consisted of water (A) and acetonitrile (B). The binary gradient elution started at 25% B in 1 minute, then linearly increased to 50% B in 5 minutes, and at the end, initial conditions were applied, 25% B for 7 minutes. The maximum wavelength of 215 nm was used.

## Results and discussion

### Influence of adsorption dosage

Figure 1. Shows that, a number of adsorbents (0.50, 0.75, 1.00, 1.50 and 2.00 g) at equilibrium decreased from 0.47 mg/g to 0.12 mg/g with an increase in the adsorbent dosage. The statistical analysis showed that there is a significant difference ( $P \leq 0.05$ ) between selected clay mass at pH 3.0 and contact time of 30 min. This can be due to the competitive adsorption between the free adsorption sites and the saturated adsorption sites. Moreover, although the number of adsorption sites per unit mass of adsorbent should remain constant independently of the total adsorbent mass, increasing the adsorbent capacity in a fixed volume reduces the number of available sites as the effective surface area is likely to decrease [6].

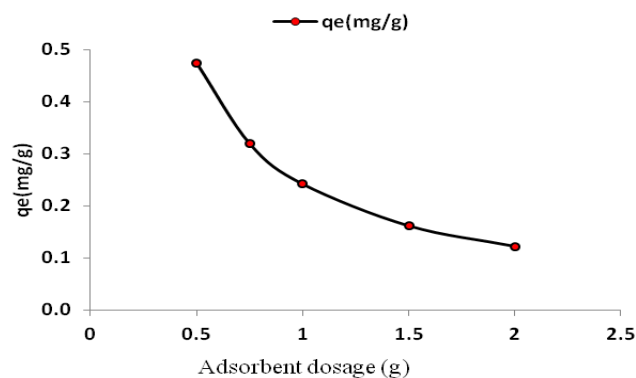


Figure 1. Effect of adsorbent dosage on adsorption of carbendazim (pH= 3,  $C_0= 5$  mg/l, cont.time=30 min)

### Influence of pH on carbendazim removal

One of the most important factors affecting the capacity of an adsorbent in aqueous solution treatment is pH. The effect of pH on carbendazim removal by BC is shown in Figure 2. The adsorption of carbendazim amount on BC increased from 0.19 mg/g to 0.44 mg/g with decrease in pH from 9.0 to 3.0 at 0.50 g of BC, and the adsorption of carbendazim amount on BC increased from 0.17 mg/g to 0.24 mg/g with decrease in pH from 9.0 to 3.0 at 1.00 g. Maximum carbendazim removal was observed at pH value 3.0. The lowest adsorbed amount was obtained at the highest pH value 9.0. The explanation of these results was that the pH value affects the ionization status of carbendazim. For instance, it can be suggested that the pH 3.0 was optimum.

Fractions of carbendazim molecules became positively charged molecules and consequently large adsorbed amount was obtained. At high pH value 9.0, a large fraction of carbendazim molecules became negatively charged or non-charged molecules. In this case BC particles cannot absorb a negatively charged carbendazim molecule due to repulsion between the negatively charged BC surfaces and carbendazim. Furthermore, the hydrophilic BC surfaces cannot adsorb large fraction from carbendazim molecules due to the hydrophobicity of carbendazim at high pH value.

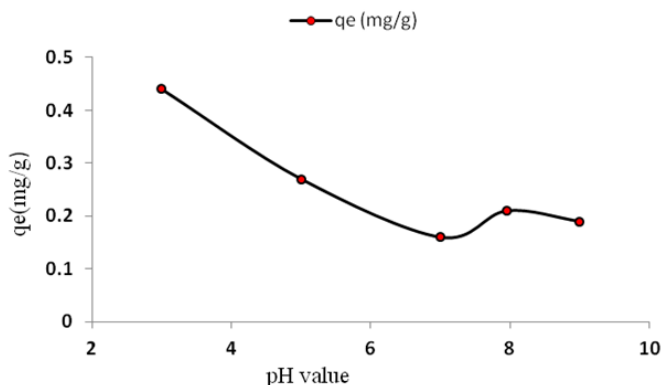


Figure 2. Effect of pH on adsorption of carbendazim by BC ( $C_0=5$  mg/l, dosage= 0,5 g and cont.time= 10 min)

### Influence of contact time

Adsorption of carbendazim on BC at various contact times in the solution with an initial carbendazim concentration of 5 mg/L is shown in the Figure 3. It can be clearly observed that the adsorption capacity was rapidly at the beginning of the adsorption time. The adsorption of carbendazim amount on BC reached 0.47 mg/g and 0.24 mg/g, respectively at doses 0.50 g and 1.00 g of BC when the pH value was 3.0. Prolonging the contact time could not improve carbendazim adsorption capacity significantly. There is no significant difference ( $P \leq 0.05$ ) found between 5 min, 30 min and 40 min, and between 10 min and 20 min, and between 20 min, 30 min and 40 min. 60 min and 80 min showed the lowest  $q_e$  value at 0.50 g, pH = 3.

According to our statistical results 10 min showed the best removal of carbendazim from aqueous media when the pH value was 3.0 and the mass of BC was 0.5 g and 1.0 g.

Figure 3. also depicts the evolution of the amount of carbendazim uptake with the contact time. The adsorption capacity of carbendazim increased with time and reached equilibrium after 10 min. The adsorption is quiet fast and attained a maximum after 5 min of contact, then followed a gradual decrease with time until it reached equilibrium. This may be due to the fact that, at the beginning, the surface adsorption sites were readily available and consequently, adsorption proceeded at very high rate, then, with increasing coverage, the number of sites became less and carbendazim ions had to fiercely compete among themselves for getting.

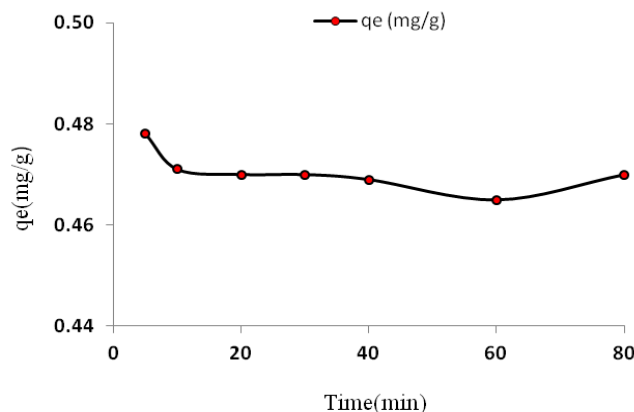


Figure 3. Effect of contact time on adsorption of carbendazim by BC ( $c_0=5$  mg/l, dosage=0,5 g, pH 3)

### Influence of initial concentration

Figure 4. show the adsorption uptake versus initial concentration for an equilibrium time at 10 min. The amount of carbendazim removed at equilibrium decreased from 0.50 mg/g to 0.21 mg/g at 0.50 g of BC with the increase in concentration from 2 mg/L to 10 mg/L. There is no significant difference ( $P \leq 0.05$ ) between concentrations 2.0 (mg/L) and 4.0 (mg/L) .and between 5.0 (mg/L) and 6.0(mg/L). 10 (mg/L) possessed the lowest  $q_e$  value when the pH value was 3.0 and the mass of BC was 0.50 g.

The highest  $q_e$  value ( $P \leq 0.05$ ) was registered at 2 (mg/l) when the mass of BC was 1.00 g and the pH value was 3.0 and contact time 10 min.

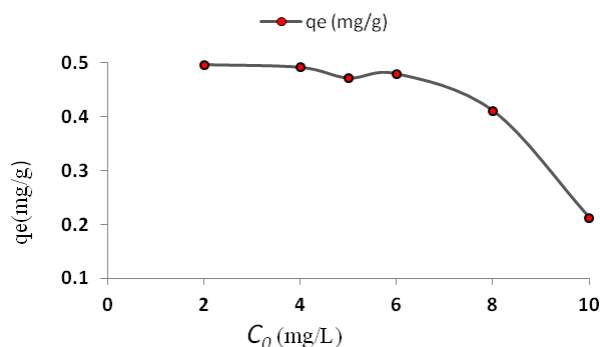


Figure 4. Effect of initial concentration on adsorption of carbendazim by BC (cont.time=10 min, dosage=0,5 g, pH 3)

The amount of carbendazim removed was 0.25 mg/g at equilibrium for 1.0 g of BC and was no significant difference in concentration from 2 mg/L to 10 mg/L. It is clear that the adsorption capacity depends on the initial concentration and amount of BC. This is due to the fact that, the initial carbendazim concentration provided the necessary driving force to overcome the resistances to the mass transfer of carbendazim ions between the solution and adsorbent [7].

### Conclusion

The study shows that BC, natural material, can be used as an adsorbent for removal of carbendazim from aqueous solutions. The adsorption characteristics of carbendazim in aqueous solution were shown to be influenced by several factors. The adsorption was highly dependent on the dosage of BC, pH and concentration of carbendazim. The result of the present investigations showed that BC has higher adsorption efficiency. The adsorbed amount of carbendazim increased as initial carbendazim concentration decrease.

In our study, carbendazim adsorption from aqueous solution was carried out by bentonite clay (BC). The mechanisms of carbendazim adsorption onto BC could be attributed to ion-exchange, surface complexion, and surface precipitation. The economic evaluation implied that adsorption process was cost-effective.

### Acknowledgement

Authors would like to thank Provincial Secretariat for Science and Technological Development, for financial support Project No. (III46009). Ali Mohammed Hgeig would like to thank the Ministry of Higher Education in Libya for his PhD grant supporting this research.

### References

- [1] A. Nennemann, S. Kulbach, G. Lagaly, *Appl Clay Sci.* 18(2001), pp. 285-298.
- [2] A. Gürses, Ç. Doğar, M. Yalçın, M. Açıkyıldız, R. Bayrak, S. Karaca. *J Hazard Mater.* 131(2006), pp. 217-228.
- [3] R. Celis, M.C. Hermosín, L. Cox, J. Cornejo. *Environ Sci Technol.* 33(1999), pp. 1200-1206.
- [4] V. Addorisio, S. Esposito, F. Sannino, *J Agric Food Chem* 58(2010), pp. 5011-5016.
- [5] M. Fouodjouo, H. Fotouo-Nkaffo, S. Laminsi, F.A. Cassini, L. Octávio de Brito-Benetoli, N. Angelo Debacher. *Appl Clay Sci.* 142(2017), pp.136-144.
- [6] Kassim, A. Tarek, B.R.T. Simoneit. Vol. 5. Springer Science & Business Media, 2001.
- [7] B.H. Hameed, A. A. Ahmad. *J Hazard Mater.* 164(2009), pp: 870-875.



REMOVAL OF *CANDIDA ALBICANS* FROM WATER BY ADHESION TO AMINOPHOSPHOROUS GROUPS GRAFTED ONTO POLY(STYRENE-CO-DIVINYLBENZENE)

Ileana Nichita<sup>1</sup>, Adriana Popa<sup>2</sup>, Smaranda Iliescu<sup>2</sup>, Gheorghe Ilia<sup>2</sup>, Valentin Radu Gros<sup>1</sup>

<sup>1</sup>, „Banat” University of Agricultural Science and Veterinary Medicine, 119 Calea Aradului, 30465, Timisoara, Romania,

<sup>2</sup> Institute of Chemistry Timisoara of Romanian Academy, 24 Mihai Viteazul Blv., 300223 Timisoara, Romania,

E-mail: nichita\_ileana@yahoo.com ; apopa\_ro@yahoo.com

### Abstract

*Candida albicans* is a fungal pathogen capable of causing opportunistic infections that may be lethal. The purpose of this study was to establish the removal percent of a *Candida albicans* culture from a water solution by using some polymers with antimicrobial activity. The mechanism of action is based on yeast adhesion on aminophosphorous active groups.

### Introduction

*Candida albicans* is considered a dimorphic fungus. *Candida albicans* is a natural inhabitant of the upper respiratory, alimentary and genital tracts in healthy humans and animals. Fungal infections with this specie are frequent because it can cause opportunistic infections in hosts who are compromised by underlying local or systemic pathological processes.

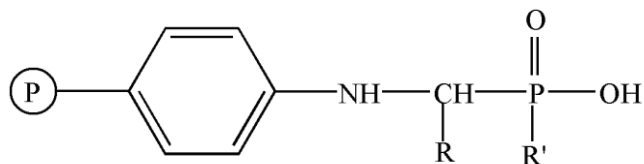
In United State, infection with *Candida albicans* is considered to be the fourth cause of disease on the bloodstream and the mortality rate exceeds that of bacteremia [2, 9].

In many countries, the intra-hospital infections with *Candida albicans* have reported as association of these microorganisms with the formation of biofilms on implantable medical devices [1, 4]. These devices support biofilm formation and *Candida albicans* have the property to form biofilm, so they are responsible for a considerable percentage of clinical candidiasis cases [1, 3, 4].

The purpose of this study was to establish the removal percent of a *Candida albicans* culture from a water solution by using some polymers with antimicrobial activity. The mechanism of action is based on yeast adhesion on aminophosphorous active groups.

### Experimental Part

Aminophosphorous groups grafted onto styrene–6.7% divinylbenzene copolymers are presented in Scheme 1.



Scheme 1. Aminophosphorous groups grafted onto poly(styrene-co-divinylbenzene); where: 3BA (R=benzyl, R'=phenyl; 4BA (R=propyl, R'= phenyl)

Aminophosphorous groups grafted onto styrene–6.7% divinylbenzene copolymers were obtained by “one-pot” reaction with copolymer grafted with amino group, phenylphosphinic

acid, benzaldehyde (or propionaldehyde) in tetrahydrofuran. The reaction was maintained under stirring for 24 h at 55°C. After cooling, the polymer was separated by filtration, washed with methanol, acetone and diethyl ether and dried at 50°C for 24 hours.

### Study of the removal of the *Candida albicans* from water

The experiment was carried out in a batch system with magnetical stirring. A quantity of each sample (3BA and 4BA) was introduced to 29 ml of sterile water. The concentration of reactive groups was 1 mmoles in every experiment. Into thus prepared mixture, 1 mL of microbial culture of *C. albicans* containing  $10^7$  CFU/mL was added in turn, and each mixture was stirred continuously (at room temperature) for 18 hours. At intervals of one hour, 3 hours, 6, 9 and 18 hours the number of bacterial cells of each system was determined. Then the number of colonies that grew on the Petri dishes was counted. The number of colonies/mL was established as an average value for the two plates by standard procedures [6, 7, 8].

### Results and discussions

The Fourier transform infrared spectra of the functionalized copolymer were obtained in KBr pellets on a Jasco FT-IR spectrophotometer (see Figure 1).

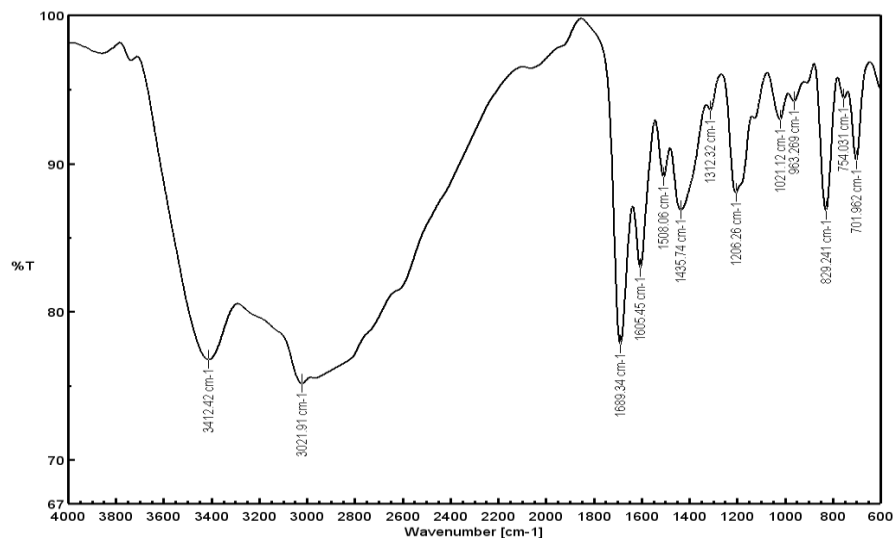


Figure 1. FTIR spectra of 3BA sample.

The bands from  $1206\text{ cm}^{-1}$  and  $1021\text{ cm}^{-1}$ , from the spectrum were assigned to group P=O and P-OH, they shows that reactions occurred with the formation of aminophosphorus groups grafted on copolymer.

In Figure 2 can be concluded that the copolymer 3BA and 4BA shows a very limited effect on yeasts.

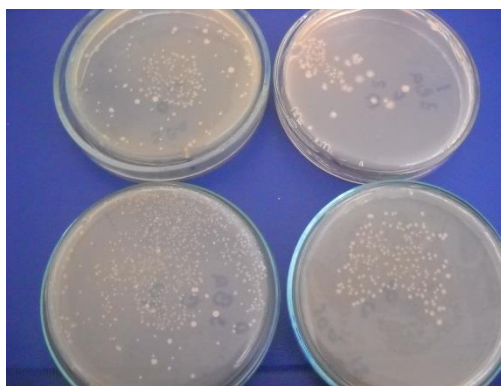


Figure 2. Removal of the microbial culture of *C. albicans* with aminophosphorous groups grafted onto poly(styrene-co-divinylbenzene).

The ability of aminophosphorous polymeric materials for the removal of *Candida albicans* from waste water was studied using the removal coefficient [5].

$$R_{coef} = V / W_t \times \log[N(0) / N(t)]$$

Rcoef is Removal coefficient where are : N(0) is the initial viable cell count, N(t) is the viable cell count at contact time t, V is the volume of viable cell suspension, W is the dry weight of aminophosphorous polymeric materials, and t is the contact time.

Table 1. The Viable cell count at contact time t (h)

<b>N(t) for 3BA</b>					
0	1	3	6	9	18
213285	62540	60146	55500	53961	53285
<b>N(t) for 4BA</b>					
213285	80535	74568	63271	61245	58256

Table 2. Removal coefficient of *Candida albicans* at different intervals of time (hours) for 3BA sample.

<b>Candida albicans</b>	Removal coefficient of at different intervals of time (hours)					
	0	1	3	6	9	18
Removal coefficient	<b>0</b>	<b>10.25</b>	<b>15.98</b>	<b>17.01</b>	<b>17.38</b>	<b>17.54</b>

Where: V = 30 mL; W<sub>t</sub> = 1.03 grams; N(0) = 2.13 · 10<sup>5</sup>.

Table 3. Removal coefficient of *Candida albicans* at different intervals of time (hours) for 4BA sample

<b>Candida albicans</b>	Removal coefficient of at different intervals of time (hours)					
	0	1	3	6	9	18
Removal coefficient	<b>0</b>	<b>11.32</b>	<b>12.22</b>	<b>14.13</b>	<b>14.51</b>	<b>15.09</b>

Where: V = 30 mL; W<sub>t</sub> = 1.12 grams; N(0) = 2.13 · 10<sup>5</sup>.

This relation can be seen in Figures 3.

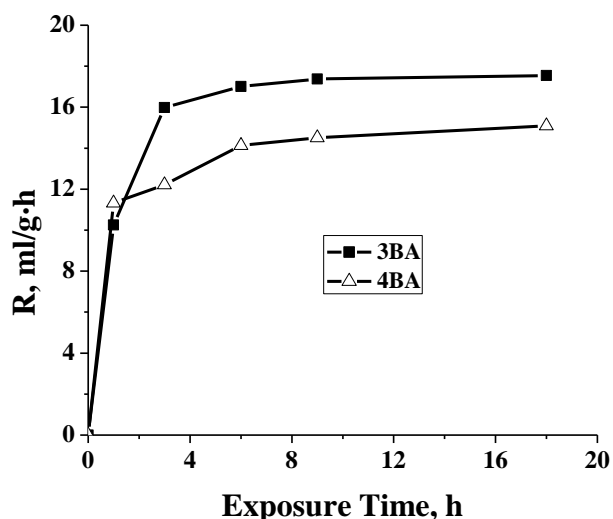


Figure 3. Removal coefficient of *Candida albicans* using 3BA and 4BA copolymer sample.

The antimicrobial activity was evaluated by the removal coefficient,  $R_{\text{coef}}$ , of the microbial culture. The results are showed in Figure 3. The copolymer 3BA had a better antimicrobial activity than the copolymer 4BA for the removal of the microbial culture of *C. albicans*. The antimicrobial activity is obtained at the interaction aminophosphorous active groups with the cell wall of *C. albicans*; so is explained the ability of the removal of the culture of *C. albicans*.

### Conclusions

The copolymers with aminophosphorous active groups were characterized by FTIR and they are considered that present antimicrobial activity. Batch treatment was used in the study of the removal of the *Candida albicans* from water. The copolymer 3BA had a better antimicrobial activity than the copolymer 4BA for the removal of the microbial culture of *C. albicans*.

### References

1. T. Coenye, K. De Prijck, H. Nailis , H. J. Nelis , The Open Mycology Journal, 2011, 5, 9-20.
2. A.S. Kao, M.E. Brandt, W.R. Pruitt, L.A. Conn, B.A. Perkins, D.S. Stephens, W.S. Baughmann, A.L. Reingold, G.A.Rothrock , M.A.Pfaller , R.W. Pinner, R.A. Hajjeh, Clin Infect Dis, 1999, 29, 1164-1170.
3. N. Kawabata, T. Hayashi, T. Matsumoto, Appl.Environ.Microbiol., 1983, 46(1), p. 203-210.
4. C.A. Kumamoto, Curr Opin Microbiol, 2002, 5, 608-611.
5. K. Nariyoshi, H. Takaya, M. Tsuguo, Applied and Environmental Microbiology, July 1983, p. 203-210
6. I. Nichita, A. Popa, E.S.Dragan , S. Iliescu, G. Ilia, J. Biomater. Sci. Polym. Ed., 2015, 26(8), 483-496.
7. I. Nichita, A. Popa, R. V. Gros, S. Iliescu, M. Stoia, M. Seres, A. Morar, Proceedings of 22<sup>nd</sup> International Symposium on Analytical and Environmental Problems, Szeged, Hungary, 10 October, 2016, p. 243-246, ISBN 978-963-306-507-5
8. H. Raducanescu, V. Bica-Popii, Bacteriologie veterinara, Bucuresti, Ceres, 1986, 123–125.
9. M.D. Richardson , J Antomicrob Chemother, 2005, 56, 5-10.

## FIBER HEMP RESPONSE TO FOLIAR APPLICATION OF GROWTH REGULATORS

**Biljana Kiprovski<sup>1</sup>, Anamarija Stojanović<sup>1</sup>, Vladimir Sikora<sup>1</sup>, Tijana Zeremski<sup>1</sup>, Bojan Konstantinović<sup>2</sup>, Dragana Latković<sup>2</sup>, Senka Vidović<sup>3</sup>**

<sup>1</sup>*Institute of Field and Vegetable Crops, Makisma Gorkog 30, 21000 Novi Sad, Serbia*

<sup>2</sup>*University of Novi Sad, Faculty of Agriculture, Trg Dositeja Obradovića 8, 21000 Novi Sad, Serbia*

<sup>3</sup>*University of Novi Sad, Faculty of Technology, Bulevar Cara Lazara 1, 21000 Novi Sad, Serbia*

*e-mail: bkiprovski@gmail.com*

### **Abstract**

The aim of this paper was to test the effect of three plant growth regulators (PGR) on fiber content of hemp cultivar Helena. Applied PGRs, Cycocel<sup>®</sup>, Regalis<sup>®</sup> and Moddus<sup>®</sup> had impact on fiber content in hemp cultivar Helena in medium concentrations: 1-2, 1.25-2.5 and 0.4-0.5 kg/ha, respectively. Further analysis of fiber quality, after application of various PGRs concentrations, should explain which PGR should be used in hemp fiber production.

### **Introduction**

Plant growth regulators (PGR) are synthetic compounds used to regulate/retard the shoot length of plants. This is achieved by reducing cell elongation and by lowering the rate of cell division [1]. Most plant growth retardants inhibit the formation of active gibberellins and can be used to reduce shoot elongation [2]. Cycocel<sup>®</sup> (chlormequat chloride) is a synthetic growth retardant that is extensively used for dwarfing of plants. Studies have indicated that Cycocel<sup>®</sup> is effective in stimulating the production of secondary metabolites [3]. Regalis<sup>®</sup> (prohexadione-Ca or 3-oxido-4-propionyl-5-oxo-cyclohexenecarboxylate), primarily used for the control of shoot growth in pome and other fruit trees, is a multifunctional plant bio-regulator that mimic of 2-oxoglutarate, inhibiting dioxygenases, which catalyse distinct steps in the biosynthesis of the growth hormone gibberellin [1]. Moddus<sup>®</sup> (trinexapac-ethyl) is effective anti-gibberellin PGR marketed primarily for the control of lodging.

Plants cells sense the environment and make appropriate adjustments to gene expression, metabolism and physiology using oxidative stress or oxidative signaling, which could be regarded as interactions between reactive oxygen species (ROS) and the antioxidative system, which set signal intensity, to relay the oxidative message and to determine its physiological outcome [4].

Hemp cultivar Helena is primarily grown for grain production, however it is rich in fiber and can reach up to 4 m height. To achieve complete use of the plant, it is important to understand in which way it is possible to enhance yield of its usable parts.

The purpose of this work was to determine response of hemp cultivar Helena to foliar application of different concentrations of mentioned PGRs with a view to test their impact on plant membrane integrity and the fiber yield.

### **Experimental**

Plants were grown in the experimental field of the Institute of Field and Vegetable Crops (Novi Sad, Serbia). Four concentrations of growth regulators, previously tested on other plant

species, were applied: Cycocel<sup>®</sup> (C1: 0.5, C2: 1, C3: 2, C4: 3 kg/ha), Regalis<sup>®</sup> (R1: 1, R2: 1.25, R3: 2.5, R4: 3 kg/ha) and Moddus<sup>®</sup> (M1: 0.2, M2: 0.4, M3: 0.5, M4: 0.8 kg/ha). Plants were treated at the beginning of a period of intensive vegetative growth, after which samples for biochemical analysis were collected. Quantification of investigated biochemical parameters was performed using Perkin Elmer Lambda 25 UV/Visible spectrophotometer. One g of fresh leaves was ground with cooled mortar and pestle and then homogenized with 5 ml 20% trichloroacetic acid for lipid peroxidation determination (LP) or total amount of TBARS (TBA-reactive substances) and expressed as nmol malondialdehyde (MDA) equivalents/g fresh weight (fw). Malondialdehyde (MDA) is a secondary end-product of the oxidation of polyunsaturated fatty acids, and reacts with thiobarbituric acid (TBA) to yield a pinkish-red chromogen with maximal absorbance at 532 nm [5]. Correction for non-specific turbidity at 600 nm was measured due to interference of other compounds including sugars, anthocyanins and other phenolics. Fiber yield [6], as well as plant heights and width were recorded. All statistical analysis were performed by STATISTICA for Windows version 13 (Dell Software).

### Results and discussion

There is no registered product that is used for hemp growth regulation, the reason of which three commonly applied PGRs are used in this study. As it is showed in the Figure 1, control represented 100% of lipid peroxidation intensity, and plants reacted differently to various PGRs concentrations. Lipid peroxidation products such as MDA (malondialdehyde) are considered useful and reliable indicator of membrane damage and oxidative signalling, due to the susceptibility of membranes to reactive oxygen species (ROS). Only higher concentrations of Cycocel<sup>®</sup> had impact on hemp leaves, while Regalis<sup>®</sup> and Moddus<sup>®</sup> induced oxidative stress in lower concentrations (Figure 1).

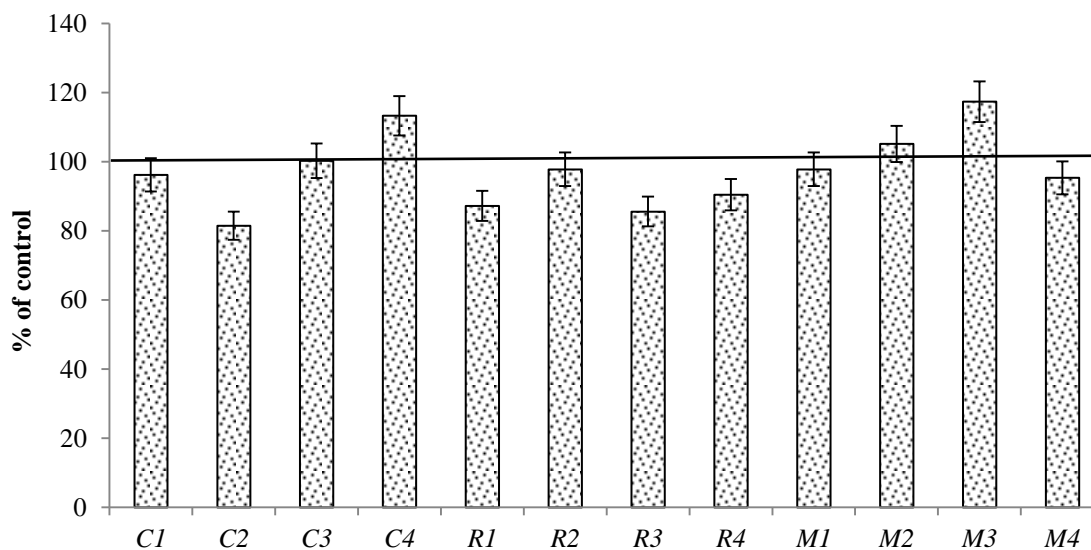


**Figure 1.** Lipid peroxidation intensity in leaves of hemp 'Helena' treated with growing concentrations of growth regulators (C-cycocel, R-regalis and M-modus, concentrations in Experimental section). Results expressed as percent of control, control represents 100%.

Shoot height (2.5-3 m) and width (approx. 2 cm) were unaffected by the treatment and however were the differences among treatments, there was no correlation between shoot

length and width parameters and fiber content. Higher fiber content was recorded for the second and third concentration of all tested PGRs.

**Table 1.** Fiber content of ‘Helena’ plants treated with growing concentrations of growth regulators (concentrations in Experimental section).

	C - Cycocel®				R - Regalis®				M - Moddus®						
	contr ol	C 1	C 2	C 3	C 4	contr ol	R 1	R 2	R 3	R 4	contr ol	M 1	M 2	M 3	M 4
% fiber content	34	33	35	35	33	32	33	35	35	33	33	31	32	33	32

### Conclusion

Applied PGRs had impact on fiber content in hemp cultivar Helena. Further analysis of fiber quality after application of various PGRs concentration should explain which PGR should be used in hemp fiber production.

### References

- [1] W. Rademacher, *Annu. Rev. Plant Physiol. Plant Mol. Biol.* 51 (2000) 501.
- [2] A.K. Singh, *Indian J. Agr. Sci.* 74 (2004) 130.
- [3] A.H.A. Farooqi, S. Fatima, A. Khan, S. Sharma. *Plant Growth Regul.* 46 (2005) 277.
- [4] H.C. Foyer, G. Noctor, *Plant Cell Environ.* 28.8 (2005) 1056.
- [5] D.M. Hodges, J.M. DeLong, C.F. Forney, R.K. Prange, *Planta* 207(4) (1999) 604.
- [6] G. Bredeman, *Faserforschung* 16 (1942) 14-39.



## EFFECT OF STORAGE TIME ON THE FATTY ACID PROFILE OF KOMBUCHA FERMENTED MILK PRODUCT

**Snežana Kravić, Spasenija Milanović, Dajana Vukić, Ana Đurović, Tanja Brezo, Zorica Stojanović, Zvonimir Suturović**

*Department of Applied and Engineering Chemistry, University of Novi Sad, Faculty of Technology Novi Sad, Bulevar cara Lazara 1, 21000 Novi Sad, Serbia  
e-mail: sne@uns.ac.rs*

### **Abstract**

Kombucha fermented milk products are the new functional dairy products that are obtained by applying non-conventional starter culture-kombucha. The health aspect of fermented milk beverages depends on the fatty acid composition of milk fat, as one of the most important components of these products. In this investigation kombucha fermented milk product was produced from milk with 2.8% milk fat using 10% (v/v) kombucha inoculums cultivated on black tea. Effect of storage time on fatty acid profile of kombucha fermented milk product was investigated. The fatty acid composition of kombucha fermented milk product was determined after production and during 7, 14 and 21 days of storage. Fatty acids analysis was performed by capillary gas chromatography - mass spectrometry after previous extraction of lipids and derivatization. The main fatty acids encountered in kombucha fermented milk product were: palmitic, oleic, stearic and myristic with mean contents of 32.63; 26.65; 11.11 and 10.80%, respectively. During 14 days of storage content of saturated fatty acids (SFA) slightly increased, while contents of monounsaturated (MUFA) and polyunsaturated fatty acids decreased (PUFA). However, after 21 days of storage the content of SFA, MUFA and PUFA in kombucha fermented milk product was very similar with those obtained after production of fermented beverage. Results showed that the storage time has not significant influence on the fatty acid profile of kombucha fermented milk product.

### **Introduction**

Fermented milk products possess various nutritional and therapeutic properties. They are characterized by easy digestibility, appropriate dietary properties (changed colloidal structure of fat and protein compared to milk, as a consequence of lactic acid production), good sensory properties, extended shelf life and a wide range of products that are enriched with the addition of fruits, grains, vitamins, mineral materials [1]. Recent studies presented the technological and nutritional potential of kombucha as an innovative starter culture in dairy industry [2-4]. Kombucha is a symbiotic association of several yeast species (*Schizosaccharomyces*, *Saccharomycodes*, *Saccharomyces*, *Zygosaccharomyces*, *Candida*, *Pichia*, *Kloeckera*, *Brettanomyces* and *Torulopsis*) and acetic acid bacteria (*Acetobacter* and *Gluconobacter*) whose metabolic activity on tea sweetened with sucrose produces a pleasant refreshing beverage [1-3, 5]. Kombucha fermented product contains ethanol, carbon dioxide, a high concentration of acid (gluconic, acetic and lactic) and a number of other health-promoting metabolites. Therefore, it is considered to be beneficial beverage in cases of: digestive ailments, diabetes, hypercholesterolaemia, high blood pressure, combating stress and cancer as well as body vitalisation, among others [2]. As the result of milk fermentation by kombucha inoculums, products similar to yoghurt or kefir are produced. Milk fat, as one of the most important components of fermented milk beverages, have great influence on the health aspect

of these products. Milk lipids represent a good dietary source of the liposoluble vitamins such as  $\alpha$ -tocopherol, retinol, and  $\beta$ -carotene, as well as the essential fatty acids. The fatty acid composition of milk is not only effective on physical properties, oxidative stability and organoleptic quality of dairy products, but also has positive effects on human health. Various fatty acids have different effects on plasma lipids. While short and medium chain fatty acids do not affect plasma lipoproteins, consumption of saturated fatty acids specifically, saturated fats with 12–16 carbon atoms tend to increase plasma total and low density lipoprotein (LDL) cholesterol levels. Fatty acid composition of milk fat, especially owing to short-chain fatty acids present in relatively big amount, is ideal for the human organism because triacylglycerol's containing short-chain fatty acids can be more easily attacked by the digestive enzymes. Milk fat contains relatively small amount of unsaturated fatty acids, despite this it can contain considerable amount of essential fatty acids needed to satisfy the requirements of the human organism. Besides, milk fat can contain conjugated linoleic acids in considerable quantity, which have according to the latest researches many useful physiological effects. Thus, recent clinical studies have focused on the bioactive fatty acids such as butyric acid, oleic acid and conjugated linoleic acid which may show key roles in the prevention of certain diseases [6]. The fatty acid content of milk is affected by numerous factors such as the geographical location, the breed type and the genetic and physiological factors of the animals. In addition, milk processing conditions like the heat treatment, the added starter culture and the storage conditions also affect the fatty acid composition of different dairy products. Therefore, the aim of this work was to study the effect of storage time on fatty acid composition of kombucha fermented milk.

### **Experimental**

Pasteurized and homogenized milk with 2.8% milk fat (Dairy Subotica, Subotica, Serbia), was used for the laboratory manufacture of kombucha fermented milk. Kombucha inoculum was obtained by cultivation of Kombucha on black tea (1.5 g/l) with sucrose concentration of 70 g/l. The tea was cooled at the room temperature, after which inoculum from a previous fermentation was added in concentration of 10%. Incubation was performed at 25°C for 7 days [4]. Kombucha inoculum in concentration of 10% was applied for milk fermentation. The fermentation was performed at 42°C and it lasted until the pH value of 4.5 was reached. Milk gel was then cooled to the temperature of 4°C, homogenized by mixer, packed in polypropylene glasses and stored in refrigerator at 4°C [2]. The extraction of fat from kombucha fermented milk product was carried out as described by Havemose et al. [7], while the methylation of fatty acid and was performed according to the methodology of Kravić et al. with minor modifications [8]. Fatty acid profile of the kombucha fermented milk product was determined by gas chromatography-mass spectrometry in accordance to our previously published experimental results [9].

### **Results and discussion**

The fatty acid composition of the kombucha fermented milk product after production (0 day) and during 7, 14 and 21 days of storage are given in Table 1, as relative ratio of total fatty acid content. The presented results represent the mean of three replications for each sample. The distribution of saturated, monounsaturated and polyunsaturated fatty acids in analysed samples is presented in Figure 1.

As can be seen from Table 1 predominant fatty acids in all analysed samples of kombucha fermented milk product were palmitic (C16:0), oleic (C18:1c), stearic (C18:0) and myristic

acid (C14:0), with mean contents of 32.63; 26.65; 11.11 and 10.80%, respectively. These fatty acids comprised about 81% of the total fatty acids. These results are in accordance with the results presented by other research [1, 10]. The content of branched-chain fatty acids, characteristic minor fatty acids of ruminants, was ranged from 1.29% to 1.53%, and this percentage was made up of five different acids: iso- and anteiso-C15, iso- and anteiso-C17 and iso-C16. Recent studies have shown that branched-chain fatty acids have anti-cancer activity. The cytotoxicity of branched-chain fatty acids was comparable to that of conjugated linoleic acid, a generally lesser component of milk fat which has received much greater attention as a potential anti-cancer agent. These fatty acids inhibited fatty acid synthesis in tumour cells, which is recognised as a useful route for developing cancer treatments since cancer cells are more dependent on fatty acid biosynthesis than healthy cells [11]. The highest content of branched-chain fatty acids was detected in kombucha fermented milk product after 21 day of storage.

Table 1. Fatty acid profile of kombucha fermented milk product during storage

<b>Fatty acid</b>	<b>0 day</b>	<b>7 day</b>	<b>14 day</b>	<b>21 day</b>
<b>4:0</b>	1.22	1.19	1.07	1.15
<b>6:0</b>	1.11	1.08	1.03	1.12
<b>8:0</b>	0.78	0.76	0.75	0.80
<b>10:0</b>	2.22	2.19	2.20	2.18
<b>12:0</b>	2.89	2.93	2.96	2.82
<b>14:0</b>	10.88	11.24	11.44	10.89
<b>14:1</b>	0.74	0.73	0.79	0.86
<b>15:0i</b>	0.18	0.19	nd	0.20
<b>15:0a</b>	0.39	0.36	0.40	0.41
<b>15:0</b>	1.14	1.09	1.15	1.16
<b>16:0i</b>	0.21	0.20	0.20	0.22
<b>16:0</b>	33.01	34.13	34.54	32.50
<b>16:1</b>	1.45	1.40	1.46	1.56
<b>17:0i</b>	0.22	0.20	0.33	0.30
<b>17:0a</b>	0.37	0.34	0.37	0.40
<b>17:0</b>	0.60	0.56	0.62	0.66
<b>17:1</b>	nd	nd	nd	0.21
<b>18:0</b>	11.15	11.34	11.56	10.96
<b>18:1t</b>	2.13	1.64	1.02	2.29
<b>18:1c</b>	26.13	25.69	26.26	25.65
<b>18:2c</b>	2.86	2.73	2.88	2.98
<b>18:3n3</b>	0.32	nd	nd	0.35
<b>20:0</b>	nd	nd	nd	0.18
<b>20:1</b>	nd	nd	nd	0.15

nd – not detected; t-trans; c-cis; i-iso; a-anteiso

Results presented in Fig 1. show that during 14 days of storage content of saturated fatty acids slightly increased, while contents of monounsaturated and polyunsaturated fatty acids decreased. After 21 days of storage the content of SFA; MUFA and PUFA in kombucha fermented milk product was very similar with those obtained at starting point, i.e. immediately after production of fermented beverage. Results showed that the storage time has not significant influence on the fatty acid profile of kombucha fermented milk product.

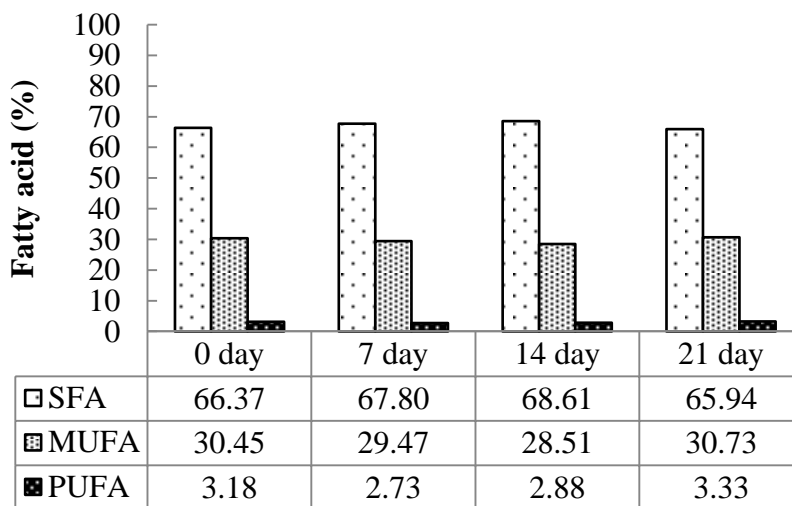


Figure 1. Distribution of saturated (SFA), monounsaturated (MUFA) and polyunsaturated (PUFA) fatty acids in kombucha fermented milk product during storage

### Conclusion

This study examined the fatty acid profile of novel functional dairy products, kombucha fermented milk product, during storage. Based on the results it can be concluded that predominant fatty acids in all samples were saturated fatty acids. The most common was palmitic acid, followed by stearic and myristic acid. Of unsaturated fatty acids, the dominant were monounsaturated fatty acids, primarily oleic. The obtained results showed that fatty acid composition of kombucha fermented milk product was not changed during 21 days of storage.

### Acknowledgements

This study was financially supported by the Ministry of Education, Science and Technological Development of the Republic of Serbia (Grant III 46009).

### References

- [1] Malbaša, R., Vitas, J., Lončar, E., Kravić, S. (2011). Influence of fermentation temperature on the content of fatty acids in low energy milk-based kombucha products. *Acta Periodica Technologica (APTEFF)* 41, 81-90.
- [2] Hrnjez, D., Vaštag, Ž., Milanović, S., Vukić, V., Iličić, M., Popović, Lj., Kanurić, K. (2014). The biological activity of fermented dairy products obtained by kombucha and conventional starter cultures during storage. *Journal of Functional Foods* 10, 336–345.
- [3] Vukić, V., Hrnjez, D., Kanurić, K., Milanović, S., Iličić, M., Torbica, A., Tomić, J. (2014). The effect of kombucha starter culture on the gelation process, microstructure and rheological properties during milk fermentation. *Journal of Texture Studies* 45, 261–273.

- [4] Malbaša, R., Milanović, S., Lončar, E., Đurić, M., Carić, M., Iličić, M., Kolarov, Lj. (2009). Milk-based beverages obtained by Kombucha application. *Food Chemistry* 112, 178-184.
- [5] Dufresne, C., Farnworth, E. (2000). Tea, kombucha and health: A Review. *Food Research International* 33, 409-421.
- [6] Yilmaz-Ersan, L. (2013). Fatty acid composition of cream fermented by probiotic bacteria. *Mljekarstvo* 63, 132-139.
- [7] Havemose, M., Weisbjerg, M., Bredie, W., Neilsen, J. (2004). Influence of feeding different types of roughage on the oxidative stability of milk. *International Dairy Journal* 14, 563-570.
- [8] Kravić, S., Marjanović, N., Suturović, Z., Švarc-Gajić, J., Stojanović, Z., Pucarević, M. (2010). Determination of trans fatty acid content of Serbian shortening by gas chromatography-mass spectrometry. *Acta Alimentaria* 39, 413-423.
- [9] Šarić, Lj., Šarić, B., Mandić, A., Kevrešan, Ž., Ikonić, B., Kravić, S., Jambrec, D. (2014). Role of calcium content in antibacterial activity of donkeys' milk toward *E. coli*. *European Food Research and Technology* 239, 1031-1039.
- [10] Brezo, T., Kravić, S., Suturović, Z., Karišik-Đurović, A., Vitas, J., Malbaša, R., Milanović, S. (2011). Influence of kombucha inoculum on the fatty acid composition of fermented milk products. *Food Industry, Milk and dairy products* 22, 21-24.
- [11] Vlaeminck, B., Fievez, V., Cabrita, A.R.J., Fonseca, A.J.M., Dewhurst, R.J (2006). Factors affecting odd- and branched-chain fatty acids in milk: A review. *Animal Feed Science and Technology* 131, 389-417.

## METAL POLLUTION BIOMONITORING IN MINING AREAS USING PERENNIAL RYEGRASS (*LOLIUM PERENNE*)

**Levente Levei<sup>1</sup>, Maria Alexandra Hoaghia<sup>1</sup>, Alexandru Ozunu<sup>2</sup>**

<sup>1</sup>INCDO-INOE 2000, Research Institute for Analytical Instrumentation, 400293 Cluj-Napoca, 67 Donath, Romania

e-mail: levente.levai@icia.ro

<sup>2</sup>Babes-Bolyai University, Faculty of Environmental Sciences and Engineering, 400294 Cluj-Napoca, 30 Fântânele, Romania

e-mail: alexandru.ozunu@ubbcluj.ro

### Abstract

The uptake of metals (Pb, Cu, Cd, Zn, Ni, Cr) by perennial ryegrass (*Lolium perenne*), grown on tailings situated in Central and NW Romania, was investigated by calculating the transfer factors (TFs). The mean TFs decreased as follows:  $TF_{Pb} > TF_{Cd} > TF_{Zn} > TF_{Ni} > TF_{Cr} > TF_{Cu}$ . The metal concentrations in tailings ranged between 19.9-2640 mg/kg Cu, 11.4-5156 mg/kg Pb, 9.10-5328 mg/kg Zn, 0.200-89.6 mg/kg Cd, 3.15-77.6 mg/kg Cr, 1.90-58.9 mg/kg Ni and in ryegrass between 2.25-58.6 mg/kg Cu, 0.129-4815 mg/kg Pb, 5.12-174 mg/kg Zn, 0.010-3.50 mg/kg Cd, 0.410-6.20 mg/kg Cr and 0.440-3.71 mg/kg Ni. The linear relationship between the metal content in ryegrass and tailings indicated a significant correlation for Pb and Zn. Metal concentrations in ryegrass differ in the three areas (Certej, Baia Mare and Aries) and can be used as a biomonitor for Pb, Zn pollution.

### Introduction

Extraction and use of ores in industrial processes produced significant environmental pollution with metals, which pose a serious threat to human health and ecosystems, due to their toxicity, tendency to bioaccumulate and high persistence [1]. Although some metals (such as Mn, Zn, Cu, Cr, Ni, Fe) act as micronutrients for living organisms, they could induce toxic effects at higher concentrations. Other metals (such as Hg, Cd, As, Pb) are non-essential and are highly toxic even at low concentrations [2].

Different plants have been used to monitor pollution, because they can accumulate toxic compounds without any deleterious effects. Among them, perennial ryegrass (*Lolium perenne*) is suitable as accumulative biomonitor for assessing atmospheric or soil levels of metals [3, 4, 5]. Grass takes up metals via the roots and is also influenced by atmospheric dust impact [4].

The relationship between metal concentrations in tailings and plant is highly specific to the plant species, substrate and metal chemistry, and is generally described by empiric equations [6]. The relationship between contaminant concentration in plant and the concentration in soil is described using Transfer Factor (TF), which is defined according to Equation 1.

$$TF = \frac{Conc_{\text{lolium}}}{Conc_{\text{tailings}}} \quad \text{Eq. 1}$$

where the concentrations are expressed as mg/kg.

The TF values quantify the relative differences in bioavailability of metals to plants and identify the efficiency of a plant species to accumulate a given metal [7].

## **Experimental**

### *Description of the sampling areas*

The environmental impact of nonferrous mining activities is considerable in the Central and Northwestern parts of Romania, where centuries of ore extraction and exploitation generated large amounts of mining waste [8]. The study was conducted in three former mining areas: Baia Mare (NW Romania) and Aries and Certej (Central West Romania), where mining wastes were collected in tailings management facilities [9, 10].

### *Sample collection and preparation*

In autumn 2016, a number of 15 ryegrass samples and the subadjacent tailings collected from the old tailings ponds that are partially revegetated by spontaneous flora. The samples were collected as follows: 5 from Certej, 8 from Baia Mare (BM) and 2 from Aries areas using a hand auger. Samples of tailings were thoroughly mixed, air dried, grounded to pass through 2 mm and then 250  $\mu\text{m}$  sieve. Plant samples were washed in distilled water, dried at 40°C until constant weight and ground to obtain a homogenized powder.

### *Determination of metals content*

The metal contents in tailings were determined after aqua regia (HCl 37.5% and HNO<sub>3</sub> 65%) extraction for 16 hours at room temperature and then, 2 hours, at reflux conditions, according to SR ISO 11466:1999 [11]. The extract was analyzed by inductively coupled plasma optical emission spectrometer (ICP-OES) using a SPECTRO FLAME spectrometer (SPECTRO, Kleve, Germany).

An amount of 0.5 g of plant sample was digested in 5 ml HNO<sub>3</sub> 65% and 2 ml H<sub>2</sub>O<sub>2</sub> 30% in closed PTFE vessel microwave digestion system, Berghof MWS-3+ (Eningen, Germany). Metals concentrations were measured by inductively coupled plasma mass spectrometer (ICP-MS) ELAN DRC II, Perkin Elmer, USA.

The quantification of ICP-OES and ICP-MS was performed using an external calibration with multi-elemental Merck (Darmstadt, Germany) standard solution. Throughout the experiments, ultrapure water (Millipore from a Direct Q UV 3 Millipore system) was used.

## **Results and discussion**

Descriptive statistics for metal contents in ryegrass in Certej, Baia Mare and Aries areas are shown in Table 1. All concentrations are reported on a dry-weight basis.



Table 1. Descriptive statistics for total metal contents in ryegrass (mg/kg) in Certej, Baia Mare and Aries areas

	Cu	Pb	Zn	Cd	Cr	Ni
<i>Certej area</i>						
min	2.85	0.139	5.12	0.010	0.410	1.00
max	13.7	49.8	49.9	0.840	6.29	3.11
mean	5.65	10.5	25.6	0.374	2.60	2.02
<i>Baia Mare area</i>						
min	2.50	3.34	15.7	0.036	0.645	0.440
max	58.6	4815	174	3.50	5.49	3.71
mean	21.2	1233	84.7	1.56	2.03	1.50
<i>Aries area</i>						
min	2.25	0.129	22.2	0.139	1.71	2.10
max	2.98	0.935	31.4	0.218	2.84	2.29
mean	2.61	0.532	26.8	0.179	2.28	2.20

The obtained concentrations in ryegrass were constantly much higher in Baia Mare area than in Certej and Aries areas (except for 1 sample). In three of the ryegrass samples collected from Baia Mare area, the content of Pb exceeded 500 mg/kg and in 2 samples exceeded 1000 mg/kg. Also, Zn concentration exceeded 100 mg/kg in 3 samples collected in Baia Mare area. The maximum tolerant levels set by the European Commission (Directive 2002/32/EC, 2002: Pb: 10 mg/kg, Cd: 1 mg/kg) [12] for animal feed such as grass and fodder were exceeded for Pb in one sample from Certej area and in 7 samples collected from Baia Mare area and for Cd in 4 ryegrass samples collected from Baia Mare area.

Descriptive statistics for metals contents in tailings in Certej, Baia Mare and Aries areas are shown in Table 2. All concentrations are reported on a dry-weight basis.

Table 2. Descriptive statistics for total metal contents in tailings (mg/kg) in Certej, Baia Mare and Aries area

	Cu	Pb	Zn	Cd	Cr	Ni
<i>Certej area</i>						
min	19.9	11.4	9.10	0.200	3.15	2.39
max	291	170	180	6.09	32.1	38.4
mean	115	70.1	73.6	1.72	16.5	14.8
<i>Baia Mare area</i>						
min	114	501	343	3.40	9.80	1.90
max	2640	5156	5328	89.6	65.1	28.9
mean	1181	1960	1405	18.7	33.5	14.2
<i>Aries area</i>						
min	30.5	16.08	100	4.11	38.8	33.1
max	32.2	32.3	140	5.98	77.6	58.9
mean	31.3	24.1	120	5.05	58.2	46.0

Similar to metals content in plants, the concentration in tailings was much higher in Baia Mare area than in Certej and Aries areas, for all the investigated elements. In three of the samples, the concentrations of Cu exceeded 1000 mg/kg and in two samples, slightly less than this value. Also, Pb contents were higher than 2000 mg/kg in four samples and around 1000 mg/kg in three samples, all in Baia Mare area.

The values of TF calculated for all metals are graphically represented in Figure 1.

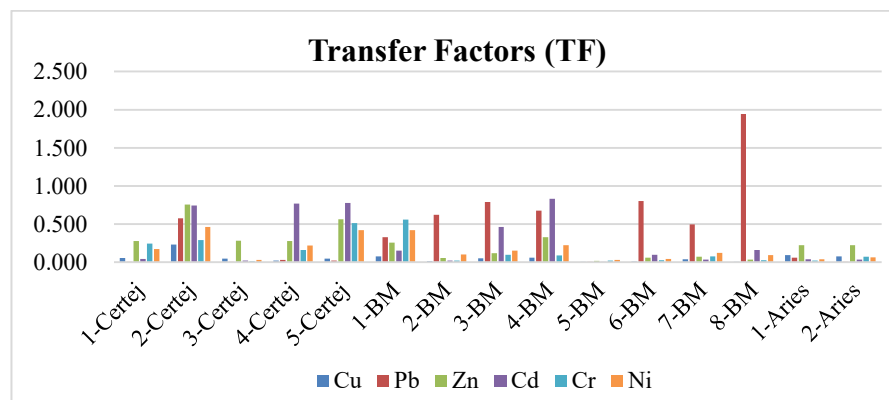


Figure 1. Values of transfer factors for metals in all the sampling points

The values of TF varied largely, over 5 orders of magnitude, from 0.0006 to 1.94, both values for Pb, in Baia Mare area. All the values of TF were lower than 1, except for Pb (1.94) in one sample. The mean values of TF decreased as follows:  $TF_{Pb} > TF_{Cd} > TF_{Zn} > TF_{Ni} > TF_{Cr} > TF_{Cu}$ . The relationships between metal concentration in ryegrass and tailings were performed for each metal as linear regressions. The obtained equations are showed in Table 3.

Table 3. Relationships between metal concentration in ryegrass and tailings

Metal	Regression equation	Regression coefficient, $R^2$
Cu	$y = 16.79x + 444.69$	0.11
Pb	$y = 1.21x + 541.46$	0.57
Zn	$y = 22.64x - 507.20$	0.64
Cd	$y = 9.91x + 1.48$	0.27
Cr	$y = -3.35x + 38.68$	0.07
Ni	$y = 2.87x + 13.58$	0.03

For Pb and Zn, the regression coefficients  $R^2$  are higher than 0.5, assuming a significant linear correlation. For the rest of the investigated metals (Cu, Cd, Ni, Cr), non-linear transfer functions could be supposed.

### Conclusions

In this study, high levels of Cu, Pb, Zn, Cd, Cr, Ni contents were recorded in tailings and ryegrass, especially in Baia Mare area (NW Romania). The metal content in tailings contributed significantly to metal content in ryegrass. Metal concentrations in ryegrass differ in the three investigated areas (Certej, Baia Mare and Aries), and could be used as biomonitor of metal pollution. Even after decommissioning, tailings deposits represent a continuous pollution source for the surrounding environment.

### **Acknowledgements**

This work was supported by a grant of the Romanian National Authority for Scientific Research and Innovation, CCCDI – UEFISCDI, project number 91BM/2017 (IMPAACT).

### **References**

- [1] M. Shahid, C. Dumat, S. Khalid, E. Schreck, T. Xiong, N.K. Niazi, J. Hazard Mater. 325 (2017) 36.
- [2] M. Jaishankar, T. Tseten, N. Anbalagan, B.B. Mathew, K.N. Beeregowda, Interdiscip. Toxicol. 7 (2014) 60.
- [3] A. Rey-Asensio, A. Carballeira, Environ. Int. J. 33 (2006) 583.
- [4] I. Suchara, J. Sucharova, M. Hola, C. Reinmann, R. Boyd, P. Filzmoser, P. Englmaier, Sci. Total Environ. 409 (2011) 2281.
- [5] D. Malschi, C. Roman, M. Miclean, M. Senila, L. Stefanescu, B. Florian Malschi, A. Bolony, G. Ghira, D. Brahaita, A. Crihan, Environ. Eng. Manag. J. 12 (2013) 1103.
- [6] Y.N. Jolly, A. Islam, S. Akbar, Springerplus, 2 (2013) 385.
- [7] A. Kachenko, B. Singh, SuperSoil 2004: 3rd Australian New Zealand Soils Conference, 5-9 December 2004, University of Sydney, Australia.
- [8] J. Zobrist, M. Sima, D. Dogaru, M. Senila, H. Yang, C. Popescu, C. Roman, B. Abraham, L. Frei, B. Dold, D. Balteanu, Environ. Sci. Pollut. Res. 16 (2009) S14.
- [9] M. Sima, B. Dold, L. Frei, M. Senila, D. Balteanu, J. Zobrist, J. Hazard. Mater. 189 (2011) 624.
- [10] E. Levei, T. Frentiu, M. Ponta, C. Tanaselia, G. Borodi, Chem. Central J. 7 (2013) 5.
- [11] SR ISO 11466:1999. Soil Quality – Extraction of Trace Elements Soluble in Aqua Regia. Romanian Standards Association.
- [12] European Commission. Directive 2002/32/EC of the European parliament and the council of 7 May 2002 on undesirable substances in animal feed. Off. J. 2002; 1140:10-21.

## GREEN FRESH SMOOTHIE – SOME PHYSICO-CHEMICAL AND NUTRITIONAL ASPECTS

Velciov Ariana – Bianca\*, Popescu Georgeta – Sofia\*, Cozma Antoanela, Stoin Daniela, Riviş Adrian, Bujancă Gabriel, Pinteă Marius

*University of Agricultural Sciences and Veterinary Medicine of Banat "King Mihai I of Romania" Timisoara*

*Faculty of Food Processing Technology Food Science Department 300645, Timisoara, Calea Aradului, nr. 119, Roumania*

*Authors e-mail address: sofiaopescu@yahoo.com, ariana.velciov@yahoo.com*

### Abstract

Increasing tendency for fresh food - fruits, vegetables, and herbs consumption worldwide and also in our country, shows the weight that they have held or hold them in the diet. In their case, not only good looks, nice color or taste and aromas are considered to be important, but especially their nutritional value, rich in sugars, vitamins and minerals needed in the diet of the human body. They also have the advantage that it can be consumed without any processing who could reduce the nutritional value.

The purpose of the study was to obtain and reveal some physico-chemical and nutritional properties of some fresh foods: green apple (*Golden delicious – Malus domestica.*), baby spinach (*Spinach oleracea*), pineapple (*Ananas comosus*) and mint leaves (*Mentha piperita*) and the juice that we obtain from them, while achieving a characterization highlighting their dietary and healing properties.

The study presents important application not only for food industry, but also for other areas, because it addresses to special categories of consumers such as vegetarians and people with lactose intolerance and fasting period.

**Keywords:** fresh food, juices, physical-chemical characteristics, healing properties

### Introduction

Nowadays, for nutritional reasons, it is necessary to increase the amount of fresh food in the daily diet due to the current nutritional habits of the society, based on increased intellectual effort, which demands larger amount of vitamin and mineral and less amount of carbohydrates and fat. Consumption of fresh fruits and vegetables provide a healthy diet that can prevent some chronic diseases, (e.g. Cardiovascular and coronary diseases, diabetes (type 2), different types of cancer, cancer, prevent developing kidney stones, help decreases bone loss, obesity [5,6].

In the category of fresh food products are included vegetal food products that are basic components of human diet, due to their increased nutritional value [3].

Mint is a perennial herb, from Lamiaceae family, well-known in history because of bioactive compounds, such as mint-oil and L-menthol and L-carvone, which is used in both pharmaceutical industry but also in food industry, as flavour [8].

Smoothies are blended drinks consisting of a number of ingredients including fruit (or less commonly vegetables), fruit juice, ice, yoghurt and milk [4, 7]. There are three main types of smoothies: fruit only, fruit and dairy, and functional.

## Experimental

### *Samples preparation*

In this study, we used 3 different types of samples (pineapple and green apple fruits, baby spinach and mint leaves) bought from a Romanian hypermarket, from west of Romania – Timisoara city.

The smoothie sample was obtained by mixing the fruits with baby spinach and mint leaves in ratio 1/1/1/0,01 (pineapple/green apple/ baby spinach/mint leaves- w/w/w/w).

### *Analytical procedures*

**Humidity** of fresh food samples was evaluated thermo-gravimetrically by using Sartorius thermo-balance.

Total dry weight content (TDW, %) can be determined from moisture content as below:

$$\text{Total dry weight content (TDW, \%)} = 100 - \text{Total moisture content (M, \%)}$$

The method for determination of **acidity** was by titration with NaOH 0,1 N in the presence of phenolphthalein [1]. The results were expressed in acidity degrees.

**Ascorbic acid** is extracted from samples by means of weak acids (2% oxalic acid solution) in the presence of hydrochloric acid, followed by titration with 2,6 – dichlorofenolindofenol until a pink color appeared [1, 2].

All determinations were performed in triplicate, calculating their arithmetic mean of three separate determinations. The data were statistically analyzed using the program Microsoft Excel.

## Results and discussion

In fig. 1 we are presenting total moisture contents (M, %) and total dry weight content (TDW, %) values.

The moisture contents of analyzed samples were of 75.85 % (leaves of mint) up to 93.18 % (baby spinach). From the analysed data presented above, we can observe that the lowest value of the total dry weight content was found baby spinach (6.32 %) and the highest value was found in mint leaves – 24.15 %.

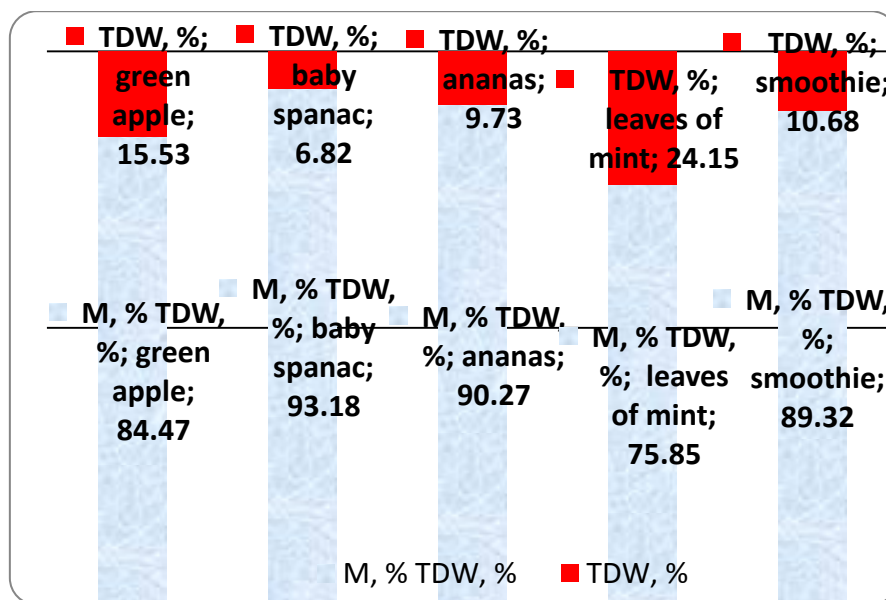


**Fig. 1** Total dry weight content (TDW, %) and total moisture content (M, %) in all samples. The different values in water content are depending on the season in regions with high relative humidity, physical properties of samples during storage processes, but also could be modified during processing.

Determination of acidity ( $^{\circ}$ ), in fresh food samples and smoothie samples were presented in Fig. 2.

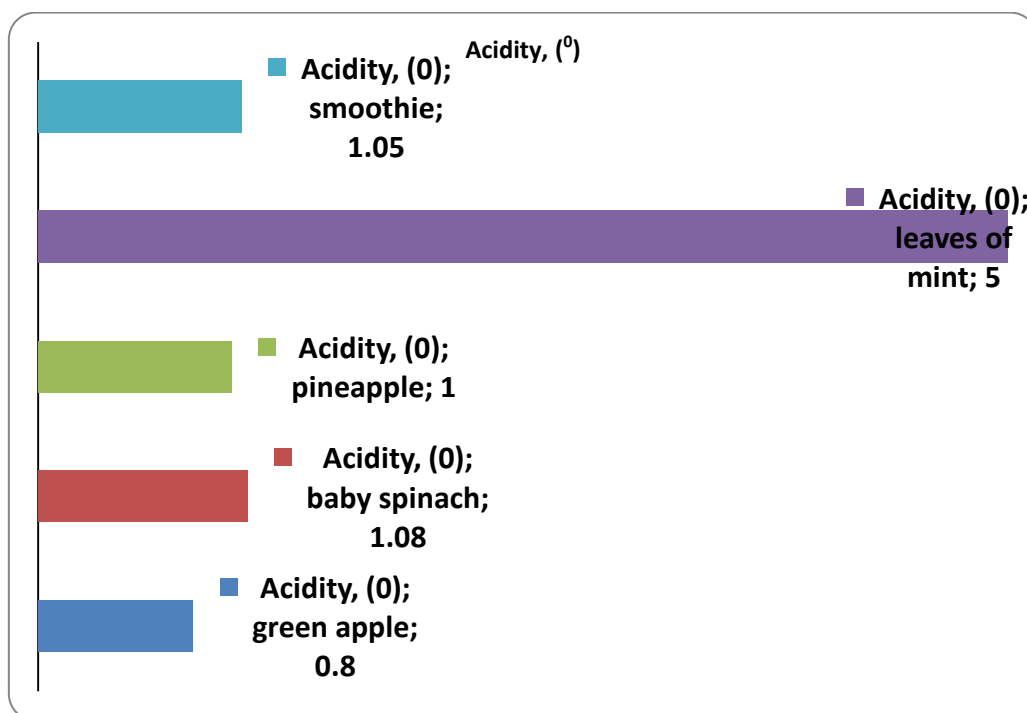


**Fig. 2** Acidity degrees in all samples. The values of acidity were between 0.8 to 5 acidity degrees (in green apple respectively in mint leaves).

From the fig. 3 presented data it can be observed the values of vitamin C concentrations in all samples (fruits, vegetables and smoothie).

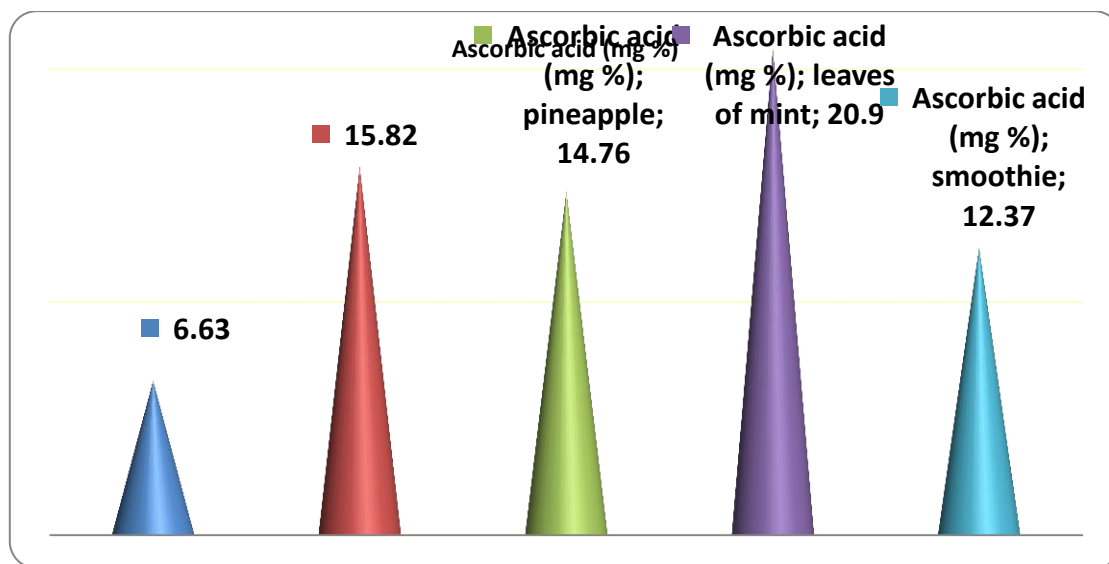


**Fig. 3** Ascorbic acid content in all samples

Ascorbic acid contents of analysed samples were found to range from 6.63 mg/100g (green apple) to 20.9 mg/100 g (mint leaves).

### Conclusions

Beverages are an ideal food format to deliver bioactive compounds to consumers.

In this study, complex beverages formulas, smoothies were formulated containing green fresh food and mint leaves as medicinal herb.

The obtained data could be used for future research because of obtained results that are under lightning once more the fact that minimally processed foods are important source of fruits, vegetables and even medicinal plants with superior quality and no additives.

### Acknowledgement

The corresponding author is Georgeta-Sofia Popescu.

### References

1. Ahmadi M., Velcirov A.B. – Biochimie și Biochimie alimentară. Metode de laborator, Ed. Eurobit, Timisoara, 2010.
2. AOAC (Association of Official Analytical Chemists), Official Methods of Analysis International, (17<sup>th</sup> Ed.) AOAC, Washington, DC, USA, 2000.
3. Baiyeri K.P., Ugehe F.D. – Tropical fruits and vegetables: physical properties, pp. 925- 934 in Encyclopedia of Agrophysics, Springer Netherlands, 2011.
4. Castillejo N., Martinez-Hernández G.B., Monaco K., Gomez P.A., Aguayo E., Artés F., Artés-Hernández F., Preservation of bioactive compounds of a green vegetable smoothie



- using short time-high temperature mild thermal treatment, *Food Sci Technol Int.*, 23(1), 46-60, 2017.
5. Corpaş L., Velciov A.B., Riviş A., Olariu L., Grăvilă C., Ahmadi M. – Physico-chemical characterisation of some fruit juices from Romanian hypermarket fruits, *Journal of Agroalimentary Processes and Technologies*, 18 (1), 95-99, 2012.
  6. Hussain I., Khan L., Marwat, G.A., Ahmed N., Saleem M., Comparative study of vitamin C contents in fruits and medicinal plants. *J. Chem. Soc. Pak.*, 30(3), 406-409, 2008.
  7. Pasvanska K., Varzakas T., Proestos C. – Minimally Processed Fresh Green Beverage Industry (Smoothies, Shakes, Frappes, Pop Ups), pp. 513-536 In Fatih Yildiz, Robert C. Wiley eds., *Minimally Processed Refrigerated Fruits and Vegetables*, 2nd ed., Springer, 2017.
  8. Taneja S.C., Chandra S. – Mint, pp. 366-387 in Peter K.V. ed. *Handbook of herbs and spices* (2nd ed.), vol. I, Woodhead Publishing Series in Food Science, Technology and Nutrition, 2012.

## THE RECYCLING OF FLY ASH IN FITOREMEDIATION PROCESSES OF SOILS POLLUTED WITH PETROLEUM PRODUCTS

**Amanda Izabela Siminic, Dorian-Gabriel Neidoni , Mihaela Dragalina, Smaranda Mășu**

*National Research and Development Institute for Industrial Ecology ECOIND, Timisoara  
Subsidiary, Timisoara, street Bujorilor, no. 115, Romania  
e-mail: amanda\_izabela@yahoo.ro*

### **Abstract**

The purpose of the paper was to implement / produce in situ crops of annual technical plants, of the species. The study was conducted on soils heavily polluted with petroleum products in the vicinity of active railways. In order to attenuate the polluting nature of the soil, adsorbent materials were used: the ascent of the thermal power plant or the indigenous volcanic tuff. For the elaboration of the experimental models, a comparative analytical-synthetic study of a data bank resulting from the installation and development of a crop of annual plantations of inlaid plants on unproduced polluted soil / fertilized soil sludge in the absence / presence of ash thermocentral or indigenous volcanic tuff. The efficiency of installing / maintaining plant crops on experimental soil variants and the TPH (Total Petroleum Hydrocarbon) petroleum products efficiency on polluted and fertilized soil with urban sludge and ash thermal power plants have been compared with the efficiency obtained in in the case of the use of the amendment as an addition to urban sludge, indigenous volcanic tuff.

### **Introduction**

Total Petroleum Hydrocarbon (TPH) comprise a mixture of hydrocarbons that pollute petrochemical areas, petroleum storage areas, petroleum waste areas, refineries, oil extraction wells. TPH are considered persistent hazardous waste that can reach food chains. These substances may have acute and / or chronic toxic effects. Acute toxic substances are benzene, benzoprene. These substances are recognized as having mutagenic and carcinogenic characteristics. The TPH class comprises chemical compounds having different physico-chemical characteristics[1]. It has been divided into two main categories:

1. GRO GROUP (gazoline range organics), boiling in the range of 60 to 170 ° C. Among these are the following very toxic substances: iso pentane, 2-3-dimethylbutane, n-butane and others. In addition to these C6-C10 short chain alkanes in this category are also included monoaromatic hydrocarbons: benzene, toluene, ethylbenzene and xylene (BTEX).
2. The DRO category (diesel range organics) in this category includes the following substances: C10 - C40 long chain alkanes and complex substances such as polycyclic aromatic hydrocarbons HAP.

These chemical compounds (TPHs) are generally released from antropogenic activity and lead to pronounced pollution of soil and deep water. Polluted sites often contain a high concentration of TPH. Pollutants in the BTEX category are highly mobile in the environment, whereas those in the HAP category strongly bind to the soil particles and near the source where they are discharged into the environment and remain there as an organic phase. Phytoremediation of hydrocarbon-contaminated soils: principles and applications [2].

## Experimental

The purpose of the experimental work was the recycling of thermal power ash for the optimization of phytoremediation processes of soils polluted with petroleum products. In the case of using technical plants, inulin.

Experimental investigations were conducted in situ on experimental lots located on strongly polluted land with petroleum products (TPH) in the range of 61.1-82.82g / kg s.u.

The objectives pursued in this phase were:

- Determination of the ash influence of the thermal power as an amendment in the phytoremediation of polluted and fertilized soils with urban sludge, compared with another amendment, namely the volcanic tuff
- Evaluation of tolerance characteristics of the annual plant species selected for phytoremediation variants in the absence / presence of ash of thermo-central by the parameters:
  - the degree of plant growth,
  - Growth rate of plants,
  - the degree of vegetation occupation of the sown area,
  - plant health

The study was conducted with a crop of annual plant, inulin. Also, comparative studies were carried out on the effect of the ash of the thermal power used as an amendment in the mixture with urban sludge in the phytoremediation process on the development of plants versus urban sludge. the effect of another amendment added to the fertilizer agent, the indigenous volcanic tuff.[3]

The degree of coverage of the cultivated area was determined in accordance with the Braun-Blanquet Scale[4]

**Table 1** Braun-Blanquet's assessment scale and completed by Ellenberg

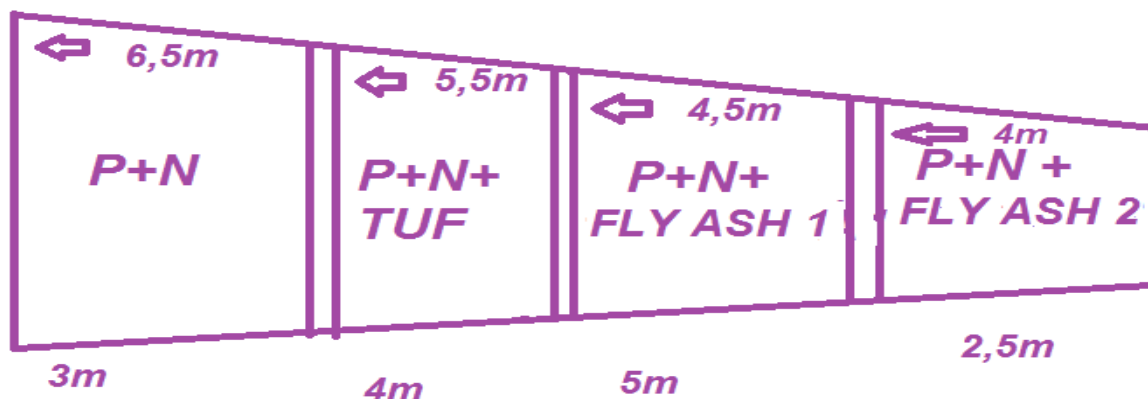
No	Scale of appreciation	Coverage range [%]
1	+ (Very rare individuals)	0.1-1
2	1 (low coverage)	1-10
3	2 (covering 1/20 of the surface)	10-25
4	3 (covering 1/4-1/2 of the surface)	25-50
5	4(covering 1/2-3/4 of the surface)	50-75
6	5 (covering >3/4 of the surface)	75-100

## Results and discussion

1. Biometric parameters of plants
2. Variation of petroleum products in cultivated soils
3. Influence of the ash amendment of the thermal power plant in the process of phytoremediation with technical plants, oil, soils polluted with petroleum products,
4. Comparative studies on the effectiveness of in-situ phytoremediation in fertilized soil variants of fertilized soil in the presence / absence of various amendments used,
5. Develop a phytoremediation model

The experimental block of study

In figure no. 1 experimental groups are presented



Based on the results obtained from the experimental studies and the analytic-synthetic analysis of the parameters of the inland culture characteristics and the variation of the oil content of the soil, experimental models of in situ phytoremediation were developed with annual technical plants

1. experimental model of in situ phytoremediation with annual technical plants on soils polluted with petroleum products 61,1-82,82g / kg s.u ..., fertilized with 60 t / ha biological sludge from a municipal wastewater treatment plant;

2. experimental model of in situ phytoremediation with annual technical plants in soils polluted with petroleum products 61,1-82,82g / kg su, fertilized with 60 t / ha biological sludge from a municipal wastewater treatment plant and treated with 50-100 t / hacenus from burning of lignite in thermal power plants;

3. experimental model of in situ phytoremediation with annual technical plants on soils polluted with petroleum products 61,1-82,82g / kg su., Fertilized with 60 t / ha biological sludge from a municipal wastewater treatment plant treated with 5t / ha indigenous volcanic tuff. [5]

## Conclusion

- The conclusions of the plant culture monitoring are:

The lot cultivated with plants of the species in which an amendment was used on the basis of indigenous volcanic tuff, as an addition to the organic fertilizer, the sludge resulting from a municipal wastewater treatment plant, shows the highest increase in plant height (50- 60 cm) as well as the highest coverage of the sown area (70%)

The use of an optimal quantity of ash of 60 t / ha as an amendment for the treatment of soils polluted with petroleum products fertilized with urban sludge generated similar effects to the effects obtained on the variant treated with urban sludge mixed with indigenous volcanic tuff

The use of a larger sludge mud mixture (100 t / ha) resulted in inferior results to the urban sludge variant and the optimal dose of the ash of the thermal power plant and of the soil variant in which urban sludge was used in the absence of amendments

• The characterization of crops according to Braun Blanquet's abundance-dominant index led to the following conclusions:

1. When the plant rose, the abundance-dominance index was superior when using indigenous volcanic tuff or ash amendment as an addition to the organic fertilizer;
2. The dominance-abundance indices uniform for all variants of soil cultivated with in after the 4th week of vegetation
3. After 9 weeks of flax cultures vegetation, the abundance-dominant index was slightly reduced in the case of the culture installed on the experimental variant of polluted soil, fertilized and fined with an ash overdose of 100 t / ha compared to the other 3 lots.

### References

- [1]Alkorta, I., & Garbisu, C. (2001). Phytoremediation of organic contaminants in soils. *Bioresource Technology*, 79(3), 273–276.
- [2]R. KKamath, J. A h, J. A. Rentz, J. L. Schnoor and P.J.J. Alvarez, Phytoremediation of hydrocarbon-contaminated soils: principles and applications Department of Civil and Environmental Engineering Seaman Center, University of Iowa City, Iowa U.S.A. 52242, 1-32
- [3]Gerhardt, K. E., Huang, X. D., Glick, B. R., & Greenberg, B. M. (2009). Phytoremediation and rhizoremediation of organic soil contaminants: potential and challenges. *Plant Science*, 176(1), 20–30
- [4]Ellenberg, H., Zeigerwerte der Gefäßpflanzen Mitteleuropas, *Scripta Geobot.*, 1974, vol. 9.
- [5]Aprill, W. and R.C. Sims, 1990. Evaluation of the use of prairie grasses for stimulating polycyclic aromatic hydrocarbon treatment in soil. *Chemosphere*, 20: 253-265

## ACCUMULATION OF ESSENTIAL METALS IN LEAVES AND ROOTS OF CUCUMBER GROWN IN THE PRESENCE OF SOLID RESIDUES FROM A BIOGASS PLANT

**Ivana Maksimović, Marina Putnik-Delić, Milica Perišić, Rudolf Kastori, Žarko Ilin, Milena Daničić**

*University of Novi Sad, Faculty of Agriculture, Trg D. Obradovića 8, 21000 Novi Sad, Serbia  
e-mail: ivanam@polj.uns.ac.rs*

### **Abstract**

Large amounts of solid residues (SR) remain after the process of energy production in a biogas plant. This material may be utilized directly or after composting (CSR) as organic fertilizers. The study was conducted to investigate the influence of various amounts of SR and CSR from biogas plant on growth, accumulation and distribution of essential metals in the leaves and roots of young cucumber plants. In both leaves and roots, concentration of K was the most responsive to treatments of macronutrients, and concentration of Mn of micronutrients. Overall, concentrations of all micronutrients, apart from Zn, were under optimal level in all treatments. Even though the concentration of nutrients in SR and CSR were limited, they significantly influenced content of essential metals and their distribution in leaves and roots of cucumber.

### **Introduction**

The use of renewable sources in process of energy production is getting more attention over time due to the need to replace fossil fuels with renewable sources of energy. Therefore, the use of biomass of various origins (harvest residues, manure, municipal waste or plants produced to be used in biogas plants) has become favored and stimulated by policies. Since the features of input material in biogas plants may vary, the composition of residues after the usage of this material to produce biogas may vary as well. Apart from the nutritive value of residues from biogas plants, they can also contribute to improvement of the soil structure since they are rich in organic matter [1].

One of the biogas facilities on the territory of Vojvodina is “Mirotin-Energo” in Vrbas, which produces 36.000 t of fermented and composted fermented residues per year. Due to their chemical composition, solid and composted solid residues (SR and CSR, respectively) have the potential to be used as organic fertilizers in agriculture [2], [3]. Therefore, the main aim of the present study was to investigate the potential use of SR and CSR from biogas facility “Mirotin-Energo” as source of nutrients in cucumber production.

### **Experimental**

The experiment was conducted in semi-controlled conditions of a greenhouse. Seeds of cucumber (*Cucumis sativus* L., cultivar “Tajfun”), were sown in pots V=750 mL, containing a mixture of 400 mL agroperlite (Agroperlit Extra, Termika Zrenjanin) and SR or CFR (either 5, 25 or 50 g), as described in Tab. 1. Each treatment was divided into two sub-treatments: one watered with deionized water (DW) and the other with ¼ strength solution after Hoagland and Arnon [4] (H) (Tab. 2). Additional two groups of plants were grown only in agroperlite (without addition of SR or CSR) and watered with either ¼ or ½ strength H (controls). The experiment was set in 3 replications, with 7 plants per replication.

Table 1. Composition of solid residue (SR) and composted solid residue (CSR) from biogas plant “Mirotin-Energo”, Vrbas. Results are averages of six replications and refer to contents of ash and mineral elements in dry matter. DM, dry matter.

Residue from biogas plant	DM	Ash	K	Ca	Mg	Fe	Zn	Cu	Mn
	%					ppm			
SR	29.16	9.45	0.11	1.16	0.45	580	63.24	5.20	127.99
CSR	27.65	34.56	0.51	8.35	1.26	980	91.91	15.62	351.71

One month after sowing, plants were harvested, roots were briefly rinsed with deionized water (DI), excess liquid removed by blotting paper, and plant material dried at 70 °C until constant mass. Dry mass (DM) of leaves, stems and roots were measured. Concentrations of essential metals in leaves and roots were assessed by flame photometry (K and Ca) and by atomic absorption spectro-photometry (Mg, Fe, Zn, Cu and Mn).

Table 2. Nutrient treatments to which cucumber was exposed. To each pot containing 400 mL of agroperlite were added 5, 25 or 50 g of solid residue (SR) or composted solid residue (CSR). DW, deionized water; ¼H and ½H, ¼ and ½ strength nutrient solution after Hoagland and Arnon [4].

Composition of nutrient medium	Treatments													
	1	2	3	4	5	6	7	8	9	10	11	12	13	14
SR (g)			5	5	25	25	50	50						
CSR (g)									5	5	25	25	50	50
DW				*		*		*		*		*		*
¼ H (control)	*		*		*		*		*		*		*	
½ H (control)		*												

### Results and discussion

Concentration of K increased in the presence of 25 and 50 g of SR and CSR in both leaves and roots, but it was about 10% higher in leaves (Tab. 3, Fig. 1). Cucumber has high requirements for K (higher than for N). According to [5], in leaves of treatments 6, 7, 8 concentration of K was optimal, in treatments 5, 12, 13 and 14 it was low and in 1-4 and 9-10 K was deficient. Concentration of Ca increased in the presence of SR and CSR in both leaves and roots, it was in the optimal range and its concentration in leaves varied less than concentrations of K and Mg (Fig. 1). The concentration of Mg in leaves increased in the presence of SR and CSR, whereas in roots 6-8 and 12-14 it was lower than in the ¼ H control. Overall concentration of Mg was in the optimal range, according to [5]. Concentration of Fe was suboptimal in all leaves except for those of treatment 13, where in was just above the threshold according to [5]. Interestingly, the treatments reduced concentration of Fe in both leaves and roots with respect



to the ¼ H control, except in treatments 10 and 13 in leaves. The average reduction of Fe concentration in leaves of plants treated with SR was 30% and in the roots of both SR and CSR as much as 57% (Fig. 1). Concentration of Zn was in the optimal range. However, in the presence of SR it slightly increased and in the presence of SCR slightly decreased in leaves, whereas it significantly decreased in SR and especially in CSR treated roots. Concentration of Cu in all treatments was low, less affected by SR and CSR in leaves but about three times lowered in roots with the respect to the ¼ H control (Fig. 1). According to [5], concentration of Mn was low in treatments 2-4 and deficient in all the others (Tab.3, Fig. 1). In treatments 3 and 4 in leaves, however, and 3, 5, 8, 11, 13 and 14 in roots it was higher than in the respective ¼ H controls suggesting that both SR and CSR can serve as a source of Mn.

Table 3. Concentration of essential metals in dry matter of leaves and roots of cucumber, grown in the presence of SR or CSR. For reference to treatments, please see Table 2.

Plant part	Treatment	K	Ca	Mg	Fe	Zn	Cu	Mn
		%			ppm			
Leaf	1	1.3	4.2	0.6	36.6	46.9	5.6	12.9
	2	1.8	6.4	0.8	48.6	50.8	6.9	18.0
	3	1.4	5.2	0.9	29.9	45.9	4.7	16.0
	4	0.8	6.7	1.3	34.2	74.1	5.6	16.9
	5	2.4	5.6	1.1	20.4	42.8	4.5	5.6
	6	3.0	6.0	1.3	20.2	51.4	5.9	4.5
	7	3.1	6.4	1.3	20.3	42.4	4.9	6.0
	8	3.7	6.8	1.5	29.4	55.1	5.6	7.9
	9	1.5	6.6	0.9	37.0	33.7	4.4	9.6
	10	0.8	7.0	1.2	37.7	48.3	4.6	9.2
	11	1.6	6.6	1.1	32.9	34.4	4.5	8.7
	12	2.0	6.6	1.1	25.0	42.8	4.6	6.3
	13	2.7	6.6	1.1	53.9	49.0	6.7	10.0
	14	2.6	5.9	0.9	29.2	39.5	4.7	6.7
Root	1	2.3	2.5	0.3	129.3	95.4	24.4	3.3
	2	2.5	3.9	0.3	61.2	93.7	13.8	1.5
	3	2.7	3.6	0.5	54.9	72.9	7.0	6.6
	4	2.5	4.3	0.6	41.9	87.4	8.9	2.9
	5	4.1	4.1	0.4	81.3	67.7	7.1	6.0
	6	6.5	8.2	0.3	40.9	67.8	8.9	1.9
	7	5.7	3.6	0.3	48.4	65.0	7.6	3.2
	8	6.6	4.8	0.3	63.8	72.5	8.1	4.4
	9	2.3	3.6	0.4	50.8	60.5	7.5	3.4
	10	2.7	3.9	0.6	40.1	67.6	8.0	2.0
	11	3.9	3.6	0.4	67.3	54.2	7.1	5.3
	12	4.8	3.6	0.3	48.4	61.3	7.5	3.1
	13	4.1	4.2	0.3	65.8	70.0	9.0	5.0
	14	4.5	4.5	0.3	62.9	64.1	8.1	4.8

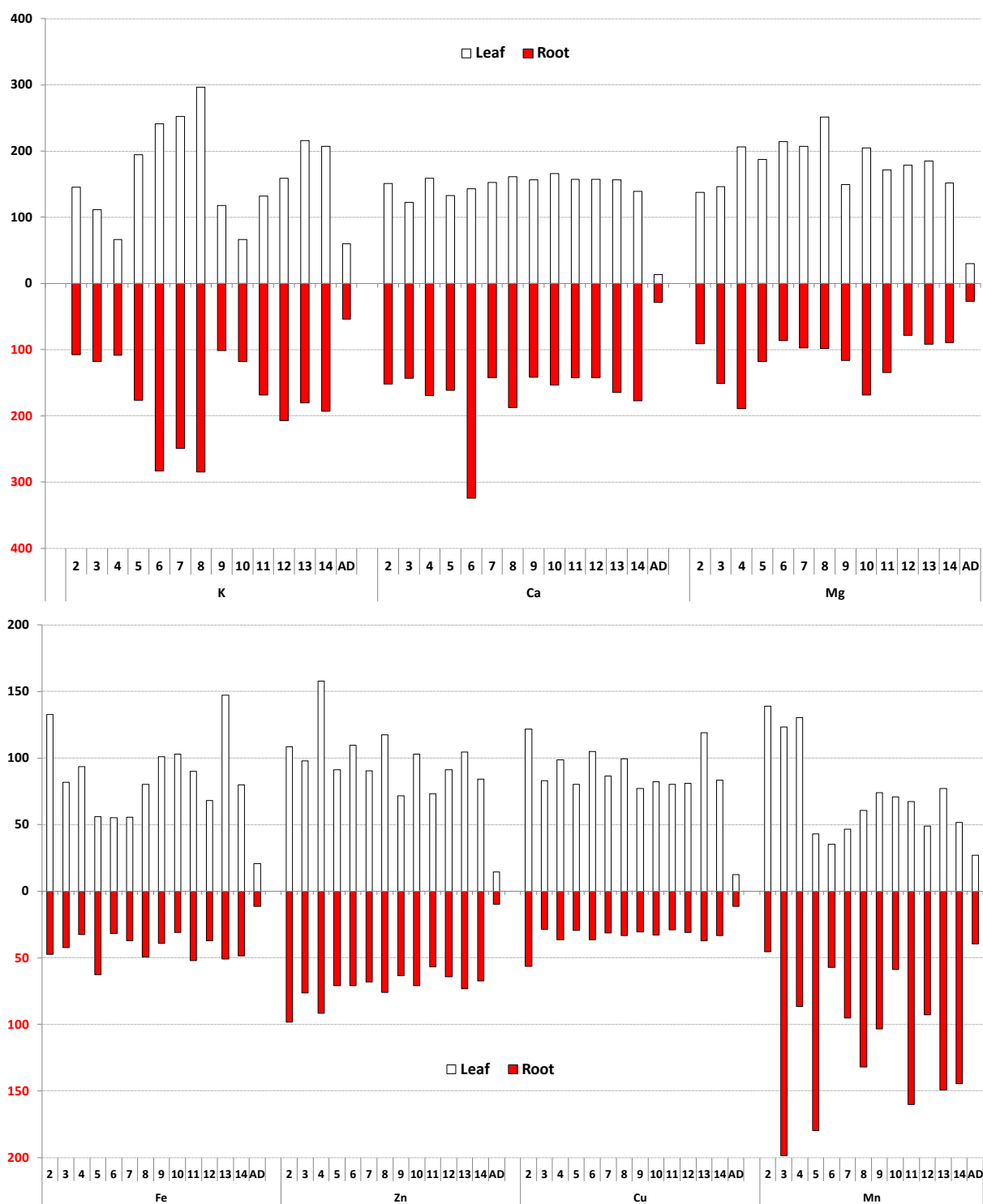


Figure 1. Concentration of essential metals in leaves and roots of cucumber, grown in the presence of SR and CSR, expressed in percents of the  $\frac{1}{4}$  H control (100%). For reference to treatments, please see Table 2. AD, average deviation.

## **Conclusion**

Even though in this experiment cucumber was not supplied with sufficient sources of all the analyzed essential metals, it was found that cucumber can utilize nutrients supplied by SR and CSR. The amounts of elements found in plants depended both on applied amount of residues and on their processing (composted or not). Besides concentration, the treatments influenced distribution of some elements between roots and shoots (e.g. Mg, Zn, Cu, and Mn) and reduced concentrations of the others (e.g. Fe and Cu). Therefore, application of solid residues in cucumber production has to be conducted carefully.

## **Acknowledgements**

This work was financially supported by Ministry of Education, Science and Technological Developments of the Republic of Serbia (TR 31036).

## **References**

- [1] B. Karki, In: H.R. Doelle, S. Rokem, M. Beruvic (Eds.), *Biogas as Renewable Energy from Organic Waste*, Eolss Publishers Co. Ltd., Canada, 2009.
- [2] W. Schäfer, M. Lehto, F. Teye. *Dry Anaerobic Digestion of Organic Residues on-farm – a feasibility Study*. Agrif. Res. Rep. 77 (2006) 98.
- [3] Ministry of Agriculture, Fisheries and Food (MAFF)/Agricultural Development and Advisory Service (ADAS), *The Analysis of Agricultural Materials*, 3rd Ed., HMSO, London, 1986.
- [4] D.R. Hoagland, D.I. Arnon. *The Water-culture Method for Growing Plants without Soil*. Calif. Agric. Exp. Stat. Pub. 347 (1950) 1-32.
- [5] <http://www.haifa-group.com/files/Guides/Cucumber.pdf> (18.08.2017.)

## EFFECT OF $\text{Cu}^{2+}$ IONS ON NITROGEN ASSIMILATION AND METABOLISM ENZYMES IN SELECTED FIELD CROPS

Djordje Malenčić

*Faculty of Agriculture, Department for Field and Vegetable crops, University of Novi Sad,  
SRB-21000 Novi Sad, Trg D. Obradovića 8, Serbia  
e-mail: malencic@polj.uns.ac.rs*

### Abstract

The effect of  $\text{Cu}^{2+}$  ions on nitrogen assimilation and metabolism enzymes (nitrate reductase, glutamine synthetase and glutamate dehydrogenase) in leaves of young plants of wheat and maize has been investigated.  $\text{Cu}^{2+}$  concentrations used were  $10^{-8}$  (control),  $10^{-7}$ ,  $10^{-5}$  and  $10^{-3}$  mol  $\text{dm}^{-3}$ . Enzymology of nitrogen assimilation and metabolism was significantly different between examined genotypes: in wheat, NR activity decreased with the increased  $\text{Cu}^{2+}$  concentrations while the GS activity increased (except for the  $10^{-3}$  mol  $\text{dm}^{-3}$   $\text{Cu}^{2+}$  concentration). In maize, NR activity was at its minimum while GS activity was not detected. GDH activity varied in both species examined. The obtained results also indicate that the investigated maize hybrid is more Cu-sensitive in the sense of nitrogen assimilation and metabolism, compared to wheat. In wheat, two nitrogen assimilation pathways were established (GS/GOGAT- and GDH-pathway). In maize, only GDH-pathway was present.

### Introduction

Plant world is becoming more endangered due to increasing contamination of the environment. Among other pollutants, heavy metals (HM) in soils very often affect cultivated plants. The assimilation, transport, distribution, accumulation and physiological properties of those elements are very important for high yield and quality of cultivated plants. Beside that, HM are of great importance from the ecological aspect because they enter the food chain through plants. Knowing the ecology and mechanisms of uptake, accumulation, distribution and effects of HM on life processes of plants is of great importance, both from physiological and ecological aspect [1].

Increased concentrations of HM, where copper (Cu) is classified, cause phytotoxicity. One of the primary effects of HM on plants is changing the structure and function of cell membranes and organelles. HM at higher concentrations could also cause increased reduction of molecular oxygen ( $\text{O}_2$ ), and therefore produce toxic oxygen species [1]. In this study, Cu was chosen because of its double effect on the plant metabolism processes. It belongs to the group of microelements - essential for plants in low concentrations, but when found in excess it may become phytotoxic. Primary effects of Cu toxicity are the inhibition of enzyme activity and damaging the membrane system. This can result in depressed photosynthesis, direct inhibition of growth processes and decreased nutrient uptake and transport which can ultimately cause the death of plants.

The assimilation and metabolism of inorganic nitrogen in plants is a complex process involving a series of enzymes. Nitrate is reduced to  $\text{NH}_4^+$  by the reaction of nitrate reductase (NR) and nitrite reductase (NiR) (Fig. 1). The cytosolic NR is the first enzyme in the pathway of nitrate assimilation, and its activity is highly regulated. Sufficient NR activity is a prerequisite for optimal utilization of soil N. NR has a major role in incorporation of N for plant yields under field conditions and it is widely known to be substrate inducible [2].

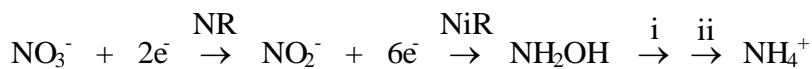


Figure 1. Reduction of  $\text{NO}_3^-$  to  $\text{NH}_4^+$  by the reaction of nitrate reductase (NR) and nitrite reductase (NiR)

Glutamine synthetase (GS) is the key enzyme responsible for the assimilation and reassimilation of ammonia (Fig. 2). In higher plants GS is one of the major enzymes responsible for the assimilation of ammonium absorbed from the growth medium, generated by nitrate reduction or reassimilated after release of endogenous  $\text{NH}_4^+$  by ammonium-evolving processes such as photorespiration [3, 4].

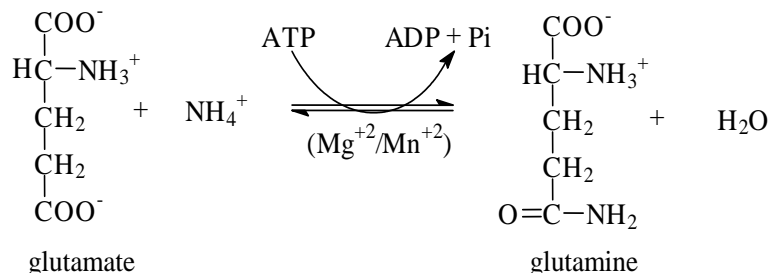


Figure 2. Reductive amination of glutamate (Glu) to glutamine (Gln)

The conversion of  $\text{NH}_4^+$  into glutamate (Glu) proceeds *via* two pathways. In the GS/GOGAT pathway,  $\text{NH}_4^+$  is incorporated into glutamine (Gln) by glutamine synthetase (GS) (Fig. 2), which is then converted with 2-oxoglutarate (2-OG) to Glu by glutamate synthase (GOGAT). Glutamate dehydrogenase (GDH) catalyzes the incorporation of  $\text{NH}_4^+$  into Glu by reversible reductive amination of 2-OG [5,6].

The aim of this study was to investigate and determine NR, GS and GDH activities in two major field crops in the regions of Central Europe - wheat (*Triticum aestivum* L.), and maize (*Zea mays* L.), affected by different concentrations of copper ions ( $\text{Cu}_2^+$ ).

## Experimental

One cultivar of wheat (*Evropa 90*) and maize hybrid (*NSSC 640*) were chosen for the experiment. Material for the investigations were leaves of young plants. Seeds were germinated for 48 h in thermostat at 25-27°C. Seedlings were grown on nutrient solution Reid and York, pH 5.5 (controlled every second day), under conditions of glass-house. There were eight plants of wheat, and six plants of maize in the pots, respectively. After 25 days, plants were treated with three concentrations of Cu ( $10^{-7}$ ,  $10^{-5}$  and  $10^{-3}$  mol dm<sup>-3</sup>), for six days.  $\text{Cu}^{2+}$  was supplied in the form of  $\text{CuSO}_4 \cdot 5\text{H}_2\text{O}$ .

The enzyme extract was prepared by homogenizing 1.0 g of fresh leaves in 10 cm<sup>3</sup> of extraction buffer containing 5 mM imidazole, 5 mM 2-mercaptoethanol and 0.5 mM EDTA, pH 7.2, followed by centrifugation at 10000 g for 10 minutes. After centrifugation, the supernatant aliquots were used to measure enzyme activities. The NADH-dependent NR activity was determined *in vivo* according to Inokuchi et al. [7], in which the formation of nitrite from nitrate was measured spectrophotometrically at 540 nm. The GS activity was assayed using the reverse-glutamyl transferase reaction, which measured the formation of glutamyl hydroxamate [5]. Measurement of GDH activity was based on decrease of absorbance at 340 nm, caused by NADH oxydation. Calculation of activity was done

according to changes in NADH concentration in presence and absence of ammonium acetate. NADH concentration was established according to NADH absorbance at 340 nm [8]. Statistical evaluation was performed using software Statistica, Version 10.0. The experiments were repeated four times, and differences between treatments were determined using LSD test for 0.05 significance level.

### Results and discussion

The initial step of  $\text{NO}_3^-$  reduction is catalyzed by the NR enzyme, which is considered a cytoplasmic enzyme in higher plants. This enzyme plays an important role in the regulation of nitrogen metabolism, and it is labile *in vivo* under the environmental stress. Our results for NR activities under conditions of excess of Cu showed, both in wheat and maize, a decrease in the enzyme activity, with the increased  $\text{Cu}^{2+}$  concentrations (Fig. 3). In maize they were much lower. Although the NR is substrate-induced enzyme, its activity may be suppressed by different ecological factors, such as HM, herbicides, UV-radiation etc. [1]. Inhibition of the activity could be promoted by 1) non-competitive enzyme inhibition, 2)  $\text{Cu}^{2+}$  reaction with -SH groups of the NR protein, and 3)  $\text{Cu}^{2+}$  reaction with  $\text{O}_2$  where oxygen free radicals are produced [9]. It seems that the main nitrogen source for maize is not  $\text{NO}_3^-$ , but  $\text{NH}_4^+$ , which could be seen from the GDH activities as well.

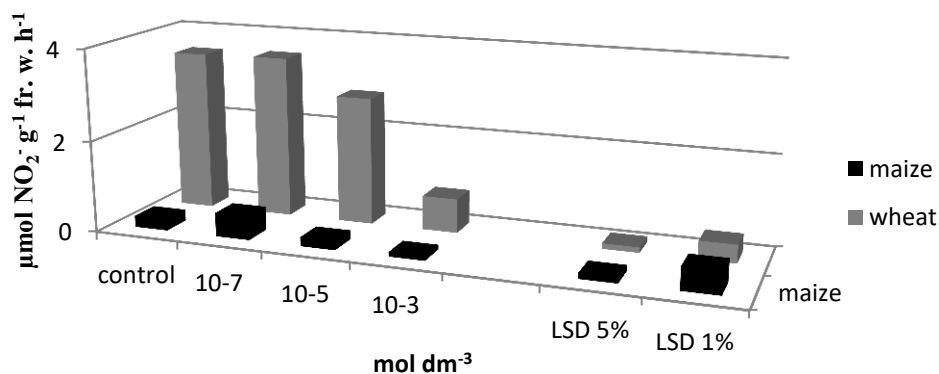


Figure 3. NR activity ( $\mu\text{mol NO}_2^- \text{ g}^{-1} \text{ fr. w. h}^{-1}$ ) in leaves of wheat and maize treated with different  $\text{Cu}^{2+}$  concentrations

GS activities in wheat increased with the increasing  $\text{Cu}^{2+}$  concentrations in the range of control -  $10^{-5} \text{ mol dm}^{-3}$ , but not at the highest concentration ( $10^{-3} \text{ mol dm}^{-3}$ ; Fig. 4). This could be reaction on nitrogen translocation from older to younger leaves in water stress conditions [10]. HM in excess can cause this as a result of decrease in root cells permeability [11]). In maize there was no GS activity. Absence of GS activity in maize point out that the nitrogen was not utilized to amino acids by GS/GOGAT-pathway, but the other pathway - GDH. GDH activity was inhibited in wheat by the  $10^{-7}$  and  $10^{-3} \text{ mol dm}^{-3} \text{ Cu}^{2+}$  probably due to SH-groups oxidation and in the non-competitive manner, but not by the  $10^{-5} \text{ mol dm}^{-3} \text{ Cu}^{2+}$  (Fig. 5). In maize, GDH activity was highest at the  $10^{-5} \text{ mol dm}^{-3} \text{ Cu}^{2+}$ . Induction of GDH at  $10^{-5} \text{ mol dm}^{-3} \text{ Cu}^{2+}$  in both genotypes could be result of metal-induced stress. In both examined genotypes GDH-pathway of nitrogen assimilation was present. In wheat it represented a side way but in the maize it was a fundamental/major metabolic way, especially because the NR activity was minimal while there was no GS activity.

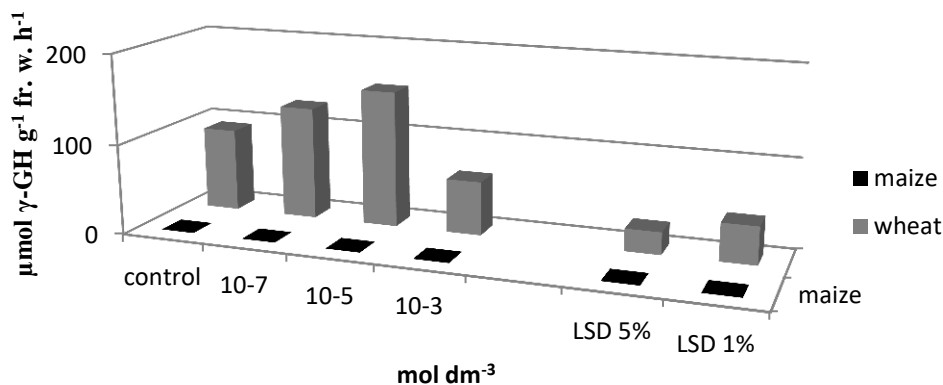


Figure 4. GS activity ( $\mu\text{mol } \gamma\text{-glutamyl hydroxamate g}^{-1} \text{ fr. w. h}^{-1}$ ) in leaves of wheat and maize treated with different  $\text{Cu}^{2+}$  concentrations

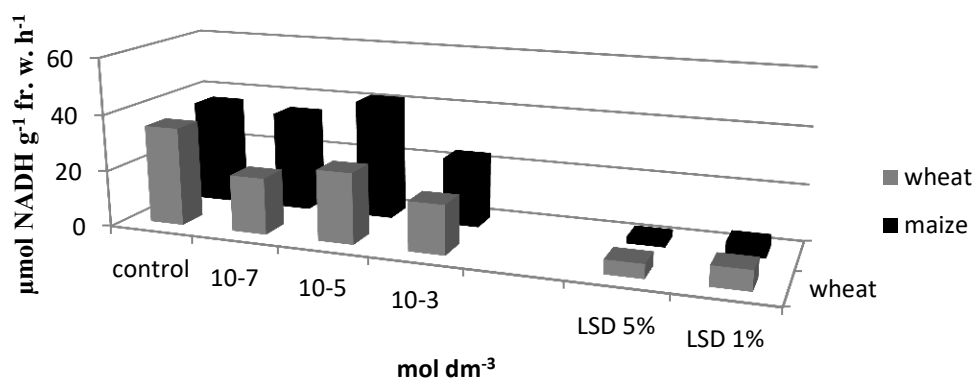


Figure 5. GDH activity ( $\mu\text{mol NADH g}^{-1} \text{ fr. w. h}^{-1}$ ) in leaves of wheat and maize treated with different  $\text{Cu}^{2+}$  concentrations

### Conclusion

Enzymology of nitrogen assimilation and metabolism was significantly different between examined genotypes: in wheat, NR activity decreased with the increased  $\text{Cu}_2^+$  concentrations while the GS activity increased (except for the  $10^{-3} \text{ mol dm}^{-3} \text{ Cu}_2^+$  concentration). In maize, NR activity was at its minimum while GS activity was not detected. GDH activity varied in both species examined. The obtained results also indicate that the investigated maize hybrid is more Cu-sensitive in the sense of nitrogen assimilation and metabolism, compared to wheat. Also, the dominant nitrogen assimilation pathway in wheat was GS/GOGAT-pathway, while in the maize that was GDH-pathway.

### Acknowledgements

This work is a part of a project financed by the Ministry of Science and Technological Development, Republic of Serbia, TR-31022.



## **References**

- [1] Malenčić, Đorđe: Effect of Cu<sup>2+</sup> ions on the activity of antioxidant enzymes and nitrogen metabolism enzymes in young plants of wheat and maize, 1996.
- [2] C. Bergareche, E. Simon, *J. Plant Physiol.* 132 (1988) 28.
- [3] P.A. Fentem, P.J. Lea, G.R. Stewart, *Plant Physiol.* 71 (1983) 496.
- [4] W. Claussen, F. Lenz, *Plant and Soil* 208 (1999) 95.
- [5] R. Inokuchi, M. Okada, *Plant Sci.* 161 (2001) 35.
- [6] J.L. Cruz, P.R. Mosquim, C.R. Pelcani, W.L. Ara'ujo, F.M. DaMatta, *Biol. Plant.* 48 (2004) 67.
- [7] R. Inokuchi, K. Motokima, Y. Yagi, K. Nakayama, M. Okada, *J. Phycol.* 35 (1999) 1013.
- [8] J. Coombs, in: J. Coombs, D.O. Hall (Eds.), *Isolation of enzymes. In: Techniques in Bioproductivity and Photosynthesis*, Oxford: Pergamon Press, 1982, pp. 142.
- [9] S. Uddin, S. Ahmad, *Biochem. Edu.* 23 (1995) 2.
- [10] R. Manderscheid, H. Jager, *J. Plant Physiol.* 141 (1993) 494.
- [11] J. Barcelo, Ch. Poschenrieder, *J. Plant Nutr.* 13 (1990) 1.

**EFFECT OF CARBON NANOFIBER ONTO TiO<sub>2</sub>-MODIFIED  
POWDER/GRANULAR ACTIVATED CARBON FOR ADVANCED WATER  
TREATMENT**

**Corina Orha<sup>1</sup>, Carmen Lazau<sup>1</sup>, Florica Manea<sup>2\*</sup>, Daniel Ursu<sup>1</sup>**

<sup>1</sup>*National Institute for Research and Development in Electrochemistry and Condensed Matter,  
no 144 A. Paunescu Podeanu Street, Timisoara 300569*

<sup>2</sup>*“Politehnica” University of Timisoara, P-ta Victoriei, No. 2, Timisoara e-mail:  
florica.manea@upt.ro*

**Abstract**

In this work, the influence of carbon nanofiber on the performance of TiO<sub>2</sub>-modified activated carbon (TiO<sub>2</sub>-AC) as photocatalyst for advanced water treatment was studied. TiO<sub>2</sub>-modified carbon nanofiber/activated carbon in powder form (TiO<sub>2</sub>-CNF/PAC) and in granular form (TiO<sub>2</sub>-CNF/GAC) were prepared by sol-gel method. Comparative morphological characterization studies for TiO<sub>2</sub>-CNF/PAC and TiO<sub>2</sub>-CNF/GAC and their testing for 25 mgL<sup>-1</sup> humic acid (HA) degradation showed a better performance of the overall sorption-involved photocatalysis using TiO<sub>2</sub>-CNF/GAC.

**Introduction**

Natural organic matters presence in drinking water source is responsible for membrane fouling in ultra- or nano-filtration steps of the advanced drinking water treatment technology. For this reason, various approaches have been investigated for the development of cheaper and more effective materials characterized by advanced properties suitable for the adsorption and photocatalysis applications in the water treatment.

Photocatalysis, one of the advanced water treatment processes, has been extensively studied to eliminate natural pollutants from water in the presence of semiconductor catalyst and UV illumination [1]. It is obviously that semiconductor catalyst is responsible for photocatalysis performance and among various materials used as semiconductors, titanium dioxide (TiO<sub>2</sub>) has been widely used for a broad range of applications because it is cheap, non-toxic, very active and stable in chemical reactions [2-4].

Various carbonaceous materials, e.g., activated carbon (AC), carbon nanotubes and carbon nanofibers (CNFs) have been intensively tested as sorbents, composite filters, antifouling membranes and support for photocatalysis processes. Composite materials based on titanium dioxide and activated carbon are receiving increasing attention for the degradation of humic, phenolic compounds, pesticides, chlorinated compounds and dyes because the activated carbon possesses high surface area, suitable pore structure and as consequence, high adsorption capacity and nano-sized TiO<sub>2</sub> facilitates photocatalysis [5-7]. However, the size of activated carbon influences the sorption characteristics and its combination with a nanostructured carbon should improve its performance.

The aim of this paper is to explore the role of CNF as support for TiO<sub>2</sub> in conjunction with powder and granular activated carbon, in form of TiO<sub>2</sub>-CNF/GAC and TiO<sub>2</sub>-CNF/PAC synthesized by sol-gel method and tested for the removal and the degradation of humic acid, the main constituent of natural organic matters from water.

## Experimental

All the chemicals were of analytical purity grade and used as received. Composite materials based on titanium dioxide-modified carbon nanofiber and activated carbon were prepared using 5 mL titanium tetraisopropoxide with a purity of 97 % (TTIP, Aldrich) as titanium precursor, 2 g of powder/granular activated carbon (Flochem Industries) and 1 g carbon nanofiber (Nanocyl, Belgium) as matrix. The mixture was vigorously magnetic stirring (700 rpm, IKA RCT basic stirrer) in the presence of 30 ml ethanol and 30 ml distilled water, and pH solution value of 2 was adjusted with HNO<sub>3</sub>. After three hours of continuous stirring the composite materials were filtered, washed, and dried at 60°C for 4 hours. The thermal treatment was realized at 400°C for 3 hours.

The morphology of the TiO<sub>2</sub>-CNF/PAC and TiO<sub>2</sub>-CNF/GAC composites was studied by a scanning electronic microscope (SEM, Inspect S PANalytical Model) coupled with the energy dispersive X-Ray analysis detector (EDX).

The photocatalytic experiments were carried out under magnetic stirring at 20°C into a RS-1 photocatalytic reactor (Heraeus, Germany), which consisted of a submerged UV lamp surrounded by a quartz shield.

For each experiment, an adsorption step of 30 minutes was assured under the same hydrodynamic conditions without UV irradiation.

At certain running time, the suspension was sampled and filtered through a 0.4 µm membrane filter. The concentration of humic acid was measured in terms of absorbance at 254 nm (A<sub>254</sub>) using a Carry 100 Varian spectrophotometer.

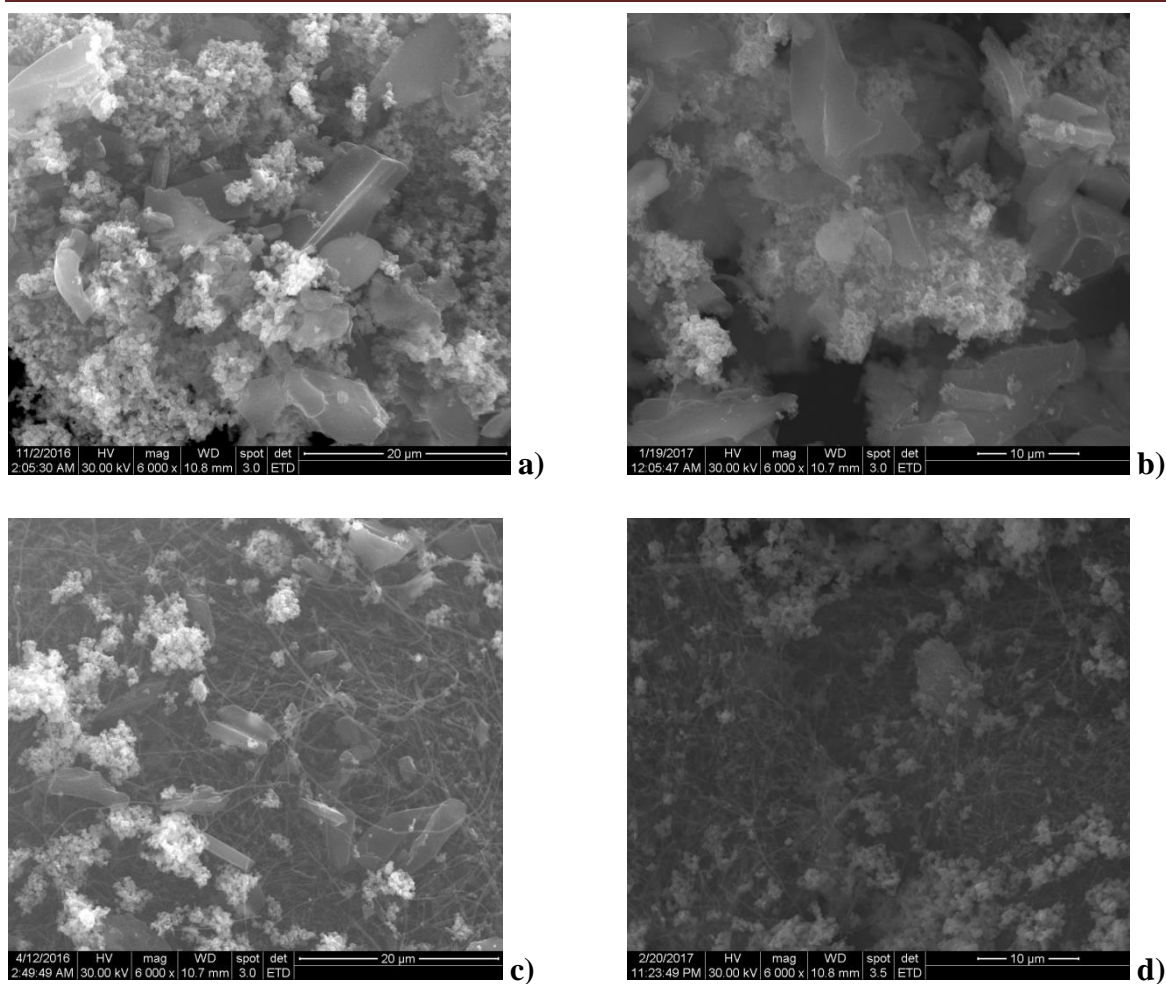
The HA removal efficiency was calculated using the following equation:

$$\text{Removal efficiency} = \frac{c_0 - c_t}{c_0} \times 100 \quad (\%) \quad (1)$$

where: C<sub>0</sub> and C<sub>t</sub> are the concentrations of HA in aqueous solution in term of A<sub>254</sub> at initial time and at any time t, respectively (mgL<sup>-1</sup>).

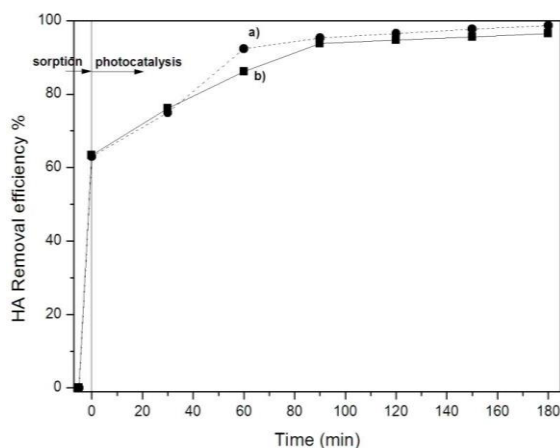
## Results and discussion

Figure 1 a-d presents SEM images for TiO<sub>2</sub>-PAC, TiO<sub>2</sub>-GAC, TiO<sub>2</sub>-CNF/PAC and TiO<sub>2</sub>-CNF/GAC. From SEM images, it is clearly seen that PAC and GAC have a layered structure, CNF have covered complete and uniform the both forms of activated carbon, forming a mesh on which TiO<sub>2</sub> nanoparticles characterized by spherically shape are distributed more uniform in comparison with PAC and GAC modified with TiO<sub>2</sub>.



**Fig.1. SEM/EDX images for a)  $TiO_2$ -PAC, b)  $TiO_2$ -GAC, c)  $TiO_2$ -CNF/PAC and d)  $TiO_2$ -CNF/GAC**

The performance of the  $TiO_2$  modified powdered activated carbon is tested for HA removal and degradation by the sorption and the photocatalysis process, with the mention that the sorption was considered as a prerequisite step of the photocatalysis process. The role of CNF in the composition of  $TiO_2$  modified activated carbon was checked for the performance of the photocatalysis process. Figures 2 and 3 show the results of the photocatalysis involving sorption step applied for HA removal and degradation expressed as the HA removal efficiency, using  $TiO_2$ -CNF/PAC and  $TiO_2$ -CNF/GAC in comparison with  $TiO_2$ -PAC and  $TiO_2$ -GAC, respectively. It can be noticed that the presence of CNF as support for  $TiO_2$  improved the sorption performance for  $TiO_2$ -GAC while no effect on the  $TiO_2$ -PAC is found. Also, the overall performance of the sorption step-involved photocatalysis was better in the presence of CNF. A slight enhancement of  $TiO_2$ -PAC performance was found by introduction of CNF as support for  $TiO_2$  that showed no necessity of CNF integration into  $TiO_2$ -PAC composition for the degradation of  $25\text{ mgL}^{-1}$  HA.



**Fig. 2. Evolution of HA removal ( $25\text{mgL}^{-1}$ ) efficiency versus time by sorption step-involved photocatalysis under UV irradiation using a)  $\text{TiO}_2\text{-CNF/PAC}$  and b)  $\text{TiO}_2\text{-PAC}$**

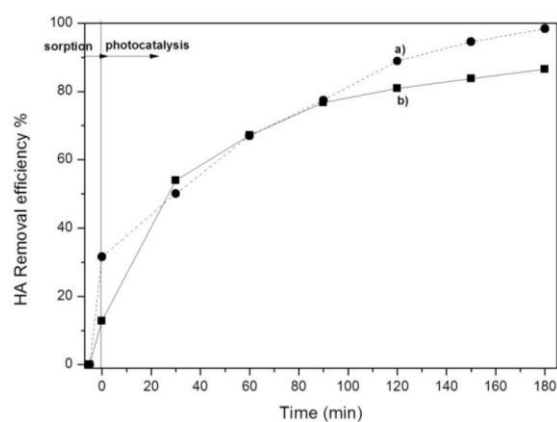


**Fig. 3. Evolution of HA removal ( $25\text{mgL}^{-1}$ ) efficiency versus time by sorption step-involved photocatalysis under UV irradiation using a)  $\text{TiO}_2\text{-CNF/GAC}$  and b)  $\text{TiO}_2\text{-GAC}$**

Due to the overall photocatalysis contains sorption and photocatalysis component, an assessment of the photocatalysis component was done by subtracting sorption component from the overall performance and the comparative results are presented in Figure 4. It can be noticed that the highest performance of photocatalysis was obtained for  $\text{TiO}_2\text{-GAC}$  composite with the mention that these materials were tested only for  $25\text{mgL}^{-1}$  HA and the overall photocatalysis performance was higher than 90%, which imposes further studies for higher HA concentrations.

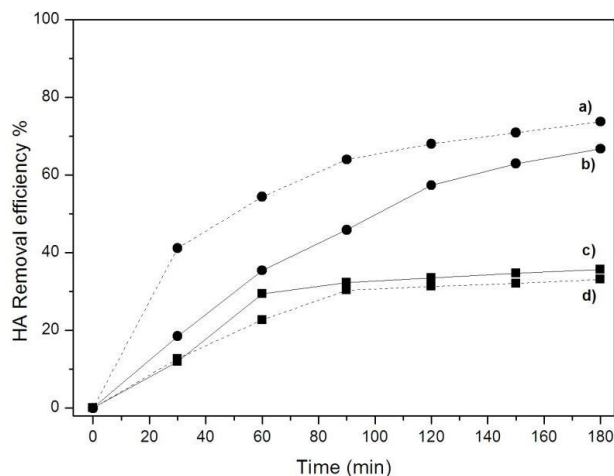


**Fig. 4. Evolution of HA removal ( $25\text{mgL}^{-1}$ ) efficiency versus time by photocatalysis under UV irradiation using a)  $\text{TiO}_2\text{-GAC}$ ; b)  $\text{TiO}_2\text{-CNF/GAC}$ ; c)  $\text{TiO}_2\text{-CNF/PAC}$  and d)  $\text{TiO}_2\text{-PAC}$**

A very important aspect is the stability of the material and their morphologies were tested also, after the photocatalysis application. The SEM images of  $\text{TiO}_2\text{-CNF/PAC}$  and  $\text{TiO}_2\text{-CNF/GAC}$  are gathered in Figure 5a and b, and it can be noticed the presence of  $\text{TiO}_2$  and CNF into catalyst composition, which denotes their good stability.

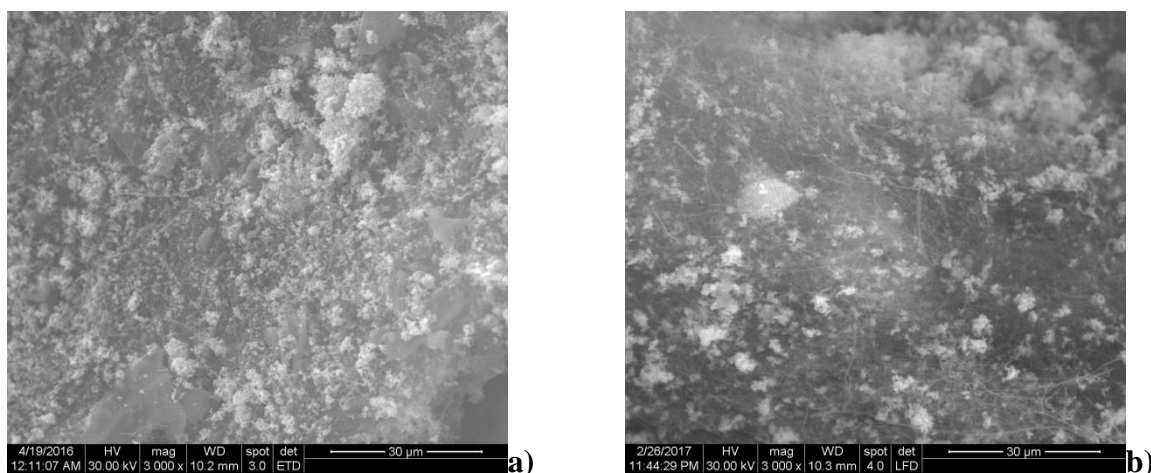


**Fig.5. SEM/EDX images recorded after photocatalysis application of a)  $\text{TiO}_2$ -PAC, b)  $\text{TiO}_2$ -GAC**

### Conclusion

$\text{TiO}_2$ -CNF/PAC and  $\text{TiO}_2$ -CNF/GAC composite materials were successfully synthesized by sol-gel method. CNF covered activated carbon forming a mesh layer that assured a better and more uniform distribution of  $\text{TiO}_2$  onto carbonaceous support.  $\text{TiO}_2$ -CNF/PAC,  $\text{TiO}_2$ -CNF/GAC,  $\text{TiO}_2$ -PAC and  $\text{TiO}_2$ -GAC acted as photocatalyst towards humic acid degradation and allowed the removal of  $25 \text{ mgL}^{-1}$  HA with an overall photocatalysis performance higher than 90%. The presence of CNF into composite allowed a slight enhancement of sorption properties of granular activated carbon without any effect onto the powdered activated carbon for removal of  $25 \text{ mgL}^{-1}$  HA. The morphology characterization of the composite after their application in the photocatalysis proved a good stability of the material that reclaim their potential for the further studies, which will envisage more concentrated humic acid removal from water.

### Acknowledgements

This work was supported by the Romanian National Research Programs PN 16 14 02 02 and PN-III-P2-2.1-PED-2016, 69PED/2017.

### References

- [1] M. H. Baek, J. W. Yoon, J. S. Hong, J. K. Suh, *Applied Catalysis A: General* 450 (2013) 222.
- [2] S. Helali, E. Puzenat, N. Perol, M.J. Safi, C. Guillard, *Appl. Catal. A: Gen.* 402 (2011) 201.
- [3] Y. Li, L. Li, C. Li, W. Chen, M. Zeng, *Appl. Catal. A: Gen.* 427 (2012) 1.
- [4] A. A. Vega, G.E. Imoberdorf, M. Mohseni, *Appl. Catal. A: Gen.* 405 (2011) 120.
- [5] M. Munner, M. Qamar, M.Saquib, D.W.Bahnemann, *Chemosphere* 61 (2005) 457.
- [6] S. Liu, M. Lim, R. Fabris, C. Chow, K. Chiang, M. Drikas, R. Amal, *Chemosphere* 72, (2008) 263.
- [7] X.Wang, Y.Liu, Z.Hu, Y.Chen, W.Liu, G. Zhao, *J. Hazard. Mater.*, 169, (2009) 1061.



## IMPROVEMENT OF WATER QUALITY WITH HIGH FLUORIDE CONTENT

Monica Ihos and Mihaela Dragalina

*National Research and Development Institute for Industrial Ecology ECOIND, Timisoara  
Subsidiary, Street Bujorilor no. 115, code 300431, Timisoara, Romania  
e-mail: monica\_ihos@yahoo.com*

### Abstract

The improvement of water quality with high fluoride content was carried out by precipitation of pollutant with  $\text{Ca}(\text{OH})_2$  and post-treatment by electrocoagulation. The applied current densities were 100, 200 and  $300 \text{ A/m}^2$  and the electrolysis time was 60 minutes. The fluoride concentration was lowered from 1000 mg/L to 407 mg/L after the precipitation and to 97 mg/L after the post-treatment by electrocoagulation at  $300 \text{ A/m}^2$ . The specific energy consumption was calculated and it was in the range of  $2.34 - 13.2 \text{ kWh/m}^3$ .

### Introduction

High concentration of fluoride can be found in effluents originated from different industries such as glass, fertilizers, solar photovoltaic cells, semiconductor or metals manufacturing industries. In these effluents, the fluoride concentration may range from hundreds to thousands of ppm [1,2].

Because of these high concentrations of fluoride in the industrial effluents, it is necessary to treat them before discharge. Conventionally, precipitation with lime is used to remove high concentrations of fluoride as  $\text{CaF}_2$  from wastewaters [3]. Experiments were also performed with magnesium salts [4] and it was found out that as precipitator they exhibited better settle ability when compared with calcium salts in fluoride precipitation.

However, the wastewaters treated by the precipitation do not meet the strict regulations requirements and post-treatment has to be done. Thus, processes like adsorption [5-8], electro dialysis [9] or coagulation [3] were able to reach this goal.

Alongside adsorption and membrane processes, electrocoagulation can be used as post-treatment of high fluoride concentration effluents and also this process exhibits some advantages from technical point of view: mechanical stirring is not necessary, reagents amount and settling time are lower than in other processes, high current efficiencies can be reached (~90%) in well-designed systems and short electrolysis time are required [10].

The aim of this paper was to remove the high concentration of fluoride from aqueous solutions envisaging the improvement of water quality by using the electrocoagulation as post-treatment.

### Experimental

All reagents were of analytical grade and the solutions were prepared with distilled water. Aqueous solution of 1000 mg/L fluoride was prepared.  $\text{Ca}(\text{OH})_2$  was used to remove the fluoride. The precipitate was removed by filtration and the pH of resulting solution was adjusted to 5 with HCl and it was sent to electrocoagulation.

The electrocoagulation experiments were carried out in a plexiglass cell with horizontal electrodes. The sacrificial anode of  $5.6 \times 14 \text{ cm}$  was made on aluminium and the cathode was a wire mesh grid made up of 3 mm diameter stainless steel wires. The distance between the electrodes was 5 mm.



Volumes of 500 ml working solutions were introduced in the cell, and the applied current densities were 100, 200 and 300 A/m<sup>2</sup>. Electrolysis duration was 60 minutes and samples were taken at every 10 minutes. The supporting electrolyte was 0.01 M NaCl.

The fluoride concentration was determined by using a Thermo Scientific Orion fluoride ion selective electrode (range: from 0.02 ppm to saturated). TISAB II solution was used as a buffer to maintain the pH and background ion concentrations.

### Results and discussion

The fluoride concentration in the solution resulted after the precipitation with lime followed by filtration was 407 mg/L. This solution was post-treated by electrocoagulation and Tables 1-3 show the residual concentration of fluoride under various working conditions.

Regardless of current density the process was more effective as the electrocoagulation time increased and the best results were obtained at 60 minutes. This finding is in agreement with the theoretical aspects regarding the electrocoagulation.

Electrocoagulation is a process consisting of producing metallic hydroxide flocks within the solution by the electro-dissolution of soluble anodes, usually made of metallic iron or aluminium. Metallic cations are being generated at the anode, via the electrochemical oxidation of iron or aluminium, whereas at the cathode typically molecular H<sub>2</sub> evolves. The metallic ions react with the OH<sup>-</sup> ions yield at cathode during the hydrogen evolution, and thus insoluble poly-oxo-hydroxides are generated. The pollutants from solution are adsorbed onto poly-oxo-hydroxides and the gas bubbles carry the pollutant to the surface solution. The increase of current density yields to higher amount of metallic hydroxide and as a consequence the adsorbed pollutant amount will be larger.

**Table 1.** Working conditions and fluoride residual concentration  
 C<sub>fluoride ini</sub>: 407 ppm; pH<sub>ini</sub>=5; current density: 100 A/m<sup>2</sup>; cell voltage: 1.5 V

Electrolysis time / min	Fluoride residual concentration / ppm	Fluoride removal efficiency / %
10	353	13.27
20	328	19.41
30	271	33.42
40	254	37.59
50	226	44.47
60	212	47.91

**Table 2.** Working conditions and fluoride residual concentration  
 $C_{\text{fluoride ini}}: 407 \text{ ppm}; \text{pH}_{\text{ini}}=5; \text{current density: } 100 \text{ A/m}^2; \text{cell voltage: } 2.0 \text{ V}$

Electrolysis time / min	Fluoride residual concentration / ppm	Fluoride removal efficiency / %
10	302	25.75
20	246	39.68
30	218	50.58
40	201	46.40
50	171	58.00
60	151	62.88

**Table 3.** Working conditions and fluoride residual concentration  
 $C_{\text{fluoride ini}}: 407 \text{ ppm}; \text{pH}_{\text{ini}}=5; \text{current density: } 100 \text{ A/m}^2; \text{cell voltage: } 2.8 \text{ V}$

Electrolysis time / min	Fluoride residual concentration / ppm	Fluoride removal efficiency / %
10	283	30.38
20	197	51.69
30	170	58.23
40	151	62.87
50	117	71.31
60	97	76.16

The specific energy consumption for 60 min of electrolysis is given in Table 4 and it was calculated according to equation 1. As it was expected the higher value was recorded for the current density of  $300 \text{ A/m}^2$ .

$$Q = UIt \cdot 10^{-3} / V \cdot 3600 \quad (1)$$

where:

Q = specific energy consumption, kWh/m<sup>3</sup>

U = cell voltage, V

I = current intensity, A

t = electrolysis time, s

V = electrolysed solution volume, m<sup>3</sup>

**Table 4.** Specific energy consumption for 60 min of electrolysis

Current density / A/m <sup>2</sup>	Cell voltage / V	Current intensity / A	Treated groundwater / m <sup>3</sup>	Specific energy consumption / kWh/m <sup>3</sup>
100	1.5	0.78	0.0005	2.34
200	2.0	1.56		6.24
300	2.8	2.35		13.2

### Conclusion

The electrocoagulation was effective for the removal of fluoride from aqueous solutions of 1000 mg/L fluoride as post-treatment stage.

The fluoride removal efficiency from an aqueous solution of 407 ppm fluoride originated from an aqueous solution of 1000 ppm fluoride after the precipitation with Ca(OH)<sub>2</sub> was of 47.91% at 100 A/m<sup>2</sup>, 62.88 % at 200 A/m<sup>2</sup> and 76.16 % at 300 A/m<sup>2</sup>.

The overall efficiency was of 78.8% at 100 A/m<sup>2</sup>, 84.9 % at 200 A/m<sup>2</sup> and 90.3 % at 300 A/m<sup>2</sup>.

### Acknowledgements

This work was supported by a grant of the Romanian National Authority for Scientific Research – Core Program 38N/2016, Environmental Research – priority in sustainable industrial development based on knowledge and innovation – ECO MEDIND, Project code PN 16 25 03 07.

### References

- [1] L. Gurtubay, I. Danobeitia, A. Barona, J. Prado, A. Elías, Chem. Eng. J. 162 (2010) 91.
- [2] N. Drouiche, F. Djouadi-Belkada, T. Ouslimane, A. Kefai, J. Fathi, E. Ahmetovic, Desalin. Water Treat. 51 (2013) 5965.
- [3] S. Aoudj, N. Drouiche, M. Hecini, T. Ouslimane, B. Palaouane, Procedia Engineer. 33 (2012) 111.
- [4] H. Huang, J. Liu, P. Zhang, D. Zhang, F. Gao, Chem. Eng. J. 307 (2017) 696.
- [5] Z. Zhang, Y. Tan, M. Zhong, Desalination 276 (2011) 246.
- [6] T. Wajima, Y. Umata, S. Narita, K. Sugawara, Desalination 249 (2009) 323.
- [7] C.-F. Chang, C.-Y. Chang, T.-L. Hsu, Desalination 279 (2011) 375.
- [8] E. Kumar, A. Bhatnagara, U. Kumar, M. Sillanpää, J. Hazard. Mater. 186 (2011) 1042.
- [9] E. Ergun, A. Tor, Y. Cengeloglu, I. Kocak, Sep. Purif. Technol. 64 (2008) 147.
- [10] C. An, G. Huang, Y. Yao, S. Zhao, Sci. Total Environ. 579 (2017) 537.

## DIMENSIONAL DISTRIBUTION OF PM<sub>2.5</sub> AND PM<sub>10</sub> IN THE ROAD PROXIMITY

Cristina Mosoarca<sup>1</sup>, Radu Banica<sup>1</sup>, Petrica Linul<sup>1,2</sup>, Alexandra Ioana Bucur<sup>1</sup>

<sup>1</sup>*Department of Applied Electrochemistry, National Institute for Research and Development for Electrochemistry and Condensed Matter, Dr. A. Păunescu Podeanu Street, no.144, 300569 Timișoara, Timiș, România*

<sup>2</sup>*University Politehnica Timisoara, Piata Victoriei 2, 300006 Timisoara, Romania  
e-mail: mosoarca.c@gmail.com*

### Abstract

The particulate matter (PM) is comprised of two kinds of particles, classified after their dimensions, the PM<sub>2.5</sub> which encompasses particles with sizes smaller than 2.5 μm and the PM<sub>10</sub> with particles ranging in size from 2.5 μm to 10 μm. As previous studies have shown, PMs have an undeniable influence, dependent on the exposure time, upon the health of the human cardiopulmonary system. In this study we focused on the dimensional distribution of PMs and the influence of altitude on their numbers. Our detailed investigation lead us to the conclusion that the particle number is increasing at higher altitudes and also that PM<sub>2.5</sub>, which represents a greater health risk factor, is much more abundant than PM<sub>10</sub>.

### Introduction

World Health Organization (WHO) is estimating that air pollution is contributing at approximately eight hundred premature deaths every year, being among the first causes of premature mortality worldwide [1]. Particle sizes, that are part of the surrounding air we breathe, are in direct correlation to the health hazards they cause. The particulate matter (PM) is divided into two categories: PM<sub>2.5</sub> which encompasses particles with sizes smaller than 2.5 μm and PM<sub>10</sub> with particles ranging in size from 2.5 μm to 10 μm [2,3].

PM is a mixture with many different constituents, as follows: sulfates, nitrates, ammonium, and other inorganic ions like sodium, potassium, calcium, magnesium and chloride; elemental and organic carbon, metals (including cadmium, copper, nickel, vanadium and zinc) and also aromatic cyclic hydrocarbons [4]. Additionally to the components previously mentioned, PM has biological elements as well, like allergens and microbial compounds. Due to their small sizes, PM<sub>2.5</sub> and PM<sub>10</sub> are breathable particles capable of penetrating the thoracic region of the respiratory system. Short PM<sub>10</sub> exposure has harmful health effects on a global scale, but mortality is caused in the greatest extend on account of long PM<sub>2.5</sub> exposure. Therefore PM<sub>2.5</sub> embodies a much higher health risk factor than PM<sub>10</sub>. It is estimated that the mortality rate on account of PM<sub>10</sub> will increase by 0.2-0.6 % per 10 μg/m<sup>3</sup> [5]. Conversely, long time exposure to PM<sub>2.5</sub> is associated with the increase of morbidity caused by cardiopulmonary diseases by 6-13 % per 10 μg/m<sup>3</sup> PM<sub>2.5</sub> [6]. PM can have both anthropogenic (man-made) and non-anthropogenic (natural) origins. Among the anthropogenic sources of air pollution, combustion processes and industrial activities have a major negative effect upon the air quality. Erosion of the pavement by road traffic and abrasion of brakes and tires have a less important role as a pollution source, however cannot be ignored. Agriculture is another harmful anthropogenic air pollution cause being the main source of ammonium [6,7]. Among the non-anthropogenic pollutants, Radon gas from radioactive decay within the Earth's crust; sulfur, chlorine, and ash particulates from volcanic activity, can be mentioned [8].

## Experimental

The analyzes were performed using a PC200 Particle Counter (Trotec) that detects size fractions and concentrations of air particles along with the measurement of environmental factors such as air temperature, humidity, dew and wet-bulb temperature. The particle counter has 6 particle size channels: 0.3  $\mu\text{m}$ , 0.5  $\mu\text{m}$ , 1.0  $\mu\text{m}$ , 2.5  $\mu\text{m}$ , 5.0  $\mu\text{m}$ , 10.0  $\mu\text{m}$  with a counting efficiency of 50% at 0.3  $\mu\text{m}$  and 100% for particles larger than 0.45  $\mu\text{m}$ . The light source is a laser class 3B with 780 nm wave length at 90 mW. The sample inlet is represented by an isokinetic probe; the flow rate is 2.83 l/min (0.1 ft<sup>3</sup>/min), controlled by an internal pump with a coincidence loss of 5%, 2 million particles per ft<sup>3</sup> (28.3 litres). The measurement temperature was in the range between 27°C and 30°C with a dew point of 9.3°C, 27.6 % humidity and 17.9 % WB (wet-bulb). PC200 was placed at different heights with the aid of an in laboratory made lifting device that made possible the data collection at ground level (0.1 m), at 2.5 m and 5 m above ground. In order to ensure the experimental reproducibility, the data collection time was set at 120 s and made in two cycles thus obtaining 42 different acquisitions for each point calculation. PM concentration in each dimensional range was calculated as an arithmetic average of the collected data in the case of the two cycles for the purpose of minimizing errors. For more accurate results, all experiments were performed in the differential mode of the PC200 analyzer.

## Results and discussion

The data was collected from a national road in both longitudinal and perpendicular direction. 0.3  $\mu\text{m}$ , 0.5  $\mu\text{m}$ , 1  $\mu\text{m}$  and 2.5  $\mu\text{m}$  channels corresponding to PM<sub>2.5</sub> class (figures 1, a,b and 2 a, b) are depicted in relation to the sampling height and to the distance from point zero of the chosen area in which the measurements took place.

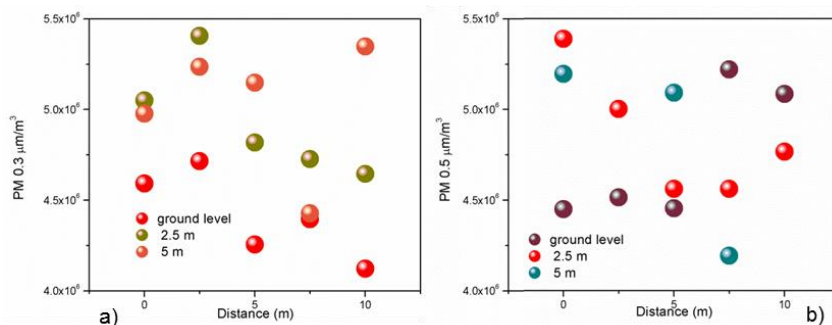


Figure 1. PM<sub>2.5</sub> concentration a) 0.3  $\mu\text{m}$  size particles; b) 0.5  $\mu\text{m}$  size particles, at ground level, 2.5 m and 5 m.

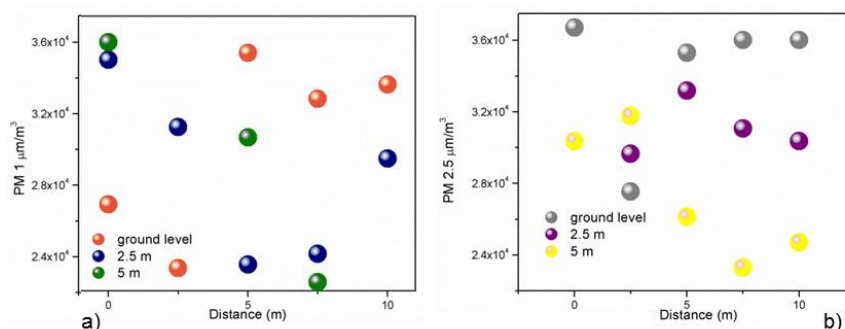


Figure 2. PM<sub>2.5</sub> concentration a) 1  $\mu\text{m}$  size particles; b) 2.5  $\mu\text{m}$  size particles, at ground level, 2.5 m and 5 m.

5  $\mu\text{m}$  and 10  $\mu\text{m}$  channels corresponding to  $\text{PM}_{10}$  class (figure 3, a,b) are depicted in relation to the sampling height and to the distance from point zero (situated at the edge of the road) of the intense traffic urban area in which the analyzes took place.

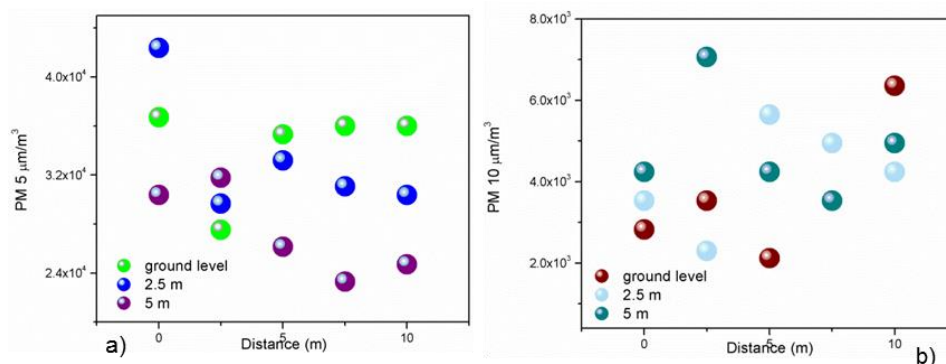


Figure 3.  $\text{PM}_{10}$  concentration a) 5  $\mu\text{m}$  size particles; b) 10  $\mu\text{m}$  size particles, at ground level, 2.5 m and 5 m.

In figure 4 is depicted the 3D mapping of the PM concentration/ $\text{m}^3$  air in relation to the dimensional distribution at three different altitudes (0.1 m, 2.5 m and 5 m), the experimental points and their corresponding projections can be noticed. The concentration of 0.3  $\mu\text{m}$  particles is increasing with the increase of the collection height. The particles concentration variation of 0.5  $\mu\text{m}$  channel is on the same direction as the previous mentioned one.

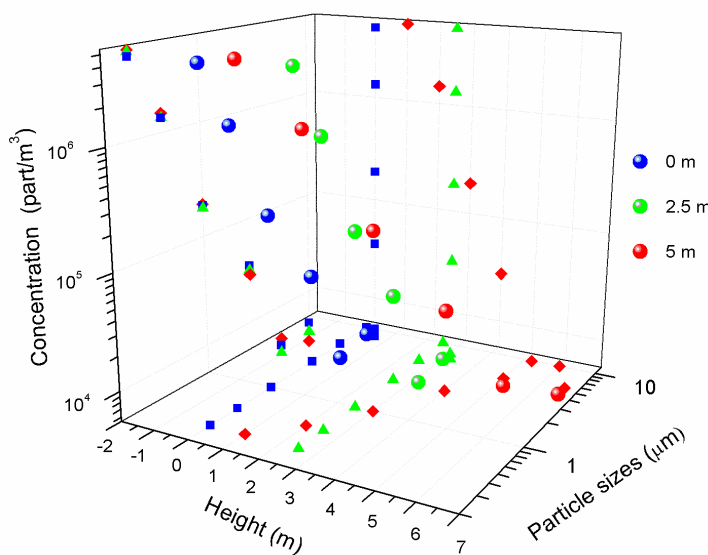


Figure 4. 3D mapping of PM concentrations depending on the data collection height and their sizes; their plan projections are also visible

With the PM dimension increase, a clear correlation between the PM sizes and their concentration dependent on the collection height it is not noticeable anymore.

As shown in figure 4, the  $\text{PM}_{2.5}$  concentration is decreasing while moving farther away from the edge of the road which is lying near buildings higher than 10 m. This decrease is obvious

only for the sampling that occurred at ground level and at 2.5 m high. For the 5 m high sampling area, the decrease in PM<sub>2.5</sub> concentration is not relevant anymore. We are considering that this effect is due to the swirling currents of air formed in the buildings proximity. The distance between the nearest building and the first traffic band is higher than 5 m, so most likely the swirling currents are formed due to the wind and not because of the passing by motor vehicles. All measurements were performed on a real time monitoring system, on a randomly chosen urban road characterized by intense traffic, during day time, at low humidity levels.

### **Conclusion**

PMs which are correlated with a high occurrence of pulmonary cancers, cardio-vascular diseases and a high rate of mortality were determined as follows: **PM<sub>2.5</sub>** with particles of 0.3 μm, 0.5 μm, 1 μm and **PM<sub>10</sub>** ranging from 2.5 μm to 10 μm. A 3D mapping of the analyzed PMs, from an urban area characterized by intense traffic, was depicted. The concentration of small particles, up to 0.3 μm, is increasing directly proportional with the sampling altitude, from approximately 4.47 million/m<sup>3</sup> air at the ground level to 5.04 million/m<sup>3</sup> air at 5 m.

At ground level (0.1m) PM<sub>2.5</sub> average number is slightly above 6 million, while PM<sub>10</sub> average number is much lower, having the value of 8.5 thousand, as compared to 5 m height were the PM<sub>10</sub> is decreasing at 7.7 thousand and PM<sub>2.5</sub> is exhibiting a significant increase at an average of 6.7 million.

So we can conclude that, on an urban road with intense traffic, the particle number is increasing at higher altitudes and PM<sub>2.5</sub>, which is more likely to cause serious health problems, is much more abundant than PM<sub>10</sub>.

### **Acknowledgements**

This work was supported by a grant of the Romanian Ministry of National Education, CNCS – UEFISCDI, project number PN 16 14 02 09.

### **References**

- [1] H. Horvath, First Ibero-American Conference on the Atmospheric Environment, 27 (1993) 293-317.
- [2] S. Rovelli, Andrea Cattaneo, F. Borghi, A. Spinazzè, D. Campagnolo, A. Limbeck, D.M. Cavallo, *Aerosol and Air Quality Research*, 17 (2017) 1142–1155.
- [3] M. Tasic, B. Djurić-Stanojevic, S. Rajšić, Z. Mijić, V. Novaković, *Acta Chim. Slov.* 53 (2006) 401–405.
- [4] M.G. Perrone, M. Gualtieri, V. Consonni, L. Ferrero, G. Sangiorgi, E. Longhin, D. Ballabio, E. Bolzacchini, M. Camatini, *Environmental Pollution*, 176 (2013) 215–227.
- [5] E. Samoli, R. Peng, T. Ramsay, M. Pipikou, G. Touloumi, F. Dominici, R. Burnett, A. Cohen, D. Krewski, J. Samet, K. Katsouyanni, *Environmental Health Perspectives*, 116 (2008) 1480–1486.
- [6] D. Krewski, M. Jerrett, R.T. Burnett, R. Ma, E. Hughes, Y. Shi, M.C. Turner, C.A. Pope, G. Thurston, E.E. Calle, M.J. Thun, Health Effects Institute, (2009) HEI Research Report 140.
- [7] D.A. Vallero, *Fundamentals of Air Pollution*, Fourth Edition, Ed. Elsevier, 2007, pp. 93-99.
- [8] C. Li, S. Kang, P. Chen, Q. Zhang, G.C. Fang, *Environmental Science and Pollution Research*, 19 (2012) 1620-1628.



## CROP RESIDUES AS FUELS FOR SMALL SCALE HEAT GENERATION IN SERBIA – POTENTIAL, ISSUES AND PERSPECTIVES

**Natasa Dragutinovic<sup>1</sup>, Branka Nakomcic-Smragdakis<sup>1</sup>**

<sup>1</sup>*Faculty of Technical Sciences, Department of Environmental Engineering, 21000 Novi Sad, Trg Dositeja Obradovića 3, Serbia  
e-mail: n.dragutinovic@uns.ac.rs*

### **Abstract**

Crop residues represent significant source of renewable energy in agricultural regions and their energetic utilization could contribute to decreased energy dependence on fossil fuels, increased utilization of local, low-cost fuels, facilitate sustainable development of rural communities, improve air quality and decrease negative environmental impact of energy sector. Total potential of biomass in Serbia amounts to 12.5 million tons a year, and in Vojvodina (northern Province) 9 million tons or 72%. Within than, crop husbandry in AP Vojvodina generates more than 6 million tons of biomass waste every year. Most common crop residues in Serbia are wastes from cereal cultivation, such as wheat straw, corn stover and corn cobs, soy straw, etc., corn being the most cultivated crop. Despite their significant energetic potential, combustion of crop residues is associated with several issues, such as increased gaseous and particulate emissions, ash sintering/melting, fouling in the combustion chamber, etc. By applying discussed primary and secondary measures for increasing combustion efficiency and reduce emissions, crop residues can be utilized as fuels for small scale heat generation in agricultural regions.

### **Introduction**

Biomass is the renewable energy source (RES) with the biggest potential in Serbia, amounting to 64% of total RES potential in Serbia. Biomass originates from forestry, wood processing industry, agriculture, municipal solid waste etc. In Vojvodina, the northern part of Serbia, and a predominantly agricultural region, residues from cereal cultivation and the most abundant and important biomass source. Furthermore, commercial production of biomass (or energy crops) for energy purposes is not yet common practice in Serbia. Having in mind that significant amounts of waste biomass must be disposed of in an adequate manner, and that solid biomass wastes have considerable heat value and energy content, thermochemical conversion of solid agricultural wastes presents promising way of solving two issues [1]. Crop residues could be utilized for heat generation in small and medium sized consumers in rural communities, since they could be sourced locally, are cheap, renewable, and sustainable, moreover since crop residues are wastes from agricultural sector and there is no competition with food cultivation. On the contrary, thermo-chemical utilization of crop residues for energy generation simultaneously manages bio waste and minimizes the amount of organic waste to be landfilled. However, thermochemical utilization of crop residues is associated with several operational and environmental issues. Given the fact that these solid fuels contain ten times higher amounts of ash than woody fuels, and significantly higher K, Na, and Cl contents, combustion of agricultural residues is associated with ash sintering and slag formation, fouling and corrosion in the combustion chamber, and elevated PM emissions. Therefore, these fuels cannot be combusted in conventional units for woody fuels, causing blockages, malfunctions

and process interruptions. Main approaches for mitigating and/or eliminating aforementioned issues are discussed in this paper.

Against this background, the aim of this paper is to give overview of crop residue potential for energetic utilization in Serbia, issues associated with combustion of crop residues, possibilities for improvement and perspectives for future research.

### Results and discussion

The total potential of biomass in Serbia amounts to 12.5 million tons a year, and in Vojvodina 9 million tons or 72%. Of this amount, 1/4 of biomass can be plowed back into the soil or as bedding for the production of manure, with the purpose of increasing fertility of the soil, 1/4 can be used for the production of fodder, 1/4 for the production of heat energy and 1/4 for other purposes [2]. Out of the total amount of biomass intended for heat production in Serbia ( $3.880,57 \times 10^3$  tons),  $2.794 \times 10^3$  tons could replace an equivalent amount of  $948.6 \times 10^3$  tons of extra light fuel oil. This is the amount of diesel fuel consumed by the entire agricultural production in Vojvodina [2]. Overview of energy potential of biomass in Serbia is given in table 1.

Table 1. Overview of most common agricultural biomass wastes generated in Serbia (available for energy production) [2]

Nb.	Type of biomass	Potential for energy purposes ( $10^3$ t)	Lower heating value (MJ/kg)
1	Wheat straw	743.75	14
2	Corn stover	1787.5	13.5
3	Corn stover of seed corn	21.56	13.85
4	Corn cobs	357	14.7
5	Sunflower stover	200	14.5
6	Sunflower shells	30	17.55
7	Barley straw	103.13	14.2
8	Soy straw	80	15.7

In AP Vojvodina crop husbandry generates more than 6 million tons of biomass waste every year, most of which is corn residue (stalk and cobs) with 54.8%, then wheat straw with 18.7% and sunflower residue (stalk, head and husk) with 13% [1, 2]. Despite their significant energetic potential, combustion of crop residues is associated with ash related operational problems (i.e. ash melting and sintering, fouling in the combustion chamber, corrosion of heat transfer tubes) as well as increased particulate matter (PM) emissions, ash sintering/melting, fouling in the combustion chamber, corrosion etc.

Despite its significant potential, energetic utilization of biomass is not straightforward, especially when taking into account negative environmental influence of combustion and PM emissions on air quality. In comparison with wood, crop residues have higher share of critical elements such K and Cl, and about ten times higher ash content, resulting in considerably lower ash melting temperatures (i.e. unfavorable ash melting behavior) [3, 4]. High share of ash and PM-forming elements in crop residues are the consequence of nutrients needed for plant growth, meaning that the deposition of trace elements within the organic matter of annual crops is often strongly influenced by the utilized mineral fertilizer [5]. This behavior might vary considerable between different crop species as well as specific crop components, various climatic conditions, different plant production measures and varying management

schemes [6]. Contamination of inorganic impurities incorporated into the organic material due to harvesting processes as well as due to transportation and storage procedures may add up to this [7]. Problematic elements K, Cl, and S build several gaseous compounds during combustion at high temperatures. After saturation, cooling or chemical reaction with other elements gaseous compounds can condense and become PM [3]. Alkalis are mostly released as gaseous hydroxides, chlorides, and sulfates during combustion. K is the key element regarding PM generation and it causes formation of problematic species at different temperatures. K-salts (KCl,  $K_2SO_4$  and  $K_2CO_3$ ) are the primary components of the sub-micrometer particulate matter in the flue gas from biomass combustion [3, 8, 9]. Regarding ash sintering/melting, melting point of K-silicates lies in the range 750-1,400 °C, depending on K and Si content. Compounds containing trace amount of Na, i.e. K-Na-Si eutectics have even lower melting points, as low as 540 °C [10]. These molten compounds show acidic effects and accelerate corrosion and deposition by sticking of non-melted particles to the layer of melted particles [11]. Furthermore, when  $K_2SO_4$  is produced, during reaction between KCl and  $SO_2$ , corrosive HCl is released in the furnace. In addition to this, KCl and  $K_2SO_4$  account for 80 to 90 wt.% of total inorganic aerosol amount [3].

There are two general approaches to increase combustion efficiency and reduce pollutant generation, primary and secondary measures. Primary measures include modification of combustion and/or fuel, including improvement of the fuel feeding system, the fuel bed arrangement grate design, air supply strategy, burning chamber geometry, process control concepts, fuel conditioning etc. Since current automated pellet stoves and boilers cannot combust agricultural residues successfully due to high ash content and ash melting, combustion units have to be modified. High ash content causes problems during ash removal process as well as clogging of air feeding system. Second ash related problem is sintering/melting on the grate, which could possibly be resolved using vibrating grates, water-cooled grates etc., by preventing agglomeration of the ashes on the grate or reducing temperature in the bed zone. Among most important primary measures are air staging, provision of intensive mixing of the combustion and the flue gases in the secondary combustion chamber, long enough residence time in the secondary combustion zone at temperature above 800 °C. These measures can be implemented in all types of common residential biomass combustion systems (stoves, boilers) [12]. It should be noticed that primary measures increase combustion efficiency as well as decrease pollutant emissions, especially pollutants resulting from incomplete combustion (e.g. unburned hydrocarbons). From fuel conditioning perspective there are various approaches to reduce and/or minimize ash related operational problems during agricultural residues combustion, including fuel leaching, fuel blending and using metal/mineral additives. Additives are especially useful in abating two issues: sorption of alkali metals in the ashes to reduce PM emissions, and bind alkalis with earth alkalis in high temperature melting silicates (e.g. kaolinite).

Secondary measures include fuel gas treatment using cyclones, baghouse filters, electrostatic precipitators (ESPs), catalysts, scrubbers etc. Secondary measure have been successfully applied in large scale plants, however due to high price relative to heat generator price, they are still not common practice in small scale combustion devices. Not all separation principles are also used for small capacities. For example, the principle of the flue gas scrubber is only used for larger installations. Cyclones are rarely used in very small biomass combustion plants. They are particularly useful, when coarse ash particles caused by air movement in the bed (eg feed grate) are carried away into the exhaust gas. For ESPs various separation performances have been demonstrated in bench tests, depending on the type, they average

between 50 and 80%. A distinction is made between deep and surface filters in the filter separators. In the case of very small firing capacities, built-in ceramic inserts (deep filter) are used in the combustion chamber (for fireplace and stoves). The cleaning is carried out thermally by burnout or through removal and manual cleaning. Conventional surface filters are, on the other hand, problematic due to the possible dew point drop and the condensation of organic particles (risk of sticking). By using metal with an internal electrical heating of the filter cartridge these problems could be reduced. However, research is still being performed in this area [13, 14].

No emission limit values for the combustion of crop residues exist in Serbia. However, updated emission limit values for solid fuel combustion include woody biomass combustion (from 2016). They are classified according to unit capacity and age, as presented in the following table.

Table 2.

	Pollutant	Fuel type	Heat capacity (kWth)	ELV (mg/Nm <sup>3</sup> )
Existing units	Carbon monoxide - CO	Log wood, woody briquettes/pellets	50-150	4000
	Particulate matter	Log wood		150
	Particulate matter	Log wood, excluding woody briquettes/pellets	≥ 4	100
New installations		Woody briquettes/pellets	≥ 4	60
	Carbon monoxide - CO	Log wood, excluding woody briquettes/pellets	4-500	1000
		Woody briquettes/pellets	4-500	800

Emission limit values for small scale biomass combustion in Serbia [15]. However, it is expected that the emission limit values for crop residue combustion will also be included and controlled by the legislation in the near future.

### Conclusion

From the aforementioned reasons, research should be focused on development of specialized heat generators designed for the combustion of fuels with high ash content and low ash sintering temperature, on one hand. Modification and adjusting of combustion units requires further research, although significant efforts have been undertaken and progress has been achieved. On the other hand, low-cost fuel conditioning measures (additives, leaching and pelletizing) could improve the quality of fuel by artificially bringing composition of agro fuels closer to the composition of woody biomass and “imitating “ its behavior, whereas pelletizing reduces transport and storage costs and creates fuel of standardized quality and uniform properties. Combination of stated measures would lead to the development of highly efficient combustion devices with lowered emissions of pollutants, tailored to the crop residues as fuels.

Since biomass represents the crucial and most abundant RES in Serbia, research in the field of crop residue combustion in small scale heat generators could facilitate its wider use, more efficient utilization and reduced emissions of pollutants.

### **Acknowledgements**

This paper is partially financed within III-42004, III-42006, and III-46009 Projects of the Ministry of Education and Science of Republic of Serbia.

### **References**

- [1] B. Nakomcic-Smaragdakis, Z. Cepic, N. Dragutinovic, *Renewable and Sustainable Energy Reviews* 57 (2016) 186–191.
- [2] M. Brkic, M. Tesic, T. Furman, M. Martinov, T. Janic, Potentials and possibilities of brickquetting and pelletizing of waste biomass in the territory of the province of Vojvodina, Faculty of agriculture, University of Novi Sad, Novi Sad, 2007.
- [3] M. Kaltschmitt, H. Hartmann, H. Hofbauer, *Energie aus Biomasse Grundlagen, Techniken und Verfahren*, 3., aktualisierte Aufl. 2016, Springer Verlag.
- [4] H. Hartmann, K. Reisinger, P. Turowski, P. Roßmann. *Handbuch Bioenergie – Kleinanlagen, Leitfaden. FNR e. V. 3., vollständig überarbeitete Auflage*, 2013.
- [5] J. Knudsen, P.A. Jensen, K. Dam-Johansen. *Energy & Fuels* (2004), 18, 1385-1399.
- [6] Y. Niu, Z. Wang, Y. Zhu, X. Zhang, H. Tan, S. Hui. *Fuel* (2016), 179, 52–59.
- [7] L. Wang, O. Skreiberg, M. Becidan. *Applied Thermal Engineering* (2014), 70, 1262 – 1269.
- [8] X. Wang, Y. Liu, H. Tan, L. Ma, T Xu, *Ind. Eng. Chem. Res.* (2012), 51, 12984–12992.
- [9] D. Bostrom, N. Skoglund, A. Grimm, C. Boman, M. Ohman, M. Brostrom, R. Backman. *Energy Fuels* (2012), 26, 85–93.
- [10] M. Blander, A.D. Pelton. *Biomass Bioenergy* (1997), 12 (4), 295–8.
- [11] V.E.M. Schmitt, Dissertation - Brennstofftechnische Eigenschaften fester Biomassepellets, Charakterisierung, Beeinflussung, Vorhersage, Technische Universität Hamburg, 2014.
- [12] T. Brunner, I. Obernberger, R. Scharler, Primary measures for low-emission residential wood combustion – comparison of old with optimized modern systems, *Proceeding of 17th European Biomass Conference & Exhibition*, Hamburg, 2009
- [13] H. Hartman, K. Reisinger, P. Turowski, P. Roßmann, 3., *Handbuch Bioenergie Kleinanlagen, vollständig überarbeitete Auflage*, FNR, Gülzow, 2013
- [14] K. Kubica, B. Paradiz, P. Dilara, *Small combustion installations: Techniques, emissions and measures for emission reduction*, European Commission, Joint Research Centre, Institute for Environment and Sustainability, Luxembourg, 2007
- [15] Regulation about the limit values of emissions of pollutants into atmosphere from combustion plants ("Official Gazette of the Republic of Serbia", no. 6/2016)

## LICHENS TRANSPLANT FROM AN UNPOLLUTED AREA IN TIMISOARA CITY

**Dorian-Gabriel Neidoni, Amanda Izabela Siminic, Mihaela  
Dragalina, Smaranda Mășu**

*National Research and Development Institute for Industrial Ecology ECOIND, Timisoara  
Subsidiary, Timisoara, street Bujorilor, no. 115, Romania  
e-mail: neidoni\_dorian94@yahoo.com*

### **Abstract**

In this paper, was followed the accumulation of heavy metals (Cd, Ni, Pb, Cu, Mn, Zn and Cr) in the tissue of lichen species, transferred from an unpolluted area to an intersection with medium traffic in the city of Timisoara (Romania). The lichen species studied were *Flavoparmelia caperata* (L.) Hale and *Hypogymnia physodes* (L.) Nyl., harvested from a forest located at 70km from the city. The study also took into account the affinity of these two species for the various heavy metals in the atmosphere. Of the study, results that lichen species had accumulated metals in the range 2.16-172%, from the initial moment. Some metals have been removed from lichenic tissue by up to 30% from baseline.

### **Introduction**

Biomonitoring can be divided into 3 categories: the transplant method, methods of laboratory testing and in situ testing. Under the transplant procedure, appropriate organisms (mainly lichens) are transplanted from unpolluted areas to the site considered polluted. Transplantation techniques are particularly useful at relatively high levels of pollutants. A distinct advantage compared to the use of indigenous species is that of well-defined exposure time. The technique does not seem to be satisfactory for the absorption rate. [1].

The epiphytic lichen, *Flavoparmelia caperata*, has been used as a heavy metal bioaccumulator (Cd, Cr, Cu, Hg, Ni, Pb and Zn) in the surrounding area of Pistoia in the north-central area of Italy. Concentrations of Cd, Cr, Ni, Hg and Pb were compared with those found in areas where there is no atmospheric pollution. Copper and especially zinc have been found in quite high concentrations. Fertilizers and pesticides have been the main source of atmospheric contamination [2].

Guttova [3], conducted a study illustrating the response of epiphytic lichens to changes in atmospheric conditions in Central Europe, where air pollutant emissions have dropped significantly since 1990 in and around Bratislava. The variation of 7 metals (Cu, Cd, Cr, Mn, Ni, Pb and Zn) was assessed in the talls of *Evernia prunastri*, *Hypogymnia physodes* and *Parmelia sulcata*.

Another study on the accumulation of metals by lichens was carried out by Affum [4], and it collected lichens from an unpolluted forest in November 2004, which were transplanted into 41 sites along the road Madina-Tetteh Quarshie. In 2005, February, samples were analyzed and found to contain higher concentrations of Mn, V, Pb, Cd, Cr and Ni than the initial samples. Observations showed that in all the samples studied, the Mn concentration was highest with maximum values around traffic lights, an intersection and a car workshop.

Transplants of epiphytic lichens from the natural environment to polluted sites are commonly used in bioindication studies. Individuals are transferred into new sites together with substrata on which they previously grew or attached on the new substrate, with carefully. [5].



An advantage of using lichens is that they continue to accumulate metals throughout the year [6]. Starting from the above, we realised a study on the accumulation of heavy metals in the tissue of the species *Flavoparmelia caperata* and *Hypogymnia physodes*.

### Experimental

The species *Flavoparmelia caperata* and *Hypogymnia physodes*, taken from an unpolluted forest located at 70 km from Timisoara, have been transplanted into an intersection with medium traffic. Heavy metal determinations were made both at the sampling time and after a month in which samples stood around this intersection. The lichens were collected from the oak (*Quercus robur*), all with substrate, from a height of 1-1.5m and transferred to the city, being watered once a few days with tap water.

After a month, the lichens were detached from the substrate and washed well with distilled water and dried. The dry tissue was weighed 0,25-0,50 g and were calcined at 550 °C. The ash was digested with a mixture of HCl+HNO<sub>3</sub> 3:1 (aqua regia). The residue was taken with 3ml HCl 1:1. The crucible was washed 3 times with 3ml of HCl 1:1. Solutions to take over the residue and solutions for washing were filtered through paper Sartorius filter papers 2-206 FT and quantitative moved in flasks of 25 ml. They were filled to sign with the HCl 1:1. Determination of metals was carried out with a spectrometer type Avanta AAS.

### Results and discussion

In Table 1, the concentration of heavy metals in lichenic tissue is presented. It should be mentioned that for Cd and Cr there was no variation of the concentration in the conditions in which the experiments were performed for none of the lichen species being taken into work.

The initial concentration in Table 1 represents the concentration determined on 02.08.2017, and the final one is the concentration determined after a month, the period during which the lichens were placed in an intersection with medium traffic.

The data in Table 1 reveals an increase in concentration for Cu, Mn and Zn in the case of *Flavoparmelia caperata*. For *Hypogymnia physodes*, the increase in concentration was recorded for Cu, Mn, Zn and Ni.

However, due to their large surface area, relatively low growth rate, and lack of waxy cuticle and stomata, lichens can also absorb and accumulate inorganic and organic contaminants such as heavy elements directly from the air. Moreover, several authors have shown that a direct relationship exists between heavy element concentrations in thalli and those in the environment [7].

**Table 1. Concentration of heavy metals in species *Flavoparmelia caperata* and *Hypogymnia physodes***

Species	Concentration of heavy metals [mg/kg D.M.]									
	Cu		Mn		Zn		Ni		Pb	
	Initial	Final	Initial	Final	Initial	Final	Initial	Final	Initial	Final
<i>Flavoparmelia caperata</i>	3,55	5,98	97,9	100	47,9	130	1,54	1,22	8,23	7,61
<i>Hypogymnia physodes</i>	5,23	7,14	269	542	76,7	132	2,46	3,33	4,92	3,45

In table 2 it is observed that within 30 days, heavy metals accrued in the range of 2,16-172%, with the exception that *Flavoparmelia caperata* eliminated Ni in a proportion of 21% and Pb



in a proportion of 7,5%, and the *Hypogymnia physodes* eliminated Pb in a proportion of 30% from baseline.

From table 2 shows that *Flavoparmelia caperata* has an affinity to accumulate Cu and Zn by up to 50% higher than *Hypogymnia physodes*, and the latter has a much higher affinity to accumulate Mn and Ni with up to 100% of *F. caperata*.

As Backor and Loppi [8] said, the ideal exposure time for accumulation of metals is 1-3 months. This study has shown that in a short period (one month), lichens have the ability to accumulate some heavy metals. After longer exposures, they become saturated with elements, lose biomass, and change their surface structures and physiological performance [8].

**Table 2. Increase / decrease of heavy metal quantities, in percent (%), after a month in an intersection with medium traffic**

Species	Cu	Mn	Zn	Ni	Pb
<i>Flavoparmelia caperata</i>	68,5%	2,16%	172%	-21%	-7,5%
<i>Hypogymnia physodes</i>	36,5%	102%	72%	35,5%	-30%

### Conclusion

This study shows that for more efficient monitoring of air pollution with heavy metals, several species of lichens must be used, because each species has a higher or lower affinity for some metals. As can be seen above, in order to monitor the pollution with Cu, Mn, Zn and Ni, *Flavoparmelia caperata* and *Hypogymnia physodes* can be used.

After a month, this lichens have the ability to accumulate heavy metals in rather high proportions. The ideal exposure time is 1-3 months.

The loss of metals in the lichens may be due either to the insufficient exposure time or to the fact that the atmosphere in which they were kept for one month does not present such heavy metals and in conclusion they have been eliminated, because it is known that there is a direct relationship between the concentration of heavy metals in the lichen thalli and the concentration in the air.

### References

- [1] D. Ceburnis, D. Valiulis, Sci. Total Environ. 226 (1999) 247
- [2] S. Loppi, F. Chiti, A. Corsini, L. Bernardi, Environ. Monit. Assess. 29 (1) (1994) 17
- [3] A. Gutova, A. Lackovicova, I. Pisut, P. Pisut, Environ. Monit. Assess. 182 (2011)
- [4] H. A. Affum, K. Oduro-Afriyie, V. K. Nartey, D. Adomako, B. J. B Nyarko, Environ. Monit. Assess. 137 (2008) 15
- [5] D. Zarabaska-Bozejewicz, E. Studzinska-Sroka, W. Faltynowicz, Fungal Ecol. 16 (2015) 34
- [6] J. Asplund, M. Ohlson, Y. Gauslaa, Fungal Ecol. 16 (2015) 1
- [7] F. Nannoni, R. Santolini, G. Protano, Waste Manag.. 43 (2015) 353
- [8] M. Backor, S. Loppi, Biol. Plant. 53 (2) (2009) 214

**MONITORING OF INORGANIC CHEMICAL PARAMETERS IN RIVER DANUBE,  
NOVI SAD, SERBIA**

**Boris Obrovski<sup>1\*</sup>, Jovan Bajić<sup>2</sup>, Ivana Mihajlović<sup>1</sup>, Mirjana Vojinović Miloradov<sup>1</sup>, Miljan Šunjević<sup>1</sup>, Veselin Bežanović<sup>1</sup>, Dragan Adamović<sup>1</sup>, Vladimir Rajs<sup>2</sup>**

*<sup>1</sup>University Of Novi Sad, Faculty Of Technical Sciences, Department Of Environmental Engineering, TrgDositeja Obradovića 6, 21000 Novi Sad, Serbia*

*<sup>2</sup>University Of Novi Sad, Faculty Of Technical Sciences, Department of Power, Electronic and Telecommunication Engineering, TrgDositeja Obradovića 6, 21000 Novi Sad, Serbia  
e-mail: borisobrovski@uns.ac.rs*

**Abstract**

Because of the importance Danube river has on the region and the population affected by it is essential to maintain constant monitoring. With new emerging pollutants every day and regular threats one of the crucial goals is to investigate the causes of possible contamination with the acquisition of new, until then unknown information. To be able to achieve quality investigation and to acquire new information special monitoring has been conducted, in which quantitative analysis of key physical-chemical parameters in water body was carried out with laboratory methods.

**Introduction**

River Danube is one of the most important rivers in Europe. It passes through 10 countries (starting from Germany then going through Austria, Slovakia, Hungary, Croatia, Serbia, Romania, Bulgaria, Moldova and Ukraine) and is basin for a large number of tributaries from 9 more countries, thus connecting 19 countries all together and around 90 million inhabitants. It represents waterway for those countries and main route from Germany to Black sea.

In many ways Danube gives life to all countries it influences. Firstly around 30 % of inhabitants affected by it use Danube water (partly purified) for drinking. Furthermore large amount of water is used in agriculture for watering crops. It is also home of more than 20 national nature parks with unique fauna and flora. Fishing industry is also very developed on Danube river and represents part of its life. Taking all of this into account we come to realization that river Danube is essential part of everyday's life for these countries as well as very influential economical factor. With wide range of usages and water circulation through various different systems but still ending up in river basin the problem of pollution emerges.

Because it represents main waterway (easier and cheaper method for transportation) many factories has been build on river banks. Most of those factories directly and indirectly pollutes river (by direct discharge of pollutants in water or vicinity). Also boats used for transport directly pollute and disturbs normal river biota. Since it river represents and gives life, many big cities are build on its banks and large number of them is still disposing waste water directly into the river. Beside this one of the main emerging problems is use of pesticides for crops, and they are directly or through its tributaries in water circulation affiliated.

To be able to preserve biota and maintain sufficient quality of water constant monitoring is from crucial importance. Also, adequate monitoring provides us data about river changes and possibilities on how to improve water quality and to mitigate pollution. The aim of this paper is to monitor important physico-chemical parameters in the Danube River. Also multivariate statistical method (hierarchical cluster method) was also applied to confirm the current state of

the Danube River, as well as investigate the causes of possible contamination with the acquisition of new, until then unknown information.

### **Experimental**

Samples of surface water for laboratory analysis were collected from six locations on river Danube in the city of Novi Sad, Serbia. Three locations are located before the discharge of wastewater (Location 1, Location 3, and Location 5) and three locations are located after the discharge of wastewater (Location 2, Location 4 and Location 6). Thirty-six samples were collected, six samples from each locations. Samples are poured into 1 L bottles, stored in hand refrigerator at 4 °C, and transported to the laboratory. Analyses were carried out in accredited Laboratory for monitoring of landfills, wastewater and air, Department of Environmental Engineering and Occupational Safety and Health in Novi Sad.

Chemical parameters that were monitored in surface water are: orthophosphate, sulfate, nitrite, nitrate, chromium, total chlorine, fluoride, chloride and ammonia. Concentrations of orthophosphate in samples were analyzed according to the Standard Methods of Environment Protection Agency (EPA 365.3). Chromium, sulfate, nitrite, nitrate, total chlorine, fluoride, chloride and ammonia were analyzed according to the HACH Methods (HACH 8023 for chromium, HACH 8021 for sulfate, HACH 8507 for nitrite, HACH 8192 for nitrate, HACH 8167 for total chlorine, HACH 8023 for fluoride, HACH 8113 for chloride and HACH 8155 for ammonia). The concentrations of all parameters were measured with UV-VIS spectrophotometer (DR 5000, HACH, Germany).

Multivariate statistical method used in this research are Hierarchical cluster analysis (CA). Statistical processing will be carried out using the program IBM SPSS statistic 20.

### **Results and discussion**

Quantitative analysis of key physical-chemical parameters in water body was carried out with laboratory methods. Research monitoring of the Danube River is necessary for the development of a database that will contain physico-chemical parameters that disturb the quality of the water body. The assessment of the influence of selected inorganic parameters on the quality of the Danube River at selected locations enables us to confirm the level of contamination of the observed river.

The data obtained from the analysis of water quality will provide information about contamination of the examined surface water bodies. However, a specific problem in monitoring of surface water quality is the complexity associated with the analysis of a large number of variables and high variability due to anthropogenic and natural impacts. By applying various multivariate techniques, interpretation of complex data matrices will be simplified in order to better understand the state of water quality of the examined area. These techniques will enable identification of possible sources of pollution affecting water bodies and represent useful tools for reliable water resources management.

Cluster analysis is a statistical technique used to identify relatively similar groups of objects. Cluster analysis does not know the association of the object or the final number of groups, but the goal is to establish similar groups or clusters. The cluster analysis group observed location into classes so that the locations with the most similar concentrations for the examined parameters are in the same class (cluster). Grouping of locations is carried out based on the concentration for analyzed physico-chemical parameters for each location separately.

The results were presented by dendrogram graphic (Figure 1) based on cluster analysis.

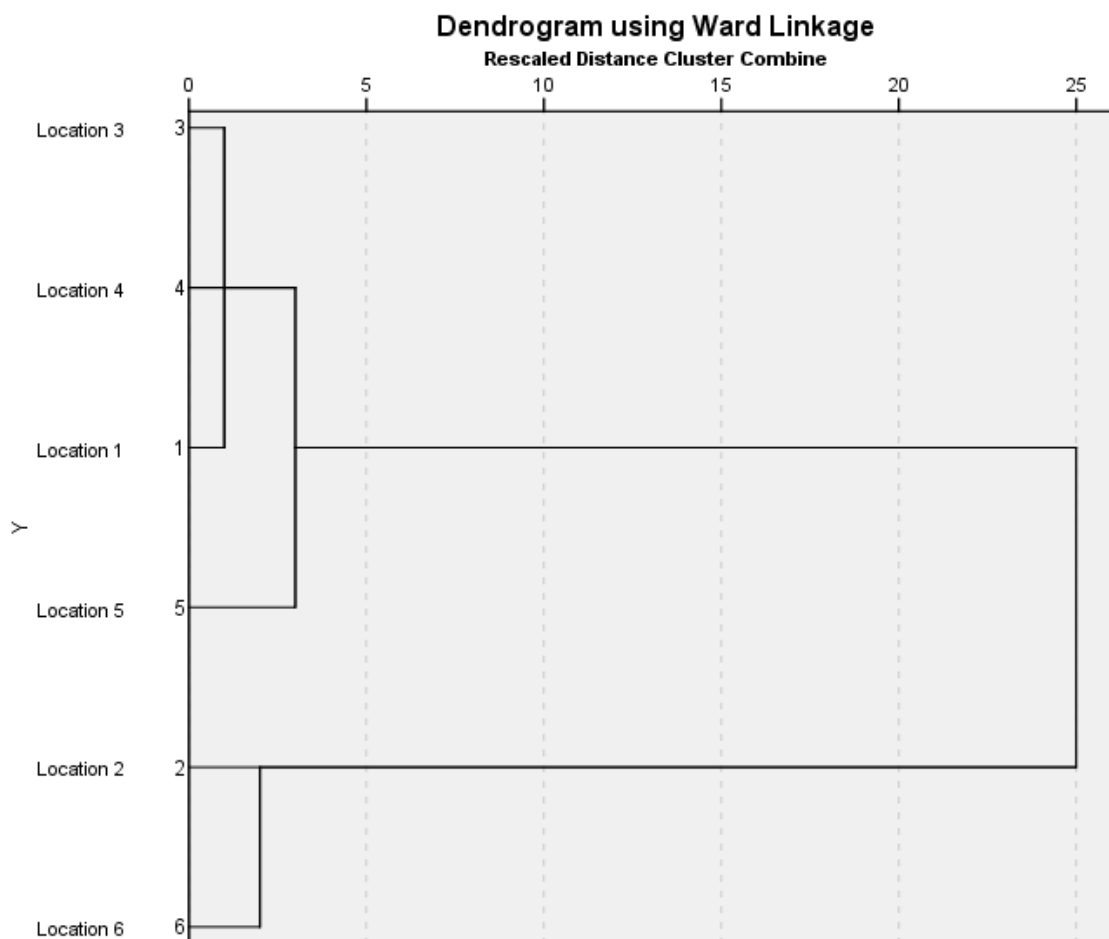


Figure 1. Dendrogram graphic for six locations

Analyses of cluster method are in full compliance with the obtained analytical results. On the dendrogram, two main clusters are shown. First cluster is for locations: 3, 4, 1 and 5. Location 1, 3 and 5 are situated before the discharge of wastewater and the concentration of the parameters is approximately the similar and within the allowed limits. Location 4 is placed 150 meters after the discharge of wastewater, but this location is specific in relation to other locations that are located after the discharge. The concentration of the analyzed parameters at this location depends on the time passed since wastewaters were discharged, as well as the flow velocity. Huge flow and large distances allow dilution of wastewater, and concentrations of parameters are relatively low. In second cluster are locations 2 and 6. These locations are placed 20 meters after discharge of wastewater. Concentrations of all parameters are higher on these two locations compared to other locations. Concentrations of ammonia and orthophosphate are quite elevated and indicate that organic matter from municipal wastewater is broken down and affects the quality of the river Danube.

### Conclusion

The river Danube is the most important river in Serbia, which is why it is of great importance to monitor the quality of the river. Level of contamination of the river is of great importance especially at locations where wastewater is discharged in river. In this paper is used multivariate statistical method which helps us to understand the processes within the river as

well as to obtain information of importance that can serve us for the planning of further monitoring. Environmental protection, especially surface water, is a multidisciplinary technique where in addition to the improvement of the monitoring system, it is necessary to use other methods (such as statistics) that will improve the quality of the environment.

### **Acknowledgements**

The authors acknowledge for the funding provided by the Ministry of Education, Science and Technological Development of Republic of Serbia under project 'Development of methods, sensors and systems for monitoring quality of water, air and soil', number III43008.

### **References**

- [1] Y. Ouyang, P. Nkedi-Kizza, Q.T. Wu, D. Shinde, C.H. Huang, Assessment of seasonal variations in surface water quality, *Water Research*, 2006 Vol. 40, Issue 20, pages 3800-3810
- [2] C. Filik Iscen, Ö. Emiroglu, S. Ilhan, N. Arslan, V. Yilmaz, S. Ahiska, Application of multivariate statistical techniques in the assessment of surface water quality in Uluabat Lake, Turkey, *Environ Monit Assess*, 2008, Issue 144, Page 269.
- [3] M. Vojinovic-Miloradov, I. Mihajlovic, O. Vyviurska, F. Cacho, J. Radonic, N. Milic, I. Špánik, Impact of wastewater discharges to Danube surface water pollution by emerging and priority pollutants in the vicinity of Novi sad, Serbia, *Fresenius Environmental Bulletin*, 2014, Issue 23, pages 2137-2145.
- [4] M. Markovic, M. Vojinovic-Miloradov, Lj. Ignjatovic, B. Obrovski, A. Cavic, I. Mihajlovic, Ecological status of artificial accumulation lake Vruci case study, Serbia *Fresenius Environmental Bulletin*. 2017, Vol. 26 Issue 8, pages 5184-5189
- [5] V. Micić, M. Krüge, P. Körner, N. Bujalski, T. Hofmann, Organic geochemistry of Danube River sediments from Pančevo (Serbia) to the Iron Gate dam (Serbia–Romania), *Organic Geochemistry*, 2010, Issue 41, pages: 971-974
- [6] S. Kolarevic, J. Knezevic-Vukcevic, M. Paunovic, J. Tomovic, Z. Gacic, B. Vukovic-Gacic, The anthropogenic impact on water quality of the river Danube in Serbia: Microbiological analysis and genotoxicity monitoring, *Archives of Biological Sciences*, 2011, Issue 63, pages: 1209-1217
- [7] B. Stanic, N. Andric, S. Zoric, G. Grubor-Lajsic, R. Kovacevic, Assessing pollution in the Danube River near Novi Sad (Serbia) using several biomarkers in sterlet (*Acipenser ruthenus* L.), *Ecotoxicology and Environmental Safety*, 2006, Vol. 65, Issue 3, pages 395-402,
- [8] A. K.T. Kirschner, G. G. Kavka, B. Velimirov, R. L. Mach, R. Sommer, A. H. Farnleitner, Microbiological water quality along the Danube River: Integrating data from two whole-river surveys and a transnational monitoring network, *Water Research*, 2009, Vol. 43, Issue 15, pages 3673-3684
- [9] B. Vrana, V. Klučárová, E. Benická, N. Abou-Mrad, R. Amdany, S. Horáková, A. Draxler, F. Humer, O. Gans, Passive sampling: An effective method for monitoring seasonal and spatial variability of dissolved hydrophobic organic contaminants and metals in the Danube river, In *Environmental Pollution*, 2014, Vol. 184, pages 101-112
- [10] M. Djogo, J. Radonic, I. Mihajlovic, B. Obrovski, D. Ubavin, M. Turk-Sekulic, M. Vojinovic-Miloradov, Selection of optimal parameters for future research monitoring programmes on MSW landfill in Novi Sad, Serbia, *Fresenius Environmental Bulletin*, 2017, Vol. 26, Issue 7, pages 4867-4875

## DETERMINING SEASONAL CORRELATION AMONG ANOXIC NITROGEN TRANSFORMATION CONDITIONS

Marija Perović<sup>1</sup>, Vesna Obradović<sup>1</sup>, Boris Obrovski<sup>2</sup>, Milan Dimkić<sup>1,2</sup>

*1 Institute for the Development of Water Resources, Jaroslava Černog 80, Pinosava-Belgrade  
2 2 University of Novi Sad, Faculty of Technical Sciences, Department of Environmental  
Engineering and Occupational Safety and Health, Trg Dositeja Obradovića 6, Novi Sad,  
Serbia*

*e-mail: okukamarija@gmail.com;*

### **Abstract:**

We examined seasonal change in physicochemical parameters  $\text{NH}_4$ ,  $\text{NO}_3$ ,  $\text{Cl}$ ,  $\text{SO}_4^{2-}$ ,  $\text{Fe}^{2+}$ ,  $\text{Mn}$  and  $\text{TOC}$  for anoxic alluvial groundwater from the first drainage line at Kovin-Dubovac and Danube water level. To evaluate the results of four year monitoring programme Principal Component Analysis (PCA) and Cluster Analysis (CA) were performed. Principal component analysis (PCA) as a multivariate statistical method was used for data filtering in order to indicate if there is a connection between groundwater chemistry, surface water levels and sampling season.  $\text{NH}_4$ ,  $\text{NO}_3$ ,  $\text{Fe}^{2+}$ ,  $\text{Mn}$ ,  $\text{SO}_4^{2-}$  and  $\text{TOC}$  were chosen as important indicators of nitrogen transformation potential.  $\text{Cl}$  and Danube levels were included in analysis as indicators of groundwater recharge. Cluster analysis (CA) was applied for grouping the months of groundwater sampling with similar pattern.

### **Introduction:**

Kovin-Dubovac is an alluvial plain of the left coast of Danube river, characterized as area with intensive agricultural production and shallow anoxic groundwater. Because of intensive agricultural production, nitrogen fertilizers are applied. Nitrogen in Kovin-Dubovac groundwater is dominantly present in reductive form of ammonium ion, whose concentration varies during the year. Conducting PCA and CA we wanted to determine if there is a correlation between alluvial groundwater chemistry, surface water levels and sampling season. Examined data are physicochemical analysis of groundwater from the first drainage line. Danube water level is presented as average value for Banatska Palanka profile, because of supposed direct influence of the river on groundwater in the first drainage line for the 2010-2014 year period. Groundwater sampling was done in april, june, july, september and october for the purposes of elaboration of different studies, under the Project No. TR37014 in the period 2010-2013 year.

### **Materials and method:**

Thickness of the aquifer sediments under the Kovin-Dubovac plain range from 1.5 to 35 m, with an average value of 20 m. The absolute height above sea level of alluvial Danube plain of Kovin -Dubovac is around 73 m in the western part and around 68 m in the central part. The average width of the alluvial plain is 8 km. Corn, sunflower, soybeans and wheat are dominantly grown crops in this area. Nitrogen fertilizers are applied in autumn for basic fertilization (september, october, november) and in pre-season (march, april). Groundwater was sampled from 16 facilities (wells and piezometers) over the 2010 to 2013 time period (B-19/d-2, B-19/p-2, B-19/P-2, B-19/P-1, B-19, B-16/P-1, B-16, B-12/d-2, B-12/p-2, B-12/P-1, B-



12, B-17, Bp-9, Bp-13, Bp-24, Bp-2). Physicochemical analysis presented in the paper are  $\text{NH}_4$ ,  $\text{NO}_3$ ,  $\text{Cl}$ ,  $\text{SO}_4^{2-}$ ,  $\text{Fe}^{2+}$ ,  $\text{Mn}$  and TOC concentration. Surface water level is presented as average value for 2010-2014 period for Banatska Palanka profile.

**Results and discussion:**

Degradation pathways, mobility and solubility of different compounds and pollutants are mainly affected by redox conditions, controlled by dissolved oxygen and the availability of electron donors. After oxygen is depleted, nitrate, manganese, iron, sulfate and  $\text{CO}_2$  are the next favorable electron acceptors, respectively. Conditions which promote respiratory denitrification are the absence of oxygen with presence of organic carbon or the absence of oxygen with the presence of iron-sulfide. Sulfate originating from denitrification can be transformed back to sulfide if electron donor-organic carbon is available in the sulfate reducing zone. The degree of nitrogen conservation in anoxic groundwater environments depends on the relative partitioning between the two major pathways of nitrate ( $\text{NO}_3^-$ ) reduction [3,4]. Depending on prevailing conditions: pH, redox potential, dissolved oxygen, the ratio of redox couple compounds and present microorganisms, some of these processes will become dominant or some of them will happen simultaneously.

**Table 1.** Principal component loadings of these variables with the variances

	Component	
	1	2
Ammonium	-,148	<b>-,791</b>
Nitrate	-,050	<b>-,720</b>
Chloride	,287	<b>,839</b>
Sulfate	<b>-,898</b>	-,401
Iron	<b>,979</b>	,178
Manganese	<b>-,897</b>	,404
TOC	<b>,796</b>	,271
Danube level	<b>,782</b>	,372
<b>Total</b>	3,921	2.416
<b>% of Variance</b>	49,012	30,196
<b>Cumulative %</b>	49,012	79,207

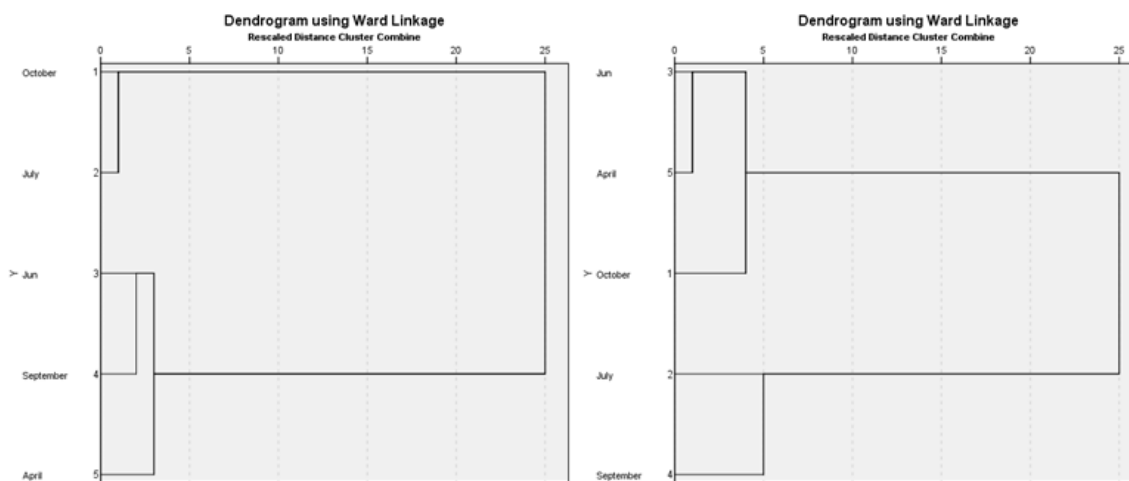
Conducted PCA and CA analysis included 8 parameters for 5 months and revealed 2 factors which explain 79, 207% of data variation (Figure 1). The first factor is presented in cluster 1 and it shows the relation between  $\text{SO}_4^{2-}$ ,  $\text{Fe}^{2+}$ ,  $\text{Mn}$ , TOC and Danube water level (Figure 2). The first subcluster groups October and July. For these months, Danube water level was the lowest. Sulfate concentrations are around 17 mg/l,  $\text{Fe}^{2+}$  around 1.5,  $\text{Mn}$  around 0.7 and TOC 2.3 mg/l. On the second subcluster June, September and April are grouped. Sulfate



concentrations are around 7 mg/l,  $\text{Fe}^{2+}$  around 2,2, Mn around 0.45 and TOC 2.4 mg/l, while Danube level is high.

The second factor shows the relation between  $\text{NH}_4^+$ , Cl and  $\text{NO}_3^-$  concentration. In the first subclacter june, aprile and october are connected.  $\text{NH}_4^+$  concentration is around 0.85 mgN/l, Cl around 20 mg/l, and  $\text{NO}_3^-$  around 0.15 mgN/l. In the second subclacter july and september are connected.  $\text{NH}_4^+$  concentration is around 1.05 mgN/l, Cl around 17 mg/l, and  $\text{NO}_3^-$  around 0.25 mgN/l. Intersection of two factors shows increase in  $\text{NH}_4^+$  concentration in july and september with moderate  $\text{SO}_4^{2-}$ , and  $\text{Fe}^{2+}$  concentrations. For these months Danube water level is low and groundwater recharge is mainly from the direction of the hinterland. Those conditions are suitable for secondary metabolism of sulfate reducers (DNRA) and/or nitrate dependent  $\text{Fe}^{2+}$  oxidation coupled with DNRA [1,2]. For aprile, june and october,  $\text{NH}_4^+$  and  $\text{SO}_4^{2-}$  concentrations are lower, while  $\text{Fe}^{2+}$  concentration shows an increase. Fero ion is in alternation with nitrate and sulfate ions as electron acceptor. Generally microorganisms and bacteria present in groundwater are characterized by a very large diversity of metabolic possibilities. Variable availability of electron acceptors induces sulfate reducing bacteria activity, which depending on availability, as electron acceptors can utilize sulfate, nitrate and fero ion, as well as doing fermentation without using inorganic acceptors.

**Figure 2.** PCA and CA analysi for sampling months for the first drainage line



### Conclusion:

Intersection of two factors shows increase in  $\text{NH}_4^+$  concentration in july and september. This could be correlated with time of fertilizer application, lower Danube level and groundwater recharge from the direction of the hinterland. Generally bacteria are characterized by a wide diversity of metabolic possibilities. Seasonal variation of availability of electron acceptors induces bacterial activity related with nitrate, fero and sulfur cycles. Sulfate reducing bacteria as well as nitrate dependent acidophiling bacteria depending on redox potential and availability as electron acceptors can utilize  $\text{SO}_4^{2-}$ ,  $\text{NO}_3^-$  or  $\text{Fe}^{3+}$  ion. Fulfillment of conditions for nitrogen loss ( $\text{N}_2$ ,  $\text{N}_2\text{O}$ ) probably by autotrophic denitrification is observed in aprile, june and october. For these months Danube water level is high, indicating recharge of surface oxie water in anoxic aquifer and fulfillment for nitrogen loss by autotrophic denitrification or anammox. Nitrogen transformations can be correlated with organic matter bioavailability, which is also seasonally conditioned. Therefore, organic matter complexity and availability

as well as precipitation and irrigation impact could be the subject of future more detail research on this topic.

### **Acknowledgements**

The authors express their gratitude to the Ministry of Education, Science and Technology Development of the Republic of Serbia for financially supporting Project No. TR37014.

### **References**

- [1] M. Rivett, S. Buss, P. Morgan, J. Smith, C. Bemment. *Water research* 42 (2008) 4215 – 4232.
- [2] M. Oshiki, S. Ishii, K. Yoshida, N. Fujii, M. Ishiguro, H. Satoh, S. Okabe. *Appl. Environ. Microbiol* 79 (13) (2013) 4087-4093.M.
- [3] A. Soonmo, W. Gardner. *Mar. Ecol.: Prog. Ser.*, 237(2002), 41-50.
- [4] J. Tiedje. A. J. B., Ed. (1988) John Wiley and Sons: New York.

## MAPPING NITROGEN TRANSFORMATION POTENTIAL IN ANOXIC ALLUVIAL AQUIFER USING PCA AND CA ANALYSIS

Marija Perović<sup>1</sup>, Vesna Obradović<sup>1</sup>, Boris Obrovski<sup>2</sup>, Milan Dimkić<sup>1,2</sup>

*1 Institute for the Development of Water Resources, Jaroslava Černog 80, Pinosava-Belgrade*

*2 University of Novi Sad, Faculty of Technical Sciences, Department of Environmental Engineering and Occupational Safety and Health, Trg Dositeja Obradovića 6, Novi Sad, Serbia*

*e-mail: okukamarija@gmail.com;*

### **Abstract:**

Increase in worldwide population has led to increase in food production. Increased food production consequently increased pesticide and fertilizers use. In fertilizers, nitrogen is in form of nitrate, ammonia or amide. Nitrates expressed solubility as well as inability of negatively charged ions to sorb on sediment particles, are usually the reasons why nitrates are considered as the final mobile compound of nitrogen transformation in soil. Information about the final compound of nitrogen resulting from transformation in water is important as an indication of aquifer potential for nitrogen conservation ( $\text{NH}_4^+$ ) or loss ( $\text{N}_2\text{O}$ ,  $\text{N}_2$ ). To evaluate the results of groundwater quality monitoring, during four years period, Principal Component Analysis (PCA) and Cluster Analysis (CA) were performed. Displayed map, developed as part of this study, presents an intersection of the conclusions based on two main factors, revealed by PCA analysis. Mapped local potential for nitrogen conservation or loss in the first drainage line of Kovin-Dubovac aquifer could be useful for managing the fate of nitrate entering the anoxic groundwater systems.

### **Introduction:**

Inadequate fertilizers use, in terms of overuse, time of use, or application on inadequate soil type, could result in nitrogen leaching to surface and groundwater. The complexity of transformation and transport processes of nitrogen compounds in the unsaturated and saturated environment is reflected in many physicochemical and biological transformations, which depend on prevailing conditions of environment. pH, redox potential, dissolved oxygen, the ratio of redox couple compounds and present microorganisms will determine which transformation processes will become dominant or which of them will happen simultaneously. In reducing environment nitrate is usually reduced by respiratory denitrification to gaseous products, mainly to  $\text{N}_2$  gas and a smaller fraction to nitrous oxide ( $\text{N}_2\text{O}$ ). If nitrogen is preserved in bioavailable, less mobile form ( $\text{NH}_4^+$ ), there is a potential for nitrogen enrichment of the hydraulically connected surface water bodies (eutrophication). If nitrogen is transformed into  $\text{N}_2$  /  $\text{N}_2\text{O}$  (denitrification) it is considered as permanent removal, decreasing the pollution risk and the need for required potable water treatment [1]. In anoxic conditions, nitrogen will be subject of reductive transformations: assimilation into biomass, respiratory denitrification, anaerobic ammonium oxidation (anammox), and dissimilatory nitrate reduction (DNR), usually associated with ammonium production (DNRA).

In order to determine the dominant redox process and final nitrogen compound present in certain conditions in individual facilities in anoxic groundwater it is necessary to quantify concentrations of electron acceptors ( $\text{O}_2$ ,  $\text{NO}_3^-$ ,  $\text{Mn}^{4+}$ ,  $\text{Fe}^{3+}$ ,  $\text{SO}_4^{2-}$ ) and products ( $\text{N}_2$ ,  $\text{NH}_4^+$ ,  $\text{Mn}^{2+}$ ,  $\text{Fe}^{2+}$ ,  $\text{H}_2\text{S}(\text{g})$ ,  $\text{CH}_4(\text{g})$ ) and to qualify their mutual interdependence. For this purpose we

applied Principal Component Analysis (PCA) and Cluster Analysis (CA) to examine 13 physico-chemical parameters in groundwater for 16 facilities (wells and connected piezometers), from the first drainage line in Kovin-Dubovac. Presented data were collected with different frequency for the purposes of elaboration of different studies, under the Project No. TR37014 in the period 2010-2013 year.

#### **Materials and method:**

Kovin-Dubovac is an alluvial plain of the left coast of Danube river between two settlements, Kovin and Dubovac. The deeper layers of the Danube's alluvial plain are composed of gravels and sandy gravels, with some cobbles even over 120 mm in diameter, with medium-grained sands, finely-grained silty sands, coal, alevrites and clay layers at their base. The upper part consists of semi-permeable sediments - silty sands, alevrites, silty clays and clay. In the paper, physicochemical results are presented for 16 wells and piezometers situated at locations across the first drainage line in Danube alluvial sediments.

Principal component analysis (PCA) as a multivariate statistical method was used for data filtering in order to classificate the facilities with different potential for nitrogen transformation. Cluster analysis (CA) was applied for grouping the sampling locations on the first drainage line in Danube alluvial aquifer, in accordance with the obtained values of physico-chemical parameters. PCA is a suitable statistical tool that explains the variance of the intercorrelated variables, transferring them into smaller groups of independent variables [2]. In this study, PCA was conducted on the physicochemical parameters in order to extract significant PCs and to reduce the variables with low significance. Information obtained by CA has enabled the estimation of fulfillment of requirements for certain nitrogen transformation reaction in individual localities. CA is a suitable chemometric tool for compiling the objects according to their characteristics [2]. In this paper, hierarchical clustering using Wards method was performed on obtained dataset, in order to indicate the relation between examined physicochemical parameters.

#### **Results and discussion**

Using the PCA four principal components were revealed, explaining 78.491 % of the total variance, from which the first two factors which explains 54.461% are presented. Principal component loadings of these variables with the variances are presented in Table 1.

**Table 1.** Principal component loadings of these variables with the variances

Parameters	Component	
	1	2
NH <sub>4</sub>	,204	<b>,900</b>
NO <sub>3</sub>	,151	,196
NO <sub>2</sub>	-,159	-,434
TN	,176	<b>,853</b>
C:N	-,143	<b>-,885</b>
TOC	<b>,808</b>	,329
SO <sub>4</sub>	-,009	,135
H <sub>2</sub> S	-,348	,017
Mn	-,447	<b>,532</b>
Eh	<b>-,789</b>	-,180
O <sub>2</sub>	-,153	-,421
Fe	<b>,942</b>	,083
Fe total	<b>,936</b>	,102
<b>Total</b>	3,526	3,185
<b>% of Variance</b>	27,124	24,49
<b>Cumulative %</b>	27,124	51,622

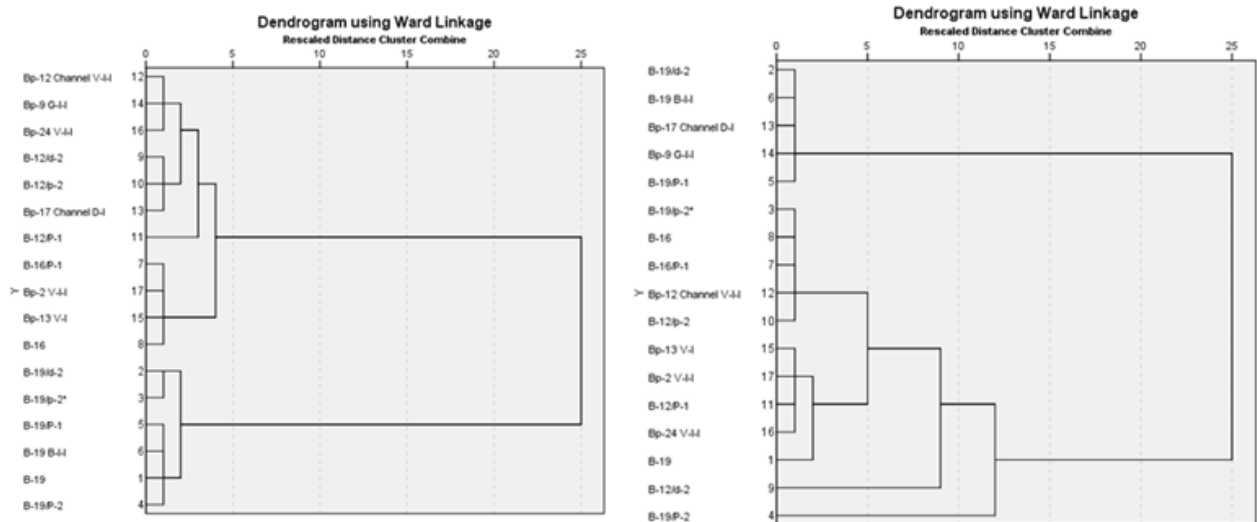


**Figure 1.** PCA and CA analysi for facilities on the first drainage line

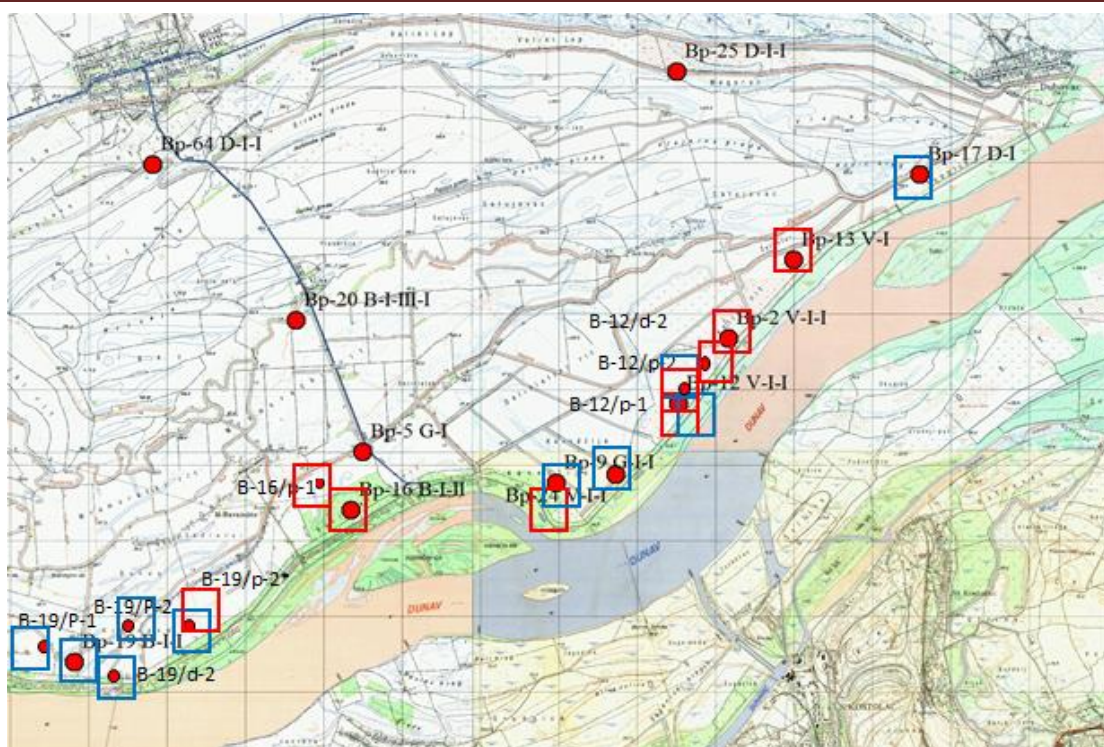


**Figure 2.** Kovin-Dubovac area with mapped facilities for local nitrogen transformation potential (blue square denotes nitrogen loss ( $N_2/N_2O$ ) while red square denotes nitrogen conservation potential ( $NH_4$ )).

Presented are the first two factors which explain 54.461% of total data variation. Factors 1 and 2 explains 35.9 % and 18.5% of total data variance, respectively. The first factor is the most significant and shows a relation between total organic carbon (TOC), fero ion (Fe), total iron concentration ( $Fe_{tot}$ ) and standard redox potential (Eh) (Figure 1). On the first dendrogram are visible two main clusters and 2 subclusters. The first subclaster connects Bp-12, Bp-9, Bp-24, B-12/d-2, B-12/p-2, Bp-17 and B-12/p-1 facilities. TOC concentration values are around 2.2, redox value is around 80 mV, fero ion concentration around 2.5 and total iron concentration around 4 mg/l. The second subclaster connects Bp-16, Bp-16/P-1, Bp-2 i Bp-13. Those objects are characterised by higher concentration of TOC, around 3.5 mgC/l, and Fetot around 5 mgN/l, while Fe and Eh are around 2.5 mgN/l and around 90mV. On the third subclaster Bp-19/d-2 i Bp-19/p-2\* are correlated. Those facilities are characterised as higher redox (over 120 mV) and low iron concentration facilities, with TOC concentration around 2. On the fourth subclaster facilities B-19/p-1, B-19, B-19/p-2 are connected. TOC concentration is the lowest, around 1, Eh values are the highest (around 200 mV) and there is no iron.

The second factor shows a relation between ammonium ( $NH_4$ ), total nitrogen ( $TN = NO_3 + NO_2 + NH_4$ ), manganese concentrations (Mn) and C:N ratio (as TOC : TN) (Figure 1). On the second dendrogram are visible two main clusters. The first subclaster connects Bp-19/d-2, Bp-19, Bp-17, Bp-9, B-19/P-1 facilities. TN is around 0.45 mgN/l,  $NH_4$  is around 0.2 mgN/l, Mn is around 0.3 mg/l, C:N ration is around 9. The second subclaster connects objects Bp-19/p-2\*, Bp-16, Bp-16/P-1, Bp-12, Bp-12/P-2, Bp-13, Bp-2, B-12/p-1, B-24, B-19.  $NH_4$  concentration is around 1.4 mgN/l, TN around 1.5 mgN/l (indicating that almost all nitrogen is in ammonium form), Mn around 0.5 mg/l and C:N ratio is around 2. The third subclaster is B-



19/P-2 facility.  $\text{NH}_4$  concentration is around 1.3 mgN/l, TN around 1.4 mgN/l, Mn shows increased concentration around 2.6 mg/l and C:N ratio is around 1.8.

We have made an intersection of summary conclusions from two examined factors and mapped aquifer local potential for nitrogen loss/conservation (Figure 2). The facilities: Bp-19, Bp-19/p-1, Bp-19/p-2 and B-19/d-2 are characterized as low TOC, low TN low iron and high redox facilities. Bp-17 and Bp-9 has low  $\text{NH}_4$  and high Fe concentration. This means that any nitrogen input in these conditions would probably be lost by respiratory denitrification processes. The facilities: B-19/p-2\*, Bp-16, Bp-16/p-1, Bp-12/p-1, B-12/d-2, Bp-2, Bp-13 are mostly characterized as high TOC, high  $\text{NH}_4$ , high Fe and low Eh, indicating fulfillment of conditions for DNRA and nitrogen conservation. Potential for both processes, nitrogen loss and conservation, depending on prevailing conditions of local environment are determined for objects: Bp-12, Bp-12/p-2, Bp-24.

### **Conclusion**

Knowledge about the final compound of nitrogen resulting from transformation in water is important for two main reasons: health and environmental hazard and indication of aquifer potential for nitrogen conservation or loss. Based on simultaneous observation of local nitrogen transformation potential from both examined factors, we concluded that the most of observed objects could be mapped for dominant potential. The comparative analysis of 13 water quality parameters for 16 anoxic facilities has been presented trying to clarify which parameters might be the most important in determining the nitrate fate. The conclusion is that ammonium increase can be correlated with high TOC, TN and Fe concentration and attributed to iron and sulfur cycles in the environment [3,4]. N loss (evaporation of  $\text{N}_2$ ,  $\text{N}_2\text{O}$ ) is probably related to low C content, where  $\text{Fe}^{2+}$  concentration will determine whether the nitrate will undergo reduction by Fe-oxidation or it will be subject to respiratory denitrification or respiratory denitrification with anammox.

### **Acknowledgements**

The authors express their gratitude to the Ministry of Education, Science and Technology Development of the Republic of Serbia for financially supporting Project No. TR37014.

### **References**

- [1] M. Perovic, V. Obradovic, S. Kovacevic, D. Mitrinovic, N. Zivancev, T. Nenin. *Water Environ Res.* 89 (1) (2017) 4-16.
- [2] M. Djogo, J. Radonic, I. Mihajlovic, B. Obrovski, D. Ubavin. M. Turk Sekulic, M. Vojinovic Miloradov. *Fresenius Environmental Bulletin* 26 (7) (2017) 4867-4875.
- [3] A. Burgin, S. Hamilton,. *Front. in Ecol. Environment.* 5(2), (2007) 89–96.
- [4] M. Oshiki, S. Ishii, K. Yoshida, N. Fujii, M. Ishiguro, H. Satoh, S. Okabe. *Appl. Environ. Microbiol* 79 (13) (2013) 4087-4093.



**TICK INFESTATION (ACARI: IXODIDAE) OF APODEMUS FLAVICOLLIS  
MELCHIOR, 1834 (RODENTIA: MURIDAE) IN VOJVODINA (SERBIA)**

**Aleksandra Petrović<sup>1</sup>, Aleksandar Jurišić<sup>1</sup>, Ivana Ivanović<sup>1</sup>, Tijana Stojanović<sup>1</sup>,  
Aleksandra Popović<sup>1</sup>, Vojislava Bursić<sup>1</sup>, Branka Ljevnaić-Mašić<sup>2</sup>**

<sup>1</sup>*Department of Environmental and Plant Protection, University of Novi Sad, Faculty of  
Agriculture, Trg Dositeja Obradovića 8, Serbia*

<sup>2</sup>*Department of Field and Vegetable Crops, University of Novi Sad, Faculty of Agriculture,  
Trg Dositeja Obradovića 8, Serbia  
e-mail: petra@polj.uns.ac.rs*

**Abstract**

The vector potential of rodents as hosts of mainly larval and nymphal stages of ixodid ticks is influenced by a large number of factors. Considering the confirmed role of mice as important reservoirs and vectors of zoonotic diseases, the aim of the study was to determine the qualitative and the quantitative diversity of ectoparasiting ticks. The total number of trapped mice was 238, and the total number of collected ticks was 449. Six species from four genera of ixodid ticks were identified: *Ixodes ricinus*, *I. trianguliceps*, *Dermacentor marginatus*, *Haemaphysalis concinna*, *H. punctata* and *Rhipicephalus sanguineus*. The average number of ticks per mouse was  $2.211823 \pm 0.157862$ . The highest values for the selected parameters were: the prevalence for *I. ricinus* larvae (8.241%), the average infestation intensity for *D. marginatus* larvae (4.714), the abundance and the infestation index for *I. ricinus* larvae (0.236; 0.022). Based on the seroprevalence and prevalence of infested rodents, the level of potential risk for human and animal could be predicted.

**Introduction**

Most rodent species represent a specific type of an "epidemiological bridge" due to their wide ranges of activity, seasonal migrations and population size fluctuations. That is the reason why they are responsible for the maintenance of high population density of ecto- and endoparasites within certain habitats, but more importantly, their spatial transfer beyond present boundaries. The vector potential of rodents as hosts of mainly larval and nymphal stages of ixodid ticks is influenced by a large number of factors, such as the preference of certain tick species to certain species of rodents or specific characteristics of habitats. These factors also determine the behavior of certain tick species, their population densities and their possibility to survive and maintain their presence in the habitats.

The density of large mammal populations also have a crucial role in maintenance of tick populations as they serve as hosts and vectors of nymphal and adult stages, and thus the role in defining the rate of larvae mortality within the certain habitat. The great influence on the survival rate of larval and nymphal stages of three-host tick species, beside microclimatic characteristics of the habitats, has the density of rodent populations as the transition hosts, because mice have characteristic diurnal and seasonal rhythms and variances in spatial distribution and dispersions.

For the parasites, the host represents a place to live, feed and reproduce, and therefore can be considered as a habitat in the narrow sense. In order to achieve the reproductive maximum ectoparasite selects among the different hosts by choosing its optimal microhabitat, which depends on a large number of factors: age of the individual, reproductive group, sex, body

weight, intensity of infestation with the same or other type of ectoparasite [1, 2]. In natural populations, higher number of ectoparasites are found on certain host specimens, which means that their distribution can not be described as a random and indicates the presence of an ectoparasite preference for certain (appropriate) host [3].

During their life cycle, ixodid ticks have frequent contacts with a large number of hosts (amphibians, reptiles, birds and mammals), in which they can overtake, maintain and transmit a large number of infectious agents relevant to human and animal health [4].

Mammals are the main hosts for 511 ticks species, four more species parasite on mammals and birds and two on mammals and reptiles [5]. Of this number, 87 tick species are associated with rodents. Some rodent species, although not synanthropic, can reach high urban populations (especially along the river banks, in the parks, gardens and yards), and therefore based on seroprevalence and prevalence of infested rodents, the potential risk and level of the infestation influence on people and domestic animals could be predicted [6].

In Vojvodina province *Apodemus flavicollis* (Melchior, 1834) demonstrates the preference for the deciduous forests with a high production of seeds and fruits for consumption, although some authors state that it could be present in mixed forest ecosystems and open habitats such as urban or agro ecosystems.

Considering the confirmed role of mice as the important reservoirs and vectors of zoonotic diseases, the aim of the study was to determine the qualitative and the quantitative diversity of ectoparasiting ticks.

### Experimental

The study was conducted at three localities in Vojvodina (Northern Province of Serbia): Apatin, Bogojevo and Labudnjača. The localities were selected according to their floristic composition and anthropogenic influence. Each trapped specimen of yellow-necked mouse was weighted, the body and tail length were measured, and the sex was determined. According to obtained measurements, specimens were classified in seven age groups: early and late pre reproductive, early, middle and late reproductive and early and late post reproductive group. Each individual was systematically and thoroughly inspected using palpatory technic. The collected ticks were properly labelled and transported to the laboratory till examination and identification.

Ticks were identified up to species level according to the standard identification keys [7, 8]. The ixodid tick infestation was described using four parameters: the prevalence (P), the average infestation intensity (AII), the abundance (A) and the infestation index (II) [9]. The results were statistically analyzed using ANOVA and Fisher's post-hoc test (Statistica 12, StatSoft, University license).

### Results and discussion

The total number of trapped mice was 238, and the total number of collected ticks was 449. Six species from four genera of ixodid ticks were identified: *Ixodes ricinus* Linnaeus, 1758, *I. trianguliceps* Birula, 1895, *Dermacentor marginatus* Sulzer 1776, *Haemaphysalis concinna* Koch 1844, *H. punctata* Canestrini & Fanzago 1878 and *Rhipicephalus sanguineus* (Latreille 1806).

Ticks were collected from 21.67% specimens of the total number of mice and 3.94% specimens did not have any species of ectoparasite. The average number of ticks per mouse was  $2.211823 \pm 0.157862$  (for  $\sigma = 2.249193$  and  $\sigma^2 = 5.058869$ ). The highest number of ticks (14)

per one mouse was detected on male specimen of late post reproductive group, trapped in Apatin.

The highest prevalence was calculated for *I. ricinus* larvae (8.241%) and the lowest for *D. marginatus* nymphs (2.004%). The highest values of average infestation intensity was obtained for *D. marginatus* larvae (4.714), and the abundance and the infestation index for *I. ricinus* larvae (0.236; 0.022) (Table 1.).

**Table 1.** Tick infestation of *A. flavicollis*

Tick species	Stage	n	B	P	AII	A	II
<i>I. ricinus</i>	larval	118	37	8.241	3.189	0.263	0.022
	nymphal	36	29	6.459	1.241	0.080	0.005
<i>I. trianguliceps</i>	larval	30	15	3.341	2.000	0.067	0.002
	nymphal	0	0	0.000	0.000	0.000	0.000
<i>D. marginatus</i>	larval	99	21	4.677	4.714	0.220	0.010
	nymphal	10	9	2.004	1.111	0.022	0.000
<i>H. concinna</i>	larval	54	26	5.791	2.077	0.120	0.007
	nymphal	14	14	3.118	1.00	0.031	0.001
<i>H. punctata</i>	larval	36	17	3.789	2.118	0.080	0.003
	nymphal	20	18	4.009	1.111	0.045	0.002
<i>R. sanguineus</i>	larval	19	13	2.895	1.462	0.042	0.001
	nymphal	13	13	2.895	1.000	0.029	0.001
<b>Total</b>		449	212				
<b>C</b>		449					
<p><b>n</b> – the total number of one tick species  <b>B</b> - the number of hosts infested with certain tick species  <b>C</b> – the total number of examined hosts  <b>P</b> – the prevalence  <b>AII</b> - the average infestation intensity  <b>A</b> - the abundance  <b>II</b> - the infestation index</p>							

Similar results were published [10] where on 12 rodent species (*A. agrarius*, *A. flavicollis*, *A. sylvaticus*, *A. uralensis*, *M. glareolus*, *Micromys minutus*, *M. arvalis*, *M. subterraneus*, *M. musculus*, *M. spicilegus*, *R. norvegicus* and *Spermophilus citellus*) from six counts in Romania, eight tick species were detected: *I. ricinus*, *I. redikorzevi*, *I. apronophorus*, *I. trianguliceps*, *I. laguri*, *D. marginatus*, *R. sanguineus* and *H. sulcata*. According to these authors the average prevalence for all tick and rodent species was 29.55%, the average infestation intensity was 3.86 and the average abundance was 1.14. The most abundant species was *I. ricinus* with the highest level of infestation on *M. arvalis*, *A. uralensis*, *A. flavicollis* and *M. glareolus*. The high statistical significances in the prevalence and the tick infestation intensity on rodents, especially for *I. ricinus* and *Dermacentor reticulatus* Fabricius 1794 were obtained in forest and meadow ecosystems in northeast Poland [11].

The one-way ANOVA did not emphasize any statistical significance regarding tick infestation paired with age or sex group ( $p_{ag}=0.320987$  and  $p_s=0.107251$  for  $p<0.05$ ). However, it could be noticed that tick infestation was slightly higher in all three reproductive groups and in male specimens of *A. flavicollis*. These results could be explained by the fact that specimens of the

reproductive groups have higher activity and wider home range, especially males. A study [12] has statistically proved that the number of tick larvae, nymphs and adults is in a positive correlation with the rodent body mass, that the number of all developmental stages of ticks on hosts decreases with the increase of the rodent population density and that there is no reliable data on the tick preference to the host's sex.

From the total number of collected ticks, only 27 (6.01%) were found on the heads (on 25 specimens of yellow-necked mouse). The grooming as a specific behavior of mice has also a significant role in the level of tick infestation. Furthermore, the grooming has a lot of functions such as body surface cleaning, ectoparasite removal, thermoregulation, auto-stimulation and the transfer of antibacterial agents from the saliva to the hair and skin and also the transmission of secondary signals from one individual to another [13]. This method of grooming is distinctive for rodents comparing to other mammal species. Mice usually clean their heads, ears and necks using their front legs and paws with intensive and fast movements, which could be the reason for small number of ticks in this body region.

The percentage of tick infestation of rodents could be extremely high [14]. Due to the reproductive strategies of tick females who usually lay (depending on species) about 2000-3000 eggs in one place, the microdistribution of the host seeking larvae in the habitats usually depends on their dense distribution and the small area of activity limited to only a few meters.

### Conclusion

Six tick species sampled from the 238 individuals of *A. flavicollis* were identified: *I. ricinus*, *I. trianguliceps*, *D. marginatus*, *H. concinna*, *H. punctata* and *R. sanguineus*. The average number of ticks per mouse was 2.2. The highest values for the selected parameters were: prevalence for *I. ricinus* larvae, the average infestation intensity for *D. marginatus* larvae, the abundance and the infestation index for *I. ricinus* larvae. Based on the seroprevalence and prevalence of infested rodents, the level of potential risk for human and animal could be predicted.

### Acknowledgements

The authors acknowledge the financial support of the Ministry of Education and Science, Republic of Serbia, Project Ref. TR31084.

### References

- [1] S. Mears, F. Clark, M. Greenwood, K.S. Larsen, Bulletin of Entomological Research. 92 (2002) 375-384.
- [2] H. Hawlena, I.S. Khokhlova, Z. Abramsky, B.R. Krasnov, Parasitology. 133 (2006) 187-193.
- [3] H. Hawlena, Z. Abramsky, B.R. Krasnov, Oecologia. 146 (2005) 200-208.
- [4] A. Jurisic, A. Petrovic, D. Rajkovic, S. Nicin, Exp. Appl. Acarol. 52 (2010) 101-109
- [5] G.V. Kolonin, Entomological Review. 87(4) (2007) 401-412.
- [6] L.A. Reparent, D. Hegglin, I. Tanner, C. Fischer, P. Deplazes, Parasitology Research. 136 (2009) 329-337.
- [7] J. Nosek, W. Sixl, Central European Ticks (Ixodoidea) – Key for determination. In collaboration with Kvcicala P. & Waltinger H. Mitt. Abt. Zool. Landesmus. Joanneum Jg., Graz, 1972, pp. 61-92.

- [8] A. Estrada-Peña, A. Bouattour, J.L. Camicas, A.R. Walker, Ticks of domestic animals in the Mediterranean Region. A guide to identification of species. University of Zaragoza. Spain, 2004.
- [9] A. Petrović, Seasonal fluctuations of voles and mice (Rodentia: Muridae) and their role as vectors of ixodid ticks (Acari: Ixodidae). PhD thesis, Faculty of Agriculture, University of Novi Sad, 2015.
- [10] A.D. Mihalca, M.O. Dumitrache, A.D. Sándor, C. Magdaş, M. Oltean, A. Györke, I.A. Matei, A. Ionică, G. D'Amico, V. Cozma, C.M. Gherman, Parasites and Vectors. 5 (2012) 26.
- [11] A. Paziewska, L. Zwolińska, P.D. Harris, A. Bajer, E. Siński, Exp. Appl. Acarol. 50 (2010) 79-91.
- [12] C. Kiffner, T. Vor, P. Hagedorn, M. Niedrig, F. Rühle, Parasitol. Res. 108 (2011) 23-335.
- [13] M.H. Ferkin, Chemical Signals in Vertebrates. 10 (2005) 64-69.
- [14] R.J. Eisen, L. Eisen, R.S. Lane, Exp. Appl. Acarol. 33 (2004) 215-233.

## WATER FROM THE TIMOK RIVER IN SERBIA: ESTIMATION OF ITS SUITABILITY FOR ARABLE SOIL IRRIGATION

**Radmila Pivić<sup>1</sup>, Aleksandra Stanojković-Sebić<sup>1</sup>, Zoran Dinić<sup>1</sup>, Jelena Maksimović<sup>1</sup>, Milan Pešić<sup>1</sup>, Dragana Jošić<sup>1</sup>**

<sup>1</sup>*Institute of Soil Science, Belgrade, Teodora Drajzera 7, Serbia  
e-mail: drradmila@pivic.com*

### **Abstract**

This paper presents the results of analysis of the content of hazardous and harmful substances in the water for irrigation, sampled during the vegetation season 2012/2013 in the basin of the Timok River, from Knjaževac to Visočni hill (Mokranja). The investigation was carried out in three cycles of monitoring on 17 selected sites, which gravitate on the an arable soil that was irrigated. During the mentioned period in the water samples it was determined the values of pH (potentiometrically), EC<sub>w</sub> (conductiometrically), TDS (gravimetrically); determination of the content of trace elements and heavy metals Cr, Ni, Pb, Cu, Zn, Cd, B, As and Fe was done according to ICP methodology, using ICAP 6300 ICP optical emission spectrometer; heavy metal Hg was determined by a flame atomic adsorption analyzer SensAA Dual.

The content of trace elements and heavy metals in the samples of water is generally below the maximum allowable concentration (MAC), except in one sample, during the first cycle of sampling, where it was recorded increased Cu content, exceeding the recommended limits (0.2509 mg l<sup>-1</sup>). One water sample from the Timok River, sampled in the second cycle of monitoring, showed a slight increase in the Ni content above the recommended limits (0.124 mg l<sup>-1</sup>). Since the location of this sample was also in the vicinity of the village, the assumption is that it is caused by an anthropogenic activity. Based on the obtained data of the content of hazardous and harmful substances in the water for irrigation of the Timok River, it can be concluded that the water is usable for irrigation of agricultural crops and soils, with frequent quality checks during the summer months.

### **Introduction**

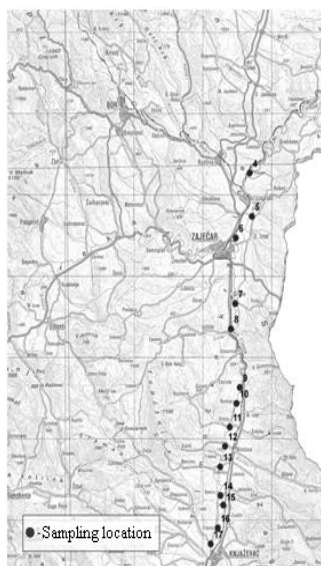
The scope of the research conducted in this paper is the study of quality of irrigation water from the Timok River, complies with the requirements of FAO, 1954 and U.S. Salinity Laboratory classification [8], designed for usability evaluation of irrigation water. Irrigation means the artificial feeding water into the soil in order to rhizosphere wetting layer at a time when the amount of available soil moisture is insufficient to meet the optimum energy crops. Irrigation is a hydro reclamation measure that aims to improve the physical properties of the soil by adding water to achieve an optimum moisture during the growing season and thus achieve optimum yield. It may be applied during part of the growing season or during the growing season. Irrigation of cultivated plants on arable soils involves the use of water of appropriate physical, chemical and biological properties, so it is very important to examine the quality of water used for its intended purpose in order to assess the impact on soil and plants. Intensification of irrigation depends primarily on the provision to the required amount of water of adequate quality. The major pollutants of surface water in the country are industrial enterprises, farms and settlements with sewage systems, without built facilities for waste water treatment, and such with acting, but technically outdated [18]. Anthropogenic impacts and natural processes can affect the quality of surface waters and threaten their use as drinking



water, and for use in industry, agriculture, and for other purposes [6,15,22]. The accumulation of metals in an aquatic environment has direct consequences to man and ecosystem [12]. The aim of this study is to assess the current water quality of the Timok River to be used for irrigation of an arable soil near the streams and highlight the pollution risk. Pollution risks are mainly the direct consequence of the discharge of waste water from industrial plants, agricultural intensification or anthropogenic factors. Relief of Timok basin is characterized by a variety of forms resulting from the highly complex genesis and evolution of this area. The formation of the relief was influenced by tectonic processes, volcanic eruptions, sea, lake and river flows. The effect of these forces is protracted and squeezing through many geological periods. The whole area is inclined towards the north and is exposed to the influence of the continental climate of the Pannonia, while the south and east sides surrounded by high mountain ranges, and to the west by high and medium-high mountains. Based on that, several special units in this area can be extracted, varying in altitude, soil and environmental conditions for the development of agriculture [2]. Agricultural soils that have the greatest significance in the observed region are Vertisols with its subtypes and varieties, Eutric Cambisols, brown soils (Distric Cambisols), which are formed on different geological substrates, Fluvisols and Luvisols [23].

### Experimental

Timok River flows through the Republic of Serbia, and the last 15 km represents the boundary between Serbia and Bulgaria. Estuary is located at an altitude of 28 m, which is the lowest point in the Republic of Serbia. Timok is part of the Black sea basin, with an average flow rate of  $24 \text{ m}^3\text{s}^{-1}$ , and the maximum that can be  $40 \text{ m}^3\text{s}^{-1}$ . In geographical terms Timok River basin lies between  $43^{\circ}30'$  and  $44^{\circ}45'$  north latitude and  $19^{\circ}30'$  and  $20^{\circ}30'$  east longitude (Figure 1).



Sampling point	Easting	Northing	Sampling point	Easting	Northing
1	7628790	4889690	10	7604960	4844430
2	7627190	4886910	11	7603970	4841500
3	7626120	4885580	12	7603300	4839140
4	7606860	4872750	13	7602590	4836620
5	7607200	4867420	14	7602620	4833080
6	7604850	4864780	15	7603020	4831910
7	7604770	4856700	16	7602230	4829100
8	7604160	4853590	17	7601200	4827130
9	7605420	4846380			

Figure 1. Location map of Timok valley with selected sample sites

A total of 51 water samples were collected from seventeen sampling points. Water samples were collected in three cycles of sampling, in July and October 2012 and April 2013., using 2000 ml plastic bottles. The sampling bottles for heavy metal determination were pre-soaked overnight with 10% HCl, rinsed with distilled water and then rinsed using river water before sample collection. Sampling bottles for the determination of physicochemical parameters were



cleaned and rinsed using distilled water only. Preservation of water samples was done by adding 2 drops of concentrated HNO<sub>3</sub> to each water sample before storage below 4°C until they were analyzed.

The measured parameters were determined by the following methods: pH - potentiometric [16], electrical conductivity (EC<sub>w</sub>) - conductimetric [7], total dissolved solids (TDS) - gravimetric [4]. The acid-available fraction of heavy metals and other toxic elements (As, B, Cd, Cr, Cu, Hg, Fe, Ni, Pb, Zn) was determined using EPA 200.7 methods [10], as well as an ICAP 6300 ICP optical emission spectrometer (ICP-OES). The concentration of Hg was determined by a flame atomic adsorption analyzer SensAA Dual (GBC Scientific Equipment Pty Ltd, Victoria, Australia).

The experiment data were presented with mean of three tests with the presented summarized basic statistics of the dataset. Analysis of the interdependence of variables was carried out by calculating a linear Pearson correlation coefficients.

### Results and discussion

The seasonal and annual averages of physico-chemical characteristics are given in Table 1.

Table 1. Average values of the water quality parameters, along with the standard limits by irrigation water US and FAO and by Republic of Serbia

Parameters	Mean±STDEV	Standard limits			
		US irrigation water quality[10]	OfficialGazette, [18,19]	Ayers et al.[5]	Duncan et al. [8]
pH	7.83±0.38	6.5-8.4		6.5-8.4	6.0-9.0
EC <sub>w</sub> 25°C (dSm <sup>-1</sup> )	0.45±0.149	<0.7	<1.0 <sup>#</sup>	<0.7	
TDS (mg·l <sup>-1</sup> )	441.76±156.23	<450		0-2000	
As (mg·l <sup>-1</sup> )	0.0046±0.0037		0.05	0.1	
B (mg·l <sup>-1</sup> )	0.069±0.09862		1.0	0-2	2.0
Cd (mg·l <sup>-1</sup> )	0.00037±0.00063	0.01	0.01	0.01	
Cr (mg·l <sup>-1</sup> )	0.001079±0.0013	0.1	0.5	0.1	
Cu (mg·l <sup>-1</sup> )	0.020±0.0471	0.2	0.1	0.2	0.2
Fe (mg·l <sup>-1</sup> )	0.0813±0.1228	5.0		5.0	5.0
Ni (mg·l <sup>-1</sup> )	0.0057±0.01812	0.2	0.1	0.2	
Pb (mg·l <sup>-1</sup> )	0.0032±0.0146	5.0	0.1	5.0	
Zn (mg·l <sup>-1</sup> )	0.0102±0.0146	2.0	1.0	2.0	2.0
Hg (mg·l <sup>-1</sup> )	bdl		0.001		

\*References (listed below in reference list); bdl-below detection limit

<sup>a</sup> - in me/l = mill equivalent per liter (mg/l ÷ equivalent weight = me/l); in SI units, 1 me/l=1 mill mol/liter adjusted for electron charge.

The pH value is a measure of basicity and acidity of the water (Figure 2). If the value is less than seven, the water or the aqueous solution is acidic, and if it is higher, then it is basic. Plants for growth and development favor the slightly acidic solution, the pH should be around 5.5. The pH is an important factor which determines the suitability of water for a variety of purposes, inter alia, for irrigation. The tested samples had pH values from neutral to slightly alkaline during the second cycle of sampling and showed a growing trend. This may be

affected by drought and an increased flow of wastewater agriculture and households, as well as microbial activity.

Conductivity is a measure of the ability of an aqueous solution to carry an electric current. Increasing levels of conductivity and cations are the products of decomposition and mineralization of organic matter [1]. The aqueous salt solution and dissociated are broken down into positive and negative ions. Natural water are with electrical conductivity values generally less than unity. Measurement of the conductivity is performed at a specific temperature and it corresponds to the presence of dissolved salts. These are most commonly sodium chloride, and there may be also a sodium sulphate, calcium chloride, calcium sulfate, magnesium chloride, etc. Absolutely demineralized water does not conduct electricity, but even with small additions becomes a good conductor. Salts dissolved in the water increase its conductivity. In this study the conductivity was obtained by indirectly calculation of the amount of salt (Figure 3). According to all reference values (US, FAO and Republic of Serbia), the conductivity values of all samples showed good quality of this water for soil irrigation. Total dissolved solids (TDS) are an important characteristic for the determination of the quality of water for irrigation because it expresses the total concentration of soluble salts in water. Dissolved solids in water include all inorganic salts, silica and soluble organic matter. Pure water must be free from most suspended particles, which are responsible for turbidity. TDS was the highest in summer due to evaporation and reduced intake, which contributed to an increase in concentration, and was with the minimum value in the rainy season, due to the increased entry of rain and a corresponding reduction in concentration at all locations (Figure 4). The content of trace elements and heavy metals in the samples of water is generally below the MAC, maximum allowable concentration [19]. In sample No. 4 in the first series of sampling it was recorded an increased copper content (Figure 5) and above the MAC ( $0.2509 \text{ mg l}^{-1}$ ). Besides the vicinity of the village, with a sampling of wastewater gravitate to the sampling points, it is possible that the reason for the increased concentration is the use of a preparation based on copper. In the other series on this site it was not registered higher content of this element above the MAC. Sample No. 5, sampled in the second series (Figure 6) showed a slight increase in the nickel content above the MAC ( $0.124 \text{ mg l}^{-1}$ ) and how it is in the zone below the rural village, it is possible that this was caused by increasing anthropogenic activity, as in other series was not registered an increased content of this element.

The diversity in the results and demonstrated dynamic variations, suggests impact of a number of various environmental factors on the pattern of metals distribution in the water. In this regard [21], reported that the concentrations of metal ions strongly depend on the biological processes, redox potential, ionic strength, pH, the activity of organic and inorganic chelators and the purification processes in water.

By analyzing the correlation parameters, the conclusion is that there is a correlation between the samples and the characteristics of the water where the pH value has a significant negative correlation to all studied parameters except to the concentration of B [13]. EC<sub>w</sub> values were positively correlated to all studied parameters except to the concentration of Pb. TDS values showed a positive correlation to the concentration of B, Cu, Fe, Pb, Zn and negatively to the concentration of As, Cd, Cr, Pb in the samples of water. As, Cd, Cu, Fe, Pb and Zn each have a positive correlation which can be interpreted as they have the same potential sources of pollution; the correlation to other parameters is negative.

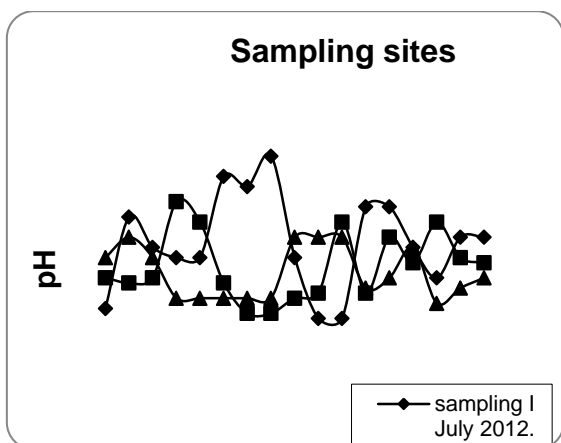


Figure 2. pH value of test water samples in batches of monitoring

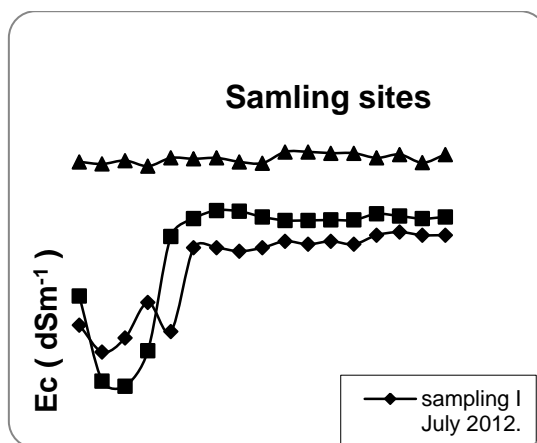


Figure 3. ECw value of test water samples in batches of monitoring

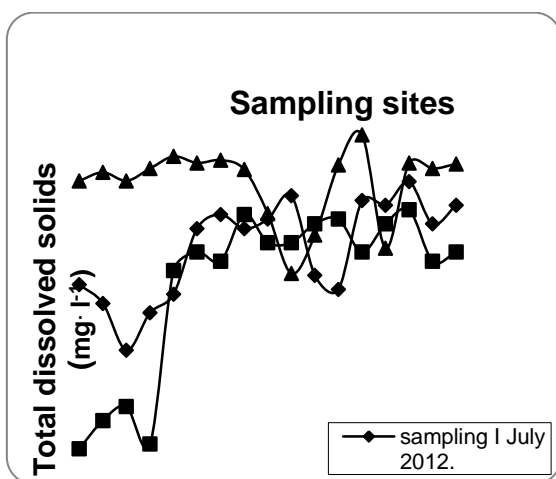


Figure 4. TDS value of test water samples in batches of monitoring

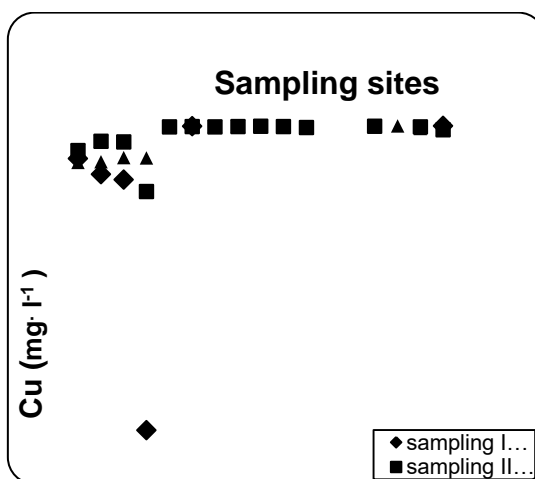


Figure 5. Cu concentration of test water samples in batches of monitoring

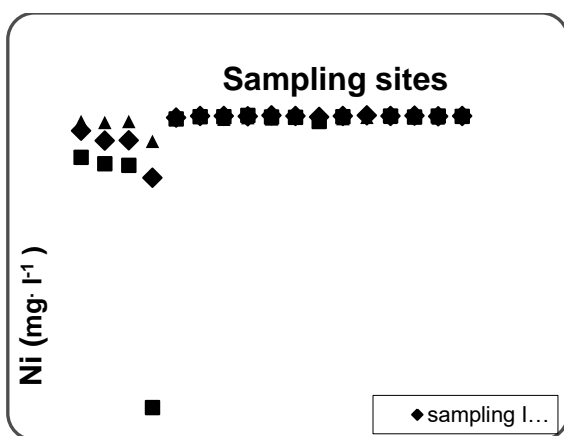


Figure 6. Ni concentration of test water samples in batches of monitoring

## Conclusion

Results from water samples showed that the content of heavy metals in the water of the Timok River in most of the samples analyzed in this study was within the MAC. Variations in the content of heavy metals in the water are the result of a wide range of human activities (primarily agriculture) in the study area and water levels throughout the year. Based on the presented it can be concluded that the water from Timok river can be used for irrigation of crops and soil in the vicinity of water flow to the restrictions and frequent quality checks during the summer months.

## Acknowledgements

This research was supported by the Ministry of Education and Science, Republic of Serbia [TP 37006].

## References

- [1] B. Abida, R. HariKrishna, E-Journal of Chemistry, 5, (2):(2008):377-384.
- [2] G. Antonović, V. Nikodijević, Đ. Tanasijević, Lj.Vojinović, N. Pavićević, Ž. Aleksić, Đ. Filipović, M. Jeremić : Zemljišta basena Timoka, Centar za poljoprivredna istraživanja, Institut za proučavanje zemljišta, Beograd (in Serbian) (1974).
- [3] APHA Standard methods for the examination of water and wastewater. In A.E.(1992)
- [4] A.E. Greenberg, L.S. Clesceri, A.D. Eato,(Eds.) American Public Health Association, 18<sup>th</sup> ed.,Washington, U.S.A.(1998)
- [5] R.S. Ayers, D.W. Westcot: Irrigation and Drainage paper 29, Rev.1, (1994) 174 p.
- [6] S.R.Carpenter, N.F.Caraco, D.L. Correll, R.W. Howarth, A.N. Sharpley, V.H. Smith, Ecol Appl 8(3) (1998):559–68.
- [7] Determination of electrical conductivity SRPS EN 27888:1993
- [8] L.D. Doneen, D.W. Westcot: FAO.Irrigation practice and water management Irrigation and Drainage Paper 1, Rev. 1. FAO , (1988) Rome. 71 pp.
- [9] R.R. Duncan, R.N. Carow, M. Huck. USGA Green Section Record: (2000)14-24
- [10] EPA METHOD 200.7. (2001): Determination of Metals and Trace Elements in Water and Wastes by Inductively Coupled Plasma-Atomic Emission Spectrometry.
- [11] FAO (1954). U.S. Salinity Laboratory Staff.
- [12] O.S. Fatoki, N. Lujiza, O.A.Ogunfowokun, Water S.A. 28(2) (2005) pp.183.
- [13] D. Gong, X. Gao, T. Ntakirutimana, J.Guo, K. Li, Pol J Environ Stud Vol. 22, No. 4, (2013)1061-1067.
- [14] <http://sh.wikipedia.org> Accessed on 20/09/2017.
- [15] H.P. Jarvie, B.A. Whitton, C. Neal, Sci Total Environ 210–211: (1998),79–109.
- [16] Measurement of pH - Potentiometric method SRPS H.Z1.111:1987.
- [17] D.W. Nelson, L.E. Sommers In: D. L. Sparks (Ed.), Methods of Soil Analysis, part 3 (SSSA, Madison, Wisconsin, USA) 961 (1996).
- [18] G. Konstantinova, N. Georgieva, Z. Yaneva, G. Petkov, M. Todorova, Ch.Miteva Bulg JAgric Sci, 19 (No 4) (2013), 635-643.
- [19] Official Gazette of Republic of Serbia, (1994):23.
- [20] Official Gazette of Republic of Serbia, (2012):50.
- [21] H. Ozmen, F. Kulahc, A. Cukuroval, M. Dogru: Chemosphere, 55: (2004), 401–408.
- [22] V.J. Simeonova, A. Stratis, C. Samara, G. Zachariadis, D. Voutsas, A. Anthemidis, M. Sofoniou, Th. Kouimtzis, Water Research 37 ( 2003), 4119–4124.
- [23] World Reference Base for Soil Resources, 2014, <http://www.fao.org/3/a-i3794e.pdf>

**RESPONSE OF *Sinapis nigra* L. AND *Sinapis alba* L. TO THE PRESENCE OF NaCl AND SILICON IN NUTRIENT SOLUTION**

**Marina Putnik-Delić, Ivana Maksimović, Dragan Lazić, Milena Daničić, Rudolf Kastori, Žarko Ilin**

*University of Novi Sad, Faculty of Agriculture, Trg Dositeja Obradovića 8, 21000 Novi Sad, Serbia*

*e-mail: putnikdelic@polj.uns.ac.rs*

**Abstract**

Stress caused by salt is one of the most important abiotic stresses for plants. It is well known that silicon can alleviate this abiotic stress in some plant species. In this experiment we analyzed *Sinapis nigra* and *Sinapis alba* growing in the presence of 50 and 100 mM NaCl and influence of Si on tolerance of this two species to salinity. The results showed that salinity had significant effect on growth, concentration of photosynthetic pigments and free proline. The smallest effect of NaCl and NaCl combined with Si was on transpiration intensity.

**Introduction**

Soil salinity is a problem that is growing in many regions where irrigation is a regular agrotechnical measure, as well as in arid and semiarid regions. Stronger mineralized water and reclaimed water utilities are often used for irrigation [1]. Cultivated plants react to increased concentrations of salt and salinity may significantly affect the quality and the yield [2].

Silicon (Si) is the second most abundant element in Earth crust. It is well known that although Si is not usually considered to be an essential element it could be beneficial for plant growth and production [3]. Many studies show that the addition of Si increases the resistance of plants to biotic and abiotic stress [4].

Black and white mustard are grown for seeds that are used as spices. Oil of black mustard has strong antibacterial activity and white mustard is also used as feed and green manure. They are very important for the production of honey, too. The diverse purposes and unexplored possibilities of mustards for analyzing those species with respect to excessive NaCl and role of silicon.

The aim of experiments was to examine the influence of different concentrations of NaCl and the effects of silicon on growth, physiological and chemical properties of black and white mustard.

**Experimental**

In this paper, we studied how the continuous presence of 0 (control), 50 and 100 mM NaCl and NaCl combined with silicon (2 ml/L) affects on fresh weight (leaf, stem, root), concentration of free proline (shoot and root) and photosynthetic pigments, and transpiration intensity, in white mustard (*Sinapis alba* L.) and black mustard (*Sinapis nigra* L.). All treatment were set in five repetitions, eight plants per repetition. Plants were grown in semi-controlled conditions of a greenhouse, in water cultures, using one half strength Hoagland solution [5] as nutritive medium. Fifty days after sowing analyses were done. Fresh weight were measured, the intensity of transpiration was measured gravimetrically, free proline were analyzed spectrophotometrically (Beckman, USA Duferies 60) [6], as well as concentration of photosynthetic pigments (following procedures [7] [8]).

Statistical analysis of data was performed by Statistica 13. Significance of obtained differences between means was established by LSD test for all parameters.

### Results and discussion

Salinity caused a reduction of growth of above-ground parts of plants, contributed to reduction of the leaf surface, which further effect was the reduction of photosynthesis intensity. The obtained results are in accordance with this experiment. White mustard didn't show significant differences in the FW leaf between treatments, while in the black mustard there were significant differences in plants grown in the presence of 100 mM NaCl+Si (Figure 1). Significant differences were between treatments, especially in FW of stems of white mustard. FW of roots was not significant compared to the control in any plant species.

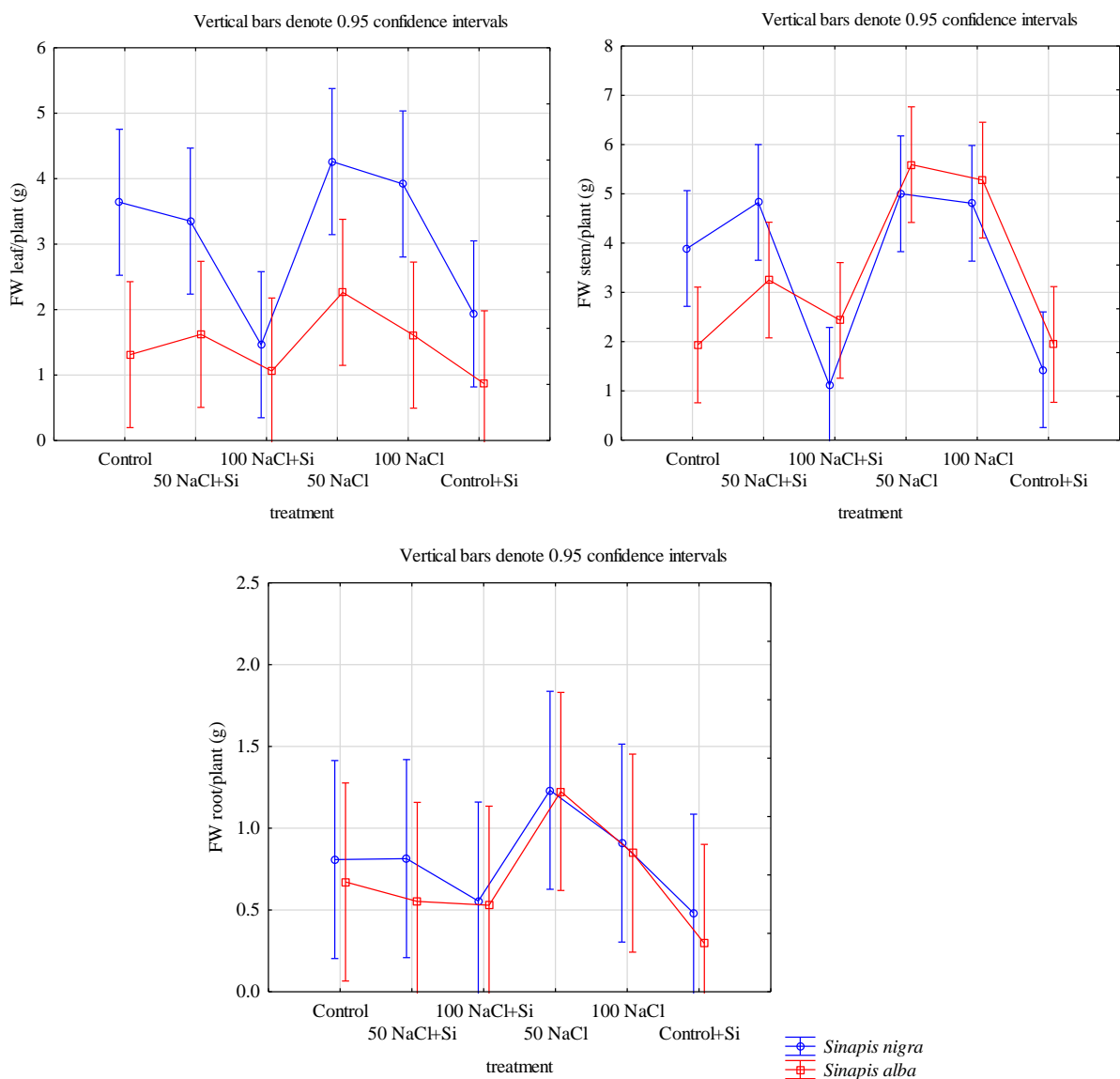


Figure 1. Fresh weight (FW) of *Sinapis nigra* and *Sinapis alba* under NaCl and Si treatment

According to previous studies (Blohina et al., 2003) Si may affect the recovery of the chlorophyll content of rapeseed caused by salinity, which suggested that Si had a positive

influence on the oxidative stress, the concentration of the photosynthetic pigments does not change significantly compared to the control. Treatment by Si in this experiment is enabled that the concentration of the pigments remained at the control level (Figure 2). The concentration of all analyzed pigments in both plant species was significantly different compared to the control, for example in treatment with 50 NaCl, concentration of Chl a was 45% higher than in the control. Quite opposite results are obtained from two varieties of corn [4] where the use of Si lead to an increase of chlorophyll, compared to plants grown in presence of NaCl, and it was defined a positive effect of Si on reduction of chlorophyll degradation.

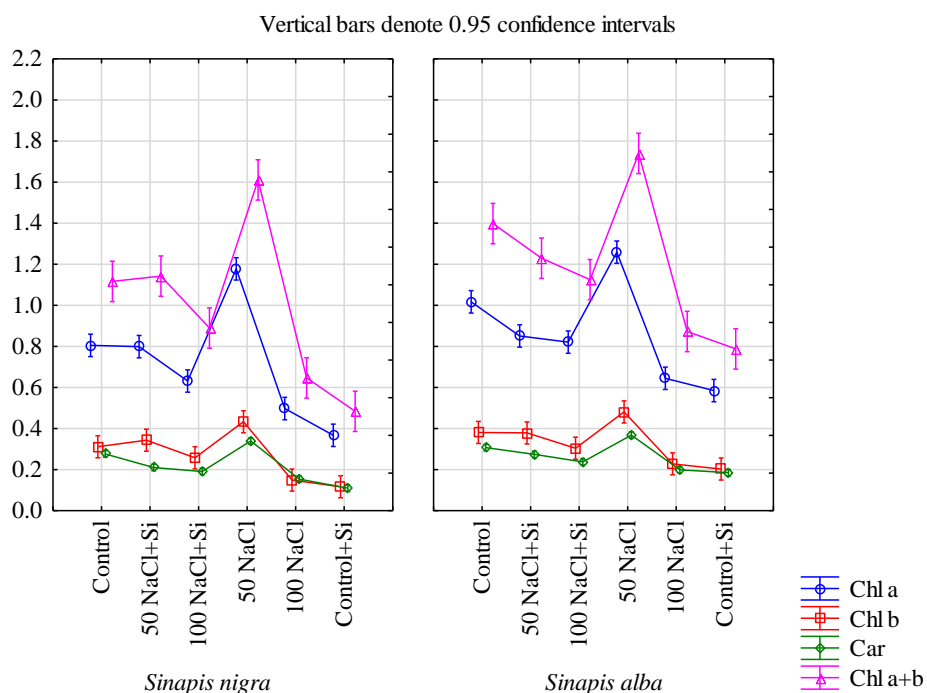


Figure 2. Photosynthetic pigments (mg/g FW) of *Sinapis nigra* and *Sinapis alba* under NaCl and silicon treatment

The content of free proline in the root was the similar in both plants species. The biggest difference compared to respective controls induced treatment 100NaCl+Si where concentration of free proline was 13 times higher in *Sinapis nigra* and about 5 times higher in *Sinapis alba* (Figure 3).



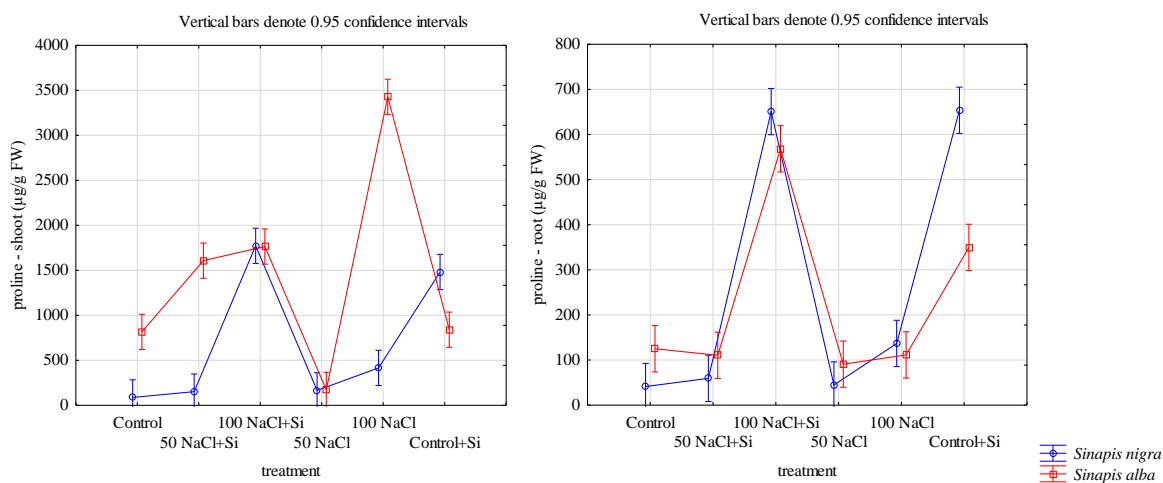


Figure 3. Concentration of free proline of *Sinapis nigra* and *Sinapis alba* under NaCl and silicon treatment

In shoots were larger differences between plant species, the difference of the concentration of free proline compared to the control was the biggest in *Sinapis alba*, 4.2 times more in the treatment of 100 NaCl, while the largest difference in *Sinapis nigra* was observed applying treatment 100NaCl+Si, 20 times higher concentrations compared to the control (Figure 3).

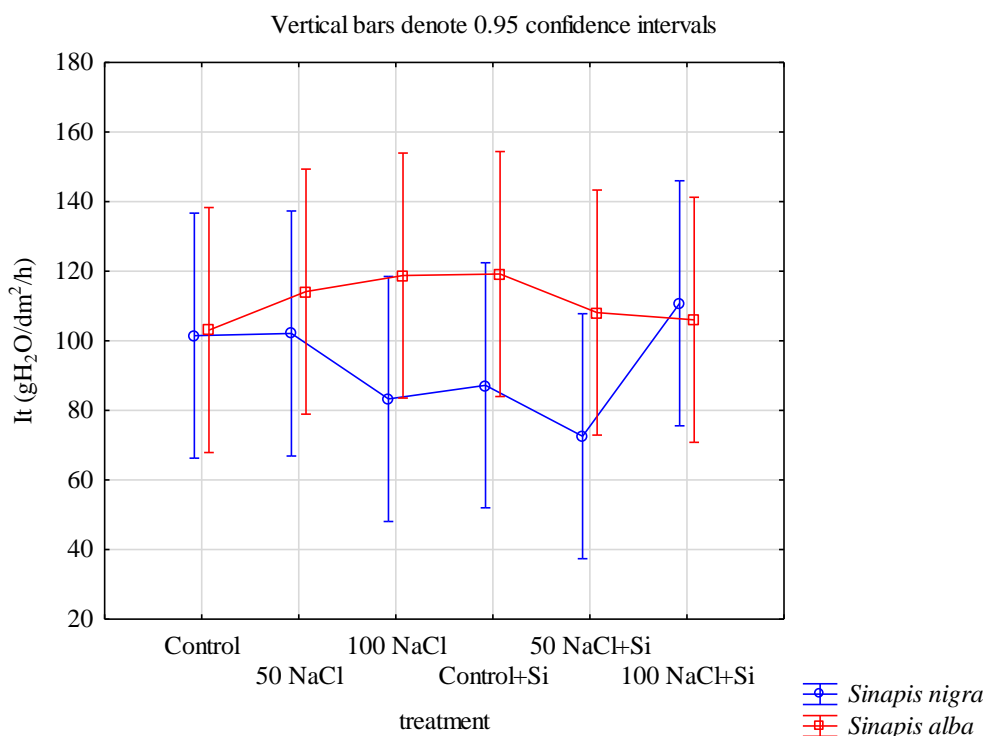


Figure 4. Transpiration intensity of *Sinapis nigra* and *Sinapis alba* under NaCl and silicon treatment

In contrast to the results of research on the oilseed rape, in which at high concentrations of salt concentration of free proline increased and upon the addition of Si proline content declined,

suggesting that Si reduced the negative effect of salinity on the concentration of proline [10]. Applied concentration of salts and of silicon had not significant influence on transpiration intensity (Figure 4). The results obtained on *Sinapis nigra* (Figure 4) are in accordance with the previous research [11] [2], which have established that salinity in peas, reduced the leaf, transpiration surface, which further reduced transpiration.

### Conclusion

Salinity significantly affected growth, concentration of photosynthetic pigments and free proline in black and white mustard, whereas intensity of transpiration changed only slightly. However, applied concentration of Si alleviated negative effects of salt in plants grown at lower salt concentration (50 mM NaCl). It would be good to examine the impact of application of different concentrations of silicon on vegetative growth, grain yield and quality of *S. nigra* and *S. alba* in the future.

### Acknowledgements

We thank Ministry of Education, Science and Technological Development of the Republic of Serbia (TR 31036 and TR 31016) for financial support.

### References

- [1] I.K. Kalavrouziotis, P.H. Koukoulakis. Elemental antagonism in vegetables under treated municipal wastewater. *J. Plant Interact.* 5 (2010) 101-109.
- [2] I. Maksimović, M. Putnik-Delić, I. Gani, J. Marić, Ž. Ilin. Growth, ion composition and stomatal conductance of peas exposed to salinity. *Cent. Eur. J. Biol.*, 5 (2010) 682-691.
- [3] Y.C. Liang, W.C. Sun, Y. G. Zhu, C. Peter. Mechanisms of silicon-mediated alleviation of abiotic stresses in higher plants: A review. *Environ. Pollut.* 147 (2007) 422-428.
- [4] E. Sacala. The influence of increasing doses of silicon on maize seedlings grown under salt stress. *J. Plant Nutr.*, 40 (2017) 819-827.
- [5] D.R. Hoagland, D.I. Arnon. The water-culture method for growing plants without soil. *Calif Agric Exp. Stat. Circ.*, 347 (1950) 1-32.
- [6] L.S. Bates. Rapid determination of free proline for water-stress studies. *Plant Soil*, 39 (1973) 205-207.
- [7] G. Holm. Chlorophyll mutations in barley. *Acta Agr. Scand.*, 4 (1954) 457.
- [8] D. Von Wettstein. Chlorophyll-letale und submikroskopische formwechsel der plastiden. *Exp. Cell Res.*, 12 (1957) 427-433.
- [9] O. Blokhina, E. Virolainen, K.V. Fagerstedt. Antioxidants, oxidative damage and oxygen deprivation stress. *Ann. Bot.*, 91 (2003) 179-194.
- [10] M.T. Nezami, A. Bybordi. Effects of silicon on photosynthesis and concentration of nutrients of *Brassica napus* L. in saline-stressed conditions. *J. Food Agric. Environ.*, 9 (2011) 655-659.
- [11] I. Maksimović, S. Belić, M. Putnik-Delić, I. Gani. The effect of sodium concentration in the irrigation water on pea yield and composition. *ECO Conference, Novi Sad* (2008) 231-235.

## A SPECTROSCOPIC AND SEMIEMPIRICAL QUANTUM CHEMICAL STUDY OF COPPER(II) PHTHALOCYANINATE

**Andrei Racu<sup>1,2\*</sup>, Mihai-Cosmin Pascariu<sup>1,3</sup>, Zoltán Szabadai<sup>1,4\*</sup>, Mircea Mracec<sup>5</sup>**

<sup>1</sup>Renewable Energies - Photovoltaic Laboratory, National Institute of Research & Development for Electrochemistry and Condensed Matter – INCEMC Timișoara, 144 Dr. Aurel Păunescu-Podeanu, RO-300569 Timișoara, Romania

<sup>2</sup>Institute of Applied Physics of the Academy of Sciences of Moldova, 5 Academiei, MD-2028 Chișinău, Moldova

<sup>3</sup>Faculty of Pharmacy, “Vasile Goldiș” Western University of Arad, 86 Liviu Rebreanu, RO-310414 Arad, Romania

<sup>4</sup>Faculty of Pharmacy, “Victor Babeș” University of Medicine and Pharmacy of Timișoara, 2 Eftimie Murgu Sq., RO-300041 Timișoara, Romania

<sup>5</sup>Department of Computational Chemistry, Institute of Chemistry Timișoara of Romanian Academy, 24 Mihai Viteazul Av., RO-300223 Timișoara, Romania  
e-mail: andrei.racu@gmail.com, szabadai@umft.ro

### Abstract

Copper(II) phthalocyaninate (CuPc) was studied using both the PM3 and PM7 semiempirical molecular orbital methods, and the results were compared with its XRD, FTIR and Raman experimental properties.

### Introduction

Organic semiconductors are intensively studied for applications in electronics, optics and spin-based information technology (spintronics) [1]. Among these materials, the blue pigment copper(II) phthalocyaninate (CuPc) is a common, low-cost and chemically modifiable p-type organic semiconductor [1,2].

CuPc (Fig. 1) exhibits a planar molecule consisting of a central metal atom bound to a ligand with extended  $\pi$  conjugated system [2,3]. It shows good thermal and chemical stability and can be easily deposited as a thin film [2] when its performance proves to be superior to that of single-molecule magnets over the same temperature range [1]. It thus holds promise for quantum information processing and medium-term storage of classical bits in all-organic devices on plastic substrates [1]. CuPc nanoribbons can also be fabricated using vapor phase deposition and these were studied for photoluminescence, with significant differences in the luminescent behavior being found between  $\alpha$ -CuPc and  $\beta$ -CuPc nanostructures [3].

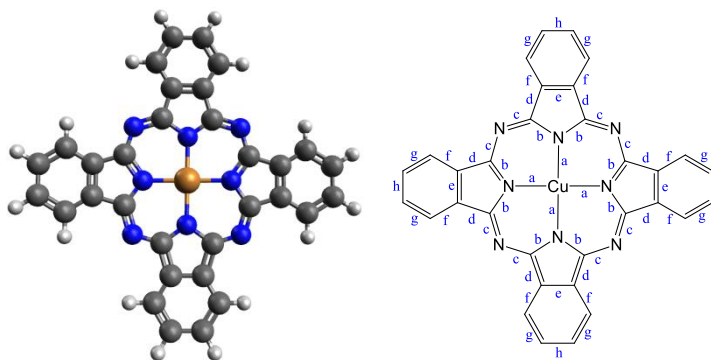


Figure 1. Molecular model (PM7) and notation of bonds for CuPc

In the past decades, the organic light-emitting diodes (OLEDs) based on CuPc as a buffer, hole injection or emitting layer, the organic solar cells (OSCs) based on CuPc as a donor material and the organic field-effect transistors (OFETs) based on CuPc as an active layer have been extensively studied due to this compound's interesting photoelectric properties: an optical gap ( $\sim 1.7$  eV) very suitable for visible absorption (i.e., usage in photovoltaic devices) and a transport gap ( $\sim 2.3$  eV) fit for electronic devices [2,3]. Near-infrared (NIR) photosensitive organic field-effect transistors based on CuPc/ErPc<sub>2</sub> heterojunction exhibit better properties when compared with the ErPc<sub>2</sub> single-layer ones, and thus good NIR photoresponsive layers can be obtained [2]. Also, the NIR light is intimately linked to industrial applications, such as NIR photodetectors and night vision [2].

In this paper, we use the PM3 and PM7 semiempirical molecular orbital methods to calculate some molecular properties of CuPc, like the bond lengths and the vibrational spectrum. We also compare the obtained results with the experimental spectroscopic data.

### Experimental

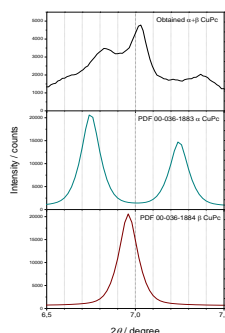
CuPc was obtained by using phthalic anhydride, copper(I) chloride, urea and ammonium molybdate, as described in the literature [4].

The UV/Vis spectrum (250–1000 nm) was acquired using an M-2000 (J.A. Woollam Co., USA) spectroscopic ellipsometer by diluting the sample with KBr, as pellets. The FTIR spectrum (400–4000 cm<sup>-1</sup>) was also acquired using KBr pellets, on a Vertex 70 (Bruker, Germany) FT-IR spectrometer. The Raman spectrum was obtained at room temperature on a Multi Probe Imaging – MultiView 1000 scanned probe microscopy (Nanonics Imaging, Israel) system, which incorporates the Shamrock 500i Spectrograph (Andor, UK). A laser wavelength of 514.5 nm was used as the excitation source, with a 20 s exposure time and a 300 l mm<sup>-1</sup> grating. The XRD diffraction pattern was obtained on a X'Pert PRO MPD (Philips-FEI PANalytical Company, Netherlands) diffractometer.

The PM3 [5] optimization was performed by using the HyperChem software [6]. The SCF “Convergence limit” was set at 10<sup>-5</sup> with an iteration limit of 100 and without using the “Accelerate convergence” procedure. For geometry optimization, the “Polak-Ribière (conjugate gradient)” algorithm was selected with an RMS gradient of 0.001 kcal/(Å mol).

For PM7 [7], the MOPAC2016 software [8] was used with the following keywords: CHARGE=0, PM7, DOUBLET, EF (or BFGS), OPT, BONDS, AUX, GRAPHF, PDBOUT, SCFCRT=1.D-10, PRECISE, GNORM=0.001, CYCLES=5000, LARGE. The BFGS (Broyden-Fletcher-Goldfarb-Shanno) algorithm gave very similar results with those obtained with the EF (Eigenvector Following) algorithm. Discarding the OPT keyword also gave very similar results in all cases. The Jmol [9] and Avogadro [10] programs were used for visualizing the molecular geometries.

## Results and discussion



The powder XRD peaks (Fig. 2) indicate that the synthesized CuPc is a mixture of  $\alpha$  and  $\beta$  phases, as seen when compared with the reference PDF data. The  $\beta$ -CuPc phase crystallizes in the monoclinic crystal system with space group P21/n and lattice parameters  $a=14.64 \text{ \AA}$ ,  $b=4.69 \text{ \AA}$ ,  $c=17.31 \text{ \AA}$ ,  $\alpha=90.00^\circ$ ,  $\beta=105.49^\circ$ ,  $\gamma=90.00^\circ$  [11].  $\alpha$ -CuPc crystallizes in the orthorhombic crystal system with lattice parameters  $a=12.97 \text{ \AA}$ ,  $b=12.15 \text{ \AA}$ ,  $c=6.66 \text{ \AA}$  and  $\alpha=\beta=\gamma=90^\circ$  [12]. The selected  $6.5\text{--}7.5^\circ 2\theta$  domain is suitable for the identification of  $\alpha$  and  $\beta$  phases of CuPc.

Figure 2. Comparison between the obtained diffractogram and standard CuPc patterns. Differences between  $\alpha$  and  $\beta$  phases of CuPc can also be revealed using optical absorption spectroscopy [3,13,14]. The obtained spectrum of CuPc (Fig. 3) consists of absorption peaks in the UV (B band) and red (Q band) spectral regions. One of the B band peaks is located at 330 nm, while the Q band has two peaks, located at 620 and 696 nm, in close agreement with the literature [3,15]. The peak at 620 nm in the Q band is assigned to the  $\pi\text{--}\pi^*$  transition of the CuPc molecule, while assignment of the peak from 696 nm is still under discussion: a  $\pi\text{--}\pi^*$  transition, an exciton peak, a surface state, a vibrational structure, and a Davydov splitting are possible candidates [15]. The difference between  $\alpha$  and  $\beta$  phases of CuPc can be observed via the shape change of the Q band [3].  $\alpha$  phase shows a more intense absorption at lower wavelengths, while a pronounced absorption at a higher wavelength is specific for the  $\beta$  phase [12,14]. Taking in consideration the literature reported results, we can confirm that the obtained absorbance spectrum is an evidence that the obtained compound is a mixture of  $\alpha$ - and  $\beta$ -CuPc [3].

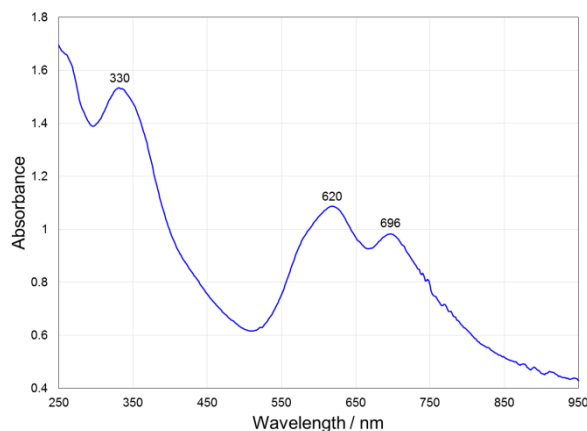


Figure 3. UV/Vis absorption spectrum of CuPc

The obtained Raman spectrum (Fig. 4) confirms the CuPc compound's formation, as seen in Table 1. The vibrational modes of Raman bands can be attributed to vibrations of the macrocycle, of the isoindole moieties, to C–H bendings and to the metal–nitrogen stretch.

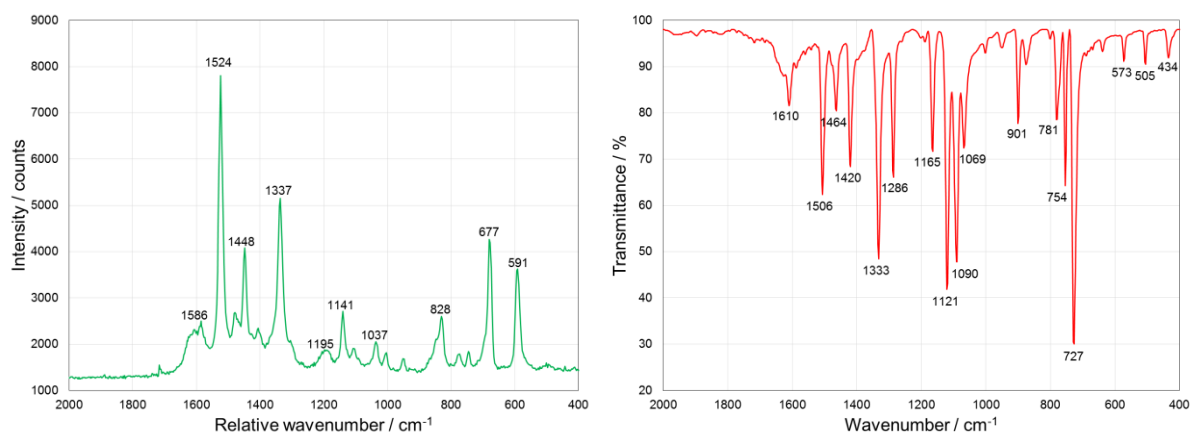


Figure 4. Raman (left) and FTIR (right) spectra of CuPc

Table 1. Raman lines identification and interpretation for CuPc

Our results	Literature results [16,17]			Interpretation
	$\beta$ -CuPc powder	$\alpha$ -CuPc film	$\beta$ -CuPc film	
$\alpha + \beta$ CuPc powder	$\beta$ -CuPc powder	$\alpha$ -CuPc film	$\beta$ -CuPc film	
Peak position (cm <sup>-1</sup> )	Peak position (cm <sup>-1</sup> )	Peak position (cm <sup>-1</sup> )	Peak position (cm <sup>-1</sup> )	
591	593	591	590	-
677	677	684	681	16 membered inner ring breathing
771	773	-	-	macrocycle deformation
828	830	839	833	C-N stretching (aza groups)
841	848	-	-	-
1004	1008	1010	1010	isoindole in-plane bending
1037	1036	1041	1040	C-H bending-isoindole group
1102	1108	1109	1104	C-H bending out of plane
1195	1193	-	-	isoindole in-plane bending
1337	1336	1338	1339	C $_{\alpha}$ -C $_{\beta}$ stretching pyrrole group
1403	1408	1414	1409	C-N stretching pyrrole group
1448	1448	-	-	C-N stretching
1524	1523	1527	1523	C $_{\alpha}$ -C $_{\beta}$ stretching pyrrole group
1586	1586	1589	1586	-

However, due to the small shift in the peak positions attributed to the  $\alpha$ - and  $\beta$ -CuPc phases, this technique is not relevant for the identification of the CuPc phase.

The computed vibrational frequencies (PM7) and bond lengths (PM3 and PM7) for CuPc are shown in Table 2 and, respectively, Table 3.

Table 2. Simulated (PM7, with or without using the OPT keyword) and experimental vibrational frequencies for CuPc; the Raman and FTIR spectra of CuPc are shown in Fig. 4

EF		BFGS		Experimental FTIR/Raman*
w/ OPT	w/o OPT	w/ OPT	w/o OPT	
493.04 (1.2)	502.45 (1.0)	502.72 (1.1)	503.71 (1.1)	505 (w)/495 (w)
563.78 (2.0)	558.19 (1.8)	558.54 (1.9)	558.50 (1.8)	573 (w)/565 (sh)
				-/591 (s)
				681 (w)/677 (s)
726.59 (5.5)	727.91 (5.6)	728.04 (5.5)	727.56 (5.6)	727 (vs)/-
745.99 (1.0)	758.70 (1.3)	759.15 (1.3)	759.08 (1.3)	754 (m)/743 (w)
				781 (w)/771 (w)
819.83 (1.3)	822.18 (1.3)	820.21 (1.3)	823.04 (1.3)	800 (w)/828 (m)
				901 (w)/-
				1032 (w, sh)/1037 (w)
				1069 (m)/-
1101.13 (1.0)	1105.76 (0.8)	1105.30 (0.8)	1106.17 (0.8)	1090 (s)/1100 (w)
				1121 (s)/1124 (w, sh)
				-/1141 (m)
				1165 (m)/1157 (w, sh)
				1192 (w)/1195 (w)
1227.80 (1.4)	1227.36 (1.5)	1227.64 (1.4)	1227.76 (1.4)	
1276.59 (1.8)	1277.30 (1.9)	1276.76 (1.8)	1277.06 (1.9)	1286 (m)/-
1289.63 (2.4)	1291.75 (1.9)	1292.46 (2.0)	1291.97 (1.9)	
				1333 (s)/1337 (s)
1369.80 (2.5)	1373.59 (2.2)	1373.53 (2.1)	1373.93 (2.2)	
1403.36 (2.5)	1403.97 (3.8)	1404.40 (3.9)	1402.99 (3.9)	1420 (m)/1422 (w)
				-/1448 (s)
				1464 (w)/1477 (w)
				1506 (m)/-
				1518 (w)/1524 (vs)
1540.67 (2.4)	1541.27 (2.8)	1540.49 (3.5)	1541.00 (2.9)	
1559.21 (16.6)	1562.96 (15.6)	1561.26 (15.0)	1563.30 (15.5)	
				1587 (w)/1586 (w)
				1610 (w)/1601 (w)
1651.88 (8.5)	1647.03 (9.0)	1647.34 (8.6)	1646.89 (8.8)	
1712.49 (7.5)	1715.20 (6.7)	1714.84 (6.8)	1715.62 (6.8)	
1727.13 (7.8)	1729.34 (9.7)	1728.93 (9.7)	1729.61 (9.8)	

\*w – weak, m – medium, s – strong, vs – very strong, sh – shoulder



Table 3. Computed and experimental bond lengths (in Å) for CuPc

Bond (see Fig. 1)	PM3 ( $\Delta H_f = 132.641$ kcal/mol)	PM7 ( $\Delta H_f = 240.303$ kcal/mol)	Experimental
a	1.899-1.900	1.982	1.950-1.953
b	1.401-1.487	1.367-1.423	1.379-1.389
c	1.331-1.353	1.326-1.341	1.344-1.371
d	1.443-1.464	1.469-1.485	1.441-1.490
e	1.417-1.420	1.425	1.407
f	1.387-1.397	1.377-1.381	1.377-1.399
g	1.394-1.399	1.403-1.405	1.372-1.401
h	1.398-1.403	1.393	1.399-1.412
C-H	1.094-1.096	1.089-1.091	-

### Conclusion

CuPc was synthesized and spectroscopically analyzed. The XRD, Raman, FTIR and UV/Vis spectra confirmed the compound's identity. Both PM3 and PM7 gave good results regarding the molecular geometry. The vibrational spectra obtained with the PM7 method was only partially confirmed by the experimental FTIR and Raman spectra.

### Acknowledgements

This work was supported by the Romanian National Authority for Scientific Research (CNCS-UEFISCDI) through project PN 16 14 03-10. We are gratefully acknowledging the generous support of J.J.P. Stewart for providing an academic license for the MOPAC2016.

### References

- [1] M. Warner, S. Din, I.S. Tupitsyn, G.W. Morley, A.M. Stoneham, J.A. Gardener, Z. Wu, A.J. Fisher, S. Heutz, C.W.M. Kay, G. Aeppli, *Nature* 503 (2013) 504.
- [2] J. Zhang, Y. Li, Y. Tang, X. Luo, L. Sun, F. Zhao, J. Zhong, Y. Peng, *Synth. Met.* 218 (2016) 27.
- [3] W.Y. Tong, H.Y. Chen, A.B. Djurišić, A.M.C. Ng, H. Wang, S. Gwo, W.K. Chan, *Opt. Mater. (Amsterdam, Neth.)* 32 (2010) 924.
- [4] F. H. Moser, A. L. Thomas, *Phthalocyanine Compounds*, Reinhold, New York, 1963.
- [5] J.J.P. Stewart, PM3, in: *Encyclopedia of Computational Chemistry*, Wiley, 2002.
- [6] HyperChem™ Professional, Hypercube, Inc., 1115 NW 4th Street, Gainesville, Florida 32601, USA, version 8.0.10 for Windows.
- [7] J.J.P. Stewart, *J. Mol. Model.* 19 (2013) 1-32.
- [8] J.J.P. Stewart: MOPAC2016 (Version: 16.035W), Stewart Computational Chemistry, Colorado Springs, CO, USA, <http://OpenMOPAC.net/>.
- [9] Jmol: an open-source Java viewer for chemical structures in 3D, <http://www.jmol.org/>.
- [10] (a) Avogadro: an open-source molecular builder and visualization tool. Version 1.1.0, <http://avogadro.cc/>; (b) M.D. Hanwell, D.E. Curtis, D.C. Lonie, T. Vandermeersch, E. Zurek, G.R. Hutchison, *J. Cheminf.* 4 (2012) 17.
- [11] L. Ruiz-Ramirez, A. Martinez, J. Mendieta, J.L. Brioso, E. Estop, J.S. Chinchon, *Afinidad* 44 (1987) 45.
- [12] R. Prabakaran, R. Kesavamoorthy, G.L.N. Reddy, F.P. Xavier, *Phys. Status Solidi B* 229 (2002) 1175.

- [13] W.Y. Tong, A.B. Djurišić, M.H. Xie, A.C.M. Ng, K.Y. Cheung, W.K. Chan, Y.H. Leung, H.W. Lin, S. Gwo, *J. Phys. Chem. B* 110 (2006) 17406.
- [14] E.A. Lucia, F.D. Verderame, *J. Chem. Phys.* 48 (1968) 2674.
- [15] A.T. Davidson, *J. Chem. Phys.* 77 (1982) 168.
- [16] R. Prabakaran, R. Kesavamoorthy, G.L.N. Reddy, F.P. Xavier, *Phys. Status Solidi B* 229 (2002) 1175.
- [17] W. R. Scheidt, W. Dow, *J. Am. Chem. Soc.* 99 (1977) 1101.

## FUZZY LINEAR PROGRAMMING IN INVESTMENTS

Nebojsa M. Ralevic<sup>1</sup>, Vladimir Dj. Djakovic<sup>2</sup>, Goran B. Andjelic<sup>3</sup>, Jelena S. Kiurski<sup>4</sup>

<sup>1</sup>*University of Novi Sad, Faculty of Technical Sciences, Department of Fundamentals Sciences, Novi Sad, Serbia*

<sup>2</sup>*University of Novi Sad, Faculty of Technical Sciences, Department of Industrial Engineering and Management, Novi Sad, Serbia*

<sup>3</sup>*Educons University, Faculty of Business Economy, Sremska Kamenica, Serbia*

<sup>4</sup>*University Business Academy, Faculty of Economics and Engineering Management, Novi Sad, Serbia*

*e-mail: nralevic@uns.ac.rs, v\_djakovic@uns.ac.rs, goran.andjelic@educons.edu.rs, jelena.kiurski7@gmail.com*

### Abstract

The possibility of the investment performances assessment is especially important in the dynamic business conditions. Hence, the appropriate methodology enables an optimal investment decision. The main objective of the research is to test and analyse the possibility of fuzzy linear programming application in the investment processes with special attention to the investment performances. The methodology used in the research understands the methods of analyses and synthesis and also application of the fuzzy linear programming. The quantitative and qualitative results of the research imply that the application of fuzzy linear programming provide important information about the effects from the investment activities.

**Keywords:** fuzzy, fuzzy linear programming, investment performances, investments.

### Introduction

The application of the contemporary engineering methods, techniques and tools present a necessity in the management processes, particularly in the investment processes. Namely, the investments processes are influenced by the dynamic nature of the investments, regarding its risk and return characteristics. The complexity of the investment environment induces the application of wide variety of mathematical methods in the function of formulating, implementation and evaluation the adequate investment strategy. In that way, investors are provided with the quality, scientific based information about the investments, determining different investment scenario effects, that is, outcomes from the investment activities. Solid, scientific based information is the key for acquiring and maintaining the competitive advantage.

When describing the fuzziness of certain system, it is important to observe it as an inherent characteristic, that is, phenomena originating from a fuzzy structure (Ralevic et al, 2011). Fuzzy linear programming presents an advantage while enabling the adequate investment decision making process. By its application it is possible to determine whether concrete investment provide the expected (requested) return from the investment activities. Specificities of the transitional markets, especially the market of the Republic of Serbia, require special attention while analysing the effects from the investment activities. Turbulent and dynamic business conditions understand the presence of high risk level and often even high level of uncertainty. Consequently, it is essential to gather high quality information about the planned investment and thus enabling the optimal investment decision.

Having in mind all mentioned above, the determination of the possibility and specificities of the fuzzy linear programming application on the transitional market of the Republic of Serbia present solid base for the academic and investment community, while recognizing its place, role and importance in the contemporary investment processes.

### Methodology

The methodology used in the research comprises the application of the fuzzy linear programming on the data acquired from the Belgrade Stock Exchange (official internet site). The research sample present the Prime listing daily data of the following stocks:

- AERO - Aerodrom Nikola Tesla a.d., Beograd;
- NIIS - NIS a.d., Novi Sad.

The general type of fuzzy linear programming is formulated as follows:

$$\begin{aligned} & \max \sum_{j=1}^n \hat{c}_j \hat{x}_j \\ & \sum_{j=1}^n \hat{a}_{ij} \hat{x}_j \leq \hat{b}_i, i = 1, \dots, m \\ & \hat{x}_j \geq 0, j = 1, \dots, n \end{aligned} \quad (1)$$

where  $\hat{a}_{ij}, \hat{b}_i, \hat{c}_j$  are fuzzy numbers, and  $\hat{x}_j$  are variables whose states are fuzzy numbers, the operation of addition and multiplication are operations of fuzzy arithmetic and  $\leq$  denotes the ordering of fuzzy numbers.

Special cases are considered:

$$\begin{aligned} & \max \sum_{j=1}^n c_j x_j \\ & \sum_{j=1}^n a_{ij} x_j \leq \hat{b}_i, i = 1, \dots, m \\ & x_j \geq 0, j = 1, \dots, n \end{aligned} \quad (2)$$

Let fuzzy numbers  $\hat{b}_i$  have the form

$$\hat{b}_i(x) = \begin{cases} 1, & x < b_i \\ \frac{b_i + d_i - x}{d_i}, & b_i \leq x \leq b_i + d_i \\ 0, & x > b_i + d_i \end{cases} \quad (3)$$

Lower and upper of the optimal values are calculated,  $z_l$  and is  $z_u$  is obtained by solving the standard programming problems, respectively.

$$\begin{aligned} & \max \sum_{j=1}^n c_j x_j \\ & \sum_{j=1}^n a_{ij} x_j \leq b_i, i = 1, \dots, m \\ & x_j \geq 0, j = 1, \dots, n \end{aligned} \quad (4)$$

$$\begin{aligned} & \max \sum_{j=1}^n c_j x_j \\ & \sum_{j=1}^n a_{ij} x_j \leq b_i + d_i, i = 1, \dots, m \\ & x_j \geq 0, j = 1, \dots, n \end{aligned} \tag{5}$$

The fuzzy sets of optimal values  $G$  fuzzy subset of  $R^n$  is defined by

$$G(x) = \begin{cases} 1, & \mathbf{c}x < z_u \\ \frac{\mathbf{c} \cdot \mathbf{x} - z_l}{z_u - z_l}, & z_l \leq \mathbf{c}x \leq z_u, \\ 0, & \mathbf{c}x > z_l \end{cases} \tag{6}$$

The problem becomes the classical problem

$$\begin{aligned} & \max \lambda \\ & \lambda(z_u - z_l) - \mathbf{c} \cdot \mathbf{x} \leq -z_l \\ & \lambda d_i + \sum_{j=1}^n a_{ij} x_j \leq b_i + d_i, i = 1, \dots, m \\ & \lambda, x_j \geq 0, j = 1, \dots, n \end{aligned} \tag{7}$$

The above problem is a problem of finding  $\mathbf{x} \in R^n$  such that

$$\left( \bigcap_{i=1}^m D_i \right) \cap G(x) \tag{8}$$

(where  $D_i(x) = \hat{b}_i \left( \sum_{j=1}^n a_{ij} x_j \right)$ ) reaches the maximum value.

### Results and discussion

In order to overcome shortcomings in stock trading due to the uncertainty of the stock prices i.e. their volatility, in the simplified model considered, usually solved using linear programming (LP), fuzzy linear programming (FLP) is applied. Coefficients and unknowns which are crisp values in LP, in FLP are fuzzy numbers.

Such problem, as it is to be seen, is reduced to solving multiple linear programs, usually by classic simplex method using software, except in simple cases where the graphic method can also be applied.

The practical application of fuzzy linear programming is considered on AERO and NIIS stocks. Let the stock market price of AERO 1350 RSD and NIIS 680 RSD. Investment capital available for the investment activities is in the following range: 1 mil RSD to 1,2 mil RSD. Expected earnings for AERO is 5 RSD and for NIIS is 7 RSD.

The limitation of the investment is the following:

- Trade volume: 1000 to 1200;
- Investment capital: 1 mil RSD to 1,2 mil RSD.

The problem is to solve the next fuzzy FLP in the described way.

$$\begin{aligned} \max z &= 5x_1 + 7x_2 \\ x_1 + x_2 &\leq \hat{b}_1 \\ 1350x_1 + 680x_2 &\leq \hat{b}_2 \\ x_1, x_2 &\geq 0 \end{aligned}$$

$$\hat{b}_1(x) = \begin{cases} 1, & x < 1000 \\ \frac{1200-x}{100}, & 1000 \leq x \leq 1200, \\ 0, & x > 1200 \end{cases}$$

$$\hat{b}_2(x) = \begin{cases} 1, & x < 1000000 \\ \frac{1200000-x}{200000}, & 1000000 \leq x \leq 1200000, \\ 0, & x > 1200000 \end{cases}$$

### Conclusion

Research results point to the adequacy of the fuzzy linear programming application on the transitional market of the Republic of Serbia. It is important to adequately determine the specificities of the investment focusing on the effects from the investment activities. Thus, the investment limitations, particularly trade volume and investment capital, affect the application performance of the fuzzy linear programming.

Further research in the subject field understand the continuous application of the fuzzy linear programming while focusing to the required return and investors risk preference while recognizing the dynamic conditions of the environment.

### Acknowledgements

The authors acknowledge the financial support of the Ministry of Education, Science and Technological Development of the Republic of Serbia, within the Project No. TR34014.

### References

- [1] N.M. Ralević, V.Dj. Djaković, G.B. Andjelić, I.M. Kovačević, J.S. Kiurski, L.Lj. Čomić, Fuzzy Prediction Based on Regression Models: Evidence from the Belgrade Stock Exchange – Prime Market and Graphic Industry, SISY 2011, IEEE 9th International Symposium on Intelligent Systems and Informatics, September 8-10, 2011, Obuda University, Budapest, Hungary; Subotica Tech, Serbia; University of Novi Sad; Subotica, Serbia, pp. 151-156.
- [2] D.F. Li, S.P. Wan, Fuzzy linear programming approach to multiattribute decision making with multiple types of attribute values and incomplete weight information, Appl. Soft. Comput. 13(11), 2013, pp. 4333-4348.
- [3] D. Dubois, H. Prade, Fuzzy Sets and Systems: Theory and Applications, Academic Press, New York, 1980.
- [4] H. Tanaka, H. Ichihashi, K. Asai, A formulation of fuzzy linear programming problem based on comparison of fuzzy numbers, Control Cybern. 3(3), 1991, pp. 185-194.
- [5] R.C. Wang, T.F. Liang, Application of fuzzy multi-objective linear programming to aggregate production planning, Comput formulation Ind Eng. 46(1), 2004, pp. 17-41.

## HIGH PERFORMANCE MASS SPECTROMETRY FOR ADVANCED INTERACTOMICS STUDIES

**Adrian C. Robu<sup>1,2</sup>, Laurentiu Popescu<sup>1,2</sup>, Daniela G. Seidler<sup>3</sup>, Alina D. Zamfir<sup>1,4</sup>**

<sup>1</sup>*Mass Spectrometry Laboratory, National Institute for Research and Development in Electrochemistry and Condensed Matter, Plautius Andronescu Str. 1, RO-300224, Timisoara, Romania*

<sup>2</sup>*Faculty of Physics, West University of Timisoara, Blvd. Vasile Parvan 4, RO-300223, Timisoara, Romania*

<sup>3</sup>*Institute for Physiological Chemistry and Pathobiochemistry, University of Münster, Waldeyer Str. 15, D-49149, Münster, Germany*

<sup>4</sup>*Department of Chemical and Biological Sciences, "Aurel Vlaicu" University of Arad, Revolutiei Blvd. 77, RO-310130, Arad, Romania  
e-mail: alina.zamfir@uav.ro*

### **Abstract**

Fibroblast growth factor-2 (FGF-2) is a glycosaminoglycan (GAG) binding protein, involved in different biological processes, such as angiogenesis, bone signaling, embryonic development, morphogenesis or cartilage metabolism. GAGs, one of its binding partners, are long-unbranched polysaccharides exhibiting a repeating disaccharide unit. Moreover, preceding studies have shown that GAGs play an important role in tissue development, cellular behavior or extracellular matrix (ECM) organization. The FGF-GAG noncovalent interactions are of high importance in the biological and biomedical fields of research, as a result of their influence in the tissue regeneration and cell proliferation processes. Here, we have employed one of the most advanced mass spectrometric (MS) techniques consisting of fully automated chip-nano electrospray (nanoESI), coupled to a quadrupole time-of-flight (QTOF) MS for studying the FGF-GAG noncovalent complexes.

The experiments were conducted in 10 mM ammonium acetate/formic acid, pH 6.8, by incubating FGF-2 and CS disaccharides dissolved in buffer; aliquots were collected after 5, 10, 30, 60 and 90 minutes and further submitted to chip-based MS analysis. For the first time, a CS disaccharide was involved in a binding assay with FGF-2. The detected complexes in the screening experiments were further characterized by top-down fragmentation in tandem MS (MS/MS) using collision induced-dissociation (CID) at low ion acceleration energies. CID MS/MS provided data showing for the first time that the binding process occurs via SO<sub>3</sub> located at C4 in the GalNAc moiety.

### **Acknowledgements**

This project was supported by the Romanian National Authority for Scientific Research, UEFISCDI, project PN-III-P4-ID-PCE-2016-0073 granted to ADZ.



**ALLELOPATHIC EFFECT OF *Xanthium strumarium* L. AND *Abutilon theophrasti* Med. EXTRACTS ON GERMINATION OF MAIZE AND SOYBEAN SEED**

**Nataša Samardžić<sup>1\*</sup>, Bojan Konstantinović<sup>1</sup>, Milena Popov<sup>1</sup>, Milan Blagojević<sup>1</sup>, Branimir Pavlič<sup>2</sup>, Jelena Vladić<sup>2</sup>**

<sup>1</sup>University of Novi Sad, Faculty of Agriculture, Department for Environmental and Plant Protection, Trg Dositeja Obradovića 8, 21000 Novi Sad, Serbia

<sup>2</sup>University of Novi Sad, Faculty of Technology, Bulevar Cara Lazara 1, 21000 Novi Sad, Serbia

e-mail: natasam@polj.uns.ac.rs

**Abstract**

During 2014 allelopathic effects of *Xanthium strumarium* L. and *Abutilon theophrasti* Med. extracts to germination and initial development of maize (*Zea mays* L.), and soybean (*Glycine max* L.) were studied in laboratory conditions. In addition to the Water extracts out of dry mass of the tested weed species, extracts made by use of hexane, ethyl acetate and methanol in different concentrations were also used. The applied concentrations were 10, 20, 30 and 40 g/l of dry matter made out of weed species in the 3-4 leaf stage of development. Inhibiting effect of water extract from dry matter of *X. strumarium* and methanol extract from which methanol part was evaporated to maize seed epicotyls and hypocotyls length was established. In comparison to the control, the maximum concentration of 40 g / l of the extract made from Water solution of *A. theophrasti* showed inhibitory effect on soybean seed epicotyls and hypocotyls length. The applied extracts made out of dry matter of the both of the studied weed species *X. strumarium* and *A. theophrasti* reduced maize seed germination for 14.8-26.83% and soybean seed germination for 18.5-35.82%, in comparison to the control in which it was 95% and 92%, respectively. After germination in a climate chamber, epicotyls' and hypocotyls' length of maize and soybean seeds was measured three, six and ten days following spraying by extracts.

**Introduction**

Weeds effect harmfully to crops by releasing phytotoxines from seeds, by decomposition of remainings, leaching and exudates [1]. Plants release harmful chemicals into the environment, reducing growth and establishment of other plants near them: the process known as allelopathy. Allelopathy is natural ecological phenomenon of relationship between organisms which can be applied for control of weeds, pests and diseases in field crops [2]. High allelopathic potential of *A. theophrasti* is shown due to inhibition of germination and growth of competitive plants, by which it reaches superior position. Although allelopathic interactions of *A. theophrasti* with other crops have been known for several decades, weak attention is paid to the biochemical interactions of this weed species, [3], that indicates negative allelopathic effect of *A. theophrasti* to soybean, maize and tomato crops [4]. Shajie and Saffari (2007) [5] established that extract made of leaves and petioles of *X. strumarium* significantly reduced germination and growth of *Zea mays* L, *Brassica napus* L, *Sesamum indicum* L, *Lens culinaris* Medic. and *Cicer arietinum* L. seedlings. Some researchers studied the effects of Water solutions made from different parts of plants, as well as their impact on other plant species [6] [7]. Different allelopathic activity of different parts of the same weed species also differs in its capabilities of harmful effects to germination and beginning growth of cultivated plants [8] [9]. Plant can

show inhibiting, but also stimulating effect to germination and growth of the nearby plants. In addition to examples of biochemical competition between weed and crop plants, there are examples of allelopathic interference between cultivated plants. This is the best illustrated by long time applied rotation system *Zea mays* (maize), *Glycine max* (soybean). It is observed that the rotation of these crops provides up to 20% higher yields [10].

### Experimental

In 2012, at locality Kać near Novi Sad plant parts of *Abutilon theophrasti* Med. and *Xanthium strumarium* L. (stem and leaf) were collected. Water extract was prepared in the following manner: in 0.5 l of water, 150 g of chopped green mass of leaves and stems of *Abutilon theophrasti* Med. and *Xanthium strumarium* L were immersed. Plant material was left in water for 96 hours at room temperature, after which it was removed, and the extract was filtered by vacuum filter. Filter paper in Petri dishes (150 mm x 25 mm) with germinated seed of the assayed soybean and maize crops was saturated by 8 ml of the extract. Control was moistened by distilled water. The assay was performed according to the method of Šćepanović *et al.*, 2007 [11]. In addition to the applied aqueous extracts, extracts made by use of methanol, hexane and ethyl acetate, from which by evaporation methanol, hexane and ethyl acetate were thrown, were also applied. All four extracts made of the above ground parts of *Abutilon theophrasti* Med. and *Xanthium strumarium* L. were made in concentrations of 10, 20, 30 and 40 g/l. By extracts treated soybean and maize seed were germinated in climatic chamber [12] and seed surface was sterilized according to Elemaru and Filhou (2005) [13].

The assays were set up according to the randomized block design with 4 replications. Each Petri dish contained 25 soybean and maize seeds, i.e. 100 seeds per treatment. All measurements were conducted third, sixth and tenth day after moistening of the studied crops seed. The existence of allelopathic activity of these two studied weed species to the soybean and maize crops were established by measurement of the crops seed epicotyls (mm) and hypocotyls (mm) length and germination (%) [11].

### Results and discussion

Experimental data confirm results of other authors [14] [2], in which allelopathic effects were reflected in inhibition of germination, that was even more pronounced for the growth of seedlings. Germination of the studied maize seed was 95% and soybean seed 92%. (Statistica 10) The significant difference of average values of hypocotyls length was tested by statistical data analysis after treatment with extracts made of the above ground parts of *A. theophrasti* and *X. strumarium*. In the study, allelopathic effect of weed species *A. theophrasti* and *X. strumarium* to the beginning growth stages and development of soybean and maize hypocotyls was confirmed, while epicotyls growth was not statistically significantly different from control values for soybean. Water extracts of the above ground (leaves and stem) parts of *A. theophrasti* in concentrations of 20, 30 and 40 g/l showed inhibiting effects to the length of soybean hypocotyls in values (3.88mm; 4.01mm; 4.3mm), lower in comparison to the control value of 20.98mm. All concentrations of methanol extract, hexane and ethyl acetate showed statistically significant difference in comparison to the control. The highest difference in comparison to the control showed hexane extracts made of *A. theophrasti* in concentration of 40 g/l, with measured hypocotyls length of 13.46mm, and control value of 20.98mm (Figure 1).

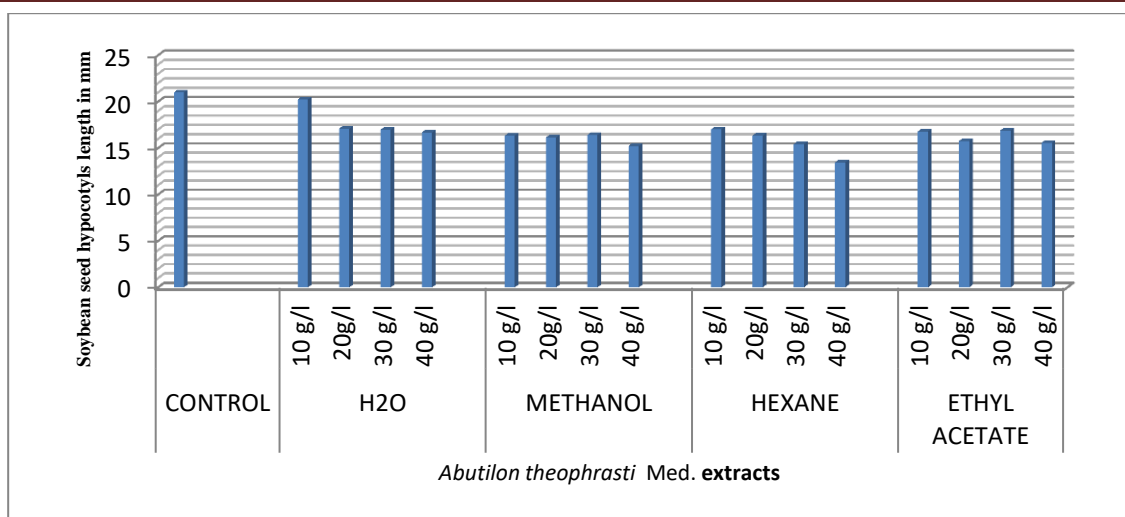


**Figure 1** Measured values of soybean seed hypocotyls after treatment with *Abutilon theophrasti* Med. extracts.

All concentrations of extractions of hexane and ethyl acetate made of *X. strumarium* had inhibiting effect of the growth of maize hypocotyls. Hexane extraction of 40 g/l reduced hypocotyls growth for 22.57% in comparison to the control value, while ethyl acetate extract in concentration of 40g/l reduced maize seed hypocotyls for 24% in relation to the control. Water extracts of *X. strumarium* had statistically significant effect to the hypocotyls growth in higher concentrations of 30 and 40 g/l, reducing hypocotyls for 14.8% and 16.29%, respectively. Methanol extraction of *X. strumarium* did not show statistically significant effect in concentration of 10g/l, but in remaining three concentrations it inhibited maize seed hypocotyls length. Methanol extraction of *X. strumarium* in concentration 40g/l showed the best effect, reducing maize seed hypocotyls growth for 26.83% in comparison to the control (Figure 2).

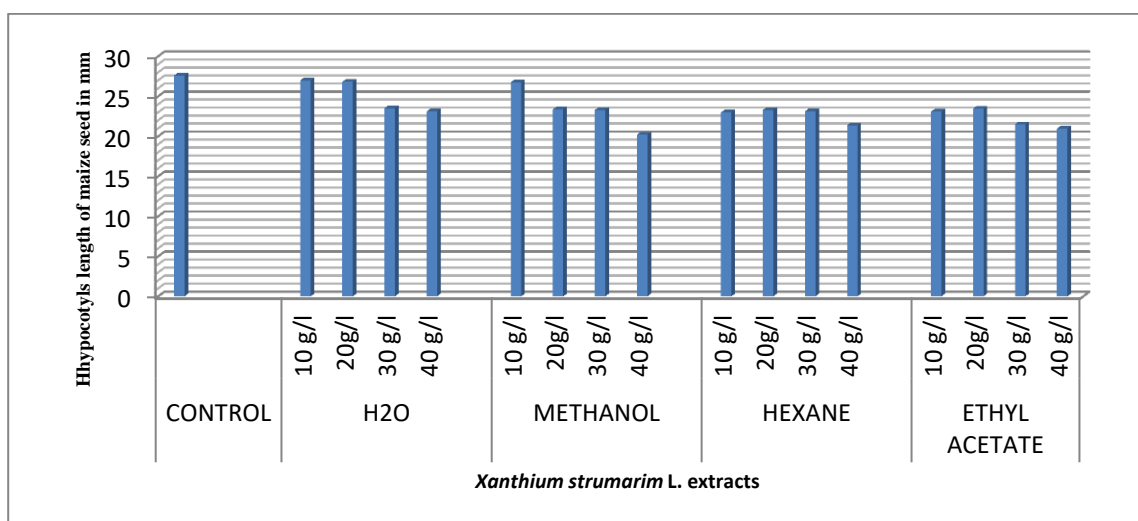


**Figure 2** Measured values of maize seed hypocotyls, after treatment with *Xanthium strumarium* L. extracts.

The increase of maize seed hypocotyls statistically differed in comparison to the control value only in extracts with hexane and methanol in the highest concentrations of 40g/l. Epicotyls length of maize seed treated by hexane extract made of *X. strumarium* was 6.17mm and control value was 8.43mm. Epicotyls length of maize seed treated by methanol extract made of *X. strumarium* was 5.83mm, and control value was 8.43mm.

### Conclusions

Based upon conducted studies, data were obtained on the effect of effect of *Abutilon theophrasti* Med. and *Xanthium strumarium* L. extracts on hypocotyls and epicotyls length of soybean and maize seed. Effect of *Abutilon theophrasti* Med. extract in tested concentrations of 10, 20, 30 and 40 g/l to the growth of soybean seed hypocotyls was between 18.5% in water extract, up to 35.82% in hexane extract, which was lower in comparison to the control. Effect of *Xanthium strumarium* L. extract in tested concentrations of 10, 20, 30 and 40 g/l to the growth of maize seed hypocotyls was between 14.8% in water extract, up to 26.83% in methanol extract, which was lower in comparison to the control. The tested concentrations did not show significant deviations in epicotyls length except for the two *Xanthium strumarium* L. extracts in the highest concentration of 40g/l.

### References

- [1] S. S. Narwal, Scienlific Publishers, Jodhapur, India, 2004.
- [2] Z. Ashrafi, H. Mashhadi, S. Sadeghi, Pakistan Journal of Weed Science Research, 13(1-2) (2007) 99 -112.
- [3] J. B. Gressel, L.G. Holm, Weed Research 4 (1) (1964) 44-53.
- [4] J.R. Qasem, C.L. Foy, Allelopathy in Agroecosystems, (2001) 43-119.
- [5] E. Shajie, M. Saffari, Allelopathy Journal. 19 (2007) 501-506.
- [6] G. Kazinczi, I. Beres, J. Mikulas, E. Nadasy, Journal of Plant Diseases and Protection, 19 (2004) 301-308.
- [7] B. Konstantinović, N. Samardžić, M. Blagojević, Bo. Konstantinović, The 7<sup>th</sup> International symposium, Temisoara, (2013), pp. 36-37.
- [8] A. Aziza, A., Tanveer, M., Ali, B., Yasin, H., Babar, M.A. Nadeem, Allelopathy Journal, 22 (2008) 25-34.
- [9] B. Konstantinović, M. Meseldžija, M. Blagojević, N. Samardžić, Bo. Konstantinović, 9 Kongres o korovima, Zlatibor, (2012) 132-133.
- [10] S. J.H. Rizvi, V. Rizvi, Chapman & Hall. London (1992).
- [11] M. Šćepanović, N. Novak, K. Barić, Z. Ostojić, N. Galzina, M. Goršić, Agronomski glasnik 6/2007, Izvorni znanstveni članak (2007):.
- [12] S.U. Chon, Y-M. Kim, J-C. Lee, European Weed Research Society Weed Research, 43,(2003), 444–450.
- [13] V. Elemar, V. Filho, Brazilian Society on Weed Science. Congress Xs 24, Svaio Pedro, BRESIL, 40(1) (2005) 217.
- [14] M. Turk, A. Tawaha, Pakistan Journal Agronomy, 1(2002), 28-30.

ALLELOPATHIC EFFECT OF *Cannabis sativa* L. ESSENTIAL OIL ON INITIAL GROWTH OF *Chenopodium album* L.

Konstantinović Bojan<sup>1</sup>, Vidović Senka<sup>2</sup>, Stojanović Anamarija<sup>3</sup>, Kojić Mirjana<sup>4</sup>, Samardžić Nataša<sup>1\*</sup>, Popov Milena<sup>1</sup>, Blagojević Milan<sup>1</sup>, Gavarić Aleksandra<sup>2</sup>, Pavlić Branimir<sup>2</sup>

<sup>1</sup> University of Novi Sad, Faculty of Agriculture, Department of Environmental and Plant Protection, Trg Dositeja Obradovića 8, 21000 Novi Sad, Serbia

<sup>2</sup> University of Novi Sad, Faculty of Technology, Bulevar cara Lazara 1, 21000 Novi Sad, Serbia

<sup>3</sup> Institute of field and vegetable crops, Maksima Gorkog 30, 21000 Novi Sad, Serbia

<sup>4</sup> PhD grant student of Ministry of education science and technological development  
e-mail:natasam@polj.uns.ac.rs

### Abstract

Allelopathy is increasingly gaining importance due to the tendency to avoid the use of synthetic herbicides. Research is increasingly focused on the finding of plant compounds that have allelopathic properties to weed species. The aim the study is to examine the allelopathic potential of *Cannabis sativa* L. essential oil in relation to the initial growth of the weed species of *Chenopodium album* L. The essential oil was obtained by the process of distillation of dry plant material collected during the ripening phase. The concentrations of essential oil were 200, 400, 600 and 800ml/l, while distilled water was used in the control. The parameters that were studied were the length of the hypocotyl and the length of the epicotyl *C. album* L. All investigated concentrations of essential oil exhibited an inhibitory effect. The average length of hypocotyl *C. album* L. in control was 2.67cm while in the smallest concentration it was 1.9cm. The average length of epicotyl *C. album* L. in control was 2.7cm and in the lowest applied concentration of 1.67cm. Increasing concentrations of essential oil increased the inhibitory effect. The obtained results indicate that it is possible to use *C. sativa* L. essential oil as bioherbicides for the control of *C. album* L.

### Introduction

The potential damage to human health and the environment from herbicides is regarded as a real problem today. This problem has resulted in an increase in interest in alternative methods that lead to the discovery of biodegradable compounds [1]. The properties of certain compounds to inhibit the germination of weed seeds and suppress their growth are attributed to allelopathy, which is very important and can be considered an alternative, non-chemical measure of weed control [2]. Interfering the normal functioning and suppressing growth of cultivated plants, weeds lead to yield reductions of up to 34% [3]. The exploitation of allelopathic properties in plants may give promising results [4]. Certain compounds derived from plants are used as repellents and pesticides, and the best known examples are compounds obtained from the following plant species: *Allium sativum* L., *Ricinus communis* L., *Tagetes patula* L., *Tanacetum vulgare* L., *Azadirachta indica* L., *Chrysanthemum cinerariifolium* (Trevir.) Vis., *Nicotiana tabacum* L., *Strychnos nux-vomica* L. [5]. Aromatic and medicinal plants are investigated as crops with pronounced allelopathic properties [2]. *Cannabis* also has the potential to be used as a repellent and pesticide [5]. The aim of the study is to determine

the allelopathic effect of *Cannabis sativa* L. essential oil on the initial development of the weed species *Chenopodium album* L.

### **Experimental**

*Cannabis sativa* L. essential oil was obtained in the process of distillation of dry plant material, which represents the above-ground part of the plant collected during the period of ripening. The essential oil was obtained by distilling 60g of dried plant material which was placed in a flask with 800 ml of distilled water. The distillation process lasted 2.5 hours. *C. sativa* L. essential oil was used in concentrations of 200, 400, 600 and 800ml/l.

The experiment was set up in 2017 in laboratory conditions. The biotest consisted of placing the *C. album* L. in Petri dishes with filter-paper. It was set in 15 seeds in two repetitions for each concentration of essential oil, while distilled water was used in the control. The Petri dishes were placed in an air-conditioned chamber for conditions of 24 °C during a fourteen-hour period (400 micrometer photons  $m^{-1} s^{-1}$ ) and then a temperature of 22 °C over a ten-hour dark period. After 5 days of follow-up, the length of the hypocotyl and the length of the epicotyl in each Petri dish were measured.

### **Results and discussion**

#### **Effect of essential oil on the length of hypocotyl**

By examining the effect of *Cannabis sativa* L. essential oil on the initial development of the *Chenopodium album* L. species, allelopathic effect was established. Increasing the concentration of essential oil increased the inhibitory effect. Unlike the control in which the average length of the hypocotyl was 2.67cm in the lowest applied concentration of essential oil, the average length of the hypocotyl was 1.9cm. A concentration of 400ml/l gave an average length of the hypocotyl of 1.6cm, a concentration of 600ml/l length of 0.77cm while a concentration of 800ml/l showed the strongest inhibitory effect with the average length of the hypocotyl was 0, 67cm (Figure 1).

#### **Effect of essential oil on the length of the epicotyl**

The *C. sativa* L. essential oil exhibited an inhibitory effect on the length of the epicotyl of the test species *C. album* L. The highest inhibitory effect exhibited concentrations of essential oil of 600 and 800ml/l, with the average length of the epicotyl being 0.63cm in difference from a control in which the average length was 2.7cm. The inhibitory effect also exhibits the smallest applied concentration of 200ml/l with an average length of epicotyl *C. album* L. of 1.67cm, while the concentration of 400ml/l gives an average length of 1.2cm (Figure 1).



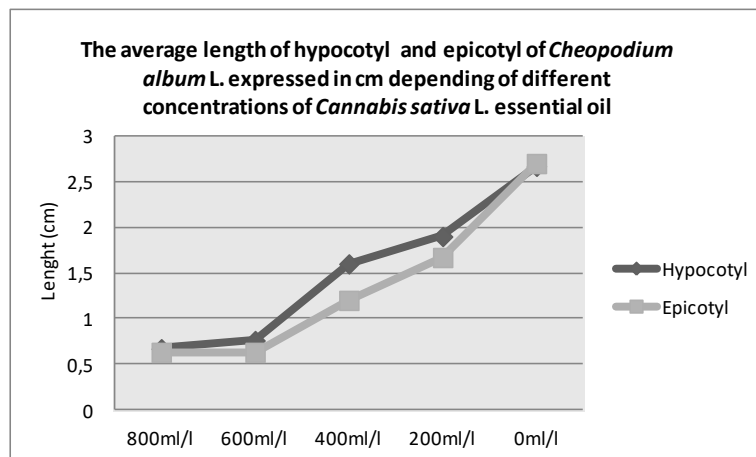


**Figure 1.** The average length of hypocotyl and epicotyl *Chenopodium album* L. expressed in cm depending on the application of different concentrations of *Cannabis sativa* L. essential oil.

### Conclusion

The obtained results in the conducted research clearly indicate the allelopathic inhibitory effect of *C. sativa* L. essential oil on the initial development of the weed species of *C. album* L. All investigated concentrations of essential oil inhibit the increase in *C. album* L., which is observed through the observed parameter of the average length of the hypocotyl, but also through average length of the epicotyl. The obtained results indicate the possibility of the use of *C. sativa* L. essential oil for the control of weed species *C. album* L. Due to increasing public pressure due to the harmful effects of synthetic herbicides on the environment, the application of biological measures to control weed species is gaining in importance makes it remarkable.

### References

- [1] N. Dudai, A. Poljakoff-Mayber, A. M. Mayer, E. Putievsky, H. R. Lerner, *Journal of Chemical Ecology*, 1999, 25, 5.
- [2] R. Baličević, M. Ravlić, T. Živković Tea, *Herbologia*, 2015, 15, 1.
- [3] K. Jabran, G. Mahajan, V. Sardana, B. S. Chauhan, *Crop Protection*, 2015, 72, 57-65.
- [4] J. K. Ahn, S. J. Hahn, J. T. Kim, T. D. Khanh, I. M. Chung, *Crop Protection* 24, 2005, 413-419.
- [5] J. M. McPartland, *Journal of the International Hemp Association*, 1997, 4, 2, 87-92.



## DETERMINATION OF THE PHENOL COMPOUNDS IN CONCRETE USING GC-MS

**Branislava Savić<sup>1</sup>, Ivana Mihajlović<sup>2</sup>, Tanja Brdarić<sup>1</sup>, Nevena Krivokapić<sup>1</sup>, Mina Seović<sup>1</sup>, Željka Nikolić<sup>1</sup>**

<sup>1</sup>*Vinča Institute of Nuclear Sciences, University of Belgrade, Mike Petrovića Alasa 12–14, 11000 Belgrade, Serbia*

<sup>2</sup>*University of Novi Sad, Faculty of Technical Sciences, Department of Environmental Engineering, Trg Dositeja Obradovića 6, 21000 Novi Sad, Serbia  
e-mail: savicbrislava87@gmail.com*

### **Abstract**

Organic contaminants from building materials negatively affected people's health. This study presents the validation of the analytical method, developed for the simultaneous identification and quantification of 9 phenolic compounds: phenol, 2-chloro phenol, 2,4-dimethyl phenol, 2,4-dichlorophenol, 2,6-dichlorophenol, 4-chloro-3-methyl phenol, 2,4,6-trichlorophenol, 2,3,4,6-tetrahydrophenol, pentachlorophenol in solid-solid concrete by gas chromatographic method with mass spectrometric detection (GC-MS). By comparing the MS spectra of the test compounds with MS spectra of analytical standards, reliable identification was achieved. The method can be applied in a given range (from 0.01 to 7.5 mg/kg) with the appropriate parameters precision, accuracy, repeatability and linearity. The developed method could be used for the quality control testing of phenols in concrete during the construction of new buildings and the old residences.

### **Introduction**

Phenol and phenol derivatives represent a very important group of pollutants due to their toxicity and carcinogenicity, as well as possibilities accumulation in the environment [1]. Nowadays, considerable attention has been devoted to the problem of phenols' emission into the indoor area of buildings. The quality of the indoor air depends largely on outdoor air quality, but it can be affected by a number of other factors such as emissions from building materials (concrete, coatings, paint, lacquer) [2]. To date, due to the various sources of indoor air pollutants, there is no EU legislation relating to indoor air quality.

Although, EU-LCIWORKING GROUP has made the proposal of LCI (Lowest concentrations of interest) for dangerous substances emitted from building materials into indoor air [3]. Concrete is a composite building material made up of water, aggregate (rock, crushed stone, sand, or gravel), a binder or paste such as cement and may contain additives [4]. As such, it presents a complex and challenging matrix for phenols analysis. The aim of the presented study is to develop and validate GC-MS method for determination of 9 phenol compounds from samples of solid-solid concrete that were prepared by solid-liquid extraction. The main emphasis is on assessing the parameters of validation such as selectivity, linearity, limit of detection (LOD), limit of quantification (LOQ), accuracy and precision. This method could be used for control testing of phenols in buildings material during construction, porous concrete pavements or any other construction which contain concrete. Also, the validated method could be used for evaluation of phenol removal process.

## **Experimental**

The following chemicals were used: Helium 5.0 (Messer Tehnogas), Phenol calibration mix 15, Phenol-Mix 15 2000 mg/L in methanol (Dr. Ehrenstorfer GmbH), Cyclohexane, HPLC grade (Fisher chemical), Methanol, CH<sub>3</sub>OH (Macron Fine Chemicals), Potassium carbonate, K<sub>2</sub>CO<sub>3</sub>, pro analysis (Lach:ner), Hydrochloric acid, 36.5-38.0% (Sigma-Aldrich), Acetic acid anhydride, (CH<sub>3</sub>•CO)<sub>2</sub>O, (Mercks reagenzien), Sodium hydroxide, NaOH, 99% (Hemos), Sodium sulphate anhydrous, Na<sub>2</sub>SO<sub>4</sub>, 99% (Centrohem).

Chromatographic analyses were carried out on the Gas chromatograph with mass detector - Agilent Technologies 7890B GC System, Agilent Technologies 5977MSD.

Sampling of the concrete walls was carried in the dimensions 10×10 cm, with a drill, with diamond plate, to the depth of 2 cm. The concrete was then collected in a hermetically sealed container and transported to the laboratory. Furthermore, the sample was homogenized to the particle size <1 μm by the hydraulic press without heating.

The basic standard solution of phenolic compounds (phenol, 2-chloro phenol, 2,4-dimethyl phenol, 2,4-dichlorophenol, 2,6-dichlorophenol, 4-chloro-3-methyl phenol, 2,4,6-trichlorophenol, 2,3,4,6-tetrahydrophenol, pentachlorophenol) in methanol in concentration of 2000 mg/L was supplied from the manufacturer in liquid form. Working solution of 50 μg/ml was prepared by diluting the basic solution of phenol in methanol. In 10 g of dry sample (dry matter determined according to SRPS EN 14346: 2012), working standard solution of phenol was added at concentrations of 0.1 mg/L, 0.5 mg/L and 1.0 mg/L (7.50, 3.75 and 1.88 mg/kg). In a measured 10 g sample - dry mass (dry matter determined according to SRPS EN 14346: 2012), an intermediate standard solution of phenol was added at concentrations of 0.1 mg/L, 0.5 mg/L and 1.0 mg/L (7.50, 3.75 and 1.88 mg/kg). The sample preparation was performed by a modified solid-liquid extraction as described in literature [25]. 75 ml of methanol was added to each spike and pH <3 was adjusted by adding concentrated hydrochloric acid (for a concrete 1 ml of HCl, for a country 0.5 ml of HCl). Extraction was performed by strong shaving for 10 minutes on an ultrasonic bath, then 30 minutes on a mechanical shaker (200-300 rpm). After the particles settled, the supernatant was filtered. An aliquot of 10 ml was transferred to a separation funnel of 100 ml and 50 ml of aqueous potassium carbonate solution (0.1M) was added. Then, 2 ml of sodium hydroxide (0.5M) and 1 ml of acetic anhydride were added to the extract. Extract was trembled for 2 minutes with the release of carbon dioxide that occurs in the separating funnel, left 10 minutes to stand with occasional shaving. After the timeout, 10 ml of cyclohexane was added. It was intensely shaken and the two phases were separated. The cyclohexane phase (upper phase) was transferred to a head space of 20 ml in which 2 g of anhydrous sodium sulfate was previously dosed. The extract was stored in a refrigerator at 4 [deg.] C. and analyzed before 48 h. 1 ml of GC-MS extract was taken. Blank sample was prepared in the same way as a real sample. Identification of compounds from the standard was performed by comparing the characteristic mass spectrum of the compound from the library with the characteristic MS spectrum of the individual phenol in the standard solution.

## **Results and discussion**

This paper presents a validated and developed a modern, precise and accurate, analytical GC-MS method for identification and quantification of phenol compounds in concrete. By comparing the MS spectra of the test compounds with MS spectra of analytical standards, reliable identification was achieved. The selectivity of the method was tested by calculation of the resolution successive peak at chromatogram of the spiked sample of concrete (Figure 1.).

A good resolution of the analyzed peaks was achieved using the GC-MS technique. The linearity of the method was tested by regression analysis. Limits of detection (LOD) and quantification (LOQ) were determined statistically using regression analysis functions obtained for linearity. Recovery test was used to check the accuracy of the method. The precision of the presented analytical method is expressed as the relative standard deviation (RSD (%)) of measurements under repeatability conditions when an analysis is performed by a single analyst using the same equipment over a short timescale. The main validation parameters of method are presented in Table 1. MS detector shows a linear response in a concentration range of 0.05 to 1 mg/L (0,01 to 7,5 mg/kg) with correlation coefficients  $R \geq 0.98$ . The accuracy of method is proved by the relative standard deviation below 5.0%. Reproducibility of the method is, indicated by a relative standard deviation of below 10.0%.

Table 1. Summary of the method validation data

Phenol	Rt± s (min.)	Regression equation	R	LOD (mg/kg)	LOQ (mg/kg)	Repeatability of the method RSD	Precision of the method RSD	Recovery %
phenol	2,959± 0,05	y=493433,108*x	0,992	0,0033	0,01	0,04	0,08	78,8
2-chloro phenol	3,703 ± 0,05	y=416100,92*x-9887,796	0,999	0,004	0,01	0,037	0,081	87,02
2,4-dimethyl phenol	3,926 ± 0,05	y=500446,669*x-10495,35	0,997	0,025	0,08	0,0303	0,0635	33,72
2,4-dichlorophenol	4,647 ± 0,05	y=394625,602*x-10262,29	0,998	0,025	0,08	0,05	0,07	86,61
2,6-dichlorophenol	4,510 ± 0,05	y=343841,22*x-6017,669	0,999	0,003	0,01	0,048	0,095	91,03
4-chloro-3-methyl phenol	4,561 ± 0,05	y=201366,61*x-4856,93	0,998	0,003	0,01	0,035	0,068	83,88
2,4,6-trichlorophenol	5,402 ± 0,05	y=246943,03*x-6070,09	0,997	0,003	0,01	0,041	0,0631	88,4
2,3,4,6-tetrahydrophenol	7,153 ± 0,05	y=109197,001*x-4218,06	0,992	0,025	0,08	0,027	0,0907	89,03
Pentachlorophenol	8,664 ± 0,05	y=82373,24*x-5042,42	0,985	0,03	0,1	0,049	0,068	85,13

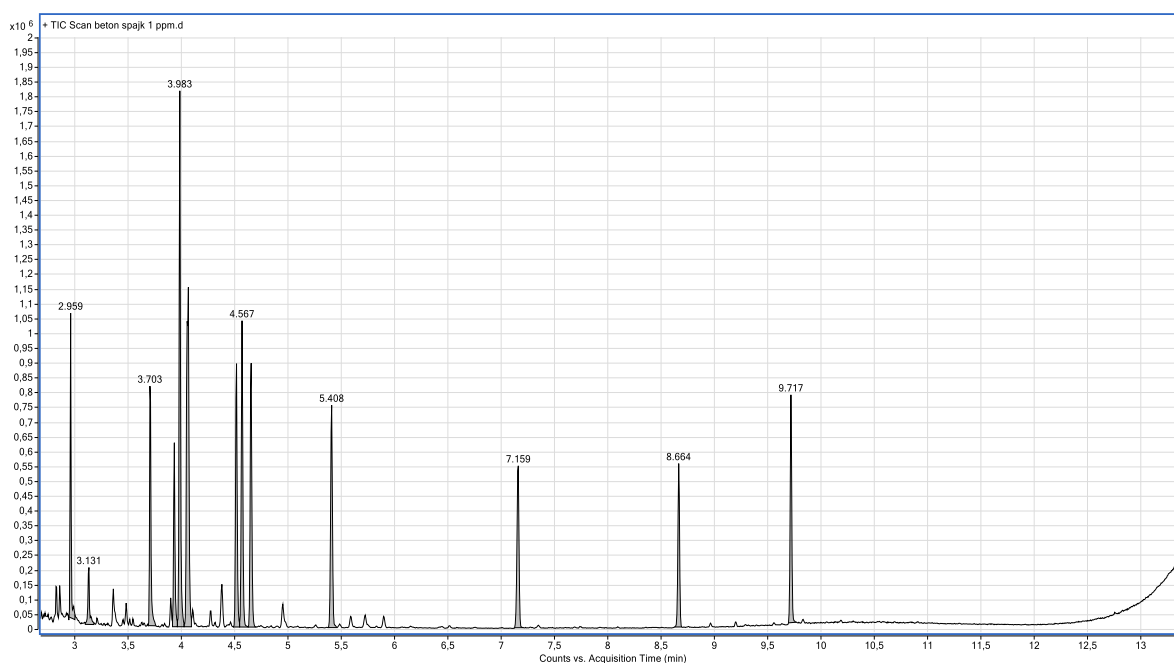


Figure 1. The chromatogram of concrete spiked with phenols solution (7,5 mg/kg)

### **Conclusion**

The method for the simultaneous identification and quantification of the nine phenols compounds in solid–solid concrete by gas chromatographic method with mass spectrometric detection analytical technique was developed and validated in presented study. Based on precision, accuracy, repeatability and linearity, it can be concluded that the measuring range of developed method ranged from 0.01 to 7.5 mg/kg. Good resolution of the analyzed peaks was achieved using the GC-MS technique. The developed method will be used for the control testing of phenols in concrete in new buildings and old buildings associated with a sick-building syndrome.

### **Acknowledgements**

This study was financially supported by the "Serbian Ministry of Education, Science and Technological Development" (Grants No. 172045 and 37021).

### **References**

- [1] J. Michałowicz, W. Duda, *Pol. J. Environ. Stud.* **16** (2007) 347–362.
- [2] J.C. Chuang, S.R. Cao, Y.L. Xian, D.B. Harris, J.L. Mumford, Chemical characterization of indoor air of homes from communes in Xuan-Wei, China, with high lung-cancer mortality-rate, *Atmos. Environ. Part A-General Top.* 26 (1992) 2193–2201, lw0345.pdf.
- [3] Current list of substances with EU-LCI values, n.d <http://www.eu-lci.org/EU-LCI Website/EU-LCI Values.html> (Accessed 9 December 2015).
- [4] S. Kubba, *Handbook of Green Building Design and Construction: LEED, Butterworth-Heinemann, BREEAM, and Green Globes*, 2012.

## BENTONITE AS ENVIRONMENTAL FRIENDLY SORPTION MATERIAL FOR SUGAR BEET MOLASSES PURIFICATION

Miljana Djordjević<sup>1</sup>, Zita Šereš<sup>1</sup>, Marijana Djordjević<sup>1</sup>, Dragana Šoronja Simović<sup>1</sup>, Nikola Maravić<sup>1</sup>, Tatjana Došenović<sup>2</sup>

<sup>1</sup>*Department of Carbohydrate Food Engineering, Faculty of Technology, University of Novi Sad, bul. cara Lazara 1, Novi Sad, Serbia*

<sup>2</sup>*Department of Basic Engineering Disciplines, Faculty of Technology, University of Novi Sad, bul. cara Lazara 1, Novi Sad, Serbia  
e-mail: zitas@tf.uns.ac.rs*

### Abstract

Search for efficient, inexpensive and environmental friendly sorption material for application in the sugar industry was always been in the research focus. Bentonite as natural material with great affinity for binding inorganic and organic compounds could fulfill the previous requirements. This study investigates application of two different sodium-calcium bentonites (Claris p30 and Claris p50) as adsorbents in the purification of sugar beet molasses. Box-Behnken experimental design was employed and the effect of 3 independent variables pH (3, 5, 7), molasses dry substance (30, 40, 50°Bx) and bentonite suspension concentration (9, 15, 21 g/L) on the sugar beet molasses color and turbidity reduction were studied. Positive results regarding color reduction (22% with Claris p30 and 48% with Claris p50) and turbidity reduction (90% with Claris p30 and 99% with Claris p50) of sugar beet molasses were obtained upon treatment with corresponding bentonites indicating their applicability as environmental friendly adsorbents of non-sugars from the sugar industry.

### Introduction

Sugar beet molasses as the final residue from the sugar crystallization unit represents a stream in which all non-sugars including colorants are concentrated. Reduction of non-sugars in sugar beet molasses is desirable in order to facilitate sugar recovery from molasses by chromatographic process and minimize changes that may occur during storage and further industrial. Decrease in sugar beet molasses non-sugars content could be achieved through treatment with different adsorbents. Application of activated carbon for juice and sugar beet molasses purification was well established but inevitable problem represents his regeneration and disposal. Adsorbents disposal problems could be diminished with the application of bentonite since he is applicable in soil fertilization [1]. Bentonite application is widespread since represents a natural material with large specific surface area and high cation exchange capacity which provides exceptional adsorption capacity for various inorganic and organic compounds [2]. Presence of dominant exchangeable ion in bentonite structure determines bentonite type and among most commonly used in the industry are sodium (Na) and calcium (Ca) bentonites [1]. Enhancement of desired bentonite properties could be obtained through bentonite modification. Combined sodium-calcium bentonite (Na-Ca bentonite) is obtained after treatment of Ca bentonite with sodium carbonate as a result of calcium ions substitution with sodium ions. This way exceptional swelling and water absorption capabilities of Na bentonite can contribute to overall expanding ability of produced Na-Ca bentonite. Another way to enhance adsorption capacity of bentonite is hydration treatment prior to application which is highly recommended [3]. Previous studies on sugar beet juice purification with

bentonite alone or in combination with other materials, reported great improvement in the juice quality [3-5]. Nevertheless, literary data concerning bentonite application in molasses treatment are scarcely. Therefore, the objective of this study was to determine the effects of Na-Ca bentonite treatment on changes in sugar beet molasses color and turbidity.

### Experimental

Molasses purification treatment was conducted according to the Box-Behnken experimental design (Table 1) with independent variables: pH (3, 5, 7), molasses dry substance (30, 40, 50°Bx) and bentonite suspension concentration (9, 15, 21 g/L).

Molasses used in this research was sampled from the sugar beet factory “Šajkaška” (Žabalj, Serbia) during the sugar beet campaign in 2016. Two different types of fine powder formulated Na-Ca bentonite, Claris p30 and Claris p50 (montmorillonite content 88-92%, moisture content 9-10%, Bentoproduct, Bosnia and Herzegovina) were used for molasses treatment. For the purpose of corresponding experiments and experimental design, molasses samples were adjusted to 30, 40 and 50°Bx using distilled water. Measurements of color and turbidity in samples were conducted prior to every set of experimental runs.

Bentonite suspensions were prepared according to the producer’s recommendations Claris p30: 100 g in 5 L of water, Claris p50: 100 g in 1 for L of water. Hydration is achieved through steeping of bentonite into distilled water heated at 40°C-50°C with intense mixing in the initial stage of hydration until uniform suspension is obtained. Bentonite suspension were stored for 12 hours at room temperature (25°C) in order to reach the best effectiveness [3].

Bentonite suspension was added to 200 ml of diluted molasses (30, 40 and 50°Bx) in order to achieve the selected concentration (9, 15 and 21 g/L). Selected pH was adjusted with citric acid (50 g/100 mL) (Lach-Ner s.r.o., Neratovice, Czech Republic) upon bentonite addition. Erlenmeyer flasks containing prepared blends were closed and placed into the water bath (VelpScientifica®, Italy) heated at 60°C and mixed for 30 min. Cooled blends (25°C) were filtered through filter paper (Selecta faltenfilter) and the obtained filtrate was used for color and turbidity measurements.

Color of samples was quantified by the absorbance measured on a spectrophotometer (Spectrophotometer MA 9522-Spekol 220, Iskra, Slovenia) at the wavelength of 420 nm according to the method given by the International Commission for Uniform Methods of Sugar Analysis (ICUMSA) and calculated using equation:

$$Color [IU] = \frac{A \times 1000}{c \times b} \quad (1)$$

where  $C$  is the colour in ICUMSA unit (IU),  $A$  is the absorbance of the solution at 420 nm,  $b$  is the cuvette length or path length in cm (1 cm cuvette for molasses) and  $c$  is dry substance content in  $g/cm^3$  calculated by using brix-density tables for sugar solutions. The turbidity of the samples was directly measured using turbidimeter WTW Turb 550IR (Germany) and given in NTU units.

Changes in molasses colour and turbidity were calculated using following equation:

$$Reduction [\%] = [(QP_i - QP_f) / QP_i] \times 100 \quad (2)$$

where  $QP_i$  is the value of initial quality parameter of diluted molasses and  $QP_f$  is the value of final quality parameter of the molasses sample after treatment.

### Results and discussion

In Table 1 are presented experimentally obtained values for each response under different experimental conditions according to the Box-Behnken experimental design.

*Influence of bentonite treatment on colour reduction*



Increase in molasses color reduction is observed at low pH values regardless of applied bentonite and his concentration (Figure 1). In samples treated at pH 3 when Claris p30 was applied (runs 1, 3, 5, and 7, Table 1) molasses color reduction percentage was three to four times higher than in samples treated with same bentonite at pH 7. Similar trend in molasses color reduction was noticed upon Claris p50 application where reduction percentage was about two times higher in samples treated at pH 3 in comparison to samples treated at pH 7. It could be concluded that pH is one of the main factors that affect bentonite adsorption capacity due to the modification of its charge [6] and the ionisation equilibrium of non-sugar compounds dissolved in the diluted molasses in acidic environment. As a result, strong electrostatic interaction between bentonite and non-sugars is enabled and molasses color reduction is more pronounced.

Table 1 Box-Behnken design with three independent variables at three levels and responses

Standard run	pH	DS [°Bx]	BC [g/L]	Color reduction [%]		Turbidity reduction [%]	
				Claris p30	Claris p50	Claris p30	Claris p50
<b>1</b>	3.0	40	9	21.75	40.57	0	0.63
<b>2</b>	7.0	40	9	7.92	26.53	66.97	48.90
<b>3</b>	3.0	40	21	17.51	42.86	0	55.04
<b>4</b>	7.0	40	21	6.66	24.92	90.20	92.65
<b>5</b>	3.0	30	15	22.34	48.93	30.87	97.45
<b>6</b>	7.0	30	15	1.51	31.62	67.65	99.08
<b>7</b>	3.0	50	15	19.34	38.29	0	0.50
<b>8</b>	7.0	50	15	0.22	14.06	80.31	52.77
<b>9</b>	5.0	30	9	0.12	24.31	0	97.08
<b>10</b>	5.0	30	21	11.54	20.6	57.32	98.37
<b>11</b>	5.0	50	9	10.18	25.68	25.46	1.12
<b>12</b>	5.0	50	21	18.14	38.17	54.59	63.27
<b>13</b>	5.0	40	15	5.14	33.02	47.75	54.73
<b>14</b>	5.0	40	15	2.38	19.25	63.35	73.34
<b>15</b>	5.0	40	15	3.22	27.23	45.88	64.40

DS-dry substance; BC-bentonite concentration;

Influence of bentonite concentration on molasses color reduction is not strongly expressed but still in samples treated with larger amount of bentonites increase in molasses colour reduction was recorded.



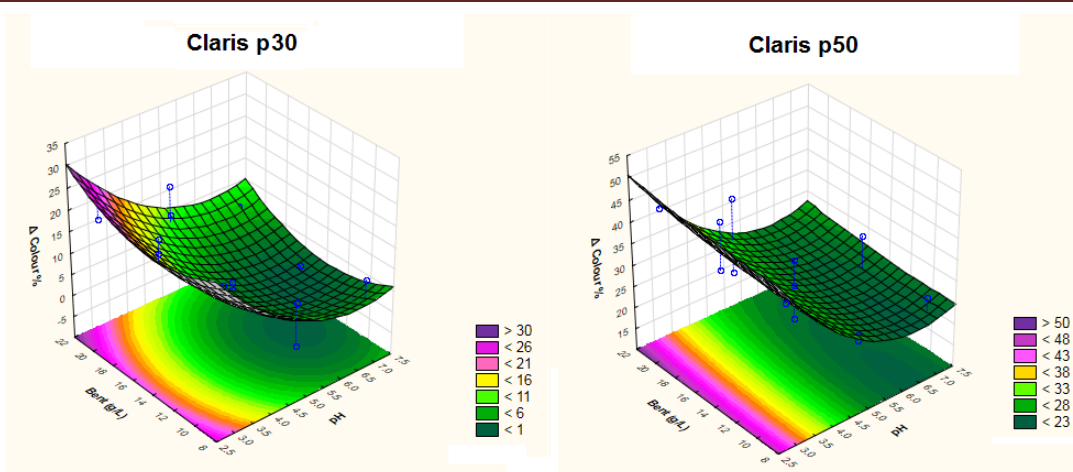


Figure 1. Influence of pH and bentonite concentration on molasses color reduction

In molasses samples with dry substance content 30°Bx and 40°Bx higher percentage in molasses color reduction was reached upon both bentonite addition probably because increase in molasses dry substance led to increase in non-sugars content.

In general, obtained results indicate that with Claris p50 application higher percentage in molasses color reduction is reached regardless of bentonite concentration and molasses dry substance.

*Influence of bentonite treatment on turbidity reduction*

Bentonite concentration and pH were the main factors which affect the molasses turbidity reduction. As presented in Figure 2 with increase in bentonite concentration and pH value reduction of molasses turbidity also increased regardless of applied bentonite. In samples treated at pH 3 (runs 1, 3, 5, and 7, Table 1) molasses turbidity reduction was almost 100% lower than in samples treated at pH 7 regardless of applied bentonite. Nevertheless, considerable molasses reduction percentage was also recorded in all samples treated at pH 5 upon both bentonites addition. Furthermore, molasses turbidity reduction increased with the increase in bentonite concentration at constant pH and molasses dry substance (runs 1 and 3; 2 and 4; 9 and 10, Table 1).

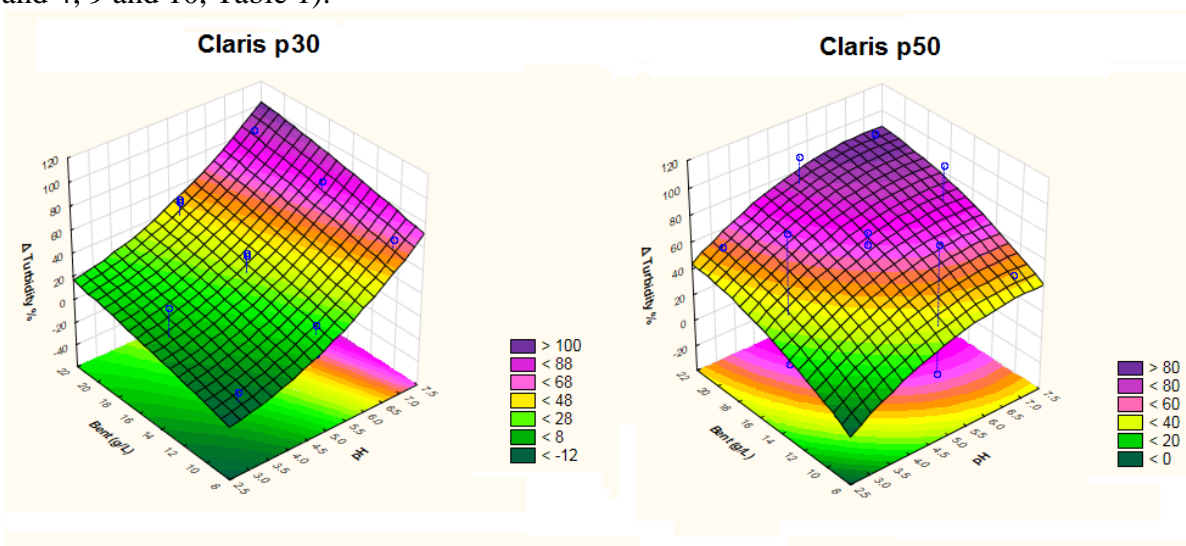


Figure 2. Influence of pH and bentonite concentration on molasses turbidity reduction

Highest molasses turbidity reduction percentage is observed when treated molasses had lowest dry substance content (30°Bx) indicating that increase in molasses dry substance content contributes to turbidity increase.

### **Conclusion**

This study showed that bentonite adsorption potential could be utilized for sugar beet molasses treatment since reduction of non-sugar compounds content, particularly colorants, is achieved upon his application. Based on the obtained results of molasses colour and turbidity reduction it can be stated that bentonite concentration and pH greatly affected the aforementioned parameters. Maximal molasses color reduction was obtained in acidic environment (pH 3-5) with the increase of bentonite concentration while the highest molasses turbidity reduction was observed at pH 7 with medium (15 g/L) and high (21 g/L) bentonite concentrations. The obtained results also drive on to conclude that Claris p50 was more efficient in molasses color and turbidity reduction in comparison to Claris p30. Therefore, corresponding bentonites can be successfully applied in the purification treatments in sugar industry without concerning of possible environmental problems.

### **Acknowledgements**

All authors express their thanks to “Bentoproduct” d.o.o. Banjaluka, Bosnia and Herzegovina for bentonite samples donation and sugar factory JSC “Šajkaška” Žabalj, Serbia for providing sugar beet molasses. Funding for Miljana Djordjević was received through scholarship granted by The Ministry of Education, Science and Technological Development of the Republic of Serbia.

### **References**

- [1] I. Savic, S. Stojiljkovic, I. Savic, & D. Gajic, in L.R. Wesley (Ed), *Clays and Clay Minerals: Geological Origin, Mechanical Properties and Industrial Applications*. Nova Science Publishers Inc., 2014, pp. 379–402.
- [2] S.M.R Shaikh, M.S.Nasser, I.A. Hussein, & A. Benamor, *Chem. Eng. J.* 311 (2017) 265. <http://doi.org/10.1016/j.cej.2016.11.098>
- [3] E. Jahed, M.H.H. Khodaparast, & A. Mousavi Khaneghah, *Appl. Clay Sci.* 102 (2014) 155. <http://doi.org/10.1016/j.clay.2014.09.036>
- [4] B. Erdođan, ř. Demirci, & Y. Akay, *Appl. Clay Sci.* 11 (1996) 55. [http://doi.org/10.1016/0169-1317\(96\)00012-9](http://doi.org/10.1016/0169-1317(96)00012-9)
- [5] P. Laksameethanasana, N. Somla, S. Janprem, & N. Phochuen, *Procedia Engineering* 32 (2012) 141. <http://doi.org/10.1016/j.proeng.2012.01.1248>
- [6] S. Ismadji, F.E. Soetaredjo, & A. Ayucitra, in: S. Ismadji, F.E. Soetaredjo and A. Ayucitra (Eds.), *Clay Materials for Environmental Remediation*, Springer International Publishing AG Switzerland, 2015, pp. 5-37. [http://doi.org/10.1007/978-3-319-16712-1\\_2](http://doi.org/10.1007/978-3-319-16712-1_2)

## A RAPID METHOD FOR PESTICIDE RESIDUES DETECTION AND QUANTIFICATION IN MAIZE, WHEAT AND RAPE

**Mariana Nela Ștefănuț<sup>1</sup>, Marius Dobrescu<sup>1</sup>, Firuța Fițișău, Adina Căta, Ioana Ienașcu<sup>1,2</sup>**

<sup>1</sup>Department of Chemistry and Electrochemistry, National Institute for Electrochemistry and Condensed Matter, INCEMC-Timișoara, Aurel Păunescu Podeanu 144, 300569 Timisoara, Romania, e-mail: mariana.stefanut@gmail.com

<sup>2</sup> "Vasile Goldiș" Western University of Arad, Faculty of Pharmacy, 86 Liviu Rebreanu, 310045, Arad, Romania

### Abstract

In order to ensure food security of cereals from Banat, we developed a rapid method HPLC for pesticide residues detection and quantification in maize, wheat and rape. All samples of maize, wheat and rape were obtained from Timiș County. We followed some pesticides from commercial *Nuprid AL 600 FS* (insecticide, active compound imidacloprid), *Buctril Universal* (herbicide, active compound bromoxynil), *Sekator Progress OD* (herbicide, active compound amidosulfuron) and *Decis* (*Decis 25 WG* or *Decis Mega 50 EW*, insecticide, active compound deltamethrin). Calibration curves for imidacloprid, bromoxynil, amidosulfuron and deltamethrin were performed using Pestanal standards and an HPLC-DAD apparatus, Dionex Ultimate 3000, equipped with quaternary pump LPG 3400A, thermostat of columns TCC-3000 and a C-18 Acclaim® 120 Silica-reversed-phase column. Extraction and concentration of pesticide residues were made in methanol, acetonitrile and mixture water-acetonitrile solvents, by ultrasonication in two steps, at 59 kHz, 30±2°C, during 30 and 15 min., respectively. Time of analyses was between 5-10 min. The residual pesticides' concentration were higher than MRLs authorized by UE laws in some of the samples.

**Key words:** imidacloprid, bromoxynil, amidosulfuron, deltamethrin, HPLC-DAD analysis

### References

- [1] Directive EU 491/2014 amending Annexes II and III to Regulation CE 396/2005 and 91/414/EEC, J. Official Com. Eur. L 146, 2014, p.53 (RO).
- [2] S. Polati et al., HPLC-UV and HPLC-MS<sup>n</sup> multiresidue determination of amidosulfuron, nicosulfuron, rimsulfuron, thifensulfuron methyl, tribenuron methyl and azoxystrobin in surface waters. *Analytica Chimica Acta* 579, 2006, 146.
- [3] R. Zanella et al., An overview about recent advances in sample preparation techniques for pesticide residues analysis in cereals and feedstuffs, in: *Pesticides-Recent trends in residue pesticide assay* (Ed.R.P. Soundararajan) CC BY 3.0 licence, 2012, 149.
- [4] I. Jaabiri et al., Development and method validation for determination of deltamethrin residue in olive oil using reversed-phase high performance chromatography, *J. Appl. Chem. (IOSR-JAC)* 6(3), 2013, 1.

## **CHEMICAL COMPOSITION EVALUATION OF SOME FLOUR MIXTURES WITH HIGH NUTRITIONAL VALUE**

**Stoin Daniela, Jianu Calin, Velciov Ariana – Bianca, Negrea Monica, Pintilie Sofia, Cozma Antoanela, Trasca Teodor**

*University of Agricultural Sciences and Veterinary Medicine of Banat "King Mihai I of Romania" Timisoara  
Faculty of Food Processing Technology Food Science Department 300645, Timisoara, Calea Aradului, nr. 119, Roumania  
author's email address: danielastoin@yahoo.com*

### **Abstract**

Cereals, fruits and vegetables have interesting nutritional properties and their inclusion in the diet is encouraged, their incorporation in bakery products could be a good way to increase consumption. In this study, the influence of the partial replacement of wheat flour (WF) with four types of flour: rye flour (RF), whole rye flour (WRF), quinoa flour (QF), buckwheat flour (BF) and goji fruit GFr) in eight mixtures obtained therefrom, was analyzed. The wheat flour was blended with rye flour, whole rye flour, quinoa flour, buckwheat flour and goji fruit in the ratios of 25:25:25:25 and 25:50:25. The studied samples were subjected to the following analyzes: determination of moisture, protein content, ash content, fat content, fiber content and total carbohydrate content. The resulting mixtures had high protein content (12.35% at M7 and 13.30% at M2), fiber (4.11% at M5 and 7.76% at M4), ash (1.79% at M8 and 2.15% at M1) fat (1.63% at M8 and 3.57% at M1) and low carbohydrates (62.35% at M2 and 65.68% at M7) and moisture ranged between 11.20% at M7 and 12.37% at M2. This study determined the optimum proportions to form these high nutritional flour mixtures. Centralizing the data obtained in this study, the high nutrient intake of the analyzed mixtures can be seen, and on the basis of these, we can recommend their use on the industrial scale in the recipes for the production of finely produced products with superior nutritional value.

### **Introduction**

In recent decades, there has been growing concern about diversification in the production and renewal of the range of products in the food industry and an increase in the consumption of high nutritional food by the population. Obtaining foods with high nutritional value means either restoring the natural concentration of the ingredients or supplementing with nutrients above the natural concentration of the product [1]. Food pyramid is a graphical representation of nutritional recommendations, quantities and types of foods to be consumed daily in order to maintain health and reduce the risk of developing various dietary diseases [1, 2]. Indications are expressed in portions of food, whose daily consumption will provide all the essential nutrients. Cereals, vegetables and fruits are best represented in the food pyramid as the basis of balanced nutrition, calling them the "basis" for proper nutrition and health, noting that they can reduce the risk of chronic disease [2].

In this context, the importance of rye flour, quinoa and buckwheat derives from their complex chemical composition, implicitly from their food value, but also from the fact that in some countries they are considered basic foods [3, 4]. High content in proteins, some essential amino acids and mineral substances of pseudo-cereals leads to improvement of the nutritional

composition of the products obtained after their processing and of their food value, respectively [5, 6].

Goji fruits have the highest concentration of antioxidants, they have a high content of vitamins, minerals, polysaccharides, amino acids, essential oils that strengthen the immune system and keep the body healthy [7]. Starting from the described premises, this work aimed at optimizing some blends of high nutritional flours.

## **Experimental**

### ***Materials***

Flours and goji fruits analyzed in this study have been purchased from hypermarkets and specialized stores.

### ***Steps in the preparation of flour mixtures***

In determining the proportion of each flour assortment that formed a mixture, was taken account of both the physical and chemical characteristics of these flours. For example, because rye flour, buckwheat flour and quinoa flour are gluten-free, to ensure the formation of the three-dimensional gluten skeleton of the dough, 25% wheat flour has been added. In the formation of the 8 mixtures, rye flour, whole rye flour and pseudocereal flour (buckwheat and quinoa flour) were used, as it is known that these flour assortments have a high nutritional value, being rich in essential amino acids, antioxidants, minerals and vitamins [3, 4, 5]. It is worth mentioning that out of the 8 mixtures, 4 of them contain only mixed flour according to the established proportions (25WF:50RF:25QF; 25WF:50WRF:25QF; 25WF:50RF:25BF; 25WF:25WRF:25BF) and the other 4 blends, contain 25% goji fruit beside the established flour mixtures (25WF:25RF:25QF:25GFr; 25WF:25WRF:25QF:25GFr; 25WF:25RF:25BF:25GFr; 25WF:25WRF:25BF:25 GFr). Goji fruit has been added in a proportion of 25%, taking into consideration that goji fruit has a high nutritional value due to the significant content of antioxidants, vitamins and minerals [7].

### ***Analytical procedures***

#### **Proximate composition of flours, flour mixtures and goji fruit**

For determining the average chemical composition of flours, flour mixtures and goji fruit, respectively, the following chemical characteristics were determined: moisture, acidity, fat content, ash content, fiber content and carbohydrate content- according to standard method A.O.A.C. 1995 [8] and protein content by the Kjeldahl method- according to standard method A.A.C.C. 2000, No. 46-10 [9]. All determinations were performed in triplicate, calculating their arithmetic mean of three separate determinations. The data were statistically analyzed using the program Microsoft Excel.

## **Results and discussion**

The results obtained from the proximate analysis of flours and goji fruit are shown in Table 1. The results obtained with regard to the chemical composition of the four types of flour analyzed and GFr compared to wheat flour highlight their nutritional potential as a result of the higher protein, fiber, fat and ash content. RF showed high levels of fat - 1.92% compared to 1.62% in WF, fiber - 3.99% compared to 1.56% in WF, ash - 2.60% compared to 0.65% in WF and lower protein level - 11.77% compared to 12.65% in WF and carbohydrates - 65.50% compared to 69.25% in WF [3]. Regarding the chemical composition of whole rye flour, quinoa flour and buckwheat flour, this was superior for all constituents analyzed as compared

to wheat flour. Fat content ranged from 1.74% to WRF to 6.24% at QF compared to 1.62; protein content ranged from 12.92% in WRF to 13.93% in QF compared to 12.65% in WF; fiber content ranged from 5.09% in WRF to 8.21% in BF compared to 1.56% in WF; ash content ranged from 1.94% in BF to 2.42% in QF compared to 0.65% in WF [3, 4, 5, 6]. Compared with other studies [3, 4, 5, 7], the carbohydrate content is lower for the four types of flour and GFr in comparison with WF, ranging from 56.85% in GFr to 65.50% in RF compared to 69.25% in WF, which contributes to the lowering of the glycemic index of the products obtained from these flours. The moisture of all four types of flour was lower than that of WF, ranging from 11.69% in BF to 14.02% in RF compared to 14.27% in WF. The chemical composition of GFr was superior to that of WF, too, exhibiting a protein content of 13.72%, fat content of 4.52%, fiber content of 16.18% and ash of 2.89%, respectively [3,4,5,6].

**Table 1.** Chemical composition of flours and goji fruit

<b>Analysis (%)</b>	<b>Wheat flour (WF)</b>	<b>Rye flour (RF)</b>	<b>Whole rye flour (WRF)</b>	<b>Quinoa flour (QF)</b>	<b>Buckwheat flour (BF)</b>	<b>Goji fruit (GFr)</b>
Moisture	14.27±0.36	14.02±0.21	13.82±0.08	11.88±0.67	11.69±0.16	5.84±0.14
Fat	1.62±0.31	1.92±0.14	1.74±0.20	6.24±0.26	2.43±0.19	4.52±0.21
Protein	12.65±0.3	11.77±0.38	12.92±0.15	13.93±0.11	13.24±0.13	13.72±0.09
Fiber	1.56±0.16	3.99±0.25	5.09±0.11	6.86±0.19	8.21±0.14	16.18±0.08
Carbohydrates	69.25±0.13	65.50±0.22	64.63±0.33	58.67±0.23	62.49±0.24	56.85±0.16
Ash	0.65±0.36	2.60±0.32	2.30±0.21	2.42±0.14	1.94±0.16	2.89±0.20

The flour mixtures were marked as:

**M1** - 25% WF + 25%RF + 25%QF + 25%GFr; **M2** - 25% WF + 25% WRF + 25%QF + 25%GFr; **M3** - 25% WF + 25%RF + 25%BF + 25%GFr; **M4** - 25%WF + 25%WRF + 25%BF + 25%GFr; **M5** - 25%WF + 50% RF + 25%QF; **M6** - 25%WF + 50%WRF + 25%QF; **M7** - 25% WF + 50%RF + 25%BF; **M8** - 25%WF + 50% WRF + 25%BF.



**Table 2.** Chemical composition of the studied flour mixtures

Mixtures	Moisture (%)	Fat (%)	Protein (%)	Fiber (%)	Carbohydrates (%)	Ash (%)
M1	11.92±0.36	3.57±0.11	13.01±0.06	7.14±0.57	62.56±0.10	2.15±0.12
M2	12.37±0.31	3.40±0.12	13.30±0.40	7.42±0.23	62.35±0.19	2.11±0.21
M3	11.65±0.33	2.52±0.28	12.84±0.25	7.48±0.14	63.52±0.03	1.98±0.01
M4	12.15±0.16	2.45±0.15	13.13±0.12	7.76±0.19	63.30±0.24	1.94±0.08
M5	11.52±0.13	2.92±0.32	12.47±0.33	4.11±0.41	64.73±0.24	2.06±0.16
M6	12.25±0.36	2.58±0.02	13.05±0.11	4.65±0.14	64.29±0.16	2.07±0.20
M7	11.20±0.16	1.97±0.52	12.35±0.41	4.43±0.19	65.68±0.08	1.94±0.12
M8	12.01±0.22	1.63±0.12	12.93±0.11	4.98±0.16	65.25±0.19	1.79±0.26

Comparing the moisture values (Table 2) corresponding to the eight analyzed mixtures of flour, it can be seen that the moisture ranged between 11.20% (**M7**) and 12.37% (**M2**). It can also be noticed that the moisture of RF and BF blends is lower (11.65% for **M3** and 11.20% for **M7**) than for blends with WRF and QF (11.92 % for **M1** and 11.52% for **M5**), which makes the use of RF and BF blends in bread making technology, to prolong the freshness of the products [3, 4, 5, 6].

The fat content of the analyzed samples varies between 1.63% (**M8**) and 3.57% (**M1**), and it can also be observed that for QF mixtures the fat content is higher (3.57% for **M1** and 2.92% for **M7**) than in the case of blends with BF (2.45% for **M4** and 1.63% for **M8**) [3, 4, 5, 6, 7]. According to the results presented in table 2, the studied mixtures (**M1** ÷ **M8**) can be considered as important "protein sources", "fiber sources" and "mineral sources", thus, the protein content varies between 12.35% for **M7** and 13.30% for **M2**, the fiber content between 4.11% for **M5** and 7.76% for **M4** and the ash content between 1.79% for **M8** and 2.15% for **M1**, results that are consistent with those obtained by Hansen, (2004), Vojtiskova (2012), Faizullah (2013) and Filho (2017) [3, 4, 5, 6].

The addition of GF<sub>r</sub> increases the nutritional value of mixtures, namely the mineral content (1.94% ÷ 2.15%), compared to the mixtures that do not contain these fruits (1.79 ÷ 2.07%). Regarding the carbohydrate content of the analyzed mixtures (**M1** ÷ **M8**) (Table 2), it can be observed that mixtures not containing GF<sub>r</sub> exhibit higher values (64.29% for **M6** and 65.68% for **M7**) compared to mixtures containing GF<sub>r</sub> (62.35% for **M2** and 63.52% for **M3**) [3, 4, 5, 6, 7].

## Conclusions

This study showed that rye flour, whole rye flour, quinoa flour, buckwheat flour and goji fruit are important sources of protein, fiber, minerals and fat compared to wheat flour. Based on the results obtained in this study we can assume that the proportions established for each



assortment of flour and goji fruit lead to the obtaining of some flour mixtures that comply with the quality standards provided by the specialized STAS. Also based on these results, the following recommendation can be made, namely, the use of these blends in both the biscuit production technology and the technology of other pastry and bakery products. The results in this research confirm that this mixture is a good source of many important nutrients that appear to have a very positive effect on human health and could be used to obtain potentially functional foods.

### **References**

- [1] Chwang, L. C., "Nutrition and dietics in aged care". *Nutrition and Dietics*, vol. 69 (3), pp 203–207. doi:10.1111/j.1747-0080.2012.01617.x. Retrieved March 31, 2015.
- [2] Vitamin and mineral requirements in human nutrition: report of a joint FAO/WHO Expert Consultation, Bangkok, Thailand, 1998.
- [3] Hansen H., Moller B., Andersen S., Jorgensen J., Hansen A., Grain Characteristics, Chemical Composition, and Functional Properties of Rye (*Secale cereale* L.) As Influenced by Genotype and Harvest Year, *J. Agric. Food Chem.*, vol. 52, pp 2282–229, 2004.
- [4] Vojtiskova P., Kmentova K., Kuban V., Kracmar S., Chemical composition of buckwheat plant (*Fagopyrum esculentum*) and selected buckwheat products, *Journal of Microbiology Biotechnology and Food Sciences*, vol. 1 (February Special issue), pp 1011-1019, 2012.
- [5] Filho A.M., Pirozi M.R., Borges J.T., Pinheiro Sant'Ana H.M., Chaves J.B., Coimbra J.S., Quinoa: Nutritional, functional, and antinutritional aspects, *Crit Rev Food Sci Nutr.*, vol. 57(8), pp 1618-1630, 2017.
- [6] Faizullah K., Muhammad A., Tariq Umar K., Muhammad I. K., Javed A. B., Nutritional evaluation of common buckwheat of four different villages of Gilgit-Baltistan, *ARPN Journal of Agricultural and Biological Science*, vol. 8, no. 3, 2013.
- [7] Niro S., Fratianni A., Panfili G., Falasca L., Cinquanta L., Rizvi Alam M.D., Nutritional evaluation of fresh and dried goji berries cultivated in Italy, *Ital. J. Food Sci.*, vol. 29, pp 398 - 408, 2017.
- [8] A.O.A.C., "Official Methods of Analysis" Association Official Analytical Chemists of the 16<sup>th</sup> Ed. International, Washington, D.C., U.S.A., 1995.
- [9] AOAC (Association of Official Analytical Chemists) Official Methods of Analysis International. 17<sup>th</sup>, Ed. Washington, DC: AOAC, 2000.

## NICKEL-FILM BASED GLASSY CARBON ELECTRODE AS AN ELECTROCHEMICAL SENSOR FOR HISTAMINE DETERMINATION

Zorica Stojanović<sup>1</sup>, Jaroslava Švarc-Gajić<sup>1</sup>, Snežana Kravić<sup>1</sup>, Ana Đurović<sup>1</sup>

<sup>1</sup>University of Novi Sad, Faculty of Technology, Department of Applied and Engineering Chemistry, Bulevar cara Lazara 1, Novi Sad, Serbia  
e-mail: zorica.stojanovic@uns.ac.rs

### Abstract

In recent years, new trends in food safety together with the consumers demand for good quality and healthier products have encouraged the search for compounds with harmful repercussions on human health. Among them, the presence of histamine in fermented foods, such as sausages, wine, beer, cheese and other dairy products has received considerable interest owing to its undesirable physiological effects in sensitive humans. Histamine is a neurotransmitter and a product of the microbial degradation of the amino acid histidine due to the action of histidine decarboxylase. The formation of high levels of histamine correlates strongly with the number of microorganisms present in histidine rich foods (vegetables, fermented foods and certain fish species). At high concentrations, histamine is a risk factor for food intoxication, whereas moderate levels may lead to food intolerance. The symptoms of histamine poisoning generally resemble the symptoms encountered with IgE-mediated food allergies. The symptoms include nausea, vomiting, diarrhea, an oral burning sensation or peppery taste, hives, itching, red rash, and hypotension. Due to the potential hazardous effects to humans, the development of analytical methodology for the determination of histamine is an important subject.

In present study, electrochemical behaviour of histamine on nickel-film based glassy carbon electrode (NiGCE) investigated and a sensitive chronopotentiometric method was developed. Electrochemical oxidation of histamine at NiGCE is achievable at moderate potentials of the working electrode providing good reproducibility and sensitivity of histamine determination. Experimental parameters affecting the oxidation process, including type and concentration of supporting electrolyte, initial potential, oxidation current, temperature and concentration time, were optimized. Chronopotentiometric determination of histamine on NiGCE can be performed in wide concentration range from 0.5-110 mg/L. Using a 240 s accumulation time, limit of detection and quantitation were 0.11 mg/L and 0.29 mg/L of histamine, respectively. The results obtained offer promising evidence that the simple chronopotentiometry on a nickel electrode can be used as a convenient analytical tool for histamine determination.

### Acknowledgements

This work was supported by the Ministry of Science and Technological Development of Republic of Serbia (Project TR 31014).

### References

- [1] S. Bodmer, C. Imark, M. Kneubühl, *Inflammation Res.* 48 (1999) 296-300.
- [2] B. Akbari-adergani, P. Norouzi, M.R. Ganjali, R. Dinarvand, *Food Res. Int.* 43 (2010) 1116-1122.
- [3] L. Maintz, N. Novak, *Am J Clin Nutr* 85 (2007) 1185-1196.
- [4] Z. Stojanović, J. Švarc-Gajić, *Electroanalysis* 24 (2010) 2031-2939.

**SCREENING OF NEONICOTINOIDS IN SURFACE WATER SAMPLES BY LIQUID CHROMATOGRAPHY QUADRUPOLE TIME-OF-FLIGHT MASS SPECTROMETRY**

**Zoran Stojanovic<sup>1</sup>, Ivana Dersek-Timotic<sup>1</sup>, Vojislava Bursic<sup>2</sup>, Bojana Spirovic-Trifunovic<sup>3</sup>, Gorica Vukovic<sup>4</sup>, Tijana Zeremski<sup>5</sup>**

<sup>1</sup>*National Reference Laboratory Department, Serbian Environmental Protection Agency, 11160 Belgrade, Ruze Jovanovica 27a, Serbia*

<sup>2</sup>*University of Novi Sad, Faculty of Agriculture, 21000 Novi Sad, Trg Dositeja Obradovica 8, Serbia*

<sup>3</sup>*University of Belgrade, Faculty of Agriculture, Nemanjina 6, 11080 Zemun, Serbia*

<sup>4</sup>*Public Health Institute of Belgrade, 11000 Belgrade, Blvd. despota Stefana 54a, Serbia*

<sup>5</sup>*Institute of Field and Vegetable Crops, Maksima Gorkog 30, Novi Sad*

*e-mail: zoran.stojanovic@sepa.gov.rs*

**Abstract**

The EU Decision 2015/495 concerning the watch list of substances for Union-wide monitoring in the field of water policy pursuant to Directive 2008/105/EC, among others, includes neonicotinoid insecticides, as well. The LC-QToF-MS technique was used for screening analysis of the surface water samples from Serbia. The residues of thiamethoxam, acetamiprid and imidacloprid were detected.

**Introduction**

Water is one of the essential resources for life and its multiple uses are indispensable for a series of activities, such as agriculture, generation of energy, public and industrial supply, among others. However, the technological development of mankind has not taken into account the risks to the environment. The pollution of surface and groundwater worldwide has become a major topic of discussion among scientists and experts in the field of environmental protection. Unfortunately, this problem has been observed relatively late (late eighties of the previous century), after the hazardous substances caused many damages to the aquatic ecosystems. Pesticides deserve special attention because they can migrate to the surface and ground water, after their application to the plants or the soil [1].

Very often farmers after the pesticides application throw empty packaging into the local channels or leave them next to the fields, which is another source of pollution [2, 3].

In the European Union, Directive 2000/60/EC sets out the basis for joint action in the field of water policy (Water Framework Directive - WFD). WFD constitutes the legal framework for the protection and improvement of the quality of all water resources such as rivers, lakes, groundwater, water and other coastal waters in the European Union. The main goal is to achieve "good chemical and ecological status in all waters" by 2015. The presence of priority and priority hazardous substances in water is regulated under Directive 2008/105/EC and Directive 2013/39/EU amending Directives 2000/60/EC and 2008/105/EC as regards priority substances in the field of water policy.

Directive 2013/39/EC [4] brings us environmental quality standards (EQS) for 45 hazardous substances in surface water, including 21 pesticides (atrazine, simazine, terbutryn, isoproturon, diuron, etc.). The presence in the environment of the pesticides that are not encompassed in this Directive is regulated by maximum allowable concentration of 0.1 µg/L (sum 0.5 µg/L).

The latest Commission implementing Decision (EU) 2015/495 [5] from 20 March 2015, established a watch list of substances for union-wide monitoring in the field of water policy pursuant to Directive 2008/105/EC. This Decision establishes additional substances and their maximum acceptable method detection limits like oxadiazon (8.8 ng/L), methiocarb (10 ng/L) and neonicotinoids (9-500 ng/L). Neonicotinoids are nowadays the most widely used insecticides in the world and include imidacloprid, thiamethoxam, acetamiprid, thiacloprid and clothianidin, as well as a metabolite 6-chloro nicotinic acid.

The multi-residue methods, lately, have been using LC/MS-MS which gives high sensitivity and selectivity operating in selective reaction monitoring mode. Triple quadrupole is the primary choice for pesticides because of the selectivity and sensitivity, as well as the wide dynamic range. Mass detectors with high mass resolution and high mass accuracy coupled with liquid chromatography allows us to get valuable information for substance identification. Time of flight (TOF) detectors are used for the identification of transformation products. Their intrinsic characteristic of highly accurate mass measurement and sensitivity in full-scan acquisition mode allows the reliable identification of a large number of degradation products in a single chromatographic run. The hybrid systems are also used for the identification of non-target and transformation products. In our work, we have investigated the surface water samples for the presence of neonicotinoids, by liquid chromatography with quadrupole time-of-flight mass spectrometry (LC-QTOF-MS) [6].

## **Experimental**

### **Samples and chromatographic conditions**

One hundred surface water samples were taken from rivers in Serbia according to ISO 5667-6 during autumn 2016. Samples are taken in 1L amber glass bottles, transported to the laboratory and kept in the refrigerator on 4 °C until the analysis. Before analysis samples are filtered through 1µm glass fiber filters and off-line pre-concentrated on Oasis HLB cartridges. The pesticides were eluted from cartridges with 5 ml of dichlormethane and 5 ml methanol. Extracts were evaporated to dryness at 40 °C on TechneDry-block under stream of nitrogen and reconstituted in 0.5 ml of initial mobile phase. Then, they were filtered through the 0.22 µm PTFE filters into the auto-sampler vials for LC-QTOF-MS. The LC-QTOF-MS conditions are given in Table 1.

Table 1. The LC-QToF-MS conditions

<b>LC1290Agilent Tehn.</b>	
Column	Eclipse Plus C18 150x2,1mm, 1,8µm
Flow	0.400 ml/min
Mobile phase composition	A:95% Acetonitrile + 0,1% Formic acid
	B: Water +0.1% Formic acid
<b>LC6550 QTOF Agilent Tehn.</b>	
<b>LC6550 QTOF Agilent Tehn.</b>	
Auto MS/MS settings	
<ul style="list-style-type: none"> <li>• Full Scan, Mass range 10-450 m/z, Absolute threshold 500 Acquisition rate 3 spectra/sec</li> </ul>	
MS/MS	
<ul style="list-style-type: none"> <li>• Inclusion list 125 pesticides, <math>\Delta</math> m/z 20 ppm, <math>\Delta</math> Rt 0.35 min</li> <li>• Isolation width 1.3 m/z, Mas range 35-450 m/z, Acquisition rate 2 spectra/sec, Absolute threshold 50, Max 5 precursor per cycle</li> </ul>	

The validation was done in accordance with SANTE/11945/2015 [7].

Limit of detection (LOD) and Limit of Quantification (LOQ) are defined by the regulation and experimentally confirmed through the spiking of real water sample with pesticide mix solution. The final concentration was from 4 to 25ng/L for different pesticide. S/N ratio was calculated with software in obtained chromatograms for LOQ. LOD values are obtained through statistical calculation.

Tabela 2: Accurate masses for  $[M + H]^+$  ions, LOD and LOQ for neonicotinoid pesticides

<b>Compound</b>	<b>Precursor ion</b>	<b>LOD (ng/L)</b>	<b>LOQ (ng/L)</b>
Thiamethoxam	292.0270	10	25
Clothianidin	250.0164	10	25
Imidacloprid	256.0597	2	5
Acetamiprid	223.0748	10	25
Thiacloprid	253.032	10	25

## Results and discussion

Data obtained from this investigation are given in Table 3. The most frequent found pesticide was imidacloprid in 39% of all analyzed samples. Eight water samples have got values which were above PNEC value. Other four pesticides are detected in amount less than 10% of all analyzed samples, and their concentrations are under the PNEC value for each of them.

Table 3. Pesticide residue detected in analyzed samples of surface water samples (ng/L)

Compound	PNEC value*	Max found concentration	Number of Postive results
Thiamethoxam	140	15	4
Clothianidin	130	12	5
Imidacloprid	9	16	39 (8 over limit)
Acetamiprid	500	19	9
Thiacloprid	50	47	6

\*The Predicted no effect concentration (PNEC) is the concentration of a chemical which marks the limit at which below no adverse effects of exposure in an ecosystem are measured

## Conclusion

For the extraction of pesticides and other contaminants from surface water samples, solid phase extraction techniques have been employed, which is a well-known technique used for the extraction of numerous compound classes in water, with high accuracy and precision. The polymeric Oasis HLB sorbent are the most used for extraction of pesticides. The use of LC-QToF-MS technique for qualitative and quantitative analyses of aqueous samples is growing. The rapid investigation in the field of LC-MS have transformed this technique into a key technique for the analysis of pesticides in environmental matrices.

EU Decision 495/2015 extends the standards pertaining to environmental quality in water protection of surface water, including neonicotinoid group of insecticides. LC-QToF-MS analysis of surface water samples is very helpful to detect low concentrations of neonicotinoids inspite of their very low PNEC values (for imidacloprid 9 ng/L). The results of the study suggest the need for constant monitoring of surface waters, especially if the water will be used for human consumption or recreation – bathing.

## Acknowledgements

This work was founded and a part of the project IPA 2012 Establishment of an integrated environmental monitoring system for Air and Water Quality capacity of air and water monitoring in Serbia.

## References

- [1] B.S. Ismail, H.S. Humaira, M.T. Latif, Int. J. Basic & Applied Sci. 12(6) (2012) 850.
- [2] V. Bursić, S. Gvozdenac, G. Vuković, M. Pucarević, S. Lazić, S. Vuković, T. Zeremski, D. Inđić D. 3rd International Conference of Ecology “Essays on Ecosystem and Environmental Research”, May 31- June 5.2013. Tirana, Albania, Proceeding book (2013) 870.
- [3] V. Bursić, G. Vuković, Z. Stojanović, S. Gvozdenac, T. Zeremski, M. Meseldžija, A. Petrović XXI Savetovanje o biotehnologiji, Proceedings 21(23) (2016) 359.

- [4] European Union, Directive 2013/39/EC of the European Parliament and of the Council, Official Journal of the European Communities, L226/1.
- [5] European Union, Directive 2015/495/EC of the European Parliament and of the Council, Official Journal of the European Communities, L348.
- [6] LC-QTOF-MS/MS method for the simultaneous full scan and MS/MS analysis of pesticides in fruit and vegetables, EURL-FV.
- [7] SANTE 11945/2015. Guidance document on analytical quality control and validation procedures for pesticide residues analysis in food and feed.



## GLASSY CARBON ELECTRODE MODIFIED WITH GRAPHENE OXIDE AND GOLD NANOPARTICLES FOR ASCORBIC ACID DETECTION

Árpád F. Szóke<sup>1</sup>, Liana M. Mureşan<sup>1</sup>, Graziella L. Turdean<sup>1</sup>, Zoltán Zsebe<sup>1</sup>,  
Kamila Ablaeva<sup>2</sup>

<sup>1</sup>*Faculty of Chemistry and Chemical Engineering, Babeş-Bolyai University, 400028 Cluj-Napoca, Arany János str. 11, Romania*

<sup>2</sup>*Al-Farabi Kazakh National University, 050040 Almaty, al-Farabi Ave 71, Kazakhstan  
e-mail: szokearpad@chem.ubbcluj.ro*

### Abstract

Glassy carbon electrodes modified with graphene oxide (GO), gold nanoparticles (AuNP) and methylene blue (MB) were produced by drop casting method for ascorbic acid (AA) determination. Nafion was used as a polymeric immobilizing matrix. The GCE/GO-AuNP-MB-Nafion and GCE/GO-AuNP-Nafion electrodes were characterized by using cyclic voltammetry and electrochemical impedance spectroscopy to investigate electrocatalytic effect, stability and reproductibility. After optimization, the analytical parameters of the modified electrodes were determined by amperometry. The limit of detection for ascorbic acid at GCE/GO-AuNP-Nafion modified electrode was 2.4 µM and the linear domain from 5 to 50 µM. The electrodes showed significant electrocatalytic effect with good stability and reproductibility.

### Introduction

Previous studies show, that glassy carbon electrodes have an anodic potential limit of approximately +1 V, depending on the electrolyte solution. Applying higher potentials will lead to polarization of the working electrode [1,2]. Thus, determining analytes with high oxidation potentials can lead to errors. This effect can be prevented by lowering oxidation potentials of analytes using modifying agents with electrocatalytic effect. Previously, graphene oxide, reduced graphene oxide and gold nanoparticles have been used as modifying agents with proven electrocatalytic effect [3,4,5,6].

L-ascorbic acid (vitamin C) is an important vitamin found in plants. It is an essential nutrient in human diet; insufficient levels of vitamin C can lead to the disease scurvy. It is also important in oxidative protection - being a potent antioxidant and reducing agent that functions in fighting bacterial infections - and in the formation of collagen for various tissues. L-ascorbic acid is widely available as a dietary supplement. Based on these, quantitative determination of ascorbic acid in biological and non-biological samples is of high importance [7]. Due to its relatively high oxidation potential (approximately 0.7 V, depending on the electrode used), analysis by electrochemical methods can be problematic and affected by interferences. For a reliable determination of ascorbic acid, lowering of the oxidation potential is needed.

In this context, our goal was to develop and optimize modified glassy carbon electrodes with a new synthesized graphene oxide (GO), gold nanoparticles (AuNP) and methylene blue (MB) using the drop-casting method for efficient ascorbic acid determination.

Immobilization of the modifying agents on the electrode surface can be achieved through a polymer matrix using Nafion or chitosan.

### **Experimental**

The glassy carbon electrode surface was cleaned by polishing, using a 2.5  $\mu\text{m}$  and a 0.3  $\mu\text{m}$  particle size  $\text{Al}_2\text{O}_3$  polishing powder from Buehler followed by three minutes of sonication in distilled water to clean it of any powder residue. The graphene oxide (GO) was prepared by dr. C. Cotet at the Faculty of Chemistry and Chemical Engineering by graphite exfoliation method [8], the  $\text{Na}_2\text{HPO}_4 \cdot 2 \text{H}_2\text{O}$ ,  $\text{NaH}_2\text{PO}_4 \cdot 12 \text{H}_2\text{O}$  and a 5 w/w% Nafion in ethanol solution were supplied by Sigma Aldrich. The methylene blue was provided by Merck, 100% ethanol was provided by Reactivul Bucuresti, the 100% L-ascorbic acid was supplied by Madal Bal kft.

A 1 w/w% graphene oxide dispersion was prepared by sonication of the solid GO in distilled water for 5 hours and a further 30 minutes of mixing using a Vortex mixer. A sol of approximately 40 nm particle size gold nanoparticles was prepared using the Turkevich-Frens method. A 0.125 w/w% alcoholic Nafion solution was prepared by diluting the 5 w/w% solution. A 1 mM methylene blue solution was prepared by dissolving the powder in ethanol. A 0.1 M phosphate buffer solution was prepared by dissolving appropriate amounts of  $\text{Na}_2\text{HPO}_4$  and  $\text{NaH}_2\text{PO}_4$  and adjusting the pH value to 7 with 0.1 M  $\text{H}_3\text{PO}_4$  or NaOH solutions, respectively.

Modified glassy carbon electrodes have been produced by the drop-casting method. Mixtures of the prepared solutions have been sonicated for two minutes before drop casting on the glassy carbon electrode surface. Solvent evaporation was performed by air drying at room temperature for a minimum of 3 hours. The GO was then reduced by cyclic voltammetry during a pretreatment phase which consisted in potential cycling between -1 and 0 V. Electrochemical measurements were using a PGSTAT-302 Autolab potentiostat (The Netherlands). Optimization studies were performed using cyclic voltammetry, calibration curves were obtained using amperometry.

### **Results and discussion**

Optimization studies have been conducted to determine the ideal amount of the modifying agents (GO, AuNP) and of the immobilizing agent (Nafion) in the presence of MB. Adding methylene blue did not yield the expected results and was kept constant (5  $\mu\text{L}$  of 1 mM solution in ethanol) during the optimization procedure. Ideal results have been obtained by drop casting 2.5  $\mu\text{L}$  of GO dispersion, 5  $\mu\text{L}$  of AuNP sol and 3  $\mu\text{L}$  of 0.125 % Nafion solution.

The oxidation potential of ascorbic acid at the bare glassy carbon and at GCE/GO-AuNP-Nafion modified electrode was 670 mV and 275 mV, respectively (Figure 1.). This shift of approximately 400 mV in oxidation potential suggests a strong electrocatalytic effect of the modifying agents.

A further study shows that the slope of the calibration curve for ascorbic acid determined using cyclic voltammetry has increased from 4.46  $\mu\text{A}/\text{mM}$  in the case of the bare electrode to

6.06  $\mu\text{A}/\text{mM}$  in the case of the GCE/GO-AuNP-Nafion modified electrode (results not shown).

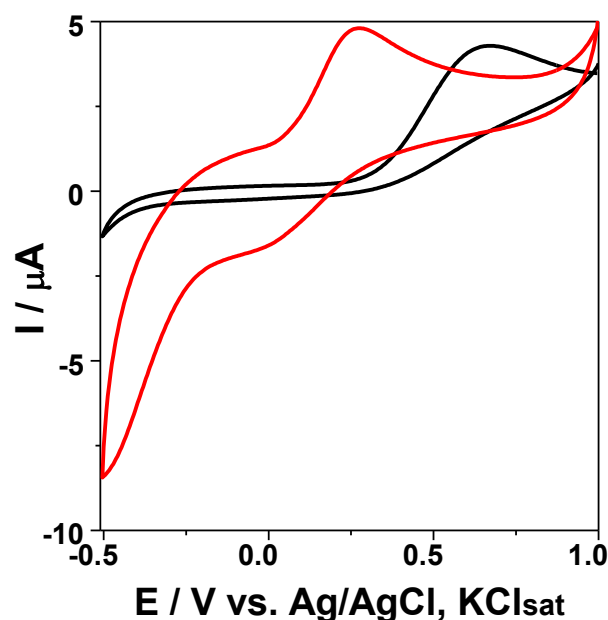


Figure 1. Cyclic voltammograms of 500 mM AA measured using a bare glassy carbon electrode (black) and a modified GCE/GO-AuNP-Nafion electrode (red). Experimental conditions: electrolyte, phosphate buffer, pH 7; starting potential, +1 V vs. Ag/AgCl,  $\text{KCl}_{\text{sat}}$ .

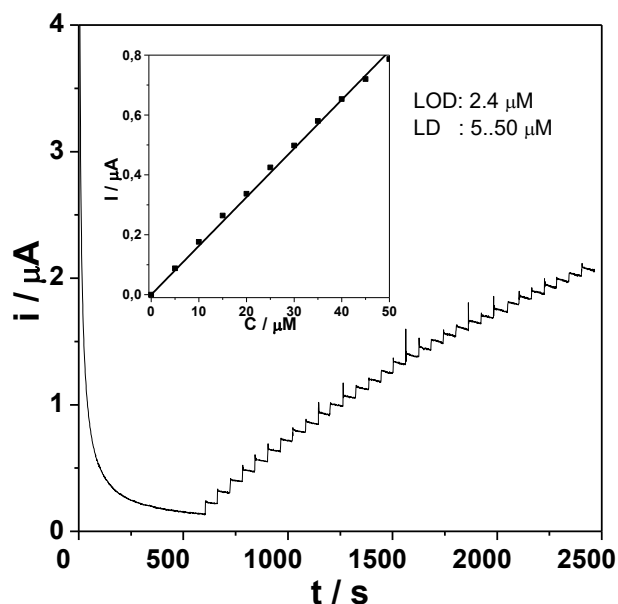


Figure 2. Amperometric measurement and calibration curve of AA using GCE/GO-AuNP-Nafion modified electrode. Experimental conditions: electrolyte, phosphate buffer, pH 7; applied potential, +0.2 V vs. Ag/AgCl,  $\text{KCl}_{\text{sat}}$ , rotating speed, 500 rpm.

The amperometric calibration curve (Figure 2.) shows a good linear range measured up to 50  $\mu\text{M}$  ascorbic acid ( $R^2 = 0.9994$ , no. of points = 11), with a low detection limit of 2.4  $\mu\text{M}$  (signal/noise = 3).

EIS measurements show that impedance is increased by the immobilizing layer of Nafion and decreased by the GO and AuNPs (results not shown).

### Conclusion

A novel, GCE/GO-AuNP-Nafion modified electrode for ascorbic acid detection has been produced, optimized and characterized. Using simple methods, we have managed to significantly decrease the oxidation potential and to increase peak height.

Further studies need to be made to determine short and long term stability and selectivity when measured in the presence of coexisting chemicals (interferents) with similar oxidation potentials, such as uric acid and dopamine.

### Acknowledgements

We would like to thank the support of the KMEI and SHA scholarships for their financial aid and Dr. Adriana Vulcu (INCDTIM) for supplying the gold nanoparticles.

### References

1. M. Gross, J. Jordan, *Voltammetry at glassy carbon electrodes*, Pure & Appl. Chem., 56 (8), (1984), 1095—1129  
T. Shigemitsu, G. Matsumoto, *Electrical properties of glassy-carbon electrodes*, Med. & Biol. Eng. & Comput., 17, (1979), 465-470
2. Á. F. Szőke, G. L. Turdean, G. Katona, L. M. Muresan, *Electrochemical determination of dopamine with graphene-modified glassy carbon electrodes*, STUDIA UBB CHEMIA, LXI, 3, Tom I, (2016), 135-144
3. W. Huan, X. Li-Guang, C.Xue-Feng, C.Yao-Dan, Y. Xiao-Tian, *Rational Design of Gold Nanoparticle/graphene Hybrids for Simultaneous Electrochemical Determination of Ascorbic Acid, Dopamine and Uric Acid*, Chinese Journal of Analytical Chemistry, 44 (12), (2016), 1617–1625
4. X. Tiana, C. Cheng, H. Yuan, J. Dua, D. Xiao, S. Xiec, M. M.F. Choi, *Simultaneous determination of l-ascorbic acid, dopamine and uric acid with gold nanoparticles—cyclodextrin–graphene-modified electrode by square wave voltammetry*, Talanta, 93, (2012), 79–85
5. J. Song, L. Xu, R. Xing, Q. Li, C. Zhou, D. Liu, H. Song, *Synthesis of Au/Graphene Oxide Composites for Selective and Sensitive Electrochemical Detection of Ascorbic Acid*, Scientific reports, 4 (7515), (2014), 1-7
6. L-ascorbic acid, *National Center for Biotechnology Information. PubChem Compound Database*, accessed sept. 17, 2017
7. L.C. Cotet, K. Magyari, M. Todea, M.C. Dudescu, V. Danciu, L. Baia, *Versatile self-assembled graphene oxide membranes obtained in ambient conditions by using a water-ethanol suspension*, J. Mat. Chem. A, 5, (2017), 2132-2142

## ACTIVITY EVOLUTION OF NANOCRYSTALLINE ZINC-INDIUM-OXIDE POWDER

**Tamara Ivetić<sup>1</sup>, Nina Finčur<sup>2</sup>, Biljana Abramović<sup>2</sup>, Ljubica Đaćanin Far<sup>1</sup>, Svetlana Lukić-Petrović<sup>1</sup>**

<sup>1</sup>*University of Novi Sad, Faculty of Sciences, Department of Physics, 21000 Novi Sad, Trg Dositeja Obradovića 4, Serbia*

<sup>2</sup>*University of Novi Sad, Faculty of Sciences, Department of Chemistry, Biochemistry and Environmental Protection, 21000 Novi Sad, Trg Dositeja Obradovića 3, Serbia*  
*e-mail: tamara.ivetic@df.uns.ac.rs*

### Abstract

In this work, the photocatalytic activity evolution of the mixed zinc-indium-oxide (ZIO) nanocrystalline powders (NCPs) was presented depending on the alterations in its solid-state preparation procedure and different concentrations of the starting precursors. The activity of the obtained ZIO NCPs as photocatalysts was examined through the degradation of two pharmaceutically active compounds (PhACs), the potential organic water pollutants, under simulated solar irradiation (SSI).

### Introduction

The presence of PhACs in drinking and environmental waters was found in many countries and mainly this pollution originates from the wastewater treatment plants [1]. Residual traces of PhACs after the usual treatment of the waste and contaminated waters are an increasing pollution problem that needs a prompt solution in the form of the supplementary methods for further purification, like heterogeneous photocatalysis (HPC). HPC is one of the alternative wastewater treatment technologies known as advanced oxidation processes (AOPs) [2, 3]. HPC generally implies the presence of a metal oxide semiconductor in the contaminated waters and simultaneous illumination with either ultraviolet (UV) or even better visible (Vis) light source. Through higher oxidation processes, and the formation of highly reactive oxidizing agents (mainly hydroxyl radicals  $\bullet\text{OH}$ ), the organic pollutants in water are transformed over time to less toxic chemicals, inorganic ions, or totally harmless carbon dioxide and water. The efficiency of the metal oxide semiconductor catalyst is measured by the time it takes to degrade the organic substance under the influence of the applied electromagnetic light (UV or Vis). The best efficiency of the photocatalyst is when it takes a shorter time for the organic substance to decompose in the presence of a given photocatalyst, and for the sake of the cost-efficiency if possible under the influence of the sunlight. Zinc-indium-oxide system is a promising candidate that supports the photodegradation of the organic pollutants and could replace the most used material for this application, titanium dioxide (TiO<sub>2</sub>) Degussa P25 [4].

### Experimental

The mixtures of ZIO NCPs were prepared using the environmentally friendly solid-state method. Starting precursors were commercial zinc oxide (ZnO) and indium oxide (In<sub>2</sub>O<sub>3</sub>) powders purchased from Sigma-Aldrich (purity 99.9%). The preparatory procedure varied for the different samples but generally included following processing steps: mechanical activation by grinding, pressing (50 kg/cm<sup>2</sup>), annealing, and grinding. Here are presented the results of

the two samples where indium was at a doping level (marked as  $\text{In}_2\text{O}_3(3\text{wt.})/\text{ZnO}(97\text{wt.})-700^\circ\text{C}/1\text{h}$  and  $\text{In}_2\text{O}_3(3\text{wt.})/\text{ZnO}(97\text{wt.})-950^\circ\text{C}/1\text{h}$ ) and one sample where the starting precursors had molar ratio around  $\text{ZnO}:\text{In}_2\text{O}_3=2:1$  (marked as  $\text{In}_2\text{O}_3(54\text{wt.})/\text{ZnO}(46\text{wt.})-700^\circ\text{C}/2\text{h}$ ). The analytical standard of used PhACs, alprazolam ( $\text{C}_{17}\text{H}_{13}\text{ClN}_4$ ) and amitriptyline hydrochloride ( $\text{C}_{20}\text{H}_{24}\text{ClN}$ ) were purchased from Sigma-Aldrich. All chemicals were analytical grade. The NCPs loading was 1 mg/mL and the initial concentration of the investigated PhACs was 0.03 mmol/L. Before performing the photocatalytic experiment, samples were stirred in dark in order to achieve the adsorption-desorption equilibrium. Photocatalytic efficiency was measured after different time intervals. Samples were first filtrated through a Millipore (Millex-GV, 0.22  $\mu\text{m}$ ) membrane filter in order to remove ZIO NCPs from the aqueous solution, and then the appropriate aliquots (0.5 mL) were transferred into the vials and analyzed by ultra fast liquid chromatography with UV/Vis diode array detector (UFLC-DAD, Shimadzu) set at 222 nm and 206 nm which are the wavelengths of the alprazolam and amitriptyline maximum absorption, respectively. Scanning electron microscope, SEM (JEOL JSM-6460LV) was used to investigate the microstructure of the obtained ZIO NCP samples.

### Results and discussion

The first results of the efficiency of ZIO NCPs in photocatalytic degradation of PhACs under simulated solar irradiation showed promising results [5]. Here are presented the comparative results of the photocatalytic degradation efficiency of three different ZIO NCPs and standard  $\text{TiO}_2$  Degussa P25 in the degradation of alprazolam and amitriptyline (Fig. 1 shows the removal efficiency depending on the irradiation time).

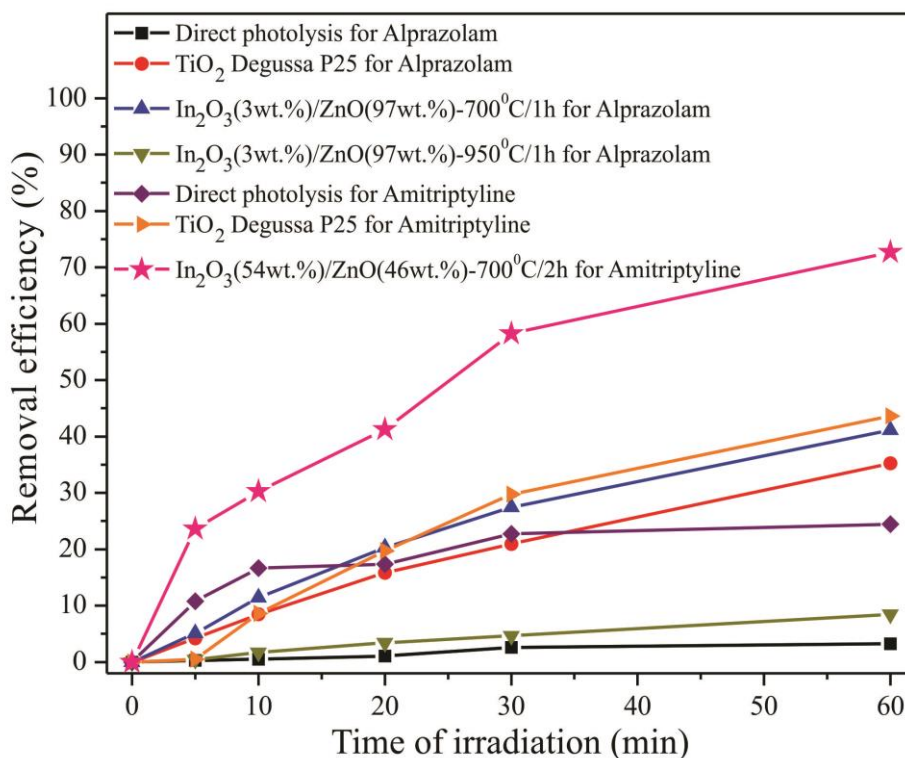


Figure 1. The removal efficiency of ZIO NCPs and  $\text{TiO}_2$  Degussa P25 under SSI in the degradation of alprazolam and amitriptyline.



The ZIO NCP prepared at 950 °C showed no photocatalytic efficiency, while the sample marked as  $\text{In}_2\text{O}_3(3\text{wt.}\%)/\text{ZnO}(97\text{wt.}\%)-700^\circ\text{C}/1\text{h}$  removed 41% of PhAC after the 60 min of SSI irradiation (Fig. 1). The most satisfactory removal of PhACs (73% of amitriptyline) was achieved in the presence of ZIO NCP which was prepared by grinding the starting precursor in the molar ratio of about 2:1, which were then annealed at 700 °C in air for two hours, and ground again, and was marked as  $\text{In}_2\text{O}_3(54\text{wt.}\%)/\text{ZnO}(46\text{wt.}\%)-700^\circ\text{C}/2\text{h}$  (Fig. 1). Intensified indium incorporation at the higher annealing temperature (950 °C) should significantly reduce the particle size and shift the optical band gap towards the visible region when the starting indium concentration is at a doping level (samples with 3 wt.% of  $\text{In}_2\text{O}_3$  and 97 wt.% of ZnO in Fig. 1). However, the occurrence of the unfavorable for the photocatalysis, the loss of the intrinsic defects such as oxygen vacancies and the formation of unstable  $\text{In}^{2+}$  ions, for the samples prepared at temperatures higher than 700 °C, could also accelerate the recombination rate and diminish the photocatalytic performance. The morphology and microstructure of the ZIO NCPs with significant photocatalytic efficiency,  $\text{In}_2\text{O}_3(3\text{wt.}\%)/\text{ZnO}(97\text{wt.}\%)-700^\circ\text{C}/1\text{h}$  and  $\text{In}_2\text{O}_3(54\text{wt.}\%)/\text{ZnO}(46\text{wt.}\%)-700^\circ\text{C}/2\text{h}$  were investigated by SEM and the example images are shown in Fig. 2.

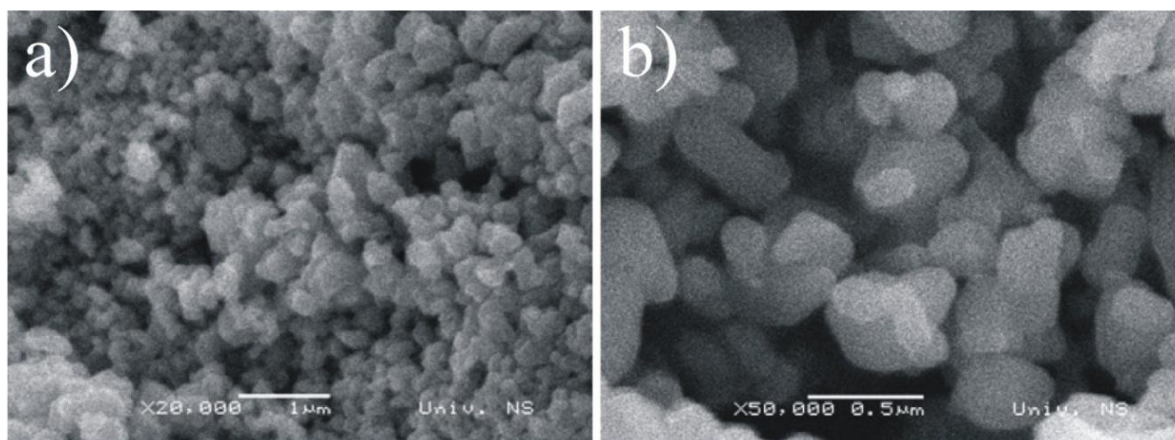


Figure 2. SEM images of ZIO NCPs, a)  $\text{In}_2\text{O}_3(3\text{wt.}\%)/\text{ZnO}(97\text{wt.}\%)-700^\circ\text{C}/1\text{h}$ , and b)  $\text{In}_2\text{O}_3(54\text{wt.}\%)/\text{ZnO}(46\text{wt.}\%)-700^\circ\text{C}/2\text{h}$ .

### Conclusion

According to the obtained results, the ZIO NCP with ~46 wt.% of ZnO and ~54 wt.% of  $\text{In}_2\text{O}_3$  is the most suitable for the photocatalytic degradation of the investigated PhACs. Its better photocatalytic performance compared to the other tested and differently prepared ZIO NCPs is believed to be a result of the synergetic effect of achieving better visible light activation through  $\text{In}_2\text{O}_3$  absorption and charge separation mechanism obtained by ZnO and  $\text{In}_2\text{O}_3$  band gap coupling, at the same time.

### Acknowledgements

The authors are grateful to the APV Provincial Secretariat for Higher Education and Scientific Research for partly financing this work (Project number 114-451-1821/2016-03) and acknowledge the support of the Ministry of Education, Science and Technological Development of the Republic of Serbia (Project numbers ON 172042 and III 45020).



**References**

- [1] M. Wu, J. Xiang, C. Que, F. Chen, G. Xu, *Chemosphere* 138 (2015) 486.
- [2] S. Sarkar, R. Das, H. Choi, C. Bhattacharjee, *RSC Adv.* 4 (2014) 57250.
- [3] A. Gajović, A.M.T. Silva, R.A. Segundo, S. Šturm, B. Jančar, M. Čeh, *Appl. Catal. B. Environ.* 103 (2011) 351.
- [4] S.G. Kumar, K.S.R.K. Rao, *RSC Adv.* 5 (2015) 3306.
- [5] T. Ivetić, N. Finčur, Lj. Đačanin, B. Abramović, S. Lukić-Petrović, 22nd International Conference on Materials and Technology, 20-22 October 2014, Portorož, Slovenia, Program and Book of Abstracts p. 99.

## HIGHLY EFFICIENT REMOVAL OF PHARMACEUTICALS FROM AQUEOUS WASTES: EVALUATION OF OPTIMAL PROCESS PARAMETERS

Maja Turk Sekulić<sup>1</sup>, Nikola Bošković<sup>1</sup>, Dragan Adamović<sup>1</sup>, Jelena Garunović<sup>1</sup>,  
Aleksandar Slavković<sup>1</sup>, Jelena Radonić<sup>1</sup>, Sabolč Pap<sup>1</sup>

<sup>1</sup>*Faculty of Technical Sciences, Department of Environmental Engineering and Occupational Safety and Health, University of Novi Sad, Trg Dositeja Obradovića 6, 21 000 Novi Sad, Serbia, majaturk@uns.ac.rs*

### Abstract

This study investigates the competitive adsorption potential of activated carbon prepared from cherry kernels (CScPA) to remove sulfamethoxazole, carbamazepine, ketoprofen, naproxen, diclofenac and ibuprofen from aqueous solution. The effect of operational parameters including initial pH, adsorbent dose, contact time and initial pharmaceutical concentration were studied in batch adsorption experiments. The results indicate that CScPA can be used as an alternative, effective and low-cost adsorbent that presents basis of sustainable technology for efficient pharmaceuticals wastewater remediation and decontamination.

### Introduction

In recent years, the presence of pharmaceuticals and personal care products (PPCPs) discharged into the water environment has been recognized as one of the common emerging issues worldwide because their residues may damage or have other adverse effects on the environmental ecology [1]. Pharmaceutical antibiotic sulfamethoxazole (SMX) is produced in large quantities and extensively used in the farming industry as veterinary therapeutics and growth promoters [2]. Diclofenac (DCF) and carbamazepine (CBZ) are two of the most frequently detected pharmaceutical residues in aquatic environments. DCF is a non-steroidal anti-inflammatory drug (NSAIDs) commonly used for the treatment of arthritis, whilst CBZ is an antiepileptic drug used for the treatment of psychomotor and temporal lobe epilepsy and also for the treatment of trigeminal neuralgia [3]. Ketoprofen (KP) is a non-steroidal anti-inflammatory drug, widely used for the treatment of rheumatoid arthritis, osteoarthritis, ankylosing spondylitis, and also for non-rheumatoid diseases or postoperative pain [4]. Naproxen (NPX) is a member of the arylacetic acid group that exhibits anti-inflammatory and analgesic effects in medical treatments [5]. Ibuprofen (IBP) is one of the most highly utilized NSAIDs worldwide and therefore it has been one of the most commonly detected pharmaceuticals in the environment, with concentrations up to micrograms per liter [6].

Recently there has been a growing concern about the elimination of pharmaceutical compounds from wastewater, and technologies studied include photo-catalytic degradation [7], biodegradation [8], biofiltration [9] and membrane filtration [10]. Advanced oxidation processes and other chemical treatments, can break down organic molecules into simple compounds, but they have many disadvantages; for instance, the high capital and operational cost and possible generation of secondary pollutions resulting in high disposal costs [11]. In contrast, adsorption technique is one of the preferred methods due to its simplicity as well as the availability of wide range of adsorbents. The cost of adsorption technology application can be reduced, if the adsorbent is cheap. Previous studies have revealed adsorption of PPCPs onto various adsorbents, such as activated carbon [12–14], carbon nanotubes [15], mesoporous nanocomposite [16] and agricultural waste[17,18].

So far, activated carbon is the widely used adsorbent for the removal of PPCPs. In recent years growing research interest in the production of low-cost and highly efficient activated carbons. The suitable application of activated carbon depends on its properties which vary with used raw precursor and preparation technique [19]. Recently, activated carbons are derived from relatively cheap and effective raw materials with a high carbon and low inorganic content, such as agro-industrial wastes, fruit industry waste and various solid organic substances for a lower adsorption system cost.

In the current study, the green activated carbon from fruit processing industry waste (cherry/sweet cherry kernels) was investigated for PPCPs removal capacity from aqueous solutions following batch experiments. The effects of pH (2-9), adsorbent dosage (0.04-4 g/L), initial concentration of PPCPs in the solution (1-50 mg/L) and contact time (5-300 min) were evaluated. The goal of this work is to evaluate the performance of the CScPA for the competitive removal of PPCPs from aqueous wastes and to simulate complex pollutant conditions encountered in wastewater treatment plant influent.

### Experimental

About 140,000 tons of sweet and sour cherry are produced in Serbia every year. Because of that prepared activated carbon was made from sour cherry/sweet cherry kernels which were washed with distilled water, crushed and dried. Phosphoric acid (50 wt.%) was used for thermochemical impregnation. Further procedure is shown in previously work [20].

Five PPCPs (CBZ, DCF, NPX, KP and IBP) were purchased from Sigma–Aldrich (Germany) while SMX was purchased from Fluka (Buchs, Switzerland). Water used for all standards were milli-Q prepared with Easypure II, Thermo Scientific. The stock solutions containing of SMX, CBZ, DCF, NPX, KP and IBP were prepared dissolving standards with 10 mL of water (milli-Q) and then 10 mL acetonitrile (HPLC grade, Sigma-Aldrich, Germany). After that 10 mL of 0.05% CH<sub>3</sub>COOH, 250 mL of glacial CH<sub>3</sub>COOH (Zorka Pharma, Serbia), diluted in volumetric flask of 500 mL filled with milli-Q water, and another 10 mL of acetonitrile were added. Standard solution concentration of pharmaceuticals was determined by HPLC (High Performance Liquid Chromatography, Agilent 1200 series).

Pharmaceuticals in filtered solution were detected by previously described chromatographic technique. The principle is states the separation and quantification of pharmaceuticals using XDB-C18 column and mobile phase, acidic solution with acetonitrile, with detection at various wave length. Separation was achieved with a type-C18 chromatography column (Zorbax Eclipse XDB-C18, 4.6 mm x 150 mm, particle size 5 μm); flow rate: 1 mL/min; column temperature: 30°C; injection volume: 15 μL; mobile phase: 0,05% CH<sub>3</sub>COOH: acetonitrile (HPLC grade, Sigma-Aldrich, Germany) = 55:45; run time = 18 min; detection: 280, 220, 230 and 254 nm [21].

Adsorption tests were performed by shaking the flasks at 140 rpm for fixed time using mechanical stirrer Heidolph Unimax 1010 (Germany) in order to achieve equilibrium. The mixtures were then filtered through FIORONI qualitative filter paper (Grade 115) and residual concentrations of pharmaceuticals were measured using HPLC. Two important equations are used to calculate amount of adsorbed pharmaceuticals on activated carbon  $q_e$  (mg/g) and to determine percent of removal of pharmaceuticals from solution  $R_e$  (%):

$$q_e = \frac{(C_0 - C_e) \cdot V}{m} \quad (1)$$

$$R_e (\%) = \frac{(C_0 - C_e)}{C_0} \cdot 100 \quad (2)$$

Where  $C_0$  is the initial pharmaceutical concentration (mg/L) and  $C_e$  is the pharmaceutical concentration at equilibrium (mg/L),  $V$  is the volume of solution (L) and  $m$  is the mass of activated carbon (g).

The effect of pH on pharmaceutical adsorption onto CScPA was investigated as following procedure: 0.1 g (2.0 g/L) of CScPA were added to 50 mL solution using initial concentration of 10 mg/L of each pharmaceutical for 60 min at room temperature ( $22\pm 1$  °C). In order to study the effect of pH on pharmaceutical adsorption, the initial pH of the solutions varied from 2 to 9, by adding appropriate amounts of diluted  $\text{NH}_4\text{OH}$  and HCl solutions.

Influence of activated carbon dosage was studied by using CScPA concentration ranging from 2, 10, 20, 50, 80, 100, 150, 200 mg, (0.04-4 g/L) in 50 mL solution of 10 mg/l each pharmaceutical at optimal pH 6, for contact time of 60 min. Whole experiment was done at room temperature ( $22\pm 1$  °C).

The effect of contact time was studied at various time intervals (5, 15, 30, 60, 120, 180, 240, 300 min) with initial concentration of 10 ml/L of each pharmaceutical at pH 6.0 and room temperature ( $22\pm 1$  °C). In 50 ml solution CScPA dose was 0.1 g (2.0 g/L).

In order to assess the effect of pharmaceutical concentration on adsorption efficiency, initial adsorbate concentrations were varied at 1, 2, 5, 10, 20, 30, 40, 50 mg/L of each pharmaceutical with optimal pH (6.0), CScPA dose of 0.1 g (2.0 g/L), contact time 60 min at temperature ( $22\pm 1$  °C).

## Results and discussion

Fig. 1a shows the effect of pH on the removal of pharmaceutical into CScPA for different pH values. Generally, the adsorption of pharmaceuticals depends strongly on the pH of the solution [22]. From the Fig. 1a, it may be concluded that the retention of pharmaceuticals after adsorption onto CScPA is remarkably influenced by the pH. This parameter has very important role in adsorption process and in particular on the adsorption capacity [23]. In fact, the adsorption efficiency of SMX, CBZ, DCF, NPX, KP and IBP decreases when pH was increased from 6 to 9. The  $\text{pK}_a$  of KP, NPX, DCF and IBP are 4.45, 4.2, 4.15, 4.91, respectively, when pH is above  $\text{pK}_a$ , acidic pharmaceuticals have negative charge while surface of adsorbent becomes more negatively charged, leading to an electrostatic repulsion between them. The  $\text{pK}_{a1}$  and  $\text{pK}_{a2}$  of SMX are 1.6 and 5.7 which indicates that this molecule has zero charge which indicates that there is no electrostatic bonding. CBZ has  $\text{pK}_a$  13.9 showing that it has a positive charge leading to potential electrostatic interaction between pharmaceuticals and surface groups of the CScPA.

Adsorption of acidic PPCPs decrease gradually for basic pH values. Dissociation degree of the surface functional groups and PPCPs is high, so the adsorbent and the solutes KP, NPX, DCF and IBP are in their negatively charged forms. In case of CBZ, it's neutral compound in the pH tested range; its binding onto CScPA is solely attributable to a non-electrostatic interaction involving hydrogen bonding probably through a nitrogen groups, oxygen groups of esters, carbonyl groups from aldehyde and ketones, methyl groups for hydrophobic bonding and Van der Waals interactions [24].

Adsorption efficiency is strongly affected by the adsorbent dosage, due to availability of the surface area and exchangeable sites. Fig. 1b presents results of the experiments with varying activated carbon concentrations. With the increase of activated carbon mass, from 2 mg to 200 mg, (0.04 - 4 g/L), the amount of adsorbed SMX, CBZ, DCF, NPX, KP and IBP decreases from 17.87 to 2.72 mg/g, 84.40 to 2.49 mg/g, 39.70 to 2.59 mg/g, 21.33 to 2.73 mg/g, 21.11 to 3.35 mg/g, 38.99 to 2.44 mg/g, respectively. After dosage of 2.0 g/L, the removal efficiency

was not increased rapidly. This dosage was adopted because the aim was to find optimal removal efficiency, while retaining minimal operating costs, for economic application for wastewater treatment plant.

The effect of contact time on the adsorption of SMX, CBZ, DCF, NPX, KP and IBP on the CScPA is presented in Fig. 1c. It is revealed, as expected, that increasing in contact time increased removal of PPCPs. In the first step of adsorption over 85% of pharmaceuticals are bounded in first 15 min and in the second phase equilibrium is attained within 60 min. It is easy to spot fast adsorption of every pharmaceutical on CScPA. CBZ showed in Fig. 1c represents that contact time is not strictly correlated with the adsorbate removal, because of its molecule nature. The amount of adsorbed pharmaceutical increased with time at initial stage of adsorption and after some point in time almost remained constant. Dynamic equilibrium was reached by the amount of adsorption from adsorbent, at this point. The time required to attain the state of equilibrium is termed the equilibrium time, and the amount of pharmaceutical adsorbed at the equilibrium time reflects the maximum adsorption capacity of the adsorbent under a given operation condition [25].

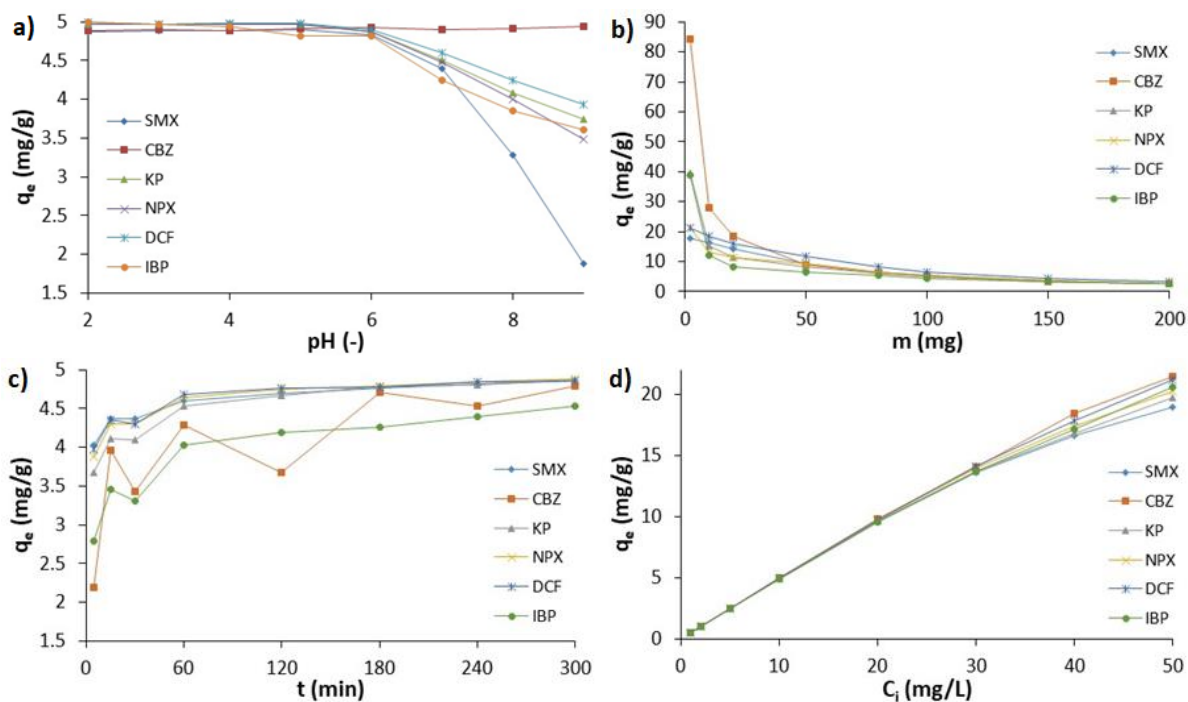


**Figure 1.** Effect of pH (a), adsorbent concentration (b), contact time (c) and initial concentrations (d) of SMX, CBZ, KP, NPX, DCF and IBP onto adsorption process

Varying pharmaceutical concentrations of 1-50 mg/L on optimal conditions showed decreasing in removal efficiency, for every pharmaceutical it was almost the same, up to 10 mg/L. After that, the removal efficiency was slightly decreasing up to 30mg/L, after which it decreased significantly. In whole process (Fig. 1d) of adsorption SMX, CBZ, DCF, NPX, KP and IBP removal efficiency dropped from 98.35 to 75.92%, 98.88 to 85.99%, 98.70 to 78.91%, 98.38 to 81.02%, 98.98 to 84.93%, 97.90 to 82.25%, respectively. Decrease in predicted process efficiency may be attributed to the lack of sufficient adsorption sites on surface area to accommodate more pharmaceutical available in the solution. Initial concentration of pharmaceuticals effected adsorption rate and capacity. Necessary driving

force was supplied by minimized mass transfer of initial concentration. In general, initial concentration boosts the adsorption of pharmaceuticals irrespective of the nature of adsorbent surface such as microporous, mesoporous, negatively or positively charge surface. The concentration increases the accessibility of pores for adsorbate molecules, as well as interactions at solid–liquid interface [26].

### Conclusion

This paper describes the adsorption of six pharmaceuticals (SMX, CBZ, KP, NPX, DCF and IBP) onto green activated carbon CScPA in multi-solute solutions. The batch adsorption experiments showed that the optimal operation conditions at 140 rpm, pH 6.0, CScPA dosage 2 mg/L and contact time 60 min have removal efficiency over 95 % for SMX, CBZ, KP, NPX, DCF and IBP. According to obtained results, the CScPA was found to be a promising low-cost solution for PPCPs contaminated water remediation and decontamination.

### Acknowledgements

This study has been financially supported by Ministry of Education, Science and Technological Development, Republic of Serbia (III46009)

### References

- [1] C. Nebot, R. Falcon, K.G. Boyd, S.W. Gibb, *Environ. Sci. Pollut. Res.* 22 (2015) 10559–10568.
- [2] L. Ji, Y. Wan, S. Zheng, D. Zhu, *Environ. Sci. Technol.* 45 (2011) 5580–5586.
- [3] Y. Zhang, S.U. Geißen, C. Gal, *Chemosphere* 73 (2008) 1151–1161.
- [4] R. Baccar, M. Sarrá, J. Bouzid, M. Feki, P. Blánquez, *Chem. Eng. J.* 211–212 (2012) 310–317.
- [5] Z. Hasan, J. Jeon, S.H. Jhung, *J. Hazard. Mater.* 209–210 (2012) 151–157.
- [6] S.P. Dubey, A.D. Dwivedi, M. Sillanpää, K. Gopal, *Chem. Eng. J.* 165 (2010) 537–544.
- [7] L. Rizzo, S. Meric, M. Guida, D. Kassinos, V. Belgiorno, *Water Res.* 43 (2009) 4070–4078.
- [8] K.M. Onesios, J.T. Yu, E.J. Bouwer, *Biodegradation* 20 (2009) 441–466.
- [9] V. Matamoros, C. Arias, H. Brix, J.M. Bayona, *Water Res.* 43 (2009) 55–62.
- [10] C. Sheng, A.G.A. Nnanna, Y. Liu, J.D. Vargo, *Sci. Total Environ.* 550 (2016) 1075–1083.
- [11] G. Moussavi, A. Alahabadi, K. Yaghmaeian, M. Eskandari, *Chem. Eng. J.* 217 (2013) 119–128.
- [12] J. V. Flores-Cano, M. Sánchez-Polo, J. Messoud, I. Velo-Gala, R. Ocampo-Pérez, J. Rivera-Utrilla, *J. Environ. Manage.* 169 (2016) 116–125.
- [13] G.Z. Kyzas, E.A. Deliyanni, *Chem. Eng. Res. Des.* 97 (2015) 135–144.
- [14] J. Lladó, M. Solé-Sardans, C. Lao-Luque, E. Fuente, B. Ruiz, *Process Saf. Environ. Prot.* 104 (2016) 294–303.
- [15] D. Wu, B. Pan, M. Wu, H. Peng, D. Zhang, B. Xing, *Sci. Total Environ.* 427–428 (2012) 247–252.
- [16] Z. Qiang, X. Bao, W. Ben, *Water Res.* 47 (2013) 4107–4114.
- [17] S. Pap, T.Š. Knudsen, J. Radonić, S. Maletić, S.M. Igić, M.T. Sekulić, *J. Clean. Prod.* 162 (2017) 958–972.
- [18] M. Turk Sekulić, S. Pap, Z. Stojanović, N. Bošković, J. Radonić, T. Šolević Knudsen, *Sci. Total Environ.* 613–614 (2018) 736–750.



- [19] S.Á. Torrellas, R. García Lovera, N. Escalona, C. Sepúlveda, J.L. Sotelo, J. García, *Chem. Eng. J.* 279 (2015) 788–798.
- [20] S. Pap, J. Radonić, S. Trifunović, D. Adamović, I. Mihajlović, M. Vojinović Miloradov, M. Turk Sekulić, *J. Environ. Manage.* 184 (2016) 297–306.
- [21] G. Pavalache, V. Dorneanu, A. Popescu, *Farmacia* 6 (2015) 366–370.
- [22] S.M. Rivera-Jiménez, S. Méndez-González, A. Hernández-Maldonado, *Microporous Mesoporous Mater.* 132 (2010) 470–479.
- [23] H. Khazri, I. Ghorbel-Abid, *J. Environ. Anal. Chem.* 3 (2016) 1–7.
- [24] I. Turku, T. Sainio, E. Paatero, *Environ. Chem. Lett.* 5 (2007) 225–228.
- [25] Y.X. Wang, H.H. Ngo, W.S. Guo, *Sci. Total Environ.* 533 (2015) 32–39.
- [26] J. Akhtar, N.A.S. Amin, K. Shahzad, *Desalin. Water Treat.* 57 (2016) 12842–12860.



## **WASTE TREATMENT TECHNOLOGIES: APPROACH TO GHG EMISSION AND COST**

**Višnja Mihajlović**

*Department of Environmental Engineering and Occupational Safety, Faculty of Technical Sciences, University of Novi Sad, 21000 Novi Sad,, Trg Dositeja Obradovica 6, Serbia  
e-mail: visnjamihajlovic@uns.ac.rs*

### **Abstract**

Municipal solid waste may have a negative impact on the environment, causing pollution and greenhouse gas emissions (GHG) that contribute to climate change, if it is not treated. Treatment of waste is a key for sustainable development. Composting, anaerobic digestion and incineration are proven technologies for treatment of municipal solid waste. Selection of waste treatment depend on many factors, mainly cost, local conditions. Aim of this paper is to analyze different scenarios for waste treatment and their impact on environment and their cost.

### **Introduction**

The municipal waste management landscape in EU accession countries will change, due to legal obligation regarding waste management. [1,2,3]. Serbia is a candidate country for European Union membership (EU), must transpose and implement the total body of EU legislation, including chapter 22 Environment.

In developing countries, and Serbia as well, main deficiencies in waste management are weak and inefficient law enforcement mechanism, lack or weak capacity or motivation of staff, lack of finances for investments, lack of incentives for both local community and for the citizens. High share of biodegradable municipal waste going to landfill, like in South Eastern Europe countries [4,5,6]. Almost all packaging waste from the household which is sent to recycling is collected by an informal sector. Separate collection is not established.

In EU Member States where the disposal of waste is not high, and where there are no fees and charges for waste disposal, diversification of waste, particularly biodegradable waste from landfills and implementation of waste treatment technologies has been more slowly, unlike in countries where fee for waste disposal was introduced and gradually started to build the necessary infrastructure for waste management [6]. In addition, new member states e.g. Poland, Bulgaria, Romania, Croatia, still depend on landfilling, and treatment options are rarely in place. Therefore, still a large amount of waste is disposed of in landfills

The transposition and implementation of the Directive provisions legislation will be an extremely challenging task for the country. The aim of this paper is Aim of this paper is to analyze different scenarios for waste treatment and their impact on environment and cost, in Novi Sad Waste Management Centre.

### **Experimental**

The input for the analysis is morphological composition of MSW in NSWMR and generated MSW waste. In 2009. total amount of generated waste was 189.000 tones [7]. Out of this, 44% is biodegradable waste (see Figure 1).

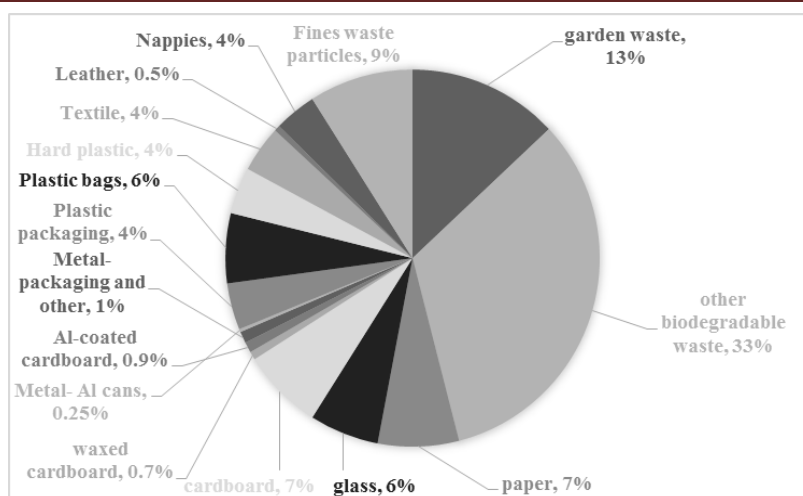


Figure 4: Morphological composition of MWS in the region [6]

For the projected waste generation growth rate we have used GDP in Serbia, which was around 2% [8].

Analysed technologies in are composting and incineration with CHP. Composting is used for the treatment of the biodegradable fraction. Composting considers open-air process in a box, which include composting and the stage of maturation and main products are compost, wastewater and residues are produced during the process. Incinerator, with energy recovery, produces electricity and heat from the waste treated; bottom ash, fly ash and filter cake are exported for disposal and reduces the amount of waste sent to landfill.

In this paper we have analysed two scenarios. Scenario 1 is treatment of only biodegradable waste, to reduce the emission of GHG from landfill, and Scenario 2 is treatment of biodegradable waste and treatment of residual waste in incinerator, to reduce the amount of waste which is landfilled. Parameters used environmental and cost analysis for Scenario 1 and Scenario 2 are given in Table 1. Environmental analysis includes the potential saving in term of CO<sub>2</sub> emission from selected treatment plants. Cost analysis include investment and operational cost for treatment plant, based on amount of treated waste.

Table 1: Analyzed technologies for the MSW treatment [10,11,12]

Technology	Investment and operating cost		GHG emission (t CO <sub>2</sub> eq)
Composting	$y=2000 (x)^{0.8}$	$y=2000(x)^{-0.5}$	0.012
Incineration CHP	$y=5000 (x)^{0.8}$	$y=700 (x)^{-0.3}$	0.378

## Results and discussion

In 2035. total amount of generated municipal waste will be 322,769 tones with 2% increased rate. In order to reach the EU biodegradable waste goals, it will be necessary to treat 97.509 tons of biodegradable waste in composting plant. Furthermore, to reduce the GHG emission, and protect the environment, 161.398 tons of residual waste should be treated. Also, 64.977 of packaging waste, must be recycled to reach the EU recycling goals [1] Cost of the analyzed technologies are given in Table 2. Incineration costs, investment and operating, are higher compared to composting, eight and ten times, respectively. Also, incineration is superior compared to composting, in terms of GHG emission.

**Table 2: Environmental and cost analysis of waste treatment**

	Investment cost (€)	Operating cost (€)	GHG emission (t CO <sub>2</sub> eq)
Composting	19,439,281	11,838,866	20,095
Incineration	73,326,217	73,326,215	974,487

In Table 3, are given costs for Scenario 1 and Scenario 2. Incineration plant, increase the cost, but also increase the savings in terms of GHG emission. Treatment of biodegradable waste will reduce only biodegradable waste for landfill, while residual waste will increase. Selection of incineration, will reduce the amount of waste sent to landfill as well, but will increase the cost of by-products treatment (fly ash and bottom ash). However, scenario 2 has a better GHG “balance” than scenario 1, thus contribute to reduction of GHG emission. Selection of waste treatment plant (scenario) will depend on many factors. One of the important factors will be the investment cost of the plant and economic sustainability of the plant. However, any of scenarios for waste treatment must be tailored to local conditions, because many proven technologies have fallen due to difficulties to adapt waste treatment to local conditions.

**Table 3: Cost and GHG emission of analyzed scenarios**

	Investment cost (€)	Operating cost (€)	GHG emission (t CO <sub>2</sub> eq)
Scenario 1	19,439,281	11,838,866	20,095
Scenario 2	92,765,498	85,165,081	994,582

### Conclusion

Both analyzed technologies are proven waste treatment. Implementation of those technologies will be challenging task for the Novi Sad region. Decision makers will have to implement and introduce different mechanisms e.g. landfill ban, landfill taxes in order to divert the waste to treatment and reduce the GHG emission from landfill.

### References

- [1] European Commission, Directive 1999/31/EC on the landfill of waste, European Parliament and of the Council, Official Journal L 182, 16/07/1999, p 1-19, Luxembourg.
- [2] European Commission, Directive 94/62/EC on packaging and packaging waste, European Parliament and of the Council, Official Journal L 365, 20/12/1994, p. 10.-23., Luxembourg
- [3] European Commission, Directive 2009/98/EC on waste and repealing certain Directives, European Parliament and of the Council, Official Journal of the European Union L 312/3, 19/11/2008, p 3-30, Luxembourg
- [4] Official Gazette of Republic of Serbia, Decree on landfilling. Official Gazette of RS 69/10 (2010)
- [5] I.STANIC-MARUNA, J. FELLNER: Solid waste management in Croatia in response to European Landfill Directive. Waste Management and Research, 30(8), 825 (2012)
- [6] K. LASARIDI : Implementing the Landfill Directive in Greece: problems, perspectives and lessons to be learned, The Geographical Journal, 175 (4): 261 (2009)
- [7] BiPRO, Support to member states in improving waste management based on assessment of member states’ performance 070307/2011/606502/SER/C2. Final report to the European

Commission, Beratungsgesellschaft für integrierte Problemlösungen (BiPRO), Brussels, Belgium, (2013)

[8] Vujić G, Jovičić N, Redžić N et al., A fast method for the analysis of municipal solid waste in developing countries – case study of Serbia. *Environmental Engineering and Management Journal* 9:1021–1029 (2010).

[9] World Bank (2015) Economic indicator database <http://data.worldbank.org/indicator/NY.GDP.MKTP.PP.KD> (Accessed 10 July 2017)

[10] Alevridou A, Venetis C, Mallini D et al. Guidelines for development of alternative waste management, Project: Waste Network for sustainable solid waste management planning and promotion of integrated decision tools in the Balkan Region (2011)

[11] IPPC, Reference Document on Best Available Techniques for the Waste Treatments Industries, European Commission - Integrated Pollution Prevention and Control (2006)

[12] Le Bozec A, Costs models for each municipal solid waste process, Deliverables 5 & 7. Aid in the Management and European Comparison of Municipal Solid Waste Treatment methods for a Global and Sustainable Approach (AWAST) (2004)

VALIDATION OF ANALYTICAL METHOD FOR DETERMINATION OF  
TERBUTHYLAZINE AND S-METOLACHLOR RESIDUES IN SOIL

Sanja Lazić, Dragana Šunjka and Slavica Vuković

<sup>1</sup>*Department of Environmental and Plant Protection, Faculty of Agriculture, University of  
Novi Sad, 21000 Novi Sad, Trg Dositeja Obradovića 8, Serbia  
e-mail: draganas@polj.uns.ac.rs*

**Abstract**

Terbuthylazine and s-metolachlor are commonly used herbicides, especially after prohibition of some other triazine and chloracetanilide herbicides. However, often used pesticides pose the risk of soil contamination due to their persistence, toxicity and bioaccumulation. The trace determination of herbicide residues, generally in environmental samples, presents a challenging analytical problem. The present work was carried out to analyze terbuthylazine and s-metolachlor residues in soil based on high performance liquid chromatography (HPLC), and QuEChERS extraction method. The method was optimized and validated according to the parameters of precision, accuracy, linearity, limits of detection and limits of quantification. Analysis was carried out using an HPLC-UV diode array detection system (Agilent 1100, USA), with an Agilent Zorbax Eclipse C18 column (50 mm × 4.6 mm, 1.8 μm) and mobile phase consisting of ultrapure water and acetonitrile (55/45, v/v). Mean recoveries obtained from soil samples fortified at three different levels ranged from 81 to 92%. The method detection limits ranged from 0.01 to 0.05 mg kg<sup>-1</sup>. Obtained results completely fulfilled the SANCO/825/00 rev. 8.1 16/11/2010 criteria.

**Introduction**

Commonly used pesticides pose the risk of soil contamination due to their persistence, bioaccumulation and toxicity. The fate of pesticides in soil is influenced by the physico-chemical properties of pesticide, the properties of the soil (presence of clay materials, organic matter, pH), climate, biology, and other factors [1]. Some herbicides can remain active in the soil for weeks, months or years. This can be an advantage, as it ensures long-term weed control and at the same time, if the herbicide stays in the soil longer than intended, it may damage susceptible crops sown in subsequent years. E.g. chlorsulfuron is used in wheat and barley, but can remain active in the soil for several years and damage legumes and oilseeds.

A real problem represents the difficulty in identifying herbicide residues before they cause a problem. Once the crop has emerged, diagnosis is difficult because the symptoms of residual herbicide damage can often be confused with and/or make the crop vulnerable to other stresses, such as nutrient deficiency or disease.

The trace determination of herbicide residues, generally in environmental samples, presents a challenging analytical problem [2]. The low dosage used requires the application of highly sensitive analytical techniques to detect trace concentrations of residues in soil [3]. Due to the low level present and complexity of sample, clean-up and enrichment before analysis is necessary and become a crucial step for the determination of herbicides in environmental samples.

Thus, the present work was carried out to analyze terbuthylazine and s-metolachlor residues in soil based on liquid chromatography and QuEChERS extraction method.

Terbutylazine and s-metolachlor are commonly used herbicides, especially after prohibition of some other triazine and chloracetanilide herbicides. Terbutylazine (2-N-tert-butyl-6-chloro-4-N-ethyl-1,3,5-triazine-2,4-diamine) is a triazine herbicide and s-metolachlor (2-chloro-N-(2-ethyl-6-methylphenyl)-N-[(2S)-1-methoxypropan-2-yl]acetamide) belong to the chloroacetanilide group of herbicide (Figure 1). They are used as a pre emergence herbicides, for control of broad spectrum weeds in maize.

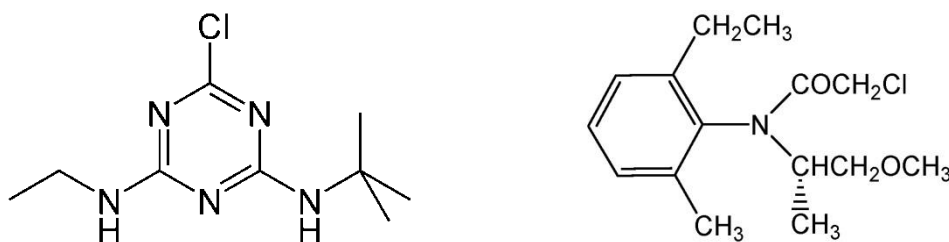


Figure 1. Structural formula of terbutylazine and s-metolachlor

## Experimental

### *Standards and reagents.*

Certificated analytical standards of terbutylazine (99.1%), and s-metolachlor (96%) were purchased from Dr Ehrenstorfer (Augsburg, Germany). QuEChERS dispersive SP extraction kits were from Agilent (USA). For the extraction, standard dissolution and mobile phase, acetonitrile (MeCN) (J.T. Baker) was used. Ultra pure water, used as a mobile phase, was produced by a Milli-Q system (Milli-pore, USA).

### *Standard solutions.*

A stock solutions of terbutylazine and s-metolachlor were prepared from the appropriate amount of analytical standards in MeCN, while working standard solutions, used for recovery and other validation parameters, were prepared by further dilution with MeCN covering the concentrations between 1.5 to 10  $\mu\text{g ml}^{-1}$ .

### *Extraction procedure.*

Soil sample used in this study was purchased from area without pesticide application. Freshly-spiked soils were prepared by weighing 10.0 g of soil into polypropylene tube 50 ml volume. Soil samples fortified with mixture of herbicides working standard solutions at three levels, 1.5, 5.0 and 10  $\mu\text{g/ml}$ . The mixture was then homogenized and the sample was allowed to stand at room temperature over night until analysis. After that, 10 ml of acetonitrile was added, shaken vigorously for a 1 min and vortexed for a 1 min. In the next step, a mix of buffered salts (1000 mg of sodium citrate, 500 mg of sodium hydrogen citrate sesquihydrate, 4000 mg magnesium sulphate and 1000 mg sodium chloride) from separate pouches was added, shaken for 1 min and vortexed 1 min. The tube was placed in an ultrasonic bath for 10 min and centrifuged at 4000 rpm for 5 min (Sigma, Germany). The supernatant was transferred through  $\text{Na}_2\text{SO}_4$  and filtered into an autosampler vial for HPLC-DAD analysis.

### *Chromatographic parameters.*

Simultaneous determination of terbutylazine and s-metolachlor residues in soil was performed with high-performance liquid chromatography system, equipped with a diode array detector (HPLC-DAD, 1100 Series, Agilent Technologies). The reversed phase

chromatographic separation was performed on ZORBAX Eclipse XDB-C18 (50 mm, 4.6 mm, 1.8  $\mu\text{m}$ ) column in an isocratic working regime with mobile phase acetonitrile/deionized water 55/45. The flow rate was  $0.92 \text{ ml min}^{-1}$ , injector volume  $20 \mu\text{l}$  and the column temperature was  $40 \text{ }^\circ\text{C}$ .

#### *Validation of the analytical method.*

The developed and optimized method for quantitative analysis of terbuthylazine and s-metolachlor in soil was validated in terms of linearity, precision, recovery, limit of detection (LOD) and limit of quantification (LOQ), according to SANCO/825/00 rev. 8.1 16/11/2010 [4].

#### **Results and discussion**

Chromatographic determination of terbuthylazine and s-metolachlor was carried out on a HPLC using reversed phase procedure and UV detection at 230 nm. HPLC/DAD chromatogram of terbuthylazine and s-metolachlor standard in acetonitrile is shown in figure 2.

The developed and optimized method for simultaneous determination of terbuthylazine and s-metolachlor herbicides in soil was validated in terms of linearity, precision, LOD, LOQ and recovery. Calibration of working standard solution was used to test the ability of procedures and instruments for determination of terbuthylazine and s-metolachlor. Linearity of calibration was assessed from a linear regression of response (area) versus concentration terbuthylazine and s-metolachlor in solution. Result showed that procedure and instrument used had good ability in separating terbuthylazine and s-metolachlor indicated by calibration curve. Response of terbuthylazine was linear at concentrations of  $1.5$  to  $10 \mu\text{g ml}^{-1}$ , with a correlation coefficient of 0.9996 and 0.9997 for terbuthylazine and s-metolachlor, respectively. Chromatogram of standard mixture is shown in Figure 2.

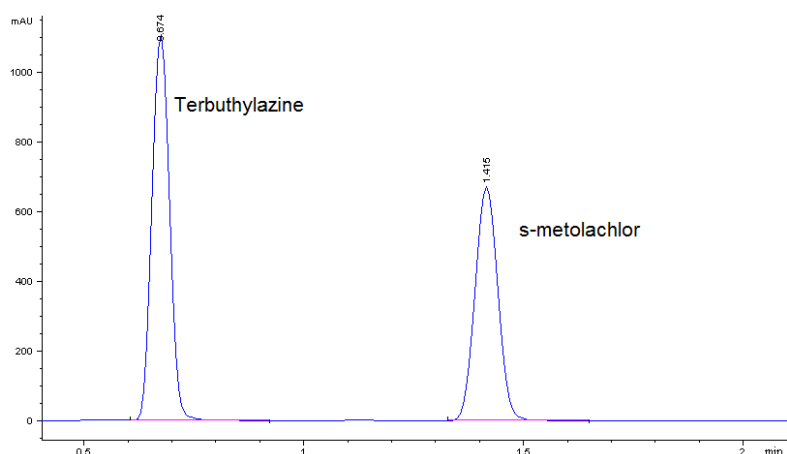


Figure 2. Chromatogram of terbuthylazine and s-metolachlor standard mixture in acetonitrile

LOD and LOQ for terbuthylazine and s-metolachlor was estimated from the fortified samples. LOD established as  $0.010 \text{ mg/kg}$  and LOQ at  $0.060 \text{ mg/kg}$ , for both analyzed herbicides.

The precision of measurement of an analyte can be evaluated as repeatability or reproducibility. In this study, precision is expressed as repeatability. Precision was checked by



matrix matched terbuthylazine and s-metolachlor standard (6.0 µg/ml) five times on the same day. Relative standard deviations (RSD) of the peak areas were 1.23 and 1.41% for terbuthylazine and s-metolachlor, respectively, fulfilling with criteria for of chromatographic measurements of  $RSD \leq 2\%$ .

The accuracy of the method was evaluated by recovery studies. For recovery studies, a soil sample was spiked before the extraction procedure with terbuthylazine and s-metolachlor herbicides at three levels. The mean recoveries for spiked sample ranged from 81 to 92%.

### **Conclusion**

In this study, a simple and precise method for simultaneous determination of terbuthylazine and s-metolachlor residues in soil samples was described. Reverse phase and isocratic elution based liquid chromatographic conditions are used for simultaneous determination of terbuthylazine and s-metolachlor. Considering the obtained values of analytical parameters, the proposed method proved to be an efficient and sensitive method for determination of terbuthylazine and s-metolachlor herbicides residues in soil samples.

### **Acknowledgements**

This research is a part of project financed by the Serbian Ministry of Education and Science, Grant No. III43005.

### **References**

- [1] R.P. Singh. Bull. Environ. Contam. Toxicol. 67 (2001) 126.
- [2] S. Lazić, D. Šunjka. Research Journal of Agricultural Science, 46 (2) (2014) 132.
- [3] G. Ye, W. Zhang, P. Cui, C. Pan, S. Jiang. Chinese Journal on Analytical Chemistry, 34 (2006) 1207.
- [4] EU COMMISSION, Directorate General Health and Consumer Protection, SANCO/825/00 rev. 8.1 16/11/2010, Guidance document on pesticide residue analytical methods.

## PURIFICATION OF MAGENTA DYE AQUEOUS SOLUTION WITH FENTON-LIKE OXIDATION PROCESS

**Vesna Kecić<sup>1</sup>, Đurda Kerkez<sup>2</sup>, Miljana Prica<sup>1</sup>, Sanja Rapajić<sup>3</sup>, Milena Bečelić-Tomin<sup>2</sup>, Anita Leovac-Maćerak<sup>2</sup>, Saša Petrović<sup>1</sup>**

<sup>1</sup>*Department of Graphic Engineering and Design, University of Novi Sad, Faculty of Technical Sciences, Trg Dositeja Obradovića 6, 21000 Novi Sad, Serbia.*

<sup>2</sup>*Department of Chemistry, Biochemistry and Environmental Protection, University of Novi Sad, Faculty of Sciences, Trg Dositeja Obradovića 3, 21000 Novi Sad, Serbia.*

<sup>3</sup>*Department of Mathematics and Informatics, University of Novi Sad, Faculty of Sciences, Trg Dositeja Obradovića 4, 21000 Novi Sad, Serbia.*

*e-mail: kecic@uns.ac.rs*

### Abstract

In this study, heterogeneous Fenton oxidation processes is applied, with the usage of nZVI as a catalyst. Greener than the conventional Fenton process, it combines the advantages of nZVI reduction and Fenton oxidation. According to the central composite design and the analysis of variance, the model presents medium  $R^2$  value of 73.02% for the Magenta removal. At the 60 min of contact time, dye removal efficiency raised more than 40% and 70% with the increase of hydrogen peroxide concentration and pH decrease, respectively. The experimental results indicate that the oxidation process leads to the reduction in dye concentration up to 97%, confirming the application possibility of Fenton-like oxidation process for the dye removal from the aqueous solution.

### Introduction

High efficiency in the flexographic printing industry is achieved with the usage of CMYK dyes (Cyan, Magenta, Yellow and Key), whereby Magenta flexo dye is commonly used. Upon completion of the printing process and during the cleaning of dye delivery and storage systems, a great amount of colored effluent can be generated. A discharge of wastewater without proper treatment into recipient contributes to the ecosystem problems, inhibiting the penetration of sunlight into water, enabling the ingress of the dye contaminants, therefore disturbing aquatic and terrestrial life [1, 2]. Numerous physical and chemical methods can be applied in order to increase water quality by reducing dyes quantity, such as ozonation, coagulation, reverse osmosis, photodegradation, membrane separation, biosorption and adsorption [3 - 5]. Amongst these methods, advanced oxidation processes (AOPs) present a great alternative for the treatment of dye contaminated water, due to the generation of oxygen-based radicals, where these species take part in different reactions in order to degrade dye molecules completely. Within the AOPs processes, dyes can totally be decomposed to low-molecular-weight compounds, carbon dioxide, water and inorganic components, or they can be transformed into harmless products [6]. In the present study a central composite design has been employed to model the process condition for efficiently removal of Magenta dye from aqueous solution by using Fenton-like oxidation process, supported with "green" synthesized nano zero valent iron.

## Experimental

**Materials.** The Magenta wastewater used in the present study was obtained from flexographic printing facility located in Novi Sad, Serbia. Magenta dye (C.I.: PR57:1, chemical formula:  $C_{18}H_{12}N_2O_6$ , MW: 352 g mol  $L^{-1}$ ,  $\lambda_{max}$ : 573 nm) as a pollutant was purchased from Flint group. All sample analyzes were carried out directly without special pre-treatment, and the chemicals used during the laboratory test were analytically pure (Merck, Germany).

**Preparation of iron nanoparticles.** The synthesis of iron nanoparticles combined with aqueous oak leaf extract was carried out as described by Machado et al., 2013. Briefly, 37 g of dried oak leaves (*Quercus Peatrea*) was mixed up with 1L of deionized water. The resulting mixture was heated to 80 °C for 20 min on a magnetic stirrer, allowed to cool and then vacuum filtered through a 0.2 mm filter paper. 0.1M  $FeCl_3 \cdot 6H_2O$  solution was slowly introduced using a burette ensuring a 3:1 ratio v/v of oak leaves extract to  $FeCl_3$ , respectively [7]. The colour of the solution changed to black indicating the synthesis of nanoparticles. In that way, a Fe(0) concentration of 1.395 g  $L^{-1}$  in synthesized nanomaterial was obtained.

**Dye decolorization.** Decolorization activity was expressed in terms of decolourization efficiency (%) and was calculated as follows (1):

$$E(\%) = A_0 - A / A_0 * 100 \quad (1)$$

where  $A_0$  is absorbance of Magenta dye aqueous solution without nanomaterial, whereas  $A$  represents absorbance of Magenta dye aqueous solution with nanomaterial. Decolorization efficiency was determined by measuring the absorbance of the aqueous solutions at 573 nm by using UV/VIS spectrophotometer (UV 1800 Shimadzu, Japan).

**Statistical analysis.** In order to investigate the effect of various operational parameters, including the catalyst dosage,  $H_2O_2$  concentration, initial Magenta concentration and pH on the dye removal efficiency, response surface methodology (RSM) based on central composite design (CCD) was employed. Each variable was coded in five levels (Table 1). The experiments were done for different combinations of these parameters using statistically designed experiments in 60 min of the reaction time.

Table 1. Process variables with experimental levels

Variables	Unit	Symbol coded	Levels				
			-2	-1	0	1	2
nZVI concentration	mg $L^{-1}$	$X_1$	0.75	15.38	30	44.63	59.25
$H_2O_2$ concentration	mM	$X_2$	1	3.5	6	8.5	11
Dye concentration	mg $L^{-1}$	$X_3$	20	60	100	140	180
pH	-	$X_4$	2	4	6	8	10

## Results and discussion

Obtained results for Magenta removal from aqueous solution indicated decolorization efficiency between 3.64 and 96.61%. The data were fitted with various models and subsequent ANOVA test showed that reaction of Magenta removal was most suitably described by quadratic polynomial model. The final model to predict the percentage of Magenta removal by enhanced Fenton process is shown in Eq. (1):

$$\begin{aligned}
 Y = & 207.2321 + 1.7674x_1 - 0.0245x_1^2 - 8.4953x_2 + 0.1053x_1x_2 + 0.7114x_2^2 - \\
 & -0.6120x_3 - 0.0160x_1x_3 - 0.0223x_2x_3 + 0.00647x_3^2 - \\
 & -38.0163x_4 + 0.1206x_1x_4 + 0.0971x_2x_4 + 0.01232x_3x_4 + \\
 & + 1.7260x_4^2
 \end{aligned}
 \tag{1}$$

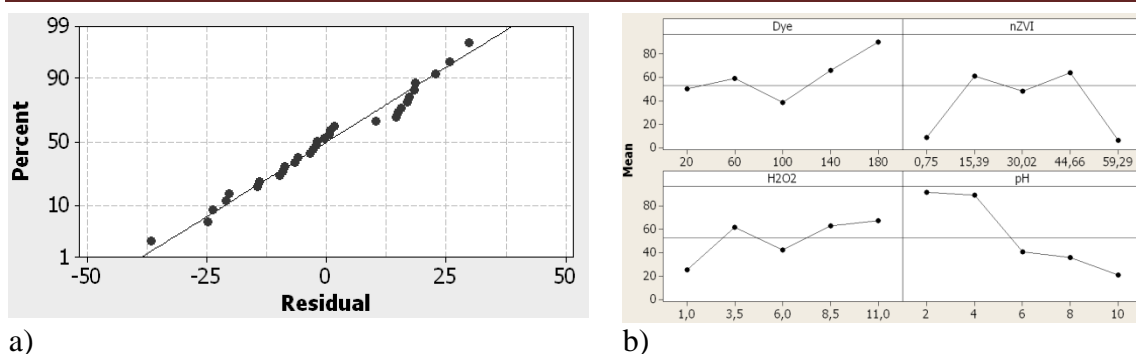
where Y is the percentage of Magenta removal efficiency and  $x_1$ ,  $x_2$ ,  $x_3$  and  $x_4$  are the values of the nZVI dosage,  $H_2O_2$  concentration, initial Magenta concentration and pH, respectively. According to the ANOVA results, the model presents high  $R^2$  value of 73.02% dye removal, indicated the medium accuracy of the polynomial model. Estimated regression coefficients, the  $T$  and  $P$  values for the Magenta removal efficiency (%) are presented in Table 2.

Table 2. Estimated regression coefficients of enhanced Fenton process

Variables	Regression Coefficient	Standard error	$T_{stat}$	P
1	207.232	105.684	1.961	0.068
$X_1$	1.767	2.164	0.817	0.426
$X_2$	-8.495	13.056	-0.651	0.524
$X_3$	-0.612	0.823	-0.743	0.468
$X_4$	-38.016	17.283	-2.199	0.043
$X_1X_2$	0.105	0.155	0.678	0.507
$X_1X_3$	-0.016	0.010	-1.655	0.117
$X_1X_4$	0.121	0.194	0.621	0.543
$X_2X_3$	-0.022	0.056	-0.392	0.700
$X_2X_4$	0.097	1.136	0.085	0.933
$X_3X_4$	0.012	0.071	0.173	0.864
$X_1^2$	-0.024	0.019	-1.237	0.234
$X_2^2$	0.711	0.679	1.046	0.311
$X_3^2$	0.006	0.003	2.436	0.027
$X_4^2$	1.726	1.062	1.625	0.124

A P-value less than 0.05 indicates the statistical significance of each term at 95% confidence level. As shown in Table 2, the regression analysis of the experimental design demonstrated that the linear model term - pH, within its tested boundaries, is the only significant independent variable. In addition, the quadratic term  $x_3^2$  were also found to be statistically significant. However, the nZVI dosage,  $H_2O_2$  concentration and initial dye concentration proved irrelevant.

In order to investigate the normality assumption of the residuals in fitted model, the normal probability plot is created (Figure 1a). A normal distribution of the points, forming fairly straight line, explains good applicability of the model for the explanation of experimental data. In order to examine differences between level means for investigated factors, the main effects plot of a two-step fractional factorial design is presented in Figure 1b. All four examined variables are displayed within five levels.



a) Figure 1. a) Normal probability plot; b) Main effects of dye concentration, nZVI dosage, H<sub>2</sub>O<sub>2</sub> concentration and pH on dye removal efficiency

Lines with higher incline indicate a greater impact of the variable on the investigated process. Based on the main effects plot it can be concluded that pH value and the dye concentration actualize the greatest impact on the decolorization process. As it can be seen from Figure 1b, Magenta removal efficiency raised about 40% with the increasing of hydrogen peroxide concentration. This can be explained by the fact that oxidation power of Fenton reaction is improved with increasing hydroxyl radical amount attained from the decomposition of hydrogen peroxide. Results also indicated that dye removal efficiency increased for 70% with the decrease of pH value from 10 to 2. In the alkaline environment, Fenton oxidation reactions are slower, unlike the acid environment. In this paper, the maximum efficiency of the decolorization process is achieved at pH 2. Furthermore, the economic cost-effectiveness of the entire process can be explained within the fact that the acidity of the nano material suspension contributes to a significant reduction of the pH value of aqueous solution, so the pH corrections are minimal, while achieving very satisfactory decolorization efficiency. Considering the findings of this study, application of enhanced Fenton process can be suggested as an efficient system to enhance the efficiency of dye removal in printing aqueous solution.

## Conclusion

The purpose of this study was to investigate the application of enhanced Fenton process using nano zero valent iron for treatment of aqueous solution containing Magenta dye, by using the response surface methodology. Based on experimental results, an empirical relationship between the response and independent variables is obtained and expressed by the quadratic polynomial model. Effect of experimental parameters on Magenta removal efficiency was established by the response surface and normal probability plot, as well as main effects plot of the model-predicted responses. High Magenta removal (97%) was obtained in the 60 min of the removal process. The greatest impact on the decolorization efficiency is achieved by the pH value. Analysis of variance showed a medium coefficient of determination value ( $R^2 = 0.730$ ), ensuring a satisfactory adjustment of the second-order regression model with the experimental data. Thus, a Fenton-like oxidation is regarded as a very effective process for treating industrial wastewater that contains dyes and other waste products.

## Acknowledgements

The authors acknowledge the financial support of the Ministry of Education, Science and Technological Development of the Republic of Serbia within the Projects No. TR 34014 and III43005.

**References**

- [1] S. Patel, Determining the Effect of Printing Ink Sequence for Process Colors on Color Gamut and Print Quality in Flexography, 2009, Doctoral Thesis.
- [2] L. Andrade, C. Míguez, M. Gomez, P. Bugallo, J. Clean. Product. 35 (2012) 214.
- [3] S. Kuppusamy, K.Venkateswarlu, P. Thavamani, Y.B. Lee, R. Naidu, M. Megharaj, Ecol. Eng. 101 (2017) 3.
- [4] S. Venkatesh, K Venkatesh, A.R. Quaff, J. Appl. Res. Technol. 15 (2017) 340.
- [5] Y. Tan, L. Sun, B. Li, X. Zhao, T. Yu, N. Ikuno, K. Ishi H. Hu, Desalination, 419 (2017) 1.
- [6] L. Bilinska, M. Gmurek, S. Ledakowicz, Process. Saf. Environ. 109 (2017) 420.
- [7] S. Machado, S. Pinto, J. Grosso, H. Nouws, J. Albergaria, C. Delerue-Matos, Sci. Total. Environ. 445 (2013) 1.

## HUMIC ACID REMOVAL FROM WATER WITH FENTON

Marjana Simonič<sup>1\*</sup>

<sup>1</sup>*Faculty of Chemistry and Chemical Engineering, University of Maribor,  
Smetanova 17, SI-2000 Maribor, Slovenia  
e-mail: marjana.simonic@um.si*

### Abstract

The aim of the research was to reduce the concentration of humic acid in water solutions. We have found that the Fenton's reaction was suitable for the treatment of synthetic wastewater with humic acid. The maximum reduction of COD for the treatment of wastewater with humic acid stood at 97.4 %, achieved at following conditions: 0.2 g FeSO<sub>4</sub>, pH = 3 and reaction time 40 min. The maximum reduction of COD was achieved if the pH of water solution was adjusted to 3 before the treatment with Fenton reagent.

### Introduction

Many wastewater including compost leachate contain humic acids. [1] Leachate could pollute the underground water sources. Surface and wastewaters are many times polluted by humic acids, heavy metals, xenobiotic and inorganic macro-compounds, such as ammonium and iron compounds from leachate [2]. Also phthalates and poly-chloro-bi-phenyls from pesticides and plastic parts were measured in increased concentrations especially in wastewaters. The limit concentration of humic acid in drinking water sources is 0.1-10 mg/L. However, if humic acid reacts with chlorine during disinfection toxic dihalo-acetonitrile (DHAN) could be formed [3]. Advanced oxidation processes are very efficient for water treatment if the pollutants are very persistent. Among them Fenton reagent could be efficient for degradation of e.g. dyes [4]. Fenton reagent is the reaction with the combination of either Fe<sup>2+</sup> and H<sub>2</sub>O<sub>2</sub> or H<sub>2</sub>O<sub>2</sub>/Fe<sup>2+</sup>/UV-rays. Hydroxyl radicals are formed at room temperature. Fe-ions represent catalyst, while H<sub>2</sub>O<sub>2</sub> represents oxidation agent. Advantages of Fenton in combination of Fe<sup>2+</sup> and H<sub>2</sub>O<sub>2</sub> are low energy demand, low toxicity of chemicals, high reaction rate, high oxidation rate and simple equipment [1, 5]. Wu et al [6] found that Fenton reagent is very important for humic acid degradation. The main drawback of Fenton process is sludge formation [7]. It is assumed that up to 50 % more sludge is formed.

In the present work the effects of Fenton reagent on organic removal from water solution was investigated. Iron sulphate in combination of hydrogen peroxide were used in experiments. The concentrations, ratio between both chemicals, the reaction time and pH influences were studied. It was found that Fenton reagent is efficient in humic acid degradation.

### Experimental

Humic acid is soluble in alkaline solutions, while at pH less than 2 it could be decomposed. Humic acid is formed from many molecules which are bounded with hydrogen and hydrophobic bonds. Humic acid was purchased by Sigma Aldrich (Germany). Working solution of humic acid was prepared by mixing 1 g of humic acid with NaOH. For each experiment the initial concentration was 30 mg/L (Fig. 1), prepared by diluting working standard solution.





Figure 1. Standard humic acid solution

Table 1 represents the analytical methods used.

Table 1: The analytical methods

Parameter	Apparatus	Method
pH	WTW Multi 3410	ISO 10523
COD(mg/l O <sub>2</sub> )	Thermoreactor Merck TR620	ISO 6060
Absorbance 254 nm	Spectrophotometer Agilent 8453	ISO 7887

The reaction between Fenton reagent and synthetic water was performed by different amounts of FeSO<sub>4</sub>·7 H<sub>2</sub>O at room temperature. It was found that the influence of temperature is negligible [1]. The mass of iron salt was chosen at 0.1 g, 0.2 g and 0.3 g. The molar ratio of FeSO<sub>4</sub>·7 H<sub>2</sub>O: H<sub>2</sub>O<sub>2</sub> was set to 1:3, 1:5 and 1:7. The reaction time was set to 20 mins, 40 mins and 60 mins. All parameters were chosen according to literature data [8]. If necessary pH was adjusted using 0,1 M HCl or 0,1 M NaOH.

### Results and discussion

The results obtained for COD are presented in Fig. 2. The best removal efficiency was determined at 0.2 g of FeSO<sub>4</sub>. The pH was measured at 10.7 due to the humic acid alkaline solution. It was prepared in NaOH for stability purposes. After the Fenton reagent addition, it decreased to 2.5 due to H<sub>2</sub>O<sub>2</sub> from Fenton reagent.

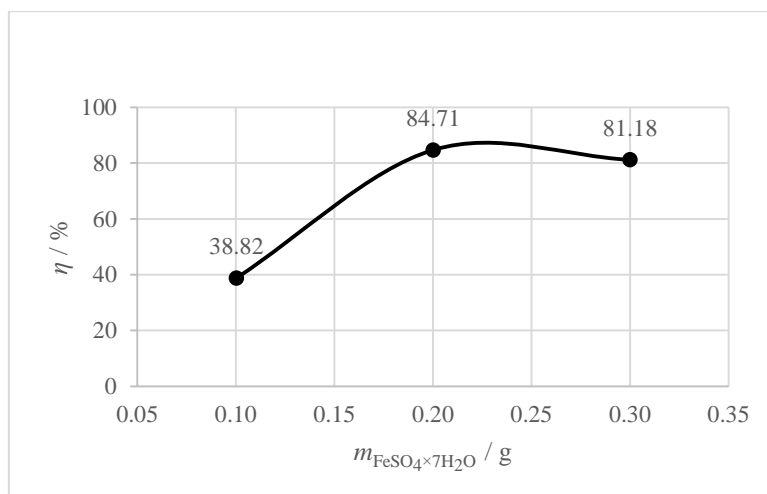
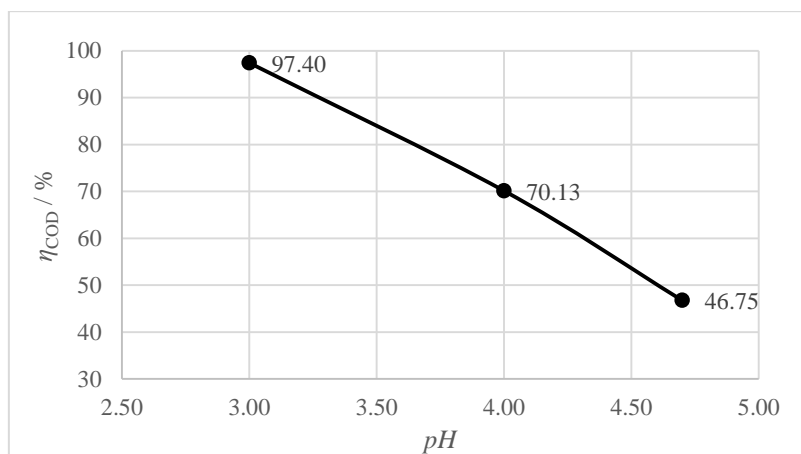
Figure 2. COD removal in dependence of amount of  $\text{FeSO}_4$ 

Figure 3. COD removal in dependence of pH

It was left as it was (pH = 4.7), then adjusted to pH = 3 and pH = 4. The best removal efficiency was achieved at pH = 3 at 97.4 % as seen from Fig. 3.

After the reaction the pH value was very similar of those solution where there was no pH adjustment. The optimum results were observed at the same values as discovered in another research [9].

The reaction time was varied from 20 mins to 60 mins. The results were very similar (not presented), with the similar removal after 60 mins at 95.7 %.

### Conclusion

Humic acid removal from water solution using Fenton reagent was studied. The main parameter was chemical oxygen demand COD. The COD was mostly reduced in synthetically prepared water for 97.4 % with the 0.2 g of Fenton reagent per 100 ml of solution at the molar ratio  $\text{FeSO}_4:\text{H}_2\text{O}_2 = 1:3$ . Very important is to adjust pH value to 3 before the reaction and that reaction last 40 mins.

### **Acknowledgements**

Author would like to acknowledge the Slovenian Research Agency for the financial support (Project No. P2-0032).

### **References**

- [1] Li W., Zhou Q., Hua T. Removal of Organic Matter from Landfill Leachate by Advanced Oxidation Processes: A Review. *International Journal of Chemical Engineering*, 2010.
- [2] Liu Z., Wu W., Shi P., et al. Characterization of dissolved organic matter in landfill leachate during the combined treatment process of air stripping, Fenton, SBR and coagulation. *Waste Management*, 41, 111–118, 2015.
- [3] Nikolaou AD, Golfinopoulos SK, Lekkas TD, Kostopoukou MN: DBP levels in chlorinated drinking water: effect of humic substances, *Environ Monit Assess*, 93(1-3):301-19, 2004
- [4] Ertugay N., Acar F.N. Removal of COD and color from Direct Blue 71 azo dye wastewater by Fenton's oxidation: Kinetic study. *Arabian Journal of Chemistry*, 2013.
- [5] Hermosilla D., Cortijo M., Huang C.P. Optimizing the treatment of landfill leachate by conventional Fenton and photo-Fenton processes. *Science of The Total Environment*, 407 (11), 3473–3481, 2009.
- [6] Wu Y., Zhou S., Ye X., et al. Oxidation and coagulation removal of humic acid using Fenton process. *Colloids and Surfaces A: Physicochemical and Engineering Aspects*, 379 (1–3), 151–156, 2011.
- [7] Neyens E., Baeyens J. A review of classic Fenton's peroxidation as an advanced oxidation technique. *Journal of Hazardous Materials*, 98 (1–3), 33–50, 2003.
- [8] Deng Y. Physical and oxidative removal of organics during Fenton treatment of mature municipal landfill leachate. *Journal of Hazardous Materials*, 146 (1–2), 334–340, 2007.
- [9] Lopez A., Pagano M., Volpe A., et al. Fenton's pre-treatment of mature landfill leachate. *Chemosphere*, 54 (7), 1005–1010, 2004.

**STUDIES ON THE PHYSICO-CHEMICAL PROPERTIES OF LANTHANUM MANGANITE PREPARED BY DIFFERENT SYNTHESIS METHODS**

P. Sfirloaga<sup>a</sup>, **C. Mosoarca**<sup>a</sup>, M. Poienar<sup>a</sup>, P. Svera<sup>a</sup>, C. Ianasi<sup>b</sup>, P. Vlazan<sup>a</sup>

<sup>a</sup>*National Institute for Research and Development in Electrochemistry and Condensed Matter, Timisoara, P. Andronescu no. 1, 300254 Romania*

<sup>b</sup>*Institute of Chemistry Timisoara of Romanian Academy,  
Bvd. Mihai Viteazul 24, Timisoara, Romania*

**Abstract:**

Perovskite  $\text{LaMnO}_3$  and related materials are technologically important for many possible applications due to their unique physical and chemical properties. It is well known that the properties of the materials depend on their synthesis processes, as have been already shown in the literature for a large class of materials [1, 2]. In this work, lanthanum manganite perovskite type materials prepared by ultrasonically method with immersed sonotrode in the reaction medium and sol-gel method, followed by heat treatment at  $600^\circ\text{C}$ , 6 h are reported. The as-prepared samples were characterized by X-ray diffraction (XRD), thermal gravimetric analysis (TGA), surface area analysis (BET), scanning / transmission electron microscopy (SEM /HRTEM/EDX), and FT-IR spectroscopy. X-ray diffraction indicates that the synthesized materials are well crystallized, with perovskite structure and without any secondary phases.

**Selective references:**

- [1]. Chen Weifan, Li Fengsheng, Liu Leili, Liu Yang, One- Step Synthesis of Nanocrystalline Perovskite  $\text{LaMnO}_3$  Powders via Microwave-Induced Solution Combustion Route, *Journal of Rare Earths* 24 (2006) 782 – 787.
- [2]. Kazuyoshi Sato, Jintawat Chaichanawong, Hiroya Abe, Makio Naito, Mechanochemical synthesis of  $\text{LaMnO}_{3+\delta}$  fine powder assisted with water vapor, *Materials Letters* 60 (2006) 1399–1402.

**Acknowledgements**

Financial support for this work was provided by the Experimental Demonstrative Project **48PED/2017**.

**EFFECT OF PD ADDITION IN LANTHANUM MANGANITE:  
MORPHO-STRUCTURAL AND ELECTRICAL PROPERTIES**

**P. Sfirloaga<sup>a</sup>, B. Taranu<sup>a</sup>, I. Malaescu<sup>b</sup>, M. Poienar<sup>a</sup>, C. N. Marin<sup>b</sup>, P. Vlazan<sup>a</sup>**

<sup>a</sup>*National Institute for Research and Development in Electrochemistry and Condensed Matter,  
Timisoara, P. Andronescu no. 1, 300254 Romania*

<sup>b</sup>*West University of Timisoara, Vasile Parvan no. 4, Timisoara, 300223 Romania*

**Abstract:**

LaMnO<sub>3</sub> is an inorganic compound with perovskite structure and partial substitution of lanthanum ions [1] or manganese ions [2] has an effect on the physical properties of materials. In the present work we report the synthesis of LaMn<sub>1-x</sub>Pd<sub>x</sub>O<sub>3</sub> (with x = 0.2 and 0.3) materials at low temperature. The doping was performed in order to improve the electrical properties by changing the crystalline structure and prevent ordering of the oxygen vacancies in these materials. The obtained materials were characterized by X-ray diffraction (XRD), transmission electron microscopy (TEM), BET analysis, energy-dispersive X-ray spectroscopy (EDX) and electrical measurements. Structural analysis shows that the obtained materials crystallize in cubic structure and have a homogeneous composition, without secondary compounds.

**Selective references:**

[1] Rodríguez-Carvajal J, Hennion M, Moussa F, Moudden AH, Pinsard L, Revcolevschi A. Neutron-diffraction study of the Jahn-Teller transition in stoichiometric LaMnO<sub>3</sub>. Phys Rev B 1998;57(6):3189.

[2] Hebert S, Martin C, Maignan A, Retoux R, Hervieu M, Nguyen N, et al. Induced ferromagnetism in LaMnO<sub>3</sub> by Mn-site substitution: the major role of Mn mixed valency. Phys Rev B 2002; 65:104420.

**Acknowledgment**

Financial support for this work was provided by the Experimental Demonstrative Project **48PED/2017**.

## FRAP CAPACITY EVALUATION OF PERENNIAL FORAGES IN THE MIDDLE OF JUNE BY PRINCIPAL COMPONENTS & CLASSIFICATION ANALYSIS

Monica Harmanescu<sup>1</sup>

<sup>1</sup>*Faculty of Agriculture, Banat's University of Agricultural Sciences and Veterinary Medicine "Mihai I al Romaniei" from Timisoara, Calea Aradului, no.119, Romania  
e-mail: monica.harmanescu@yahoo.com*

### Abstract

This main goal was to test Principal Components & Classification Analysis (PC&CA), an exploratory multivariate technique, for FRAP capacity evaluation of Romanian permanent grassland forages depending on fertilization: organic or mineral. The vegetal samples were harvested in the middle of June from hill grassland of Caras-Severin. Seven cases and fifteen variables were chosen for the multivariate data matrix. PC&CA offered the possibility to differentiate between organic fertilized cases from those fertilized exclusive mineral or unfertilized. The highest positive correlation coefficients for FRAP capacity were found for the two species from others botanical family, *Inula britannica* and *Rosa canina*. PC&CA can be considered a useful and flexible statistic instrument to evaluate the FRAP capacity of the grassland forage in the middle of June, depending on fertilization, in the soil-clime conditions of Caras-Severin.

### Introduction

Principal components analysis is a multivariate technique used to obtain few artificial variables as principal components based on a high number of correlated characteristics, for extract and make accessible important information about the complex process [1, 2, 3, 4, 5, 6, 7]. In this study it was chosen a real-case for test the facilities offered by PC&CA: the data of the perennial forages FRAP capacity, soil, fertilization and the presence of some plants species in grassland covering from Caras-Severin. Why FRAP capacity of the plants from grassland? Because perennial forages offer the opportunity to obtain functional feed for animals with minimum investment, cheaper then others sources, with high benefic impact on animal's health.

FRAP capacity of plants is related to antioxidant compounds which can reduce the free radicals, responsible for many chronic diseases in human's organism [8, 9, 10]. The food safety and quality are influenced by the feed safety and quality. That's way it is important to identify parameters easy to monitor, rapid and with low cost, which can give relevant information on the quality of agricultural products used as feed and raw matter in food industry or for direct human consume. FRAP capacity of perennial forages can be in the future a parameter of feed quality, determined as routine.

### Experimental

The quantitative characteristics of fifteen variables of the seven cases (one unfertilized and six fertilized) were used as PC&CA data matrix fitted by StatSoft - STATISTICA version 10. The vegetal (perennial grassland forages) and soil samples were harvested in the middle of June 2009. The location was N: 45°12' latitude; E: 21°60' longitude. Calcic Luvisol and temperate continental with Mediterranean influences clime characterized the studied permanent grassland ecosystem. The grassland was fertilized since 2003 as experimental field with five

replications for each case. One case was kept in unfertilized ecosystem conditions (M) and six cases were fertilized. Fermented sheep manure was chosen for organic fertilization cases (O1, O2, O3) with doses varied between 20-60 t/ha, being applied at each two years. The mineral nitrogen fertilizer varied between 100-200kg/ha in M1, M2 and M3 cases, on a constant doses of potassium and phosphorus (50kg/ha), applied yearly. The 200 kg/ha of mineral nitrogen were applied in two steps.

The active variables of PC&CA matrix were fourteen: soil pH, soil humus (%), soil total nitrogen content (%), organic and mineral nitrogen fertilization data, gravimetric percents of grassland forages for *Calamagrostis epigejos* (Ce), *Festuca rupicola* (Fr), *Poa pratensis* (Pp), *Lathyrus pratensis* (Lp), *Trifolium repens* (Tr), *Inula britannica* (Ib), *Filipendula vulgaris* (Fv), *Rosa canina* (Rc) and *Galium verum* (Gv). One supplementary variable was used: the FRAP capacity of perennial forages of the seven grassland cases (\*FRAP).

Soil pH was quantified respecting the SR ISO 10390/1999 [11]. The soil humus was determined by Walkley – Black – Gogoasă method [12]. The soil total nitrogen content was measured by Kjeldahl method [13]. The grassland floristic composition was established gravimetric (%). FRAP capacity of perennial forages was estimated quantitatively by FRAP method [14], using ethanol extracts (70%) diluted 1/20 and TPTZ reagent (tripiridil-triazine). The absorbance was read at 593 nm.

## Results and discussion

The data acquired for the Calcic Luvisol pH varied in 5.4 – 6.0 range. The humus values were between 6.2% and 9.0%. Total nitrogen content of hill grassland soil was in 0.23 – 0.31% range. The recorded data for gravimetric percent of *Calamagrostis epigejos* (Ce) in grassland covering were between 5% and 13%, higher in mineral nitrogen fertilization cases (M1, M2, M3). *Festuca rupicola* (Fr) was present in 16 – 46% range, also with the highest values in the mineral nitrogen fertilization cases. *Poa pratensis* (Pp) gravimetric percents were under 5%. *Lathyrus pratensis* (Lp) was present in grassland forages under 6%, higher in organic fertilization cases (O2, O3), while *Trifolium repens* (Tr) was under 38%, the highest in O3 (the fertilization case with the highest dose of fermented sheep manure). The others two organic fertilization cases (O1 and O2) had also high quantity of *Trifolium repens*, varied in 25-27% range. The species from others diverse species as *Inula britannica* (Ib), *Filipendula vulgaris* (Fv), *Rosa canina* (Rc) and *Galium verum* (Gv) were under 5%, 9%, 18%, and respectively 7%. All these recorded data were introduced in multivariate data matrix as active variables. The FRAP capacity of the perennial grassland forages of the seven studied cases (supplementary variable) was in 122 – 278  $\mu\text{M Fe}^{2+}/\text{g}$  range. The projections on the PC1xPC2 plan of the seven studied cases and of the fifteen variables are presented in Figure 1, respectively in Figure 2:



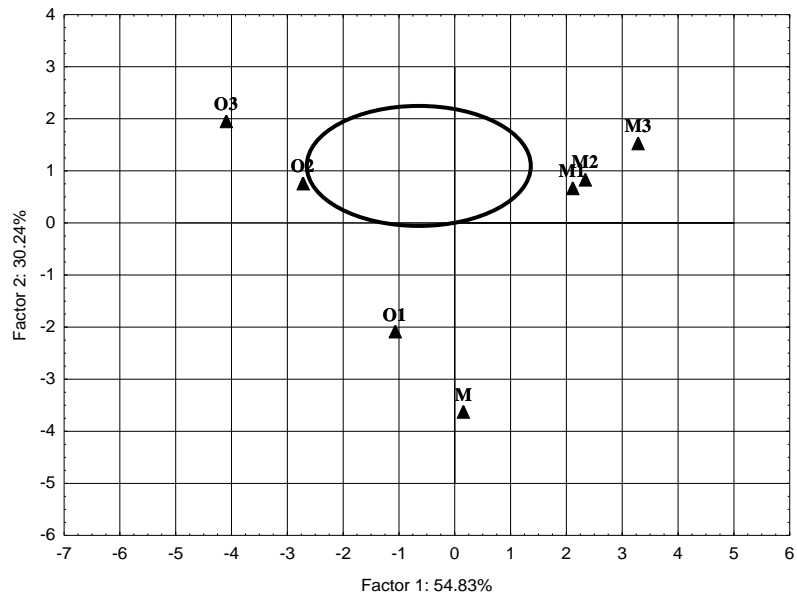


Figure 1. The projection of the seven studied cases on the PC1xPC2 plan

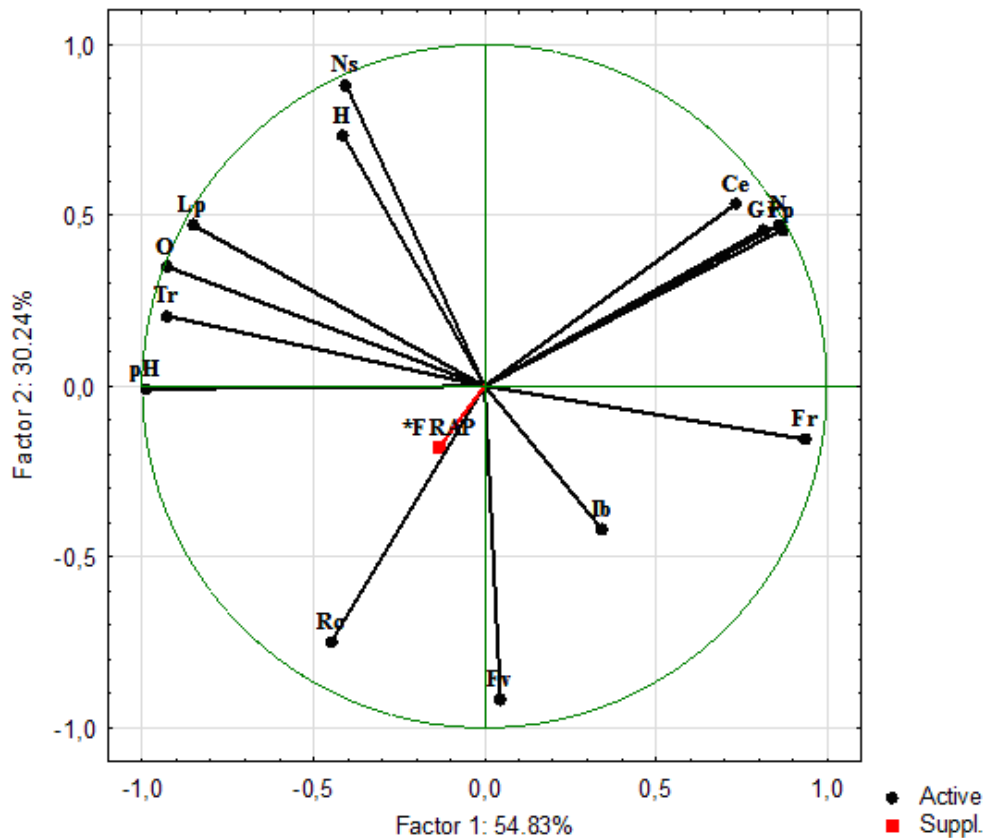


Figure 2. The projection of the fifteen variables on the PC1xPC2 plan

The PC&CA model was described 100% by six principal components. First three principal components had the eigenvalues higher than 1: 7.7 (PC1), 4.2 (PC2) and 1.3 (PC3). PC1 and PC2 described more than 85% of the PC&CA variance.

There were some variables which had a high positive influence on first principal component (PC1): the presence in permanent grassland forages of *Calamagrostis epigejos* (0.74), *Festuca*

*rupicola* (0.94), *Poa pratensis* (0.87), *Galium verum* (0.81) and mineral nitrogen fertilization data (0.86). A high negative influence on PC1 had soil pH (-0.99), *Lathyrus pratensis* (-0.85), *Trifolium repens* (-0.93), and the organic fertilization data (-0.93). In the second principal component (PC2) the highest positive influence had humus (0.73) and total nitrogen content (0.88) soil parameters. *Filipendula vulgaris* and *Rosa canina* had the highest negative impact on PC2: -0.91, respectively -0.75.

Projecting the seven cases of perennial forages harvested from the hill grassland on PC1xPC2 plan (Figure 1), it can be observed that mineral nitrogen fertilization trials were grouped distinctively (M1, M2 and M3). On the opposite side were grouped the forages from the trials fertilized with the highest doses of fermented sheep manure (O2 and O3). The smallest dose of fermented sheep manure (20t/ha) application differentiate the grassland ecosystem parameters of O2 from the others.

Figure 2 and the correlations of data matrix have shown that in the experimental field conditions of studied permanent grassland, *Lathyrus pratensis* and *Trifolium repens* had the highest presence in the fermented sheep manure application cases, the coefficients being 0.95, respectively 0.96, while in mineral nitrogen fertilization cases the coefficients were negatively: -0.50, respectively -0.68. The correlation between organic fertilization data and the *Galium verum* presence (%) had also a negative coefficient (-0.57). In mineral fertilization cases the *Poaceae* species were dominants, having high positive correlation coefficients: 0.88 for *Calamagrostis epigejos*, 0.68 for *Festuca rupicola* and 0.94 for *Poa pratensis*. *Galium verum* was also influenced significant positively by mineral fertilization, the correlation coefficient being 0.96. *Trifolium repens* was correlated negatively with mineral fertilization, the coefficient was -0.68. Between supplementary variable \*FRAP capacity of perennial forages and the gravimetric percents of *Inula britannica* and *Rosa canina* the correlation coefficients were positive in this period of the year: 0.35, respectively 0.31.

## Conclusion

PC&CA can be a flexible statistic tool to monitor the FRAP capacity of the grassland forage in the middle of June, depending on fertilization. Using this exploratory multivariate technique and the selected active and supplementary variables, it was possible to discriminate between organic fertilized trials (cases) from those fertilized exclusive mineral or unfertilized. It was possible also to highlight the correlations between fertilization data and the presence of different plants species responsible for the FRAP capacity in the middle of June, in soil-climatic conditions of experimental field from Caras-Severin hill. Organic fertilizer influenced the presence of *Lathyrus pratensis* (0.95) and *Trifolium repens* (0.96). Mineral fertilization had positive influence on the distribution of *Calamagrostis epigejos* (0.88), *Festuca rupicola* (0.68), *Poa pratensis* (0.94) and *Galium verum* (0.96). FRAP capacity of permanent grassland forages had positive correlation coefficients for *Inula britannica* (0.35) and *Rosa canina* (0.31).

## Acknowledgements

The quantitative results, used as data matrix to test the PC&CA multivariate technique facilities for FRAP capacity of permanent grassland forages depending on fertilization, were aquired with the financial support of Grant BD/CNCSIS Romania: “On the influence of substances flows on the quality of forage from grassland”, 2007 – 2009 (www.cnscis.ro).

## References

- [1] F.K. Wanga, T.C.T. Dub, Omega, 28 (2000) 185-194.
- [2] A.B.W. Manage, S.M. Scariano, Journal of Statistics Education, vol.21, no.3 (2013) 1-22.
- [3] S.C. Crespo, A.L. Moreno-Chacón, A. Rojas. L.M. Melgarejo, Braz. Chem. Soc., vol.22, no.12 (2011) 2275-2280.
- [4] G. Evgenidis, E. Traka-Mavrona, M. Koutsika-Sotiriou, International Journal of Agronomy, article ID 697879 (2011), 7 pages.
- [5] K. Rymuza, E. Turska, G. Wielogórska, A. Bombik, Acta Sci. Pol., Agricultura, vol. 11, no.1 (2012) 79-90.
- [6] P. Singh, V. Bajpai, S. Kumar, M. Srivastava, B. Kumar, Journal of Medicinal Plants Studies, vol.5, no.3 (2017) 384-391.
- [7] G. Verma, P.K. Mahajan, A. Chandel, International Journal of Applied Research, vol.2, no.7 (2016) 857-859.
- [8] C. Henriquez, S. Almonacid, I. Chiffelle, T. Valenzuela, M. Araya, L. Cabezas, R. Simpson, H. Speisky, Chilean Journal of Agricultural Research, vol.70, no.4 (2010) 523-536.
- [9] M.B. Hossain, N.P. Brunton, C. Barry-Ryan, A.B. Martin-Diana, M. Wilkinson, Rasayan J. Chem., vol.1, no.4 (2008)751-756.
- [10] R.L. Prior, X. Wu, K. Schaich, J. Agric. Food Chem., 53 (2005) 4290–4302.
- [11] SR ISO 10390 (1999), *Calitatea solului. Determinarea pH-ului.*
- [12] E. Stoica coord., C. Răuță, N. Florea, Metode de analiză chimică a solului, București, 1986.
- [13] I. Gergen, *Analiza produselor agroalimentare*, Eurostampa Ed., Timișoara, 2004, pp.40.
- [14] I.F.F. Benzie, J.J. Strain, Analytical Biochemistry, 239 (1996) 70-76.

## OXYGEN REDUCTION ACTIVITY OF COBALT-NITRIDE ON NITROGEN-DOPED GRAPHENE

**Gergő Ballai<sup>1</sup>, Tamás Varga<sup>1</sup>, Henrik Haspel<sup>1,†</sup>, Ákos Kukovecz<sup>1</sup>, Zoltán Kónya<sup>1,2</sup>**

*1 Department of Applied and Environmental Chemistry, University of Szeged, H-6720 Szeged, Rerrich Béla tér 1, Hungary*

*2 MTA-SZTE Reaction Kinetics and Surface Chemistry Research Group, H-6720 Szeged, Rerrich Béla tér 1, Hungary*

† Present address: Division of Physical Sciences and Engineering, KAUST Catalysis Center (KCC), King Abdullah University of Science and Technology (KAUST), 4700 KAUST, Thuwal, 23955-6900, Saudi Arabia.

### **Abstract:**

Fuel cells technology can offer suitable alternatives to replace one of the most important environmental issues of our days, i.e., fossil fuels. In the last decades, non-precious metal catalysts came in the view such as transition metal-oxides, -nitrides, or even metal free catalysts like N-graphene. Such systems are expected to replace high cost oxygen reduction reaction (ORR) catalysts used nowadays [1]. We hereby demonstrate a simple method for the simultaneous synthesis of cobalt-nitride nanoparticles on nitrogen-doped graphene support. The reported non-precious metal catalyst showed high electrocatalytic activity in ORR, and thus it is a promising alternative cathode-side catalyst in polymer electrolyte membrane (PEM) fuel cells. The catalyst was synthesized from lyophilized graphene-oxide and cobalt(II)-acetate in NH<sub>3</sub> flow at high temperature, and the effect of cobalt-nitride amount on catalyst properties was further examined. To this end, transmission electron microscopy (TEM) and X-ray diffractometry (XRD) were employed to monitor the morphological and structural changes in the graphene sheets and the supported cobalt-nitride particles. The electrochemical properties of the catalyst were investigated in a three-electrode cell in oxygen saturated 0.1 M potassium-hydroxide solution at different rotation rates with a rotating disk electrode (RDE) setup. The optimal amount of cobalt-nitride and nitrogen-doped graphene was determined, producing a promising non-precious metal catalyst for oxygen reduction reaction.

[1] ZHANG, JiuJun (ed.). PEM fuel cell electrocatalysts and catalyst layers: fundamentals and applications. Springer Science & Business Media, 2008., 89-134

**EXTRACTION OF ANTIOXIDANT AND POLYPHENOL COMPOUNDS FROM TOKAJI ASZÚ MARC WITH ISO-PROPANOL – WATER SOLVENT**

**Szilvia Bánvölgyi<sup>1</sup>, Fiina K. Namukwambi<sup>1</sup>, István Kiss<sup>2</sup>, Éva Stefanovits-Bányai<sup>3</sup>, Gyula Vatai<sup>1</sup>**

<sup>1</sup>*Department of Food Engineering, Szent István University, H-1118 Budapest, Ménesi str 44., Hungary*

<sup>2</sup>*Fitomark 94 Kft., H-3934 Tolcsva, Arany János utca 16/a, Hungary*

<sup>3</sup>*Department of Applied Chemistry, Szent István University, H-1118 Budapest, Villányi str 29-43., Hungary*

*e-mail: Banvolgyi.Szilvia@etk.szie.hu*

**Abstract**

The aim of this study was to determine the best parameter of extracting total phenol content (TPC) and antioxidant capacity (AC) from Tokaji Aszú using isopropanol – water solvent. The solid/liquid ratio was used 1:4. Different parameters such as solvent concentration (0, 25, 50, 75, 100%), time (0.5, 1, 2, 3, 4, 5) and temperature (30, 45 and 60 °C) were investigated. The total phenol content (TPC) and antioxidant capacity (AC) were determined in the extracts using spectrophotometric analysis. SPSS statistical software was used to determine the significant difference (One-Way ANOVA, post hoc multiple comparisons, Scheffe test at significance level 0.05). The binary solvent (a mixture of water and isopropanol) was better than mono-solvent (pure water or 100% isopropanol). The optimal extracting condition for TPC was achieved at 60 °C (temperature), 50% (isopropanol) and 4 hrs (time) 7419±36 µM GAE/L while maximized value of AC was 5228±11µM ASE/L reached at 60 °C (temperature), 25% (isopropanol) and 4 hrs (time).

**Introduction**

Wine production generates a huge amount of waste which is considered as unbeneficial and potentially causes environment problems. However, due to the advance technology, minimization of waste production in several wine industries has drawn attention to many. The necessary development of innovation and effective valorization procedures has been implemented to reduce winery waste (1). Winery wastes are regarded as a low-cost source of antioxidant and phenolic compounds (2).

Wine making residues includes organic wastes (grape pomace, seeds, pulp and skins, grape stems and leaves); wastewater; emission of greenhouse gases and inorganic wastes (1). In the present paper, organic wastes (grape pomace) were studied. This waste is produced during the production of must (grape juice) after pressing the whole fruit (1). Phenolic compounds are recovered through solvent- extraction procedure whereby isolation, identification, and quantification are performed (2).

The goal of an extraction process is to provide the maximum yield of substances and of the highest quality (concentration of phenolic compounds and antioxidant power of the extracts).

**Experimental**

The marc of Tokaji aszú was provided by the Fitomark Ltd. (Tolcsva). The marc was stored in freezer till the experiments.

### Extraction measurements

Our aim was to find the optimal conditions of the extraction from Tokaji aszú marc. Isopropanol and deionized water were used to prepare the solvent, 4:1 solvent-to-sample ratio was chosen. Continuous stirring was ensured during all experiments. The picture and flow sheet of the equipment can be seen at Figure 1.

In the experiments three parameters of the extraction were changed: the temperature, the solvent concentration and the time of the extraction. The temperature was 30 °C, 45 °C and 60 °C. To keep the temperature at constant value a Lauda Ecoline E100 Immersion Thermostat was used. The solvent contains different volumes of isopropanol (0 – 25 – 50 – 75 – 100%). The time of the extraction was half-, one-, two-, three-, four- and five-hours long.

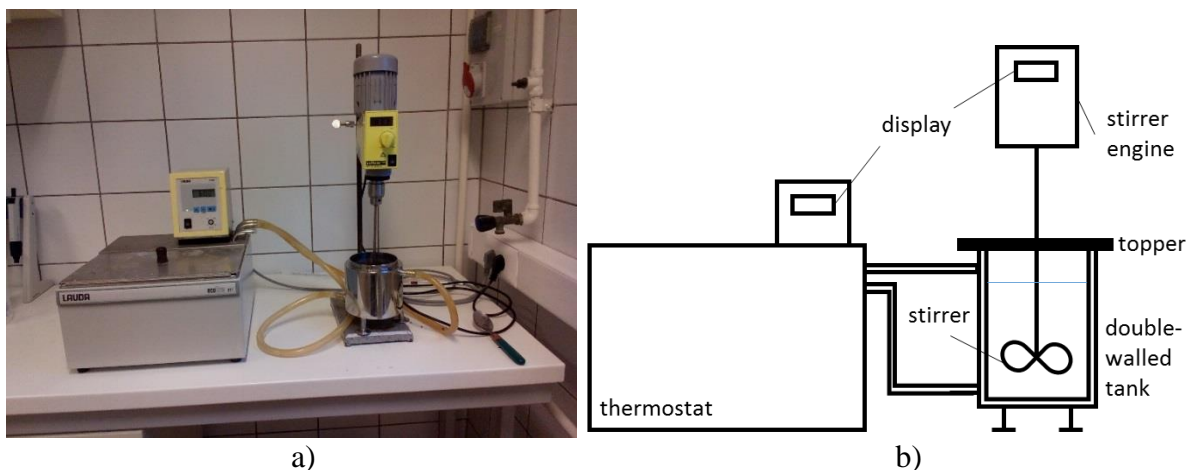


Figure 1. (a) picture of the experimental equipment and (b) flow sheet of the experimental equipment

### Analytical measurements

The TPC, FRAP assays were run with a Nicolet Evolution 300 BB type spectrophotometer (Thermo Electron Corporation, Cambridge, UK) at the respective wavelengths. Measurements were run triplicate.

#### Analysis of total phenol content (TPC)

Total phenol content was determined by the Folin-Ciocalteu assay [3] applying gallic acid as the standard at 760 nm. Total phenol content was expressed in  $\mu\text{mol}$  equivalents of gallic acid (GS)/L.

#### Antioxidant capacity measurements (AC)

The FRAP antioxidant capacity assay was run as described by Benzie and Strain [4] using ascorbic acid as standard. The absorbance was measured at 593 nm and results were determined in  $\mu\text{mol}$  equivalents of ascorbic acid (AS)/L.

SPSS Statistics 22 software was used to determine the significant difference between the samples (one-way ANOVA, post hoc multiple comparisons).

## Results and discussion

Figure 2. shows the phenol concentration (a) and antioxidant capacity (b) of the extracts in case of water solvent at different temperatures versus extraction time. At higher temperature (60 °C) the phenol concentration and antioxidant capacity were two and three times higher than at lower temperature (30 °C). The extraction time generally increased the total phenol content and the antioxidant capacity. In case of water solvent the maximum values of polyphenol concentration was  $3000 \pm 17 \mu\text{M GS/L}$  (after 5 hours), and the maximum of antioxidant capacity was  $1575 \pm 33 \mu\text{M AS/L}$  (after 5 hours).

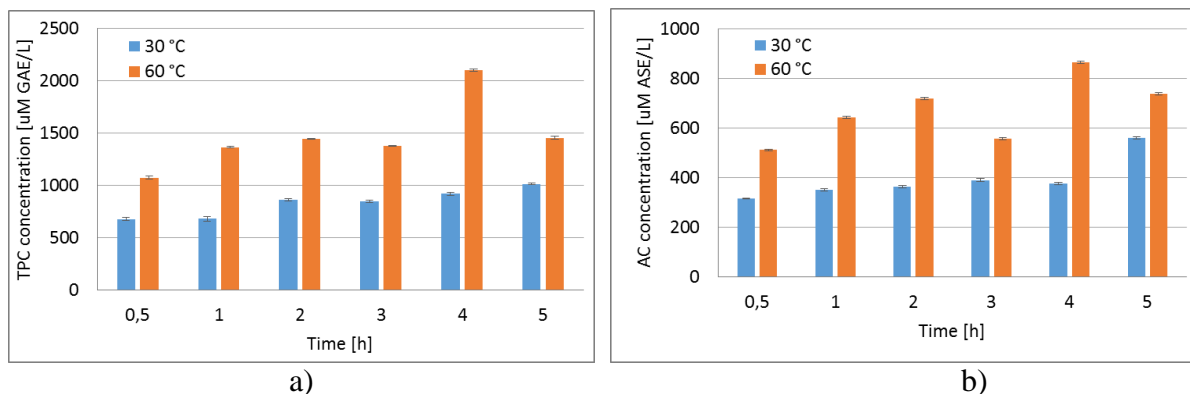


Figure 2. (a) Polyphenol concentration increase of water solvent and b) Antioxidant capacity increase of water solvent

In our experiments the phenol content and the antioxidant capacity of the extracts were much higher at 60 °C temperature than at 30 °C temperature, therefore we only represent the results at 60 °C temperature comparing the various solvent concentrations.

The total phenol content of the extracts can be seen in Figure 3. in case of 25% – 50% (a) and 75% – 100% (b) isopropanol solvent versus extraction time. The different volumes of isopropanol in the solvent reached a more varied result than the water solvent. In case of 25% isopropanol solvent the total phenol content was increased in the first 3 hours and after that it was almost constant. The Scheffe test did not show significant difference between the TPC values at 3-4-5 hrs. Using 50% isopropanol the TPC concentration in the extract was the same after one hour. Next to 75% isopropanol solvent a continuously raise was observed in TPC during the five hours. Using 100% isopropanol the TPC concentration was low like using pure water. The maximum value of total phenol content ( $7419 \pm 36 \mu\text{M GAE/L}$ ) was reached at 60 °C temperature, 50% ethanol solvent after 4 hours.



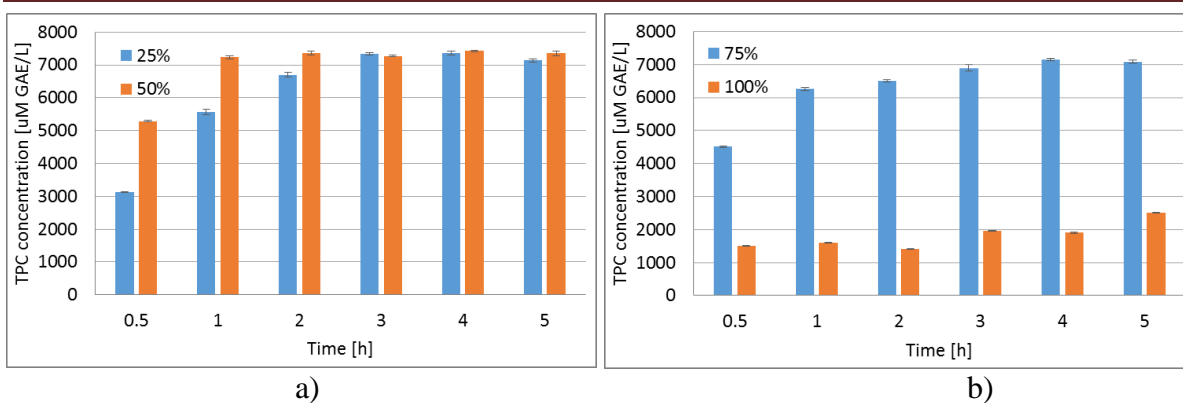


Figure 3. (a) Polyphenol concentration in case of 25% and 50% isopropanol solvent (b) Polyphenol concentration in case of 75% and 100% isopropanol solvent at 60 °C temperature

The antioxidant capacity of the extracts can be seen in Figure 4. in case of 25% – 50% (a) and 75% – 100% (b) isopropanol solvent versus extraction time at 60 °C temperature.

The interaction of water and isopropanol have shown a positive effect on antioxidant capacity in the extracts. Using 25% isopropanol solvent the AC increases directly proportional to time until 4 hours and then decrease during 5 hours of extraction.

The maximum value of antioxidant capacity ( $5228 \pm 11 \mu\text{M ASE/L}$ ) was reached at 60 °C temperature, 25% ethanol solvent after 4 hours. Applying 50-75% isopropanol solvent an almost continuously raise was observed in AC during the five hours. In all cases there are significant difference between AC concentrations. Using 100% isopropanol for the extraction resulted low AC concentrations. The AC values were almost the same values like in case of pure water.

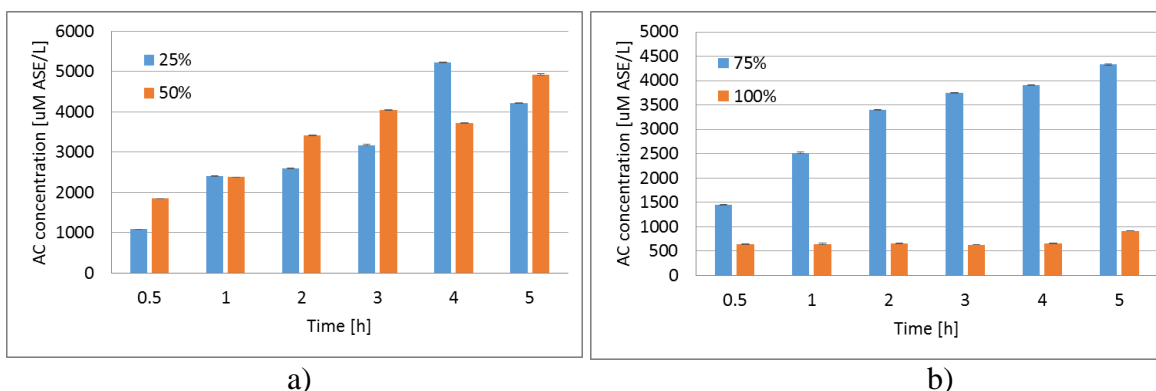


Figure 4. (a) Antioxidant capacity in case of 25% and 50% isopropanol solvent (b) Antioxidant capacity in case of 75% and 100% isopropanol solvent at 60 °C temperature

Figure 5. shows the influence of temperature on TPC and AC in case of different concentration of solvent after 3 hrs extraction. The temperature has a great impact on phenolic compounds and antioxidant recovery. TPC increased with temperature and Chew et al. [5], Wang et al. [6] reported similar results.

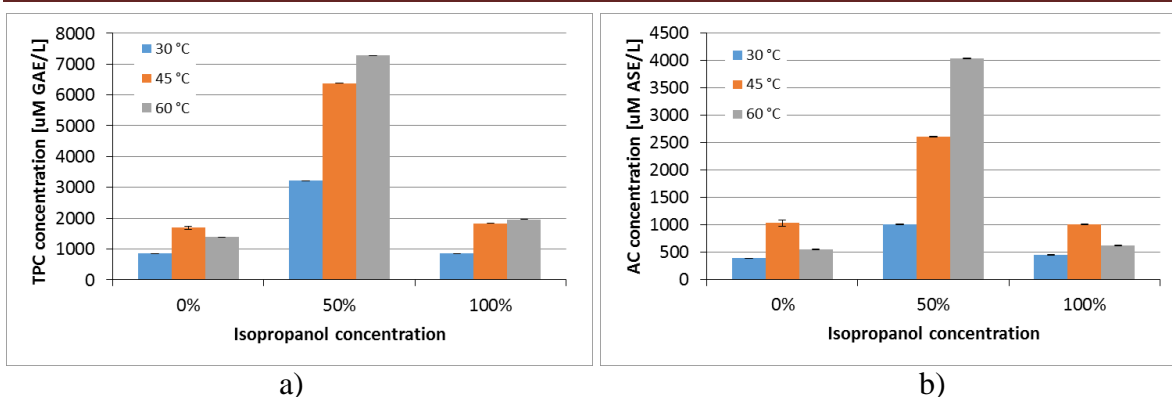


Figure 5. Effect of temperature and solvent concentration on TPC (a) and AC (b) content after 3 hours of extraction

Thoo et al. [7] mentioned that to improve phenolic compounds adequate heating is applied to promote solvent extraction by enhancing both diffusion coefficients and the solubility of polyphenol content. Wang et al. [6] findings demonstrated that high temperature has a positive impact on the extraction of phenolic compounds excluding antioxidant since it increases solubility and diffusion coefficient of any compounds.

Our results show that the extraction at 60 °C has the highest yield of total phenolic content to compare with 30 °C and 45 °C while for antioxidant capacity extracted at 45 °C was high and decreases at 60 °C except for using 50% of isopropanol. Antioxidant capacity was sensitive to high temperatures. High-temperature degrade and promote molecular collisions, favouring polymerization which reduces antioxidant compounds [8].

From the economic point of view, working at 45 °C is much better than 60 °C to maximised the yield. This need to be verified by evaluation of the energy cost of the extraction step on the overall production cost [2].

The high temperature is in favoured of the released bound of polyphenol in a sample with the breakdown of cellular constituents of plant cells which lead to increased cell membrane permeability. These bound polyphenols could further reduce the chances of polyphenol coagulating with lipoprotein, thereby enhancing the solubility of the polyphenol and diffusion increasing polyphenol yield [7].

There is no significant difference between AC extracted using 0% and 100% isopropanol concentration at all temperature (30, 45 and 60 °C), respectively. There is also no significant difference between AC values at 30 °C, 50% isopropanol and 45 °C, 0% isopropanol and 45 °C, 100% isopropanol concentration. But in all other cases, there are significantly difference. There is a significant difference between all TPC concentration except at 30 °C temperature using 0% and 100% isopropanol.

## Conclusion

Winery waste is rich in phenolic compounds. The extraction process can be used to separate these compounds from waste. The extraction experiments were achieved successfully. In all cases the concentration of total phenol content and antioxidant capacity was higher at higher temperature. The maximum recovery TPC from the grape marc using traditional solid-liquid extraction was  $7419 \pm 36$  µM GAE/L at the optimum conditions of 50% isopropanol concentration, 60 °C temperature and 4 hours, respectively. In contrast, the maximum AC was  $5228 \pm 11$  µM ASE/L under optimum conditions of 25 % isopropanol concentration, 60 °C temperature and 4 hours, respectively. These results indicate that an increase in temperature

and solvent concentration has a positive impact on both TPC and AC. There was a gradual increase in TPC and AC as the temperature rises from 30 °C to 60 °C. The TPC and AC rise during binary solvent (25-75% isopropanol concentration) and decrease in the mono-solvent system (pure water and 100 % isopropanol concentration). Determine the optimal parameters of the extraction (temperature, solvent concentration and extraction time) is not easy because of the different optimum of the total phenol content and antioxidant capacity. Our suggestion to choose the optimal operating parameters according to the more important component.

### **Acknowledgements**

Acknowledgement to the Ministry of Human Capacities of Hungarian Government (EFOP-3.6.3-VEKOP-16) for their sponsorship.

### **References**

- [1] A. Teixeira, N. Baenas, R. Dominguez-Perles, A. Barros, E. Rosa, D.A. Moreno, C. Garcia-Viguera, *Int. J. Mol. Sci.* 15(9) (2014) 15638-15678.
- [2] G. Spigno, D. M. De Faveri, *J. Food Eng.* 78(3) (2007) 793-801.
- [3] V.L. Singleton, J.A. Rossi, *Am. J. Enol. Vitic.* 16 (1965) 144-158.
- [4] F.F. Benzie, J.J. Strain, *Anal. Biochem* 239 (1996) 70-76.
- [5] K.K. Chew, M.Z. Khoo, S.Y. Ng, Y.Y. Thoo, W.M. Wan Aida, C.W. Ho, *Int. Food Res. J.* 18(4) (2011) 1427-1435.
- [6] J. Wang, B. Sun, Y. Cao, Y. Tian, X. Li, *Food Chem.* 106 (2008) 804-810.
- [7] Y.Y. Thoo, S.K. Hoa, J.Y. Liang, C.W. Hob, C.P. Tana, *Food Chem.* 120 (2009) 290-295.
- [8] Y.H. Wong, H.W. Lau, C.P. Tan, K. Long, K.L. Nyam, *Sci. World J.* 2014 (2014) ID 789346, 7 pages.

**CHARACTERIZATION OF NOVEL SURFACTIN ISOFORMS AND THE EFFECTS OF DIFFERENT CULTIVATION PARAMETERS ON THEIR PRODUCTION BY *BACILLUS SUBTILIS***

**Attila Bartal<sup>1</sup>, Anita Kecskeméti<sup>1</sup>, Bettina Bóka<sup>1</sup>, László Manczinger<sup>1</sup>, Csaba Vágvölgyi<sup>1</sup>, András Szekeres<sup>1</sup>**

<sup>1</sup>*Department of Microbiology, Faculty of Sciences, University of Szeged, 6726, Közép fasor 52, Szeged, Hungary  
e-mail: bartaloszi@gmail.com*

**Abstract**

Surfactin is a lipopeptide-type biosurfactant produced mainly by the gram-positive microorganism *Bacillus subtilis*. It consists of a peptide loop of seven amino acids and a hydrophobic fatty acid chain (C<sub>12</sub> – C<sub>16</sub>). Surfactins are proved to exhibit various biological activities, such as anti-tumor, anti-viral and anti-inflammatory effects. According to these properties, different therapeutic and environmental applications of surfactins are considered. The chemical composition of surfactins could be varied in the length of the fatty acid chain and in the sequence of the amino acids of the peptide chain generating a wide spectrum of different homologues and isomers. The chemical composition of these isoforms could be elucidated via mass spectrometry by the analysis of MS<sup>n</sup> fragmentation pattern. Furthermore, depending on the cultivation conditions, the production of surfactins are affected resulting in various rates of the different isoforms produced.

In this work a mixture of surfactins were extracted from the strain *Bacillus subtilis* (SZMC 6179J) and were examined by HPLC-ESI-IT-MS technique. To increase the separation of the components with higher masses a gradient elution was applied using a non-polar solvent system, which led to their proper elution and characterization of their structures. Both the length of the linked fatty acids and the peptide sequences were also investigated during the MS<sup>2</sup> spectra analyses of the sodiated precursor ions. The results led to the discovery of a novel, recently unknown group of surfactin forms possessing glutamic acid in as the fifth amino acid residue instead of the aspartic acid described previously at this position. To examine the effects of the culture media on the surfactin production, it was modified with various carbon sources and metal ions. It was reaffirmed that altering the cultivation parameters could enable the improved production of certain surfactin variants, which could serve possibility for their further preparative purification and structural elucidation.

The research was supported through the New National Excellence Program of the Ministry of Human Capacities.

**EFFECT OF ADAPTATION ON HEXANE BIODEGRADATION BY A  
RHODOCOCCUS STRAIN CAPABLE OF HYDROCARBON UTILIZATION**

**Attila Bodor<sup>1</sup>, Nikolett Rácz<sup>1</sup>, Sándor Mészáros<sup>1</sup>, Péter Petrovszki<sup>1</sup>, Ágnes Erdeiné  
Kis<sup>1,2,3</sup>, Krisztián Laczi<sup>1</sup>, Gábor Rákhely<sup>1,2,3</sup>, Katalin Perei<sup>1,3</sup>**

<sup>1</sup>*Department of Biotechnology, University of Szeged, H-6726 Szeged, Közép fasor 52,  
Hungary*

<sup>2</sup>*Institute of Biophysics, Biological Research Centre, H-6726 Szeged, Temesvári krt. 62,  
Hungary*

<sup>3</sup>*Institute of Environmental and Technological Sciences, University of Szeged, H-6726 Szeged,  
Közép fasor 52, Hungary  
e-mail: bodor.attila@gmail.com*

**Abstract**

Although organic solvents such as hexane have harmful effects on human health and natural environments, they are commonly used chemicals in several industrial fields. Bioremediation is an environmentally friendly and cost effective waste management technique for rehabilitation of polluted environments. A hydrocarbon-utilizing bacterial strain identified as a *Rhodococcus sp.* PAE1 was previously isolated from mazut. This new isolate was adapted to hexane in order to assess the effects of adaptation. The adapted strain exhibited a wide range of hexane tolerance and faster hexane biodegradation rate compared to the non-adapted strains. Adaptation to hexane combined with changes in cell membrane fatty acids resulted in increased cell surface hydrophobicity and elongation of cells that can promote the bioavailability of a water insoluble substrate.

**Introduction**

Despite their harmful effects, organic solvents are widely used industrial chemicals posing a serious risk to human health and natural environments [1, 2]. Although hexane is a widespread solvent applied in the production of cleaning supplies [3] and glues [4], in footwear manufacturing [5], pharmaceutical [6] and food industry [7], it can do damage to the aquatic or terrestrial wildlife, if it is emitted into the environment [8]. Since hexane is highly volatile, it can easily evaporate into the atmosphere and contribute to the formation of photochemical smog by increasing the tropospheric ozone concentration [9, 10]. Taking these facts into consideration, adequate damage prevention and remediation technologies are needed. Out of the possible strategies, bioremediation involving the use of microorganisms or plants can be one of the most suitable techniques because it is an environmentally friendly and cost-effective method [11]. As a short chain alkane, hexane is extremely toxic for cells and even hydrocarbon degrader microorganisms can be sensitive for relatively low concentration of hexane. Therefore, we aimed to examine the tolerance of this strain to hexane, the effects of adaptation on hexane biodegradation and the phenotypical changes including cell length and cell surface hydrophobicity (adhesion% or ADH%) that might be involved in increasing hexane bioavailability.

**Experimental**

*Rhodococcus sp.* PAE1 isolated from mazut was adapted to hexane as sole carbon and energy source for 6 months. Cells were incubated with various concentrations of hexane, while their

size and cell surface hydrophobicity were measured. Respiration activity and biodegradation efficacy were determined by following CO<sub>2</sub> release and remaining hexane content of each culture.

### Results and discussion

Solvent tolerance was assessed by measuring respiration in liquid minimal medium (MM) supplemented with hexane in varying concentrations as sole carbon and energy source in closed vials. *Rhodococcus sp.* PAE1 was able to tolerate and even use hexane in a range of 0.1 - 1.5 V/V% (Fig. 1).

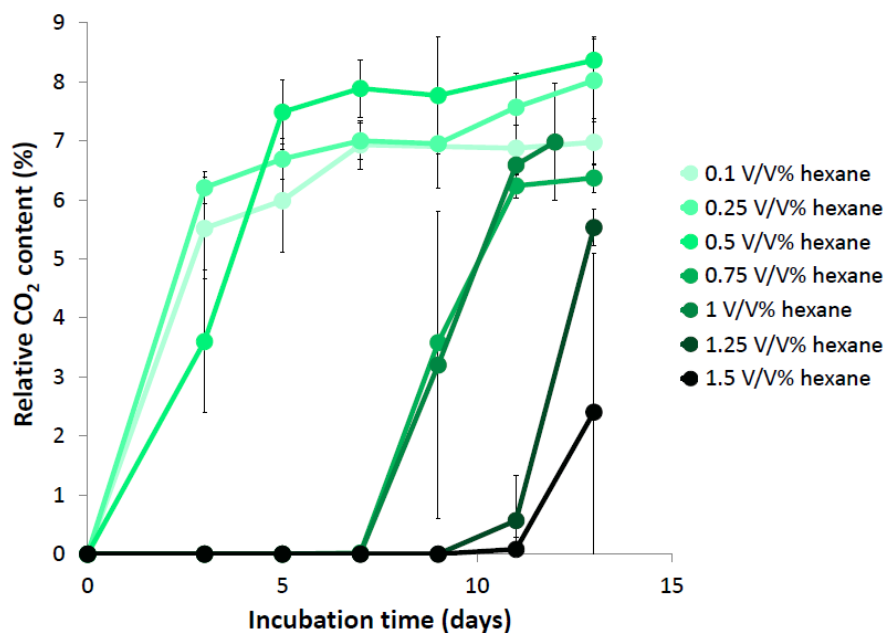


**Figure 1.** CO<sub>2</sub> production by *Rhodococcus sp.* PAE1 growing on hexane in varying amount as sole carbon and energy source

Respiration data were also used to examine the degradation of hexane by the adapted strains and the non-adapted ones (previously cultured in nutrient-rich LB medium or pregrown on hexane only once). Adapted culture was able to utilize hexane faster than the others but an increased rate of biodegradation was observed even in the cell line precultured on hexane only once compared to the non-adapted one indicating a quick adaption process to this solvent (Fig. 2.).

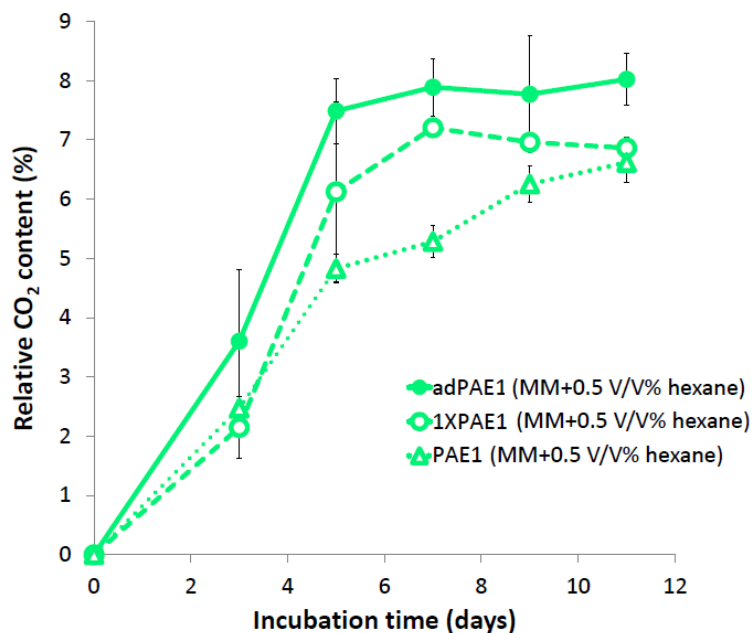


**Figure 2.** Effect of adaptation on CO<sub>2</sub> production by *Rhodococcus sp.* PAE1 growing on 0.5 V/V% hexane as sole carbon and energy source

Remaining hexane content from these samples were determined after solvent-solvent extraction and GC-MS analysis. Our results revealed that available oxygen concentration in the headspace of closed vials limited hexane biodegradation and it was only sufficient for oxidizing about 25% of the initial hexane concentration (Fig. 3.).

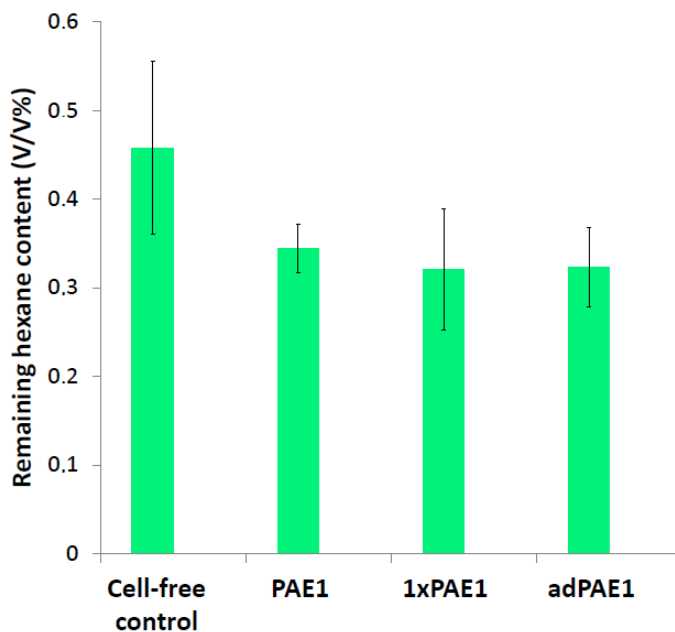


**Figure 3.** Remaining hexane content after 11 days of incubation



Cell surface hydrophobicity is a widespread phenomenon in *Rhodococci* due to chains of mycolic acid located in their cell walls. Using the method of Qiao et al. [13] and analysing bright field microscopy pictures, cell surface hydrophobicity (ADH%) and cell length of *Rhodococcus sp.* PAE1 from the previous samples were determined (Table 1.).

**Table 1.** Remaining hexane content after 11 days of incubation

	<b>non-adapted PAE1 (LB)</b>	<b>non-adapted 1xPAE1</b>	<b>long term adapted PAE1</b>
<b>ADH%</b>	41.67 ± 19.97	55.39 ± 12.02	61.89 ± 8.76
<b>Cell length (µm)</b>	2.02 ± 0.14	2.21 ± 0.16	2.38 ± 0.10

Based on our data, we suppose that properties of culturing medium and the bioavailability of carbon source essentially influence the surface parameters and length of bacterial cells grown in that specific medium. Increased hydrophobicity of the cell surface and elongation can be beneficial for utilization of a not water-soluble substrate. In accordance with our previous results (Fig. 2.), adapted *Rhodococcus sp.* PAE1 strain showed to be different from non-adapted ones (precultured in LB or on hexane only once) and exhibited higher cell surface hydrophobicity and cell length while the non-adapted strain, which was precultured on hexane only one time, seemed to have intermediate properties between the adapted *Rhodococcus sp.* PAE1 and the non-adapted PAE1 strain precultured in nutrient-rich LB medium.

### Conclusion

Hexane utilization by adapted *Rhodococcus sp.* PAE1 was increased compared to the non-adapted cells presumably caused by adaptation-induced changes, such as elongation and increased cell surface hydrophobicity facilitating hexane bioavailability. Cells were tended to be aggregated in hexane containing media. We suppose that adaptation might result in increased level of unsaturated bonds in membrane fatty acids playing a crucial role in making cells more resistant to organic solvents. These observations could be useful in future application of bacteria capable of hexane biodegradation.

### Acknowledgements

The project was supported by the European Union and Hungarian State (grant agreement no. EFOP-3.6.2-16-2017-00010) and by the Norway Grant (grant agreement no. HU09-0044-A1-2013).

### References

- [1] Wypych, G. (2001). *Handbook of solvents*. ChemTec Publishing.
- [2] Reichardt, C., & Welton, T. (2011). *Solvents and solvent effects in organic chemistry*. John Wiley & Sons.
- [3] Sack, T. M., Steele, D. H., Hammerstrom, K., & Remmers, J. (1992). A survey of household products for volatile organic compounds. *Atmospheric Environment. Part A. General Topics*, 26(6), 1063-1070.
- [4] Rastogi, S. C. (1993). Organic solvent levels in model and hobby glues. *Bulletin of environmental contamination and toxicology*, 51(4), 501-507.

- [5] Heuser, V. D., Erdtmann, B., Kvitko, K., Rohr, P., & da Silva, J. (2007). Evaluation of genetic damage in Brazilian footwear-workers: biomarkers of exposure, effect, and susceptibility. *Toxicology*, 232(3), 235-247.
- [6] Grodowska, K., & Parczewski, A. (2010). Organic solvents in the pharmaceutical industry. *Acta Pol Pharm*, 67(1), 3-12.
- [7] DeSimone, J. M. (2002). Practical approaches to green solvents. *Science*, 297(5582), 799-803.
- [8] Ferrando, M. D., & Andreu-Moliner, E. (1992). Acute toxicity of toluene, hexane, xylene, and benzene to the rotifers *Brachionus calyciflorus* and *Brachionus plicatilis*. *Bulletin of environmental contamination and toxicology*, 49(2), 266-271.
- [9] Atkinson, R. (1997). Gas-phase tropospheric chemistry of volatile organic compounds: 1. Alkanes and alkenes. *Journal of Physical and Chemical Reference Data*, 26(2), 215-290.
- [10] Fehsenfeld, F., Calvert, J., Fall, R., Goldan, P., Guenther, A. B., Hewitt, C. N., & Zimmerman, P. (1992). Emissions of volatile organic compounds from vegetation and the implications for atmospheric chemistry. *Global Biogeochemical Cycles*, 6(4), 389-430.
- [11] Fingerman, M. (Ed.). (2016). *Bioremediation of aquatic and terrestrial ecosystems*. CRC Press.
- [12] Bell, K. S., Philp, J. C., Aw, D. W. J., & Christofi, N. (1998). The genus *Rhodococcus*. *Journal of Applied Microbiology*, 85(2), 195-210.
- [13] Qiao, G., Li, H., Xu, D. H., & Park, S. I. (2012). Modified a colony forming unit microbial adherence to hydrocarbons assay and evaluated cell surface hydrophobicity and biofilm production of *Vibrio scophthalmi*. *ARS USDA Submissions*.

TRIPTOFÁN ÉS BIZONYOS METABOLITJAINAK KONCENTRÁCIÓJÁNAK  
MEGHATÁROZÁSA CREUTZFELDT-JAKOB BETEGEKNEL

THE ASSESSMENT OF CONCENTRATIONS OF CERTAIN TRYPTOPHAN  
METABOLITES IN CREUTZFELDT-JAKOB DISEASE

Edina Cseh<sup>1</sup>, Nikolett Nánási<sup>1</sup>, Gábor Veres<sup>1,2</sup>, Péter Klivényi<sup>1</sup>, Krisztina Danics<sup>3,4</sup>,  
László Vécsei<sup>1,2</sup>, Gábor G Kovács<sup>3,5</sup>, Dénes Zádori<sup>1</sup>

<sup>1</sup>*Department of Neurology, Faculty of Medicine, Albert Szent-Györgyi Clinical Center,  
University of Szeged, Szeged, Hungary*

<sup>2</sup>*MTA-SZTE Neuroscience Research Group, Szeged, Hungary*

<sup>3</sup>*Prion Disease and Neuropathology Reference Center, Semmelweis University, Budapest,  
Hungary*

<sup>4</sup>*Department of Forensic and Insurance Medicine, Semmelweis University, Budapest, Hungary*

<sup>5</sup>*Institute of Neurology, Medical University of Vienna, Vienna, Austria  
[cshedina.k@gmail.com](mailto:cshedina.k@gmail.com)*

## 1. Abstract

The kynurenine (KYN) pathway (KP), also known as the route where more than 95% of the tryptophan (TRP) is metabolized, in its steps of catabolism forms different metabolites which contribute to the neuroprotective–neurodegenerative changes in central nervous system. For this reason, TRP metabolism is extensively studied in neurodegenerative diseases (Alzheimer’s disease, Parkinson’s disease, Huntington’s disease), where the neurologically active metabolite concentration changes are followed. Kynurenic acid (KYNA), which is an endogenous N-methyl-D-aspartate receptor (NMDAR) antagonist, is considered to be a neuroprotective agent.

In the present study TRP, KYN and KYNA were determined from human serum and cerebrospinal fluid (CSF) of patients with Creutzfeldt-Jakob disease (CJD) and age- and gender-matched controls, using high performance liquid chromatography (HPLC) applying UV and fluorescent detectors. The developed method was optimized and validated according to the International Congress Harmonization Guidelines.

The precision and recovery values ranged between 1.60-4.36%, 81.61-101.09%, respectively. There were no differences between the groups with regard all the measured metabolites.

The application of the developed validated method enabled the simultaneous determination of certain metabolites of the KP of TRP metabolism, but no evident alterations were found in patients with CJD.

## 2. Bevezetés

A triptofán (TRP) a 20 aminosav egyike, mely fontos szerepet játszik a központi és perifériás idegrendszerben található, sejtek működéséért felelős fehérjék szintetizálásában [1]. A kinurenin (*kynurenine*, KYN) útvonal (*kynurenine pathway*, KP) a TRP átalakulásának fő útja, 95%-a ezen az útvonalon metabolizálódik [2]. Ennek fontossága abban rejlik, hogy a KYN útvonalon a neurodegeneratív–neuroprotektív folyamatokért felelős neuroaktív vegyületek keletkeznek, mint például a 3-hidroxi-kinurenin (3-OHK), kinolinsav (*quinolinic acid*, QUIN) és a kinurénsav (*kynurenic acid*, KYNA) [3]. A KYNA az egyik ismert endogén

kompetitív antagonistája az N-metil-D-aszpartát receptornak, ezáltal a jelátvitelt képes módosítani és így a glutamáterg neurotranszmisszió során a káros folyamatok gátlásával neuroprotektív hatást fejt ki [4].

A 3-OHK és a QUIN neurotoxikus molekulák, amelyek hatásukat részben szabadgyökök képződésén keresztül fejtik ki, ez több idegrendszeri megbetegedés hátterében állhat, mint például Alzheimer-kór, Parkinson-kór és a Huntington-kór [5]. Az említett neurodegeneratív betegségek esetén több alkalommal is leírtak különböző elváltozásokat a KP-ben, melyek főleg a neuroaktív KP metabolitok koncentrációjában, valamint ezen anyagok keletkezését befolyásoló enzimek aktivitásának megváltozásában nyilvánultak meg [3].

A Creutzfeldt-Jakob betegség (*Creutzfeldt-Jakob disease*, CJD) ugyan egy ritka neurodegeneratív kórkép, de gyors, progresszív lefolyása miatt különös figyelmet igényel, és a kórképben végzett biomarker kutatások egyre nagyobb jelentőséggel bírnak [6]. Jelen tanulmányban a triptofán egyes metabolitjainak vizsgálatát tűztük ki célul. A KP szinten történő koncentrációváltozásokat egy validált metodika segítségével végezzük, UV és fluoreszcens detektorral (FLD) ellátott nagyhatékonyságú folyadékkromatográffal.

### 3. Alkalmazott anyagok és módszerek

A standardsor készítéséhez az alábbi referenciavegyületeket alkalmaztuk: KYN, KYNA, TRP, 3-NLT, ez utóbbit, mint belső standardot (Sigma Aldrich, Saint Louis, MO, Amerikai Egyesült Államok). A humán liquor minták mérési tartománya a fent említett 4 vegyületre 100-3000 nM, 1-100 nM, 5000-50000 nM és 500-5000 nM, míg a szérum esetén 100-5000 nM, 1-100 nM, 100-5000 nM és 500-7500 nM (standardsorok). E tartományban mért görbe alatti területek értékei egyenesen arányosak az ismert koncentráció értékekkel. Így tehát, a mért vegyületek görbe alatti területeivel arányos koncentrációértékeket a fenti tartományokra kapott lineáris összefüggés segítségével számoljuk ki.

A metodika beállítása egy korábban már részletezett módszer szerint történt, kis változásokkal [7]. Röviden, a mobilfázis 0.2 M cink-acetát-dihidrát/acetonitril = 95/5 (v/v%) (Sigma Aldrich, Saint Louis, MO, Amerikai Egyesült Államok; Scharlau, Barcelona, Spanyolország) arányú elegye, melynek pH-ját 6,2-re állítottuk be ecetsavval (VWR International, Radnar, PA, Amerikai Egyesült Államok). A mobilfázis áramlási sebessége 1,2 ml·min<sup>-1</sup> volt. A liquor kicsapásához trifluorecetsavat (Sigma Aldrich, Saint Louis, MO, Amerikai Egyesült Államok), illetve a szérum kicsapásához perklórsavat (Scharlau, Barcelona, Spanyolország) alkalmaztunk. A mintákat kicsapás után 12000 rpm sebességgel centrifugáltuk, 4°C-on 10 percen keresztül (Hettich Mikro C200, Tuttlingen, Németország).

A mintákat FLD és UV/Vis detektorokkal felszerelt nagyhatékonyságú folyadékkromatográffal (Agilent Technologies, Santa Clara, CA, Amerikai Egyesült Államok) mértük. Az elválasztáshoz egy Security Guard előoszloppal ellátott fordított fázisú Kinetex C18 kromatográfiás oszlopot (Phenomenex Inc., Torrance, CA, Amerikai Egyesült Államok) használtunk. A beállított hullámhosszak UV detektor esetén a KYN és a 3-NLT mérésére 365 nm, illetve a fluoreszcens detektoron az excitációs hullámhosszak KYNA-ra valamint TRP-ra 344 és 254 nm voltak, az emissziós hullámhossz pedig 398 nm volt mindkét anyag esetében.

### 4. Kísérleti eredmények és kiértékelésük

#### 4.1. Metodika validálás

A validálás során meghatározott paraméterek eleget tesznek az ICH [8] által megfogalmazott biológiai mintákra vonatkozó követelményeknek. Ezek közé sorolható a

precizitás, érzékenység, szelektivitás, linearitás, meghatározási és kimutatási határ, illetve a visszanyerési tényező.

Először a validálás paramétereit határoztuk meg. Úgy a szérum, mind a liquor minták esetén is szükségszerű az alkalmazott metodika validálása. A kalibráló görbe linearitását a fent említett standardsorok méréséből kapott görbe alatti területek és az ismert koncentrációk közötti viszony adja meg. A méréstartományt lefedő koncentrációjú minták linearitását az  $R^2$  értékkel határoztuk meg ( $R^2 > 0,99$ , alkalmazott szoftver: R Development Core Team, 2002). Ugyanezzel az összefüggéssel az érzékenységet ( $S'$ ) is meghatározzuk, melyről pontos adatot a görbe meredeksége (deriváltja) nyújt.

1. Táblázat A mérési tartomány és az érzékenység

LIQUOR	KYN	KYNA	TRP	3-NLT
koncentráció tartomány, nM	100-3000	1-100	5000-50000	500-5000
$R^2$	0,9989	0,9985	0,9999	0,9991
$S'$	0,0127	4,7295	0,4242	4,6725
SZÉRUM	KYN	KYNA	TRP	3-NLT
koncentráció tartomány, nM	100-5000	1-100	100-5000	500-7500
$R^2$	0,9998	0,9917	0,9999	0,9999
$S'$	0,00405	1,2386	0,106	0,0022

A precíz működés igazolásához ugyanazon mintaoldat többszöri elemzésének megismétlése szükséges, végül pedig a tapasztalati szórással (*relative standard deviation*, RSD%) adjuk meg a 6-szor párhuzamosan mért natív minta (N) eredményeit. Továbbá szükséges a natív minta olyan oldatokkal való kicsapása, melyben az analitok is megtalálhatóak ismert koncentrációkban. Így az egyik oldat alacsony koncentrációban (S1), míg a másik oldat magasabb koncentrációkban (S2) tartalmazza az analitokat, és mindegyik oldat 3 párhuzamos mérésével határozzuk meg a visszanyerési tényezőt (*recovery factor*, RF%).

2. Táblázat A precizitás és visszanyerési tényező

LIQUOR	KYN	KYNA	TRP
N átlag, nM	52,07	4,01	1316,20
<b>Precizitás, RSD%</b>	3,87	4,36	1,60
S1 átlag, nM	424,49	4,37	422,59
Valós koncentráció, nM	500	5	500
<b>RF %</b>	84,90	93,06	84,52
S2 átlag, nM	861,84	19,50	914,65
Valós koncentráció, nM	1000	20	1000
<b>RF %</b>	86,18	97,52	91,46

SZÉRUM	KYN	KYNA	TRP
N átlag, nM	369,25	7,30	1605,46
<b>Precizitás, RSD%</b>	3,18	4,02	2,97
S1 átlag, nM	496	3,35	5479,32
Valós koncentráció, nM	500	4	6000
<b>RF %</b>	99,21	81,61	91,32
S2 átlag, nM	960,58	11,36	10108,60
Valós koncentráció, nM	2000	12	10000
<b>RF %</b>	96,06	94,69	101,09

A meghatározási határ (*limit of quantification*, LOQ) azt a legkisebb koncentrációt jelenti, mely még megfelelő precizitással és helyességgel meghatározható, míg a kimutatási határ (*limit of detection*, LOD) az alapzaj háromszorosának megfelelő magasságú jelet adó koncentráció. A fenti két paramétert a következő képletekkel határoztuk meg ( $\sigma$ : a vakminta szórása,  $S'$ : érzékenység)

$$\text{LOD} = 3.3 \sigma/S', \text{ illetve } \text{LOQ} = 10 \sigma/S'$$

3. Táblázat A meghatározási és a kimutatási határ értékei

		KYN	KYNA	TRP
LIQUOR	LOD (nM)	27,61	1,28	430
	LOQ (nM)	91,08	4,27	1440
SZÉRUM	LOD (nM)	160	3,21	47,8
	LOQ (nM)	484	9,73	145

1.2. Triptofánmetabolitok mérése

Az adatok feldolgozására szolgáló minták között 5 CJD, illetve 5 kontroll (CO) szérum és liquor minta található. A CJD és a CO betegek összehasonlítása a TRP metabolitjainak

koncentráció szintjén történt a 46/2014. sz. intézményi etikai engedély birtokában, az adatokat az 5. táblázat mutatja.

5. Táblázat A vizsgálat triptofánmetabolitok átlagos koncentráció szintjei

Vizsgált metabolitok		KYN	KYNA	TRP
		c (nM)	c (nM)	c (nM)
Liquor	CJD-csoport	35,95	1,48	1816,66
	CO-csoport	<LOD	2,88	1919,26
Szérum	CJD-csoport	2093,02	35,97	54646,87
	CO-csoport	1569,40	14,86	49923,38

A KP során keletkező TRP, KYN, KYNA és a koncentráció szinteket mértük, amely mérés során nem észleltünk szignifikáns változásokat, t-tesztek alkalmazásával az alábbi  $p$ -értékeket kaptuk: liquor minták esetén  $p_{KYN,LI} = 0,7558$ ;  $p_{KYNA,LI} = 0,3516$ ;  $p_{TRP,LI} = 0,9589$ . Szérum esetén  $p_{KYN,SE} = 0,919$ ;  $p_{KYNA,SE} = 0,6996$ ;  $p_{TRP,SE} = 0,6659$ .

### Következtetések

A kísérletek során sikerült validálni az alkalmazott metodikákat, melyek a humán liquor és szérum mérések kiértékelésére szolgáltak. A validálás során kapott értékek a metodikánk robusztusságára utalnak. A precizitás egyik esetben sem haladta meg az  $RSD \leq 4.5\%$  értéket, míg a visszanyerési tényezők 81%-102% közöttiek voltak. A TRP metabolizmusának KP-t tanulmányozva, a kis elemszámból adódó korlátok mellett, nem találtunk szignifikáns különbséget a vizsgált metabolitok koncentrációjában CJD-s egyének értékeit a kontroll csoport értékeivel összehasonlítva, mely eredmények ezen útvonal CJD-ben való érintettségét nem támogatják.

### Köszönetnyilvánítás

A kutatás a GINOP-2.3.2-15-2016-00034 és EFOP-3.6.1-16-2016-00008 pályázatokból valósult meg. Dr. Zádori Dénest a Magyar Tudományos Akadémia Bolyai János Kutatási Ösztöndíja támogatja.

### Irodalomjegyzék

- [1] K. Sarkhosh, E.E. Tredget, Y. Li, R.T.Kilani, H. Uludag, A. Ghahary, Wound Repair Regen., 11 (2003) 337.
- [2] H. Wolf, Scand. J. Clin. Lab. Invest. Suppl.,136 (1974) 1.
- [3] R. Schwarcz, J.P. Bruno, P.J. Muchowski, H.Q. Wu, Nat. Rev. Neurosci. 13 (2012) 465.
- [4] L. Vécsei, L. Szalárdy, F. Fülöp, J. Toldi, Nat. Rev. Drug. Disc. 12 (2012) 64.
- [5] G.J. Guillemin, FEBS J., 279 (2012) 1356.
- [6] G.G. Kovacs, U. Andreasson, V. Liman, G. Regelsberger, M.I. Lutz, K. Danics, E. Keller, H. Zetterberg, K. Blennow, E. J. Neurol, (2017) 1.
- [7] C. Herve', P.Beyne, H. Jamault, E. Delacoux, J. Chromatogr. B. Biomed. App. 675 (1996) 157.
- [8] ICH harmonised tripartite guideline, validation of analytical procedures. Fed Regist., 1995 (60) 11260.



BUCHWALD-HARTWIG CROSS COUPLING OF 13 $\alpha$ -ESTRONEDávid Szemerédi<sup>1</sup>, Ildikó Bacsa<sup>1</sup>, János Wölfling<sup>1</sup>, Gyula Schneider<sup>1</sup>, Erzsébet Mernyák<sup>1</sup>

<sup>1</sup>Department of Organic Chemistry, University of Szeged, Dóm tér 8, H-6720, Szeged, Hungary  
e-mail: bobbe@chem.u-szeged.hu

**Abstract**

Use of catalysts and alternatives of traditional heating are important part of environmentally-friendly processes and sustainable chemistry. Here we aimed to develop a suitable method for Buchwald-Hartwig amination of 13 $\alpha$ -estrone by microwave assisted synthesis.

**Introduction**

Transition-metal-catalyzed cross-coupling reactions (CUAAC<sup>1</sup>, Sonogashira<sup>2</sup>) were recently published on hormonally inactive 13 $\alpha$ -estrane core. Microwave assisted Buchwald-Hartwig reactions are described on small compounds<sup>3</sup>, but there is no example in the literature for larger molecules.

**Experimental**

Reactions were carried out in CEM Discover microwave reactor. Crude mixtures were purified and novel compounds were characterized by <sup>1</sup>H and <sup>13</sup>C NMR spectroscopy measurements.

**Results and discussion**

First we optimized the reaction conditions: solvent, applied base, temperature and palladium source. With the optimal conditions in hand we carried out coupling reactions of different amines (Figure 1.).

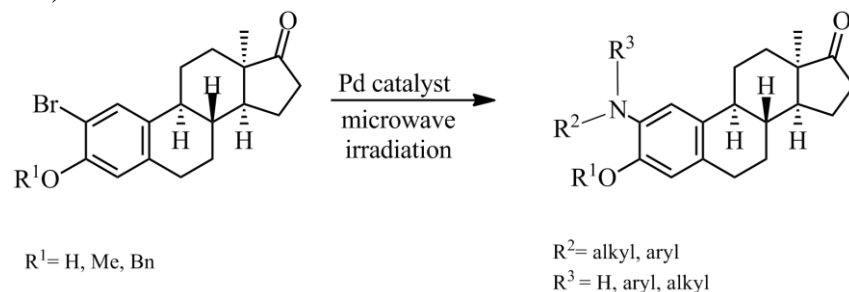


Figure 1. General method for Buchwald-Hartwig cross-coupling of 13 $\alpha$ -estrone

**Conclusion**

Novel microwave assisted method was developed for Buchwald-Hartwig coupling of steroidal compound and successfully expanded to a range of substituted amines.

**Acknowledgements**

The authors are grateful for financial support from the Hungarian Scientific Research Fund (OTKA K113150). This project has been supported by the GINOP 2.3.2-15-2016-00038 grant of the Hungarian National Research, Development and Innovation Office (NKFIH).

**References**

[1] Szabó J., Bacsa I., Wölfling J., Schneider G., Zupkó I., Varga M., Herman B.E., Kalmár L., Szécsi M., Mernyák E. Journal of Enzyme Inhibition and Medicinal Chemistry 2016, 31, 574–579.

- [2] Bacsa I., Jójárt R., Wölfling J., Schneider G., Herman B.E., Szécsi M., Mernyák E. *Beilstein Journal of Organic Chemistry*, 2017, 13, 1303-1309.
- [3] Tundel R. E., Anderson K. W., Stephen L. Buchwald S. L. *J. Org. Chem.* 2006, 71, 430–433.

**PRELIMINARY STUDY OF OPTIMAL EXTRACTION OF BIOLOGICALLY  
ACTIVE COMPOUNDS FROM SEA BUCKTHORN  
(HIPPOPHAE RHAMNOIDES L.) POMACE**

**Diána Furulyás<sup>1</sup>, Rentsendavaa Chagnaadorj<sup>1</sup>, Fanni Kis<sup>1</sup>, Katalin Bíró<sup>1</sup>,  
Mónika Stéger-Máté<sup>1</sup>, Éva Stefanovits-Bányai<sup>2</sup>**

<sup>1</sup>Department of Food Preservation, Szent István University, H-1118 Budapest, Villányi street  
29-43., Hungary

<sup>2</sup>Department of Applied Chemistry, Szent István University, H-1118 Budapest, Villányi street  
29-43., Hungary

e-mail: furulyas.diana@etk.szie.hu

**Abstract**

The processing of fruits results in high amounts of waste materials such as peels and seeds which is a critical subject in every industry. The aim of this study is to explore the best combination of drying and extraction method, to achieve the highest antioxidant content in sea buckthorn pomace (SBP), which appears as a by-product when making use of the berries. In the frame of our research the optimal drying conditions were previously tested, relying on the results vacuum drying was executed at 40 and 60 °C furthermore SBP was dried also by atmospheric dryer at 60 and 80°C. Drying curve was also determined. When extracting the antioxidant compounds, 20 and 40 % ethanol and acetone were used as solvents, applied in 1:30 proportion. Amount of total polyphenol content and antioxidant capacity (FRAP) were determined by spectrophotometry methods. Besides regarding amount of valuable components economical aspects must be considered for choosing the optimal drying technology. In case of vacuum drying duration was two times longer than in case of atmospheric technologies. The results show that the highest antioxidant capacity (4958.45 mg AAE/100g dm) was registered using 40% acetone extracted from the pomace, dried at 80°C. Further examination could reveal whether the extracted antioxidant content of the SBP, a by-product of fruit processing technologies, could be used natural food additives as bio-preservatives after appropriate clarification processes.

**Introduction**

Sea buckthorn (SB) (*Hippophae rhamnoides*) belongs to the *Elaeagnaceae* family [1]. Origin of the plant name is from Greek words: “hippos phao” means brilliant horse. Every part of SB were used in Europe and Central Asia, the fruits, leaves, bark and roots were processed to a food, dietary supplement, feed, firewood, fuel, or even to decorative elements [2]. This plant has a rich history in natural medicine [3], many of the substances that found in sea buckthorn are known to have gained increasing attention in recent years due to their high content of bioactive compounds with health benefits [4]. The SB fruits and seeds are good sources of valuable nutrients: carotenoids, tocopherols, phytosterols, phenolic acids, flavonoids, and proanthocyanidins, demonstrating various useful effects: antioxidant, antimicrobial, anti-inflammatory [5-10]. Processing of SB fruit produces high amount of pomace, which are utilized rather inefficiently or discarded as a waste, so considerable amounts of nutrients are lost [11]. The extraction schemes of pomace were developed and many option of utilization of SBP recently become research topic [12-14]. There is a growing interest in the utilization of antioxidant-rich plant extracts as dietary food supplements [15]. The aim of this study was to

explore the best combination of drying and extraction methods, to achieve the highest antioxidant content in sea buckthorn pomace, which appears as a by-product when making use of the berry and obtain phenolics preparation from sea buckthorn pomace.

### Experimental

The “Ascola” SB berries were collected from agricultural plots of Hungary. Chemicals were purchased by Sigma-Aldrich Chemie Ltd. All reagents used were of analytical grade.

SB were destemmed, and then heated to 80°C, to inactivate enzymes. The material was squeezed, resulting in juice and pomace. Drying methods were the next step by Memmert V 200 vacuum dryer (Mettler GmbH, Schwabach, Germany) at 40°C and 60°C, also by atmospheric dryer (LMIM, Esztergom, Hungary) at 60°C and 80°C. In each case 2 kg of SBP was dried in single layer on three perforated trays until moisture content became lesser than 10%. Water content was determined per every 30 minutes by drying until constant weight at 121 °C using a MAC-50 moisture analyzer (Radwag Waagen GMBH, Hilden, Germany). After this step the pomace was grinded. All samples were sealed in bag, and stored in a freezer at -20 °C until ready for extraction, which was performed at room temperature, using two different solvents: acetone and ethanol at different concentrations 20 V/V % and 40 V/V% (ratio between pomace and solvent was 1:30 proportions). After half-an-hour of extraction, supersonic bath was used for another 30 minutes, to intensify the process. The tube is centrifuged at 2500g for 10 min to the phases separate and the supernatant is recovered. Samples were further analyzed using two methods:

- The antioxidant capacity of samples was estimated according to the procedure described by Benzie and Strain [16]. Ferric reducing antioxidant power assay (FRAP) was defined in ascorbic acid equivalent (mg ascorbic acid equivalent/ 100 g dm).
- Total polyphenol content (TPC) of the einkorn extract was determined according to the Folin–Ciocalteu spectrophotometric method described by Singleton and Rossi [17]. Results were specified in mg gallic acid equivalent/ 100 g dm.

Results were calculated, statistical evaluations were performed using Microsoft Excel. Independent samples t-test were used for the statistical analyses by Student t-test at 95% confidence.

### Results and discussion

Fig. 1 shows the drying curves obtained for SBP dried.

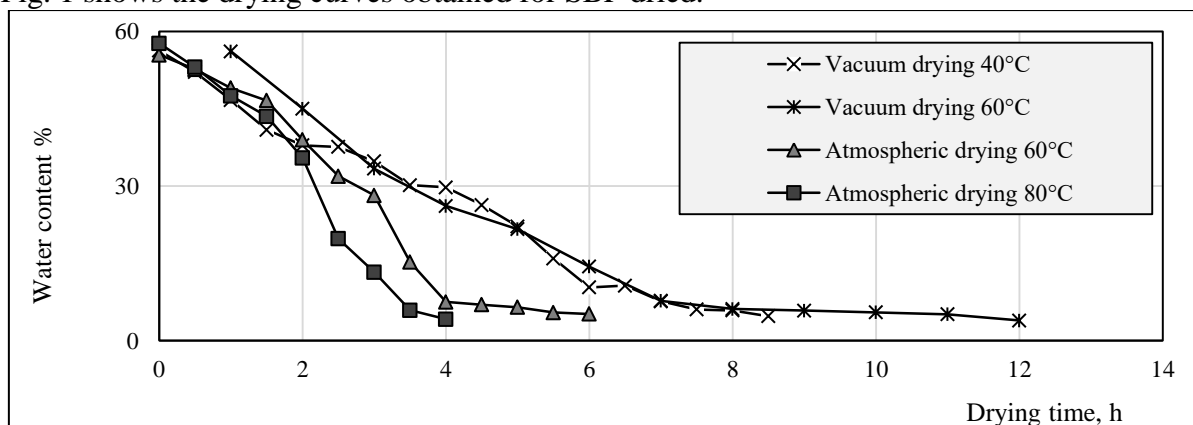


Figure 1. Drying curves

Drying mode (atmospheric or vacuum) and temperature affected dehydration speed. Initial wet content was 57.68% and time needed to reach final wet content (7-10%) was different depending on its drying method and temperature.

In case of atmospheric drying at 60°C and 80°C would require a shorter drying period to reach a moisture content under 10%. On the contrary, when vacuum drying was performed, wet content decreased slowly. The vacuum drying mode at 40°C was the longest process requiring 12 hour instead of atmospheric drying method at 80 °C dried in 4 hour (Fig. 1).

High variation was also observed for the antioxidant activity among the samples (Fig. 2). FRAP, expressed in mgAAE/100 g dm, ranged from 1156.28 to 4958.45 for dried samples.

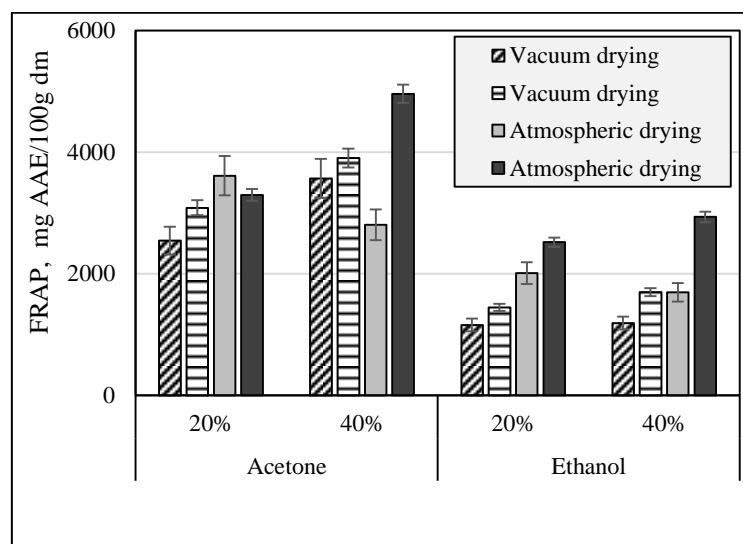


Figure 2. Average values of antioxidant capacities, evaluated using the method relying on Ferric Reducing Ability of Plasma, mg ascorbic acid equivalent/ 100g dm

FRAP value of the atmospheric dried samples at 80°C was the highest among the different drying methods.

Pomace dried at 80 °C showed significantly higher ( $p>0.05$ ) outcome, consequently, lower drying temperature affected the antioxidant compounds in a positive way. Regarding the solvents applied, acetone extracted the analyzed components with the best results. Concentration of ethanol solvent had no significant effect on FRAP value but using different concentration of acetone had significant differences of antioxidant activity yield.

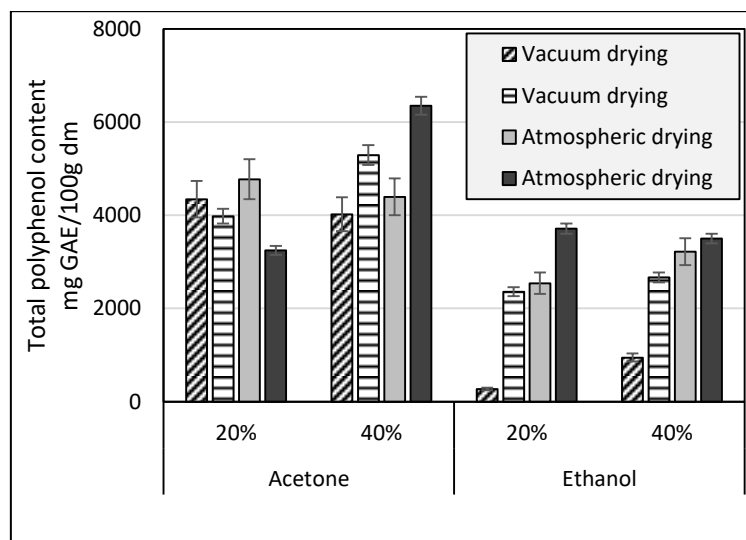


Figure 3. Total polyphenol content (TPC) average results, mg gallic acid equivalent/100g dm

The differences of total polyphenol content of SBP extracts are shown Figure 3. The TPC values had a range from 272.28 to 6351.24 mg GAE/100g dm. The highest value was reached by the sample which was dried at 80°C, extracted with 40 V/V % acetone. This result corresponds with the conclusion of the FRAP method.

The results also demonstrate the high polyphenol content of sea buckthorn pomace. The polyphenols are greatly diverse. The changes of polyphenols were influenced by many factors during food processing such as temperature, duration, presence of other components, etc. These effects can be resulted in degradation, transformation or enzymatic browning. Actual polyphenol content depends on the result of these effects [18].

When the samples were drying in atmospheric dryer the presence oxygen increase activity of polyphenol oxidase which play role keys in enzymatic browning because of product of Maillard reaction increasing the polyphenols content was higher at high temperature levels. Instead of during vacuum drying lack of oxygen inhibit these enzymes.

### Conclusion

The aim of this research was to set up an environmentally friendly technological process to obtain high-value biologically active extracts from sea buckthorn by-products, thereby helping to reduce waste from the juice industry.

In present study, many pomace extracts was prepared by different drying mode and extraction solvents to find the best method to create pomace extract with high amount of antioxidant components.

Phenolic compounds and antioxidant capacity of SBP were affected by drying temperature (40-60-80 °C) and pressure (atmospheric and vacuum drying). Highest antioxidant capacity and highest amount of phenolic compounds were observed after atmospheric drying at 80 °C, using 40 V/V% acetone extraction solvent. Our results indicated that further experiments are needed for attempt more drying mode and extraction solvent to extract antioxidant components from the pomace and more research are needed for further exploitation on the production of food additives or supplements with high nutritional value.

## **References**

- [1] J. Xing, B. Yang, Y. Dong, B. Wang, J. Wang, H.P. Kallio, *Fitoterapia*, 73 (2002) 644-650
- [2] P. Malinowska, B. Olas, *Kosmos*, 2 (2016) 285-292
- [3] A. Niesterek, H. Lewandowska, Z. Golub, R. Świsłocka, W. Lewandowski, *Kosmos*, 4 (2013) 571-581
- [4] T. S. C. Li, L.C.H. (1998) Wang, In G. Mazza (Ed.), *Functional foods, biochemical and processing aspects* (pp. 329–356). Lancaster, PA: Technomic Publishing Company Inc
- [5] L.M. Bal, V. Meda, S. Satya, *Food Research International*, 44 (2011) 1718-1727.
- [6] Yang, B., & Kallio, H. (2002). Composition and physiological effects of sea buckthorn (*Hippophae*) lipids. *Trends in Food Science & Technology*, 13 ,160-167.
- [7] T. Michel, E. Destandau, G. Le Floch, M.E. Lucchesi, C. Elfakir, *Food Chemistry*, 131 (2012) 754-760
- [8] C. Chen, X.-M. Xu, Y. Chen, M.-Y. Yu, F.-Y. Wen, H. Zhang, *Food Chemistry*, 141 (2013) 1573-1579
- [9] J. Fan, X. Ding, W. , J. Fan, X. Ding, W. Gu, *Food Chemistry*, 102 (2007) 168-177
- [10] Y.-J. Xu, M. Kaur, R.S. Dhillon, P.S. Tappia, N.S. Dhalla, *Journal of Functional Foods*, 3 (2011) 2-12
- [11] C.M. Galanakis, *Trends in Food Science & Technology*, 26 (2012) 68-87
- [12] P. Górnaś, I. Pugajeva, D. Segliņa, *European Food Research and Technology*, 239 (2014) 519-524
- [13] P. Górnaś, A. Soliven, D. Segliņa, *European Journal of Lipid Science and Technology*, 117 (2015) 773-777
- [14] R. Yakimishen, S. Cenkowski, W.E. Muir, *Applied Engineering in Agriculture*, 21 (2005) 1047-1055
- [15] C. Eccleston, Y. Baoru, R. Tahvonen, H. Kallio, G.H. Rimbach, A.M. Miniñane, *The Journal of nutritional biochemistry*, 13(6), (2002) 346-354.
- [16] I.I.F. Benzie, J.J. Strain, *Annalitical Biochemistry*, 239. (1966) 70-76
- [17] V.L. Singleton, J.A. Rossi, *American journal of Enology and Viticulture*, 16(3) (1965) 144-158.
- [18] L. Manzocco, S. Calligaris, D. Mastrocola, M.C. Vicoli, C.R. Lerici, *Trends Food Science Technology*, 39 (2001) 53-59.



## A SIMULATION STUDY TO COMPARE THE POWER OF NORMALITY TESTS

**Péter Erdélyi, Róbert Rajkó**

*Institute of Process Engineering, University of Szeged, H-6725 Szeged, Moszkvai krt. 5-7.,  
Hungary  
e-mail: erd\_pet@fastmail.jp*

### **Abstract**

A common assumption of many statistical procedures during data analysis is that the data is normally distributed. Several statistical tests have been developed for the determination of the validity of this assumption. Now, the question is: which is the most powerful? We performed an extensive Monte Carlo simulation study to answer this question. We found that compared to six other tests, the Shapiro–Wilk test performs the best under most conditions.

### **Introduction**

One of the most frequently made assumptions during data analysis (for example when performing a t-test, an F-test, an analysis of variance, or tests for the regression coefficients in a regression analysis) is that the data is normally distributed. [1]

There are graphical methods to determine the normality of the data (Q-Q plots, etc., which we will not discuss here since these are less reliable, subjective), and there are also dozens of more objective, formal statistical tests. The mere fact, that there are so many alternatives suggests that this is a hard problem without an exact, perfect solution, and also, it raises the obvious question: which one should we use, which is the best test?

The tests we have studied are based on frequentist inference: they are hypothesis tests, and the data set is tested against the null hypothesis that it is normally distributed. Therefore, it can commit either of the well-known two types of error: it incorrectly rejects the null hypothesis (type I error, “false positive”), or incorrectly fails to reject it (type II error, “false negative”).

If we generate a large number of normally distributed samples, carry out a normality test on each, then count the cases when the test incorrectly rejects the null at a given significance level ( $\alpha$ ) we can calculate the proportion of type I errors. This value is called the *size* of the test. The significance level chosen by the user is the upper bound of the size, if the test works correctly.

The *power* of a test ( $1-\beta$ ) is the complement of the type II error rate ( $\beta$ ), which can be determined similarly: by generating samples of non-normal distributions, and count the cases of the test failing to reject the null hypothesis of normality.

### **Experimental**

We performed an extensive Monte Carlo simulation study in the R statistical programming environment.[2] The tests compared were the Shapiro–Wilk test (SW for short in the following), provided by the R “stats” package, which is part of the base distribution, so it can be considered as the default normality test in R, the Jarque–Bera test (JB) from the “moments” package, and five more tests from the “nortest” package: the Shapiro–Francia (SF), Anderson–Darling (AD), Cramér–von Mises (CM) Lilliefors (LI), and Pearson's  $X^2$  (PE) tests.

We generated samples from the standard normal distribution and 17 alternative (non-normal) distributions which we divided to two groups: the symmetricals (i.e. with a skewness of zero,

like the normal distribution), and the asymmetricals (with nonzero skewness) to see if any tests perform better against one type of alternative distribution than the other.

**Symmetric distributions**

- Laplace ( $\mu=0, \sigma=0.5$ )
- Logistic ( $\mu=0, s=0.5$ )
- Student's t ( $\nu=1$ ), ( $\nu=20$ )
- Beta ( $\alpha=0.5, \beta=0.5$ ), ( $\alpha=2, \beta=2$ )
- Uniform ( $a=0, b=1$ )
- Binomial ( $n=20, p=0.5$ )

**Asymmetric distributions**

- $X^2$  ( $k=1$ ), ( $k=20$ )
- Exponential ( $\lambda=0.5$ ), ( $\lambda=1$ )
- Poisson ( $\lambda=10$ )
- Log-normal ( $\mu=0, \sigma=1$ ), ( $\mu=0, \sigma=0.1$ )
- Weibull ( $\lambda=0.5, k=1$ ), ( $\lambda=10, k=1$ )

The sample sizes were: 10, 15, 20, 25, 30, 35, 50, 100, 200, 500, the number of samples were 1.000.000 each of the ten sizes. We then evaluated all seven tests on every sample at three significance levels: 0.01, 0.05, 0.1, and calculated their power and size as explained in the introduction.

**Results and discussion**

Considering the large amount of generated data, we summarize the results on Figures 1–3. The best performing test is uniformly the Shapiro–Wilk test, closely followed by the Anderson–Darling, the Shapiro–Francia and the Cramér–von Mises test.

As seen on Figure 1, The Shapiro–Wilk test holds the set significance level almost perfectly. The Shapiro–Francia test exceeds it slightly, but that improves with the increasing sample size. The other tests' type I error rate stays under the required level, which is not optimal, but not erroneous. The behavior of the Pearson test is almost pathological, for reason unknown.

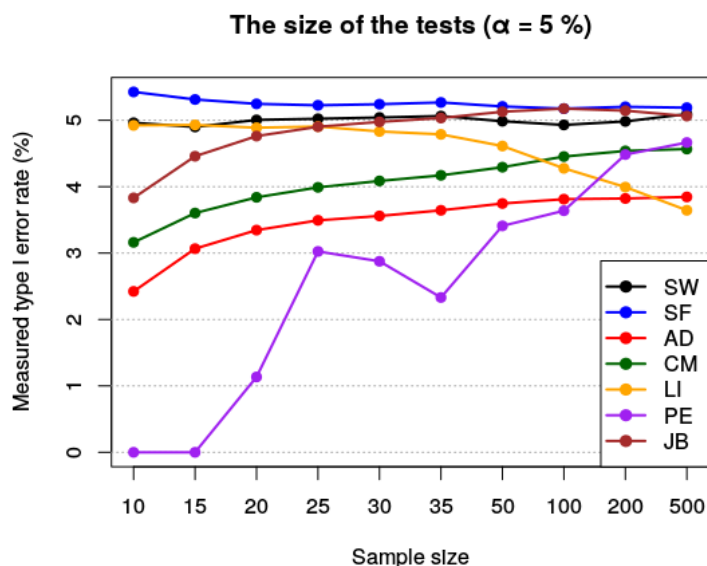


**Figure 1. The size of normality tests as a function of sample size at a significance level of 5%. (The horizontal axis is not to scale.)**

As expected, the power of every test is increasing with the sample size – there’s more information to base the decision on (Figure 2). The standard deviation is generally high, because we are averaging the results for several alternative distributions, some of them are easy to detect (e.g. Student’s t with 1 degree of freedom), and also some harder cases (e.g. Student’s t with 20 degrees of freedom). The interesting, upside down “U” shape of the SD vs.

sample size curves is due to the fact that the power at low sample sizes is usually close to its lower bound (0%), at high sample sizes it's close to its upper bound (100%), and there's simply less room for the value to vary.

If we look at the symmetrical and asymmetrical distributions separately (Figure 3), the trend is basically the same: the SW, AD, SF and CM tests have the highest power. In the asymmetrical cases the average power is higher, and also the difference between the tests is smaller, because the skewed distributions are easier to detect, they are more different from the normal distribution.

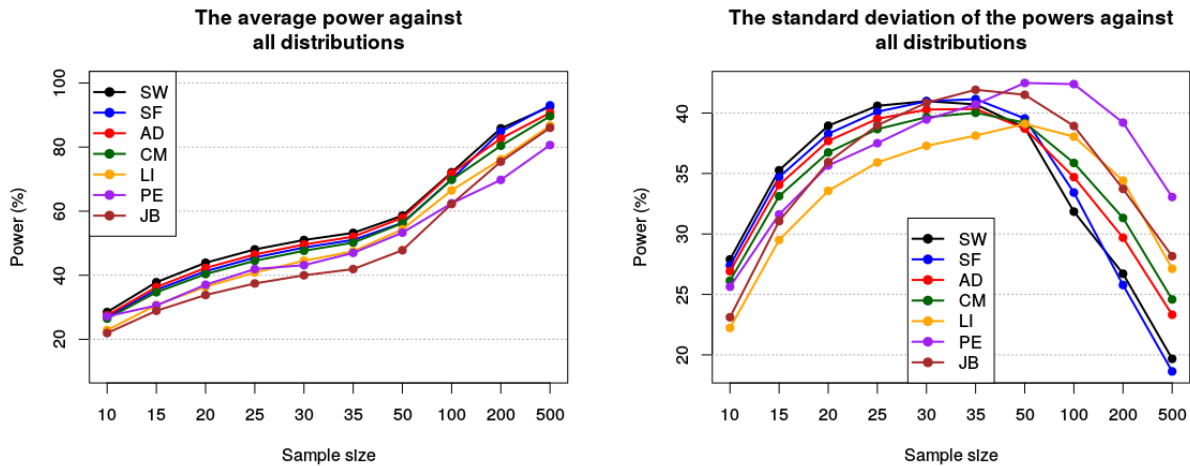
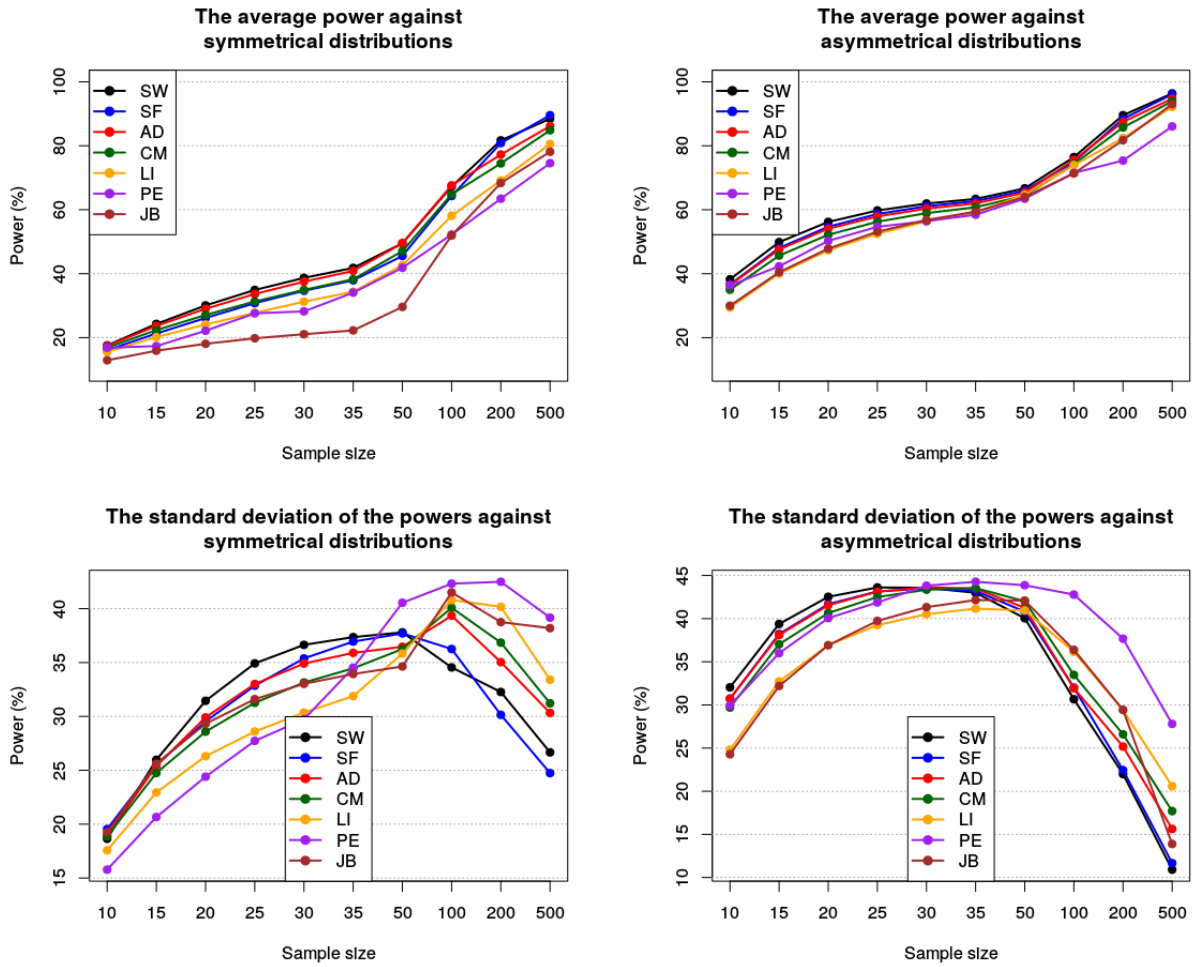


Figure 2. The average and the standard deviation of the power of normality tests against all studied distributions in the function of sample size. (The horizontal axes are not to scale.)



**Figure 3. Comparison of the average and the standard deviation of the power of normality tests against symmetric and asymmetric distributions. (The horizontal axes are not to scale.)**

### Conclusion

We compared the power of seven normality tests available in R statistical computing environment, and found that the Shapiro–Wilk test performs the best against a large variety of alternative distributions both at small and large sample sizes. This test is part of the base R distribution as a de facto default, and it seems the developers have chosen wisely, there is no need to install any other packages.

### References

- [1] Thode, Henry C.: Testing for normality. Vol. 164. CRC press, 2002. p. 1.
- [2] R Core Team, R: “A Language and Environment for Statistical Computing.” R, Foundation for Statistical Computing, Vienna, Austria, 2015. <https://www.R-project.org>

## HŐMÉRSÉKLET HATÁSA A RÉZ-ALAPÚ FOTOKATALIZÁTOROK ELŐÁLLÍTÁSÁBAN ÉS HŐKEZELÉSÉBEN

Fodor Szilvia<sup>1,2</sup>, Mucsi Kata<sup>1</sup>, Pap Zsolt<sup>2,3</sup>, Hernádi Klára<sup>1</sup>, Lucian Baia<sup>3,4</sup>

1. Department of Applied and Environmental Chemistry, University of Szeged, H-6720

Szeged, Rerrich Béla tér 1, Hungary

2. Institute of Environmental Science and Technology, University of Szeged, H-6720 Szeged,

Tisza Lajos körút 103, Hungary

3. Nanostructured Materials and Bio-Nano-Interfaces Center, Interdisciplinary Research  
Institute on Bio-Nano-Sciences, Babes,-Bolyai University, 400271 Cluj-Napoca, Romania

4. Faculty of Physics, Babeş-Bolyai University, RO-400084, Mihail Kogălniceanu 1, Cluj-  
Napoca, Romania

e-mail: fod\_szilvia@chem.u-szeged.hu

### Abstract

Nanotechnology is a highly investigated research area, which includes photocatalysis applicable for water purification. This research area offers possible solutions to remove dangerous pollutants, such as pharmaceutical residues, or to create self-cleaning systems as well. The current issue in this scientific field is the efficient utilization of the visible light spectrum of the sunlight. Our main goal was to obtain copper-based photocatalysts, such as  $\text{Cu}_x\text{O}$  and  $\text{Cu}_x\text{S}$  (applying hydrothermal crystallization). Calcination was further used at different temperatures (400 - 600 °C) to increase the crystallinity and to induce changes in the morphology and structure of the materials. The samples were examined by X-ray diffraction for detection of crystal structure and Scanning electron microscopy for determination of the morphological properties. These materials can be used as photocatalysts in visible light.

### Bevezetés

A nanotechnológia területének rohamos fejlődését a benne rejlő új lehetőségek adják, mint a heterogén fotokatalízis, amely lehetőséget nyújthat a félvezetők víz- és levegőtisztításban való alkalmazásában.

Az itt végbemenő folyamat során elengedhetetlen egy félvezető, amelynek a megfelelő hullámhosszon történő megvilágításával, kialakul egy elektron-lyuk páros, hiszen a gerjesztés során egy elektron a vegyértéksávból a vezetési sávba jut fel, maga után hagyva egy pozitív töltésű hibahelyet. A keletkezett elektron-lyuk pár hasznosulhat redox folyamatokban, amennyiben jelen van a rendszerben egy elektrondonor és egy elektron akceptor vegyület [1]. A reakció során a szerves szennyező elbomolhat oxidációval a katalizátor felületén, vagy a képződött reaktív gyökökkel.

A felhasználhatóságban mutatott számos pozitív tulajdonságának köszönhetően napjaink legkutatottabb és leggyakrabban alkalmazott félvezetője a heterogén fotokatalízisben a titán-dioxid. A  $\text{TiO}_2$  jelenlétében végbemenő fotokatalitikus folyamatok nemcsak szerves szennyezők oxidációjára használhatók fel, hanem oxigénmentes körülmények között lehetőség nyílik vizes oldatokból történő hidrogén gáz fejlesztésére is. A fotokatalitikus hidrogénfejlesztés során a rekombinációs idő meghosszabbítására több módszert vizsgáltak, amelyek közül a kompozitkészítés az egyik legígéretesebb eredményekkel kecsegtető alternatíva. A félvezetőket kompozitokba viszik más félvezető oxidokkal ( $\text{ZnO}$ ,  $\text{WO}_3$ ) [2, 3], szén nanoanyagokkal [4] és számos kutatás folyik a nemesfém nanorészecskékkel való

hatékonyság növelési kísérletekről is. Ez utóbbi esetén a vezetési sávba feljutó elektron a katalizátor felületére leválasztott nemesfémre kerül át, ahol csapdázódik, majd hasznosul és így megnöveli az elektron-lyuk pár élettartamát a rekombináció visszaszorításával.

Munkánk során ennek a folyamatnak a fejlesztését tűztük ki célul, hiszen egy aktuális probléma a hatékonyság azon módon történő feljavítása, miszerint a napfény nem csak UV tartományát szeretnék felhasználni ezeken a folyamatokban. Erre a fejlesztésre lehetőségünk lehet a  $\text{TiO}_2$  lecserélésével vagy kombinálásával egy olyan félvezetőre, mely a látható fény tartományban aktív. Ezt a megoldást szeretnénk megvalósítani munkánk során, mégpedig úgy, hogy a  $\text{TiO}_2$  helyett különböző Cu-alapú vegyületeket próbálunk alkalmazni. A réz-alapú fotokatalizátorok optikai tulajdonságainak (kis tiltottsáv-szélesség) köszönhetően, a gerjesztési katalizátorok gerjesztési küszöbe látható fény tartományba esik, vagy kompozitok esetén eltolódhat ebbe az irányába [5].

Ezeknek a megvalósítását szem előtt tartva célunk volt  $\text{Cu}_x\text{O}$  és  $\text{Cu}_x\text{S}$  vegyületek előállítása, figyelemmel kísérve az anyagszerkezeti és morfológiai tulajdonságok befolyásolhatóságát. Ezeket a tulajdonságokat első megközelítésben a hőmérséklet befolyásolásával vizsgáltuk.

## Kísérleti rész

### 1. $\text{Cu}_x\text{S}$ katalizátorok előállítása

A szintézis első lépésében 0,5 g  $\text{CuCl}_2 \cdot 2 \text{H}_2\text{O}$ , 0,4 g  $\text{CH}_4\text{N}_2\text{S}$  és 0,25 g PVP kimérését követően ezeket 40 mL etanolban, 30 perc folyamatos kevertetés mellett homogenizáljuk, majd autoklávban 6 órán keresztül hidrotermálisan kezeljük. A szakirodalmi adatokból kiindulva az előállítást több hőmérsékleten is elvégeztük (120 °C, 140 °C, 160 °C és 180 °C) és a továbbiakban vizsgáljuk a hőmérséklet befolyását az előállított minták kristályszerkezetére tekintve. Az előállítást követően háromszor vízzel, végül pedig etanollal mossuk, 10 perces centrifugálásos ciklusokban (4000 fordulat·perc<sup>-1</sup>), majd szárítószekrényben szárítjuk.

### 2. $\text{Cu}_x\text{O}$ katalizátorok előállítása

A szintézis első lépésében 60 mL (0,03 M) prekursor oldatban ( $\text{Cu}(\text{CH}_3\text{COO})_2$  vagy  $\text{CuCl}_2$ ) megfelelő mennyiségű etilén-diamint oldunk fel (1,5 g vagy 3 g) a reakció edényben, majd 60 °C-ra melegítjük fel és 10 percig várunk, folyamatos kevertetés mellett. Ez után 10 mL (3 M) NaOH oldatot csepegtetünk lassan az edénybe, majd innen számolva 8 perc elteltével 30 mL (0,33 M) glükóz oldatot csepegtetünk szintén lassan a reakcióhoz és 15 percig hagyjuk végbemenni a reakciót, tartva a 60 °C-os hőmérsékletet és a kevertetést. Az előállítást követően háromszor vízzel, végül pedig acetonnal mossuk, 10 perces centrifugálásos ciklusokban (4000 fordulat·perc<sup>-1</sup>), majd szárítószekrényben szárítjuk.



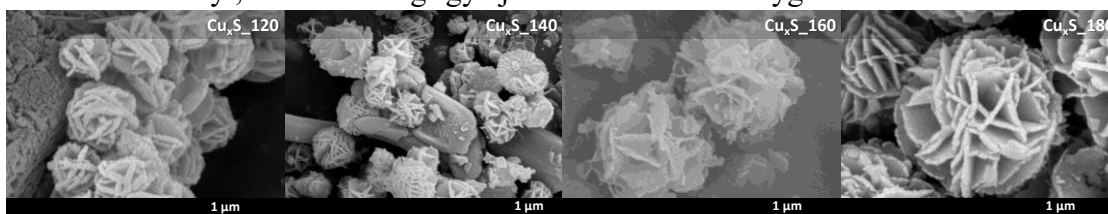
1. táblázat: A  $\text{Cu}_x\text{O}$  vegyületek előállításának kísérleti körülményei

$\text{Cu}_2\text{O}_1$	$\text{Cu}_2\text{O}_2$	$\text{Cu}_2\text{O}_3$
60 mL $\text{Cu}(\text{Ac})_2$ (0,03 M)	60 mL $\text{Cu}(\text{Ac})_2$ (0,03 M)	60 mL $\text{CuCl}_2$ (0,03 M)
1,5 g EDTA	3 g EDTA	1,5 g EDTA
10 mL NaOH (3 M)	10 mL NaOH (3 M)	10 mL NaOH (3 M)
30 mL glükóz (0,33 M)	30 mL glükóz (0,33 M)	30 mL glükóz (0,33 M)

## Eredmények

### 1. Hőmérséklet hatása az előállítási módszerek során:

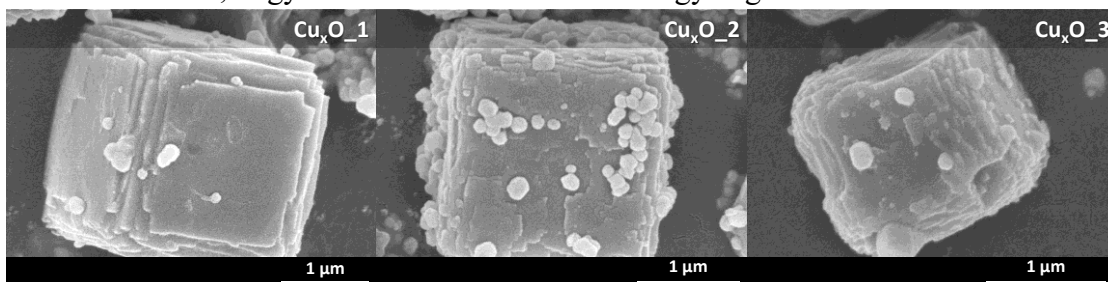
Az előállított félvezetőket elsőként pásztázó elektronmikroszkópiás módszerrel (SEM) vizsgáltuk, hogy felderítsük az előállítási módszer alakselektivitási eredményességét és az elért mérettartományt, valamint megfigyeljük a kialakult kristálygeometriákat.



1. ábra: Az előállított  $\text{Cu}_x\text{S}$  félvezetőkről készült SEM felvételek

Ahogy azt az 1. ábrán megfigyelhetjük a  $\text{Cu}_x\text{S}$  vegyületek előállítása során végzett hőmérséklet módosítás hatással volt a kapott termék morfológiai tulajdonságaira. A hőmérséklet növelésével a két alacsonyabb hőmérsékleten előállított mintában olyan ismeretlen komponens keletkezését tapasztaltuk, amelyek minőségét további EDS mérések során kiderítettük: réz-hidroxi-kloridról van szó. Az elsőre ismeretlen fázis mellett megjelenő mikroszillagok minden mintában megfigyelhetőek voltak, de a magasabb hőmérsékleteken előállított mintákban csak ez a fázis volt a jellemző. Mindemellett a részecskeméret a hőmérséklet növelésével megnőtt (0,77 - 1,48 nm).

A  $\text{Cu}_x\text{O}$  esetében a pásztázó elektronmikroszkópiás felvételek megmutatták, ahogy az a 2. ábrán is látható, hogy mikrokockák kialakulása megy végbe az előállítás során.



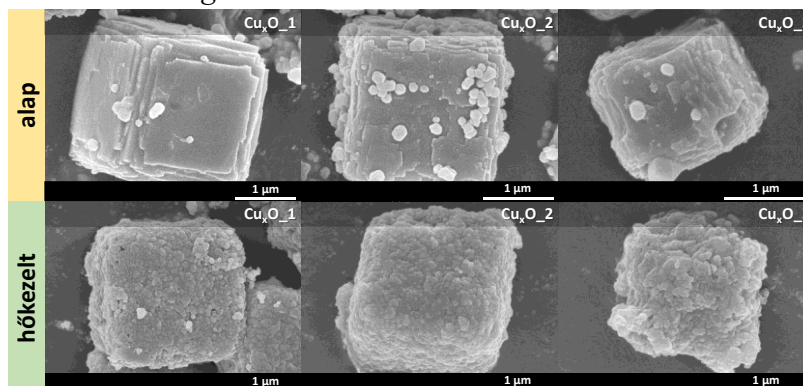
2. ábra: Az előállított  $\text{Cu}_x\text{O}$  félvezetőkről készült SEM felvételek

Megfigyelhető, hogy a kísérleti körülményektől függően sikerült előállítani szabályosabb szerkezetű mikrokockát is, melynek a szélső részén lapok figyelhetőek meg a  $\text{Cu}_x\text{O}_1$  mintáról készült felvételen. A  $\text{Cu}_x\text{O}_2$  mintán megjelennek kisebb méretű részecskék, melyek Cu kiválását jelenthetik, a harmadik kísérleti körülmények mellett végzett módszer



esetén pedig azt figyelhetjük meg, hogy a  $\text{Cu}_x\text{O}_3$  mintában a mikrokockák szélei nem annyira szabályosak ebben az esetben.

## 2. Hőmérséklet hatása az utólagos hőkezelés során:



3. ábra: Az előállított  $\text{Cu}_x\text{O}$  félvezetőről és azok 500 °C-on hőkezelt megfelelőiről készült SEM felvételek

Az előállított félvezetőket a reprodukálási kísérleteket követően hőkezelésnek vetettük alá, mely során szintén vizsgáltuk a hőmérséklet módosításának a hatását. A végzett kísérleteket tehát több hőmérsékleten végezzük el: 400 °C-on, 500 °C-on és 600 °C-on is hőkezeltünk mintákat. Az eredmények azt mutatják, hogy ezekben az esetekben is számít az alkalmazott hőmérséklet, bár lényegesen kisebb mértékben, mint az előállítási folyamat során.

A 3. ábrán megfigyelhetjük, hogy a szerkezetmódosulás a kristályszerkezet morfológiai megváltozásában nem mutatkozik meg, de ennél látványosabb viszont a hőkezelés részecskeméretre gyakorolt hatása. A felvételeken ugyanis azt láthatjuk, hogy a kockát felépítő lapok átalakulnak szemcsés szerkezetűvé és az azelőtt jól behatárolható élek ennek köszönhetően lemorzsolódnak. Ez a későbbiekben, a részecskeméret csökkentésének köszönhetően, lehetséges, hogy az aktivitás növelését fogja eredményezni.

## Következtetések

A kutatás eredményességét első sorban az adja, hogy sikeresen elő tudunk állítani réz-alapú, monodiszperz és izomorf rendszereket:  $\text{Cu}_x\text{O}$  esetén mikrokockákat,  $\text{Cu}_x\text{S}$  esetén pedig mikroszillagokat. Ezeknek az előállított szerkezeteknek a kristályfázisait, vagy a morfológiai sajátosságait is sikerült módosítani a hőmérséklet módosításának hatására. Ezt követően a minták kalcinálásakor (400-600 °C) is tapasztaltunk eltréseket a kapott félvezetők között. A következő lépésben ezeknek a változásoknak a hatását szeretnénk vizsgálni, fotokatalitikus folyamatokban.

## Köszönetnyilvánítás

A kutatás anyagi és személyi támogatásáért köszönet illeti a GINOP-2.3.2-15-2016-00013 pályázatot. Fodor Szilvia köszönetet mond a Balassi Intézet Kutatói Programban és a Makovecz Hallgatói Ösztöndíj Programban való támogatásért. Pap Zsolt köszönetet mond a Magyar Tudományos Akadémia Prémium Posztdoktori Pályázatának az anyagi támogatásért.

**Referenciák**

- [1] A. Karci, Chemosphere 99 (2014) 1-18.
- [2] I. Székely, G. Kovács, L. Baia, V. Danciu, Zs. Pap, Materials 9 (2016) 258.
- [3] K. Vajda, K. Saszet, Zs. Kedves, Zs. Kása, V. Danciu, L. Baia, K. Magyar, K. Hernádi, G. Kovács, Zs. Pap, Ceram. Int. 42 (2016) 3077–3087.
- [4] B. Réti, Z. Major, D. Szarka, T. Boldizsár, E. Horváth, A. Magrez, L. Forró, A. Dombi, K. Hernádi, J. Mol. Catal. A: Chem. 414 (2016) 140–147.
- [5] W. Siripala, A. Ivanovskaya, T. F. Jaramillo, S.-H. Baeck, E. W. McFarland, Sol. Energy Mater. Sol. Cells, 3 (2003) 229–237.

## INVESTIGATION OF SORPTION OF POTENTIAL ANTHROPOGENIC POLLUTANTS ON OIL SHALE AND ITS COMPOSITE FORMS

Miklós Molnár<sup>1,2</sup>, Renáta Rauch<sup>2</sup>, Ottó Horváth<sup>3</sup>, Rita Földényi<sup>1\*</sup>

<sup>1</sup>*Soós Ernő Water Technology Research Center, University of Pannonia Faculty of Engineering, Veszprém, Hungary*

<sup>2</sup>*Research Institute of Biomolecular and Chemical Engineering, University of Pannonia, Veszprém, Hungary*

<sup>3</sup>*Institute of Chemistry, University of Pannonia, Veszprém, Hungary*  
*e-mail: foldenyi@almos.uni-pannon.hu*

### Abstract

Sorption of three different asymmetric polar organic compounds – TEBA (benzyltriethylammonium chloride), Supragil WP (sodium diisopropyl naphthyl sulfonate) and 4-nitrophenol – was studied on Hungarian oil shale and its special composite forms. These frequently used and persistent chemicals can become anthropogenic pollutants when they get into the environment. Sorption is an appropriate method to remove these chemicals by oil shale, but the difficulty of the usage of oil shale as a sorbent is its crumbling nature. Therefore two different types of composites (oil shale–alginate and oil shale–agar) were prepared, which are more manageable, and their sorption abilities were compared to the oil shale powder. The sorbed amount of Supragil WP and 4-nitrophenol on oil shale in the oil shale–alginate composite was higher than on powder, while the sorbed amount of TEBA on oil shale in the oil shale–agar composite was almost the same as on powder.

### Introduction

Oil shale is a rock of natural origin containing no artificial chemicals, which is present in a large amount in the world, also in Hungary. Oil shale originates from the biomass of algae accumulated in the volcanic craters over 4 to 5 million years. It is widely used in agriculture as a soil-ameliorating agent because of its organic and microelement contents and low price. Usually its organic material content is between 5 and 50 %, but in some deposits the content can reach 90 %, which is mainly kerogen [1]. Unfortunately oil shale is easily crumbling, which inhibits its practical usage as a sorbent. Its sorption abilities for removing pollutants has already been investigated [1-3].

Alginate is a biopolymer, it is extracted from brown algae. It consists of 1,4-linked  $\beta$ -D-mannuronate and  $\alpha$ -L-guluronate. The ratio of mannuronate and guluronate fractions depends on the source of the alginate, thus the physical and chemical properties of alginate vary in wide ranges. In the presence of some divalent cations (such as  $\text{Ca}^{2+}$ ,  $\text{Sr}^{2+}$ ,  $\text{Ba}^{2+}$ ), the linear copolymer chains change to gel form, these cations crosslink the alginate chains [4-5]. Alginate has been used for removing environmental pollutants [6].

Agar is also a natural polysaccharide, a biopolymer, which derives from cell wall of red algae. Agar can be fractionated into two components: agarose and agarpectin. The agarose fraction has greater gelling capability. It consists of 1,3-linked  $\beta$ -D-galactopyranose and 1,4-linked 3,6-anhydro- $\alpha$ -L-galactopyranose. These repeating units form long chains. Agarpectin has essentially the same backbone structure, but with various amounts of the residues replaced by pyruvic acid ketal and different sugar units. The gel liquefies when heated and it binds when

cooled. The random coils in solution change to bundles of helices in gel form [5,7]. Agar has also been used for eliminating chemical pollutants [8].

The relatively high price of alginate and agar (compared to the oil shale) disadvances the wide usage. The combination of alginate or agar with the lower-cost oil shale sorbent results in a new composite material, which could eliminate pollutants as effectively as the oil shale powder can.

TEBA (Figure 1, left) is a popular cationic phase transfer catalyst at organic chemical syntheses, Supragil WP (Figure 1, middle) is an anionic chemical, which is widely used as a dispersant, while 4-nitrophenol (Figure 1, right) is a persistent intermediate and precursor of several pharmaceutical drugs, pesticides, and dyes. The structure of both chemicals is similar to surfactants, therefore they can be considered as asymmetric polar compounds [9].

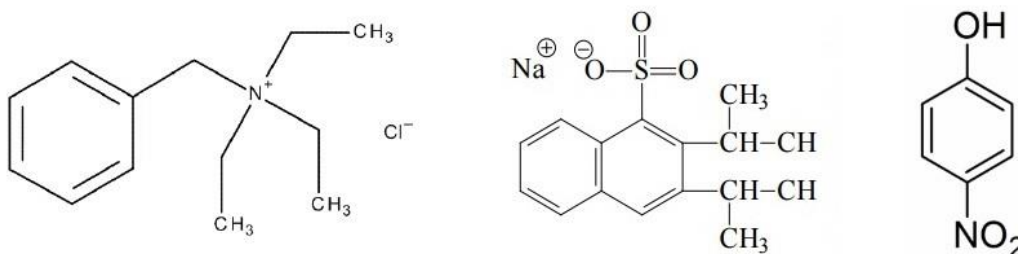


**Figure 1.** Chemical structures of TEBA (left), Supragil WP (middle) and 4-nitrophenol (right)

4-nitrophenol ( $pK_a = 7.15$ ) can be present in non-ionic and anionic forms, depending on the pH of the supernatant. During the sorption process, 4-nitrophenol was present mainly in anionic form, but the measurement was carried out at the non-ionic form.

## Experimental

Oil shale sample originated from Pula (Hungary), which was milled:  $\varnothing < 0.8$  mm.

Sodium alginate, agar, TEBA, Supragil WP, 4-nitrophenol and calcium chloride were purchased from Sigma-Aldrich Co., Naturtrade Hungary Kft., Merck KGaA., Rhodia Geronazzo Spa., Reanal Laborvegyszer Kft. and Lach-Ner, s.r.o., respectively. All chemicals were used without further purification.

UV-VIS measurements were performed on a Varian Cary 50 UV-VIS spectrophotometer, pH was determined with a Radelkis combination pH electrode.

The nonlinear least-square fitting procedure of the Origin scientific graphing and analysis software was utilized, using Levenberg-Marquardt algorithm.

### *Preparation of alginate beads*

A solution of 2.5 % (w/v) concentration was prepared by dissolution of sodium alginate in deionized water. The obtained mixture was dropped into 0.2 mol/L  $\text{CaCl}_2$  solution, and alginate beads were formed ( $\varnothing$ : ~ 5 – 6 mm) instantly. After standing in the gelation media overnight, the beads were filtered out and washed with deionized water.

### *Preparation of oil shale–alginate beads*

According to the above described procedure, sodium alginate mixture was prepared. This solution was mixed with the swollen oil shale, using 8 : 1 mass ratio of oil shale and sodium

alginate. This suspension was added dropwise into 0.2 mol/L  $\text{CaCl}_2$  solution and oil shale composite beads were formed ( $\varnothing$ : ~ 5 – 8 mm). The post-treatment is identical with that applied in the case of alginate beads.

#### *Preparation of agar sorption layer*

A solution of 0.66 % (w/v) concentration was prepared by dissolution of agar powder in boiling deionized water. Exact quantity of this mixture was poured into crystallizing dishes and cooled to room temperature.

#### *Preparation of oil shale–agar sorption layer*

According to the above described method, agar solution was prepared, and the semi-cooled solution mixed with swollen oil shale, using 30.3 : 1 mass ratio of oil shale and agar powder. This suspension was poured into crystallizing dishes and cooled to room temperature.

#### *Sorption on oil shale powder*

The sorption experiments were performed in 250 mL stoppered Erlenmeyer flasks. 5 g of oil shale powder was weighed into the flask and was left to swell in 5 mL water overnight at room temperature. Different concentrations of TEBA (from 2 to 20 mmol/L) or Supragil WP (from 50  $\mu\text{mol/L}$  to 20 mmol/L) or 4-nitrophenol (from 50  $\mu\text{mol/L}$  to 20 mmol/L) solutions were prepared with 0.01 mol/L  $\text{CaCl}_2$  (pH= 7.4). 50-50 mL of these solutions were transferred to the swollen oil shale samples. The suspension was then shaken and left to stand for 24 hours for equilibration at room temperature. Then approximately 2 mL of the supernatant was transferred into an Eppendorf tube and was centrifuged at rpm = 15000 for 20 minutes for perfect separation of the supernatant and oil shale powder. After the centrifugation, the supernatant was measured by UV-VIS spectrophotometer and the concentration was determined.

#### *Sorption on alginate and oil shale–alginate beads*

The procedure to measure the sorption on alginate and oil shale composite was almost the same as in the case of the sorption on oil shale powder. In this case, instead of oil shale powder, the alginate beads or oil shale composite beads were weighed. The weighed oil shale–alginate composite beads contained 5 g of oil shale powder. The alginate content of the weighed oil shale composite beads was equal to the weighed alginate beads at these sorption experiments.

#### *Sorption on agar and oil shale–agar sorption layer*

The method to measure the sorption on agar and oil shale–agar layer was very similar to the above mentioned procedures. The exact quantity of cooled oil shale–agar suspension in crystallizing dishes contained 5 g of oil shale powder. The agar content of the weighed oil shale–agar layers was equal to the weighed agar layers at these sorption experiments. The incubation time in this case was 48 hours.

Before the 4-nitrophenol concentration measurement, the supernatants were diluted with 0.1 M HCl in 1 : 1 ratio in every case, for the more precise concentration determination. All samples were in triplicate. The UV-VIS absorbance of the blank sample ( $c_0 = 0$  mol/L) was subtracted.

## Results and discussion

The adsorption isotherms were analyzed in terms of Langmuir or Freundlich isotherm equation, which ever fits on the data better.

$$\text{Langmuir isotherm: } q_e = Q \cdot \frac{K_L \cdot c_e}{1 + K_L \cdot c_e}$$

$$\text{Freundlich isotherm: } q_e = K_F \cdot c_e^n$$

where  $q_e$  is the adsorption capacity at equilibrium, mol of solute adsorbed per gram of adsorbent (mol/g);  $c_e$  is the equilibrium solution concentration (mol/L);  $Q$  is the maximum amount of solute adsorbed for monolayer coverage of the surface (mol/g);  $K_L$  is the Langmuir constant (L/mol);  $K_F$  ( $L^n / (\text{mol}^{(n-1)} \cdot \text{g})$ ) and  $n$  are Freundlich constants.

The adsorbed amount of the solute was calculated according to the following equation:

$$q = \frac{V \cdot (c_0 - c)}{m}$$

where  $q$  is adsorption capacity at equilibrium (mol/g);  $V$  is the volume of the equilibrium solution (0.05 L);  $c_0$  and  $c$  are the initial and the equilibrium concentrations of the solute (mol/L);  $m$  is the weighed amount of the dry adsorbent (g).

The adsorption isotherms of TEBA and Supragil WP can be seen in Figure 2. In the case of TEBA, the amount sorbed by oil shale calculated from the oil shale–agar layer (**light blue line**) is almost the same as by oil shale powder (**black line**), while the amount sorbed by oil shale calculated from oil shale–alginate beads (**blue line**) is slightly lower than by oil shale powder. The diffusion of cationic TEBA to the oil shale is hindered through the negatively charged alginate in the composite, while the diffusion of TEBA is not hindered through the relatively neutral agarose gel.

In the case of Supragil WP, the amount sorbed by oil shale calculated from the oil shale–agar layer (**light blue line**) is lower than by oil shale powder (**black line**). It can be explained by the apolar-apolar interaction between Supragil WP and agar, which hinders the solute to reach the oil shale in the composite. The amount sorbed by oil shale calculated from oil shale–alginate beads (**blue line**) is higher than by oil shale powder. It can be caused by the difference of liquid-solid ratio compared the powder to the composite. Thus, the repulsion between the anionic Supragil WP and the anionic surface-charged oil shale powder is more significant.

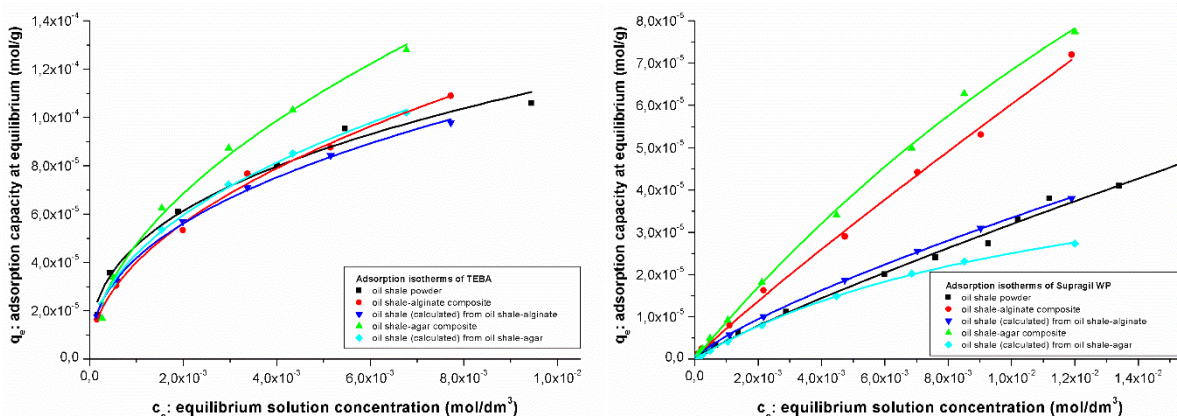


**Figure 2.** Adsorption isotherms of TEBA (left) and Supragil WP (right)



The tendency of adsorption isotherms of 4-nitrophenol is very similar to the adsorption isotherms of Supragil WP (Figure 3), although the sorbed amounts are higher in the case of 4-nitrophenol. During the sorption process, 4-nitrophenol was present not only in anionic form, but also in non-ionic (protonated) form. Thus, the electrostatic repulsion between the oil shale powder or the oil shale in the composite and 4-nitrophenol is less pronounced, which induces the higher 4-nitrophenol uptake of sorbents.

A comparison of the adsorption isotherms (Figure 3, right) demonstrates the sorption differences between the cationic TEBA, anionic Supragil WP, and, partly anionic 4-nitrophenol compounds. The sorption ability of TEBA is much higher than that of Supragil WP or 4-nitrophenol on the anionic surface-charged oil shale. The explanation is the electrostatic repulsion or attraction between the oil shale and the solute.

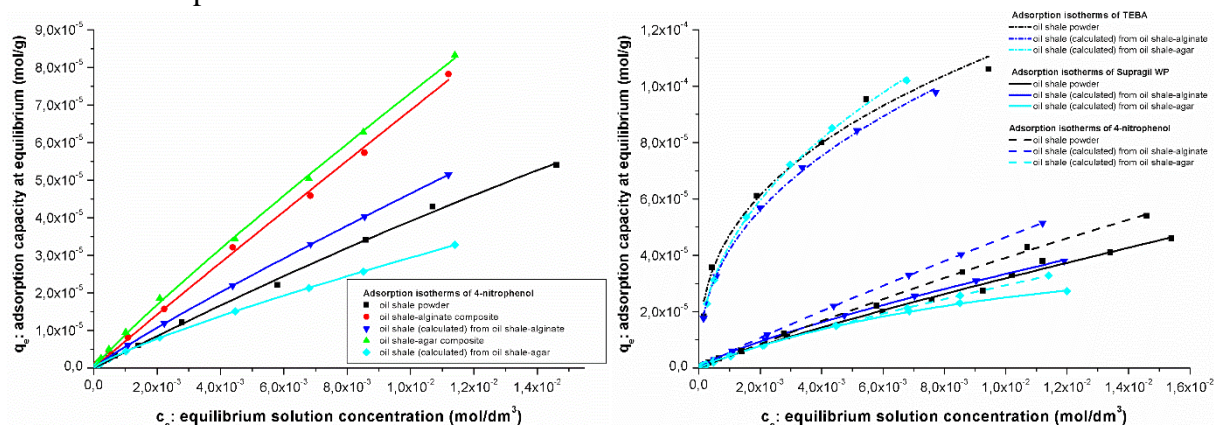


**Figure 3.** Adsorption isotherms of 4-nitrophenol (left) and comparison of adsorption isotherms of TEBA, Supragil WP and 4-nitrophenol (right)

## Conclusion

In this present work, we tried to find some manageable forms of Hungarian oil shale, the sorption abilities of which are as good as or better than those of the oil shale powder. Alginate and agar are suitable forming agents to form a workable and efficient sorbent composite with oil shale for eliminating chemical pollutants. Identifying the physical and chemical properties of the actual contaminant to be eliminated from the environment, we can choose the best forming agent, which results in a more successful retention of pollutants.

## References

- [1] R. Rauch, R. Földényi, Journal of Environmental Science and Health, Part B 47 (2012) 670.
- [2] N. Ayar, B. Bilgin, G. Atun, Central European Journal of Chemistry 6 (2008) 284.
- [3] E. T. Acar, S. Ortoboy, G. Atun, Chemical Engineering Journal 276 (2015) 340.
- [4] G. A. P. Juárez, M. Spasojevic, M. M. Faas, P. de Vos, Frontiers in Bioengineering and Biotechnology 2 (2014) 26.
- [5] P. de Vos, H. A. Lazarjani, D. Poncelet, M. M. Faas, Advanced Drug Delivery Reviews 67-68 (2014) 15.
- [6] S. Peretz, O. Cinteza, Colloids and Surfaces A 319 (2008) 165.
- [7] S. Arnott, A. Fulmer, W. E. Scott, Journal of Molecular Biology 90 (1974) 269.
- [8] B. Gupta, Z. Begum I, G. Rajput, Chemical Engineering Communication 195 (2008) 1200.
- [9] F. Szántó (Ed.), A kolloidkémia alapjai, Gondolat Könyvkiadó, Budapest, 1987.



## INVESTIGATION OF THE CHEMICAL DURABILITY AND EFFECTIVENESS OF TEXTILE PRODUCTS WITH SILVER COATING

**Dalma Fuderer<sup>1</sup>, Tünde Dudás<sup>2</sup>, Albert Kéri<sup>1</sup>, Ilona Pfeiffer<sup>3</sup>, Gábor Galbács<sup>1</sup>**

<sup>1</sup>*Department of Inorganic and Analytical Chemistry, Faculty of Natural Sciences and Informatics, University of Szeged, 6720 Szeged, Dóm sq. 7, Hungary,  
e-mail: galbx@chem.u-szeged.hu*

<sup>2</sup>*Department of Technology, Juhász Gyula Faculty of Education,  
University of Szeged, 6725 Szeged, Boldogasszony Blvd. 6, Hungary*

<sup>3</sup>*Department of Microbiology, Faculty of Natural Sciences and Informatics,  
University of Szeged, 6726 Szeged, Közép ave. 52, Hungary*

### **Abstract**

We studied the silver content and the durability of the antimicrobial effect of commercially available silver-coated textiles. The effect of cleaning cycles on these attributions was in the focus of our work. Inductively coupled plasma mass spectrometry (ICP-MS) was used to monitor the silver content of samples, while the antimicrobial activity was tested by using four types of bacteria and four types of fungi.

### **Introduction**

Nanotechnology is a very broad field, which incorporates research areas as diverse as surface science, organic chemistry, molecular biology, semiconductor physics, microfabrication, molecular engineering, etc. [1]. Nanoparticles of silver are being used as antimicrobial agents in several ways, including the sterilization of wounds, embedding them in plastic coatings of storage containers (e.g. plastic boxes, inner walls of refrigerators, etc.) to prevent the fouling of food stored in them or incorporating silver nanowires into filter units used to purify drinking water [2].

Along the same concept, silver is also used in textiles (e.g. clothing, in the household, in cars, in furniture covers, etc.) to promote self-cleaning and odor-suppression. In these applications, silver is applied either in form of silver salts (e.g. silver chloride), elemental nanoparticles or nanoscale coatings on the surface of the textile fibers. The interlaced weaving of the fabrics from polymer and silver-coated fibers is also customary. In all cases, the antimicrobial effect is caused by the slow release of silver ions that reduces bacterial growth on the textile by releasing silver ions, which are active on the fiber surface [3,4].

The widespread use of silver nanoparticles in commercial products, especially textiles, will likely result in an increase of the environmental concentration levels of silver. The problem is further intensified by the fact that water plants presently are not well equipped to remove Ag nanoparticles from drinking water. Many researchers even consider silver to be more toxic than other metals when in nanoscale form also because these particles have a different toxicity mechanism compared to dissolved silver. Nanoparticles can also become airborne easily due to their size and mass. When inhaled, nanoparticles can go deeper into the lungs reaching more sensitive areas. The mentioned experience confirm why it is crucial to investigate the textiles treated with silver and compare their chemical durability and effectiveness to those of conventional textiles.

### Samples and materials

The polymer textile samples studied were obtained from commercial circulation. Four textile samples were coated with Ag nanoparticles, three contained silver-coated fibers and one was given an undetermined treatment by the manufacturer which was referred as “silverization”. The base fibers in these textiles are cotton, elastane, polyamide and poliester.

For the quantitative determination of the silver content of textiles we used ICP-MS spectrometry on an Agilent 7700x instrument, The silver content of the textile samples was dissolved by using ultratrace purity HNO<sub>3</sub> (VWR). All solutions were prepared by using trace analytical purity deionized labwater (Millipore Elix Advantage 3+ Synergy). Cleaning (washing) cycles were modeled by using alkaline solutions prepared from with analytical grade Na<sub>2</sub>CO<sub>3</sub> (Reanal). 0.22 μm poresize PVDF syringe filters (Labex) were used for the filtration of solutions. ICP-MS calibration solutions were prepared from ICP-MS multi-elemental stock solutions (Inorganic Ventures).

Optical microscopy images were recorded with an Optika Ti600-FL microscope equipped with a high-resolution color digital camera. All statistical and graphical evaluation of the data was made in OriginLab 8.6 and Microsoft Excel software.

### Results and discussion

The optical microscopy images of the surface of the fabrics can be seen in Figure 1. The silver-coated fibers can be easily identified (ESZ-1, ESZ-2, ESZ-3). Even coatings (across the fabric) or nanoparticles of course can not be detected by optical microscopy. We also attempted to use scanning electron microscopy to detect these particles but it was not succesful due to the static charging of textiles. All in all, the presence of silver in the fabrics could only be partially confirmed by microscopy.

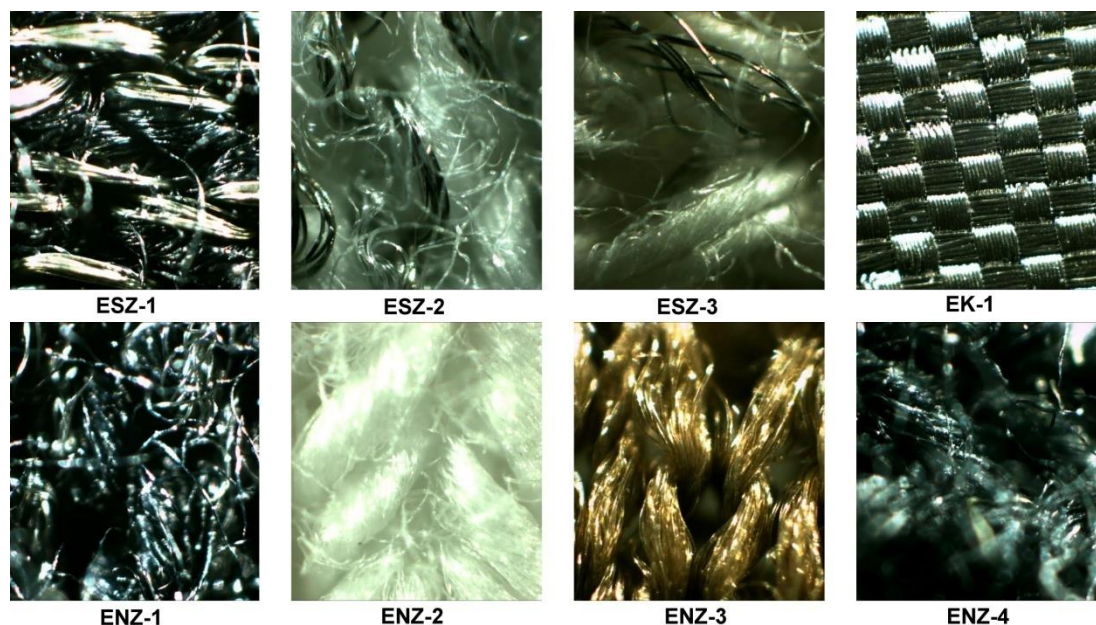


Figure 1. Optical microscope images of some silver-treated textiles (similar magnifications)

The initial microbiological activity of the textile samples was examined by preparing a suspension of suitable bacteria and fungi and incubating sub-samples (30 x 30 mm) of the

textiles together with the suspension and in agar-agar gel at 30°C for 48 hours. The activity was estimated by measuring the size of colonies and comparing them to control colonies. The results showed that the antibacterial effects of the investigated textiles are intermediate. Three samples, a nano silverized (ENZ-2), a textile with Ag-coated fibers (ESZ-2) and the textile “silverized” (EK-1) showed the best antimicrobial activity. The activity was assumed to be caused by the presence of Ag.

In order to monitor the change of silver content of textiles during washing cycles, we developed a simple sample preparation method followed by ICP-MS analysis. Again, 30 x 30 mm pieces of textile were treated with 0.2 mol/dm<sup>3</sup> nitric acid for 10, 30, 60, and 120 minutes of time, during which shaking was also employed. This routine was followed in order to establish the optimal duration of acid treatment. As an illustration, this optimization curve for sample ESZ-2 can be seen in Figure 2. Based on these data, the area-specific silver content of the fabrics could be estimated; it was found to vary in a wide range from 0.5 to 850 mg/m<sup>2</sup>.

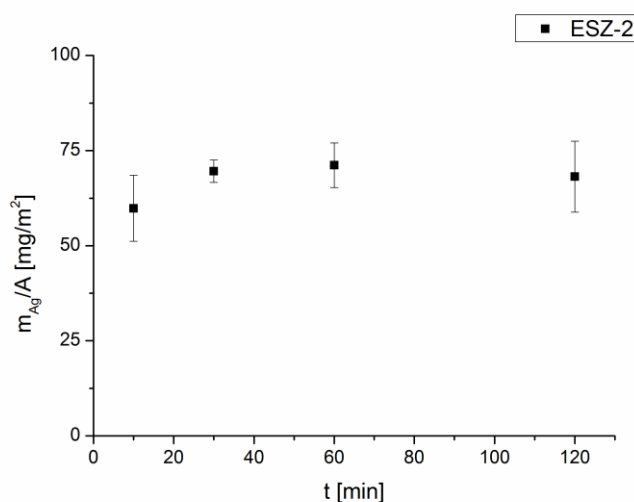


Figure 2. Optimization of the duration of nitric acid treatment of the sample ESZ-2 for the determination of the area-specific silver content. Error bars represent the standard deviation from three parallel measurements

We also performed model washing experiments, the purpose of which was to monitor the release (loss) of silver from these samples. Our first attempts with NP-treated samples involved washing with water and surveying the silver nanoparticles in the aqueous leachate by using single nanoparticle ICP-MS methodology. Unfortunately, no Ag NPs were detected, which is either the indication of that the Ag NPs used in the textile treatment are too small or that pure water can not easily remove the NPs. In further experiments we used a Na<sub>2</sub>CO<sub>3</sub> solution (one spoonful of carbonate in 5 liter water) to model the washing procedure. 100 mL solution was poured on each sub-sample and the textiles were then shaken for 15 minutes. After each treatment, the sub-samples were carefully drained and rinsed thoroughly. Following this, the residual silver content of the fabrics was determined by the ICP-MS method, as described above. This washing procedure was then repeated several times, each time starting out with a fresh piece of fabric and continuing with the washing-rinsing cycles until the required, incremental number of steps.

In accordance with the expectations, the silver content of the samples decreased with the increase of washing cycles. The extent of the loss of silver was different for different samples,

probably because of differences in the base fiber composition and the silver treatment. Figure 3. shows the loss of silver after 10 washing cycles for three textile samples. The loss was greatest for ENZ-2, where it reached almost 77%, but even the most durable fabric lost 35% of its silver content.

The investigation of the remaining antimicrobiological activity of the washed samples is in progress now. We will present the detailed results in our poster contribution.

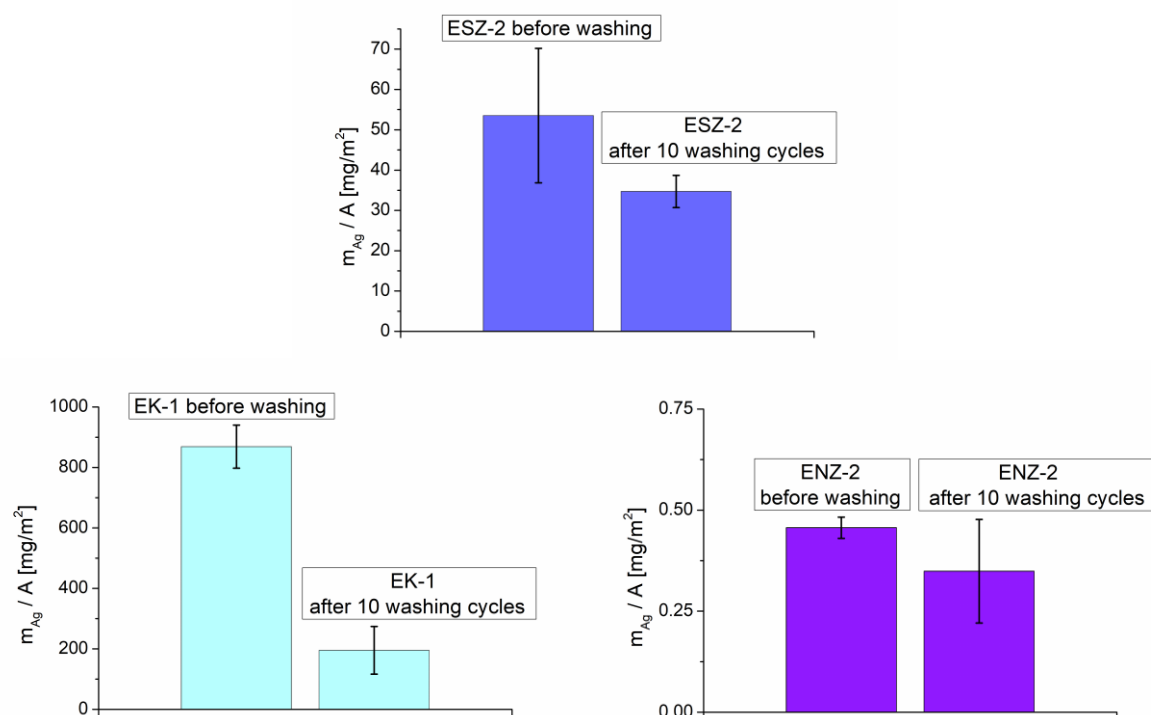


Figure 3. Change of the silver content of textiles as a result of  $\text{Na}_2\text{CO}_3$  washing cycles. Error bars represent the standard deviation from three parallel measurements

## References

- [1] R. Saini, S. Saini, S. Sharma, J. Cutan. *Aesthet. Surg.* 3 (2010) 32.
- [2] S. Iravani, H. Korbekandi, S.V. Mirmohammadi, B. Zolfaghari, *Res. Pharm. Sci.* 9 (2014) 385.
- [3] C. Som, B. Nowack, P. Wick, H. Krug, *Nanomaterialien in Textilien: Umwelt-, Gesundheits- und Sicherheits-Aspekte, Fokus: synthetische Nanopartikel*, Empa und TVS Textilverband Schweiz, St. Gallen, 2010
- [4] C. Som, M. Halbeisen, A. Köhler, *Integration von Nanopartikeln in Textilien Abschätzungen zur Stabilität entlang des textilen Lebenszyklus*, Empa und TVS Textilverband Schweiz, St. Gallen, 2009

## ÜREGES SZERKEZETŰ TITÁN-DIOXIDOK ELŐÁLLÍTÁSA SZÉNGÖMB TEMPLÁT SEGÍTSÉGÉVEL

### PREPARATION OF TITANIUM DIOXIDE HOLLOW STRUCTURES BY THE APPLICATION OF CARBON SPHERE TEMPLATES

**Tamás Gyulavári<sup>1,2\*</sup>, Gábor Veréb<sup>2,3</sup>, Zsolt Pap<sup>2,4,5</sup>, Klára Hernádi<sup>1,2</sup>**

<sup>1</sup>Szegedi Tudományegyetem, Természettudományi és Informatikai Kar, Alkalmazott és Környezeti Kémiai Tanszék, Magyarország, HU-6720 Szeged, Rerrich Béla tér 1.

<sup>2</sup>Szegedi Tudományegyetem, Természettudományi és Informatikai Kar, Környezettudományi és Műszaki Intézet, Környezatkémiai Kutatócsoport, Magyarország, HU-6720 Szeged, Tisza Lajos krt. 103.

<sup>3</sup>Szegedi Tudományegyetem, Mérnöki Kar, Folyamatmérnöki Intézet, Magyarország, HU-6725 Szeged, Moszkvai krt. 9.

<sup>4</sup>Babeş-Bolyai Tudományegyetem, Interdiszciplináris Bio-Nano Tudományok Intézete, Románia, RO-400271 Kolozsvár, Treboniu Laurian 42.

<sup>5</sup>Babeş-Bolyai Tudományegyetem, Fizika Kar, Románia, RO-400084 Kolozsvár, M. Kogalniceanu 1.

\*e-mail: gyulavarit@chem.u-szeged.hu

#### Abstract

In the present study carbon spheres were used as templates to synthesize titanium dioxide hollow structures. The synthesis of the photocatalysts were based on the synthesis method of our previous, highly efficient (peroxo group enhanced) titanium dioxide.

Carbon sphere templates were characterized by XRD, SEM, and IR measurements, while titanium dioxide hollow structures were characterized by XRD and SEM measurements, respectively. The photocatalytic activity was determined by the degradation of phenol under visible light irradiation. Self-made hollow sphere TiO<sub>2</sub> (denoted as 'Rutile-H2\_HS') possessed superior photocatalytic efficiency compared to commercial Evonik Aeroxide P25 and self-made reference photocatalyst synthesized without shape tailoring.

#### Bevezetés

Napjaink ígéretes alternatív vízkezelési módszerei a nagyhatékonyságú oxidációs eljárások, melynek egyik típusa a heterogén fotokatalízis. Lényege, hogy félvezető fotokatalizátorok fényel történő gerjesztése következtében egy elektron a vegyértéksávból a vezetési sávba lép át miközben a vegyértéksávban egy pozitív töltésű lyukat hagy maga után. A gerjesztett fotokatalizátor felületén, összetett gyökös folyamatok révén a szerves szennyező anyagok lebonthatók. Fotokatalizátorként az esetek döntő többségében titán-dioxidot alkalmaznak számos előnyös tulajdonsága miatt (olesó, fotostabilis, biokompatibilis stb.).

Korábbi publikációnkban [1] egy rutil fázisú titán-dioxid kiemelkedő fotokatalitikus aktivitása a felületén lévő Ti-O-O-Ti (peroxo) csoportok jelenlétének, vagyis a „peroxidált” felületnek volt tulajdonítható. Vizsgálataink alapján a peroxidált felület a fényelnyelés vöröseltozódását is eredményezi. Egy másik publikációnkban [2-3] széngömb templát felhasználásával üreges titán-dioxid gömbhéjakat állítottunk elő, melyek fotokatalitikus aktivitása meghaladta a nem gömbhéjas szerkezetű referencia TiO<sub>2</sub> fotokatalitikus aktivitását. A megnövekedett fotokatalitikus aktivitást annak tulajdonítottuk, hogy a gerjesztéshez



használt fény gömbön belüli többszöri visszaverődése lehetőséget teremthet a gerjesztett állapot többszöri létrejöttéhez.

Jelen tanulmányban a felületi peroxo-csoportok és gömbhéjas morfológia együttes kialakításával kívánunk nagy fotokatalitikus aktivitású titán-dioxidot előállítani.

### Alkalmazott anyagok és módszerek

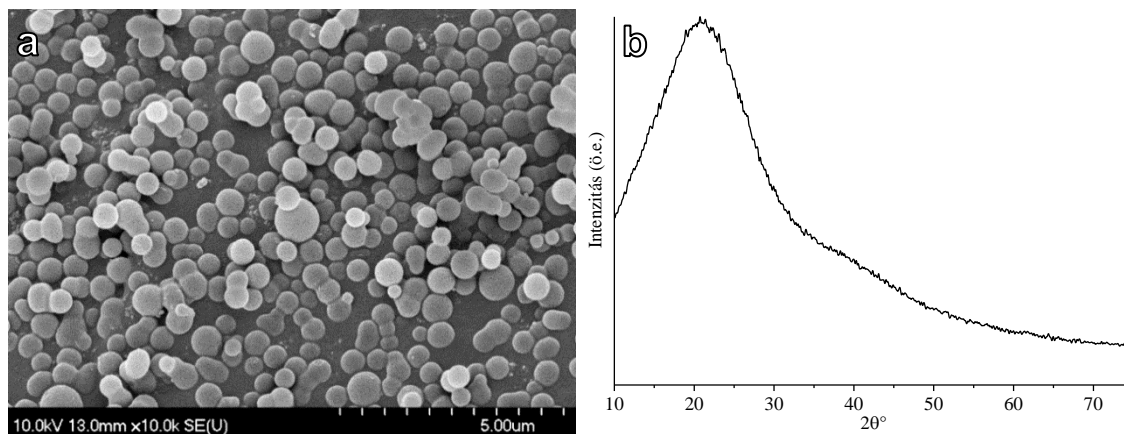
A széngömb (CS) templátokat hidrotermális módszerrel állítottuk elő. Egy 0,15 M-os szacharóz oldat pH értékét 2 M-os NaOH-dal 12-re állítottuk be majd 180 °C-on 12 órán át autoklávban hőkezeltük. A keletkező terméket aceton felhasználásával centrifugálással tisztítottuk a szintézis során képződő aromás vegyületek és oligoszacharidok eltávolítása érdekében, majd szárítást követően achát mozsárban porítottuk. A peroxo-csoportokat tartalmazó, rutil fázisú titán-dioxid bevonat szintéziséhez [1] az alkalmazott reaktánsokat a következő molarányban alkalmaztuk:  $\text{Ti}(\text{OC}_4\text{H}_9) : \text{H}_2\text{O}_2 : \text{HCl} : \text{H}_2\text{O} = 1 : 2 : 3 : 50$ . Az említett korábbi publikációban [1] leírtak szerint kinyert szervesetlen fázishoz hozzáadtuk az előzetesen elkészített széngömb templátokat, és 5 perces ultrahangos homogenizálást alkalmaztunk. 48 órás 55 °C-on történő öregítés során a titán-dioxid nanorészecskék kikristályosodtak a széngömbök felületén, majd a keletkező szuszpenziót szárítottuk és achát mozsárban porítottuk. Ezt követően a templátokat 4 óra 400 °C-on történő kalcinálással távolítottuk el, mely eredményeképp üreges gömb szerkezetű titán-dioxidot kaptunk.

A részecskeméretet és kristályfázis összetételt egy Rigaku Miniflex II típusú röntgen diffraktométerrel határoztuk meg. Az infravörös spektrumokat egy „FRA 106 Raman” modullal kiegészített „Bruker Equinox 55” típusú spektrométerrel rögzítettük. A morfológia vizsgálatát egy Hitachi S-4700 típusú pásztázó elektronmikroszkóppal végeztük.

A fotokatalitikus aktivitást fenol modellszennyező ( $c=10^{-4}$  M) bomlásának sebességével jellemeztük. A látható fényt sugárzó lámpákkal felszerelt fotoreaktorból vett minták fenol koncentrációját egy Merck Hitachi típusú HPLC berendezéssel határoztuk meg. Referencia fotokatalizátorként Evonik Aeroxide P25 titán-dioxidot alkalmaztunk.

### Eredmények és kiértékelésük

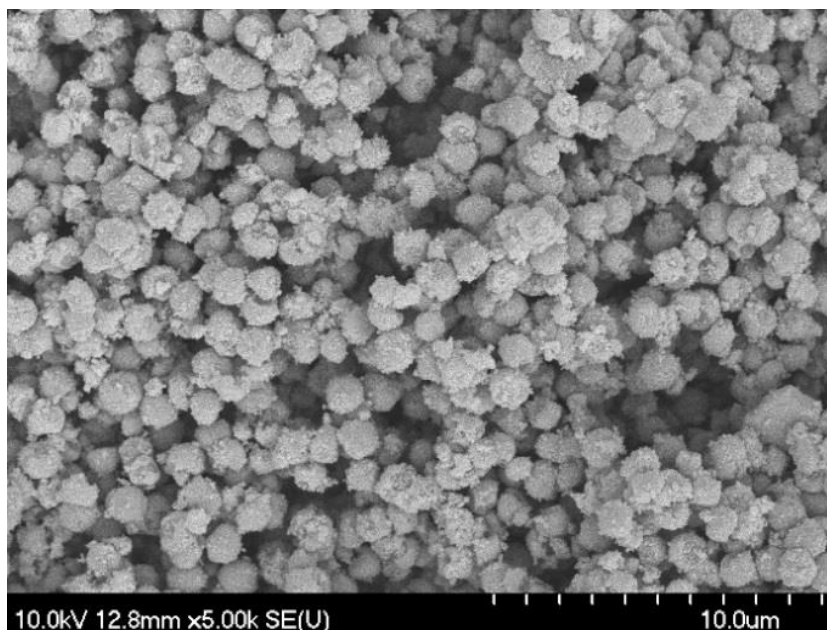
A centrifugálással tisztított széngömböket „CS\_0” jelöléssel láttuk el. A széngömbökről készült SEM felvétel és röntgendiffraktogram (XRD) az **1. ábrán** látható.



**1. ábra:** A CS\_0 széngömbökről készített SEM (a) és XRD (b) felvételek

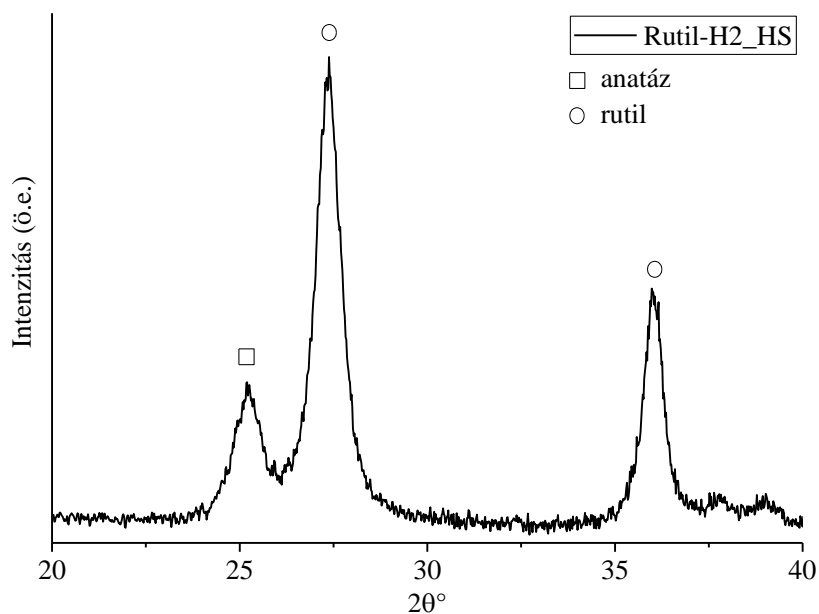
A SEM képek alapján jól definiált gömb morfológia figyelhető meg, a grafikus módszerrel meghatározott részecskeméret 472 nm. A röntgen diffraktometriával történő jellemzés során a  $\sim 22^\circ$ -nál mért széles reflexió amorf szénnek feleltethető meg, grafitos ( $26,5^\circ$ ) szerkezetre, vagy egyéb kristályos anyag jelenlétére utaló reflexió nem figyelhető meg.

Az elővizsgálatok után a CS\_0 széngömb-templát felhasználásával elkészített  $\text{TiO}_2$ -szén nanokompozitból kalcinálással eltávolítottuk a szenet és előállítottuk az üreges  $\text{TiO}_2$  gömbhéj szerkezetű fotokatalizátort, melyet „Rutil-H2\_HS” jelöléssel láttunk el. A pásztázó elektronmikroszkópos felvételek (**2. ábra**) alátámasztják, hogy az üreges gömb morfológia kialakulása sikeresen végbement, törmelékes régió megjelenése nem tapasztalható. A Rutil-H2\_HS mintáról készített röntgendiffraktogram a **3. ábrán** látható.



**2. ábra:** Az üreges gömbhéj morfológiájú titán-dioxidról készített SEM felvétel

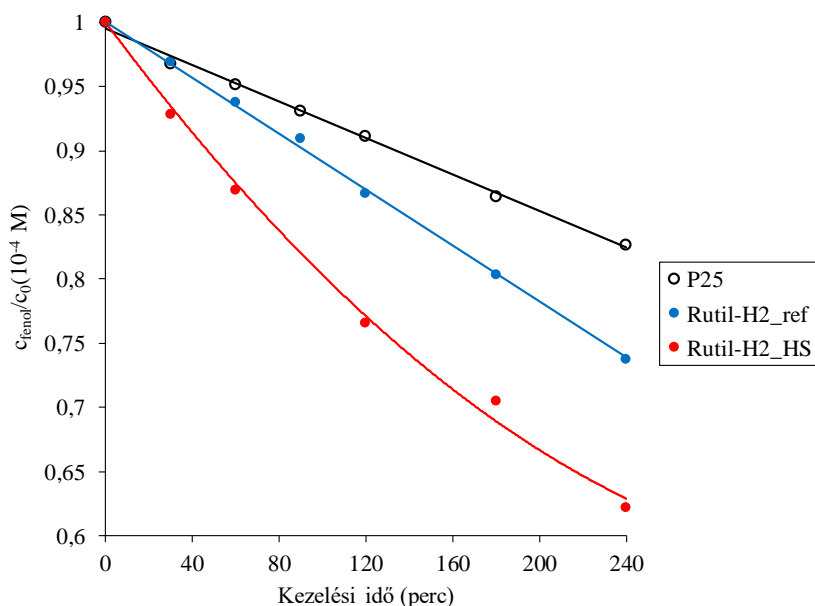




**3. ábra:** A Rutil-H2\_HS titán-dioxidról készített XRD felvétel

Az előállított titán-dioxid kristályos fázisa 80% rutilt és 20% anatázt tartalmaz, a grafikus módszerrel meghatározott közepes részecskeméret 880 nm. Az anatáz a kalcinálás során az amorf titán-dioxid átkristályosodásából eredeztethető.

A fotokatalitikus aktivitásokat bemutató **4. ábra** alapján az alakirányított szintézissel előállított Rutil-H2\_HS minta fotokatalitikus aktivitása meghaladja a referenciaként használt, nem gömb morfológiájú Rutil-H2\_ref és a P25 fotokatalitikus aktivitását is.



**4. ábra:** A fenol fotokatalitikus bontásának eredményei

## Összegzés

Jelen tanulmányban szacharóz oldatból hidrotermális módszerrel előállított széngömb templátok felhasználásával sikeresen állítottunk elő üreges gömbhéj szerkezetű titán-dioxidot. A széngömb templátok anyagszerkezeti jellemzőinek vizsgálata alapján azok amorf szerkezetűek, kristályos fázisra utaló reflexió nem jelent meg. A széngömbök felhasználásával szol-gél módszerrel titán-dioxid bevonatot állítottunk elő, majd kalcinálással a széngömb templátok eltávolításával egyidejűleg kristályos üreges gömb morfológiájú titán-dioxidot kaptunk. A fotokatalitikus aktivitást látható fényvel történő gerjesztés mellett fenol modellszennyező bontásával vizsgáltuk, mely során az üreges gömb morfológiájú Rutil-H<sub>2</sub>HS TiO<sub>2</sub> fotokatalitikus aktivitása meghaladta valamennyi vizsgált katalizátor fotokatalitikus aktivitását. Megállapítottuk, hogy a peroxo-csoportok és a gömb morfológia okozta előnyös tulajdonságokat sikeresen kombináltuk.

## Köszönetnyilvánítás

A kutatást a GINOP-2.3.2-15-2016-00013 azonosító számú projekt támogatta. A szerzők köszönetüket fejezik ki az OTKA-K-124212 azonosító számú projektnek. Veréb Gábor köszönetét fejezi ki, hogy a munka a Bolyai János Kutatási Ösztöndíj támogatásával készülhetett. A kutatáshoz szükséges infrastruktúra beszerzését részben a Svájci Alap (SH/7/2/20) biztosította.

## Irodalomjegyzék

- [1] T. Gyulavári, Z. Pap, G. Kovács, L. Baia, M. Todea, K. Hernádi, G. Veréb, Catal. Today 284 (2017) 129-136.
- [2] B. Réti, G. Kiss, T. Gyulavári, K. Baán, K. Magyar, K. Hernádi, Catal. Today 284 (2017) 160-168.
- [3] N. Justh, L. P. Bakos, K. Hernádi, G. Kiss, B. Réti, Z. Erdélyi, B. Párditka, I. M. Szilágyi, Sci. Rep. 7:4337 (2017)

**EFFECTS OF GLYPHOSATE-BASED HERBICIDES AND THEIR COMPONENTS  
ON THE EMBRYONAL DEVELOPMENT OF ZEBRAFISH (*DANIO RERIO*):  
ASSESSMENT OF THE ROLE OF RETINOIDS**

**Gergő Gyurcsó, Mária Mörtl, Eszter Takács, Ágnes Fejes,  
László Simon, Béla Darvas, András Székács**

<sup>1</sup>*Agro-Environmental Research Institute, National Research and Innovation Centre  
H-1022 Budapest, Herman Ottó út 15, Hungary  
e-mail: g.gyurcso@cfri.hu*

**Abstract**

Intensification of agricultural technologies led to a worldwide increase in the use of agrochemicals. Herbicides may exert toxicity to non-target organisms water ecosystems. In this study individual and combined teratogen effects of herbicide active ingredient glyphosate and surfactants applied in formulated herbicides were investigated on embryonal development of zebrafish. Retinoic acid-retinol (RA/ROH) and 13-cis-RA/ROH ratios are useful parameters in teratogenicity studies to assess xenobiotic effects, thus analytical determination of three retinoids were determined by HPLC method.

**Introduction**

Pesticides applied at cultivation areas may be absorbed, washed-off or leached to other environmental compartments. These chemicals can trigger harmful effects at very low concentrations on living organisms in soil or surface water, and cause teratogenic, carcinogenic or endocrine disrupting abnormalities. Upon the ban of atrazine in the EU [1], glyphosate has become the most widely used herbicide: its use has risen globally almost 15-fold since the introduction of genetically modified glyphosate-tolerant crops [2,3]. Due to the continuously expanding application of glyphosate, this herbicides active ingredient is a common pollutant in surface waters worldwide. Surfactants are used as common additives in agrochemical formulations to enhance it pesticide efficacy [4]. Surfactants are declared as inert ingredients regarding the main pesticide effect, but recent studies found that these compounds may exert toxicity, moreover, synergistic toxic effects were also indicated [5,6].

Retinoic acid (RA) is of major importance during vertebrate embryonic development and its levels need to be under strict endocrine regulation, otherwise congenital malformations will develop [7]. RA, as an active metabolite of vitamin A, is vital for vertebrate embryonic development, namely in somitogenesis, neurogenesis and organogenesis. It acts as a ligand for nuclear RA receptors, converting them from transcriptional repressors to activators. The distribution and levels of RA in embryonic tissues are tightly controlled by regulated synthesis through the action of specific retinol (ROH) and retinaldehyde dehydrogenases and by degradation via specific cytochrome P450s [8]. Possible functions of RA during embryogenesis were first inferred by studying its teratogenic effects, i.e. how the administration of excess doses of RA, either globally or by local implantation using RA-impregnated beads, interferes with normal developmental processes. Studies have been performed in a wide range of species including amphibians, zebrafish, chick and rodents [9,10]. Teratogenic effects of glyphosate-based herbicides in embryonal development of *Xenopus laevis* via disturbances in RA cell signals was reported by Paganelli et al. [11,12]. Embryotoxicity and teratogenicity by glyphosate on zebrafish embryos were also published, where cardiac and pericardiac

alterations, digest-vitelline and musculo-eskeletal malformations were detected [13]. In our study, we first report individual and combined teratogenic effects of components of formulated herbicides on zebrafish (*Danio rerio*) embryos.

## Experimental

### *Teratogen effects of glyphosate-based herbicides and their components*

Teratogenic effects of the herbicide active ingredient glyphosate, four formulated glyphosate-based herbicides and four surfactants frequently applied in herbicides were investigated based on the OECD 236 guideline [14]. Xenobiotics investigated were obtained by Lamberti S.p.A, Abizzate, Italy (Table 1).

Table 1. Chemical characteristics of xenobiotics investigated [15,16].

	Trade Name	AI	AI (%)	Present in
<b>Surfactants</b>	Emulson AG GPE 3SS	POE tallow amine	100	Roundup Classic, Glyfos
	Rolfen Bio	POE alkyl phosphate ether	70	
	Eucarol Age SS	sodium-APG sulfosuccinate	45	
	Eucarol Age EC	sodium-APG citrate	30	
		<b>Glyphosate salt</b>		<b>Surfactant (%)</b>
<b>Formulated herbicides</b>	Roundup Classic	IPA (486 g L <sup>-1</sup> )*		POEA (15.5%)
	Total	IPA (486 g L <sup>-1</sup> )*		un. (58.5%)
	Glyfos	IPA (486 g L <sup>-1</sup> )*		POEA (9%)
	Medallon Premium	DA (433 g L <sup>-1</sup> )*		APG (10-20%)
<b>AI</b>	glyphosate IPA	IPA (486 g L <sup>-1</sup> )*		

AI – active ingredient, POE – polyethoxylated, IPA – isopropylammonium salt, DA – diammonium salt, APG – alkyl polyglucoside, un. – unknown. \*Concentrations are equivalent to 360 g L<sup>-1</sup> of the free acid form of glyphosate

Authorisation of animal housing and experiments according to the corresponding legal regulation in the EU [17] have been completed prior to the study. Maintenance of the zebrafish colonies was performed in 80 litre aquaria at 26±1 °C and under 16:8 hrs light:dark photoperiods. Fish were fed daily with living and frozen food (*Artemia salina*, *Culex pipiens*) and plate fish food. Health conditions of the fish and maintenance conditions were supervised regularly by a veterinarian. In the 96-hr ecotoxicity assay, newly fertilised embryos were treated with glyphosate active ingredient, herbicides or surfactants at five concentrations. Tests were carried out in triplicates in 24-well plates. One day before the test males and females at a ratio of 2:1 per were placed in spawning tanks a few hours before the onset of darkness. Twenty embryos per concentration at 8-16-cell developmental stages were exposed to chemicals. FET control water was used as negative control and as internal plate control. A positive control 3,4-dichloroaniline at concentration of 4 mg L<sup>-1</sup> was performed. Development and mortality was recorded upon 24, 48, 72 and 96 hrs of exposure by an Olympus IX73 inverse microscope (Unicam Kft., Budapest, Hungary), LC<sub>50</sub> values were determined at 96 hrs and calculated by statistical software ToxRat<sup>®</sup> (ToxRat Solutions GmbH, Alsdorf, Germany).

*Analytical determination of retinoids in zebrafish*

For analytical determination of retinoids in full body homogenates, fish were collected at different developmental stages and sizes of 2-4 hr eggs, 10-day juveniles (DR1), 10-14 mm (DR3) and 25-30 mm fish (DR6). Eggs and fish were placed into 5 ml stabilizing buffer (0.5% ascorbic acid, 0.5% EDTA, 0.3% sodium sulphate in phosphate buffered saline, pH 7.3), then homogenised (Heidolph Silent Crusher M) for 2x1 min at 15000 rpm for eggs and DR1 group and 4x4 minutes at 26000 rpm for DR3 and DR6 groups. Chemical analyses of the samples were performed on Younglin YL9100 high pressure liquid chromatography (HPLC) equipped with a YL9150 autosampler, using a Kinetex EVO (Phenomenex) C18 core-shell column (150 mm × 4.6 mm i.d., 5µm) at 30°C and UV detector signals recorded at  $\lambda=330$  nm and  $\lambda=300$  nm for each compound. The HPLC method was optimised with standard solutions of 13-cis-retinoic acid (13-cis-RA), retinoic acid (RA) and retinol (ROH). External calibration was used in the range between 20 ng mL<sup>-1</sup> and 15 µg mL<sup>-1</sup>. The eluent flow rate was 1.2 mL min<sup>-1</sup> with isocratic elution for 5 minutes (20:80 = A:B eluents, A = 2% acetic acid in water, B = ACN). Retention times were 3.30, 3.50 and 3.77 minutes for 13-cis-RA, RA acid and ROH, respectively. Two sample preparation methods were assessed (Figure 1). Finally, the method using ethyl acetate:hexane = 1:1 mixture for the extraction was applied and recoveries were determined with standard solutions from spiked water samples at two levels (2 and 20 µg mL<sup>-1</sup>) and from fish samples (1-, 2-, 3- and 4-day old eggs) as well.

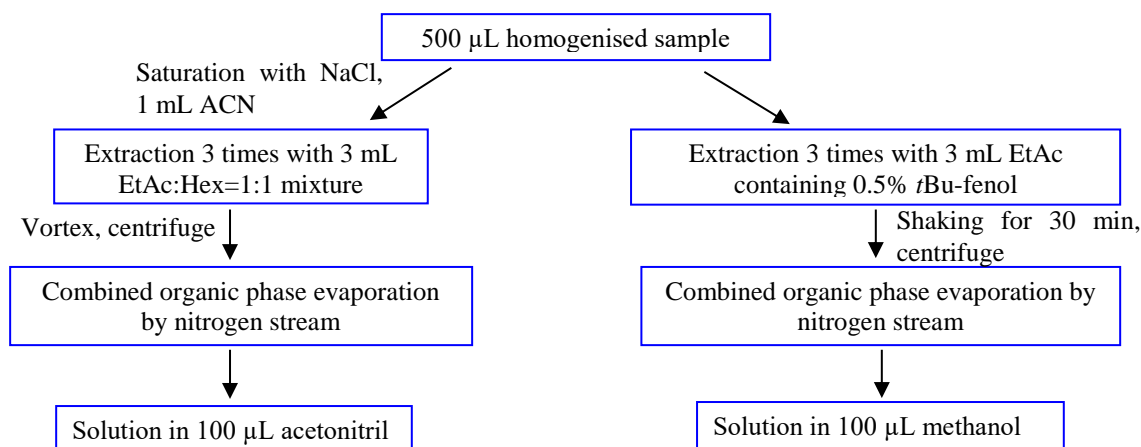


Figure 1. Extraction methods tested for preparation of *D. rerio* samples for HPLC measurement

## Results and discussion

### *Teratogen effects of glyphosate-based herbicides and their components*

Coagulation of the embryos, lack of somite formation, non-detachment of the tail and lack of heartbeat were recorded as indicators of lethality. Other deformities (e.g., inhibition of heartbeat and circulation, lack of eyes or pigmentation, scoliosis, lordosis, lack of pigmentation, oedema) were also recorded. 96-hr LC<sub>50</sub> values showed the acute toxic effects of chemicals investigated. Herbicide active ingredient glyphosate was found the least toxic on embryos. Its LC<sub>50</sub> was higher than 9.8 g L<sup>-1</sup> (glyphosate concentration in 2% Roundup Classic applied in agricultural practices). Formulated herbicides were 44-336 times more toxic than glyphosate, that were considered to be due to the chemical characteristics and quantity of the surfactants, since the nominal concentration of the active ingredient did not differ in these products. The least toxic one among formulated herbicides was Medallon Premium that

contains an alkyl polyglucoside surfactant; while the most toxic were Roundup Classic and Glyphos that contain a non-ionic surfactant polyethoxylated tallow amine. The pure surfactants were identified as the most toxic components: their LC<sub>50</sub> values were 232-2438 times lower than that to glyphosate. Below or near the LC<sub>50</sub> values, defromites, oedema (pericardial), inhibition of heartbeat and circulation were the most frequently detected non-lethal malformations in every treatments (Figure 2).



Figure 2. Pericardial oedema after 48 hrs exposition of Glyphos at concentration of 20 mg L<sup>-1</sup>.

*Analytical determination of retinoids and assessment of their roles in teratogenic effects*

The biochemical scheme for the conversion of these compounds is depicted in Figure 3. As the method using ethyl acetate:hexane=1:1 for the extraction was more efficient and resulted in higher recoveries (Table 2) and cleaner extracts, than extraction with ethyl acetate, this solvent was applied for fish samples. Limits of detections, determined with standard solutions were 50, 25 and 10 ng mL<sup>-1</sup> for 13-cis-RA, RA and ROH, respectively. Results of analytical determinations from embryos and small fish are summarised in Table 3.

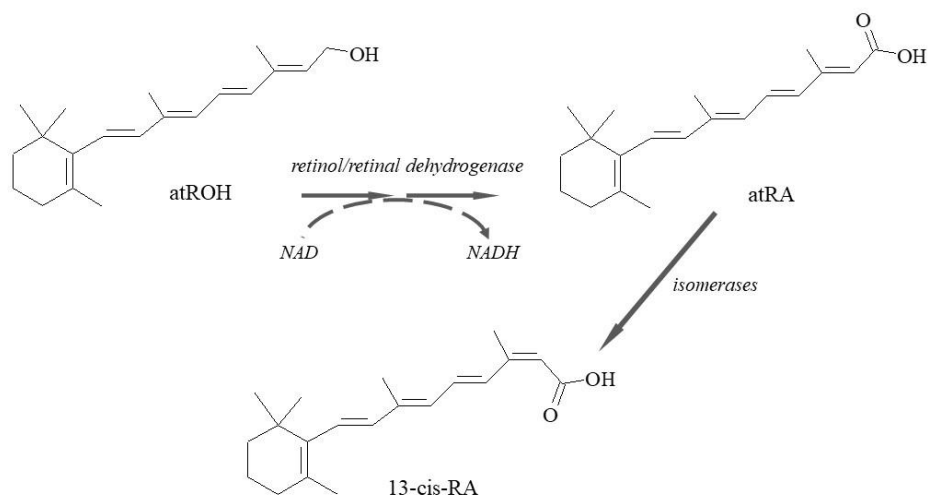


Figure 3. Enzymatic conversion of vitamin A (atROH) into all-trans-retinoic acid (atRA) and 13-cis-retinoic acid (13-cis-RA) during embryonic development.

Table 2. Recoveries (%) from spiked water samples concentrations and from fish eggs

	Spiked water samples		Fish egg samples (days after fertilisation)			
	2 $\mu\text{g mL}^{-1}$	20 $\mu\text{g mL}^{-1}$	1 day	2 days	3 days	4 days
13-cis-retinoic acid	82.3±6.7	86.5±8.7	36.9±2.4	69.3±5.1	68.2±4.5	56.6±4.9
retinoic acid	82.1±9.4	95.2±6.2	43.7±3.7	78.7±6.8	72.9±5.2	56.4±4.2
retinol	37.5±8.9	64±10.4	51.4±4.9	48.5±5.1	59.2±5.3	59.6±5.4

Table 3. Concentration of retinoids in the final extract ( $\mu\text{g mL}^{-1}$ ) of different aged and sized zebrafish. DR1 - 10-day juveniles, DR3 – 10-14 mm length, DR6 – 25-30 mm length.

	DR1	DR3	DR6
13-cis-retinoic acid	<LOD	<LOD	<LOD
retinoic acid	<LOD	<LOD	<LOD
retinol	<LOD	0.035±0.003	0.289±0.039

DR1 - 10-day juveniles, DR3 – 10-14 mm length, DR6 – 25-30 mm length.

Retinoids regulate differentiation, development and embryogenesis of vertebrates [18,19], and induce changes in their endogenous levels eventually lead to teratogenic effects. Vitamin A or all-trans-retinol (atROH) is converted enzymatically in a sequential process to all-trans-retinoic acid (atRA), and is further isomerised into its isoform 13-cis-RA. The progression of this enzymatic process triggers numerous cellular effects, the retinoic acid signalling pathway (RA pathway) [20], and is an indicator of its activation. The RA pathway has been implicated in various developmental processes, e.g. during early embryonic development, retinoids act as important morphogens, and participate in regulating apoptosis, differentiation and cell fate specification. Surfactants used in glyphosate-based herbicides and the active ingredient glyphosate itself have been indicated to interfere with the formation of retinoids and the RA pathway [11,12]. Thus, we have determined levels of atROH, atRA and 13-cis-RA in *D. rerio* embryos and young fish emerging. Retinoic acid-retinol (RA/ROH) and 13-cis-RA/ROH ratios are useful parameters in teratogenicity studies to assess xenobiotic effects. In our hand, as RA and 13-cis-RA were found to be below LODs, such ratios could not be calculated, and therefore, assessment has to rely on ROH levels detected. Nonetheless, this preliminary survey indicated that ROH (and possibly RA and 13-cis-RA, if detected by more sensitive analytical methods) are suitable biomarkers of pesticide exposure in exposed *D. rerio*.

### Acknowledgements

This research was supported by project “Mechanism-related teratogenic, hormone modulant and other toxicological effects of veterinary and agricultural surfactants” (OTKA K109865) of the National Scientific Research Fund of Hungary.

### References

- [1] European Commission, 2004/248/EC (2004)
- [2] C.M. Benbrook, Environ Sci Eur. 28 (2016) 3.



- [3] J.P. Myers, M.N. Antoniou, B.B.L. Carroll, T. Colborn, L.G. Everett, M. Hansen, P.J. Landrigan, B.P. Lanphear, R. Mesnage, L.N. Vandenberg, F.S. vom Saal, W.V. Welshons, C.M. Benbrook, *Environ. Health*. 15 (2016) 19.
- [4] M.J.L. Castro, C. Ojeda, *Environ. Chem. Letters*, 12 (2014) 85.
- [5] M.T.K. Tsui, L.M. Chu, *Chemosphere*, 52 (2003) 1189.
- [6] J. Marc, M. Le Breton, P. Cormier, J. Morales, R. Bellé, O. Mulner-Lorillon, *Toxicol. Appl. Pharmacol.* 203 (2005) 18.
- [7] H. Fernandes-Silva, P. Vaz-Cunha, V.B. Barbosa, C. Silva- Gonçalves, J. Correia-Pinto, R.S. Moura, *Cell. Mol. Life Sci.* (2017)
- [8] M. Rhinn, P. Dollé, *Development* 139 (2012) 843.
- [9] V. Avantaggiato, D. Acampora, F. Turto, A. Simeone, *Dev. Biol.* 175 (1996) 347.
- [10] A.J. Durston, J.P. Timmermann, W.J. Hage, H.F. Hendriks, N.J. de Vries, M. Heideveld, P.D. Nieuwkoop, *Nature* 340 (1989) 140.
- [11] A. Paganelli, V. Gnazzo, H. Acosta, S.L. Lopez, A.E. Carrasco, *Chem Res. Toxicol.* 23 (2010) 1586.
- [12] A. Carrasco, In: B. Breckling, R. Verhoeven (Eds.), *Theorie in der Ökologie*, Peter Lang, Frankfurt, Germany, 2013, pp. 113.
- [13] V. Bortagaray, R.C. Aramburu, L. Barrios, P. Ojeda, G. del Puerto, D. Rodríguez-Ithurralde, *J. Dev. Toxicol.* (2010).
- [14] OECD, Test No. 236, (OECD Publishing, Paris, 2013).
- [15] N. Defarge, E. Takács, V.L. Lozano, R. Mesnage, J.S. de Vendomois, G.E. Séralini, A. Székács, *Int. J. Environ. Res. Public Health* 13 (2016) 264.
- [16] Sz. Klátyik, E. Takács, M. Mörtl, A. Földi, Zs. Trábert, É. Ács, B. Darvas, A. Székács, *J. Environ. Anal. Chem.* 97 (2017) 901.
- [17] European Parliament and Council, Directive 2010/63/EU (2010).
- [18] R.K.T. Kam, Y.D., Yonglong, *Cell Biosci.* 2 (2011) 11.
- [19] M. Clagett-Dame, D. Knutson, *Nutrients* 3 (2011) 385-428.
- [20] L.M.Y. Lee, C.-Y. Leung, W.W.C. Tang, H.-L. Choi, Y.-C. Leung, P.J. McCaffery, C.-C. Wang, A.S. Woolf, A.S.W. Shum, *Proc Natl Acad Sci U S A.* 109 (2012) 13668.

## TiO<sub>2</sub>-Cu NANOKOMPOZITOK ELŐÁLLÍTÁSA ÉS VIZSGÁLATA VALÓS- ÉS MODELLSZENNYEZŐK LEBONTÁSÁRA

Hampel Boglárka<sup>1,3</sup>, Pap Zsolt<sup>2,3</sup>, Hernádi Klára<sup>1</sup>, Kovács Gábor<sup>1,3</sup>, Lucian Baia<sup>3,4</sup>

1. Department of Applied and Environmental Chemistry, University of Szeged, H-6720

Szeged, Rerrich Béla tér 1, Hungary

2. Institute of Environmental Science and Technology, University of Szeged, H-6720 Szeged,

Tisza Lajos körút 103, Hungary

3. Nanostructured Materials and Bio-Nano-Interfaces Center, Interdisciplinary Research Institute on Bio-Nano-Sciences, Babeş-Bolyai University, 400271 Cluj-Napoca, Romania

4. Faculty of Physics, Babeş-Bolyai University, RO-400084, Mihail Kogălniceanu 1, Cluj-Napoca, Romania

e-mail: hampelboglarka@chem.u-szeged.hu

### Abstract

Photocatalysis is a research field that offers a variety of environmentally friendly solutions for the degradation of organic pollutants. With this method, the different contaminants can be oxidized to carbon dioxide and water, which are obviously no longer harmful. Among the semiconductors TiO<sub>2</sub> is the most studied and used photocatalyst because of its non-toxicity, high photocatalytic performance, chemical inertness, environmentally benign nature and low cost. In the present work copper nanoparticles were deposited on two different commercial TiO<sub>2</sub> (Evonik Aeroxide P25 and Aldrich anatase). During the synthesis, the concentration of copper was systematically varied (0.5%, 1.0%, 1.5%, 5.0% and 10.0 wt.%). The morpho-structural properties were investigated using XRD, TEM, EDX and DRS methods. The photocatalytic activity was evaluated under UV-light, using methyl orange as a model- and ketoprofen as a real pollutant.

### Bevezetés

A heterogén fotokatalízis lényege, hogy ha egy félvezetőt egy megfelelő hullámhosszúságú fényel világítunk meg, akkor a szerves szennyezőt (esteleges köztitermékeken keresztül/több lépésben) CO<sub>2</sub>-ra, H<sub>2</sub>O-re és egyéb egyszerű ionokra bontja el, amelyek már a környezet számára nem veszélyesek [1]. Ha a gerjesztést kiváltó energia (pl. UV-, vagy látható fény) nagyobb vagy egyenlő a tiltottsáv-szélességének energiaértékével, akkor a vegyértéksávban található elektron gerjesztődik, majd a vezetési sávba kerül, maga után hagyva egy pozitív töltésű ún. „lyukat” [2]. Ezek a fotogenerált elektronok (e<sup>-</sup>) és lyukak (h<sup>+</sup>) redox folyamatokhoz vezetnek, amelyekben az elektron a redukciós, míg a lyukak az oxidációs folyamatokért felelősek [3], amelyek ha nem hasznosulnak végbemegy a rekombináció. A félvezető fotokatalizátorok közül számos példa található a szakirodalomban, pl: ZnO [4], WO<sub>3</sub> [5], SnO<sub>2</sub> [6], CuO [7], stb. Az összes közül a leginkább elterjedt és leggyakrabban alkalmazott a titán-dioxid, mivel nem mérgező a környezet számára, kémiailag inert, jó fotokatalitikus tulajdonsággal rendelkezik és alacsony áron megvásárolható [8]. A TiO<sub>2</sub>-nak rengeteg előnyös tulajdonsága mellett a legnagyobb hátránya, hogy csak az UV tartományban nyel el, amely a napfénynek csupán a 3-4%-a. A titán-dioxid fotokatalitikus aktivitása jelentősen növelhető, ha annak felületére különböző fémeket/nemesfémeket választanak le. A szakirodalomból számos példa található erre, a kutatók eddig Au [9], Ag [10], Pt [11], Cu [12] és Pd nanorészecskéket [13] is felvittek ezeknek a félvezetőknél a felületére és bizonyították, hogy ezáltal elérhető az aktivitás növelése.

## Kísérleti rész

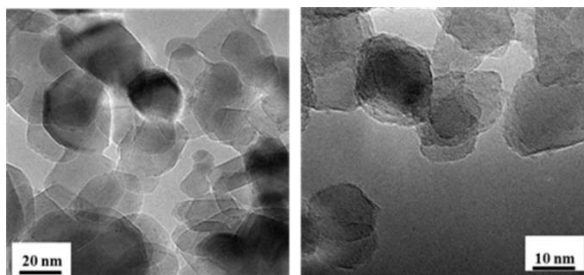
Kutatásunk során két ipari titán-dioxidot (Evonik Aeroxide P25 és Aldrich anatáz) vittünk kompozitba réz nanorészecskékkel. Az összes kompozit előállítása *in situ* módszerrel történt, tehát a szintézist a titán-dioxid szuszpendálásával kezdtük desztillált-vízben. Nátrium-citrátot adagoltunk a réz-nanorészecskék részecskeméretének a szabályozása végett, amelyeket kémiai redukcióval nyertünk  $\text{CuCl}_2$  oldatból, nátrium-borohidrid oldat használatával. Az így kapott szuszpenziót (amely tartalmazta a  $\text{TiO}_2$ -t és a réz nanorészecskéket) szárítottuk, centrifugális mosásnak vetettük alá, végül pedig ismét szárítottuk és így nyertük a por állagú mintákat. A réz tömegszázalékos tartalmát illetően 5 különböző mintát állítottunk elő mindkét alapkatalizátorra: 0,5%, 1%, 1,5%, 5% és 10% réz tartalommal.

## Eredmények

### Anyagszerkezeti jellemzések

A Cu nanorészecskék jelenlétének az ellenőrzésére elsősorban transzmissziós elektronmikroszkópiás felvételeket készítettünk. Az 1. ábrán két P25 alapú kompozit látható. A sötétebb „foltok” a réz nanorészecskéket jelölik, melyek mérete 3-8 nm, amíg a nagyobb részecskék a P25 anatáz és rutil kristályait, melyek mérete 20-40 nm.

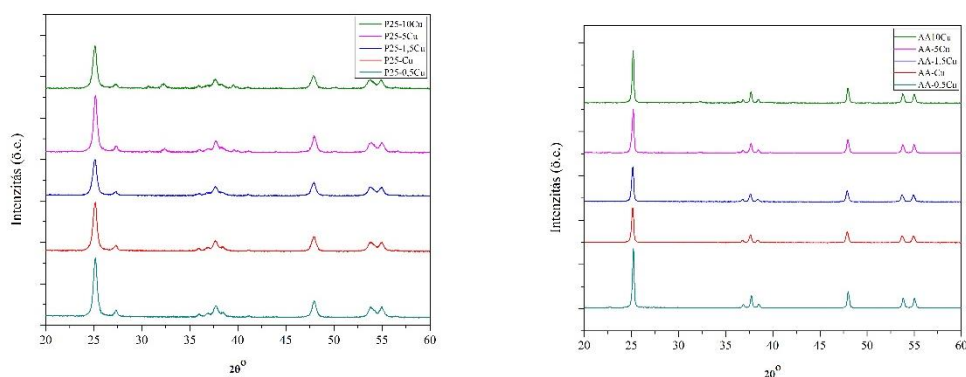
A kompozitok összetételének az ellenőrzésére energiadiszperzív röntgenspektroszkópiás méréseket végeztünk. Kiszámoltuk a réz valós tartalmát az AA alapú kompozitok esetében. Azt vettük észre, hogy amint növekszik az elméleti réz-tartalom úgy növekszik az eltérés az elméleti és valós tartalom között. Ez magyarázható azzal, hogy nem redukálódott az egész réz tartalom teljes mértékben illetve egy része átalakult  $\text{CuO}$ -dá (XRD is bizonyítja).



1. ábra: P25-10Cu TEM felvételei

A diffúz reflexiós spektrumok különböző lefutásúak a Cu tartalom függvényében, azaz minden esetben sikerült befolyásolni a gerjesztési küszöböt. Kiszámoltuk és megállapítottuk, hogy a réz jelenléte minden esetben csökkentette a tiltottsáv-szélesség értékét, ami azért jó mert ez által a katalizátorok gerjesztési küszöb értéke a látható fény irányába tolódott el.

A röntgen-diffraktogramokon észrevehető, hogy a réz nanorészecskék jelenléte nem befolyásolta a részecskeméretet és kristályszerkezetét a  $\text{TiO}_2$ -nak, azonban abban az esetben amikor a 10% Cu-t tartalmazó kompozitokat vizsgáltuk, akkor újabb reflexiók megjelenését vettük észre  $30-35^\circ 2\theta$  között, amelyek a  $\text{CuO}$ -ra jellemzőek.

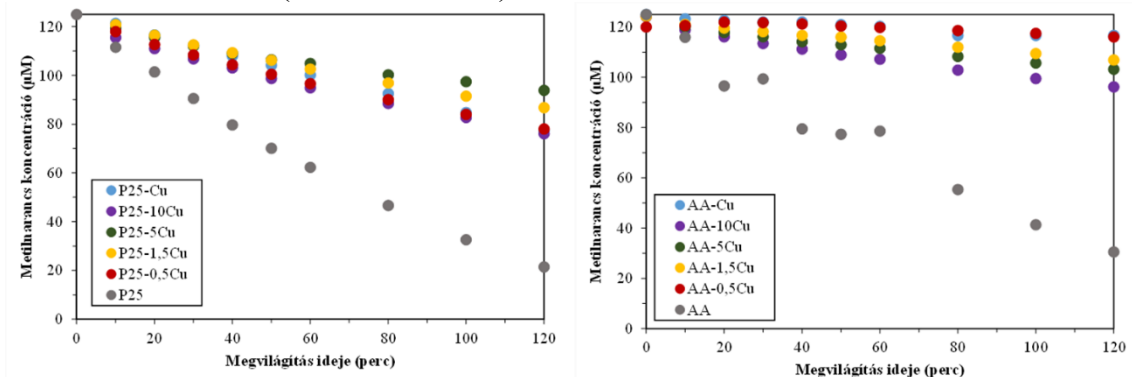


2. ábra: A kompozitok röntgen diffraktogramja

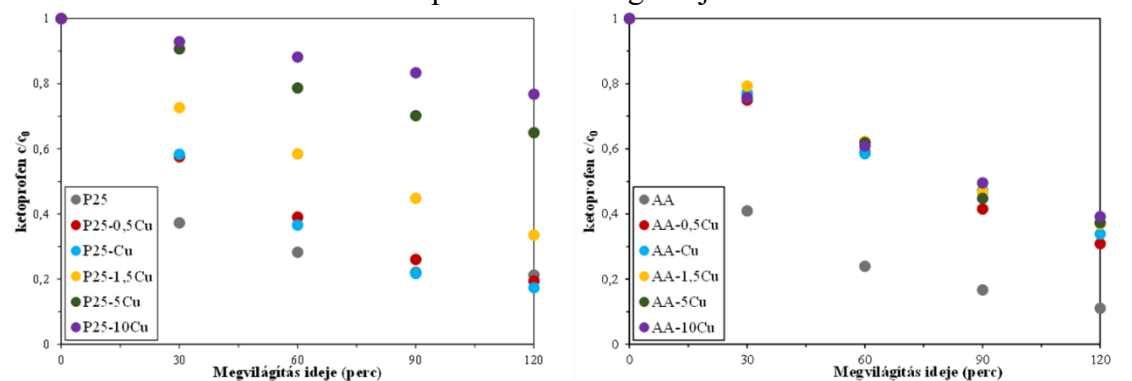
Fotokatalitikus aktivitás vizsgálata

Sajnos a rézzel módosított katalizátorok egyikének sem sikerült jobb fotokatalitikus aktivitást mutatni metilnarancs bontásra, mint az alapkatalizátoroknak. Azonban mindkét esetben a legjobb fotokatalitikus aktivitást az a kompozit mutatta, amelyik 10%-ban tartalmazott réz nanorészecskét.

A ketoprofenet mindegyik fotokatalizátor bontotta, sőt a P25 alapú anyagok egy részének sikerült jobb aktivitást elérnie, mint az alapkatalizátornak. A metilnarancs bontással ellentétben a ketoprofenre a réz tartalmának a növelése csökkentette az aktivitást mind a két esetben, a legjobb fotokatalitikus aktivitással pedig azok a kompozitok rendelkeztek, amelyek 0,5% Cu-t tartalmaznak (mindkét esetben).



3. ábra: A kompozitok bomlásgörbéje metilnarancsra



4. ábra: A kompozitok bomlásgörbéje ketoprofenre

## **Következtetések**

Az XRD és EDAX vizsgálatokból arra következtettünk hogy azon kompozitok estében, melyek több %-ban tartalmaznak rezet CuO is megjelenik a nanorészecskék mellett. A kompozitok kialakításával sikerült a gerjesztési küszöböt is eltolni a látható fény irányába. A metilnarancs bontására ugyan nem sikerült jobb fotokatalitikus aktivitást elérni a kompozit kialakítással, megfigyeltük, hogy a 10% Cu-t tartalmazó mintáknak sikerült a leginkább közel férközni az alapkatalizátorok aktivitásához. A ketoprofen bontásra a P25 alapú kompozitoknak sikerült jobb fotokatalitikus aktivitást elérni, mint az alapkatalizátornak. Mindkét esetben pedig a 0,5% rezet tartalmazó minták bontották le a leginkább a ketoprofen oldatot.

## **Köszönetnyilvánítás**

Hampel Boglárka köszönetet mond a Balassi Intézet, Márton Áron Szakkollégiumának a Tehetséggondozói Szakkollégiumban való támogatásért és a Babeş-Bolyai Tudományegyetemnek a Fialat Kutatói Kiválósági Ösztöndíjért.

## **Hivatkozások**

- [1] J. Zhao, X. Yang: Photocatalytic oxidation for indoor air purification: a literature review (Building and Environment 38 (2003) 645–654)
- [2] U. I. Gaya, A. H. Abdullah: Heterogeneous photocatalytic degradation of organic contaminants over titanium dioxide: A review of fundamentals, progress and problems (Journal of Photochemistry and Photobiology C: Photochemistry Reviews 9 (2008) 1–12)
- [3] D. Spasiano, R. Marotta, S. Malato, P. Fernandez-Ibanez, I. Di Somma: Solar photocatalysis: Materials, reactors, some commercial and pre-industrialized applications. A comprehensive approach (Applied Catalysis B: Environmental (2014))
- [4] M. A. Behnajady, N. Modirshahla, R. Hamzavi: Kinetic study on photocatalytic degradation of CI Acid Yellow 23 by ZnO photocatalyst (Journal of Hazardous Materials 133 (2006) 226-232)
- [5] A. Watcharenwong, W. Chanmanee, N. R. Tacconi, C. R. Chenthamarakshan; R. Kajitvichyanukul, K. Rajeshwar: Anodic growth of nanoporous WO<sub>3</sub> films: Morphology, photoelectrochemical response and photocatalytic activity for methylene blue and hexavalent chrome conversion (Journal of Electroanalytical Chemistry 612 (2008) 112-120)
- [6] S. K. Kansal, M. Singh, D. Sud: Studies on photodegradation of two commercial dyes in aqueous phase using different photocatalysts (Journal of Hazardous Materials 141 (2007) 581-590)
- [7] M. Farbodn, N. M. Ghaffari, I. Kazeminezhad: Fabrication of single phase CuO nanowires and effect of electric field on their growth and investigation of their photocatalytic properties (Ceram. Int. (2014) 40, 517–521)
- [8] W.-J. Ong, L.-L. Tan, S.-P. Chai, S.-T. Yong, A. R. Mohamed: Facet-Dependent Photocatalytic Properties of TiO<sub>2</sub>-Based Composites for Energy Conversion and Environmental Remediation (ChemSusChem (2014) 7, 690 – 719)
- [9] I.M. Arabatzis, T. Stergiopoulos, D. Andreeva, S. Kitova, S.G. Neophytides, P. Falaras: Characterization and photocatalytic activity of Au/TiO<sub>2</sub> thin films for azo-dye degradation (Journal of Catalysis (2003) 127–135)
- [10] J. Yu, J. Xiong, B. Cheng, S. Liu: Fabrication and characterization of Ag–TiO<sub>2</sub> multiphase nanocomposite thin films with enhanced photocatalytic activity (Applied Catalysis B: Environmental (2005) 211–221)

- [11] L. Yu, Y. Shao, D. Li: Direct combination of hydrogen evolution from water and methane conversion in a photocatalytic system over Pt/TiO<sub>2</sub> (*Applied Catalysis B: Environmental* 204 (2017) 216–223)
- [12] G. Colón, M. Maicu, M.C. Hidalgo, J.A. Navío: Cu-doped TiO<sub>2</sub> systems with improved photocatalytic activity (*Applied Catalysis B: Environmental* 67 (2006) 41–51)
- [13] O. T. Alaoui, A. Herissan, C. L. Quoca, M. M. Zekri, S. Sorgues, H. Remita, C. Colbeau-Justin: Elaboration, charge-carrier lifetimes and activity of Pd-TiO<sub>2</sub> photocatalysts obtained by gamma radiolysis (*Journal of Photochemistry and Photobiology A: Chemistry* 242 (2012) 34–43)

## MULTI-STAGE MEMBRANE PROCESSES FOR WASTEWATER TREATMENT

**Szabolcs Kertész, Péter Bor, Sándor Beszédes, Veréb Gábor,  
László Zsuzsanna, Hodúr Cecília**

*Department of Process Engineering, Faculty of Engineering, University of Szeged, H-6725  
Szeged, Moszkvai krt. 9, Hungary  
e-mail: kerteszk@mk.u-szeged.hu*

### **Abstract**

In this work the feasibility of the purification of dairy wastewater was investigated by multi-stage membrane separation techniques using ultrafiltration and nanofiltration. In order to investigate the applicability of the single and multi-stage processes, first, the permeate fluxes and flux decline rates were analyzed. Secondly, membrane rejections, based on chemical oxygen demand, conductivity and turbidity were compared. Finally, the biogas production from the concentrates were measured and compared for further utilization of the membrane separation by-products.

### **Introduction**

Before discharging into living waters or sewerage, appropriate wastewater treatment is necessary to effectively decrease the pollution, especially organic load of dairy wastewater. Effluents need to be effectively treated to meet the strickening European Union environmental regulations. Nowadays the commonly used technologies such as sedimentation or oxidation, membrane separation can offer a novel solution. Although the advantages of membrane separations are remarkable, like high flux and contaminant rejection or good mechanical strength and durability, fouling of membranes are still a critical issue which limits the application of larger scale industrial utilizations [1, 2]. Increasing the shear rate on the membrane surface by module vibration can reduce membrane fouling by altering the concentration polarization, decreasing the cake layer and to reduce the deposition of particles on the surface [3, 4]. Limited data is available from scientific articles on the application of vibratory shear enhanced processing (*VSEP*) for dairy wastewater treatment [5, 6], especially in multi-stage membrane systems [7].

Ultrafiltration (*UF*) and nanofiltration (*NF*) have been proven to be effective at dairy wastewater treatment and have many advantages: almost complete retention of proteins and clean effluent water and low energy consumption. In addition, Zhang et al. [8] have reported that the shear stress could effectively remove casein micelles and whey protein layer on the membrane surface and the cleaning temperatures of 35 and 50°C had a much greater cleaning capacity than that of 20°C. However, severe non-washable membrane fouling could form inside the pores caused by dairy particles and proteins. Recently, other studies have reported that membrane mitigation can be occurred by increasing the shear rate at the membrane surface that can scour and reduce the deposit of foulants; vibrations of the membrane can create high surface shear stresses, which can efficiently improve both the permeate flux and mass transfer [9, 10, 11].

In the present study, we investigated the efficiency of a multi-stage membrane system in terms of permeate flux, flux decline rate, membrane rejection and the concentrates biogas production performances. In the first stage a shear enhancement *UF* device was used for controlling membrane fouling in filtration dairy wastewater. In the second stage a classical cross-flow *NF*



device was tested for two possible reasons: achieving more effective foulants removal and to reach a much higher volume reduction ratio in order to compare the results with only one stage test.

### Experimental

Synthetic dairy wastewater was used for the separation experiments from skimmed milk powder (5 g/dm; InstantPack, Hungary) and anionic surfactant cleaning agent Chemipur CL80 (0.5 g/dm; Hungaro Chemicals, Hungary).

The electric conductivity and pH of the samples was determined with a C5010 type multimeter (Consort, Belgium). The turbidity was measured with a HACH2100AN turbidimeter (Hach, Germany). The samples were analysed with a chemical oxygen demand (COD) ET 108 digester and a PC CheckIt photometer (Lovibond, Germany). All of the analytical measurements were repeated three times to calculate an accurate average.

The first stage of the multi-stage membrane filtration experiments was carried out using a VSEP L Series membrane device equipped with a single circular membrane of 503 cm<sup>2</sup> with an outer radius of 13.5 cm and inner radius of 4.7 cm for UF (New Logic Research Inc., USA). Supporting the membrane housing there is a vertical shaft, which acts as a torsion spring and transmits the oscillations of a lower plate, and the housing containing the membrane oscillates azimuthally with displacement amplitude, which was adjusted to be 2.54 cm on the outer rim. In figure 1/a detailed schematic diagram description of VSEP system is given. A more detailed description of it can be found in our earlier publication [12]. The second stage of the multi-stage membrane filtration experiments was carried out with an Uwatech 3DTA classical laboratory cross-flow membrane apparatus (Uwatech GmbH., Germany) with the use of flat-sheet standard membranes with a filtering surface area of 156 cm<sup>2</sup> for both UF and NF experiments (fig. 1/b).

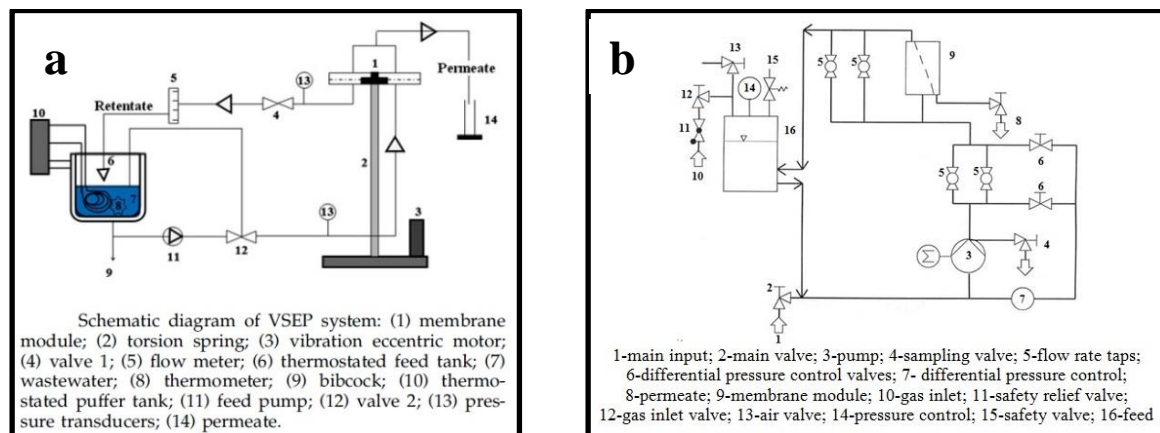


Figure 1. Diagrams of membrane separation devices (a: first stage: a vibratory shear enhanced processing [12], VSEP device; b: second stage: classical cross-flow membrane, 3DTA apparatus)

All the separation experiments were carried out at 50±1°C, transmembrane pressure was set to 0.8 MPa in case of UF, and 3 MPa for NF. Three polyethersulfone 10 kDa, 7 kDa and 5 kDa UF membranes were tested, and a thin film composite (TFC) NF membrane with a molecular weight cut-off (MWCO) of 200 Da.

Batch mesophilic anaerobic digestion tests were carried out at 37°C for 30 days to determine the biogas yield from the concentrates. Biogas production was detected by pressure increase

method in continuously stirred reactors with volume of 250mL equipped by OxiTop-C® measuring heads (WTW, Germany).

## Results and discussion

### Permeate fluxes

The single *UF* experiments were carried out three different *MWCO* in order to compare the effects of them to the second stage. The scope of the multi-stage separation experiments could be different. In one hand, when *NF* of the *UF* permeates was tested, the *UF* was practically a pre-filtration process before *NF*. By comparing the multi-stage experiments with the single filtration ones, the effect of the pre-filtration was investigated. On the other hand, when *NF* of the *UF* concentrates were carried out, the aim was to process the concentrates until a much higher volume reduction ratio (*VRR*). The volume reduction ratio, *VRR* [-], was defined as

$$VRR = \frac{V_F}{V_F - V_P} \quad (2)$$

where  $V_F$  is the volume of the feed [m<sup>3</sup>] and  $V_P$  is the volume of the permeate [m<sup>3</sup>] at any time. Since the further utilization of the membrane filtration concentrates are always an important issue, a post-treatment was also investigate. Therefore, the biogas yields of concentrates with different concentrates from different stages were tested.

The first stage *UF* and second stage *NF* experiments were carried out in order to investigate the permeate fluxes, flux decline rates, membrane rejections and biogas production of the concentrates. First, the permeate fluxes and flux decline rates were analyzed. The permeate flux,  $J$  [L/m<sup>2</sup>hbar] was defined using equation 1 in order to compare fluxes of the two different filtration devices:

$$J = \frac{dV_p}{dt} \frac{1}{A_m \times TMP} \quad (1)$$

where  $V_p$  is the volume of permeate [L],  $t$  is the membrane filtration time [h] and  $A_m$  is the effective membrane area [m<sup>2</sup>] and  $TMP$  is the transmembrane pressure [bar].

Figure 2 shows the permeate fluxes (a) and flux decline rates,  $J/J_0$  (b) of multi-stage *UF* and *NF* membrane processes as a function of filtration time.

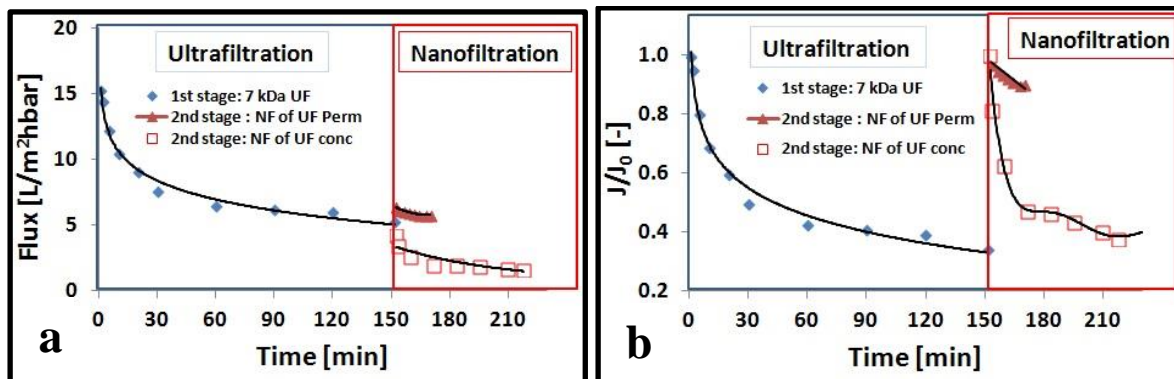


Figure 2. Fluxes of the different membrane filtration stages (a) and flux decline rates ( $J/J_0$ ) with different processes (b) (first stage: *VSEP*,  $A_{vibr} = 2.54$  cm, 7 kDa *PES* membrane; second stage: *Uwatech 3DTA*, 200 Da *TFC* membrane)

Due to membrane fouling, all of the membrane fluxes decreased during the filtration procedure. As shown in right side of the figure 2/a, the *NF* of *UF* permeate fluxes were higher than the *NF* of *UF* concentrate fluxes. Furthermore the filtration time was also shorter in the case of *UF* permeate till the end of the experiments, when achieved the same final *VRR* of 8. (The *VSEP* had a dead volume of 2 L, while *3DTA* apparatus had a significantly smaller dead volume of 0.2 L.) In the first stage 10 L of feed model wastewater was ultrafiltered to a concentrate volume of 2 L to *VRR* of 5. In second stage 1.6 L of concentrate was used for the experiments and processed to a concentrate to the volume of 0.2 L (*VRR*=8). The multi-stage concentrations resulted in a total *VRR* of 40.

In figure 2/b, the average flux decline rate was higher in case of *NF* of *UF* concentrate than *NF* of *UF* permeate, revealed that a higher fouling tendency was observed in that case. Is also visible that less time is needed to achieve the same final *VRR* when permeate of *UF* was tested by *NF*. It can be also seen that by using a new nanofiltration membranes in the beginning of the second stage the extent of membrane fouling can be lessened in both *NF*, than in the first stage *UF*.

### Membrane rejections

The original synthetic dairy wastewater had an average *COD* of 4770 mg/L, *EC* of 0.821 mS/cm and turbidity of 221.5 NTU. *COD* represents the total organic load, and *EC* shows the salts in the analyzed samples. The selectivity of the membrane, *R* [%], for a given solute was expressed by the average retention using the following equation 3:

$$R = \left(1 - \frac{c}{c_0}\right) 100 \quad (3)$$

where *c* is the average concentration of the solute in the permeate phase, and *c*<sub>0</sub> is the concentration of the solute in the feed wastewater expressed by chemical oxygen demand, conductivity or turbidity.

In figure 3/a, it can be observed that the first stage resulted 75.31, 79.92 and 52.52 % *COD* rejection using 5 kDa, 7 kDa, and 10 kDa *UF* membranes, respectively. In figure 3/b, it is visible that the *COD*, *EC* and turbidity rejections could be effectively increased by the second stage. Implementation of the multi-stage clarification stages (with 7 kDa *UF* then *NF*) the *COD*, *EC* and *Turb* rejection increased by 19.08, 20.66 and 0.11 %, respectively.

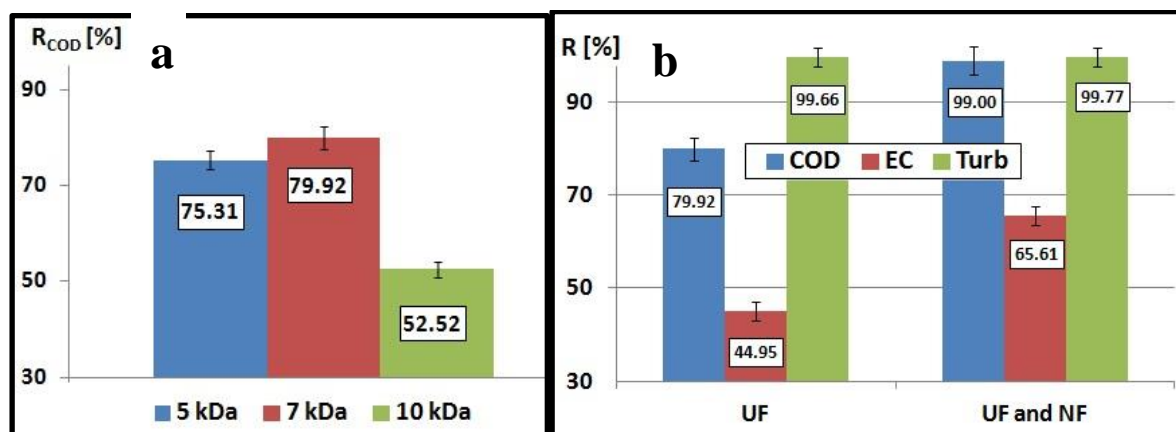


Figure 3. First stage (a) (Ultrafiltration, *UF*) and multi-stage (b) (Ultrafiltration followed by Nanofiltration, *UF* and *NF*) membrane process rejections expressed by of chemical oxygen demand (*COD*), electric conductivity (*EC*) and turbidity (*Turb*)

Figure 4 compares the biogas production of first stage of *UF* concentrates, *UF* permeate, original wastewater (fig. 4/a) and concentrates of 5 kDa *UF* followed by *NF* and 10 kDa *UF* followed by *NF* concentrates of two-stage separation tests (fig. 4/b). On the one hand, comparing the pore sizes of the *UF* membranes revealed that concentrates of the smaller pore size *UF* membrane had higher biogas production. All of the *UF* concentrates had higher, but permeate of the *UF* had lower biogas production than the original feed. On the other hand, in the multi-stage process it increased almost two times and concentrates of the 5 kDa *UF* followed by *NF* had the highest biogas production.

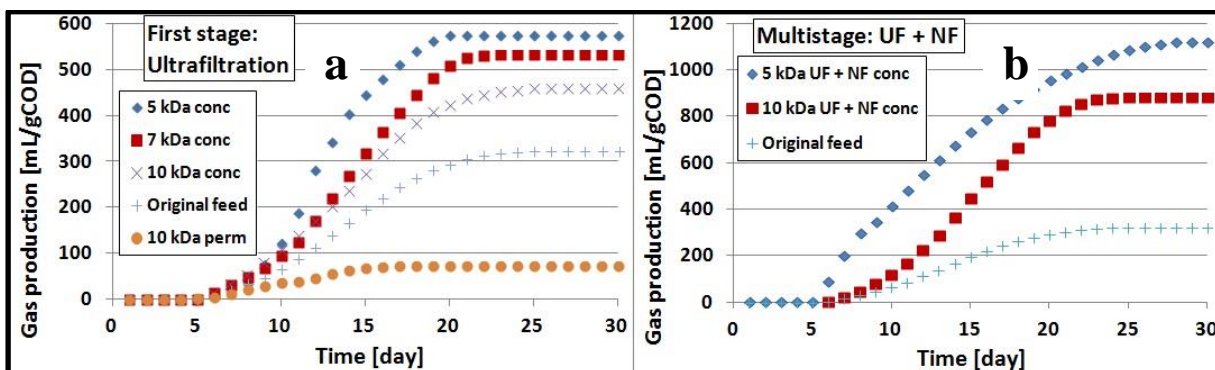


Figure 4. First stage (a) (Ultrafiltration, *UF*) and multi-stage (b) (Ultrafiltration followed by Nanofiltration, *UF* and *NF*) membrane process biogas productions from different concentrates

## Conclusion

In this study the purification of dairy wastewater was investigated by multi-stage membrane separation techniques by ultrafiltration and nanofiltration. In order to investigate the effects of the second stage of the processes, the influences of permeate fluxes, flux decline rates, membrane rejections and biogas production were measured and compared. The nanofiltration of ultrafiltration permeate fluxes were higher than the nanofiltration of ultrafiltration concentrate fluxes. It was observed that the chemical oxygen demand, conductivity and turbidity membrane rejections significantly increased by the second nanofiltration stage. Comparing the pore sizes of the ultrafiltration membranes revealed that concentrates of the smaller pore size ultrafiltration membrane had higher biogas production. All of the ultrafiltration concentrates had higher, but its permeate had lower biogas production than the feed. Furthermore, in the multi-stage process, it increased almost two times and concentrates of the 5 kDa ultrafiltration followed by nanofiltration had the highest biogas production.

## Acknowledgements



Supported by the UNKP-17-4 New National Excellence Program of the Ministry of Human Capacities. The authors are also grateful for the János Bolyai Research Scholarship of the Hungarian Academy of Sciences and the project Hungarian Science and Research Foundation (OTKA contract number K 115691).

## References

- [1] K. Wang, A.A. Abdalla, M.A. Khaleel, N. Hilal, M.K. Khraisheh, *Desalination* 411 (2017) 190.
- [2] B. Wu, R. Wang, A.G. Fane, *Water Res.* 110 (2017) 120.
- [3] L.H. Ding, M.J. Jaffrin, *Sep. Sci. Technol.* 49 (2014) 1953.
- [4] J. Luo, W. Cao, L.H. Ding, Z. Zhu, Y. Wan, M.Y. Jaffrin, *Sep. Sci. Technol.* 96 (2012) 194.

- [5] M.Y. Jaffrin, *J. Membr. Sci.* 324(1-2) (2008) 7.
- [6] O. Akoum, M.Y. Jaffrin, L.H. Ding, M. Frappart, *J. Membr. Sci.* 235 (2004) 111.
- [7] B. Farizoglu, S. Uzuner, *Biochem. Eng. J.* 57 (2011) 46.
- [8] W. Zhang, L. Ding, M.Y. Jaffrin, B. Tang, *Chem. Eng. J.* 325 (2017) 457.
- [9] T. Li, A.W.K. Law, M. Cetin, A.G. Fane, *J. Membr. Sci.* 427 (2013) 230.
- [10] F. Zhao, H. Chu, Y. Zhang, S. Jiang, Z. Yu, X. Zhou, J. Zhao, *J. Membr. Sci.* 529 (2017) 215.
- [11] M. Pourbozorg, T. Li, A.W.K. Law, *Water Res.* 99 (2016) 101.
- [12] Sz. Kertész, Á. Veszprémi, Zs. László, J. Csanádi, G. Keszthelyi-Szabó, C. Hodúr, *Desal. Water Treat.* 55 (2015) 2836.

## A KONYHASÓ-FOGYASZTÁS ÖSSZEFÜGGÉSE AZ ALACSONY ÉS A MAGAS VÉRNYOMÁSSAL

Kiss Zoltán

*Csongrád Megyei Egészségügyi Ellátó Központ Hódmezővásárhely-Makó*

*Belgyógyászati Osztály*

*H-6900 Makó, Kórház u. 2. P.: 72.*

*e-mail: kiss.zoltan@csmekhm.hu*

### Summary

According to the concerning scientific and medical literature, it is obvious that lowered salt (NaCl) intake lowers high blood pressure. Related epidemiologic randomized studies show that the pathomechanism of essential hypertension is debated, obscure and multifactorial, because inflammatory, genetic (tubular  $\text{Na}^+$ -retention because of gene mutation), civilization-environmental, life-style, endogen natriuretic factors also play a role and lowered/increased  $\text{Na}^+$ -intake – via different mechanism – similarly influences the genesis of hypertension and increased cardiovascular risk adding long-term deleterious central nervous system consequences of limited salt intake. At the same time one can not agree with expert opinion, i.e. the population-wide trials without preliminary screening are unnecessary, because their results differentiate a subgroup, in which the hypertension is salt-dependent or resistant, therefore posttrial investigations will be necessary. The 24-hour urine  $\text{Na}^+$ -excretion has a high degree of intraindividual variation, but measures of multiple urine-collections as an average provide more reliable information on  $\text{Na}^+$ -homeostasis.

### Bevezetés

Már 1 milliárd feletti a magas vérnyomásban szenvedők száma a Földön. 10%-ra becsülik azok számát, akik megfelelő, szakszerű gyógyszeres kezelésre sem reagálnak megfelelően (1). Ez részben utal arra, hogy a pathogenesis nem megoldott. Hosszas fennállás esetén súlyos szövődmények, rokkantságot is okozó szélütés-agyvérzés, dementia (multiinfarct), szív- és veseelégtelenség jelentkezhet. Arra a felismerésre, mely szerint a csökkent konyhasóbevitel (1 g NaCl-ben  $400 \text{ mg Na}^+ = 23 \text{ mmol}$  van) csökkenti a magas vérnyomást, népegészségügyi programok indultak.

### A konyhasóbevitel és a magas vérnyomás összefüggése

Elfogadott teória, hogy a sómegvonás általában csökkenti, a fokozott sóbevitel pedig növeli a vérnyomást (2). A vese csökkent  $\text{Na}^+$ -kiválasztása só- és vízretenciával jár, emelkedik a vérplazma és a cerebrospinalis folyadék, a liquor  $\text{Na}^+$ -tartalma, ami szimpatikotoniát, következményes vasoconstrictiot és perifériás ellenállás növekedést, vérnyomásemelkedést okoz. Ebben elsősorban a bőr és a vázizomzat sótartalom-növekedésének van szerepe (3). Régóta ismeretes, hogy a magas vérnyomás részben gyulladásos betegség (4).

A gyulladást az IL-17-t termelő lymphocyták közvetítik, szintjük emelkedett hypertoniában és az immunsuppressiv szerek csökkentik a vérnyomást (5). Az immunsejtek (keringő antigénprezentáló monocyták, makrofágok, dendrit sejtek, T-sejtek) beszűrik a vesét, az érrendszer és citokinek révén befolyásolják az excretiot és az ér-relaxációt. Yi és munkatársai (6) kimutatták, hogy a magas sótartalmú étel emberben növeli a keringő monocyták számát az alacsony sótartalommal összehasonlítva. A gyulladásos citokinek (IL-6 és IL-23) szintje nő, az



antiinflammatorikus (IL-10) csökken magas sóbevitel mellett. Az IL-23 növeli és fenntartja az embrionális T-sejtek, T-helper (Th17) -sejtek alakuláshoz szükséges polarizációt.

A reaktív O<sub>2</sub>-gyökök (ROS) minden sejt mitochondriumaiban képződnek és az erekben proinflammatorikus géneket aktiválnak (7). Az érbelhártya által termelt NO szerepe is fontos (8), mivel a ROS és a vasodilatator-NO egyensúly eltolódása az előbbi javára insulin-resistentiát, endothel dysfunctiot, bal kamra hypertrophiát okoz sóérzékeny magas vérnyomásban (9).

Az alacsony konyhasóbevitel kétségkívül csökkenti a vérnyomást (10), de van egy jelentős csoportja a népességnek, akikben a konyhasómegvonás vagy hosszantartó vízajtó szedése éppen emeli a renin-angiotensin-aldosteron rendszer stimulálása révén. A ROS-emelkedést az angiotensin-II okozza (11).

Az NaCl emeli az extracellularis folyadéktérfogatot és a perctérfogatot. Ennek ellensúlyozására a vese- és a perifériás vascularis rezisztencia csökken NO fokozott termelése révén só-rezisztenciában, míg só-szenzitív egyénekben ez elmarad és a vérnyomás emelkedik. Az ok az öröklött vagy szerzett endotel diszfunkció, **TGF**-béta-túltermelés, oxidatív stressz, csökkent NO. A hosszantartó, magas konyhasótartalmú étkezés viszont endotel-diszfunkcióhoz vezet még a sórezisztens egyénekben is.

Civilizációs ártalomként (környezeti toxicus fémek, Al, As és fokozott stress) jelentkezik az ionpumpa, a Na<sup>+</sup>K<sup>+</sup>ATPase bénítása endogen gátlók, ouabain (=Na<sup>+</sup>-uretikus faktor, 12), ill. a bufadienolidok révén. Utóbbi elválasztását a fokozott konyhasóbevitel még tovább fokozza, de eredendően az erek simaizmában emelkedik a citosol Na<sup>+</sup>, a kiegyenlítő Na<sup>+</sup>-Ca<sup>++</sup> antiport révén nő a citosol Ca<sup>++</sup>, vasoconstrictiot okozva (13), ami kedvezőtlen a szív-érrendszeri morbiditást és halálozást illetően is (14).

A vizelettel történő Na<sup>+</sup>-kiválasztást illetően több mint 100.000 felnőttben 90%-ban magas és mérsékelt (>5.99-, 3-5.99 g/nap) értéket kaptak. 10% <3 g/nap, 4% ennél kevesebbet ürített. A magas Na<sup>+</sup> és alacsony K<sup>+</sup>-ürítőkben direkt összefüggés volt a magas vérnyomással. A szív-érrendszeri rizikó a magas és alacsony Na<sup>+</sup> ürítésű csoportban volt magasabb átlag 3,7 éves megfigyelés alatt (15,16) a 17 országot érintő vizsgálatban. A fokozott K<sup>+</sup>-ürítés ellenkező hatású volt. A vesék szerepe etiológiától függetlenül meghatározó a magas vérnyomás kialakulásában.

A NutriCode tanulmányban (17) linearis összefüggést találtak a szív-érrendszeri halálozás és a nagymértékű konyhasófogyasztás között 1.6 millió esetet vizsgálva. Génhibára utal a disztális nephron epitheliális csatornákon (eNA<sup>+</sup>) zajló Na<sup>+</sup> absorptio kóros fokozódása miatt kialakuló, ún. sófüggő magas vérnyomás. Ray és munkatársai 300 magas és 300 alacsony vérnyomású emberben vizsgálták a gén polimorfizmust (18) 1 hetes alacsony (51.3 mM Na<sup>+</sup>/nap), ezt követő 1 hetes magas (307.8 mM Na<sup>+</sup>/nap) Na<sup>+</sup>-bevitel mellett 1906 résztvevőben. 16 génmutációt azonosítottak. Fokozott működésű csatornát 4 egyénben mutattak ki, akikben nem működő csatorna is volt. 15% só-szenzitív volt, de a vérnyomásértékek igen szórta, jelezve, hogy 1 génmutáció penetrációja rendkívül változó. A só-szenzitivitás normális vérnyomás esetén is fokozott halálozással jár (19). Öröklődő magas vérnyomást Liddle-szindrómában észleltek, amit az epitheliális vese- Na<sup>+</sup>-csatorna mutációja okoz.

### Megbeszélés

A számtalan ellentmondás között az első, hogy a mind a csökkent, mind a fokozott Na<sup>+</sup> bevitel (3000-5000 mg/nap) növeli a szív-érrendszeri betegségek előfordulását (20).

Idült vesebetegségben a csökkent sóbevitel nagyobb halálozási aránnyal jár (21), de a sóbevitel növelésével szintén nő ennek a kockázata (22). A 24 órás Na<sup>+</sup> ürítést 2 évig



vizsgálva a növekvő üritéssel együtt nőtt a szív-érrendszeri kockázat (23). Ezen belül a bal kamra hypertrophia (MR-val vizsgálva) a vérnyomástól függetlenül a bőr Na<sup>+</sup>-tartalmával mutatott összefüggést (24).

Népesség-méretű vizsgálatban (UK, Finnország, Japán) 19-64 évesekben a napi Na<sup>+</sup> bevitel 15%-os csökkentésére (560 mg) a szélütés és a iszkémiás szívbetegség halálozása 40%-al csökkent (25), miközben a szisztolés vérnyomás csak 3 Hgmm-el. 2.5 g NaCl (1000 mg Na<sup>+</sup>)/nap fogyasztásakor az átlagos szisztolás vérnyomás csökkenés 1.7 Hgmm volt (26).

Felvetődött a következő mechanizmus is: alacsony Na<sup>+</sup> bevitelre nő a koleszterin, triglicerid, renin, aldostreon, katekolamin-szint, nő a szív-érrendszeri kockázat. Ugyanakkor az aldostreeron-angiotenzin rendszer fokozott Na<sup>+</sup> és víz reabszorpcióval helyreállítja a Na<sup>+</sup>-egyensúlyt (27).

A Na<sup>+</sup> bevitel csökkentés cukorbetegekben javítja a kreatinin clearancet és csökkenti a fehérjevizelést (28). 5912 magas és normális vérnyomású egyénben a Na<sup>+</sup> bevitel csökkentése 23 %-al csökkentette a szív-érrendszeri eseményeket (29).

Eszenciális magas vérnyomásban több faktor mellett a fokozott Na<sup>+</sup> és a csökkent Ca<sup>++</sup> felvétel szerepét is kimutatták. A vörösvértestekben és limfocitákban csökkent Mg<sup>++</sup> és emelkedett Na<sup>+</sup>-koncentrációt mértek. Kísérleti körülmények között spontán hypertenziós patkányokban az aorta símaizomban alacsonyabb Mg<sup>++</sup> és magasabb Na<sup>+</sup> tartalom van a normotenzívekhez képest. Ennek az oka a Na<sup>+</sup>/Mg<sup>++</sup>-csere működészavara (Na<sup>+</sup>-dependens, Mg<sup>++</sup>-efflux). Az emelkedett intracelluláris Na<sup>+</sup> koncentrációt eszenciális hypertoniában csökkent Na<sup>+</sup>K<sup>+</sup>ATPase aktivitás (Na<sup>+</sup>-pumpa), a fokozott Na<sup>+</sup>H<sup>+</sup> csere és a Na<sup>+</sup>-Li<sup>+</sup> ellentranszport okozhatja. Ugyancsak csökkent a mitochondriális ATP synthase spontán hypertenzív patkányokban együtt a Mg<sup>++</sup>ATP-szubsztráttal. Az ér símaizmában az extracelluláris Mg<sup>++</sup> emelkedés Ca<sup>++</sup>-szint csökkenést okoz. Intracellulárisan viszont a Mg<sup>++</sup>-szint csökkentése csökkent Na<sup>+</sup>K<sup>+</sup>- és Ca<sup>++</sup>ATPase (Ca<sup>++</sup>-pumpa) működéshez vezet, ami fokozott Na<sup>+</sup>-Ca<sup>++</sup>-cserét okoz és így nő az intracelluláris Na<sup>+</sup>-Ca<sup>++</sup> koncentráció (30).

A Na<sup>+</sup>-pumpa (Na<sup>+</sup> K<sup>+</sup>ATPase) az ATP terminális foszfát hidjának hidrolízisével működik. A Na<sup>+</sup>K<sup>+</sup>ATPase alfa2 izoformjának gátlása az endogen ligand oubainnal magas vérnyomáshoz vezet (31). Az ACTH túltermelődés Cushing-szindrómában módosítja ennek működését és kísérletesen egérben és emberben is megváltozik az intracelluláris Na<sup>+</sup>, Ca<sup>++</sup>-koncentráció és a jelátviteli utak (Src, PKC, MAPKK), ami az ouabain közvetítésével magas vérnyomást okoz. Öröklött, familiáris magas vérnyomásban a repolarizációban szükség szerint nyitott-zárt-inaktivált K<sub>v</sub> csatornák közül K<sub>v</sub>B1 mutáció az Ito csökkenést, a K<sub>v</sub>B2 mutáció pedig magas vérnyomást és az életveszélyes szívritmuszavarokat okozó Brugada szindrómát vált ki.

## Következtetések

1. Az áttekintett szakirodalom szerint a népesség-szintű sóbevitel csökkentés szerepe a vérnyomáscsökkentésben önmagában kérdéses, mivel a bevitt mennyiségtől függően, illetve függetlenül a magas és az alacsony Na kiválasztás egyaránt növeli a szív-érrendszeri kockázatot. Mind a magas, mind az alacsony exkréció esetén a fokozott K<sup>+</sup>-kiválasztás ellensúlyozza a magas Na<sup>+</sup> kiválasztást Oparil vizsgálatai szerint (32).
2. Egyidejűleg kimutatták, hogy a konyhasó csökkentése az étrendben csökkenti a gyomorrák, a végstádiumú vesebetegség, a bal kamra hipertrophia, a pangásos szívelégtelenség és az osteoporosis kockázatát. Utóbbi rendkívül kérdéses, mivel a szervezet össz Na<sup>+</sup> tartalmának 30 %-a a csontokban van (33, 34). Magas vérnyomásban – állatban és emberben egyaránt – a bőrben és a vázizomzatban történő só-felszaporodás a vérben mérténél arányában nagyobb (10) és ez az immunrendszere

hatva vaszkuláris és renális gyulladás közvetítésével hipertoniához vezet. Így a szöveti Na<sup>+</sup> lehet terápiás cél.

3. Rendkívül fontos az étrend, hiszen a konyhasó közel 75 %-a kész- és félkésztelekből származik és ennek az arányát a különböző epidemiológiai vizsgálatokban nehéz meghatározni. Utóbbiak értékelésénél rendkívül fontos, hogy konyhasó vagy Na<sup>+</sup>-bevitelről van-e szó, hiszen 1g NaCl = 400 mg Na<sup>+</sup>.
4. Az 1998 óta különböző országokban 2007-ig végzett 13 multicentrikus randomizált klinikai vizsgálatokból kiderült, hogy az olyan fokú Na<sup>+</sup>-bevitel csökkentése, amely csökkenti a vérnyomást, egyúttal növeli szimpatikus aktivitást, csökkenti az inzulin-érzékenységet, aktiválja a renin-angiotenzin rendszert és fokozza az aldoszteron elválasztást (35).
5. A csökkentett sóbevitel hosszútávú következménye lehet a hyponatraemia kialakulása (szerum Na <135 mmol/l), amely kórházi beteganyagban gyakran, 15-20 %-ban, a teljes népességben 2%-ban fordul elő. A szövődmények és a halál független előjele szívelégtelenségben (36), májsugorodásban (37) és neurológiai betegségekben (38). Enyhe fokban növeli az idős korban gyakori elesés, zavartság és a kognitív diszfunkció kockázatát és az adott betegség súlyosságát is jelzi, fokozza.
6. A népesség-szintű vizsgálatok nem feleslegesek, mivel lehetőséget adnak a só-szenzitív/rezisztens alcsoportok elkülönítésére, a költséges, alig vállalható, teljeskörű előszűrés kiváltására. Több, mint 100 randomizált tanulmány bizonyítja, hogy a konyhasó bevitel csökkentése mérsékli a vérnyomást felnőttekben és csökkennek a szív-érrendszeri szövődmények is (39). Az ezt megkérdőjelező vizsgálatokban sok a metodikai hiba (40). A 24 órás vizelet-Na<sup>+</sup> meghatározás eredményei nagy egyéni variációt mutatnak, de többszörös, megismételt vizsgálattal ez a hiba mérsékelhető.

### Összefoglalás

A tudományos és az orvosi szakirodalom egységes abban, hogy a csökkent konyhasóbevitel (NaCl) csökkenti a magas vérnyomást. Az ezzel kapcsolatos népegészségügyi szintű randomizált vizsgálatok azonban rámutattak, hogy a magas vérnyomás jelenleg is tisztázatlan patomechanizmusában gyulladós, genetikai (génmutáció miatt fokozott tubuláris Na<sup>+</sup> visszatartás) civilizációs-környezeti faktorok, életmódi tényezők, endogén natriuretikus faktorok is szerepet játszanak és a csökkent vagy fokozott Na<sup>+</sup> bevitel – eltérő mechanizmussal – szerepet játszik a magas vérnyomás és a fokozott szív-érrendszeri kockázat kialakulásában, hozzáteve a csökkent sóbevitel hosszútávú kedvezőtlen idegrendszeri következményeit. Ugyanakkor nem lehet egyetérteni azokkal, akik a sok bizonytalansági tényező miatt a populációs szintű vizsgálatokat előszűrés nélkül feleslegesnek tartják, hiszen éppen ezek eredményeiből különíthető el az az alcsoport, amely sófüggő vagy sórezisztens magas vérnyomásban szenved és alapos utánvizsgálatokra érdemes. A 24 órás vizelet-Na<sup>+</sup>-ürítés nagy egyéni variációt mutat, de többször vizsgálva, átlagolva megbízható támpont a Na-homeosztázist illetően.

### Irodalomjegyzék

1. Judd, E., Calhoun, D.A.: Apparent and true resistant hypertension: definition, prevalence and outcomes. *J. Hum. Hypertens.* 28, 463-468, 2014.
2. Ha, S.K.: Dietary salt intake and hypertension. *Electrolyte Blood Press* 12, 7-18, 2014.
3. Kopp, C., Linz, P., Dahmann, A., Hammon, M., Jantsch, J., Müller, D.N., Schmieder, R.E., Cavallaro, A., Eckardt, K.U., Uder, M., Luft, F.C., Titze, J.: <sup>23</sup>Na magnetic resonance

imaging-determined tissue sodium in healthy subjects and hypertensive patients. *Hypertension* 61, 635-640, 2013.

4. McMaster, W.G., Kirabo, A., Madhur, M.S., Harrison, D.G.: Inflammation, immunity, and hypertensive end-organ damage. *Circ. Res.* 116, 1022-1033, 2015.

5. Madhur, M.S., Lob, H.E., McCann, L.A., Iwamura, Y., Blinder, Y., Guzik, T.J., Harrison, D.G.: Interleukin 17 promotes angiotensin II-induced hypertension and vascular dysfunction. *Hypertension* 55, 500-507, 2010.

6. Yi B, Titze J, Rykova M, Feuerecker M, Vassilieva G, et al. Effects of dietary salt levels on monocytic cells and immune responses in healthy human subjects: a longitudinal study. *Trans. Res.* 166, 103-110, 2015.

7. Rao, G.N., Berk, B.C.: Active oxygen species stimulate vascular smooth muscle cell growth and proto-oncogene expression. *Circ. Res.* 70, 593-599, 1992.

8. Tolins JP, Shultz PJ: Endogenous nitric oxide synthesis determines sensitivity to the pressor effect of salt. *Kidney Int.* 46, 230-236, 1994.

9. Laight, D.W., Carrier, M.J., Anggard, E.E.: Antioxidants, diabetes and endothelial dysfunction. *Cardiovasc. Res.* 47, 457-464, 2000.

10. Sacks, F.M., Svetkey, L.P., Vollmer, W.M., Appel, L.J., Bray, G.A., Harsha, D. et al.: Effects on blood pressure of reduced dietary sodium and the dietary approaches to stop hypertension (DASH) diet. DASH-Sodium Collaborative Research Group. *N. Engl. J. Med.* 344, 3-10, 2001.

11. Graudal, N.A., Galloe, A.M., Garred, P.: Effects of sodium restriction on blood pressure, renin, aldosterone, catecholamines, cholesterol and triglyceride: a meta-analysis. *JAMA.* 279, 1383-1391, 1998.

12. Blaustein MP, Physiological effects of endogenous ouabain: control of intracellular Ca<sup>2+</sup> stores and cell responsiveness. *Am J Physiol.* 264, C1367-C1387, 1993.

13. Iwamoto, T., Kita, S.: Hypertension, Na<sup>+</sup>/Ca<sup>2+</sup> exchanger, and Na<sup>+</sup>,K<sup>+</sup>-ATPase. *Kidney International* 69, 2148-2154, 2006.

14. Graudal, N.A., Hubeck-Graudal, T., Jürgens, G.: Effects of low-sodium diet vs. high-sodium diet on blood pressure, renin, aldosterone, catecholamines, cholesterol and triglyceride (Cochrane Review). *Am. J. Hypertens.* 25, 1-15, 2012.

15. Mente, A., O'Donnell, M.J., Rangarajan, S. et al.: Association of urinary sodium and potassium excretion with blood pressure. *N. Engl. J. Med.* 371, 601-611, 2014.

16. O'Donnell, M.J., Mente, A., Rangarajan, S. et al.: Urinary sodium and potassium excretion, mortality, and cardiovascular events. *N. Engl. J. Med.* 371, 612-623, 2014.

17. Mozaffarian, D., Fahimi, S., Singh, G.M. et al.: Global sodium consumption and death from cardiovascular causes. *N. Engl. J. Med.* 371, 624-634, 2014.

18. Ray, E.C., Chen, J., Kelly, T.N., He, J., Hamm, L.L., Gu, D., Shimmin, L.C., Hixson, J.E., Rao, D.C., Sheng, S., Kleyman, T.R.: Human epithelial Na<sup>+</sup> channel missense variants identified in the GenSalt study alter channel activity. *Am. J. Physiol. Renal Physiol.* 311, F908-F914, 2016.

19. Weinberger MH, Fineberg NS, Fineberg SE, Weinberger M. Salt sensitivity, pulse pressure, and death in normal and hypertensive humans. *Hypertension* 37,429-432, 2001.

20. Mente A, O'Donnell M, Rangarajan S, et al. Associations of urinary sodium excretion with cardiovascular events in individuals with and without hypertension: a pooled analysis of data from studies. *Lancet* 2016 May 20 (Epub ahead of print).

21. Cogswell ME, Zhang Z, Carriquiry AL, et al. Sodium and potassium intakes among US adults: NHANES 2003-2008. *Am J Clin Nutr.* 96, 647-57, 2012.
22. Poggio R, Gutierrez L, Matta MG, Elorriaga N, Irazola V, Rubinstein A. Daily sodium consumption and CVD mortality in the general population: systematic review and meta-analysis of prospective studies. *Public Health Nutr.* 18, 695-704, 2015.
23. Mills KT, Chen J, Yang W, et al. Sodium excretion and the risk of cardiovascular disease in patients with chronic kidney disease. *JAMA.* 315, 2200-10, 2016.
24. M.P. Scheiner, U.Raff, C.Kopp, et al: Skin Sodium Concentration Correlates with Left Ventricular Hypertrophy in CKD. *J Am Soc. Nephrol.* 28: 1867-1876, 2017.
25. He FJ, Pombo-Rodrigues S, Macgregor GA, Salt reduction in England from 2003 to 2011: its relationship to blood pressure, stroke and ischaemic heart disease mortality. *BMJ Open* 2014;4(4) :e004549.
26. Mozaffarian D, Fahimi S, Singh GM, et al. Global sodium consumption and death from cardiovascular causes. *N Engl J Med.* 371, 624-34, 2014.
27. Graudal NA, Hubeck-Graudal T, Jürgens G. Effects of low-sodium diet vs. high-sodium diet on blood pressure, renin, aldosterone, catecholamines, cholesterol, and triglyceride (Cochrane Review). *Am J Hypertens.* 25, 1-15, 2012.
28. McMahon EJ, Campbell KL, Bauer JD, Mudge DW, Altered dietary salt intake for people with chronic kidney disease. *Cochrane Database Syst. Rev.* 2, CD010070, 2015.
29. Cook NR, Cutler JA, Obarzanek E, et al. Long term effects of dietary sodium reduction on cardiovascular disease outcomes: observational follow-up of the Trials of Hypertension Prevention (THOP). *BMJ.* 334, 885-8, 2007.
30. Alvarez-Leefmans, F.J., Giraldez, F. and Gamino, S. M. Intracellular free Mg<sup>2+</sup> in excitable cells: its measurement and its biologic significance. *Can. J. Physiol Pharmacol.* 65, 915-925, 1987.
31. Kaplan H. J, The sodium pump and hypertension: A physiological role for the cardiac glycoside binding site of the Na, K-ATPase, *PNAS*, 102, 15723-15724, 2005.
32. Oparil, S: Low Sodium Intake – Cardiovascular Health Benefit or Risk?, *N.Engl. J. Med.* 677-679, 371-7, 2014.
33. Appel J. L. Anderson, A.M. Cheryl: Compelling Evidence for Public Health Action to Reduce Salt Intake, *N. Engl. J. Med.* 650-652., 362-7, 2010.
34. Alderman H. M: Reducing Dietary Sodium, The Case for Caution, *JAMA*, 303, 2010.
35. Gradual NA, Galloe AM, Garred P. Effects of sodium restriction on blood pressure, renin, aldosterone, catecholamines, cholesterol, and triglyceride: a meta-analysis. *JAMA.* 279, 1383-1391, 1998.
36. Klein, L., O'Connor, C.M., Leimberger, J.D., et al.: Lower serum sodium is associated with increased short-term mortality in hospitalized patients with worsening heart failure: results from the Outcomes of a Prospective Trial of Intravenous Milrinone for Exacerbations of Chronic Heart Failure (OPTIME-CHF) study. *Circulation* 111, 2454-60, 2005.
37. Wu, C.C., Yeung, L.K., Tsai, W.S., et al.: Incidence and factors predictive of acute renal failure in patients with advanced liver cirrhosis. *Clin. Nephrol.* 65, 28-33, 2006.
38. Bhardwaj, A.: Neurological impact of vasopressin dysregulation and hyponatremia. *Ann. Neurol.* 59, 229-36, 2006.
39. He FJ, Pombo-Rodrigues S, Macgregor GE. Salt reduction in England from 2003 to 2011: its relationship to blood pressure, stroke and ischaemic heart disease mortality. *BMJ Open* 4(4):e0045-49, 2014.

40. Cobb LK, Anderson CA, Elliott P, et al, Methodological issues in cohort studies that relate sodium intake to cardiovascular disease outcomes: a science advisory from the American Heart Association. *Circulation*, 129, 1173-86, 2014.

## COMPARATIVE EVALUATION OF VETERINARY ACTIVE INGREDIENTS AND FORMULATIONS

**Szandra Klátyik<sup>1</sup>, Gyuri Sági<sup>2</sup>, Eszter Takács<sup>1</sup>, Krisztina Kovács<sup>2</sup>, László Wojnárovits<sup>2</sup>, Erzsébet Takács<sup>2</sup>, Béla Darvas<sup>3</sup>, András Székács<sup>1</sup>**

<sup>1</sup>*Agro-Environmental Research Institute, National Research and Innovation Centre, H-1022 Budapest, Herman Ottó út 15, Hungary*

<sup>2</sup>*Institute for Energy Security and Environmental Safety, Centre for Energy Research, Hungarian Academy of Sciences, H-1121 Budapest, Konkoly-Thege Miklós út 29-33, Hungary*

<sup>3</sup>*Hungarian Society of Ecotoxicology, H-1022 Budapest, Herman Ottó út 15, Hungary*  
*e-mail: sz.klatyik@cfri.hu*

### Abstract

Chemical substances used in various fields of agriculture (e.g., veterinary medicine or crop protection) represent relevant environmental loads, and their residues, metabolites and decomposition products possibly occur in wastewater and can easily reach surface water. Adjuvants (e.g., surfactants) and other co-formulants used in veterinary medicine, feed additives, as well as in pesticide formulations have long been classified as inactive ingredients (AIs) in the aspects of the required main biological effect of the pharmaceutical or pesticide product. In wastewater management the application of the advanced oxidation processes (AOP) are in the focus of interest due to their high efficiency in the removal of persistent organic pollutants and pharmaceutical residues. To compare the toxicity of various AIs and formulations used in veterinary medicine, acute toxicity tests were performed on *Daphnia magna*. Additionally, effects of the presence of H<sub>2</sub>O<sub>2</sub> due to AOP on the toxicity of 0.1 mmol dm<sup>-3</sup> sulphamethoxazole (SMX) solutions oxidised during gamma irradiation (1 kGy, 2.5 kGy) were assessed. Ecotoxicological evaluation of the treated SMX solutions was carried out using three test organisms (*Vibrio fischeri*, *Pseudokircheriella subcapitata*, *D. magna*). Results showed significant differences in the individual acute toxicity of various veterinary AIs and formulations on *D. magna*. SMX and trimethoprim (TRI) were the least toxic investigated AIs; their evaluated EC<sub>50</sub> values were 98.06±58.67 and 93.06±33.17 mg L<sup>-1</sup>, respectively. The most toxic AI was sulphaguanidine (SGD) (EC<sub>50</sub> = 1,79±0.34 mg L<sup>-1</sup>). Significant differences were observed in the toxicity of the investigated veterinary drugs containing SMX and TRI. Their formulated veterinary pharmaceutical product SUMETROLIM was more toxic on *D. magna* (EC<sub>50</sub> = 106.17±54.86 mg L<sup>-1</sup>) compared to the COTRIUM-E. Combined toxicity was the highest when SMX and TRI were investigated together in SUMETROLIM equivalent concentrations compared to the formulated veterinary products. The untreated SMX solution resulted in 5±1% inhibition on *V. fischeri*, while higher, 30±2% inhibitions were detected in irradiated solutions due to the presence of H<sub>2</sub>O<sub>2</sub>. H<sub>2</sub>O<sub>2</sub> showed significantly high inhibition on the investigated test organisms. By the reduction of H<sub>2</sub>O<sub>2</sub> concentrations, decreased inhibition was observed on *V. fischeri* and *P. subcapitata*. The evaluated EC<sub>50</sub> for *V. fischeri*, *P. subcapitata* and *D. magna* were 0.349, 0.251 and 0.064 mmol dm<sup>-3</sup>, respectively.

### Introduction

Several chemical substances and their formulations are used in various fields of agriculture, such as veterinary medicine, animal husbandry and nutrition, and chemical plant protection;



and these compounds may have potential adverse effects on the environment. Besides the active ingredients (AIs), the registered formulations may contain various additives (e.g., surfactants), and in the aspects of the required main biological effect of the pharmaceutical or pesticide, these additives have long been considered as inactive or inert components. However, possible adverse effects of veterinary drugs and plant protection products may be caused not only by the AI(s), but also by the applied additives in these formulations. Several studies proved combined additive, synergistic or antagonistic side effects between the AIs and their additives used in the formulations, additionally the significantly higher own toxicity has been verified for several additives (e.g. polyethoxylated tallow amine, POEA) [1-7].

In the last decade the occurrence of the residues of veterinary pharmaceuticals in the aquatic environment have become a matter of concern, according to their potential risks posed to non-target organisms and the potential for human exposure via the food chain and drinking water. Thus, these compounds represent significant environmental loads due to the appearance of their metabolites and decomposition products in environmental matrices (e.g., soil, sediment, surface water) and even in wastewater [8-9]. According to Iglesias *et al.*, the most frequently detected pharmaceuticals in surface water were decoquinatone, sulphamethazine (SMZ), sulphamethoxypyridazine and trimethoprim (TRI) [10].

Advanced oxidation processes (AOPs) due to their high efficiency in the removal of persistent organic pollutants and pharmaceutical residues are in the focus of interest, as complementary or alternative methods to traditional wastewater treatment [11-12]. During AOP treatment of wastewater, hydroxyl ( $\cdot\text{OH}$ ) or sulphate ( $\cdot\text{SO}_4^{2-}$ ) radicals are generated in sufficient quantity to remove organic materials, organic and inorganic contaminants, or to increase the biodegradability of wastewater prior to biological treatment [13]. Application of AOP resulted in the appearance of  $\text{H}_2\text{O}_2$  in the treated solutions, when using particular methods (e.g.,  $\text{O}_3/\text{H}_2\text{O}_2$ ) or it forms in radical reactions (e.g., ionising radiation) [14], and can modify the inhibitory effects on living organisms [12,15].

The aim of this study was to investigate and compare the individual acute toxic effects of various veterinary AIs (e.g., sulphonamides and TRI) and veterinary formulations (e.g., SUMETROLIM, COTRIM-E) as a combination of AIs and additives on *Daphnia magna* immobilisation. Additionally, the effects of AOP and the appearance of  $\text{H}_2\text{O}_2$  on the toxicity of sulphamethoxazole (SMX) were investigated and compared on various test organisms (*Vibrio fischeri*, *Pseudokirchneriella subcapitata* and *D. magna*) using SMX solutions oxidised during gamma irradiation.

## Experimental

### *Determination of acute toxic effects of AIs and formulations used in veterinary medicine*

To assess the individual toxic effects of veterinary AIs, acute immobilisation tests were conducted on *D. magna* according to the OECD Test No. 202 guideline [16] using solutions of sulphonamides SMX, SMZ and sulphaguanidine (SGD) and TRI. Determination of acute toxic effects of veterinary drugs, as a combination of the AIs and additives, was performed on the basis of the same guideline. Both of the investigated veterinary medicines (SUMETROLIM and COTRIM-E) contain SMX and TRI as AIs: SUMETROLIM contains 400 mg of SMX and 80 mg TRI per tablet, while COTRIM-E contains 480 mg of co-trimoxazole in 5 ml (480 mg of co-trimoxazole consists of 400 mg of SMX and 80 mg of TRI). *D. magna* juveniles used for testing were less than 24 hrs and exposed to the test substances for 48 hrs.

Aerated reconstituted ISO test water was applied during the assays with known concentrations of the AIs and formulations. The pH value of the solutions remained between



the acceptable range of 6–9 during the experiments. The temperature was  $20\pm 2^\circ\text{C}$ , with 16-hr light and 8-hr dark photoperiods. In each test five concentrations of the investigated substance and an untreated control were used in four replicates at each level. Tests were performed in triplicates for each compound individually and in formulation. Immobilisation rates were recorded upon 24 and 48 hrs of exposure, and were compared to the untreated control values. The criteria of the test were verified.  $\text{EC}_{50}$  values were determined by statistics analysis at 48 hrs, calculated by statistical software ToxRat®. A theoretical value of the 48-hr  $\text{EC}_{50}$  value for SUMETROLIM was calculated using the nominal inhibitory concentrations of both AIs ( $\text{EC}_{50}[\text{AI}]$ ) as well.

#### *Determination of the effects of AOP treatment and the appearance of $\text{H}_2\text{O}_2$*

An aqueous solution of SMX was prepared at a concentration of  $0.1 \text{ mmol dm}^{-3}$ . The initial concentration was controlled by liquid chromatography tandem mass spectrometry (LC-MS/MS). Gradient type elution and positive ionisation mode was applied with electrospray ionisation. AOP was carried out at room temperature by a  $^{60}\text{Co}$  panoramic type  $\gamma$ -irradiation facility. Prior to the irradiation, unbuffered samples ( $1 \text{ dm}^{-3}$ , in amber glass bottles) were air saturated and were permanently aerated during the procedure. The solutions irradiated at 1 kGy absorbed dose contained hydroxylated products, but initial molecules were also present in low amounts [17-18]. Prolonged irradiation with 2.5 kGy led to decomposition of all initial molecules and resulted in the appearance of low molecular mass acids [18]. During the irradiation,  $\text{H}_2\text{O}_2$  was formed in radical reactions, and in purified water matrix it proved to be persistent. In order to make reliable ecotoxicity assays after irradiation,  $\text{H}_2\text{O}_2$  content was removed/reduced by catalytic decomposition with  $\text{MnO}_2$ .  $\text{H}_2\text{O}_2$  concentration was measured with the Merck  $\text{H}_2\text{O}_2$  test kit by spectrophotometric measurement of the absorbance at 454.5 nm of yellow or orange complexes formed.

To evaluate the effects of  $\text{H}_2\text{O}_2$  on *D. magna*, acute immobilisation tests were executed on the basis of the corresponding OECD guideline. The growth inhibition on freshwater unicellular microalgae *P. subcapitata* was investigated after 72 hrs of exposure according OECD Test No. 201 [19]. Reduction of cell growth was evaluated by measuring optical density changes at 750 nm by a UV/Vis spectrophotometer (JASCO 550). The samples were constantly shaken (100 rpm) and illuminated continuously (8600-8800 lux). Acute toxicity of SMX and  $\text{H}_2\text{O}_2$  on *V. fischeri* a widely used bioluminescent bacterium, was determined by Microtox® tests performed on the basis of the adequate protocol approved by US-EPA [20]. The inhibition of natural light emission was determined compared to a non-toxic control. The detected decrease in luminescence and the increase in toxicity are proportional. Inhibition was evaluated after 30 min of exposure at pH  $7\pm 0.2$ . The tests were performed in triplicates by using two parallels.

#### **Results and discussion**

On the basis of our acute toxicity testing on *D. magna* the most toxic AI was SGD ( $\text{EC}_{50} = 1.79\pm 0.34 \text{ mg L}^{-1}$ ), SMZ was less toxic ( $\text{EC}_{50} = 38.07\pm 9.52 \text{ mg L}^{-1}$ ), while the least toxic veterinary AIs were the SMX and trimethoprim (TRI) with evaluated  $\text{EC}_{50}$  values of  $98.06\pm 58.67$  and  $93.05\pm 33.2 \text{ mg L}^{-1}$ , respectively. Significant differences were observed in the toxicity of the investigated veterinary drugs containing SMX and TRI. SUMETROLIM was more toxic on *D. magna* ( $\text{EC}_{50} = 106.17\pm 54.86 \text{ mg L}^{-1}$ ) compared to COTRIUM-E (its concentration of  $250 \text{ mg L}^{-1}$  resulted in 15% immobilisation). The combined toxicity of SMX and TRI was higher when the two AIs were investigated together in equivalent concentrations, than in the

formulated product SUMETROLIM. The  $EC_{50}[AI]$  values of SMX and TRI corrected to SUMETROLIM were  $71.13 \pm 36.75$  and  $13.80 \pm 7.13$  mg L<sup>-1</sup>, respectively.

On *V. fischeri* the untreated SMX solution showed  $5 \pm 1\%$  inhibition, while  $30 \pm 2\%$  inhibition was observed in both irradiated solutions at 1 kGy and 2.5 kGy. The toxicity of SMX solutions increased in function of the quantity of absorbed dose, and was significantly higher in the presence of H<sub>2</sub>O<sub>2</sub>. It can be concluded that the presence of H<sub>2</sub>O<sub>2</sub> due to AOP has a significant impact on the exposure of the test organisms and on the results. To investigate the impact of H<sub>2</sub>O<sub>2</sub> alone on the test organisms (*D. magna*, *P. subcapitata* and *V. fischeri*), experiments have been conducted using a dilution series of H<sub>2</sub>O<sub>2</sub> aqueous solutions up to 0.5 mmol dm<sup>-3</sup>. Remarkably high inhibition was observed at the concentration of 0.5 mmol dm<sup>-3</sup> H<sub>2</sub>O<sub>2</sub> on all applied test organisms (Figure 1), resulting in  $100 \pm 0\%$ ,  $96 \pm 1\%$  and  $72 \pm 5\%$  inhibition on *D. magna*, *P. subcapitata* and *V. fischeri*, respectively. Therefore, at this concentration the presence of H<sub>2</sub>O<sub>2</sub> hinders interpretation of results targeting toxicity of products formed during the treatment. With the reduction of H<sub>2</sub>O<sub>2</sub> concentrations, decreased inhibition was observed on *V. fischeri* and *P. subcapitata*. A linear correlation was detected between the inhibition and H<sub>2</sub>O<sub>2</sub> concentrations. The inhibitory effects of H<sub>2</sub>O<sub>2</sub> (below 0.05 mmol dm<sup>-3</sup> concentration) on *V. fischeri* and *P. subcapitata* were regarded as acceptable, i.e.  $2 \pm 0\%$  and  $14 \pm 6\%$ , respectively. *D. magna* showed a different behaviour, where the concentration-response curve was sigmoidal. The toxicity was not modified with the reduction of H<sub>2</sub>O<sub>2</sub> concentration from 0.5 to 0.1 mmol dm<sup>-3</sup>. The reduction of H<sub>2</sub>O<sub>2</sub> concentration resulted in a decrease of immobilisation from  $90 \pm 9\%$  to  $24 \pm 9\%$  (Figure 1). The acceptable susceptibility of these organisms was detected when the level of H<sub>2</sub>O<sub>2</sub> was decreased to 0.01 mmol dm<sup>-3</sup> (resulting in  $6 \pm 8\%$  immobilisation) or below. The evaluated EC<sub>50</sub> values were found to be as high as 0.349, 0.251 and 0.064 mmol dm<sup>-3</sup> for *V. fischeri*, *P. subcapitata* and *D. magna*, respectively [12].

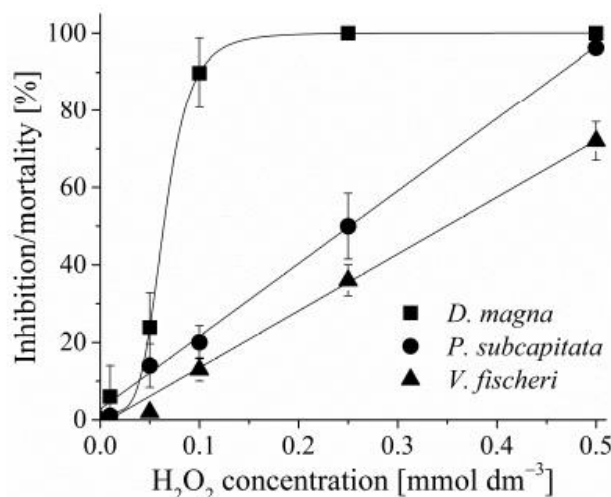


Figure 1. Concentration dependence of H<sub>2</sub>O<sub>2</sub> effects on *Daphnia magna*, *Pseudokirchneriella subcapitata* and *Vibrio fischeri* [12]

### Conclusion

On the basis of scientific data, the (eco)toxicity evaluation of surfactants and other additives is necessary for sufficient environmental risk assessment of formulations used in agriculture

including veterinary medicines, animal husbandry and plant protection. In addition, these components cannot be classified as inactive components regarding their side-effect profiles, due to their properties and their role in biological interactions. Our results emphasise the investigation and refinement of the complementary or alternative methods useable in traditional wastewater treatment, like AOP treatments. Residual H<sub>2</sub>O<sub>2</sub> in AOP may significantly modify the results of ecotoxicity assessment using living test organisms. During AOP treatments, a substantial reduction of H<sub>2</sub>O<sub>2</sub> is recommended to at least ~0.05 mmol dm<sup>-3</sup> in *V. fischeri* and *P. subcapitata* investigations due to the significant inhibition by H<sub>2</sub>O<sub>2</sub> at higher concentrations. In case of *D. magna*, complete elimination of H<sub>2</sub>O<sub>2</sub> is needed prior to tests, in order to avoid misleading results during the investigation of the effects of AOP on the toxicity of the treated solutions.

### Acknowledgements

This research was supported by project “Mechanism-related teratogenic, hormone modulant and other toxicological effects of veterinary and agricultural surfactants” (OTKA K109865) of the National Scientific Research Fund of Hungary.

### References

- [1] L.C. Folmar, H. Sanders, A.M. Julin, Arch. Environ. Contam. Toxicol. 8 (1979) 269-278.
- [2] M. T. K. Tsui, L.M. Chu, Chemosphere 52 (2003) 1189-1197.
- [3] R. Mesnage, B. Bernay, G-E. Seralini, Toxicology 313 (2013) 122-128.
- [4] I. Székács, Á. Fejes, Sz. Klátyik, E. Takács, D. Patkó, J. Pomóthy, M. Mörtl, R. Horváth, E. Madarász, B. Darvas, A. Székács, Int. J. Biol. Veter. Agric. Food Eng. 8 (2014) 213-218.
- [5] E. Takács, Sz. Klátyik, M. Mörtl, G. Rácz, K. Kovács, B. Darvas, A. Székács, Int. J. Environ. Anal. Chem. 97 (2017) 885-900.
- [6] Sz. Klátyik, P. Bohus, B. Darvas, A. Székács, Front. Vet. Sci. 4 (2017) 146.
- [7] Sz. Klátyik, E. Takács, M. Mörtl, A. Földi, Zs. Trábert, É. Ács, B. Darvas, A. Székács, Int. J. Environ. Anal. Chem. (2017).
- [8] T.P. Knepper, J. L. Berna, Compr. Anal. Chem. 40 (2003) 1-49.
- [9] U. Zoller, in: U. Zoller (Ed.), Handbook of Detergents, Part B, Environmental Impact (Surfactant Science Series), CRC Press, Boca Raton, 2004, pp. 467-485.
- [10] A. Iglesias, C. Nebot, B. I. Vázquez, J. M. Miranda, C.M.F. Abuín, A. Cepeda, Environ Sci Pollut Res Int. 21 (2014) 2367-2377.
- [11] W. Qin, Y. Song, Y. Dai, G. Qiu, M. Ren, P. Zend, Environ. Earth Sci. 73 (2015) 4939-4946.
- [12] Gy. Sági, A. Bezsényi, K. Kovács, Sz. Klátyik, B. Darvas, A. Székács, L. Wojnarovits, E. Takács, Radiat. Phys. Chem. (2017).
- [13] Y. Deng, R. Zhao, Curr. Pollut. Rep. 1 (2015) 167-176.
- [14] C. von Sonntag, Water Sci. Technol. 58 (2008) 1015-1021.
- [15] I. Talinli, G. Anderson, Water Res. 26 (1992) 107-110.
- [16] Organisation for Economic Co-operation and Development, Test No. 202: Daphnia Sp. Acute Immobilisation Test, (OECD Publishing, Paris, 2004).
- [17] Z. Guo, F. Zhou, Y. Zhao, C. Zhang, F. Liu, C. Bao, M. Lin, Chem. Eng. J. 191 (2012) 256-262.
- [18] G. Sági, T. Csay, L. Szabó, G. Pátzay, E. Csonka, E. Takács, L. Wojnárovits, J. Pharm. Biomed. Anal. 106 (2015) 52-60.

[19] Organisation for Economic Co-operation and Development, Test No. 201: Freshwater Alga and Cyanobacteria, Growth Inhibition Test, (OECD Publishing, Paris, 2011).

[20] US EPA, 2003. ETV Joint Verification Statement, Rapid Toxicity Testing System, Microtox®.

**ENVIRONMENTALLY BENIGN CATALYSIS: CHITOSAN, A NATURAL LIGAND  
FOR HIGHLY ENANTIOSELECTIVE RU CATALYZED TRANSFER  
HYDROGENATION OF KETONES**

**Vanessa Judit Kolcsár,<sup>1</sup> György Szöllösi<sup>2,\*</sup>**

<sup>1</sup>*Department of Organic Chemistry, University of Szeged, Dóm tér 8, Szeged, 6720, Hungary*

<sup>2</sup>*MTA-SZTE Stereochemistry Research Group, Dóm tér 8, Szeged, 6720, Hungary*

*\*Corresponding author: szollosi@chem.u-szeged.hu*

**Abstract**

We have studied the use of an in situ prepared Ru-chitosan complex in the transfer hydrogenation of prochiral ketones. Reaction of acetophenone and its substituted derivatives resulted in good enantioselectivities in aqueous solvent mixture. To our delight in the reduction of several cyclic ketones over 90% enantiomeric excesses were obtained, reaching up to 97% in the transfer hydrogenation of heterocyclic 4-chromanone or 4-thiochromanone derivatives. The pre-prepared Ru-chitosan complex provided identical results even after several months' storage without special precautions. The complex prepared from a natural, inexpensive, readily available chiral ligand is a convenient alternative of the synthetic ligands, and may be applied in environmentally friendly and sustainable processes for preparing optically pure chiral alcohols.

**Scope**

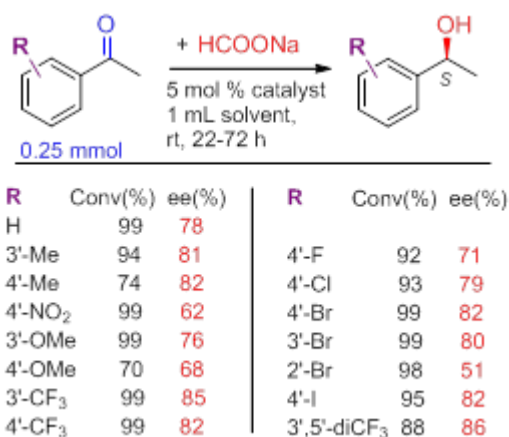
Enantioselective hydrogenations and transfer hydrogenations are among the most convenient procedures in the preparation of optically pure compounds used as intermediates in the production of pharmaceuticals, agrochemicals, flavors and fragrances.<sup>1</sup> A large variety of chiral complexes have been developed for the transfer hydrogenation of various prochiral unsaturated compounds. Recent trends in the fine chemical industry require environmentally friendly, sustainable processes. The use of chiral ligands of natural origin, such as chitosan, has multiple advantages. Chitosan may be obtained from wastes produced in the food industry, may replace the expensive chiral ligands, is biocompatible, biodegradable and due to its hydrophilic character may be used in aqueous media. Thus, is a perfect candidate for the development of catalysts used in green processes. Due to the presence of the free amino groups in this biopolymer it may be used as organocatalyst and is able to form complexes with metal cations.<sup>2,3</sup> However, only few studies have been published attempting the use of chitosan complexes in asymmetric transfer hydrogenations and the results obtained until now are far behind the values produced using synthetic chiral ligands. Satisfactory results were obtained using few chitosan derivatives,<sup>4,5</sup> however the need of functionalization of the chiral polymer decreased significantly their practical values.

Our aim was to study the transfer hydrogenation of prochiral ketones using chiral Ru catalysts prepared from unmodified chitosan as ligand in water-based solvents and to explore the applicability of this chiral complex. Determination of the structural requirements imposed to the ligand and the scope of the reaction were set as primary tasks, with the final goal of developing a highly enantioselective, economic, environmentally friendly procedure for the convenient transfer hydrogenation of prochiral ketones.

## Results and discussion

Preliminary studies were carried out with an *in situ* prepared complex from [Ru(*p*-cymene)Cl<sub>2</sub>]<sub>2</sub> and commercial high molecular weight chitosan using HCOONa as donor in the transfer hydrogenation of a few acetophenone derivatives. Short optimization of the reaction conditions and the solvent composition led us to the conclusion that a water-*i*PrOH 4-1 solvent mixture provides the best enantioselectivities in these reactions. Investigations of the ligand structure using low molecular weight chitosan, N-, O- and N-,O- functionalized chitosan, glucosamine and chitin indicated that the long polymeric chain and the free amino group is benefic for obtaining good activities and enantioselectivities. Next, we examined the transfer hydrogenation of a large library of aromatic ketones under conditions found most appropriate, selected examples are shown in Figure 1.

Figure 1. Enantioselective transfer hydrogenation of acetophenone derivatives with Ru-chitosan complex.



To our delight, results obtained in our experiments exceeded the best values reported until now by the use of chitosan derivatives as ligand. Further variation in the prochiral ketone structure showed that increasing the alkyl chain of acetophenone decreased the ee (not shown), however, the reduction of ketones having alicyclic structure connected to the aromatic ring gave surprisingly high enantioselectivities, as shown in Figure 2. Moreover, the ketones including a heteroatom in the ring, such as 4-chromanones and 4-thiochromanones provided the corresponding alcohols in even better, up to 97%, enantiomer excesses (Figure 2). The reactions were also carried out at 1 mmol scale to obtain the isolated products in excellent yields and high optical purities.

Further, we prepared the Ru-chitosan complex, which after slow evaporation of the solvent gave a dark orange film (Figure 2.), which was equally efficient in the transfer hydrogenations as the *in situ* formed catalyst. The material could be handled easier, as compared to the parent chitosan and could be stored for several months without alterations in its catalytic properties. The FT-IR spectrum of this material indicated the coordination of the Ru to chitosan.



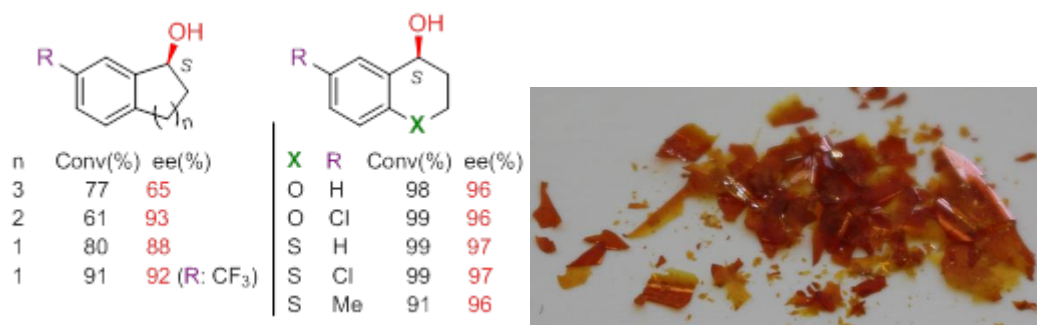


Figure 2. Results of transfer hydrogenation of cyclic ketones with the Ru-chitosan complex and the image of the prepared complex film.

Based on the results obtained using different ligands and the effect of the ketone structure on the conversion and enantioselectivity we suggested a plausible structure for the complex. It is assumed that the amino groups of different glucosamine units are involved in the coordination of the Ru(II) ion. An outer-sphere mechanism is suggested, during which the ketones' six-membered ring assure the necessary rigidity to the molecule, whereas hydrogen-bond acceptor heteroatoms in the ring are able to interact with the hydroxyl groups of the chitosan improving the orientation of the ketone.

### Conclusions

In summary, we have examined the performance of commercial chitosan as chiral ligand in the enantioselective transfer hydrogenation of prochiral ketones. Following the optimization of the reaction conditions, especially the nature of the solvent, we obtained high enantioselectivities in the reaction of a large number of acetophenone derivatives in aqueous media. The values surpassed those reported in the literature obtained with chitosan derivatives. Moreover, we obtained over 90% ee in the reaction of cyclic ketones, reaching up to 97% in the reduction of compounds having heteroatoms in the alicyclic ring. The prepared Ru-chitosan complex could be stored several month without special precautions. Based on the effect of chitosan derivatives and other ligands we suggested a plausible structure of the complex and a probable reaction mechanism, which rationalized the effect of the prochiral ketones' structure on the enantioselectivity. Finally, we mention that the highly selective chiral Ru complex was prepared using a cheap, natural material as chirality source, thus the developed method is a green, environmentally friendly and sustainable way to obtain optically enriched chiral alcohols.

### Acknowledgments

Financial support by OTKA Grant K 109278 and by the ÚNKP-16-2-II. New National Excellence Program of the Ministry of Human Capacities (V. J. K.) is appreciated.

### References

1. G. Shang, W. Li, X. Zhang, in *Catalytic Asymmetric Synthesis* (ed.: I. Ojima), 3<sup>rd</sup> ed., John Wiley & Sons, Hoboken, New Jersey, chap. 7, pp. 343-436, **2010**.
2. A. El Kadib, *ChemSusChem* **2015**, 8, 217-244.
3. E. Guibal, *Sep. Purif. Technol.* **2004**, 38, 43-74.
4. M. Babin, R. Clément, J. Gagnon, F.-G. Fontaine, *New J. Chem.* **2012**, 36, 1548-1551.
5. B. Liu, H. Zhou, Y. Li, J. Wang, *Chin. J. Org. Chem.* **2014**, 34, 2554-2558.



**ENVIRONMENTALLY BENIGN CATALYSIS:  
ASYMMETRIC MICHAEL-ADDITIONS USING HOMOGENEOUS AND  
HETEROGENIZED CHIRAL 1,2-DIAMINE DERIVATIVES**

**Viktória Kozma<sup>1</sup>, György Szöllösi<sup>2</sup>**

<sup>1</sup>*Department of Organic Chemistry, University of Szeged, 6720 Szeged, Dóm tér 8, Hungary*

<sup>2</sup>*MTA-SZTE Stereochemistry Research Group, 6720 Szeged, Dóm tér 8, Hungary*  
*e-mail: kozma.viktoria92@gmail.com*

**Abstract**

We have studied the asymmetric Michael-addition of aldehydes to maleimides using optically pure 1,2-diamine catalysts. Investigations on the effect of the structure of the catalyst, maleimide and aldehyde led to valuable conclusions as concern the steric and electronic requirements for obtaining high activities and stereoselectivities in these asymmetric reactions. Based on these observations a plausible reaction intermediate for explaining the stereoselective addition of the nucleophile to the activated olefin is suggested. Furthermore, the results were used for selecting the chiral catalyst and the appropriate linker for the preparation of heterogenized chiral materials. The activities and enantioselectivities obtained using the catalysts immobilized on a proper support approached those obtained with their soluble counterparts and kept their stereoselectivities upon reuse.

**Introduction**

Asymmetric Michael-additions are among the most often-used stereospecific reactions for coupling organic molecules, widely applied for preparing optically pure fine chemicals. Succinimide derivatives may be obtained by the enantioselective addition of nucleophiles, such as aldehydes, to maleimides.<sup>1</sup> These reactions are catalyzed efficiently by chiral diamines and derivatives thereof, among which cyclohexane-1,2-diamines, 1,2-diphenylethylene diamines, their sulfonamides and thiocarbamides are privileged chiral catalysts.<sup>2-4</sup> However, a systematic comparison of their performances in the enantioselective addition of aldehydes to maleimides is still missing. A detailed study is of paramount importance for selecting the proper catalyst structure and the linker for the immobilization of these organocatalysts in order to obtain heterogeneous, recyclable chiral catalysts. The heterogeneous catalysts obtained by immobilization of the diamines could be applied in environmentally friendly, sustainable processes as convenient alternatives of their soluble counterparts for the preparation of optically pure succinimides.

Our aim during this work was to study the effect of the chiral 1,2-diamine derivatives' structure on the results obtained in the asymmetric addition of various aldehydes to maleimides, in order to find an efficient, easily accessible catalyst for these reactions. Based on the results of this study we planned to attempt the immobilization of the selected chiral 1,2-diamine catalyst using an appropriate linker over several inorganic and organic supports. Our goal was to develop a highly efficient, reusable heterogeneous chiral catalyst for the asymmetric Michael-addition of aldehydes to maleimides.

**Experimental**

The chiral 1,2-diamine derivatives, functionalized inorganic oxides or organic polymers used as supports, maleimide derivatives and aldehydes were obtained from commercial sources and

were used as received. Asymmetric Michael-additions were carried out in closed glass reactors heated in oil bath if necessary. In reactions catalyzed by solid materials, the mixtures were stirred magnetically or mixed using shakers. In a typical run the chiral catalyst was dissolved in the proper solvent amount followed by addition of the maleimide derivative and the aldehyde. The solution or the suspension (in case of the solid chiral catalysts) was stirred at the given temperature for the desired time. Following the reactions the soluble catalysts were extracted with saturated  $\text{NH}_4\text{Cl}$  aqueous solution and the organic products were analysed. After the heterogeneously catalyzed reactions the catalyst was separated by decantation before the aqueous washing of the products. These materials were reused in several successive runs. Products resulted in the Michael-additions were analysed by GC-MSD and GC-FID using chiral capillary column. Larger scale experiments were also carried out, the resulted products were purified by column chromatography for determination of the yields. The pure compounds were characterized by  $^1\text{H}$ - and  $^{13}\text{C}$ -NMR spectroscopy.

### Results and discussion

The addition of isobutanal to N-phenylmaleimide was selected as test reaction for investigating the effect of the chiral 1,2-diamine structure. Selected results are presented in Figure 1. Cyclohexane-1,2-diamine derivatives gave the Michael adducts in few hours, however, provided lower enantioselectivities (not shown in figure) as compared with the 1,2-diphenylethylene diamine derivatives, the latter however needed

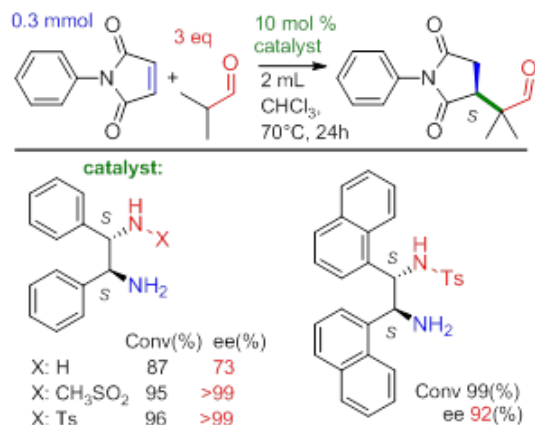


Figure 1. Results of the test Michael-addition using 1,2-diamine catalyst (Ts: p-toluenesulfonyl).

longer reaction times, up to 24 hours, for complete conversion of the maleimide. An acidic group, such as the sulfonamide group, needed to obtain high ee, however, the methanesulfonamide was equally efficient as the toluenesulfonyl derivative. Using the opposite (*R,R*) enantiomer of the catalysts resulted in identical conversion and ee values except the *R*-succinimide derivative was obtained in excess. Similar tendencies were observed using N-ethyl, N-*tert*-butyl and unsubstituted maleimides or propanal and cyclohexanecarbaldehyde nucleophiles. Reactions carried out at 1 mmol scale gave the optically pure isolated adducts in good yields. Based on the steric and electronic effect of the substituents we suggested a plausible reaction intermediate and a mechanism able to rationalize the obtained enantioselectivities.

Accordingly, we immobilized optically pure 1,2-diphenylethylene diamine using linkers having acidic, H-bond donor character, such as sulfonamide, thiocarbamide or squaramide

groups over silica or polystyrene resin supports. Selected catalysts and results obtained in the addition of isobutanal to N-phenylmaleimide using these materials are summarized in Figure 2.

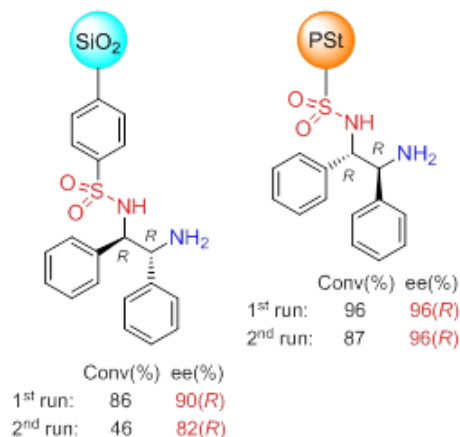


Figure 2. Selected heterogenized chiral catalysts and results obtained in the test reaction.

The success of the immobilization process of the chiral compounds was checked by FT-IR spectroscopy, absorption bands characteristic to the sulfonamide group appeared in the spectra of the materials shown in the figure. The silica-supported catalysts gave lower enantioselectivities and partially lost their activity upon reuse, which we ascribed to the unfavorable effect of the support's surface acidic sites. On the contrary, the chiral catalysts immobilized on polystyrene resins approached the performances of the soluble catalysts, affording the same conversion and only slight decrease in the enantioselectivity. Moreover, the enantiodiscrimination ability of the catalyst was kept in a 2<sup>nd</sup> run. The small decrease in conversion may be attributed to the small amount of catalyst lost during manipulations. Good results were also obtained with catalysts immobilized on polystyrene resins via thiocarbamides or squaramide groups (not shown in the figure), which will be also presented.

## Conclusion

We have studied the asymmetric Michael-addition of aldehydes to maleimides using optically pure 1,2-diamine derivatives resulting in chiral succinimides. We have investigated in detail the effect of variations in the structure of the catalysts and the reactants. Based on the results of these experiments we could deduce the structural elements of the reaction components, which have decisive influence on the stereochemical outcome of these asymmetric reactions. Based on these results we selected the proper catalyst and linker for the immobilization of the chiral catalyst in order to obtain heterogeneous chiral catalysts, which approached the performances of their soluble counterparts. The proper choice of the support allowed the reuse of the solid catalysts without enantioselectivity decrease. Finally, we note that the prepared heterogeneous catalysts are the first, which were designed for the asymmetric Michael-addition of aldehydes to maleimides. Results presented in this work are also promising starting-points of further efforts devoted to apply heterogeneous, environmentally friendly catalysts in the preparation of practically relevant chiral succinimides.

## Acknowledgements

Financial support by the ÚNKP-16-2-II. New National Excellence Program of the Ministry of Human Capacities (V. K.) is appreciated.

**References**

- [1] P. Chauchan, J. Kaur, S.S. Chimni, Chem. Asian J. 2013, 8, 328-346.
- [2] F. Xue, L. Liu, S. Zhang, W. Duan, W. Wang, Chem. Eur. J. 2010, 16, 7979-7982.
- [3] F. Yu, Z. Jin, H. Huang, T. Ye, X. Liang, J. Ye, Org. Biomol. Chem. 2010, 8, 4767-4774.
- [4] A. Avila, R. Chinchilla, E. Gómez-Bengoá, C. Nájera, Tetrahedron: Asymmetry 2013, 24, 1531-1535.

## ANALYSIS OF NEW SYNTHETIC CANNABINOID IN HUMAN URINE BY LC-MS/MS

Tímea Körmöczy<sup>a</sup>, Éva Sija<sup>b</sup>, Róbert Berkecz<sup>a</sup>

<sup>a</sup> Department of Medical Chemistry, Faculty of Medicine, University of Szeged, Dóm tér 8, H-6720, Szeged, Hungary

<sup>b</sup> Department of Forensic Medicine, Faculty of Medicine, University of Szeged, Kossuth L. Bld. 40, H-6724, Szeged, Hungary  
e-mail: kormoczi.timea@med.u-szeged.hu

### Abstract

Synthetic cannabinoids (SCs) are a group of novel psychoactive substances, which bind to cannabinoid receptors (CB1 and CB2). One of the largest groups of SCs are smoking mixtures, which are intended as legal replacements of cannabis and distributed on the illicit drug market. In 2016, 11 new SCs were reported by the European Monitoring Centre for Drugs and Drug Addiction (EMCDDA). The most commonly used techniques for quantitation of SCs in urine are high performance liquid chromatography coupled to tandem mass spectrometry (LC-MS/MS). In this study we analysed in 2016-2017 released 6 new SCs such as 5F-MN18, AMB-CHMINACA, AMB-FUBINACA, APP-CHMINACA, CUMYL-4CN-BINACA and THJ-2201. The LC-MS/MS system was optimised and the mass of identified parent ions, daughter ions and related retention time were determined. Matrix effect, extraction recovery and process efficiency were evaluated by the method proposed by Matuszewski et al.

### Bevezetés

Szintetikus kannabinoidok képezik az új pszichoaktív szerek legnagyobb csoportját. 2015-ben az Európai Unióban 98 új szert jelentettek be, melyből 24 szintetikus kannabinoid volt. 2016-ban a regisztrált új szintetikus kannabinoidok száma 11-re csökkent. A szintetikus kannabinoidok olyan szerek, melyek ugyanazon agyi receptorokra hatnak, mint a természetes kannabiszban található fő hatóanyag a delta-9-tetrahidrokannabinol (THC). A Kábítószer és Kábítószerfüggőség Európai Megfigyelőközpontja (*European Monitoring Centre for Drugs and Drug Addiction, EMCDDA*) által kiadott jelentés szerint, 2016-ban 45 súlyos következményekkel járó fogyasztás volt, melyek közül 18 halálos kimenetelű mérgezés [1-2]. A szintetikus kannabinoidok kockázata egyrészt abban rejlik, hogy jobban kötődnek a kannabinoid receptorokhoz (CB1, CB2), ezáltal sokkal aktívabbak, mint a kannabiszban található fitokannabinoidok, másrészt a pontos fiziológiai hatásuk nem ismert [3].

A törvényi szabályozások következtében a kábítószer piaca gyorsan változik, ezért minél előbb fontos az új anyag azonosítása és detektálásuk optimalizálása. Munkánk során a 2016 év végén illetve 2017 elején megjelent új szintetikus kannabinoidok vizelet mintákból történő analizálásával foglalkoztunk, melyet a gyakorlatban legtöbbször alkalmazott LC-MS/MS módszerrel végeztünk.

### Anyagok és módszerek

#### Vegyszerek és standardok

A vizsgálatokban szereplő szintetikus kannabinoidok standard mintáit a Nemzeti Szakértői és Kutató Központ biztosította, melynek tisztasága 90% feletti. A belső standardként használt

deuterált delta-9-tetrahidrokannabinol (THC-COOH-D<sub>3</sub>) oldat a Cerilliant-tól (Merk, Darmstadt, Németország) került megrendelésre. Az enzimes kezeléshez éticsigából (*Helix Pomatia*) kivont  $\beta$ -glükuronidáz enzimet (Merk, Darmstadt, Németország) használtunk. A minta előkészítéshez és a mérésekhez LC-MS tisztaságú vizet, acetonitrilt (VWR, Radnor, USA), hangyasavat (Termo Fisher Scientific, Waltham, USA), vízmentes nátrium acetátot (Reanal, Budapest, Magyarország), ecetsavat (Spektrum 3D, Debrecen, Magyarország), biokémiai felhasználásra alkalmas szilárd ammónium-szulfátot és LC tisztaságú etanolt (Merck, Darmstadt, Németország) használtunk. A vizsgálatokhoz negatív mintaként saját vizelettel dolgoztunk.

#### Vizelet minták folyadék-folyadék extrakciója

2 mL vizelet mintához 20  $\mu$ L belső standardot (10  $\mu$ g/mL), 40  $\mu$ L szintetikus kannabinoidok standard keverékét és 400  $\mu$ L  $\beta$ -glükuronidáz enzimet tartalmazó acetát puffert (pH 5) adtunk, melyet 1 éjszakán át szobahőmérsékleten inkubáltunk. Az inkubációt követően 3 mL acetonitrilt adtunk és ammónium-szulfáttal vízmentesítettük az oldatot. Ezt követően a mintát 60 másodpercig intenzíven rázattuk (Multi-Tube Pulse Vortexer, Glas Col, Terre Haute, USA), majd 8 percig centrifugáltuk (2500 rpm, MLW K-26 D, Németország). Centrifugálást követően 2,2 mL felső fázist 50°C-on 25 perc alatt bepároltunk. A bepárolt mintákat kúpos inzertbe 200  $\mu$ L 50:50 acetonitril-víz elegyében visszaoldottuk [4]. A mérések során 20  $\mu$ L-t injektáltunk.

Az új vegyületekre készítettünk egy kalibrációs sort, mely a következő koncentrációkat tartalmazta: 0,2; 0,5; 1; 1,6; 2; 5 és 10 ng/mL.

#### LC-MS/MS

Az analízishez Agilent 1100 HPLC rendszert (Waldbronn, Németország) használtunk, mely egy elektronporlasztásos ionforrású (ESI) hármass kvadrupól rendszerű tömegspektrométerrel (Finnigan TSQ 7000, Thermo Fisher Scientific, Waltham, USA) volt összekapcsolva. A kromatográfiás elválasztás egy fordított fázisú Kinetex C18 (100 x 2,1 mm, 2,6  $\mu$ m, 100 Å, Phenomenex, Torrance, USA) kromatográfiás oszlopon és egy C18 (4 x 2 mm, Phenomenex, Torrance, USA) előtét oszlopon történt. Az oszlop 50°C-os hőmérsékletét egy oszlop termosztát biztosítja. A mozgó fázis A (0,1% hangyasav vízben) és B (0,1% hangyasav acetonitrilben) eluensből állt. A 11 perces analízis idő során gradiens elúciót alkalmaztunk (**1. Táblázat**). A rendszer továbbá tartalmazott az ionforrás elszennyeződésének elkerülése érdekében egy külső mikro 10 utas váltószelepet, mely a folyadékkromatográfiás rendszer és a tömegspektrométer közé volt beépítve. A váltószelep 1-5,8 percig engedi be az eluátumot, ezen felül egy segédpumpa biztosítja a tömegspektrométer fémkapillárisának öblítését. A kapilláris- és szeleptosást segédpumpa végzi 90:10 acetonitril-víz eleggyel, míg a tūmosás 80:20 acetonitril-víz eleggyel történt.

A tömegspektrometriás mérés pozitív ionizációs módban és MRM módszerrel történt. Az analízis ESI forrással, 15 cm x 190  $\mu$ m x 75  $\mu$ m fűtött kapillárisal (230°C), porlasztó (50 psi) és segédgázzal (30 psi) történt. Ütközési gázként nitrogént használtunk 2,0 mTorr nyomáson. Detektor feszültség: 1900V. A méréshez Xcalibur 1.3 programmal és Tune-nal történt, míg az adatok kiértékeléséhez Thermo Xcalibur 2.2 programmal dolgoztunk, az alábbi paraméterekkel: simítás: 1, alapvonal: 40, terület zaj: 5, csúcs zaj: 5, minimum csúcsmagasság: 3 jel/zaj.

1.Táblázat Gradiens program

Idő (perc)	%B	Áramlási sebesség (mL/perc)
0,00	50	0,4
4,00	100	0,4
6,00	100	0,4
6,10	100	0,7
6,90	100	0,7
7,00	50	0,7
9,50	50	0,7
9,51	50	0,4
10,0	50	0,4

#### Tömegspektrometriás mérés optimalizálása és a retenció idő meghatározása

A tömegspektrometriás mérés optimalizálása során a 2016 év végén illetve 2017 elején megjelent 6 szintetikus kannabinoid fragmentációját vizsgáltuk. A legújabb szintetikus kannabinoidok: **5F-MN18**, **AMB-CHMINACA**, **AMB-FUBINACA**, **APP-CHMINACA**, **CUMYL-4CN-BINACA** és **THJ-2201**. A mérés során 10 ng/mL koncentrációjú standard mintából 1 µL-t injektáltunk kromatográfiás oszlop nélkül. Az mérés során azonosítottuk az egyszerűen töltött  $[M+H]^+$  szülőiont, majd megvizsgáltuk a fragmentációját. A legintenzívebb fragmensiont célionnak (*quantifier ion*) választottuk, amelyet a mennyiségi meghatározás során veszünk figyelembe. A későbbi azonosításhoz egy ennél kisebb intenzitású kísérőiont (*qualifier ion*) választottunk ki. Az azonosítást követően 10 és 50 eV közötti ütközési energia mellett megnéztük a csúcsterületek alakulását, és amelyik ütközési energia mellett legintenzívebb volt az adott fragmension, azt rendeltük hozzá az MRM mérés során. A retenció idő meghatározásához 2 ng/mL koncentrációjú standard oldat 20 µL-t injektáltuk a kromatográfiás oszlopra.

#### Visszanyerés, mátrixhatás és teljes folyamathatékonyág

A vizsgálatokat Matuszewski [5] és Yanes [6] által kidolgozott módszer alapján végeztük. A visszanyerés vizsgálat célja, hogy kiderítsük az általunk használt mintaelőkészítési módszerrel hány százalékát tudjuk detekálni az adott szintetikus kannabinoidoknak vizelet mintából. A mátrixhatás vizsgálat megmutatja, hogy az analizálandó komponens környezete (mátrixa), hogyan befolyásolja a vizsgált anyagok ionizálhatóságát. A folyamathatékonyág vizsgálat a visszanyerés és mátrixhatás eredményeit együttesen foglalja össze.

A méréshez 3 mintasorozatot készítettünk. Mindegyik sorozat 4 mintát tartalmazott, melyet háromszor mértünk meg. Amíg az A sorozatnál a szintetikus kannabinoidokat tartalmazó oldatot és a belső standardot a vizelet mintához adtuk hozzá az extrakció elején addig a B sorozatnál a standardokat az extrakciót követően, míg C sorozatnál nem használtunk vizeletet és extrakciós módszert, csak a tiszta oldatokkal dolgoztunk. Az eredményeket a következők szerint számoltuk ki:

$$\text{Visszanyerés (\%)} = \frac{A}{B} \times 100, \quad \text{Mátrixhatás (\%)} = \frac{B}{C} \times 100,$$

$$\text{Teljes folyamathatékonyág (\%)} = \frac{A}{C} \times 100$$

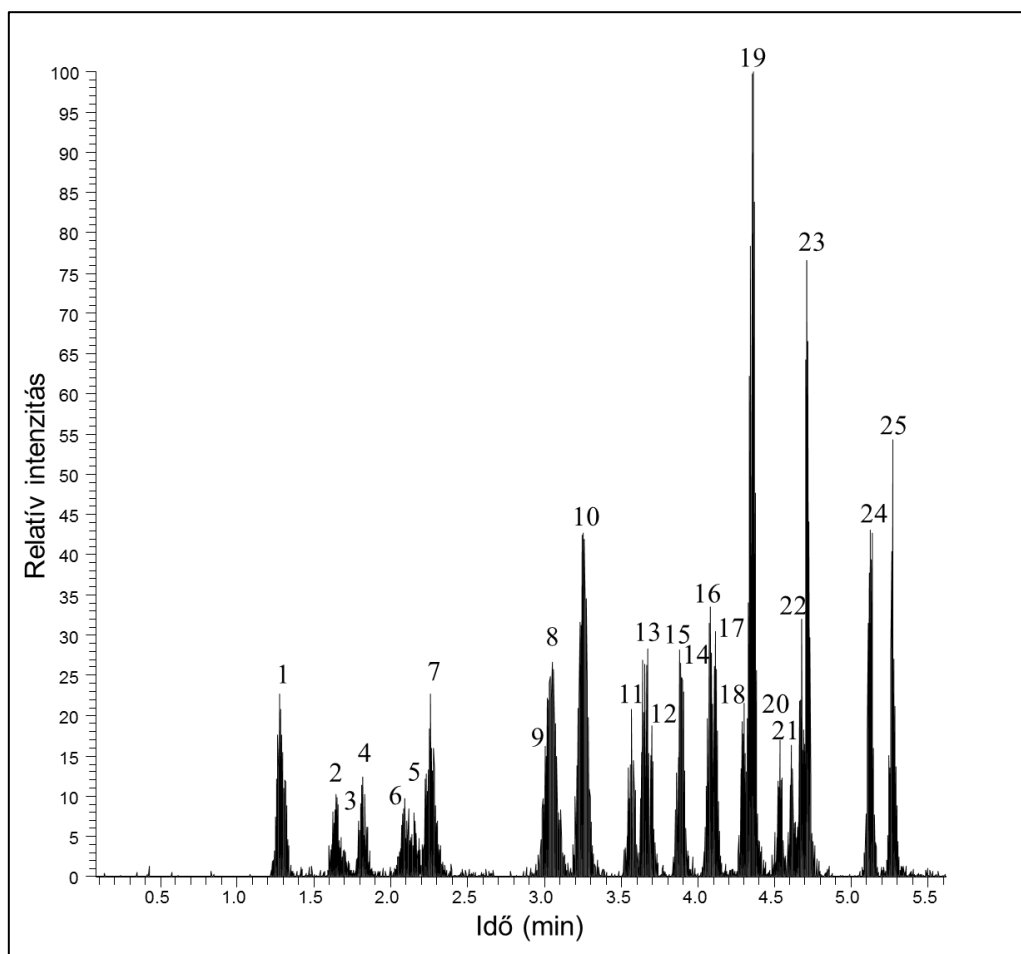


### Eredmények és értékelésük

Az ionizáció során a vizsgált szintetikus kannabinoidokra a következő egyszeresen töltött szülőionok keletkeztek: 5F-MN18 376 (m/z), AMB-CHMICA 371 (m/z), AMB-FUBINACA 384 (m/z), APP-CHMINACA 405 (m/z), CUMYL-4CN-BINACA 361 (m/z) és THJ-2201 361 (m/z). A fragmentáció során – az AMB-CHMICA kivételével – a célion mellett a pontosabb azonosítás érdekében két kísérőion került kiválasztásra: 5F-MN18 233 m/z (20eV) célion, 145 m/z (43eV) és 213 m/z (30eV) kísérőion; AMB-CHMICA 240 m/z (144eV) célion és 144 (45eV) kísérőion; AMB-FUBINACA 253 m/z (26eV) célion, 109 m/z (49eV) és 324 m/z (20eV) kísérőionok; APP-CHMINACA 241 m/z (32eV) célion, 145 m/z (50eV) és 360 m/z (20eV) kísérőionok; CUMYL-4CN-BINACA 226 m/z (29eV) célion, 119 m/z (35 eV) és 243 m/z (17 eV) kísérőionok; THJ-2201 233 m/z (20eV) célion, 145 m/z (42eV) és 213 m/z (28eV) kísérőionok. A 6 új optimalizált vegyület apolárisabb tulajdonságuknak köszönhetően később eluálódnak (**1. Ábra**). A retenciós idő 5F-MN18 4,50 perc, AMB-CHMICA 4,31 perc, AMB-FUBINACA 3,85 perc, APP-CHMINACA 3,51 perc, CUMYL-4CN-BIACA 3,19 és a THJ-2201 esetében 4,58 perc lett.

A mennyiségi meghatározás során kapott eredményekről elmondható, hogy 0,2-10 ng/mL-es koncentráció tartományban lineáris. Az  $R^2$  értéke a CUMYL-4C-BINACA kivételével (0,98) minden esetben 0,99. A belső standardra normalizált területek relatív szórása (*RSD%*) minden vegyületre 20% alatti. A kapott mérési adatok alapján a kimutatási határ (*LOD*) a 6 új pszichoaktív anyagra 0,2 ng/mL, a meghatározási határ (*LOQ*) 0,05 ng/mL.

A kapott eredmények azt mutatják, hogy az általunk használt mintaelőkészítési módszerrel a CUMLY-4CN-BINACA vegyületet lehet a leghatékonyabban, azaz 74,7%-ban visszanyerni. A többi anyagra a visszanyerés 60-70% közötti, míg az AMB-CHMICA esetében 58,5 % lett. A mátrixhatást tekintve legtöbb esetben negatív befolyásolásról beszélhetünk, melynek feltételezhető oka, hogy a mátrixban lévő nagy koncentrációjú jól ionizálódó endogén komponensek ionelnyomó hatást eredményeznek a spray képzés során. Ez látszik az 5F-MN18 (87,1%), APP-CHMINACA (88,8%), CUMYL-4CN-BINACA (99,3%) és a THJ-2201 (88,1%) esetén. Két esetben, AMB-CHMICA és AMB-FUBINACA szereknél pozitív mátrixhatásról beszélhetünk (107,0% és 120,9%), melynek feltételezhető oka, hogy a mátrixban található egyéb komponensek segítik az adott vegyület ionizálhatóságát protonátadással vagy felületi feszültséget csökkentő hatásukkal. A folyamathatékonyság vizsgálat a visszanyerés és mátrixhatás vizsgálat eredményeit együttesen mutatja. A kapott eredmények alapján elmondható, hogy az egyes szintetikus kannabinoidok terület százalécai korrelálnak a mátrixhatás eredményeivel.



**1. ábra** Az újonnan vizsgált 6 szintetikus kannabinoid és a már ismert 18 szintetikus kannabinoid, valamint a belső standard teljes ionáram kromatogramja. (1) 5F-AMBICA, (2) AMB-FUBINACA, (3) 5F3P, (4) 5F-APP-PINACA, (5) ADB-FUBINACA, (6) APP-FUBINACA, (7) AB-PINACA, (8) ADB-PINACA, (9) AB-CHMINACA, (10) CUMYL-4CN-BINACA, (11) APP-CHMINACA, (12) ADB-CHMINACA, (13) 5F-AMB, (14) AMB-FUBINACA, (15) MDMB-FUBICA, (16) THC-COOH-D<sub>3</sub>, (17) 5F-MDMB-PINACA, (18) MDMB-FUBINACA, (19) AMB-CHMICA, (20) 5F-MN18, (21) THJ-2201, (22) ADAMANTYL-THPINACA, (23) MDMB-CHMICA, (24) AKB48F, (25) FUB-AKB-48F.

### Következtetés

Munkánk során a 2016 és 2017-ben megjelent legújabb 6 szintetikus kannabinoid vizelet mintából vett HPLC-ESI-MS/MS analízisét végeztük. A tömegspektrometriás detektálás során meghatároztuk a szülő- és célionokat. A későbbi pontosabb minőségi meghatározás érdekében 2 kísérőion került kiválasztásra. A már optimalizált tömegspektrometriás paraméterekkel fordított fázisú kromatográfiás rendszerben meghatároztuk a retenciós időket. A vizelet mintákból az adott anyag azonosítása során figyelembe vesszük a retenciós idejét, a szülőion, a célion és kísérőionok tömegét ( $m/z$ ) és azok intenzitását adott ütközési energia mellett. A mennyiségi meghatározás a célionok belső standardra normalizált csúcsterülete, valamint a kalibrációs görbe alapján történik. A vizsgált szintetikus kannabinoidokat az általunk használt folyadék-folyadék extrakciós mintelőkészítési módszerrel 58-74%-ban lehet visszanyerni.

### **Köszönetnyilvánítás**

A kutatást az EFOP-3.6.1-16-2016-00008 azonosítójú, EU társfinanszírozású projekt támogatta.

### **References**

- [1] Kábítószer és Kábítószer-függőség Európai Megfigyelőközpontja: Európai kábítószer-jelentés, Tendenciák és fejlemények, 2016. Link: <http://www.emcdda.europa.eu/system/files/publications/2637/TDAT16001HUN.pdf>
- [2] Kábítószer és Kábítószer-függőség Európai Megfigyelőközpontja: Európai kábítószer-jelentés, Tendenciák és fejlemények, 2017. Link: [http://www.emcdda.europa.eu/system/files/publications/4541/TDAT17001HUN.pdf\\_en](http://www.emcdda.europa.eu/system/files/publications/4541/TDAT17001HUN.pdf_en)
- [3] W. D Wessinger, J. H Moran and K. A. Seely.: Synthetic Cannabinoids Effects on Behavior and Motivation, In: Patrizia Campolongo, Liana Fattore (Ed.), Cannabinoid Modulation of Emotion, Memory, and Motivation, Springer, 2015, 205-221.
- [4] É. Sija, R. Berkecz, S. Zsigrai, T. Janáky, É. Kereszty, T. Varga, L. Insititóris: Módszerfejlesztés szintetikus kannabinoidok kimutatására vizeletből, In: TOX'2015 Tudományos Konferencia, Harkány, Hungary, 2015.10.14-16.p. 76. 1 p. (poster).
- [5] B. K. Matuszewski, M. L. Constanzer, C. M. Chavez-Eng: Strategies for the Assessment of Matrix Effect in Quantitative Bioanalytical Methods Based on HPLC-MS/MS, In: Anal. Chem. 2003. 75, 3019-3030
- [6] E. G. Yanes, D. P. Lovett: High-throughput bioanalytical method for analysis of synthetic cannabinoid metabolites in urine using salting-out sample preparation and LC-MS/MS, In: Journal of Chromatography B, 909 (2012), 42-50.

## TÖBBVÁLTOZÓS FOLYAMATSZABÁLYOZÁS VIZSGÁLATA R KÖRNYEZETBEN

### INVESTIGATION OF MULTIVARIATE STATISTICAL PROCESS CONTROL IN R ENVIRONMENT

**József MIHALKÓ, Róbert RAJKÓ**

*Szegedi Tudományegyetem, Mérnöki Kar, Folyamatmérnöki Intézet, 6725 Szeged, Moszkvai  
krt. 5-7.*

*Institute of Process Engineering, Faculty of Engineering, University of Szeged,  
5-7. Moszkvai krt., Szeged, Hungary, H-6725*

#### **Abstract**

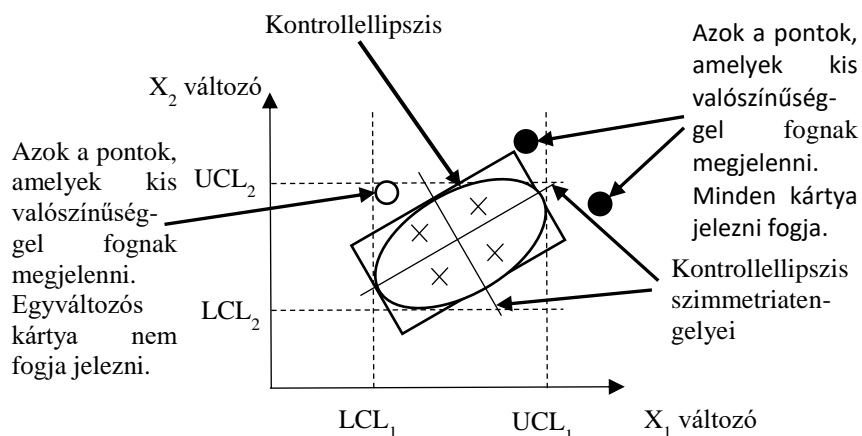
At the first stage of our work, the theoretical knowledge needed to use the multivariate statistical process control (MSPC) was explored. Last year, we clarified the sometimes confused concepts, equations and formulas (Mihalkó and Rajkó, 2016). At the second stage, R project simulation studies and some food industrial practical model investigations are carried out for confirming the MSPC advantages compared with the univariate ones. Furthermore, we analyze, using principal component analysis (PCA), what could cause the outlying values, moreover we will demonstrate how to use the MYT-decomposition.

#### **Bevezetés**

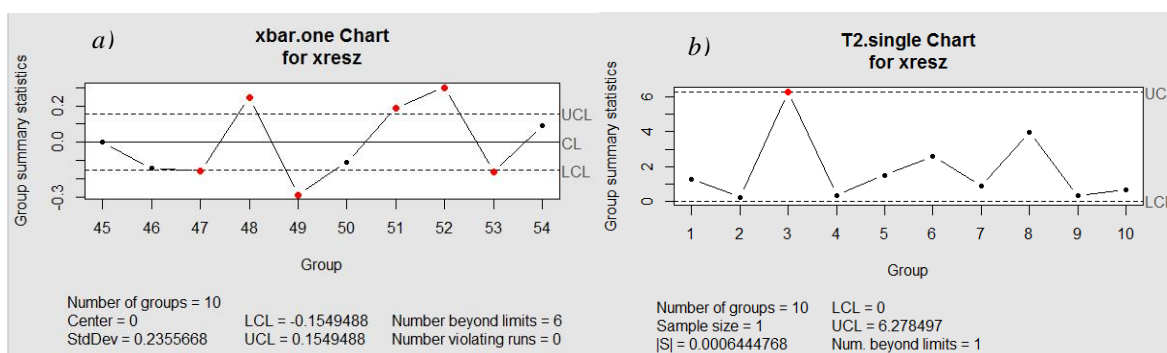
A statisztikai folyamatszabályozás (Statistical Process Control, SPC) során akkor történik beavatkozás a termékgyártás adott folyamatába, ha ismerünk olyan okot, amelynek hatására a minőségjellemző (pl. tömeg) értéke megváltozik. Az SPC fő eszközei közé az ellenőrző (más néven szabályozó) kártyák sorolhatók (Kemény et al., 1998).

#### **Módszerek**

A statisztikai folyamatszabályozáson belül elkülöníthetők az egy-, illetve a többváltozós folyamatszabályozási módszerek. A két módszer közötti fő különbség, hogy az egyváltozós módszereknél (Univariate SPC, USPC) egy ismert változónak az értelmezése történik egy vagy több ismert – nem mesterséges – változóval, míg a többváltozós módszereknél (Multivariate SPC, MSPC) a több ismert változót kevesebb számú mesterséges változóval értelmezzük (Sváb, 1979). A két módszer közötti különbséget mutatja az 1. ábra.



4. ábra: Egy- és többváltozós módszerek összehasonlítása. Forrás: Rogalewicz (2012).



2. ábra: Véletlen számok generálásával kapott a) átlag-kártya és b) T<sup>2</sup>-kártya (95%-os megbízhatósági szinten).

A T<sup>2</sup>-statisztika pontos eloszlása két szemponttól függ (Ittész, 1999):

- egyrészt attól, hogy egyedi vagy csoportosított adatokkal dolgozunk;
- másrészt attól, hogy visszatekintő elemzést végzünk (I. fázis) vagy az aktuális folyamatot felügyeljük (II. fázis).

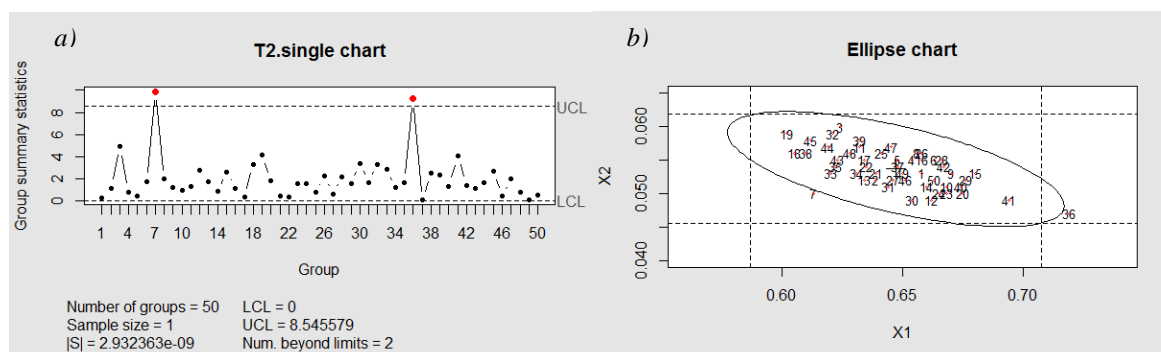
A II. fázisban azonban nehéz értelmezni, hogy mi okozhatta a jel tartományán kívülre kerülését. Lehet, hogy azt az egyik minőségjellemző, esetleg kettő vagy több változó együttműködése, vagy a kovariancia megváltozása váltja ki. Néhány módszert már kidolgoztak erre a problémára, pl. főkomponens-analízist, MYT-felbontást (Mason et al., 1997, Rogalewicz, 2012). Mason et al. (1997) az MYT-felbontás konkrét számítási sémáját írja le.

## Eredmények és értékelésük

A tavalyi, 22<sup>nd</sup> International Symposium on Analytical and Environmental Problems elnevezésű konferencián poszterelőadás keretében bemutattuk az MSPC használatához szükséges elméleti ismereteket, tisztáztuk az alkalmazható összefüggések alakjait és szerepüket, ill. összegyűjtöttük az MSPC alkalmazásának főbb előnyeit és hátrányait az USPC-vel szemben (Mihalkó és Rajkó, 2016).

A munkánk második fázisában elsőként R project-ben megvalósított szimulációs vizsgálatokat végeztünk el, amelyet a következőkben részletezünk. Az algoritmusok egyike a

100 db véletlen szám generálásával („runif” parancs segítségével történt) kapott adatsor felhasználásával elkészített egyváltozós folyamatszabályozás eszközeként használható átlag-kártya látható a 2.a) ábrán. A CL a középvonalat, az UCL az elfogadási tartomány felső határát, az LCL az elfogadási tartomány alsó határát jelenti. A 2.b) ábrán az MSPC során alkalmazható  $T^2$ -kártya látható, ahol a véletlen számok generálásáért az „rmvnorm” parancs a felelős.



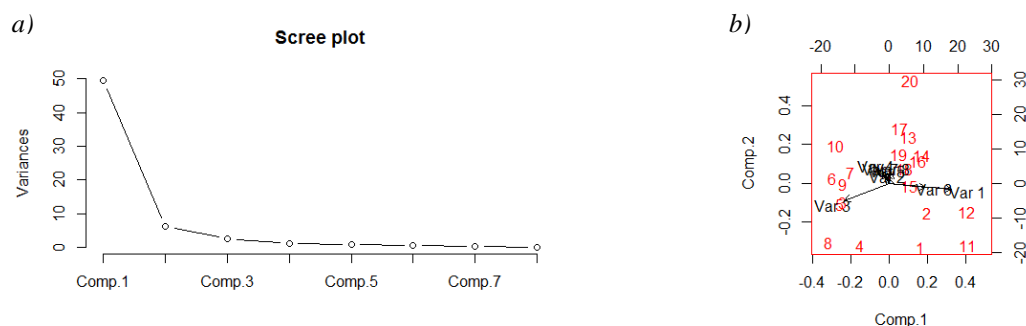
**3. ábra: Pácolt sonka víz- és sótartalma alapján készített a)  $T^2$ -kártya és b) kontrollellipszist tartalmazó ellenőrző kártya Ittész és Zukál példája alapján (99%-os megbízhatósági szinten).**

Az algoritmusok megvalósítása után Ittész András és Zukál Endre mérési adatsorának R-ben történő ellenőrzése következett abból a célból, hogy az Ittész és Zukál (1999) által publikált Hotelling-féle  $T^2$ -kártyát és a kontrollellipszist tartalmazó kártyát visszkapjuk-e (3.a) ábra).

A  $T^2$ -kártyát visszakaptuk, azonban a kontrollellipszist tartalmazó szabályozó kártyát egy hibakód („kisminták számának nagyobbak kell lennie, mint 1”) miatt nem kaptuk vissza a szakirodalomban szereplővel. Az „ellipseChart” nevű parancs forráskódjának átalakítása révén meg tudtuk jeleníteni az ellenőrző kártyát (3.b) ábra).

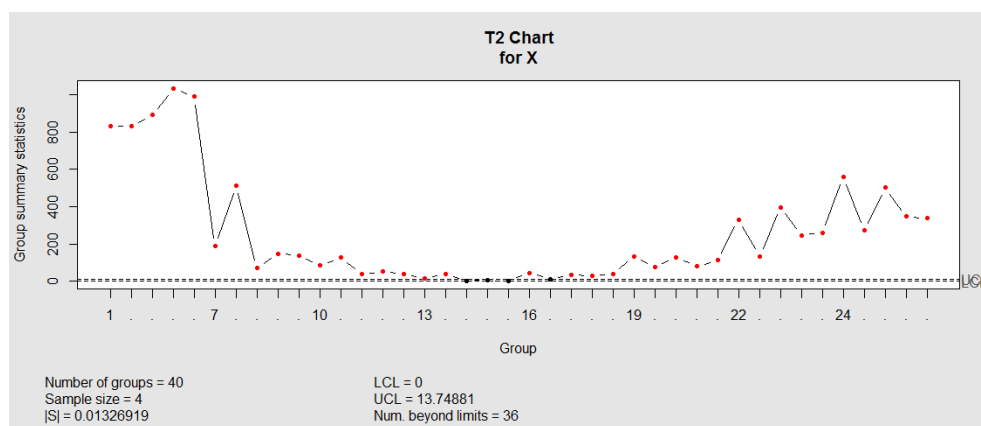
Továbbiakban gyakorlati alkalmazási illusztrációkat hajtottunk végre annak érdekében, hogy bizonyítsuk az MSPC előnyeit az USPC-vel szemben. A gyakorlati alkalmazási illusztrációk egyike a Koppenhágai Egyetem által elérhetővé tett Pármai sonka érlelésének mérési eredményeinek felhasználásával bemutatott folyamatszabályozás (models.life.ku.dk, 2016). Többek között azt sikerült megállapítani, hogy nem szükséges a sonkákat az előállításától kezdődően 15-18 hónapig érlelni, hanem elegendő csak a szűk esztendő (11-12 hónapos) érlelés, legalábbis csak az analitikai mérési eredményeket figyelembe véve.

Ezt követően a főkomponens-analízis módszerét felhasználva az R-ben megvizsgáltuk azt, hogy a 8 megmért változó – nedvesség-, só-, fehérjetartalom, 2 db érzékszervi bírálat, valamint a színérésekhez tartozó L, a és b jellemzők – közül melyeknek lesz faktorhatása. A hegyomlás ábrán (4.a) ábra) látható, hogy 3 főkomponens van. A kettős diagram (4.b) ábra) segítségével belátható, hogy a 3. változó (fehérjetartalom, ennek faktorhatása is van), az 1. és a 6. változó (nedvességtartalom és az L értékek) lényegesen eltér a másik öt változótól.



4. ábra: a) Hegyomlás ábra és b) kettős diagram a Pármai sonka érlelésének változóira nézve.

A másik gyakorlati alkalmazási illusztráció egy saját márkás szalámi érlelésének folyamatkövetése volt, amelynek mérési adatait Rostás Csabának és témavezetőjének, Dr. Eszes Ferencnek köszönünk.



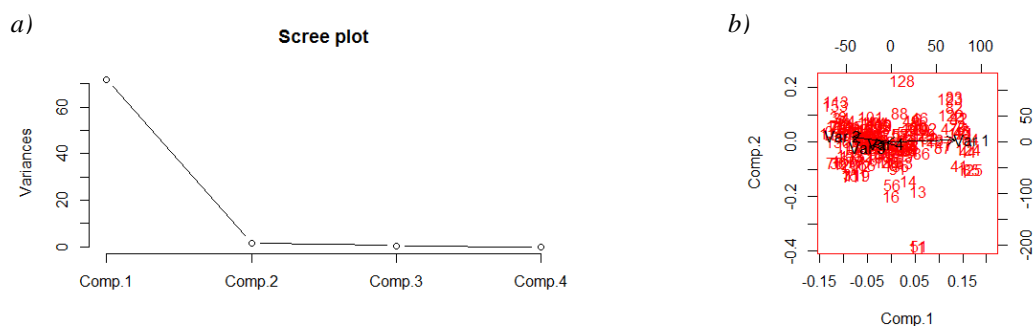
5. ábra: Folyamatkövetés a szalámi érlelésének változóira nézve (95%-os megbízhatósági szinten).

A 5. ábrán jól elkülöníthetőek a szalámi érlelésének főbb szakaszai:

- a füstölés utáni első napokban visszanedvesítés, a kéreg felpuhítása történik,
- a 7. naptól kezdődik a termék szárítása,
- a 10. naptól a 19. nap között a szalámi érlelése stabilizálódik,
- ezután pedig újfent vízelvonás történik, megszűnik a stabil folyamat.

Emellett a hegyomlás ábrán (6.a) ábra) látható, hogy 2 főkomponens van, illetve a kettős diagramról (6.b) ábra) leolvasható, hogy az első változó, illetve a második változó egymástól és a többi minőségjellemzőtől lényegesen eltér.





6. ábra: a) Hegyomlás ábra és b) kettős diagram a szalámi érlelésének változóira nézve.

Végezetül pedig egy példát mutatunk be az MYT-felbontás alkalmazására, vagyis arra keressük a kérdést, hogy mi okozhatja egy jel tartományon kívülre kerülését. Ehhez Itzész és Zukál (1999) mérési adataiból kapott  $T^2$ -statisztika eredményeit használtuk fel (3.a) ábrán látható a  $T^2$ -kártya). Ezen az ábrán látható, hogy 2 zavart jelző pont van, ez a 7. és a 36. minta. A részletezett számítást a 7. mintán keresztül mutatjuk be. Mivel kétváltozós folyamatszabályozásról van szó, ezért kétféleképpen lehet felbontani a 7. mintából kapott  $T^2$ -értéket:

$$T^2 = T_1^2 + T_{2.1}^2 \quad (1)$$

$$T^2 = T_2^2 + T_{1.2}^2 \quad (2)$$

A 7. minta  $T^2$ -értéke 9,888, a felső beavatkozási határ (angol rövidítése: UCL) pedig 8,546, vagyis látható az, hogy a  $T^2$ -érték túllépi az UCL-t, ezért ki kell számolni a feltétel nélküli  $T^2$ -értékeket ( $T_1^2$  és  $T_2^2$  értékeket) és egy új felső beavatkozási határértéket, ezen értékeket az 1. táblázatban összegezzük.

1. táblázat: Feltétel nélküli  $T^2$ -értékek és a hozzá tartozó UCL-érték.

$T_1^2$	$T_2^2$	UCL
2,038	1,544	7,326

Az 1. táblázat értékei azt mutatják, hogy a feltétel nélküli  $T^2$ -értékek az elfogadási tartományba esnek (kisebb az értékük, mint az UCL értéke), így még nem találtuk meg a zavarjelzés okát, emiatt ki kell számolnunk a feltételes  $T^2$ -értékeket (az (1) és (2) egyenlet segítségével), illetve a jellemző felső beavatkozási határértéket, amelyeket a 2. táblázatban összegzünk.

2. táblázat: Feltételes  $T^2$ -értékek és a hozzá tartozó UCL-érték.

$T_{2.1}^2$	$T_{1.2}^2$	UCL
7,850	8,344	7,491

Mivel a feltételes  $T^2$ -értékek túllépik a felső beavatkozási határértéket, ezért a 7. minta esetében a jel tartományon kívülre kerülését az okozza, hogy ennél a mintánál a víz és a sótartalom korrelációja nem követi a többi mérésnél tapasztaltat.

## Következtetések, javaslatok

Ebben a cikkben bemutatjuk az R project-ben megvalósított szimulációs vizsgálatokat és gyakorlati alkalmazási illusztrációkat, amelyekkel igazoltuk az MSPC előnyeit az USPC-vel szemben. Azonban fontos megjegyezni, hogy ezen adatok nem a folyamatszabályozásra megtervezett mérési eredmények, csupán illusztrációkként szolgálnak (mind a Pármai sonka, mind a saját márkás szalámi folyamatkövetése esetében). Ezeknél az adatoknál később megnéztük, hogy mi okozta a jel tartományon kívülre kerülését a II. fázisban, amelyhez vagy főkomponens-analízist vagy az ún. MYT-felbontást használhatjuk.

A későbbiekben elsődlegesen a célunk az, hogy ipari partner segítségével egy adott technológiai folyamat gyakorlatban megvalósuló szabályozását hajtsuk végre, amelyhez pl. optimális kísérlettervet kell kidolgozni.

## Köszönetnyilvánítás



Az Emberi Erőforrások Minisztériuma UNKP-17-2 kódszámú Új Nemzeti Kiválóság Programjának támogatásával készült.

## Irodalom

[http://www.models.life.ku.dk/ParmaHam\\_Fluor](http://www.models.life.ku.dk/ParmaHam_Fluor) (2016. 10. 25.)

Ittész A. (1999): Többváltozós statisztikai folyamatszabályozás, *Minőség és Megbízhatóság*, 33(5), pp. 226-231.

Ittész A., Zukál E. (1999): Többváltozós folyamatszabályozás alkalmazási lehetőségei a húsiparban, *A Hús*, 9(3), pp. 179-183.

Kemény S., Papp L., Deák A. (1998): *Statisztikai minőség- (megfelelőség-) szabályozás*, Műszaki Könyvkiadó – Magyar Minőség Társaság, Budapest, pp. 56-57., pp. 81-83.

Mason R.L., Tracy N.D., Young J.C. (1997): A practical approach for interpreting multivariate  $T^2$  control chart signals, *Journal of Quality Technology*, 29(4), pp. 399., pp. 404-405.

Mihalkó J., Rajkó R. (2016): Advantages and drawbacks of using multivariate statistical process control in food industry, In: *Proceedings of the 22<sup>nd</sup> International Symposium on Analytical and Environmental Problems*, Szeged, pp. 385-389., [http://www2.sci.uszeged.hu/isaep/index\\_htm\\_files/Proceedings%20of\\_ISAEP\\_2016.pdf](http://www2.sci.uszeged.hu/isaep/index_htm_files/Proceedings%20of_ISAEP_2016.pdf)

Rogalewicz M. (2012): Some Notes on Multivariate Statistical Process Control, *Management and Production Engineering Review*, 3(4), pp. 81.

Sváb J. (1979): *Többváltozós módszerek a biometriában*, Mezőgazdasági Kiadó, Budapest, pp. 16.

**E-VITAMIN MÉRÉSRE ALKALMAS NAGYHATÉKONYSÁGÚ  
FOLYADÉKKROMATOGRÁFIÁS MÓDSZEREK FEJLESZTÉSE ÉS VALIDÁLÁSA**

**DEVELOPMENT AND VALIDATION OF HIGH PERFORMANCE LIQUID  
CHROMATOGRAPHY METHODS FOR VITAMIN E MEASUREMENTS**

**Nikolett Nánási<sup>1</sup>, Edina Cseh<sup>1</sup>, Márton Szentirmai<sup>1</sup>, Gábor Veres<sup>1,2</sup>, Péter Klivényi<sup>1</sup>,  
László Vécsei<sup>1,2</sup>, Dénes Zádori<sup>1</sup>**

<sup>1</sup>*Department of Neurology, Faculty of Medicine, Albert Szent-Györgyi Clinical Center,  
University of Szeged, Szeged, Hungary*

<sup>2</sup>*MTA-SZTE Neuroscience Research Group, Szeged, Hungary*  
e-mail: nannik1026@gmail.com

**Abstract**

Tocopherols, also known as the ingredients of fat-soluble vitamin E compounds play an important role in antioxidant mechanisms. Their deficiency of tocopherols, mainly that of  $\alpha$ -tocopherol, can cause several neurological disorders, such as ataxia, myopathy, retinopathy, peripheral neuropathy. The aim of this study was to validate and establish methods applicable for the detection of  $\alpha$ -tocopherol from murine serum and certain brain regions.

In the present study we report 3 different reversed-phase HPLC methods using a single C18 column in isocratic system. The detection was carried out with 3 different detectors. For the detection of murine serum samples, a diode-array detector (DAD) was applied, whereas for murine brain samples electrochemical (ECD) and fluorescence detectors (FLD) were utilized and a detailed validation process was carried out.

The ranges of precision and recovery were the following during the validation processes: 0.61-3.57% and 66.19-105.91%, respectively.

The application of these methods provide a valuable tool for the determination of  $\alpha$ -tocopherol from murine serum and brain samples.

**Bevezetés**

Az E-vitamin csoportjába tartozó 8 vegyület ( $\alpha$ -,  $\beta$ -,  $\gamma$ - és  $\delta$ -tokoferolok, valamint a tokotrienolok) kiemelkedő szereppel bír az oxidatív stressz ellen, közülük is leginkább az aktívabb és magasabb koncentrációban megtalálható  $\alpha$ -tokoferol, mely különös tekintettel az alábbi területeken fejt ki jótékony hatását: keringési- és idegrendszer [1]. Számos neurológiai elváltozás kialakulásában, lefolyásában az antioxidáns rendszer sérült működése állhat. Többek között az ataxia izolált E-vitamin hiány (*ataxia with vitamin E deficiency, AVED*), mely esetén az  $\alpha$ -tokoferol transzporter fehérje ( *$\alpha$ -tocopherol transport protein,  $\alpha$ -TTP*) nem expresszálódik a májsejtekben [2], így nincs, ami biztosítsa a szervezet számára a megfelelő antioxidáns védelmet.

Célunk egy olyan robosztus, reprodukálható metodika fejlesztése, validálása majd alkalmazása, amely gyors és megbízható  $\alpha$ -tokoferol koncentráció méréseket eredményez, úgy az egér szérum, mint az agyi szövetekből is. Egészen az 1980-as évekre nyúlik vissza az ehhez hasonló kutatások gyökere [3], azóta több módszert is alkalmasnak találtak E-vitamin és metabolitjainak meghatározására, ám csak csekély számúban találni hiteles adatokat validálás hiányában [4-7]. Nem találtunk olyan közleményt, mely ilyen meghatározást több detektor és metodika összehasonlításával értékelné.

## Kísérleti rész

Tanulmányunk során C57BL/6 egerek szérum és egyes agyi régióinak (striatum, cortex, hippocampus, cerebellum és agytörzs)  $\alpha$ -tokoferol-szintjét határoztuk meg HPLC (Agilent 1100 és 1260 Series) segítségével. Az állatokból nyert mintákat metodikai módszereink segítségével előkészítettük. Az állatok ( $n = 6$ ) elaltatását követően a bal kamrából vért nyertünk, melyhez meghatározott mennyiségben 50 mg/ml etilén-diamin-tetraecetsav-oldatot (EDTA, Sigma-Aldrich, Saint Louis, MO, Amerikai Egyesült Államok) adtunk, 4°C-on tárolás és 30 percnyi alvadás után 3500 fordulat/perc sebesség mellett 5 percig centrifugáltuk a vérmintákat 4°C-on (Hettich Mikro 220, Tuttlingen, Németország). A felülúszókat egy 2,2 ml-es Eppendorf csöbe gyűjtöttük össze, majd vortex segítségével 20 másodpercig homogenizáltuk. A homogenizált szérumból 200  $\mu$ l-nyi mennyiségeket azonnal stabilizáltunk 200  $\mu$ l 85 mM aszkorbinsav-oldattal (Sigma-Aldrich, Saint Louis, MO, Amerikai Egyesült Államok) és 400  $\mu$ l 1,14 mM butil-hidroxi-toluol (BHT, Sigma-Aldrich, Saint Louis, MO, Amerikai Egyesült Államok) -etanol (VWR International, Radnar, PA, Amerikai Egyesült Államok) oldattal. Az így kapott  $\sim 800$   $\mu$ l stabilizált és homogenizált szérum mintákat ezt követően -80°C-on tároltuk felhasználásig.

Jelen egerek vérmentes agyi régióit is felhasználtuk, melyeket perfuzionálás útján kaptunk, melyet perisztaltikus pumpa segítségével a bal kamrába mesterséges agyfolyadékot áramoltattunk 3 percig. Az agyszöveteket jégen választottuk szét, majd 1,5 ml-es Eppendorf csövekbe helyeztük a régiókat és felhasználásig -80°C-on tároltuk őket. A szövetek feldolgozása a következő lépésekből állt. A fagyott agyi régiókat külön-külön lemértük analitikai mérlegen, majd 1020  $\mu$ l homogenizáló oldat hozzáadása után UH100 homogenizátorral (amplitúdó 100%, ciklus: 0,5) agytömegtől függően 1-2 perc alatt szétroncsoltuk a mintákat. A homogenizált agyi mintákat 10 percig 4°C-on tároltuk, majd 12000 fordulat/perc sebesség mellett 10 percen keresztül ülepítettük őket 4°C-on. A további mintaelőkészítés megegyezett a szérumnál tárgyaltakkal.

Három detektálási módszert alkalmaztunk  $\alpha$ -tokoferol meghatározásra. A vérből nyert szérumot DAD, az agyi régiókat ECD és FLD detektálás mellett mértük.

Mérés előtt felolvasztott, 4°C-os mintákhoz, mind szérum, mind agyi minta esetén 600  $\mu$ L 1,13 mM koncentrációban BHT-t és rac-tocolt (Matreya LLC., Pleasant Gap, PA, Amerikai Egyesült Államok) tartalmazó hexán (Sigma-Aldrich, Saint Louis, MO, Amerikai Egyesült Államok) oldatot adtunk. Pontosan 1 percen keresztül kevertettük vortex segítségével az oldatokat. Ezután a hexános és etanolos fázist elválasztandó 12000 fordulat/perc sebességgel 10 percig centrifugáltunk 4°C-on. A centrifugálást követően a felső, hexános fázisból 450  $\mu$ L-t bepároltunk  $N_2$  gázzal hozzávetőlegesen 15 perc alatt. Ezután a visszamaradt komponenseket 28,57 V/V% etanol (VWR International, Radnar, PA, Amerikai Egyesült Államok), 28,57 V/V% 1,4-dioxán (Sigma-Aldrich, Saint Louis, MO, Amerikai Egyesült Államok), 42,86 V/V% acetonitril (ACN, VWR International, Radnar, PA, Amerikai Egyesült Államok) elegyben oldottuk és 10 másodpercig vortexszel homogenizáltuk, így injektálásra és elválasztásra kész állapotra hozva a mintákat.

Szérum minták elválasztásához Agilent 1260-as rendszeren Kinetex C18 (150x4,6 mm; 5  $\mu$ m, Phenomenex Inc., Torrance, CA, Amerikai Egyesült Államok) oszlopot használtunk 25°C-os hőmérsékleten termosztálva. A kolonna védelme érdekében előtét kolonnát használtunk: Security Guard C18 (4x3 mm, Phenomenex Inc., Torrance, CA, Amerikai Egyesült Államok). A mobilfázis összetétele: 66,54 V/V% ACN (VWR International, Radnar, PA, Amerikai Egyesült Államok), 21,40 V/V% tetrahidrofurán (THF, Sigma-Aldrich, Saint Louis, MO, Amerikai Egyesült Államok), 6,61 V/V% metanol (Sigma-Aldrich, Saint Louis,

MO, Amerikai Egyesült Államok), 2,72 V/V% ammónium-acetát (Sigma-Aldrich, Saint Louis, MO, Amerikai Egyesült Államok) 1 vegyes százalékos oldata, 2,72 V/V% desztillált víz (injekcióhoz való víz). A mobilfázist minden mérés előtt frissen készítettük és az elkészítését követően kerámiaszűrőn 0,45 µm-es pórusméretű hidrofób PVDF membránszűrőn vízsugárszivattyú segítségével szűrtük. A mobilfázis áramlási sebessége 2,1 mL/perc volt. Minden mintából 50 µL térfogatot injektáltunk a mérések során.

Agyminták esetén Agilent 1100 rendszeren Luna C18(2) oszlopot (75x4,6 mm; 3 µm, Phenomenex Inc., Torrance, CA, Amerikai Egyesült Államok) 25°C-os hőmérsékleten termosztálva. A kolonna védelme érdekében szintén előtét kolonnát használtunk: Security Guard C18 (4x3 mm, Phenomenex Inc., Torrance, CA, Amerikai Egyesült Államok). A mobilfázis összetétele ECD méréshez: 91,25 V/V% metanol (Sigma-Aldrich, Saint Louis, MO, Amerikai Egyesült Államok), 4,25 V/V% desztillált víz, 4,50 V/V% izopropil-alkohol (VWR International, Radnar, PA, Amerikai Egyesült Államok), 0,291 vegyes% nátrium-perklorát (Sigma-Aldrich, Saint Louis, MO, Amerikai Egyesült Államok). Hasonlóan, mint DAD méréseknél, a mobilfázist minden mérés előtt frissen készítettük és az elkészítését követően kerámiaszűrőn 0,45 µm-es pórusméretű hidrofób PVDF membránszűrőn vízsugárszivattyú segítségével szűrtük. A mobilfázis áramlási sebessége 1,2 mL/perc volt. Minden mintából 10 µL térfogatot injektáltunk a mérések során mintatermosztálás mellett (4°C). A mobilfázis összetétele FLD mérés esetén az alábbi volt: 100 V/V% metanol (Sigma-Aldrich, Saint Louis, MO, Amerikai Egyesült Államok). A mobilfázis áramlási sebessége 1,8 mL/perc volt. Minden mintából 10 µL térfogatot injektáltunk a mérések során mintatermosztálás mellett (4°C)

ECD esetén a beállított munkapotenciál (előzetes feszültség vs. áramerősség görbék felvételével) +700 mV volt, FLD esetén a gerjesztési hullámhossz 292 nm, a mérési hullámhossz pedig 330 nm volt [8]. DAD esetén az α-tokoferol (Sigma-Aldrich, Saint Louis, MO, Amerikai Egyesült Államok) 292 nm-en, míg a belső standardot (rac-tokol, Matreya LLC., Pleasant Gap, PA, Amerikai Egyesült Államok) 297 nm-en regisztráltuk. A metodikákat az ICH által megfogalmazott paraméterek szerint validáltuk, így meghatároztuk a metodikák pontosságát, érzékenységét, szelektivitását, linearitását és visszanyerhetőségét.

## Eredmények

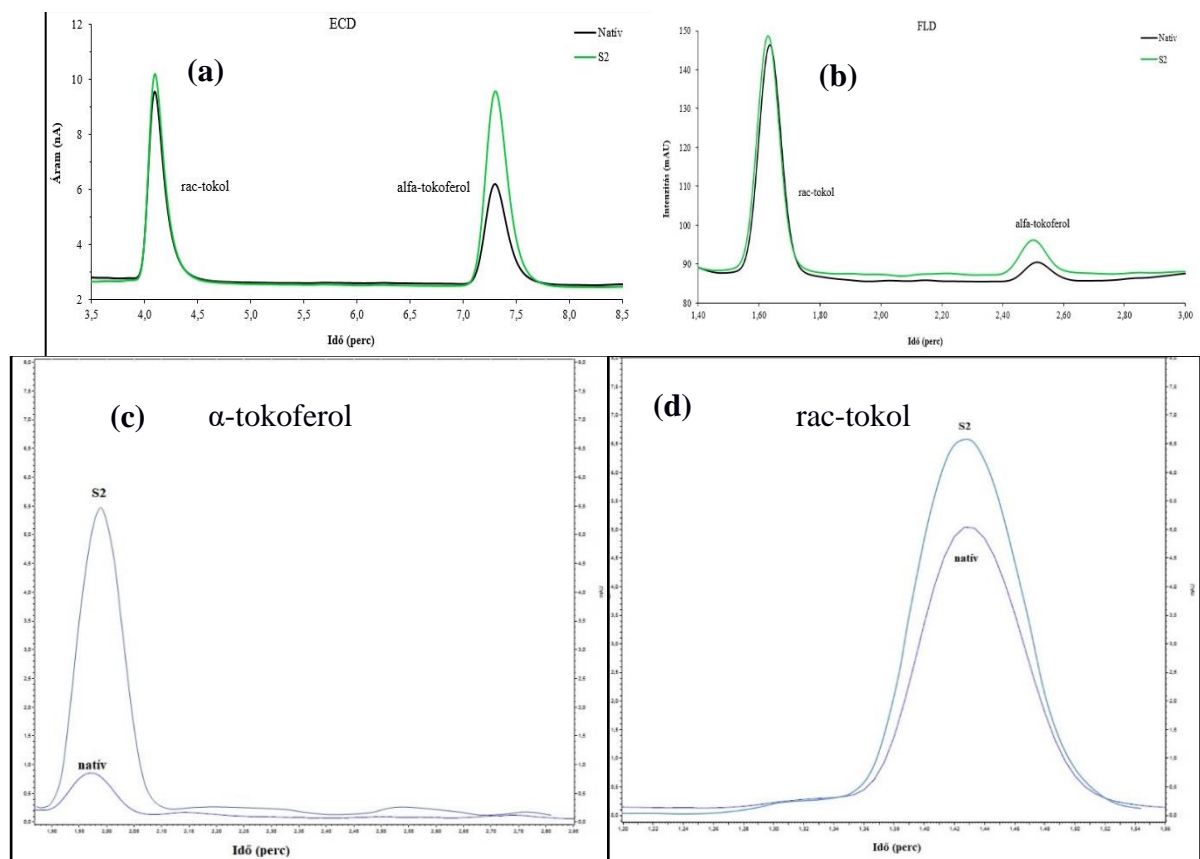
A validálás során a **1. Táblázatban** látható eredményeket kaptuk, ahol a variációs együtthatók (*coefficient of variance*, CV%) értékek láthatók, a mérési variancia és a mérés átlagának hányadosa százalékos értékben kifejezve. A visszamérési tényező (*recovery factor*, RF) kiszámítására 2 olyan oldatot készítünk, mely a natív mintához képest ismert koncentrációban hozzáadott analitot tartalmaz. A S1 oldat alacsony, míg az S2 oldat magasabb koncentrációban tartalmazza az analitokat. A mért koncentráció és az ismert koncentráció hányadosa a RF értékekkel szolgál, százalékban kifejezve. A linearitás megállapításához minden esetben 6 tagú kalibráló oldatsorozatot készítettünk. Az integrált csúcs alatti területeket a kalibráló oldat ismert koncentrációinak függvényében ábrázolva, és alkalmazva a legkisebb négyzetek módszerét, minden analitra igen jó linearitást mutattunk ki ( $R^2 \geq 0.99$ , kiértékelő szoftver: R Development Core Team, 2002). A metodikák szelektivitását az **1. ábra** mutatja be, ahol egy natív és egy S2 mintát mutatunk be. A meghatározási határ (*limit of quantification*, LOQ) azt a legkisebb koncentrációt jelenti, mely még megfelelő precizitással és helyességgel meghatározható, míg a kimutatási határ (*limit of detection*, LOD) az alapzaj háromszorosának megfelelő magasságú jelet adó koncentráció, illetve a következő képletekkel határoztuk meg ( $\sigma$ : a vakminta szórása,  $S'$ : érzékenység).

$$\text{LOD} = 3.3 \sigma/S', \text{ illetve } \text{LOQ} = 10 \sigma/S'$$

1. egyenlet. LOD és LOQ számítására alkalmas képletek.

3. Táblázat. HPLC metodikák validálási eredményei.

Metodikák validálása	Komponens	α-tokoferol			rac-tokol		
	Metodika	DAD	ECD	FLD	DAD	ECD	FLD
Precizitás	Terület	0,73%	1,46%	3,57%	0,61%	1,82%	0,75%
	c (μM)	0,73%	1,49%	3,46%	0,62%	1,84%	0,75%
Visszanyerési tényező	RF 1	71,00%	103,64%	86,86%	-	-	-
	RF 2	66,19%	105,91%	103,96%	-	-	-
Érzékenység (S')		5230	0,1086	0,0631	5520	0,0247	0,094
Kimutatási határ (nM)		23	6	69	590	148	28
Meghatározási határ (nM)		69	17	207	1790	447	83



5. ábra. (a) ECD, (b) FLD detektorral regisztrált kromatogramjai ugyanazon agyi szövetek natív és S2 mintáiból, (c) és (d) DAD detektorral regisztrált egérszérum kromatogramjai.



### **Összefoglalás**

Sikerült megfelelő mintaelőkészítést követően  $\alpha$ -tokoferolt meghatározni egér szérum és agyszövetből, sikeresen validáltuk a metodikáinkat, valamint meghatároztuk, hogy agyszövet esetén a kétféle detektálás (ECD és FLD) hasonlóan robosztus és precíz.

### **Köszönetnyilvánítás**

A kutatás a GINOP-2.3.2-15-2016-00034 és EFOP-3.6.1-16-2016-00008 pályázatokból valósult meg. Dr. Zádori Dénest a Magyar Tudományos Akadémia Bolyai János Kutatási Ösztöndíja támogatja.

### **Irodalomjegyzék**

- [1] Hacquebard M., Carpentier Y. A., Current Opinion in Clinical Nutrition & Metabolic Care, 2005; 8:133-138.
- [2] Eggermont E., European Journal of Pediatrics, 2006; 165:429-434.
- [3] R.G.Fariello, O. Ghilardi, A Pescgechera, Neuropharmacology, 1988, 10:1077-1080
- [4] M. Podda, C. Weber, M. G. Traber, L. Packer, Journal of Lipid Research, 1996, 37: 893-901.
- [5] G. T. Vatassery, H. T. Quach, W. E. Smith, Biochimica et Biophysica Acta 1782, 2008, 414-420.
- [6] S. Hagl, D. Berressem, R. Grewal, Nutritional Neuroscience, 2016, 19:1, 1-10.
- [7] K. Takahashi, S. Takisawa, K. Shimokado, European Journal of Nutrition, 2017, 56:1317-1327.
- [8] C. Yuan, M. Burgyan, D.R. Bunch, Journal of Separation Science, 2014, 2293-2299.



SYNTHESIS AND CHARACTERIZATION OF CONTROLLED-SIZE  
CU NANOPARTICLES

Ádám Nyitrai<sup>1</sup>, Levente Juhász Koppány<sup>2</sup>, András Sápi<sup>2</sup>, Ákos Kukovecz<sup>2</sup>,  
Zoltán Kónya<sup>2</sup>

<sup>1</sup> University of Szeged, Dept. of Applied & Environmental Chemistry, Rerrich Bela ter 1. ,  
Szeged, H-6720, Hungary  
e-mail:adam19960728@mail.com    telszám:+36303140254

<sup>2</sup> University of Szeged, Dept. of Applied & Environmental Chemistry, Rerrich Bela ter 1. ,  
Szeged, H-6720, Hungary

**Abstract**

In industrial applications, synthesis of monodisperse catalyst particles is problematic, therefore the effect rising from the size in catalytic processes remain unexploited. In this work, copper nanoparticles with narrow size distribution were fabricated with a wet chemistry method, in higher temperature, under argon atmosphere. In this process, 3-15 nm copper nanoparticles were produced with controlled size.

The free standing catalysts were characterized by and transmission electron microscopy, electro diffraction.

**Acknowledgements**

This paper was supported by the János Bolyai Research Scholarship of the Hungarian Academy of Sciences and the ÚNKP-ÚNKP-16-4 New National Excellence Program of the Ministry of Human Capacities as well as the Hungarian Research Development and Innovation Office through grants NKFIH OTKA PD 120877 of AS. ÁK is grateful for the fund of NKFIH (OTKA) K112531 & NN110676. This collaborative research was partially supported by the “Széchenyi 2020” program in the framework of GINOP-2.3.2-15-2016-00013 “Intelligent materials based on functional surfaces – from syntheses to applications” project.

## TiO<sub>2</sub>-WO<sub>3</sub> KOMPOZIT FOTOKATALIZÁTOROK HATÉKONYSÁGÁNAK FELTÉRKÉPEZÉSE KÜLÖNBÖZŐ SZERVES SZENNYEZŐK BONTÁSA ESETÉN

**Eszter Orbán<sup>1</sup>, Zsolt Pap<sup>1,2,3</sup>, Gábor Kovács<sup>1,2,3</sup>, Hernádi Klára<sup>2</sup>, Lucian Baia<sup>1,3</sup>**

<sup>1</sup>*Institute for Interdisciplinary Research on Bio-Nano-Sciences, Treboniu Laurian 42, RO-400271 Cluj-Napoca, ROMANIA*

<sup>2</sup>*Research Group of Environmental Chemistry, Institute of Environmental Science and Technology, University of Szeged, Szeged, HUNGARY*

<sup>3</sup>*Faculty of Physics, Babeş-Bolyai University, Mihail Kogălniceanu 1, RO-400084 Cluj-Napoca, ROMANIA*

*e-mail: eszterorban94@gmail.com*

### **Abstract**

Among the increasing water pollution, organic dyes have gained growing attention because their environmental persistence and resistance to conventional treatment technologies. The widespread use of organic dyes in textile industry produced a great damage to the environment. There are many different organic textile dyes in synthetic-cotton textile industries, for instance, reactive azo dyes or triaryl methane-based dyes, which are known to have carcinogen and mutagenic effects.

The aim of our research is to resolve the problems caused by the textile industries using TiO<sub>2</sub>-WO<sub>3</sub> composite photocatalysts. The most efficient composite was characterized by SEM, DRS and XRD and its photocatalytic activity was investigated in-detail. The reusability of the composite was also investigated showing the increased photostability of these materials. The composition of the composite and the most preferable operational pH value was optimized in order to further enhance the efficiency of the composites.

### **Bevezetés**

Az ipari forradalom következtében a textilipar a világ egyik vezető ágazatává nőtte ki magát. Emiatt azonban a hidroszféra szennyezettsége is nagymértékben megnőtt, következésképpen a különböző víztisztítási eljárások jelentősége előtérbe került. Mivel sok olyan szennyezőanyag is belekerül természetes vizeinkbe, amelyek hagyományos módszerekkel nem ártalmatlaníthatóak, fontos szerep jut az alternatív víztisztítási módszereknek, így a heterogén fotokatalízisnek is. Az eljárás lényege, hogy egy félvezető esetén gerjesztéskor az elektron a vegyértéksávból a vezetési sávba kerül, pozitív töltésű lyukat hagyva a vegyértéksávban. Az így létrejövő elektron-lyuk pár redox-reakcióban vehet részt, lebontva a vízben lévő szerves anyagokat, esetünkben szerves festékmolekulákat.

Jelen munka célja a felületi töltés megváltoztatásán alapuló módszer segítségével két félvezető oxidból álló kompozit fotokatalizátor előállításának. A továbbiakban ennek a kompozitnak a vizsgálata, majd a fotokatalitikus hatékonyságának javítása: a kompozit összetételének optimalizálása által, valamint a lebontandó festék pH tartományának változtatásával, különböző szerkezetű modellfestékek felhasználásával.

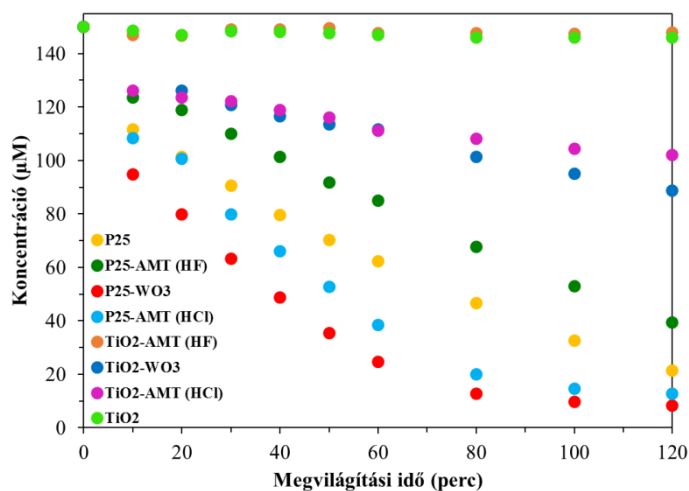
### **Kísérleti rész**

Az általam használt eljárás az egyedi oxidok izoelektromos pontjának meghatározásán alapszik, az irodalomban már leírt módszer szerint [1]. A következőkben a két oxid felületén kialakuló ellentétes töltés miatt -a két félvezető izoelektromos pontja közötti pH

intervallumban a felületi töltésük ellentétes- kialakuló elektrosztatikus vonzóerőre alapozva elkészítettük a kompozitokat, Úgy az irodalomra, mint a saját méréseinkre (SEM és EDX felvételekre) alapozva, az így kapott kompozitok homogenitása nagymértékben megnő a mechanikus keveréssel készültekhez képest [2].

### Eredmények és értékelésük

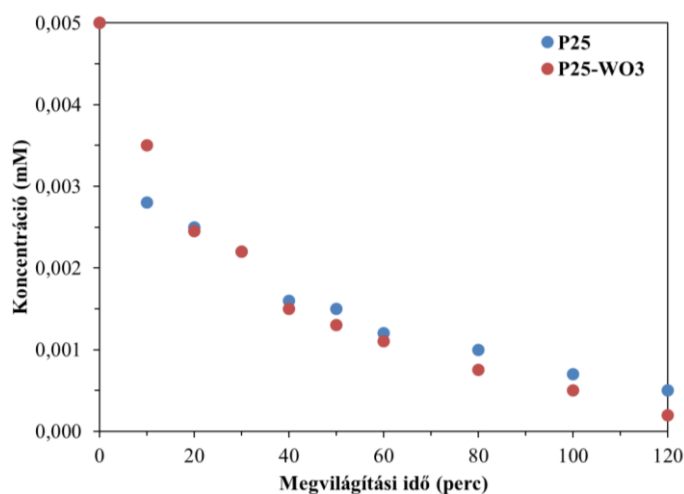
Korábbi kísérleti munkám során három féle (általunk előállított) volfrám-trioxidot és két féle (egy kereskedelemben kapható és egy általunk előállított) titán-dioxidot használtam, tesztelve hatékonyságukat metilnarancs-oldat bontásával, amelyhez egy UV fényvel működő,  $6 \times 6$  W fluoreszcens, higanygőz lámpával ellátott ( $\lambda_{\max} \approx 365$  nm) fotoreaktort használtam. A folytonos levegőáram ( $45\text{-}60 \text{ L}\cdot\text{h}^{-1}$  hozam) és keverés biztosította az oxigén-ellátást a bontás során, és a katalizátor egyenletes eloszlását a modellszennyező oldatában, ugyanakkor a termosztatálásnak köszönhetően az oldat hőmérséklete állandó  $25^\circ\text{C}$  maradt. A szuszpenzió töménysége pedig  $1 \text{ g}\cdot\text{L}^{-1}$  volt. A bontás során vett mintákat egy SPECORD 250 típusú spektrofotométerrel vizsgáltam. A katalizátorok fotokatalitikus hatékonyságát az 1. ábra szemlélteti.



1. ábra: A metilnarancs-oldat bomlási görbéi

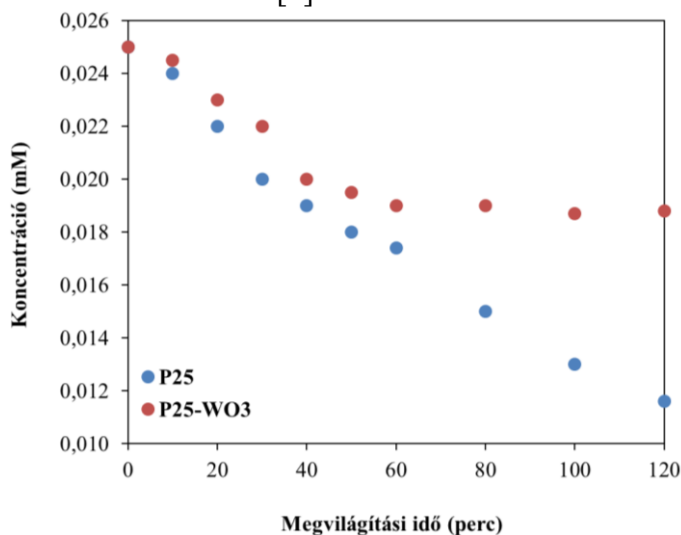
Az 1. ábrán látható, hogy a P25-WO<sub>3</sub> jelű minta hatékonysága (94,4%-os konverzió) a legjobb a kompozitok közül, sőt a referenciakatalizátornál, a P25-nél (85,7%) is hatékonyabb. Ez a hatékonyságbeli változás az egyedi félvezetők morfológiai sajátosságainak tudhatók be, hiszen korábbi elektronmikroszkópos vizsgálataink alapján nagyon eltérő formájú részecskék keletkeznek a különböző előállítási módszerek során [3].

A továbbiakban a leghatékonyabbnak bizonyult fotokatalizátorral végeztem vizsgálatokat. A metilnarancs-oldaton kívül triaril-metán festékek bonthatóságát is vizsgáltam (malachitzöld és kristályviola), melyek eredményeit a következő ábrákon illusztráltam.



2. ábra: A malachitzöld-oldat bomlászörfbéje

A malachitzöld-oldatot (2. ábra) mindkét katalizátor nagy hatékonysággal bontja, P25 esetén 88 %-os a konverzió két óra elteltével, míg a P25-WO<sub>3</sub> 98 %-os konverzióértéket mutat. A malachitzöld bomlási mechanizmusával több tanulmány is foglalkozik, de nem egyértelmű, hogy milyen folyamatok mennek végbe vagy milyen köztitermékek keletkeznek a bomlás során. A szakirodalom alapján a malachitzöldet a TiO<sub>2</sub> bázikus közegben bontja le a legkönnyebben, így az ideális pH-tartomány kiválasztása fontos lehet a kompozit hatékonyságának növelésének érdekében [4].

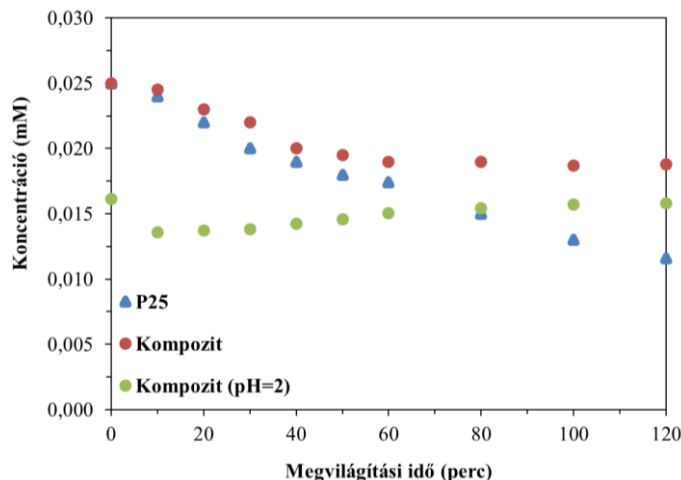


3. ábra: A kristályviola-oldat bomlászörfbéje

Ahogy a 3. ábrán jól látható, a kristályviola oldatot jobban bontja a P25, 53,3%-ban lebontja a színezéket. Ezzel ellentétben a kompozit esetén a színezék valószínűleg csak adszorbeál a WO<sub>3</sub> felületén, így a P25 a kompozitban nem tudja lebontani a kristályviolát. Az irodalomban a kristályviola degradációjának pH-függését is tanulmányozták, és arra a következtetésre jutottak, hogy savas közegben a kristályviola könnyebben lebomlik, ezért nagy jelentőség tulajdonítható a pH intervallumnak, amelyen az oldatot bontjuk [5].

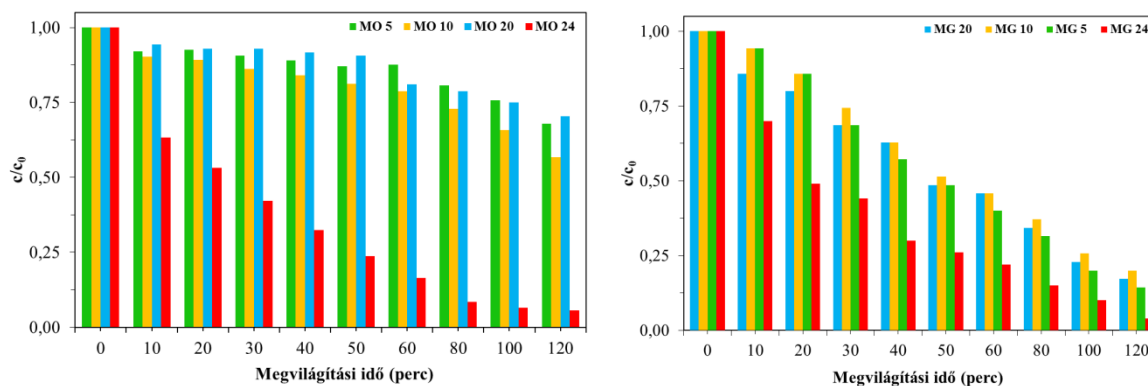
A szakirodalom alapján a platínával nanorészecskéekkel módosított kereskedelmi titán-dioxid pH = 3 értéknél, tehát savas közegben hatékonyabb fotokatalizátor, mint bázikus (pH = 9) vagy semleges közegben kristályviola-oldat esetében [5]. Ebből kiindulva sósav

segítségével beállítottuk a kristályviola-oldat savasságát (pH = 2-nél kék színű az oldat, az átsapás pH = 2,5-nél figyelhető meg), és megvizsgáltuk a fotokatalitikus aktivitását, hogy összehasonlíthassuk az alap pH-jú (pH = 5,3) kristályviola-oldat bontásának hatékonyságával (4. ábra). Referencia katalizátorként a P25-t használtuk, amely 54%-ban bontotta a kristályviola-oldatot. A pH = 5,3-as bontás esetén megfigyelhető a már említett adszorpció, ahogy az első órában csökkent az oldat koncentrációja. Méréseink során érdekes eredményre jutottunk, ugyanis a 2-es pH-jú oldat bontása során a színezék nagy százalékát (64 %-át) adszorbeálta a kompozit, már a szuszpenzió készítése közben (4. ábra). Ezen kívül a mérési adatok alapján feltételezhető, hogy a savas közegben történő protonálódás (a színváltozás ennek tudható be, batokróom eltolódást szenved a molekula) miatt egy adszorpció-deszorpció-oszcilláció következik be, ahogy az a 4. ábrán is látható.



4. ábra: A különböző pH-jú kristályviola-oldatok bomlásgörbéi

Mivel a kereskedelemben kapható  $\text{WO}_3$  az általunk vizsgált összes forgalmazó esetén drágább, mint a szintén kereskedelemben forgalmazott  $\text{TiO}_2$ , hangsúlyt fektettünk - a költségek csökkentésének céljából - a volfrám-trioxid mennyiségének csökkentésére is, figyelembe véve az elsődleges szempontot, a fotokatalitikus hatékonyságot. Összehasonlításképpen az Alfa Aesar vegyszerforgalmazó 100 g  $\text{WO}_3$  ára 54,4 Euro, míg 100 g  $\text{TiO}_2$  24,36 Euro. Előző kísérleteinkben a  $\text{TiO}_2:\text{WO}_3$  arány 76:24 volt. Ahogy az az 5. ábrán is látható, két színezék (metilnarancs- és malachitzöld-oldat) esetén is vizsgáltuk a különböző összetételű kompozitok fotokatalitikus aktivitását. Az irodalomban található adatok ellentmondásosnak bizonyultak [6,7], hiszen kiderült, hogy nem csak színezék-, de katalizátorfüggő is az optimális összetétel. A méréseink alapján megállapítható, hogy az eddig használt 76:24 tömegarány a legkedvezőbb összetétel az általunk vizsgált modell-szennyezők irányába tanúsított fotokatalitikus aktivitás szempontjából.



5. ábra: Fotokatalitikus aktivitás metilnarancs (MO X) és malachitzöld (MG X, ahol X a WO<sub>3</sub> koncentrációja) esetén különböző kompozitösszetételeknél

### Összefoglaló

Összegezve eddigi eredményeinket, elmondható, hogy sikerült reprodukálni és jellemezni úgy az egyedi oxidokat, mint a kompozitokat. A pH befolyásolását és ennek hatásait vizsgáló első kísérleti lépéseit megtettük, amelyek több kérdést is felvetettek, így további kísérleteinkben ennek a paraméternek a vizsgálatára is nagy hangsúlyt kívánunk fektetni. Ezután sikeresen optimalizáltuk a kompozit összetételét, vizsgálva a fotokatalitikus aktivitást metilnarancs- és malachitzöld-oldat esetén is. Levontuk a következtetést, hogy mindkét esetben a TiO<sub>2</sub>:WO<sub>3</sub> = 76:24 arány a leghatékonyabb, tehát a továbbiakban is érdemes ezzel az aránnyal dolgozni.

### Köszönetnyilvánítás

Köszönöm a pénzügyi támogatást a Márton Áron Tehetséggondozó Programnak, továbbá Pap Zsolt köszönetét fejezi ki a Magyar Tudományos Akadémia Prémium Posztdoktori Ösztöndíjprogramnak az anyagi támogatásért.

### Hivatkozások

- [1] E. McCafferty, *Electrochimica Acta* 55 (2010) 1630.
- [2] L. Baia et al., *Mat. Sci. in Sem. Proc.* 42 (2016) 66.
- [3] I. Székely et al., *Mat.* 9 (2016) 258.
- [4] C.C. Chen et al., *J. of Haz. Mat.* 141 (2007) 520.
- [5] H.J. Fan et al., *J. of Haz. Mat.* 185 (2011) 227.
- [6] É. Karácsonyi et al., *Cat. Tod.* 208 (2013) 19.
- [7] C. Shifu et al., *Pow. Tech.* 160 (2005) 198.

## FEASIBILITY STUDY OF CONTAMINANTS ANALYSIS IN URANIUM-CONTAINING MATERIALS BY LIBS SPECTROSCOPY

<sup>1</sup>Dávid Palásti, <sup>2</sup>Éva Kovács-Széles, <sup>3</sup>Andrey Berlizov, <sup>1</sup>Gábor Galbács

<sup>1</sup>*Department of inorganic and Analytical Chemistry,  
University of Szeged, Szeged, Hungary, email: galbx@chem.u-szeged.hu<sup>1</sup>*

<sup>2</sup>*Department of Radiation Safety, Centre for Energy research,  
Hungarian Academy of Science, Budapest, Hungary*

<sup>3</sup>*International Atomic Energy Agency, Vienna, Austria*

### Abstract

Uranium-containing samples are in the focus of analytical research for various reasons, for example with regards to nuclear safeguarding, quality management or nuclear forensic science. In our present contribution, we overview the challenges related to the analysis of contaminants in uranium-containing samples and the potential solution for overcoming them.

### Introduction

Radioactive materials are very useful, since nuclear power plants provide electrical energy for hundreds of millions people, and they are also extensively applied for diagnostic and therapeutic purposes in medicine. Nevertheless, radioactive materials can mean serious threat too. The radiation emitted by these materials may initiate apoptosis and can severe the DNA, causing tissue deformations. In the current state of the international situation, the great destructive power of nuclear materials should also not be overlooked. Consequently, the regulation and qualification of radioactive materials is an important task. Uranium is one of the most commonly used fuel in nuclear reactors and bombs, thus its properties – including chemical purity - are tested very often.

Laser-induced breakdown spectroscopy (LIBS) is a modern, versatile trace analytical atomic spectroscopic technique, which is becoming increasingly popular in recent years for both quantitative and qualitative purposes. The light from a pulsed laser is focused onto the surface of a solid sample, where it ignites a microplasma. The analytical information can be retrieved from the optical emission of this microplasma. The use of this method usually require minimal or even no sample preparation and very little sample amount, furthermore the measurements can also be accomplished in a stand-off fashion, right in the field. All these characteristics make LIBS an ideal candidate for contaminants analysis in uranium-containing materials.

### Discussion

Radioactive materials are typically analysed for three main causes by the methods of analytical atomic spectrometry.

**Quality management** is an essential part of manufacturing products, and this also goes for nuclear fuel grade uranium dioxide powder and pellets. The regulations of the international standards concerning their physical and chemical properties are very strict [1, 2]. Elemental impurities are also considered to be important, because they can effectively alter the physical properties (density, toughness, sinterability etc.) as well as nuclear properties of the powder and pellets. For example, the presence of a high concentration of boron or other neutron-capturing agents such as Gd, Eu, Dy, Sm and Cd can significantly lower the neutron flux



flowing through the uranium oxide, which in turn lowers the caloric value of the nuclear fuel. For this reason, the total boron equivalent concentration of these elements is not allowed to exceed 4 ppm. The maximum allowable concentration limits for other elements are usually in the 100-300 ppm range, but their cumulative concentration shall not exceed 1500 ppm.

Element	Maximum Concentration Limit of Uranium, µg/gU
Aluminum	250
Carbon	100
Calcium + magnesium	200
Chlorine	100
Chromium	200
Cobalt	100
Copper	250
Fluorine	100
Iron	250
Lead	250
Manganese	250
Molybdenum	250
Nickel	200
Nitrogen	200
Phosphorus	250
Silicon	300
Tantalum	250
Thorium <sup>A</sup>	10
Tin	250
Titanium	250
Tungsten	250
Vanadium	250
Zinc	250

<sup>A</sup> Thorium is primarily of concern because of the reactor production of <sup>233</sup>U.

Table 1. Traditional impurity limits in uranium dioxide according to [2]

**Nuclear forensic investigations** provide answers to questions concerning nuclear materials found outside of the regulatory control. One of such investigations is the elemental or isotopic “fingerprint-like” identification (assignment) of a “nuclear forensic signature” to a sample. This signature is characteristic for the ore, but the processing technology/facility employed will also impose its own signature onto the sample, the latter of which can then be used to identify the “manufacturer” and hence its legal status. This qualitative analytical application can allow the investigators to determine the origin of an unknown nuclear material [3].

In the case of **nuclear safeguards investigations** the analytes are ambient samples (soil, water, etc.). The average concentration of uranium in the Earth’s crust is low (only about 2-4 ppm), so if an elevated level of U concentration is found, it indicates either a leak from a nearby nuclear industry facility or the usage of nuclear weapons such as fission bombs or so called dirty bombs [4]. Due to their purpose, safeguards measurements deal with low concentrations and complex matrices [5].

Many atomic spectroscopy methods, such as graphite furnace atomic absorption spectrometry (GFAAS), spark- and arc atomic emission spectrometry, inductively coupled plasma atomic emission (ICP-AES) and mass spectrometry (ICP-MS), the latter two sometimes also combined with laser ablation sample introduction, were used in the literature for the above analyses. Unfortunately, none of these methods can be executed in the field, either because the instrumentation is bulky and costly, or because the instruments can only process liquid samples, so extensive sample preparation is needed prior to the spectroscopy measurements.

According to recent literature, LIBS has a great potential for becoming a quick, field-applicable, trace analytical technique for radioactive samples. For example, Campbell *et al.*

were able to discriminate different uranium oxides ( $\text{UO}_2$ ,  $\text{U}_3\text{O}_8$ ,  $\text{UO}_3$ ) via the comparison of the relative intensity of some well-chosen uranium and oxygen lines [6]. Barefield *et al.* had shown that uranium and thorium can be detected by LIBS in their ores [7] and the same authors could also determine low concentrations of uranium in a glass matrix severe spectral interferences [8]. Russo *et al.* developed algorithms for spectral deconvolution of uranium isotopic spectral lines and demonstrated their usefulness in soil matrices for the fairly accurate determination of the  $^{235}\text{U}/^{238}\text{U}$  isotope ratio [9]. LIBS limits of detection can also be adequate for even the most demanding technical/safeguards applications (in the sub-ppm range) [10].

It also has to be mentioned that since LIBS is an atomic emission spectrometry method, it generates line-rich spectra (it is not uncommon in complex matrices that the emission spectrum contains over 100,000 spectral lines!). If portable instrumentation with compact, conventional dispersive spectrometers are to be used for the analysis, one will face severe spectral interferences, especially in studies dealing with elements that have several isotopes. If isotope ratios are also to be determined, then the resolution of conventional spectrometers can cause problems, since atomic isotopic shifts are usually very small, on the order of pm only. In addition to this, the plasma is usually generated under atmospheric conditions (even is under a laser ablation chamber for safety reasons), which causes pressure-induced broadening of spectral lines [10].

At the moment it seems that there are two potential solutions to these problems. For isotope-resolving studies, laser ablation molecular isotopic spectrometry (LAMIS), introduced by Russo *et al.* [11], may be a solution. This approach uses LIBS experimental conditions favouring the formation/detection of molecular components and measures the molecular (e.g. oxide, fluoride) isotopic shifts instead of the atomic ones, because the former shift can be 100 times larger than the latter. The other possibility is to use advanced, compact, but high resolution spectrometer optical arrangements, such as the spatially heterodyne spectrometer (SHS) for LIBS. The first studies out in this research area [12, 13] are also promising and suggest that isotopic resolution will indeed be possible in the field by using LIBS spectrometry. At present, we are pursuing both of these approaches (LAMIS and SHS) in order to reach our goal of developing a LIBS-based method for the analysis of contaminants in uranium-containing materials.

## References

- [1] C696-99 Standard test methods for chemical, mass spectrometric, and spectrochemical analysis of nuclear-grade uranium dioxide powders and pellets (Reapproved 2005)
- [2] C753-04 Standard specification for nuclear-grade, sinterable uranium dioxide powder (Reapproved 2009)
- [3] E. Keegan, M. J. Kristo, K. Toole, R. Kips, E. Young: Nuclear Forensics: Scientific analysis supporting law enforcement and nuclear security investigations; *Analytical chemistry*, 88, (2015), 1496.
- [4] S. Boulyga, S.Konegger-Kappel, S. Richter, L. Sangély: Mass spectrometric analysis for nuclear safeguards; *Journal of Analytical Atomic Spectroscopy*, 30, (2015), 1469.
- [5] É. Széles, Zs. Varga, Zs. Stefánka: Sample preparation method development for analysis of safeguards swipe samples by inductively coupled plasma mass spectrometry, *Journal of Analytical Atomic Spectrometry*, 25, (2010), 1014.
- [6] K. R. Campbell, N. R. Wozniak, J. P. Colgan, E. J. Judge, J. E. Barefield II, D. P. Kilcrease, M. P. Wilkerson, K. R. Czerwinski, S. M. Clegg: Phase discrimination of uranium

- oxides using laser-induced breakdown spectroscopy; *Spectrochimica Acta Part B*, 134, (2017), 91.
- [7] E. J. Judge, J. E. Barefield II, J. M. Berg, S. M. Clegg, G. J. Havrilla, V. M. Montoya, L. N. Lopez: Laser-induced breakdown spectroscopy measurements of uranium and thorium powders and uranium ore; *Spectrochimica Acta Part B*, 83, (2013), 28.
- [8] I. Choi, G. C.-Y. Chan, X. Mao, D. L. Perry, R. E. Russo: Line selection and parameter optimization for trace analysis of uranium in glass matrices by laser-induced breakdown spectroscopy (LIBS); *Applied Spectroscopy*, 67, (2013), 1275.
- [9] I. Choi, G. C.-Y. Chan, X. Mao, V. Zorba, O. P. Lam, D. K. Shuh, R. E. Russo: Isotopic determination of uranium in soil by laser induced breakdown spectroscopy; *Spectrochimica Acta Part B*, 122, (2016), 31.
- [10] G. Galbács: A critical review of recent progress in analytical laser-induced breakdown spectroscopy, *Analytical and Bioanalytical Chemistry*, 407, (2015), 7537.
- [11] A.A. Bol'shakov, X. Mao, J. Ghonzalez, R.E. Russo: Laser ablation molecular isotopic spectrometry (LAMIS): current state of the art, *Journal of Analytical Atomic Spectrometry*, 1, (2016), 119.
- [12] D. J. Palásti, I. Rigó, M. Veres, G. Galbács: Construction and initial characterization of a spatially heterodyne LIBS spectrometer, PP23, IX Euro-mediterranean Symposium on LIBS, June 11-16, 2017, Pisa, Italy
- [13] I. B. Gornushkin, B. W. Smith, U. Panne, N. Omenetto: Laser-induced breakdown spectroscopy combined with spatial heterodyne spectroscopy, *Applied Spectroscopy*, 68, (2014), 1076.



SUPPORTED THROUGH THE NEW NATIONAL EXCELLENCE PROGRAM OF THE MINISTRY OF HUMAN CAPACITIES

## ANALYSIS OF THE ANTIOXIDANT PROPERTIES OF SEA BUCKTHORN JAMS DURING STORAGE

Rentsendavaa Chagznaadorj<sup>1</sup>, Diána Furulyás<sup>1</sup>, Gergely Mátravölgyi<sup>2</sup>, Gitta Ficzek<sup>2</sup>,  
Dávid Papp<sup>2</sup>, Mónika Stéger-Máté<sup>1</sup>

<sup>1</sup> Department of Food Preservation, Faculty of Food Science, University of Szent István, H-1118 Budapest, Villányi út 29-43, Hungary

<sup>2</sup> Department of Pomology, Faculty of Horticultural Science, University of Szent István, H-1118 Budapest, Villányi út 29-43, Hungary  
e-mail: furulyas.diana@etk.szie.hu

### Abstract

In the frame of this research, sea buckthorn jams were prepared by blending sea buckthorn pulp with apple pomace powder in varying proportions to achieve especially good organoleptic characteristics and texture without the addition of pectin. Apple pomace is a by-product of apple juice production, and it might be suitable for replacing pectin in jam products. Sea buckthorn is an excellent ingredient of functional foods, having outstandingly useful biologically active compounds. It has positive impact on human health primarily as a result of its high C-vitamin, flavonoid, and carotenoid content.

In this study, we compared the following quality parameters of sea buckthorn jam samples: water soluble dry matter content, titratable acid, polyphenol contents, antioxidant activity, and carotenoid components. Sea buckthorn jams were prepared from 'Leikora' berries by adding different proportions of apple pomace (0, 0.5, 1, 1.5, 2%). One jam was prepared for being used as control by adding pectin. Determination of dry matter content was fulfilled based on Codex Alimentarius 3-1-558/93 formula. Total titratable acid content was determined based on MSZ EN Nr 12147:1998 Hungarian Standard. Antioxidant status was determined by Ferric Reducing Antioxidant power (FRAP) assay and total polyphenol content using spectrophotometer; with high performance liquid chromatography (HPLC)  $\beta$  carotenoid was also identified and quantified. Consumer panel testing of the jams was carried out by sensory testing.

Significant differences were shown in the quality parameters of sea buckthorn jams. Increasing the amount of apple pomace added to the sea buckthorn -apple jams resulted in higher polyphenol content of the samples. The loss of polyphenols was decreasing during storage, the more apple pomace was added to the samples. Adding apple pomace, was also favorable as it lowered the loss of  $\beta$  carotenoid during storage. Increasing the pomace proportion resulted in higher antioxidant capacity; however, the more apple pomace was added, the antioxidant capacity was decreasing in a higher degree during storage. The pomace did not have any negative effect on the sensory attributes, but it favorably affected the changes of valuable components during the storage; thus it might be a suitable replacement of pectin.

**Key words:** *Apple pomace, Sea buckthorn, Jam, Antioxidant, Carotenoid, Polyphenol content.*

### Introduction

In the 21th century, the stress caused by being rushed every day and the lack of physical activity due to the lifestyle of the society (including sitting work) lead to such diseases as obesity, cardiovascular problems, or the diabetes. In many cases it would be sufficient to pay attention to the diverse diet, eat fruits and vegetables ordinary, and even if only to a minimal

extent, but to do some physical work every day. The treatments of those people who suffer from the previously mentioned common diseases are extremely expensive, so the preventing these problems is very important. Nowadays, more and more advertising campaign focuses on the positive effects of fruit consumption, and several scientific research pursues to confirm that also.

Special attention should be paid to those prominent fruit species which contain bioactive compounds. However we know many good sources of bioactive compounds (plants, animals, various microorganisms, or even non-natural materials), that of plant origin have the greatest potential (Guaadaoui et al. 2014; Dóka et al. 2014; Wani et al. 2016). Fruits have huge beneficial effect on human health thanks to their active ingredients, primarily to their C-vitamin, flavonoid, carotenoid, and tocopherol content (Krejcarová et al. 2015).

There are many fruit species which contain significant amount of bioactive compounds however not consumed fresh, only after processing. Among these, sea buckthorn (*Hippophae rhamnoides* L.) is an outstanding species. Due to its bioactive compounds it is especially suitable for functional food production. Several research groups are dealing with the valuable ingredients, and health benefits of sea buckthorn (Ali and Ahmad, 2015; Chakraborty et al. 2015; Song et al. 2014; Korekar et al. 2011). Sea buckthorn is mostly consumed in the form of juices, jams, dried fruits, and dietary supplements.

The aim of this research is to comprehensively analyze the health benefits of a significant sea buckthorn cultivar of the Hungarian growing, and to carry out consumer panel testing of sea buckthorn-apple jams with various compositions, at least three times during storage; furthermore, to follow the changes in the biologically active components, and in the sensory attributes during the storage.

## **Experimental**

### *Raw materials*

Pulp of the sea buckthorn (SB) cultivar 'Leikora' (provided by the Bio Berta Kft.) and the apple cultivar 'Rosmerta' was used to prepare the SB-apple jam samples. We used powder made of the pomace of 'Rosmerta' for the jams, as natural thickening agent.

### *Preparation of jam samples*

The apples were cut into four pieces and then baked on 180 °C in an oven. The sea buckthorn berries were heated to 80 °C by an induction cooker. Finally the pulp of both fruits were gained by pressing them with a high performance press.

The apple pomace, which contains skin, stalk, and seeds parts remained from the pressing, was dried in two steps. At the beginning of the process the drying was done on 70 °C and atmospheric conditions, and later the temperature was reduced to 50 °C to avoid the damage of the low moisture content materials.

The jam samples were prepared by adding apple pulp in 33 %, sea buckthorn pulp in 50 %, and sugar in 17 % proportions. First the pulps were mixed, heated to 80-85 °C, and then the sugar was added.

We weighted out 1 kilogram per sample, then the proper amount of pomace was added to the samples to set the required concentrates. We used two control jams, one was free of pomace or any other thickening agent, and one contained 1% pectin instead of pomace (table 1).

The changes of the six kinds of jams were constantly tracked during the storage. The following parameters were measured, in the 6<sup>th</sup>, 9<sup>th</sup>, and 12<sup>th</sup> month of the storage period: soluble solid content (Brix<sup>o</sup>), acid content, polyphenol content, and FRAP value by

spectrophotometry, and  $\beta$  carotenoid content by HPLC. On the same dates sensory testing were carried out, evaluating the color, taste, secondary taste, odor, secondary odor, acidity, sweetness, and texture of the samples. Data was analyzed with the SPSS 14.0 software. Univariate analysis was carried out to separate homogenous groups by the Duncan test. The RSD value was set to 5 %.

#### Experimental methods

The soluble solid content of the samples was determined by a digital refractometer in Brix %, according to the Codex Alimentarius 3-1-558/93 manual. We measured the titrable acid content according to the MSZ EN 12147:1998 Hungarian regulation. The total acid content (m/m %) was expressed in citric acid equivalent. We determined the total phenolic content with the method of Singleton and Rossi (1965). The absorption was measured on 765 nm, and the results were shown in mg gallic acid/liter (mg GS/l) dimension.

Table 1. Types and codes of jam samples

Sample code	Jam type
0	Free of apple pomace and pectin
1	0,5 % apple pomace
2	1 % apple pomace
3	1,5 % apple pomace
4	2 % apple pomace
P	1 % pectin

We used the modified method of Benzie and Strain (1996) for measuring the water soluble antioxidant capacity (FRAP) of the samples. The absorption of the samples on 593 nm was calculated from the calibration curve made with ascorbic acid, and the values were given in mmol ascorbic acid/liter (mM AS/l) dimension.

The identification and quantification of  $\beta$  carotenoid was done by HPLC method. Carotenoids were extracted from 5 g samples in dark, using 15 ml THF (tetrahydrofuran). The samples were shaken for 12 hours on 4 °C, and on 150 rpm. We placed the supernatant into 1,5 ml Eppendorf tubes and centrifugated it for 5 minutes on -5 C°. The supernatant was then filtered with micro filter and injected into the HPLC instrument. Every measurement was repeated 3 times. The retention time of  $\beta$  carotenoid was 12 minutes.

#### Results and discussion

The soluble solid content of the prepared jam samples ranged between 27 and 29 %. Fluctuation in the values with the storage time were only few tenths, the changes were not significant. The acid content of the samples ranged from 1,8 to 2% at the preparation, which neither has changed significantly during the storage.

We can characterize the antioxidant status of the jam samples excellently by analyzing the polyphenol content, antioxidant capacity, and  $\beta$  carotenoid content, and by following the changes of these during the storage period.

When the samples were prepared, there was linear relationship between the polyphenol content, and the amount of added pomace in the jams, as it is shown in Table 1. The more pomace were added, the better values the jams had. In the 6<sup>th</sup> month of storage the polyphenol content was lower in all of the samples except in sample 0 (free of pomace and pectin). In the



second period of storage the polyphenol content was decreasing even more. The least amount of reduction (25%) was measured in sample 3 (1,5 % apple pomace addition). In the case of the other samples containing apple pomace, the reduction was between 32 to 33 %; while it was 46 % (sample P) and 64 % (sample 0) in the case of those samples which did not contain any apple pomace.

In the 12 month long storage period, the antioxidant capacity showed different tendency than the polyphenol content. In the case of all samples the antioxidant capacity was increasing (by 30 to 50 %) in the first part of the storage period, then in the rest of the storage time it was decreasing. The lowest amount of reduction was showed in the samples containing apple pomace. The reduction was 5% in the sample containing 0,5 % pomace, 26% in the sample of 1 % pomace, and 38 % in that of 1,5 % apple pomace. In the case of the samples free of pomace, sample 0 and sample P, the degree of reduction was 10 and 31 %, respectively. In the case of the samples having high pomace content, 1,5 and 2 %, the antioxidant capacity was decreasing in a very high amount: 38 and 53 %, respectively.

Table 1. Changes in the polyphenol content,  $\beta$  carotenoid content, and FRAP values of sea buckthorn-apple jams during storage

		sample 0	sample 1	sample 2	sample 3	sample 4	sample P
<b>Polyphenol content (mg GS/l)</b>	freshly prepared	1919	2219	2169	2373	2673	2019
	6th month of storage	2000	1840	1927	2227	2469	1660
	12th month of storage	1169	1481	1469	1790	1794	1169
<b>FRAP (mM AS/l)</b>	freshly prepared	4,6	3,7	5,0	7,2	6,5	5,5
	6th month of storage	9,8	10,2	9,1	13,9	12,2	11,8
	12th month of storage	5,8	4,2	6,4	10,0	10,2	7,2
<b><math>\beta</math> carotenoid content (mg/ml)</b>	freshly prepared	0,188	0,145	0,122	0,101	0,093	0,084
	6th month of storage	0,133	0,102	0,097	0,082	0,115	0,112
	12th month of storage	0,067	0,144	0,147	0,062	0,116	0,045

The  $\beta$  carotenoid content of the individual samples changed differently during storage. We can see that higher apple pomace concentrates coincide with lower  $\beta$  carotenoid content. A possible explanation for this is that, according to the literature, apple does not contain  $\beta$  carotenoid at all.

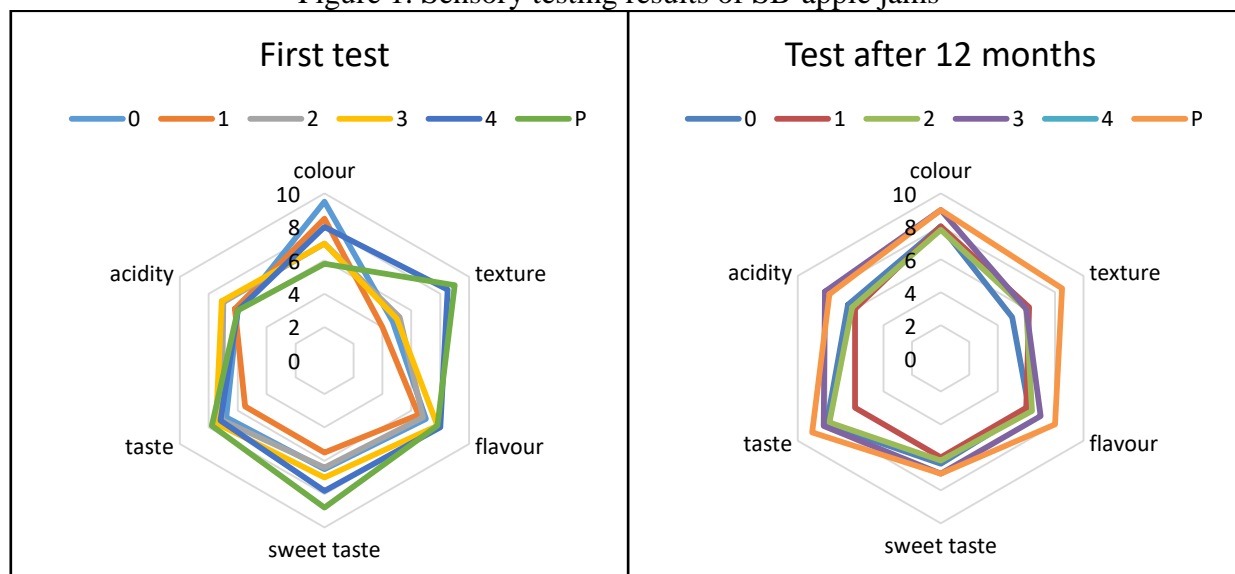
However, during storage the added pomace hinders the degradation of  $\beta$  carotenoids. In the end of the 12 month long storage, in the samples containing no apple pomace (sample 0 and P) the carotene content dropped drastically to 64 and 46 %, respectively. In contrast, no significant change was measured in the samples containing apple pomace (sample 2 and 4), or the change was very slightly (0,7%, sample 1). Sample 3 was an exception, where the reduction was 38 %; this should be clarified by further investigations.



The sensory testing data is suggesting that the lower pomace concentrate of the samples results in more preferable color. However, the samples containing high amounts of pomace had more favorable taste and odor.

Sample 3 and 4 reached outstandingly high scores. Concerning acidity, the samples containing no pomace were not preferred.

Figure 1. Sensory testing results of SB-apple jams



With the increase of added pomace the testers liked more the sweetness of the samples; the best score was given to sample 4. The results regarding the texture are very clear. The more pomace is added to the samples, the better scores were given, and the best score was given to the sample containing pectin, probably due to its gelling effect. Summarizing the data, we can say that sample 4 and P were the most favored ones by the consumers.

### Conclusion

Adding apple pomace to the SB-apple jams increases their polyphenol content. The more apple pomace is added the degree of polyphenol reduction is the less. Those jams which do not contain added apple pomace were decreasing in their  $\beta$  carotenoid content; in contrast, those which contain apple pomace lost much less  $\beta$  carotenoid. It can be concluded that high pomace content is accompanied with high proportion of antioxidant capacity loss; however, the presence of pomace in the samples resulted in high antioxidant capacity (10,0 – 10,2 mM AS/L).

We came to the conclusion, that adding 0,5 to 1 % of apple pomace to SB-apple jams affected positively the changes of valuable components during storage. Although above a certain concentration, the favorable effect can not be shown. The further investigations should focus on the flavonoid composition of the samples, and their antioxidant capacity should be analyzed with other methods, in order to confirm the protective effect of apple pomace.

### Acknowledgements

### References

- [1] Ali J, Ahmad B. (2015): Comparative antitumor and anti-proliferative activities of Hippophae rhamnoides L. leaves extracts. *Journal of Coastal Life Medicine*. 3(3):228-232.
- [2] Benzie, I.I.F., Strain, J.J. (1966): The ferric reducing ability of plasma (FRAP) as a measuring of „antioxidant power”: The FRAP assay. *Analytical Biochemistry*. 239. 70-76. DOI: 10.1006/abio.1996.0292
- [3] Chakraborty M, Karmakar I, Haldar S, Nepal A, Haldar PK. (2015): Anticancer and antioxidant activity of methanol extract of Hippophae Salicifolia in EAC induced Swiss albino mice. *International Journal of Pharmacy and Pharmaceutical Sciences*. 7(8):180-184.
- [4] Codex Alimentarius 3-1-558/93
- [5] Dóka O, Ajtony Zs, Bicanic D, Valinger D, Végvári Gy (2014): Direct quantification of carotenoids in low fat baby foods via laser photoacoustics and colorimetric index a\*. *International Journal of Thermophysics* 35: (12) pp. 2197-2205.
- [6] Guaadaoui A, Benaicha S, Elmajdoub N, Bellaoui M, Hamal A. (2014): What is a bioactive compound? A combined definition for a preliminary consensus. *International Journal of Nutrition and Food Sciences*. 3(3): 174-179.
- [7] Korekar G, Stobdan T, Singh H, Chaurasia O, Singh S. (2011): Phenolic content and antioxidant capacity of various solvent extracts from seabuckthorn (*Hippophae rhamnoides L.*) fruit pulp, seeds, leaves and stem bark. *Acta Alimentaria*. 40(4). DOI: 10.1556/AAlim.40.2011.4.
- [8] Krejcarová J, Straková E, Suchý P, Karásková K. (2015): Sea buckthorn (*Hippophae rhamnoides L.*) as a potential source of nutraceuticals and its therapeutic possibilities - A review. *Acta Veterinaria Brno* 84 (3):257-268.
- [9] MSZ EN 12147:1998
- [10] Singleton, V. L., Rossi, J. A. 1965. Colometry of total phenolics with phosphomolybdic phosphotungstic acid „reagents”. *American Journal of Enology and Viticulture*. 16:144 – 158.
- [11] Song Z Xu H, Gao J, Zhang M, Xiao R, Li W. (2014): Physicochemical properties changes of sea buckthorn cloudy juice during cold crushing, concentrating and storage. *Nongye Gongcheng Xuebao/Transactions of the Chinese Society of Agricultural Engineering*. 30(3):264-270.
- [12] Wani TA, Wani SM, a, Ahmad M, Ahmad M, Gani A, Masoodi FA. (2016): Bioactive profile, health benefits and safety evaluation of sea buckthorn (*Hippophae rhamnoides L.*): A review. *Cogent Food & Agriculture*. DOI: 0.1080/23311932.2015.1128519

## ZÖLDSÉGALAPÚ PROBIOTIKUS KÉSZÍTMÉNYEK EGÉSZSÉGVÉDŐ KOMPONENSEINEK VIZSGÁLATA

Szabó Gergely Tibor<sup>1</sup>, Bujna Erika<sup>2</sup>, Fodor Marietta<sup>1</sup>, Papp Nóra<sup>1</sup>,  
Stefanovits-Bányai Éva<sup>1</sup>, Stégerné Máté Mónika<sup>3</sup>, Furulyás Diána<sup>1,3</sup>

<sup>1</sup> Alkalmazott Kémia Tanszék, Szent István Egyetem, H-1118 Budapest, Villányi út 29-43,  
Magyarország

<sup>2</sup> Sör és Szeszipari Tanszék, Szent István Egyetem, H-1118 Budapest, Villányi út 29-43,  
Magyarország

<sup>3</sup> Konzervtechnológiai Tanszék, Szent István Egyetem, H-1118 Budapest, Villányi út 29-43,  
Magyarország

e-mail: furulyas.diana@etk.szie.hu

### Absztrakt

Napjainkban a funkcionális élelmiszer kifejezés egyre nagyobb teret hódít, azonban szervezetünk számára szükséges probiotikumok bevitelére nem minden ember számára történhet azonos úton. Azok számára, akik laktóztoleranciával vagy tejcukor érzékenységgel élnek együtt, a tej alapú probiotikus készítmények fogyasztása nem egy járható út, így számukra alternatív megoldást kell biztosítani. Kísérletünk során három kereskedelmi forgalomban kapható zöldséglevet (paradicsomlé, sárgarépalé, céklalé) vizsgáltunk, melyek mindegyikét probiotikus *Bifidobacterium lactis Bb-12* törzssel oltottunk be, majd 3 hetes tárolási kísérlet alatt vizsgáltuk az antioxidáns hatású vegyületek mennyiségét három különböző módszerrel. Mértük a polifenol tartalmát (TPC), troloxra vonatkoztatott (TEAC) és vasredukálóképességen alapuló (FRAP) antioxidáns kapacitását. Az eredmények kiértékelése után megállapítható, hogy a vizsgált módszerekkel a legtöbb esetben az antioxidáns hatású összetevőkben nem mutatható ki szignifikáns változás a fermentálást követően, valamint a céklalé kiemelkedően nagy mennyiségű antioxidáns tulajdonságú komponenseket tartalmaz, melyet a fermentálás után kisebb csökkenést mutatva, de továbbra is jelentős mennyiségben őriz meg.

### Bevezetés

A „funkcionális” élelmiszer kifejezést a japán kormány használta először az 1980-as évek közepén [1]. Olyan, a normális étrend részét képező élelmiszereket soroltak ide, melyek az alap táplálkozási értékeken túl egyéb, jól definiált, étlettanilag kedvező hatásokkal is rendelkeznek, így csökkentve a krónikus betegségek kockázatát [2-3]. A funkcionális élelmiszerekben komplex módon vannak jelen különböző bioaktív vegyületek. Ide tartoznak azok az élelmiszerek is, melyek prebiotikumokat és probiotikumokat tartalmaznak [4]. A FAO/WHO [5] a probiotikumokat olyan mikroorganizmusoknak nevezi, melyek a szervezetbe megfelelő mennyiségben bejuttatva a bél mikroflóra összetételét és ezáltal az általános egészségi állapotot kedvező irányba befolyásolhatják. A probiotikumok túlnyomó része természetes tagja a bélmikrobiótának, legtöbbjük a *Bifidobacterium* és a *Lactobacillus* nemzetségből származik, de ismertek *Saccharomyces*, *Lactococcus*, *Streptococcus* nemzetségből származó probiotikus törzsek is. A *Bifidobacterium* és a *Lactobacillus* nemzetség probiotikus törzseit elterjedten alkalmazzák tejalapú probiotikus termékekben [6]. Mivel a tejfehérje allergia és a laktóztolerancia akadályt képez a tej alapú probiotikumok korlátlan fogyasztásában, a nem tej alapú probiotikus élelmiszerek előállítására, hatalmas előny jelent azoknak a fogyasztóknak, akik ilyesfajta intoleranciával élnek együtt. Különösen a

gyümölcs és zöldség alapú probiotikus termékek jöhetnek szóba. A probiotikus baktériumok hordozó mátrixaként kiemelten vizsgálták a gyümölcs- és zöldségleveket [7-9].

A nyers és fermentált zöldségek és gabonaszármazékok fogyasztása is különösen kedvező lehet, mivel az ezekben levő tápanyagokat a probiotikus baktériumok könnyen hasznosítják [10-12].

Az egyik legígéretesebb zöldségalapú probiotikus termék a sárgarépa, ami az egyik leggyakrabban használt zöldségek közé tartozik, gazdag vitaminokban (A, D, B, E, C, K) és ásványi anyagokban (kalcium, kálium, foszfor, nátrium, vas). A sárgarépalé alkalmazhatóságát zöldségalapú probiotikus terméként, már korábban vizsgálták Kun és munkatársai [13]. Megállapították, hogy a *Bifidobacterium*-ok képesek tápanyag kiegészítés nélkül is jól szaporodni a sárgarépalében.

Kísérleteink célja, zöldség alapú probiotikus mikroorganizmussal fermentált zöldség (paradicsom, répa, cékla) készítmények vizsgálata, mely fogyasztásával elérhető a kívánt pozitív egészségügyi hatást a laktózintoleranciában szenvedő fogyasztóknak is.

### **Anyagok és módszerek**

Kutatásunk során *Bifidobacterium lactis Bb-12* törzssel dolgoztunk, mely a Chr. Hansen cégtől került beszerzésre. A törzset folyadéktenyészet formájában, TPY tápközegben 37°C-on anaerob körülmények között tartottuk fenn, anaerob jar alkalmazásával. Többszöri átoltást végeztünk a mérések előtt, hogy minél hatékonyabban szaporodjon a kísérletben részt vevő baktérium törzs. A mérések során használt BIO zöldséglevelek kereskedelmi forgalomból kerültek beszerzésre 500 ml-es kiszerelésben.

#### Erjesztés körülményei:

A zöldséglevelek kezdeti pH értékét pH=6 körüli értékre állítottuk be (Mettler-Toledo típusú elektronikus pH mérő műszerrel), 1n NaOH-dal, a mikroorganizmus optimális szaporodási tartományának elérése érdekében. A mintákat 100 ml-es steril lombikokba adagolva 100 ml-ként majd 1 ml (1v/v%) *B. lactis Bb-12* törzssel oltottuk be, ezt követően 37°C-on inkubáltuk, anaerob körülményeket biztosítva. A fermentáció során, meghatározott időközönként, mintát vettünk, a pH értékeket rögzítettük, majd további feldolgozásig hűtőszekrényben tároltuk. A mintavételek a 0. időponttól kezdve 3 óránként, illetve további 3 hétig tartó tárolási időintervallumban hetente történt.

#### Antioxidáns kapacitás vizsgálata a fermentáció során háromféle módszerrel történt:

- Az **összes polifenol tartalmat** (TPC) Folin-Ciocalteu reagens segítségével Singleton és Rossi módszerével [14] spektrofotometriás úton  $\lambda=760$  nm-en határoztuk meg, galluszsavból készült kalibrációs görbe segítségével. Az eredményeket mM GS/L-ben adtuk meg.
- **Troloxra vonatkoztatott antioxidáns kapacitás** (TEAC - Trolox Equivalent Antioxidant Capacity) mérésekor Miller és munkatársai nevéhez [15] fűzhető módszerre támaszkodtunk. A reakció az ABTS (2,2'-azino-di-(3-etilbenzotiazolin)-6-szulfoninsav) oxidációján alapszik. A reakció spektrofotometriásan nyomon követhető  $\lambda=734$  nm-en. Az eredményeket mM Trolox/L-ben adtuk meg.
- Az antioxidáns kapacitást **FRAP (Ferric Reducing Ability of Plasma)** módszerrel, spektrofotometriás úton,  $\lambda=593$  nm-en határoztuk meg [16]. A mérés lényege, hogy a ferri-(Fe<sup>3+</sup>) ionok antioxidáns aktivitású vegyületek hatására ferro-(Fe<sup>2+</sup>) ionokká redukálódnak, amelyek alacsony pH-n a tripyridil-tiazinnal (TPTZ = 2,4,6 tripyridil-s-

triazin) színes komplexet (ferro-trypiridil-triazin) képeznek. Az eredményeket aszkorbinsavval készített kalibrációs görbe segítségével mM AS/L-ben adtuk meg.

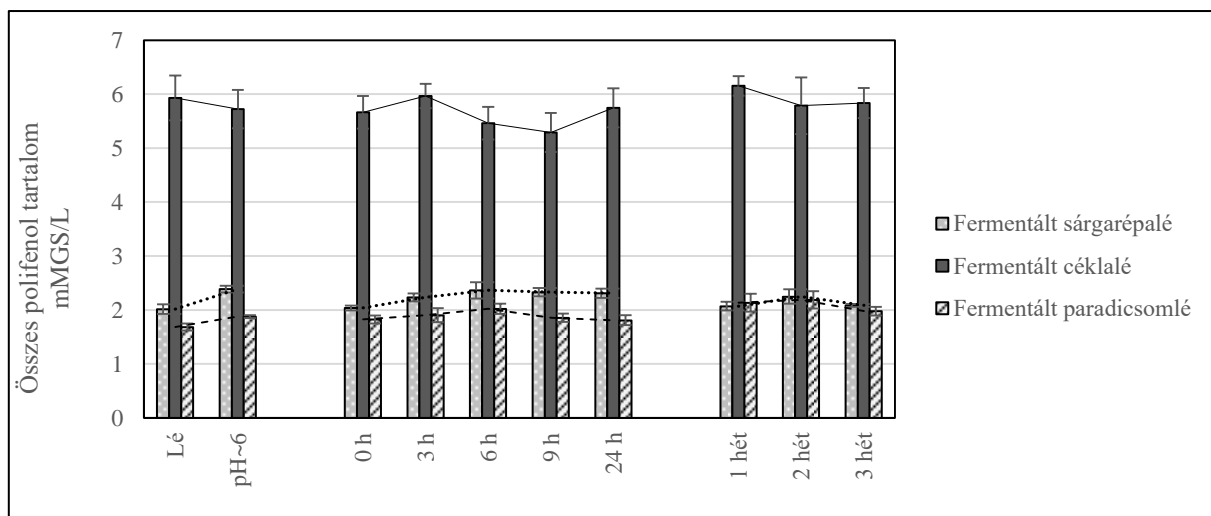
- A statisztikai kiértékelést Microsoft Excel program segítségével végeztük. AZ alkalmazott *Student t-teszt* megmutatta, hogy az eltérések statisztikai szempontból azonosnak tekinthetőek-e 95%-os konfidenciaszint mellett.

### Eredmények és értékelés

A probiotikummal beoltott zöldséglevelek sejtszámát ellenőrizve a harmadik hónap végére is  $10^8$  TKE/ml nagyságrendűek voltak, amik megfelelnek a Magyar Élelmiszerkönyv előírásának, mely szerint a probiotikumot tartalmazó élelmiszereknek a minőségmegőrzési határidőn belül legalább  $10^6$  TKE/ml probiotikus élőscsira számmal kell rendelkeznie.

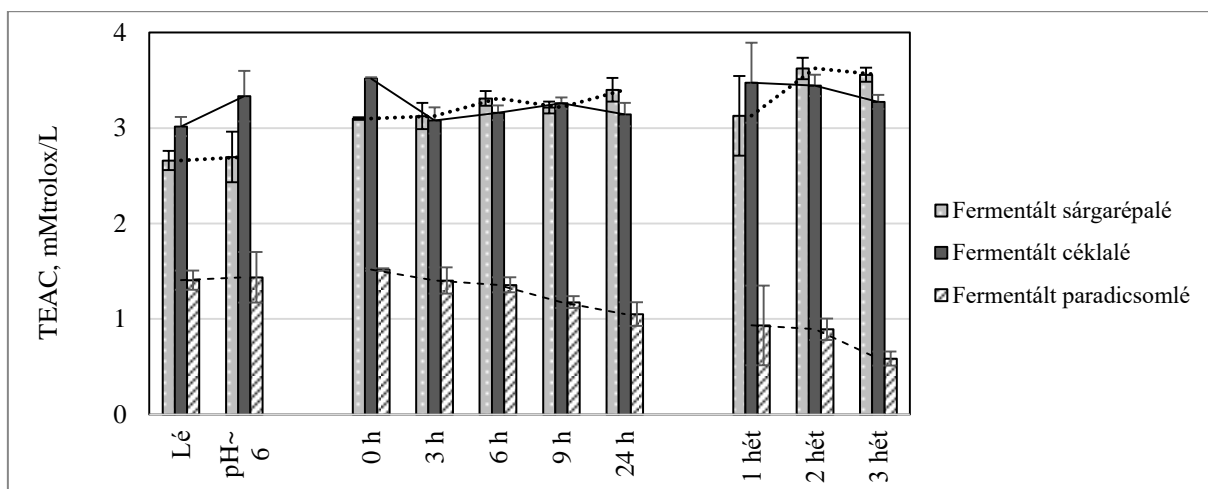
A beoltás hatására történő antioxidáns kapacitás változását három módszerrel (TPC, TEAC, FRAP) mért eredmények alapján vizsgáltuk.

A zöldséglevelekben mutakozó polifenolos vegyületekre utaló különbségek (1. ábra) alapján elmondható, hogy a céklalé mutatja a legnagyobb polifenol tartalom értéket ( $>5,29$  mM GS/L), majd a sárgarépalé ( $>2,01$  mM GS/L) és a paradicsomlé ( $>1,68$  mM GS/L) következik. Vonatkozik ez a kezdeti (*Lé*) és a pH beállítás ( $pH \sim 6,0$ ) utáni állapotra, valamint a fermentált levekre egyaránt, melyekből az első 9 órában három óránként (*0h, 3h, 6h, 9h*), majd 24 óra elteltével (*24h*) vettünk mintát. A tárolást három hétig végeztük, heti mintavételezéssel (*1 hét, 2 hét, 3 hét*).



1. ábra Zöldséglevelek összes polifenol tartalmának (TPC) alakulása *Bb-12* törzs beoltása esetén

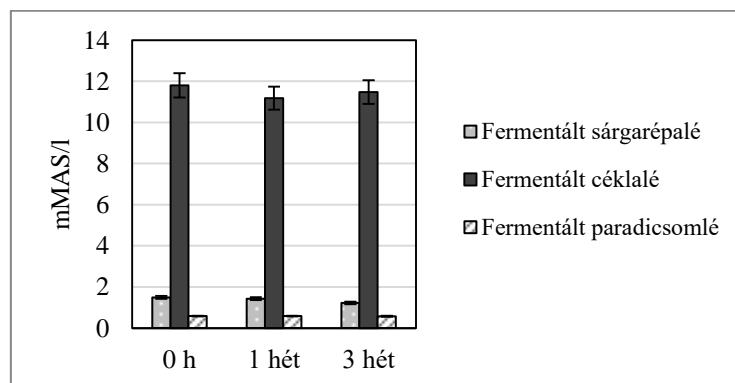
Az egyes zöldséglevelekben az oltás utáni állapotokat elemezve, a paradicsomlé egészségre kedvező hatást mutató polifenol tartalma szignifikánsan nem változott a 3 hetes tárolási idő alatt. Feltételezhető tehát, hogy a mikrobák anyagcsere tevékenysége nem befolyásolta a polifenol tartalmat. Hasonlóan kedvező, egészségvédő hatását megőrizve alakultak a polifenolos komponensek, a sárgarépalé és céklalé mintákban is.



2. ábra Fermentált zöldséglevelek gyökfogyó képességének (TEAC) alakulása *Bb-12* törzs beoltása esetén

A TEAC módszer eredményeinek (2. ábra) kiértékelésénél látható, hogy a paradicsomlé esetében a polifenol tartalomhoz hasonlóan, a fermentálás nem okozott szignifikáns változást az AOK értékekben. A sárgarépalé *Bb-12* törzsszel történő beoltásakor a harmadik hét végére statisztikailag is értékelhető növekedést mértünk a kezdeti állapothoz képest. Feltételezhetően a sárgarépalében jelenlévő, valamely AOK-ért felelős komponens/komponensek növekedésére vagy pedig valamely komponensben kedvező irányba megváltozó átalakulására utalhat ez a tendencia.

A céklalé beoltása kapcsán mért troloxra vonatkoztatott értékek a kezdeti állapothoz képest 61,28%-os csökkenést mutatott, mely jelentős nagyságrendi változást jelent (1,63mM Trolox/l-ről 0,663mM Trolox/L-re). A sárgarépalé esetében mérhető a legmagasabb TEAC érték (3,45 mM Trolox/L), ebben az esetben a fermentálás hatására szignifikáns (+14,79%) növekedés mérhető a 3. heti tárolás végére.



3. ábra Zöldséglevelek antioxidáns kapacitásának (FRAP) alakulása *Bb-12* törzs beoltása esetén

A vasredukáló képességen alapuló módszerrel mért AOK értékek kapcsán (3. ábra) a beoltás utáni (0 h) az egy hetes és a háromhetes időpontban vizsgáltuk a beoltott mintákat. A FRAP módszerrel mért antioxidáns kapacitás kapcsán elmondható, hogy mind a három zöldséglé esetében gyenge csökkenés mutatkozik, ami azt jelentheti, hogy a vasredukáló képességet befolyásolják a probiotikumok beoltása a vizsgált 3 hetes időintervallumban. A céklalé FRAP



értékét vizsgálva ismét észrevehető a kiemelkedő (>11,17mMAs/L) mértékű antioxidáns kapacitásának eredménye, amely egy nagyságrenddel nagyobb a másik két zöldséglé esetében mért értéknél.

### Következtetés

Kísérletünkben *Bifidobacterium lactis Bb-12* törzs beoltásával előállított fermentált zöldséglevek (sárgarépa, cékla, paradicsom) antioxidáns aktivitásának változását vizsgáltuk a beoltástól számítva 3 hetes tárolási időintervallumban.

Eredményeink alapján, a zöldségalapú készítmények igen innovatív megoldásnak ígérkeznek, hiszen az általunk végzett vizsgálatokból feltételezhető, hogy egészségvédő hatásukat megőrizve, megfelelő tápközegnek bizonyulnak a probiotikumok számára. A zöldséglevek közül az antioxidáns vizsgálatokban a céklalé mutatott kiemelkedő eredményeket magas polifenol és antioxidáns tartalma miatt, azonban a sárgarépalé a három hetes tárolás alatt képes volt megőrizni a benne lévő antioxidáns hatású vegyületeket, szignifikáns csökkenést egyik mérésünk esetében sem tapasztaltunk. További vizsgálatok szükségesek a zöldségkészítmények pozitív tulajdonságainak feltérképezésére, de elő kísérleteink alapján elmondható, hogy fogyasztással a probiotikus tulajdonságaik mellett az antioxidáns hatásuk is hozzájárulhat az egészségünk megővéséhez, így azok a fogyasztók is hozzájuthatnak ilyen egészségvédő termékekhez, akik egyéb tejalapú probiotikus készítményt nem fogyaszthatnak.

### Irodalomjegyzék

- [1] C.O. FOSHU Japanese regulations for probiotic foods. Enfield, CT: CRC Press, Science Publishers, 2011, pp. 33–40.
- [2] A. Cenci, W. Chingwaru, *Nutrients*, 2, (2000) 611–625.
- [3] P.C. Stringheta, T.T. Oliveira, R.C. Gomes, M.P.H. Amaral, A.F. Carvalho, M. A. P. Vilela, *Brazilian Journal of Pharmaceutical Sciences*, 43, (2007) 181–194.
- [4] G. Ares, A. Giménez, A. Gábaro, *Food Quality and Preference*, 20, (2009) 50–56.
- [5] FAO/WHO, Report of a Joint FAO/WHO Expert Consultation, (2001) Córdoba, Argentina.
- [6] M. Saarela, G. Mogensen, R. Fondén, J. Mättö, M.T. Sandholm, *Journal of Biotechnology* 84(3), (2000) 28.
- [7] C. L. Nicolesco, L.C. Buruleanu, *Bulletin UASVM Agriculture*, 67, (2010) 352–359.
- [8] S.Nualkaekul, D. Charalampopoulos, *International Journal of Food Microbiology*, 146, (2011) 111–117.
- [9] A. L. F. Pereira, T. C. Maciel, S. Rodrigues, *Food Research International*, 44, (2011) 1276–1283.
- [10] Y. Kourkoutas, M. Kanellaki, A. A. Koutinas, *WT- Food Science and Technology*, 39, (2006) 980–986.
- [11] C. M. Peres, C. Peres, A. Hernández-Mendoza, F. X. Malcata, *Trends in Food Science & Technology*, 26, (2012) 31–42.
- [12] C. R. Soccol, L. P. S. Vandenberghe, M. R. Spier, A. B. P. Medeiros, C. T. Yamagishi, J. D. Lindner, *Food Technology Biotechnology*, 48, (2010) 413–434.
- [13] Sz. Kun J. Rezessy-Szabó D.Q. Nguyen A. Hoschke, *Process Biochemistry*, 43(8), (2008) 816–821.
- [14] V.L. Singleton, J.A. Rossi, *American journal of Enology and Viticulture*, 16(3) (1965) 144–158.



- [15] N.J. Miller C. Rice-Evans M.J. Davies V. Gopinathan A. Milner, *Clinical Science*, 84(4) (1993) 407-412
- [16] I.I.F. Benzie, J.J. Strain, *Analytical Biochemistry*, 239. (1966) 70-76.

## ÚJ HPLC ELJÁRÁS AZ ALFA-AMILÁZ AKTIVITÁS ÉS GÁTLÁS MÉRÉSÉRE

István Takács\*<sup>1,3</sup>, Anikó Pósa<sup>1</sup>, András Szekeres<sup>2</sup> Gábor Endre<sup>2</sup> Gyöngyi Gyémánt<sup>3</sup>

<sup>1</sup>Élettani, Szervezettani és Idegtudományi Tanszék, SZTE, TTIK, Szeged Közép fasor 52  
Magyarország

<sup>2</sup>Mikrobiológia Tanszék, SZTE, TTIK Szeged Közép fasor 52 Magyarország

<sup>3</sup>Szervetlen és Analitikai Kémiai Tanszék Debreceni Egyetem, Debrecen Egyetem tér  
Magyarország

\*e-mail: taki.biotech@gmail.com

### Abstract

The control of the hyperglycemia is crucial in the treatment of type II diabetes and other metabolic syndromes. In these situations, the  $\alpha$ -amylases could play an important role in the increasing of the blood glucose level due the breakdown of the polysaccharides. The  $\alpha$ -amylases are the first enzymes, which take a part in the process of the releasing glucose monomers from complex polysaccharides. Therefore, the investigations of both  $\alpha$ -amylase activities and the quantity of their inhibition are important on the field of anti-diabetic drug research. Our presented research was aimed to develop a new HPLC based method for the measurement of reaction product of  $\alpha$ -amylase reaction using specially synthesized, p-nitrophenyl-labelled maltooligomer substrate. After the enzyme reaction, three product was detectable possessing the chromophore-group during the reversed-phase separation. One of them was selected to follow the enzyme kinetic of the human salivary amylase applying linear regression on the area data acquired at different time points of the reaction. Furthermore, due to the specific substrate measuring only the  $\alpha$ -amylase activity, our method could be used successfully also for the accurate measurement in the inhibition studies.

**Keywords:**  $\alpha$ -amylase, inhibition, HPLC method, diabetes

### Bevezetés

Az  $\alpha$ -amiláz (EC.3.2.1.1) a glikozid-hidrolázok családjába tartozó, a poliszaharidok glükózegységei közötti  $\alpha$ -(1,4) glikozid kötések bontásáért felelős enzim [1]. Klinikai vonatkozásban ezen enzimaktivitás emelkedése több betegség következménye is lehet pl: hasnyálmirigy-, fültőmirigy gyulladásban. Ezekben az esetekben az  $\alpha$ -amiláz mérésének differenciál diagnosztikai szerepe is van [2]. Az  $\alpha$ -amiláz gátlásának meghatározására alkalmas módszer az újabb erre az enzimre ható gyógyszerek fejlesztésben is fontos szerepet kaphat, mert az egyes jelenleg elérhető gyógyszerek jelentős mellékhatásokkal rendelkeznek. Ezért megnőtt az olyan természetes hatóanyagok iránt az érdeklődés melyek az amilázt gátolják, de nem okoznak mellékhatásokat [3]. A humán  $\alpha$ -amilázokat, mind a nyálmirigy mind a hasnyálmirigy által termelt enzimeket alaposan tanulmányozták, mivel a cukorbetegség, és az elhízás kezelésében alkalmazott gyógyszerek kutatásában fontos szerepe van [4]. Számos amiláz inhibitorot írtak le, és néhányat alkalmaznak jelenleg is a cukorbetegség kezelésében [5]. Az általunk kifejlesztett új HPLC alapú módszerrel specifikusan csak az  $\alpha$ -amiláz által hidrolizált szubsztrát mennyiségét mérjük. Szubsztrátként 2-klór-4-nitro-fenil- $\beta$ -D-maltoheptozidot (CNP-G7) használtunk. Ez a szubsztrát már elég hosszú, hogy átfedje a humán nyál amiláz (HSA) aktív helyét és a természetes szubsztráthoz hasonlóan viselkedjen. A HSA és a szubsztrát reakciója során a három felszabaduló redukáló végtermék fő

összetevője a CNP- $\beta$ -D-maltotrióz (CNP-G3) amely a szubsztrát detektálható reakciótermékeinek 50%-át teszi ki [6]. Az aglikon kromofor lehetővé teszi az UV-tartományban (302 nm) való magas érzékenységgel való detektálást, amely béta-glikozid kötéssel kapcsolódik a szénhidrát lánchoz, melyet az  $\alpha$ -amiláz nem képes hasítani. A korábbi kalorimetriás titrálási (ITC) módszerrel végzett vizsgálatok megerősítették, hogy a CNP-G7 a keményítőhöz hasonlóan hasad az enzimreakcióban [7]. A CNP-G7 szubsztrát alkalmas továbbá fotometriás amiláz meghatározásra is, ilyenkor azonban segéd enzimek alkalmazása szükséges [8,9].

### 3.0 Anyagok és módszerek

#### 3.1 CNPG-7 Szubsztrát szintézise és tisztítása

A CNP-G7 szubsztrátot kémiai szintézissel állítottuk elő [10]. A szintézis során az oligoszacharid peracetilezett származéka keletkezik, amelyből a Zemplén-féle dezacetilezéssel állítottuk elő a szabad oligoszacharidot. A további tisztítási műveleteknél 1,0 g CNP-G7-t feloldottuk 30 ml metil-alkoholban (VWR) majd 300  $\mu$ l 30% nátrium-metilátot (Merck) adtunk az oldathoz. A reakcióelegyet 0 °C-on 50 percig kevertettük majd az oldószert csökkentett nyomáson bepárooltuk és a maradékot vízben visszaoldottuk és Amberlite-H<sup>+</sup> gyanta (Sigma) hozzáadásával pH 6-ra savanyítottuk. A gyantát szűréssel távolítottuk el és a szűrletet liofilizálással szárítottuk. A terméket desztillált vízben feloldottuk és szemipreparatív HPLC segítségével választottuk el a szabad klór-nitrofeniltől. Ehhez szemipreparatív HPLC berendezést (Younglin, 6400) használtunk ami kézi mintaadagolóval UV/VIS detektorral és gáztalanítóval volt felszerelve. Állófázisként Supelcosil™ LC-18 (200 mm x 10 mm, 5  $\mu$ m) oszlopot alkalmaztunk. A mozgó fázis acetotinitril : víz (10:90) arányú keveréke volt, áramlási sebessége 5,0 ml/min. A detektálást 302 (termék) illetve 400 nm (p-nitrofenol) hullámhosszon végeztük, az injektálási térfogat 500  $\mu$ l volt. A szemipreparatív kromatográffal tisztított terméket ezután -50 °C-ra fagyasztottuk és Christ Alpha1-4 liofilizátorral fagyasztva szárítottuk 36 órát.

#### 3.2 A szubsztrát tisztaságának ellenőrzése HPLC készüléken

A tisztított CNP-G7 szubsztrát tisztaságát folyadékkromatográfiával vizsgáltuk. Az analitikai HPLC mérést (Agilent 1260 Infinity) kvaterner pumpával, degasserrel és kézi mintaadagolóval felszerelt rendszeren végeztük. A mérés UV/VIS detektorral ( $\lambda = 302$  nm) történt Genesis C-18 (150 mm x 4,6 mm, 4  $\mu$ m) oszlopon. A mozgó fázis acetonitril és víz (15:85) keveréke volt. Az áramlási sebesség 0,8 ml/perc, míg az injektált térfogat 20  $\mu$ l volt.

#### 3.3 A szubsztrát tisztaságának ellenőrzése MALDI-TOF készüléken

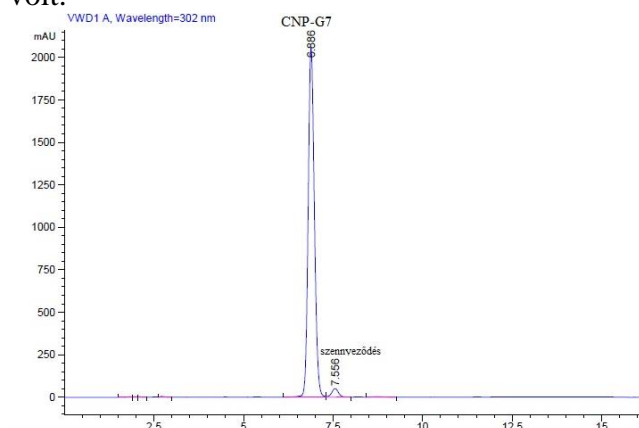
A tömegspektrometriás méréseket a MALDI-TOF (Bruker Biflex III) készülékkel végeztük, melyhez mátrixként 2,5-dihidroxibenzoésavat (2,5-DHB, Aldrich) használtunk és pozitív-ion módban mértünk. A lézerhez 19 kV, a reflektoronhoz 20 kV feszültséget alkalmaztunk. A kapott tömegspektrumok kiértékelését, a készülék X-TOF programjával végeztük.

#### 3.4 Az enzimreakció detektálása

A reakcióhoz 400  $\mu$ l 5,0 mM CNP-G7 oldatot összekeverünk 8  $\mu$ l 84 nM HSA-val és a mintát 37 ° C-on inkubáljuk. A minták vétele és az injektálás az 5., 25., 45., és a 65., percben történt. A kromatogramokat a ChemStation szoftverrel (Agilent) értékeltük.

## Eredmény és vita

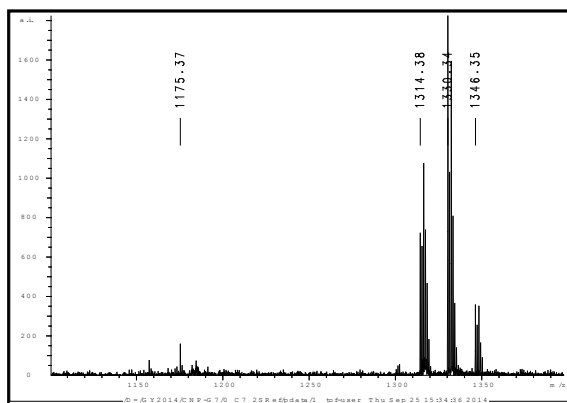
A tisztított CNP-G7 szubsztrát retenciós ideje 6.688 perc (**1. ábra**). A minta tisztasága 96,92% volt.



**1. ábra** Tisztított CNP-G7 szubsztrát HPLC kromatogramja

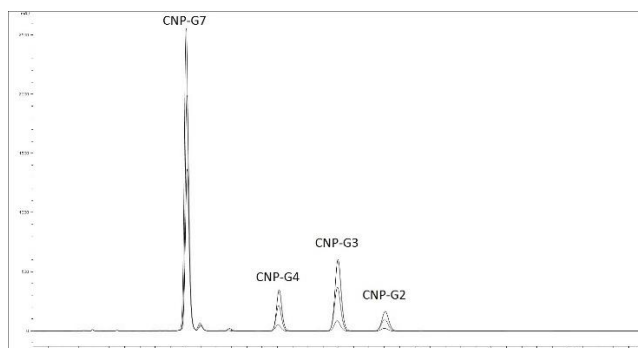
A CNP-G7 MALDI-TOF MS eredménye

A pozitív ionizációs módban felvett MALDI-TOF MS spektrumon (**2. ábra**) láthatjuk a CNP-G7 kálium és a nátrium addukt ionjait. A számított molekulatömeg a kálium addukt esetében 1346,32 Da  $[C_{48}H_{74}O_{38}NCl+K]^+$ , míg a nátrium addukt esetében 1330,34 Da  $[C_{48}H_{74}O_{38}NCl+Na]^+$  volt. Kis mennyiségű G7 oligomer is látható a spektrumokon 1175,37  $m/z$  értéknél ( $[M+Na]^+$ ), amely nem tartalmazza a krómofór csoportot.

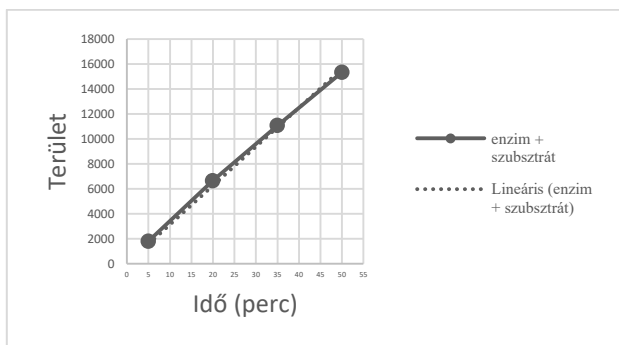


**2. ábra** CNP-G7 szubsztrát MALDI-TOF MS spektrumai

Az enzimmérésekhez a tisztított CNP-G7 szubsztrátot használtuk, amely több hatékony kötést tud létrehozni a HSA aktív centrumával ezért a kromatogramon három, különböző hosszúságú termék csúcsa is látszódik, melyek megfelelő módszerrel elválaszthatók egymástól és a szubsztráttól (**3. ábra**). Az enzimaktivitás sebességének jellemzésére a fő termék, a CNP-G3 (**4. ábra**) keletkezésének a sebességét határoztuk meg. A különböző időpontokban injektált minták kromatogramján a CNP-G3 hoz tartozó csúcs területét mértük és ábrázoltuk az idő függvényében.



3. ábra A különböző időpontokban injektált minták kromatogramja



4. ábra A CNP-G3 képződés reakciósebességének meghatározása a CNP-G7-HSA katalizálta hidrolízis reakcióban

A sebességet ( $v$ ) lineáris regresszióval határoztuk meg. Az egyenes egyenlete  $y=312,26x$  volt, és a korrelációs koefficiens  $R^2=0,9969$  volt.

### Megvitatás

A HPLC kétségtelenül az egyik legfontosabb analitikai módszer a vegyületek azonosítására és mennyiségi meghatározására. Ezzel párhuzamosan a HPLC-technikák használata az enzimatis reakciók tanulmányozásában jelentősen megnőtt. A HPLC alkalmazásával a komponensek elválasztása és mennyiségi meghatározása lehetséges és az adatokból a reakciók sebessége kiszámítható [11]. Mivel a szubsztrát és a három felszabaduló redukáló végtermék hasonló vegyület (maltooligomerek) és valamennyi tartalmaz kromofor csoportot. A fő termék (CNP-G3) mennyiségi meghatározása területi adatok alapján történt, és a reakciósebességeket a kinetikus görbék lineáris részéből számoltuk ki. Ezek az eredmények megerősítik HPLC-alapú kinetikai módszerek alkalmazhatóságát az  $\alpha$ -amiláz aktivitásának megbízható meghatározására. A CNP-G7 szintézisének kialakított  $\beta$ -konfiguráció megvédi a szubsztrátot az amiláz hasításától így a kromofor csoport mindvégig a szubsztráton marad specifikussá téve a meghatározást.

### Köszönetnyilvánítás

AZ Emberi Erőforrások Minisztériuma ÚNKP-16-4 kódszámú Új Nemzeti Kiválóság Programjának támogatásával készült (Pósa Anikó, Szekeres András)

Köszönetemet szeretném kifejezni Dr. Gyémánt Gyöngyi egyetemi docensnek, a szubsztrát előállításában és a MALDI-TOF MS spektrumok felvételében nyújtott segítségével.

### **Irodalomjegyzék**

- [1] Jacobsen N, Melvaer KL, Hensten-Pettersen A. Some Properties of Salivary Amylase: A Survey of the Literature and Some Observations. *J Dent Res* 1972 03/01; 2017/09;51(2):381-388.
- [2] Chapman R. Serum Amylase Estimations in Differential Diagnosis. *Br Med J* 1959 Oct 3;2(5152):602-606.
- [3] Gao J, Xu P, Wang Y, Wang Y, Hochstetter D. Combined effects of green tea extracts, green tea polyphenols or epigallocatechin gallate with acarbose on inhibition against alpha-amylase and alpha-glucosidase in vitro. *Molecules* 2013 Sep 18;18(9):11614-11623.
- [4] Copeland RA. Evaluation of enzyme inhibitors in drug discovery: a guide for medicinal chemists and pharmacologists. : John Wiley & Sons; 2013.
- [5] Yamagishi S, Nakamura K, Takeuchi M. Inhibition of postprandial hyperglycemia by acarbose is a promising therapeutic strategy for the treatment of patients with the metabolic syndrome. *Med Hypotheses* 2005;65(1):152-154.
- [6] Kandra L, Gyemant G. Examination of the active sites of human salivary alpha-amylase (HSA). *Carbohydr Res* 2000 Nov 17;329(3):579-585.
- [7] Lehoczki G, Szabo K, Takacs I, Kandra L, Gyemant G. Simple ITC method for activity and inhibition studies on human salivary alpha-amylase. *J Enzyme Inhib Med Chem* 2016 Apr 6:1-6.
- [8] Gillard BK, Marksman HC, Feig SA. Direct spectrophotometric determination of alpha-amylase activity in saliva, with p-nitrophenyl alpha-maltoside as substrate. *Clin Chem* 1977 Dec;23(12):2279-2282.
- [9] Junge W, Wortmann W, Wilke B, Waldenstrom J, Kurrle-Weittenhiller A, Finke J, et al. Development and evaluation of assays for the determination of total and pancreatic amylase at 37 degrees C according to the principle recommended by the IFCC. *Clin Biochem* 2001 Nov;34(8):607-615.
- [10] Farkas E, Janossy L, Harangi J, Kandra L, Liptak A. Synthesis of chromogenic substrates of alpha-amylases on a cyclodextrin basis. *Carbohydr Res* 1997 Oct 7;303(4):407-415.
- [11] Edward F. Rossomando. HPLC in Enzymatic Analysis, Third Edition - (Methods of Biochem Analysis Vol 50) (Methods of Biochemical Analysis) 3rd Edition. 2011.

PLATINUM NANOPARTICLES ON NITROGEN-DOPED GRAPHENE FOR  
OXYGEN REDUCTION REACTION

Ágnes Tímea Varga<sup>1</sup>, Tamás Varga<sup>1</sup>, Henrik Haspel<sup>1,†</sup>, Ákos Kukovecz<sup>1</sup>, Zoltán Kónya<sup>1,2</sup>

*1 Department of Applied and Environmental Chemistry, University of Szeged, H-6720 Szeged, Rerrich Bela tér 1, Hungary*

*2 MTA-SZTE Reaction Kinetics and Surface Chemistry Research Group, H-6720 Szeged, Rerrich Béla tér 1, Hungary*

† Present address: Division of Physical Sciences and Engineering, KAUST Catalysis Center (KCC), King Abdullah University of Science and Technology (KAUST), 4700 KAUST, Thuwal, 23955-6900, Saudi Arabia.

**Abstract:**

Excess use of non-renewable energy resources is a serious environmental problem nowadays. Fuel cells can be a promising alternative as they provide rather clean energy and they can be used for various purposes in many sizes. Our work focuses on the oxygen reduction reaction (ORR) in polymer electrolyte membrane (PEM) fuel cells. Generally, platinum nanoparticles are used on carbon black support which is an expensive and easily degradable catalyst. Nitrogen-doped graphene support can be an alternative solution with various advantages, which improve the ORR efficiency of the dispersed platinum. Our aim was to achieve a one step method to synthesize Pt/Nitrogen-doped graphene composite with reduced platinum content. A mixture of platinum (II)-acetylacetonate and graphene oxide was thermally treated at three different temperatures. The resulting material was examined by several characterization techniques: thermogravimetry (TGA) was used to determine the platinum content of the samples, transmission electron microscopy (TEM) was applied to examine the graphene sheets and platinum particles, and X-ray photoelectron spectra (XPS) were taken to determine the physical states of the graphitic materials and the oxidation state of Pt. Linear sweep voltammetry (LSV) and cyclic voltammetry (CV) were performed in a three-electrode cell in oxygen saturated 0.1 M HClO<sub>4</sub> solution by a rotating disk electrode (RDE) at different rotation rates to see the electrochemical behaviour of the samples, compared to a conventional Pt/CB catalyst. The results revealed the successful synthesis of the desired catalyst with promising electrochemical performances.



**HETEROGENEOUS PHOTOCATALYSIS OF OXALIC ACID, PHENOL AND COUMARIN -DETAILED INVESTIGATION OF THE EFFECT OF REACTION PARAMETERS**

**KUMARIN, MINT POTENCIÁLIS AKTINOMÉTER 185 NM HULLÁMHOSSZÚSÁGÚ VUV FOTOLÍZISÉNEK VIZSGÁLATA**

**Milán Molnár<sup>1</sup>, Máté Náfrádi<sup>1</sup>, Krisztina Schrantz<sup>1</sup>, Klára Hernádi<sup>2</sup>, Tünde Alapi<sup>1</sup>**

<sup>1</sup>*Department of Inorganic and Analytical Chemistry, University of Szeged, H-6720 Szeged, Dóm tér 7, Hungary*

<sup>1</sup>*Department of Applied and Environmental Chemistry, University of Szeged, H-6720 Szeged, Rerrich Béla tér 1.  
e-mail: alapi@chem.u-szeged.hu*

**Abstract**

In the case of heterogeneous photocatalysis the transformation of organic compounds can take place due to the hydroxyl radical (HO•) based reactions or direct charge transfer on the surface of the photocatalyst. The relative contribution of these ways to the transformation depends strongly on the chemical properties of the pollutant, and the surface properties of the photocatalyst, which can be strongly influenced by the properties of the solution, such as pH, ionic strength, etc.

In the present work the effect of various reaction parameters (methanol as non-adsorbed HO• scavenger, formic acid and Na-formate as well adsorbed HO• scavengers, NaF as surface modifier, EDTA and pH) were studied on the transformation of the phenol, oxalic acid and coumarin. The transformation of the phenol, which does not adsorb well on the TiO<sub>2</sub> surface is mainly taken place by HO• based reaction, which was confirmed by the effect of HO• scavengers. Oxalic acid adsorbs well and mainly the direct charge transfer is responsible for its transformation. The negligible effect of methanol and significant negative effect of NaF on the rate of transformation confirmed this. The relative contribution of the HO• based reaction and direct charge transfer to the transformation of coumarin depended strongly on the reaction parameters, such as pH and the presence of additives.

**Bevezetés és célkitűzés**

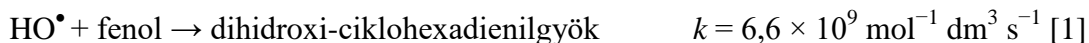
A nagyhatékonyságú oxidációs eljárások egyike a napjainkban is dinamikusan fejlődő heterogén fotokatalízis. Ennek alkalmazás során a fotokatalizátor megfelelő energiájú fotonokkal történő gerjesztése következtében töltés szeparáció (pozitív lyuk,  $h\nu_{VB}^+$  és elektron,  $e_{VB}^-$ ) jön létre. A fotogenerált töltések a felületre kijutva számos oxidatív és redukzív folyamatot indíthatnak el.

A heterogén fotokatalízis során lejátszódó folyamatok még ma is vitatottak, feltehetően az alkalmazott fotokatalizátortól és az eltávolítandó szerves vegyület tulajdonságaitól egyaránt nagymértékben függ, hogy a közvetlen töltésátmenet, vagy a fotokatalizátor felületén képződő HO•-kel való reakciók a dominánsak a szubsztrátum átalakulásában. A lejátszódó folyamatokat természetesen a reakciókörülmények is jelentősen befolyásolják.

Méréseim során a TiO<sub>2</sub> (Aeroxide P25), mint fotokatalizátor alkalmazása mellett három, megfelelően megválasztott szubsztrátum, a kumarin, a fenol és az oxálsav átalakulását vizsgáltam különböző reakciókörülmények között. Vizsgáltam egyrészt a pH mint domináns

reakció paraméter hatását, valamint a NaF mint a TiO<sub>2</sub> hidropilitását és ezen keresztül az adszorpció befolyásoló anyag, az EDTA mint a közvetlen töltésátmenettel való átalakulást gátló anyag, illetve néhány gyökfogó (metanol, terc-butanol, hangyasav és nátrium-formiát) hatását a fent említett három vegyület átalakulási sebességére, hogy a heterogén fotokatalízis során lejátszódó folyamatokról részletesebb képet kapjak.

A fenol csak kismértékben adszorbeálódik a TiO<sub>2</sub> felszínén, HO•-kel azonban az aromás vegyületekre jellemző addícióval, nagy sebességgel reagál



Az e<sub>aq</sub><sup>-</sup>-kal történő reakciója az előző folyamathoz képest két nagyságrenddel kisebb sebességi együtthatóval megy végbe:



Az adszorpció kiemelkedő jelentőségű és meghatározó a szubsztrátumok heterogén fotokatalitikus átalakulása szempontjából. Az oxálsav jól adszorbeálódik a TiO<sub>2</sub> felületén, ugyanakkor igen jó elektron donor is. Átalakulása során a h<sub>νB</sub><sup>+</sup>-kal való reakciója következtében COOH• képződik. Természetesen az oxálsav átalakulását ebben az esetben is iniciálhatja a HO•:



azonban ezen reakció sebességi állandójának értéke 2-3 nagyságrenddel kisebb a fenol és HO• közti reakcióra vonatkozó értéknél.

A kumarin HO•-kel való reakciója ( $k = 2 \times 10^9 \text{ mol dm}^{-3} \text{ s}^{-1}$  [3]) umbelliferon (7-hidroxi-kumarin) képződését eredményezi. Heterogén fotokatalitikus vizsgálatok során a képződő umbelliferon által kibocsátott fluoreszcens fény intenzitásának időbeni változását tekintik a HO• képződési sebességével arányosnak [4]. Az e<sub>aq</sub><sup>-</sup> és a kumarin reakciójára ( $k = 1,6 \times 10^{10} \text{ dm}^{-3} \text{ mol}^{-1} \text{ s}^{-1}$  [5]) vonatkozó érték azonban azonos az O<sub>2</sub> és e<sub>aq</sub><sup>-</sup> közti reakcióra ( $k = 2 \times 10^{10} \text{ dm}^{-3} \text{ mol}^{-1} \text{ s}^{-1}$  [6]) vonatkozó értékkel, és egy nagyságrenddel nagyobb, mint a kumarin HO•-kel való reakciójára vonatkozó érték így átalakulása feltehetően közvetlen töltésátmenettel is végbemehet, azaz a kumarin elektronbefogóként is viselkedhet.

### Kísérleti körülmények és módszerek

A fenol és oxálsav koncentrációját folyadékkromatográfiásan (Merck-Hitachi L-7100 típusú pumpa, L-4250 UV-Vis detektor) mértem. Az aromás vegyületek elválasztáshoz Lichrospher 100, RP-18 oszlopot (Merck), eluensként víz-metanol 50:50 arányú elegyét (0,90 cm<sup>3</sup> perc<sup>-1</sup> áramlási sebesség) használtam. A detektálás 210 nm-en történt. Az oxálsav elválasztásához GROM RESIN ZH oszlopot (Herrenberg-Kayh) alkalmaztam, az eluens 0,01 M koncentrációjú kénsav (0,7 cm<sup>3</sup> perc<sup>-1</sup>) volt. A detektálás 205 nm-en történt.

A kumarin koncentrációját 0,2 cm-es kvarcküvetében spektrofotometriásan, Agilent 8453 diódasoros spektrofotométerrel 278 nm-en ( $\epsilon_{\text{kumarin}} = 12400 \text{ mol}^{-1} \text{ dm}^3 \text{ cm}^{-1}$ ) mértem. A kumarin átalakulása során képződő umbelliferon gerjesztését követően kibocsátott fluorimetriás fény intenzitását Hitachi F4500-as spektrofluoriméterrel mértem. A gerjesztés 332 nm-es hullámhosszúságú fényvel történt. Az umbelliferon által kibocsátott fény intenzitása arányos az umbelliferon koncentrációjával, maximuma 456 nm-nél van.

A használt TiO<sub>2</sub> felületi töltésének és primer részecskék aggregációja mértékének pH függését, valamint az ionerősség beállítására használt NaCl hatását fényszórás segítségével vizsgáltuk. Az 1,0 g dm<sup>-3</sup>-es töménységű TiO<sub>2</sub> szuszpenzióból minden mérés alkalmával 100-

szoros hígítást készítettem. A pH beállítása HCl és NaOH oldatokkal történt. A méréseket Malvern típusú készüléken végeztem, mely DTS 1070 ZetaSizer típusú Zeta-cellát tartalmazott.

### Eredmények és értékelésük

A NaCl hozzáadása csökkentette a kumarin átalakulásának sebességét és megnövelte az umbelliferon képződésének sebességét. Míg a kumarin átalakulási sebessége NaCl jelenlétében inkább a lúgos oldatban, negatív felületi töltésnél mért értékhez, az umbelliferon és ezzel együtt a HO<sup>•</sup> képződésének sebessége inkább a savas oldatban mért értékhez közelít. Az eredményt a felületen adszorbeálódott ionoknak a felületi potenciálra, és ezen keresztül az ott lejátszódó folyamatokra gyakorolt hatásával értelmezhetjük. Összehasonlítva a NaCl-ot tartalmazó különböző pH-jú oldatokra vonatkozóan a kumarin átalakulásának sebességét és az umbelliferon képződésének a sebességét, mindkettőnek a pH növelése kedvez.

**1. Táblázat:** Különböző adalékanyagok hatása a kumarin kezdeti átalakulási sebessége ( $r_0^{kum}$ ) az umbelliferon által kibocsátott fluoreszcens fény intenzitása-idő függvény kezdeti meredeksége ( $m_0^{umb}$ ), és maximális értéke ( $I_{max}$ ), különböző pH-jú oldatok esetén

	$r_0^{kum}$ ( $\times 10^{-8} \text{ moldm}^{-1} \text{ s}^{-1}$ )	$m_0^{umb}$ ( $\times 1000$ )	$I_{max}$
pH = 5,5; NaCl nélkül	15	0,85	2472
pH = 5,5; NaCl	5,4	1,70	2500
NaF	25	1,10	1926
MeOH	7,0	0,44	2472
pH = 3,0; NaCl	5,8	0,74	2140
HCOOH, NaCl	0,5	0,00	215
pH = 9,0 NaCl	12	1,78	1570
NaCOOH, NaCl	1,7	0,00	187

A metanol, a hangyasav és a formiátion egyaránt igen nagy sebességi állandóval reagál el a HO<sup>•</sup>-kel, így mindhárom vegyület HO<sup>•</sup>-fogóként használható. Mérési eredményeink azonban azt mutatják, hogy, míg a metanol csupán felére csökkentette a kumarin átalakulásának sebességét (közel azonos mértékben, mint a NaCl), és az umbelliferon, azaz a HO<sup>•</sup> képződésének sebességét is, addig a hangyasav és a formiátion jóval nagyobb mértékben csökkentette a kumarin átalakulási sebességét és gyakorlatilag teljesen megakadályozta az umbelliferon, következésképpen a HO<sup>•</sup> képződését és/vagy oldatba jutását a TiO<sub>2</sub> felületéről. Mindez részben azzal értelmezhető, hogy mindkét vegyület, a metanollal ellentétben, igen jól adszorbeálódik a TiO<sub>2</sub> felületén. Feltehetően a metanol inkább az oldat fázisba kiszabaduló HO<sup>•</sup> gyökökkel reagál el, hasonlóan a kumarinhoz. A NaF a kumarin átalakulásának sebességére nem volt hatással, ami szintén alátámasztja, hogy annak átalakulása elsősorban oldatfázisban a HO<sup>•</sup>-kel való reakció során történik.

A NaF a NaCl-hoz hasonlóan egyáltalán nem befolyásolta a fenol átalakulásának sebességét, ellentétben a metanollal, ami ebben az esetben is határozottan csökkentette azt. Mindezt azzal értelmezhetjük, hogy a fenol átalakulásáért elsősorban az oldatfázisban lévő

HO<sup>•</sup>-kel való reakció a felelős. A metanolhoz hasonlóan a TiO<sub>2</sub> felszínén rosszul adszorbeálódó t-butanol is csökkentette a fenol átalakulásának sebességét, bár kisebb mértékben, mint a metanol. A TiO<sub>2</sub> felületén jól adszorbeálódó hangyasav a nátriumformiáthoz hasonlóan, a fenol esetében is nagyobb mértékben csökkentette az átalakulás sebességét, mint a metanol és terc-butanol. Az összehasonlítás minden esetben az azonos pH-jú, adott adalékanyagot nem tartalmazó fenol oldatában mért átalakulási sebességhez ( $r^{\text{fen}}(\text{ref})$ ) viszonyítva történt.

2. Táblázat: Adalékanyagok hatása a fenol kezdeti átalakulási sebességére különböző pH-jú oldatok esetén

	$r^{\text{fen}} (\times 10^{-8} \text{ mol dm}^{-3} \text{ s}^{-1})$	$r^{\text{fen}} / r^{\text{fen}}(\text{ref})$
-	12,9	-
NaCl	13,2	1,02
NaF	14,6	1,13
MeOH	2,6	0,20
t-BuOH	4,9	0,38
EDTA	0,5	0,04
pH = 3, NaCl	4,1	-
HCOOH	0,5	0,12
pH = 9, NaCl	13,2	-
HCOONa	1,5	0,11

3. Táblázat: Az oxálsav és nátrium-oxalát átalakulási sebessége ( $r$ ) és relatív átalakulási sebessége ( $r / r^{\text{ref}}$ ) valamint az adszorpció mértéke

	$r (\times 10^{-8} \text{ mol dm}^{-3} \text{ s}^{-1})$	$r / r^{\text{ref}}$	adszorpció mértéke* (%)
oxálsav, pH = 4,2	8,50	-	10
oxálsav, pH = 4,2, NaCl	12,2	1,43 <sup>1</sup>	6
oxálsav, pH = 4,2, NaF	1,27	0,15 <sup>1</sup>	1
oxálsav, pH = 4,2, MeOH	7,89	0,93 <sup>1</sup>	5
oxálsav, pH = 4,2, t-BuOH	7,66	0,90 <sup>1</sup>	5
oxálsav, pH = 5,1 EDTA	0,71	0,08 <sup>1</sup>	0
oxálsav, pH = 3,8, HCOOH	3,15	0,37 <sup>1</sup>	2
oxálsav, pH = 5,2, HCOONa	0,82	0,10 <sup>1</sup>	2
Na-oxalát, pH = 7,5	0,65	0,08 <sup>1</sup>	2
Na-oxalát, pH = 8,0, HCOONa	0,69	1,06 <sup>2</sup>	2

\*a kiindulási koncentráció ( $c_0$ ) és a TiO<sub>2</sub> szuszpenzióból 40 perces várakozás után vett felülúszóban mért koncentráció ( $c$ ) hányadosa, azaz  $c_0/c \times 100$

<sup>1</sup>referenciaként az oxálsav, pH = 4,2 ( $r^{\text{ref}^1}$ ),  $8,50 \times 10^{-8} \text{ mol dm}^{-3} \text{ s}^{-1}$  értéket használva

<sup>2</sup>referenciaként a nátrium-oxalát, pH = 7,5 ( $r^{\text{ref}^2}$ ),  $6,5 \times 10^{-9} \text{ mol dm}^{-3} \text{ s}^{-1}$  értéket használva

Az oxálsav átalakulásában az adszorpció jelentőségét igazolja, hogy NaF hatására nem csupán az átalakulási sebesség csökkent, hanem az adszorpció mértéke is. Érdekes

megjegyezni azt is, hogy a NaF-dal ellentétben a NaCl (mely nem képes a felület adszorpciós tulajdonságait oly mértékben befolyásolni mint a NaF) nem csökkentette az oxálsav adszorpciójának mértékét, átalakulási sebességét pedig kismértékben növelte. Mindez alátámasztja az adszorpciónak az oxálsav heterogén fotokatalitikus átalakulásában betöltött kiemelkedő szerepét.

A fenollal ellentétben a rosszul adszorbeálódó metanol és terc-butanol nem volt hatással az átalakulás sebességére. Ugyanakkor az EDTA a kezdeti meredek szakasz után szinte teljesen inhibíálta az átalakulást. Mindez összhangban a NaF hatásával egyértelműen arra utal, hogy az oxálsav átalakulás szinte kizárólag a TiO<sub>2</sub> felületén adszorbeálódva, elsősorban közvetlen töltésátmenettel indul.

A hangyasav, mint jól adszorbeálódó HO<sup>•</sup>-fogó, az oxálsavhoz hasonlóan a h<sub>νB</sub><sup>+</sup>-kal is elreagálhat. A metanollal és terc-butanollal ellentétben, a hangyasav szignifikánsan csökkentette az átalakulás sebességét, ami elsősorban a két szubsztrátum adszorpciója és h<sub>νB</sub><sup>+</sup>-kal való reakciói közti versengéssel értelmezhető. Összehasonlítva az oxálsav nátrium-formiát jelenlétében mért átalakulási sebességét a nátrium-oxalátéval látjuk, hogy a két érték igen közel esik egymáshoz, így ebben az esetben valószínűleg a pH önmagában is felelős az átalakulási sebesség csökkenéséért.

Az alkalmazott adalékokok hatása alapján a fenol átalakulásában a HO<sup>•</sup>-kel való reakció a domináns, az oxálsav esetében a közvetlen töltésátmenet a meghatározó, melynek előfeltétele az oxálsav adszorpciója a felületen, valamint a vegyértéksáv megfelelő potenciálja, amit a pH és a jelenlévő egyéb ionok adszorpciója jelentősen befolyásolhat.

### Összefoglalás, következtetések

- A kumarin és a fenol átalakulása szempontjából a HO<sup>•</sup>-kel való reakció, míg az oxálsav átalakulásában a közvetlen töltésátmenet a meghatározó.
- A vizsgált reakciókörülményeknek a szubsztrátum átalakulási sebességére kifejtett hatásával eldönthető, hogy a szubsztrátum átalakulásában a HO<sup>•</sup>-kel való reakció, vagy a közvetlen töltésátmenet a domináns.
- A pH és az adszorpció, valamint a jelen lévő egyéb ún. idegen ionoknak a felületi potenciálra és a HO<sup>•</sup> képződési sebességére gyakorolt hatásának jelentősége nem hagyható figyelmen kívül.

### Köszönetnyilvánítás

A szerzők köszönik a TÉT\_15\_IN-1-2016-0013 pályázat támogatását.

### Irodalomjegyzék

- [1] Field, R.J.; Raghavan, N.V.; Brummer, J.G. *J. Phys. Chem.* **86**, 2443 - 2449. (1982)
- [2] Lai, C.C.; Freeman, G.R. *J. Phys. Chem.* **94**, 302 - 308. (1990)
- [3] Getoff, N.; Schwoerer, F.; Markovic, V.M.; Sehested, K.; Nielsen, S.O. *J. Phys. Chem.* **75** 749 - 755 (1971)
- [4] Gopakumar, K.; Kini, U.R.; Ashawa, S.C.; Bhandari, N.S.; Krishnan, G.U.; Krishnan, D. *Radiat. Eff.* **32** 199 – 203 (1977)
- [5] Czili. H. Horváth A. *Appl. Catal. B: Environ.* **81** 295–302 (2008)
- [6] Land, E.J.; Truscott, T.G. *Photochem. Photobiol.* **29** 861 - 866 (1979)
- [7] Buxton G. V., Greenstock C. L., Helman W. P. and Ross A. B. *J Phys Chem Ref Data*, **17** (2), 513–886. (1988)

## VUV PHOTOLYSIS OF COUMARIN AS A POTENTIAL ACTINOMETER OF THE 185 NM VUV LIGHT

### KUMARIN, MINT POTENCIÁLIS AKTINOMÉTER 185 NM HULLÁMHOSSZÚSÁGÚ VUV FOTOLÍZISÉNEK VIZSGÁLATA

Dóra Kis, Máté Náfrádi, Krisztina Schrantz, Tünde Alapi

<sup>1</sup>*Department of Inorganic and Analytical Chemistry, University of Szeged, H-6720 Szeged, Dóm tér 7, Hungary  
e-mail: alapi@chem.u-szeged.hu*

#### Abstract

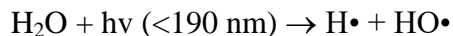
Vacuum-ultraviolet (VUV) photons are able to generate directly H• and HO• from water due to its direct photolysis. Consequently this method can be applied for the investigation of the HO• initiated reactions and the effect of the reaction parameters on the formation rate of this reactive radical having important role in the Advanced Oxidation Processes. For characterization of the light source we have to determine the photon flux of the VUV photons. The aim of this work was the investigation of the effect of dissolved oxygen, dinitrogen oxide and pH on the VUV photolysis of coumarin and formation of its hydroxylated byproduct coumarin using 185 nm VUV light.

#### Bevezetés

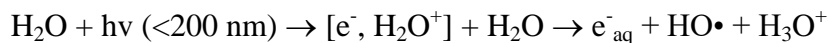
VUV-fotolízisben - akárcsak a többi elektromágneses sugárzást felhasználó nagyhatékonyságú eljárásnál - a lámpa típusa meghatározza a folyamat eredményességét. A legtöbb anyag jelentős elnyeléssel rendelkezik a VUV-tartományban. Ennek ellenére vizes oldatok VUV fotolízise során feltételezhetjük, hogy a fotonokat elsősorban a közeg, azaz a víz nyeli el, tekintettel annak koncentrációjára.

Két lámpatípust különböztetünk meg, amelynek használata elterjedt a VUV fotolízisben: a kisnyomású higanygőz lámpa és a xenon (Xe) excimer lámpa. A kisnyomású higanygőzlámpák elsősorban két hullámhosszúságon, 254 nm-en (UV) és 185 nm-en (VUV) sugároznak. A 254 nm-es fény intenzitásához képest, mely a fény formájában kibocsátott energia 85%-át hordozza, a 185 nm hullámhosszúságú fény intenzitása 8%.

A VUV-fotonok elnyelődése következtében megtörténik a vízmolekulák homolízise:



vagy ionizációja:



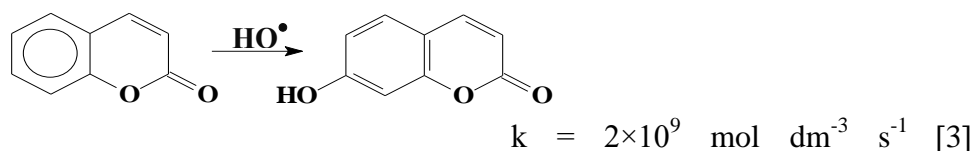
A két folyamat kvantumhasznosítási tényezője közt jelentős eltérés van. A HO•-nek a víz homolízise következtében való képződésére vonatkozó érték ( $\Phi(\text{HO}\cdot)$ ) 0,33 a 185 nm hullámhosszúságra vonatkozóan [1]. Ugyanakkor hidratált elektron ( $\text{e}^-_{\text{aq}}$ ) képződésére vonatkozó kvantumhasznosítási tényező értéke ( $\Phi(\text{e}^-_{\text{aq}})$ ), 0,045 – 0,05 [1], azaz mindkét hullámhosszúságon a pH 4 - 9 tartományban egy nagyságrenddel kisebb, mint  $\Phi(\text{HO}\cdot)$ . A fentiek értelmében a VUV fotonok elnyelődése következtében elsősorban H• és HO•



képződik. Mivel a  $\Phi(e^-_{aq})$  értéke kicsi, a jelentőségét és reakcióit vizes oldatok VUV fotolízise során többnyire elhanyagolják.

Az, hogy a VUV tartományban az anyagok moláris abszorbanációjának értéke kivétel nélkül meglehetősen nagy, megnehezíti az aktinometriás módszerek kidolgozását. Jelenleg a leginkább javasolt aktinometriás módszer a metanol vizes oldatának VUV fotolízisén alapul [2].

Az elmúlt évek során több kutató heterogén fotokatalízis során olyan nem jól adszorbeálódó aromás szerves szubsztrátumot használt a  $HO^\bullet$  kimutatására és (relatív) képződési sebességének meghatározására, melynek  $HO^\bullet$ -kel való reakciója lumineszcens, vagy fluoreszcens köztiterméket eredményez. Az egyik ilyen szubsztrátum a kumarin, melynek  $HO^\bullet$ -kel való reakciója umbelliferon (7-hidroxi-kumarin):



képződését eredményezi. Heterogén fotokatalitikus vizsgálatok során a képződő umbelliferon által kibocsátott fluoreszcens fény intenzitásának időbeni változását tekintik a  $HO^\bullet$  képződési sebességével arányosnak [4].

A kumarin  $H^\bullet$ -kel való reakciójának sebességi állandójára vonatkozó adatot nem találtunk a szakirodalomban, azonban az  $e^-_{aq}$  és a kumarin reakciójára ( $k = 1,6 \times 10^{10} \text{ dm}^{-3} \text{ mol}^{-1} \text{ s}^{-1}$  [5]) vonatkozó érték azonos az  $O_2$  és  $e^-_{aq}$  közti reakcióra ( $k = 2 \times 10^{10} \text{ dm}^{-3} \text{ mol}^{-1} \text{ s}^{-1}$  [6]) vonatkozó értékkel, és egy nagyságrenddel nagyobb, mint a kumarin  $HO^\bullet$ -kel való reakciójára vonatkozó érték.

### Kísérleti körülmények és módszerek

A VUV/UV, azaz 185 és 254 nm hullámhosszúságú fényvel való fotolízisnél alkalmazott kisnyomású higanygőzlámpa volt. A lámpa elektromos teljesítménye 15 W, a 185 nm hullámhosszúságú fény fluxusa gyári adatok alapján  $3,6 \times 10^{-7} \text{ mol}_{\text{foton}} \text{ s}^{-1}$ . A fényforrás egy dupla falú, henger alakú, üvegből készült reakcióedénybe merült. Minden alkalommal azonos térfogatú ( $250 \text{ cm}^3$ ), az áramlásos rendszerben folyamatosan keringetett oldatot sugároztunk be.

A pH-t NaOH és HCl oldatok segítségével állítottuk be a kívánt értékre (pH = 3,0, pH = 9,0, illetve a kumarin oldat saját pH-ján végzett méréseknél annak pH-ja 5,5 volt). Ezekben az esetekben az ionerősség állandó értéken tartása miatt az oldatban  $5,0 \times 10^{-3} \text{ mol dm}^{-3}$  NaCl koncentrációt állítottunk be. A kumarin oldat kiindulási koncentrációja minden esetben  $1,0 \times 10^{-4} \text{ mol dm}^{-3}$  volt.

A kumarin koncentrációjának változását spektrofotometriásan követtem Agilent 8453 diódasoros spektrofotométerrel. A kumarin átalakulása során képződő umbelliferon gerjesztését követően kibocsátott fluorimetriás fény intenzitását Hitachi F4500-as spektrofluoriméterrel mértem. A gerjesztés 332 nm-es hullámhosszúságú fényvel történt. Az umbelliferon által kibocsátott fény intenzitása arányos az umbelliferon koncentrációjával, maximuma 456 nm-nél van. Az umbelliferon képződésének sebességét az ezen a hullámhosszúságon mért fluoreszcens fény intenzitásának időbeni változásával (kezdeti szakasz meredeksége) jellemeztem.

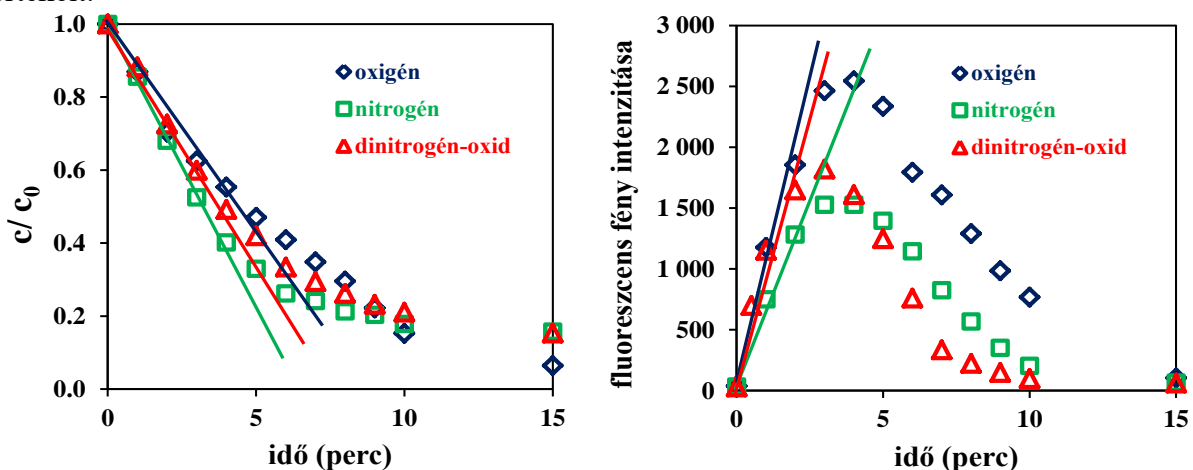


## Eredmények és értékelésük

Mivel a kisnyomású higanygőzlámpa 185 nm mellett 254 nm-en is sugároz, első lépésben megvizsgáltam, hogy a lámpa által kibocsátott 254 nm hullámhosszúságú fény hatására átalakul-e a kumarin és ez vajon együtt jár-e az umbelliferon képződésével. Ebben az esetben közönséges kvarc búrával rendelkező fényforrást használtam, mely csak 254 nm-en sugároz. A kumarin átalakulásának és az umbelliferon képződésének sebessége is elhanyagolható volt a 254 nm hullámhosszúságú fény hatására.

Az ionerősség beállítására használt NaCl mindhárom esetben (oxigén, nitrogén és dinitrogén-oxid) kismértékben csökkentette a kumarin átalakulási sebességét, és az umbelliferon képződésének a sebességét, ami feltehetően a Cl<sup>-</sup>-nak a HO<sup>•</sup> koncentrációra kifejtett hatásával értelmezhető.

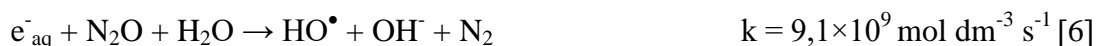
A kumarin átalakulási sebességére nem volt szignifikáns hatással az oldott oxigén és a dinitrogén-oxid jelenléte (1a. ábra), az umbelliferon képződési sebességére és maximális koncentrációjára viszont igen (1b. ábra). Oldott oxigén és dinitrogén-oxid jelenlétében az umbelliferon képződésének sebessége meghaladta a nitrogénnel oxigénmentesített oldat mért értékeit.



**1. ábra:** Oxigén és dinitrogén-oxid hatása a kumarin átalakulására és az umbelliferon által kibocsátott fluoreszcens fény intenzitására VUV/UV fényvel besugárzott, NaCl-ot tartalmazó oldatokban

Az oldott oxigén gátolja a primer gyökök, azaz a H<sup>•</sup> és HO<sup>•</sup> rekombinációját a H<sup>•</sup>-re való addíciója következtében, így megnő a HO<sup>•</sup> koncentráció. A HO<sup>•</sup> koncentráció növekedésének egy másik lehetséges oka, a HO<sub>2</sub><sup>•</sup> és O<sub>2</sub><sup>•-</sup> diszproporcionálódásával képződő H<sub>2</sub>O<sub>2</sub> UV fotolízise.

A dinitrogén-oxidot elektron-befogóként használják, mivel a



reakció szerint az e<sub>aq</sub><sup>-</sup>-nal reagálva azt HO<sup>•</sup>-ké konvertálja. Ugyanakkor sokkal kisebb sebességgel, de elreagál a H<sup>•</sup>-kel is:



mely reakció szintén HO<sup>•</sup>-öt eredményez. Vizes oldatok VUV fotolízise során így a dinitrogén-oxid az oxigénhez hasonlóan megnövelheti a HO<sup>•</sup> koncentrációt. Ugyanakkor figyelembe véve a dinitrogén-oxid oldhatóságát, a H<sup>•</sup>-el és e<sub>aq</sub><sup>-</sup>-al való reakciói sebességi

állandójának értékét, ez elsősorban az  $e^-_{aq}$ -al való reakciónak köszönhető, még akkor is, ha a víz VUV fotolízise során  $\Phi(e^-_{aq})$  értéke (0,045) egy nagyságrenddel kisebb, mint  $\Phi(HO\bullet)$  értéke (0,33) (1. Táblázat).

**1. Táblázat:**  $HO\bullet$ ,  $H\bullet$  és  $e^-_{aq}$  reakcióinak sebességi állandói, valamint azok szorzata az egyes reaktánsok kiindulási koncentrációival (adatok forrása: NIST Standard Reference Database)

	c (mol dm <sup>-3</sup> )	$HO\bullet$		$H\bullet$		$e^-_{aq}$	
		$k_{HO\bullet}$	$k_{HO\bullet} \times c$	$k_{H\bullet}$	$k_{H\bullet} \times c$	$k_{e^-_{aq}}$	$k_{e^-_{aq}} \times c$
kumarin	$1,0 \times 10^{-4}$	$2,0 \times 10^9$	$2,0 \times 10^5$	nincs adat	nincs adat	$1,6 \times 10^{10}$	$1,6 \times 10^6$
O <sub>2</sub>	$1,25 \times 10^{-3}$	-	-	$1,2 \times 10^{10}$	$1,5 \times 10^7$	$1,9 \times 10^{10}$	$2,0 \times 10^7$
N <sub>2</sub> O	$2,5 \times 10^{-2}$	-	-	$2,1 \times 10^6$	$5 \times 10^4$	$9 \times 10^9$	$2,3 \times 10^8$

Sem az oxigén, sem a dinitrogén-oxid nem változtatta meg a kumarin átalakulási sebességét szignifikánsan a nitrogénnel oxigénmentesített oldathoz képest annak ellenére, hogy a  $HO\bullet$  koncentráció feltehetően oxigénnel telített oldatban volt a legnagyobb. A kumarin  $e^-_{aq}$ -nal való reakciójának sebességi állandójának értéke egy nagyságrenddel meghaladja annak  $HO\bullet$ -kel való reakciójának, valamint összemérhető a dinitrogén-oxid és az oxigén  $e^-_{aq}$ -nal való reakciója sebességi állandójának értékével (1. Táblázat). Vagyis azt, hogy a kumarin átalakulási sebességét szignifikánsan nem befolyásolta sem az oxigén, sem a dinitrogén-oxid jelenléte, feltehetően azzal értelmezhetjük, hogy reakció körülménytől függően szerepet kaphat az átalakulásban az  $e^-_{aq}$  és a  $H\bullet$  is.

**2. Táblázat:** A kumarin kezdeti átalakulási sebessége ( $r_0^{kum}$ ) és az umbelliferon által kibocsátott fluoreszcens fény intenzitása-idő függvény kezdeti meredeksége ( $m_0^{umb}$ ), valamint maximális értéke ( $I_{max}$ ), különböző pH-jú oldatok esetén

	$r_0^{kum}$ ( $\times 10^{-7}$ moldm <sup>-3</sup> s <sup>-1</sup> )	$m_0^{umb}$	$I_{max}$
N <sub>2</sub> , pH = 3,0	1,74	207	786
N <sub>2</sub> , pH = 5,5	1,40	345	1780
N <sub>2</sub> , pH = 9,0	1,22	412	2393
O <sub>2</sub> , pH = 3,0	1,46	399	2081
O <sub>2</sub> , pH = 5,5	1,45	531	2140
O <sub>2</sub> , pH = 7,0	1,40	360	1814
O <sub>2</sub> , pH = 9,0	2,32	345	1949
N <sub>2</sub> O, pH = 3,0	2,07	773	1891
N <sub>2</sub> O, pH = 5,5	2,07	519	1563
N <sub>2</sub> O, pH = 9,0	1,88	566	1663

Az umbelliferon a kumarin  $HO\bullet$ -kel való reakciója következtében képződik. Az oxigén hatását a képződés sebességére ebben az esetben egyértelműen az oxigénnek a  $HO\bullet$  koncentrációra kifejtett pozitív hatásával értelmezhetjük. A dinitrogén-oxid kevésbé növeli

meg a HO• koncentrációt és ezen keresztül az umbelliferon képződésének sebességét, mint az oxigén, de pozitív hatása még mérhető.

A kumarin átalakulása a 3 és 5 pH-jú oldatokhoz képest a 9-es pH-jú oldatban oxigénmentes körülmények között lassabb, oxigén jelenlétében azonban gyorsabb volt (2. Táblázat). Ugyanakkor dinitrogén-oxid esetében egyáltalán nem volt mérhető hatása a pH-nak (2. Táblázat). Az umbelliferon képződésére vonatkozóan a pH hatása csak oxigénmentes körülmények között nyilvánult meg. Ebben az esetben a pH növelése szignifikánsan megnövelte azt (2. Táblázat).

A víz VUV fotolízise során az  $e^-_{aq}$  képződésére vonatkozó kvantumhasznosítási tényező ( $\Phi(e^-_{aq})$ ) értéke pH-függő, lúgos tartományban, azon belül is pH > 9-nél megnövekszik [1]. Ellenkező esetben, pH < 3 esetén  $\Phi(e^-_{aq})$  csökkenhet a H<sup>+</sup> és  $e^-_{aq}$  ( $k = 2,3 \times 10^{10} \text{ dm}^{-3} \text{ mol}^{-1} \text{ s}^{-1}$ ) [6] reakciója miatt.

Oxigénmentes oldatban a kumarin pH = 9-nél tapasztalt átalakulási sebesség növekedését értelmezhetjük a  $\Phi(e^-_{aq})$  értékének, illetve az  $e^-_{aq}$  koncentrációjának megnövekedésével. Oxigén jelenlétében a pH = 3-nál tapasztalt átalakulási sebesség csökkenését a  $\Phi(e^-_{aq})$  értékének, illetve az  $e^-_{aq}$  koncentrációjának az  $e^-_{aq}$  és H<sup>+</sup> közti reakció következtében történő csökkenésével értelmezhetjük. A képződött H• oxigén jelenléte nélkül valószínűleg a kumarinnal reagál el, oxigén jelenlétében viszont a H• nagy valószínűséggel kis reaktivitású HO<sub>2</sub>•-ké alakul át. Az umbelliferon képződési sebességének szignifikáns csökkenése a pH növekedésével oxigénmentes körülmények között megerősíti a fenti gondolatmenet helyességét.

#### Következtetések

- A 254 nm hullámhosszúságú fény jelentősége elhanyagolható a 185 nm hullámhosszúságú VUV fény mellett a kumarin átalakulása és az umbelliferon képződése szempontjából egyaránt.
- A kumarin nem csak a HO•-kel, hanem az  $e^-_{aq}$ -nal is elreagál, a két folyamat relatív hozzájárulása a kumarin átalakulásához oxigénmentes körülmények között függ az oldat pH-jától.
- Az umbelliferon képződésére alapozva a VUV tartományban használható aktinométer fejleszthető.

#### Köszönetnyilvánítás

A munka a DAAD 151955 bilaterális szerződés támogatásával készült.

#### Irodalomjegyzék

- [1] Gonzalez M. C., Oliveros E., Worner M. and Braun A. *J Photochem and Photobiol C*: **5** (3), 225–246. (2004)
- [2] Oppenländer T. and Schwarzwälder R. *J Adv Ox Technol*, **5** (2), 155–163. (2002)
- [3] Gopakumar, K.; Kini, U.R.; Ashawa, S.C.; Bhandari, N.S.; Krishnan, G.U.; Krishnan, D. *Radiat. Eff.* **32** 199 – 203 (1977)
- [4] Czili. H. Horváth A. *Appl. Catal. B: Environ.* **81** 295–302 (2008)
- [5] Land, E.J.; Truscott, T.G *Photochem. Photobiol.* **29** 861 - 866 (1979)
- [6] Buxton G. V., Greenstock C. L., Helman W. P. and Ross A. B. *J Phys Chem Ref Data*, **17** (2), 513–886. (1988)
- [7] Czapski, G.; Peled, E. *Isr. J. Chem.*, **6**, 421-436. (1968)

## **DETECTION OF SLUDGE DISINTEGRATION PROCESS BY DIELECTRIC CONSTANT MEASUREMENT**

**Sándor Beszédes, Balázs Lemmer, Zoltán Jákói, Gábor Keszthelyi-Szabó, Cecilia Hodúr**

*Department of Process Engineering, University of Szeged Faculty of Engineering, H-6725  
Szeged, Moszkvai krt. 9, Hungary  
E-mail: beszedes@mk.u-szeged.hu*

### **Abstract**

Microwave irradiation has a good potential for sludge pre-treatment. Several studies concluded that microwave pre-treatments increase the disintegration degree and biogas production of waste activated sludge. However, dielectric parameters are not commonly measured for wastewater and sludge, especially for sludge produced in food industry. Moreover, the efficiency of continuously flow microwave sludge conditioning process has not been analyzed in details. Therefore our research aimed to examine the disintegration efficiency of the microwave treatments for sludge originated from food industry carried out in continuously flow reactor. Another aspect of research was to investigate the relationship between the dielectric parameters and the change of disintegration degree.

### **Introduction**

Because of environmental aspects and the need for energy sludge utilization by biological method, such as anaerobic digestion, has been become more and more popular. Wastewater sludge has theoretically good biodegradability. But in practice, because of the flocculants dosed in wastewater treatment technology, or disinfection agents used in food industry together with organic macromolecular components form a complex sludge structure resistant to direct biological degradation. Therefore an appropriate pre-treatments stage is need before further biological utilization of sludge.

There are known several pre-treatments methods. Among them the thermal process are widely used because of their good controllability and flexibility for varying quality and quantity of sludge production. Microwave (MW) irradiation is considered as more effective compare to the conventional thermal processes. MW pretreatments are suitable to increase the organic matter solubility and, therefore, the bioavailability of substrate. This strong disintegration effects of MW irradiation can manifested in higher biogas production, for instance [1] [2]. Considering the promising results related to microwave treatment for municipal sludge further analysis is needed to investigate the applicability of the method for other types of sludge. Beside this, further examination is needed to determine the dielectric parameters of sludge exposed to MW irradiation.

Dielectric polarization and ionic conduction play role in the heat generation mechanisms of microwave irradiation. At microwaves frequencies the polarity of electromagnetic field vary with high frequency, therefore the ionic and dipolar molecules are moving in time. If molecules with dipolar characteristics lag behind the electromagnetic field heat is generated in the materiel, due to the energy dissipation. In high water contented systems the dipole movement is influenced by the strength of hydrogen bonds. For free water, the movement is occurred in the gigahertz frequency range. Dipolar movement is the dominant mechanism for bound water in the megahertz frequency range and for ice at kilohertz frequencies [3].

In order to assess the energetic efficiency of sludge treatment by microwave irradiation investigation of dielectric behavior of processed material is needed. Moreover, deeper analysis of dielectric behavior is necessitated if dielectric parameters are assumed to vary during MW pre-treatments due to thermal effects and/or structural and physicochemical changes. Dielectric constant and dielectric loss factor determined the penetration depth of electromagnetic waves into the materials, as well. In high water contented materials, such as sludge, the moisture content and the physicochemical state of water has a dominant effect of dielectric behavior [4]. During thermal and thermochemical pre-treatments partial hydrolysis of macromolecules is also occurred. Decomposition of high molecular weight components into smaller molecules, especially if it produces compounds with polar characteristics or led to increase of the concentration of ionic components with high migration ability. Increasing of polar characteristic and amount of ionic components can have effect on dielectric behaviors of processed materials.

Measurement of apparent dielectric parameters enable to the fast determination of moisture content during dehydration of agricultural and food product [5] and composting process [6]. Main advantages of dielectric measurements over the conventional methods are the fast detection and the possibility for in-situ and non-destructive measurements. By dielectric technique the ripening of apple [7], maturation of meat [8] is controllable.

### Experimental

For the experiments primary sludge produced in the wastewater purification line of a meat processing work was used. Volatile solid (VS) and total solid (TS) content of sludge was and  $6560 \pm 281 \text{ mgL}^{-1}$  and  $53 \pm 3.5 \text{ gL}^{-1}$ , respectively. Total chemical oxygen demand (TCOD) and COD of soluble phase (SCOD) was  $28300 \pm 690 \text{ mgL}^{-1}$  and  $3250 \pm 212 \text{ mgL}^{-1}$ .

Microwave treatments were carried out a custom made continuously flow microwave unit equipped magnetron with a frequency of 2450 MHz. Sludge was pumped through the toroidal cavity resonator by a peristaltic pump. Volumetric flow rate was varied in the range of 6-35  $\text{Lh}^{-1}$ .

Microwave related process parameters for sludge pre-treatments was the microwave power level (W) and the specific microwave energy intensity ( $E_s$ ,  $\text{Jg}^{-1}$ ).  $E_s$  was given from the power of magnetron (P), the volumetric flow rate ( $Q_v$ ), the quantity of sludge in microwave reactor (m) and the effective volume of PTFE spiral in the cavity resonator (V).

$$E_s = \frac{P}{m Q_v} V \quad [\text{Jg}^{-1}] \quad (1)$$

For the MW-alkali pre-treatment NaOH dosage was applied. The dosage was given in  $\text{g}_{\text{NaOH}}/\text{g}_{\text{TS}}$  unit.

Structural and chemical change of sludge was characterized by the disintegration degree (DD). DD was calculated from soluble chemical oxygen demand measured from the raw ( $\text{SCOD}_0$ ) a pre-treated sludge ( $\text{SCOD}_t$ ) and the COD of the total sludge matrix (TCOD).

$$DD = \frac{\text{SCOD}_t - \text{SCOD}_0}{\text{TCOD} - \text{SCOD}_0} 100 \quad [\%] \quad (2)$$

COD was measured photometrical method using special COD test cuvettes containing potassium dichromate. Soluble phase was separated from particulate organic matters by centrifugation (10000 rpm for 10 minutes) and pre-filtration ( $0.45 \mu\text{m}$ ).

Dielectric constant ( $\epsilon'$ ) was measured by a special designed, tailor made dielectrometer. For dielectric measurements the same frequency -2450 MHz- was used that of applied for microwave pre-treatment of sludge. Diode power sensors were positioned in a distance of  $\lambda/8$  to detect the perturbation of waveform and form of standing waves.

Power was measured by a dual channel power meter (NRVZ, Rohde&Schwarz). From the voltage standing wave ratio the reflection coefficient and phase shift was calculated. From the geometry of waveguide and positioning of sample holder with the phase shift and reflection coefficient the dielectric constant was derived.

### Results and discussion

Effects of microwave-alkaline treatment on sludge disintegration was characterized by DD. Alkaline dosage and irradiated microwave energy - as control parameters - have significant effects on DD. Results of ANOVA show that linear and quadratic terms and interaction of variables can be considered significant at the level of 95%. Increasing of  $E_s$  and alkali addition increased the DD, but over certain values of energy intensity and NaOH dosage disintegration start to decrease (Fig. 1.). Initial DD of meat processing sludge was 11%, maximum achievable DD was 27.2% if alkaline dosage and irradiated microwave energy was in the range of 0.35-0.55  $g_{NaOH}/g_{TS}$ , and 6000-8000  $Jg^{-1}$ , respectively.

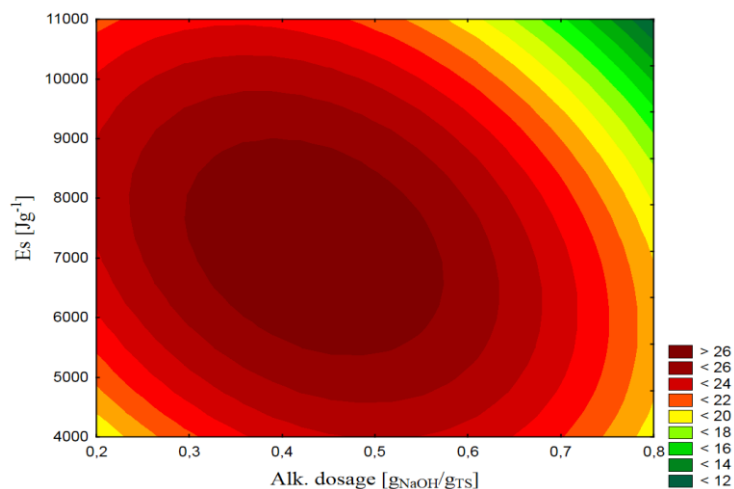


Fig.1. Effect of alkaline dosage and  $E_s$  on DD

Our results verified, that microwave irradiation combined with alkaline dosage was suitable to increase the disintegration degree of meat processing wastewater sludge. During the microwave heating under alkaline condition the sludge particles are break up, and the macromolecular components are partially hydrolyzed [1]. These effects are manifested in higher solubility of organic matters, which was detected by SCOD measurements.

Physicochemical change of sludge structure can provoke the change of dielectric parameters. Our results verified that dielectric constant of microwave-alkaline pre-treated sludge has been changed and the tendency of the change of dielectric behaviors was similar that obtained for DD (Fig. 2.). In order to investigate the relationship between the dielectric behavior and disintegration process dielectric constant ( $\epsilon'$ ) was depicted as a function of DD. It was found that in the DD range of 13-28% a strong linear correlation was found between the DD and dielectric constant (Fig. 3.a.).



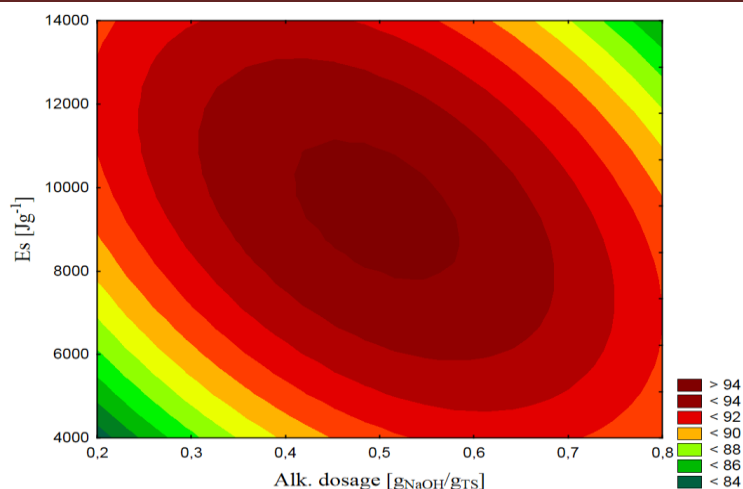


Fig.2. Dielectric constant as a function of  $E_s$  and alkaline dosage (temperature= $25^\circ\text{C}$ )

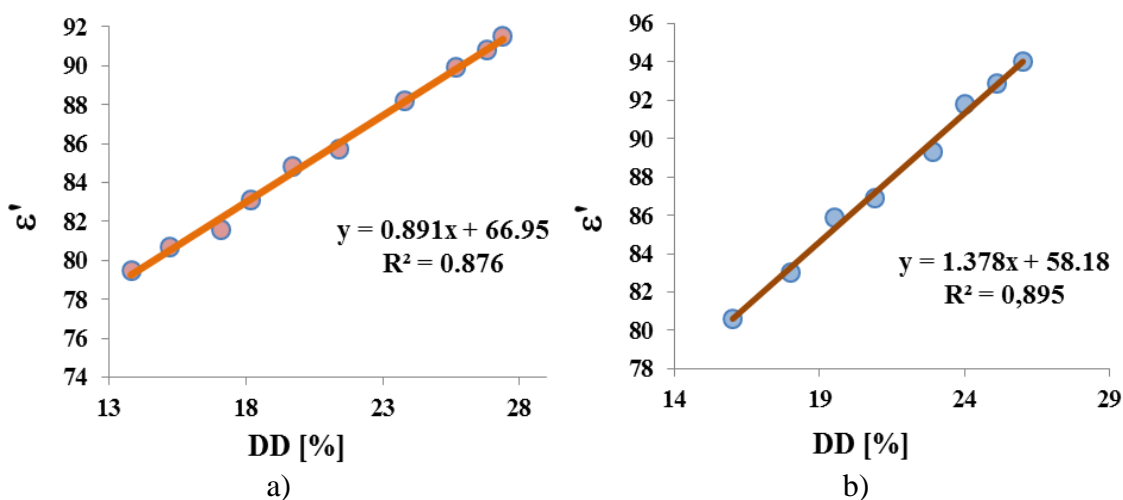


Fig.3. Relationship between dielectric constant and DD for fresh collected (a) and freeze stored sludge (temperature= $25^\circ\text{C}$ )

To test the validity of dielectric measurements for detection of the change of DD, in the next stage of experiments measurements were carried out for freeze stored sludge sample, as well. Independently from the freezing-thawing process the linear connection of dielectric constant with DD has been also revealed (Fig.3.b).

Disintegration of sludge particles increase the ratio of free to bounded water content. Increasing of free water with higher smaller molecular weighted components produced during thermochemical treatment of sludge enhances the orientation ability of compounds in high frequency electromagnetic field [4]. Enhanced polarization ability was detected by the change of dielectric constant.

## Conclusion

Efficiency of microwave pre-treatment for municipal waste activated sludge was verified in numerous studies. But suitability of microwave treatments for sludge produced in food industry wastewater purification is not investigated in details. Generalization of experimental results and scale-up of microwave sludge pre-treatment for pilot and industrial system has difficulties, mainly the experiences from continuously flow microwave sludge treatment



process is missing. Further investigations are needed to analyze the energetic efficiency of microwave irradiation. Energy need and payback period of microwave sludge treatment is depended by several factors. From the aspects of material characteristic, the composition and dielectric parameters determined mainly the energetic efficiency. Sludge has high water content and, therefore, good microwave power dissipation. But dielectric parameters of sludge have not been investigated deeply, moreover, during sludge treatments the dielectric behavior can be changed due to the physicochemical changes of sludge.

Therefore, in our work the applicability of the continuously flow microwave treatment combined with alkaline addition was investigated for meat processing wastewater sludge. Our results verified, that microwave irradiation was suitable to increase the disintegration degree of sludge.

Enhanced disintegration can manifest in higher concentration of soluble organic matter content. Higher bioavailability of soluble organic substrate provoke that efficiency of a subsequent biological degradation process can be increased, as well.

Higher biodegradability is suitable to intensify the controlled biological utilization of sludge, in composting or anaerobic digestion process, respectively. Improvement of biogas yield provoked by the microwave pre-treatment could led to enhanced energetic efficiency and shortened overall payback period of sludge pretreatment-digestion technology.

Another aspect of our research was to determine the dielectric constant for meat processing sludge. Our results verified that dielectric behavior was influenced by the disintegration efficiency of microwave-alkaline treatment. Dielectric constant has a good linear correlation with disintegration degree in the investigated range.

Therefore dielectric measurements can be considered suitable to the fast, reliable and non-destructive detection of the change of organic matter solubility in laboratory scale batch and continuously flow process and, however, for in-line and real time characterization of the disintegration efficiency of sludge pre-treatments.

### **Acknowledgements**

This project was supported by the János Bolyai Research Scholarship of the Hungarian Academy of Sciences and the UNKP-17-4-I-SZTE-5 New National Excellence Program of the Ministry of Human Capacities.

### **References**

- [1.] Dogan, F.D. Sanin, *Water Res.* 43 (2009) 2139–2148.
- [2.] Serrano, JA: Siles, M.A. Martin, A.F. Chica, FS: Estevez-Pastor, E. Toro-Baptista, J. *Env. Manag.* 177 (2016) 231-239
- [3.] G. Brodie, R. Destefani P.A. Schneider, L. Airey, L., M.V. Jacob, J. *Microw. Power Electromagn. Energ.* 48 (2014) 147–157.
- [4.] O.D. Afolabi, M. Sohail, J. *Env.Manag.* 187 (2017) 401-415.
- [5.] M. Castro-Giraldez, U. Tylewicz, PJ. Fito, M. Dalla Rosa, P. Fito, J. *Food Engineering* 102 (2011) 34-42.
- [6.] L. Cai, TB. Chen, D. Gao, HT. Liu, GD. Zheng, *Waste Manag.* 33 (2013) 12-17.
- [7.] M. Castro-Giraldez, PJ. Fito, C. Chenoll, P. Fito, *Agr. Food Chem.* 58 (2010) 3761-3766.
- [8.] JL: Demez, S. Clerjon, S. Abouelkaram, J. Lepetit, J. *Food Eng.* 85 (2008) 1116-1122.

## BIZMUT-VANADÁT FOTOKATALIZÁTOROK ELŐÁLLÍTÁSA ÉS STABILITÁSVIZSGÁLATA

Zsolt Kása<sup>1\*</sup>, Zsolt Pap<sup>1,2</sup>, Klára Hernádi<sup>3</sup>, Lucian Baia<sup>2,4</sup>

<sup>1</sup>Research Group of Environmental Chemistry, Institute of Environmental Science and Technology, University of Szeged, Szeged, HUNGARY

<sup>2</sup>Institute of Interdisciplinary Research in Bio-Nano Sciences, Babeş-Bolyai University, Cluj-Napoca, ROMANIA

<sup>4</sup>Department of Applied and Environmental Chemistry, University of Szeged, Szeged, HUNGARY

<sup>3</sup>Faculty of Physics, Babeş-Bolyai University, Cluj-Napoca, ROMANIA  
e-mail: kasa.zsolt@chem.u-szeged.hu

### Abstract

In this study, bismuth vanadate with different cube-like structured morphologies were crystalized by one-step hydrothermal method with pH modulation without additives. The as-prepared BiVO<sub>4</sub> products were systematically characterized with various techniques to prove their crystallographic, morphological, chemical and optical properties. The photocatalytic activities of the synthesized BiVO<sub>4</sub> were assessed by the photodegradation of rhodamine B (RhB) and oxalic acid under UV and visible light irradiation. The recyclability was investigated as well and found that the bismuth vanadate microcrystals were transformed.

### Bevezetés

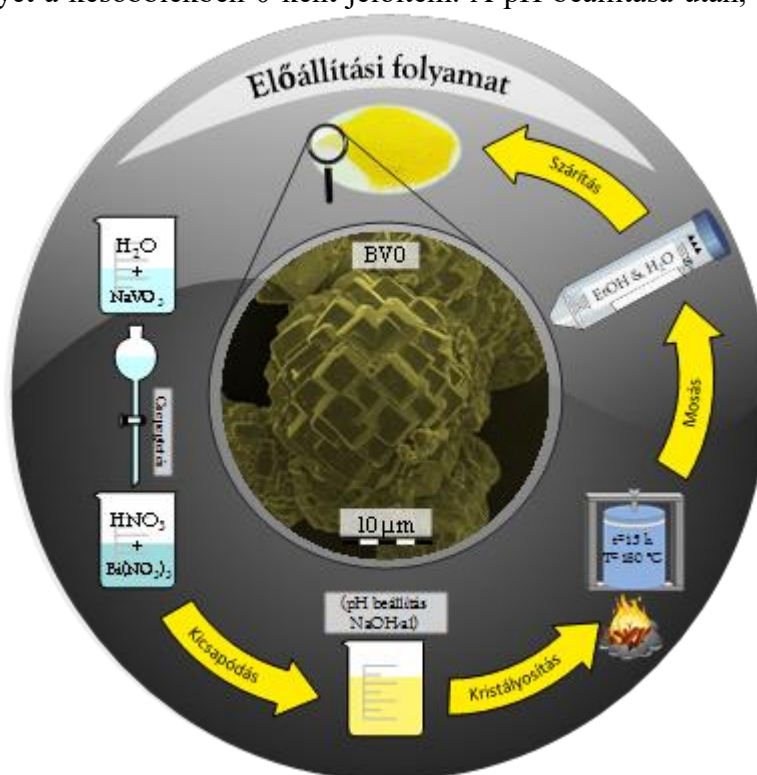
A fotokatalízis a nagyhatékonyságú oxidációs eljárások (AOP's) egyik fajtája, egy alternatív víztisztítási eljárás, mely során egy félvezető fotokatalizátor segítségével képesek lehetünk a vízben vagy a levegőben lévő, nehezen eltávolítható szerves szennyező anyagokat lebontani, ideális esetben széndioxiddá, vízzé, valamint szervesetlen ionokká oxidálni [1]. A folyamat lényege, hogy ha egy félvezető részecskét a megfelelő energiájú elektromágneses sugárzással gerjesztünk, akkor a vegyérték sávból a vezetési sávba „kényszerítünk” egy elektront, ez által hátramarad egy pozitív töltésű „lyuk”. Ez az „elektron-lyuk” pár képes a felület közelében lévő szerves szennyezőket gyökös folyamatok által oxidálni [2]. Fontos, hogy ha megfelelően megválasztott félvezetőt alkalmazunk (például titán-dioxid, volfrám-trioxid, bizmut oxid tartalmú vegyesoxidok), akkor a folyamat elindításához kizárólag csak napfényre van szükség. A kiválasztott katalizátor esetében elvárás, hogy kedvező fizikai-kémiai, optikai, és morfológiai tulajdonságokkal rendelkezzen, melyek szorosan összefügghetnek a fotokatalitikus aktivitással. Így, ha képesek vagyunk a számunkra kedvező irányba módosítani a félvezető kristály tulajdonságait, mint például a méretét, alakját, fajlagos felületét, kristályfázisát, akkor a fotokatalitikus degradációs kapacitás nagymértékben megnövelhető [3]. E tulajdonságok a szintéziselegy pH-jának változtatásával, adalékanyagok hozzáadásával, vagy éppen utólagos hőkezeléssel befolyásolhatók. Ezt nevezzük irányított kristályosításnak, melynek lényege, hogy egy adott előállítási/kristályosítási paramétert optimalizálunk, így a fotokatalizátor egy kedvező tulajdonságát kihangsúlyozzuk, ez által növelve meg a katalizátor hatékonyságát.

A bizmut-vanadát egy olyan bizmut-oxid tartalmú vegyesoxid, mely könnyen előállítható, kelően olcsó, valamint a tiltott sáv szélessége elég kicsi ahhoz, hogy látható fényben gerjeszhető legyen. Mindemellett az irányított kristályosítás könnyen megvalósítható

a szintéziselegy pH-jának befolyásolásával [4] [5]. Ugyanakkor előzetes vizsgálataink arra engedtek következtetni, hogy a katalizátor egyes szerves anyagokkal/savakkal szemben UV megvilágítás mellett korántsem elég stabil ahhoz, hogy hatékonyan használható legyen ipari körülmények között

### Kísérleti rész

Munkám során hidrotermálisan állítottam elő különböző morfológiájú bizmut-vanadát mikrorészecskéket. Az irányított kristályosítást a szintéziselegy pH-jának változtatásával értem el. A mikrorészecskék előállítását az alábbi recept szerint történt: 2,5 mmól bizmut-nitrát pentahidrátot ( $\text{Bi}_2(\text{NO}_3)_3 \cdot 5 \text{H}_2\text{O}$ ) feloldottam 55,7 mL 2 mólos salétromsavban (A oldat). Ezalatt egy másik edényben 2,5 mmól nátrium-metavanadátot ( $\text{NaVO}_3$ ) oldottam fel 55,7 mL nagy tisztaságú Milli-Q vízben (B oldat), majd 30 perc kevertetés után hozzácepegettem az A oldatot. További 30 perc kevertetés után 0,2 mólos, 2 mólos, valamint 20 mólos NaOH oldattal beállítottam a pH-t. A pH értékek a következők voltak: 1, 2, 3, 5, 7, és 9. A NaOH mentes oldat pH-ja ~0,7 volt, melyet a későbbiekben 0-ként jelöltem. A pH beállítása után, a kicsapódó sárga, amorf bizmut-vanadát szuszpenziót egy acél köpenyes teflon autoklávba töltöttem, majd 15 órára 180 °C-ra programozható szárítószekrénybe tettem. A hidrotermális kezelést követően az autoklávot szobahőmérsékletre hűtöttem és a keletkező kristályos bizmut-vanadát abszolút etanollal és Milli-Q vízzel mostam és 40 °C-on 12 órán át szárítottam. A mintákat a következő képpen kódoltuk: BV0-tól BV9-ig, ahol a BV a kristályos bizmut-vanadatra utal, míg a szám, a beállított pH értéket jelöli. A szintézis vázlata, valamint a pH beállítás nélküli minta pásztázó elektronmikroszkópos felvétele az 1. ábrán látható.



1. ábra  $\text{BiVO}_4$  előállítása

### Fotokatalizátorok jellemzése

A kristályos anyagokat számos anyagvizsgálati módszerrel jellemeztük: pásztázó elektronmikroszkópia (SEM), röntgendiffraktometria (XRD), valamint diffúz reflexiós spektroszkópia (DRS).

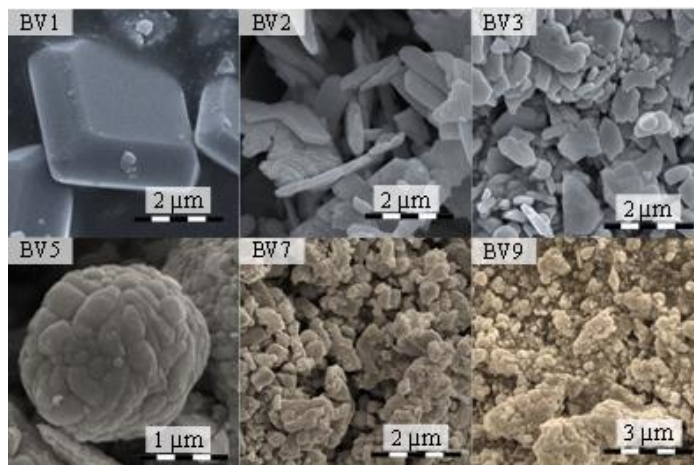
A létrehozott anyagok fotokatalitikus aktivitását látható fény megvilágítása mellett teszteltem 25 °C-on. A fényforrás 4 darab 24 W-os hagyományos energiatakarékos izzó volt ( $\lambda_{\text{max}} > 400 \text{ nm}$ ). A modellszennyező egy festékanyag, a rhodamin B, valamint oxálsav volt. A tesztek során 100 mg fotokatalizátort szuszpendáltam 100 mL,  $1 \cdot 10^{-5}$  M-os rhodamin B oldatban, vagy  $5 \cdot 10^{-4}$  M-os oxálsav oldatban, majd 30 percig sötétben kevertettem, hogy a

szorpciós folyamatok egyensúlyba kerüljenek. A lámpák felkapcsolását követően 30 percenként mintát vettem, amelyet lecentrifugáltam. A rhodamin B mennyiségének változását UV-vis spektrofotométerrel követtem nyomon (detektálási hullámhossz = 553 nm), míg az oxálsav fogyását nagyhatékonyságú folyadékkromatográfiás elválasztástechnikával határoztam meg. A detektálás hullámhossza ekkor 206 nm volt.

### Eredmények és értékelésük

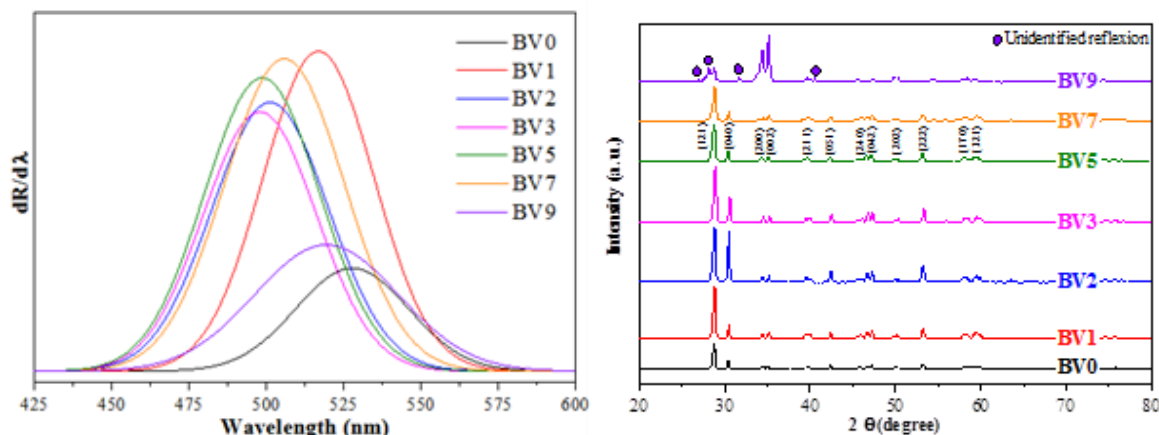
A fent felsorolt mérés technikákkal vizsgáltuk meg a keletkezett részecskéket, hogy többet megtudjunk a morfológiáról, a kristálytani és optikai tulajdonságairól, valamint az anyagok fotokatalitikus tulajdonságairól.

A SEM felvételekből egyértelműen látszik (2. ábra), hogy extrém alacsony pH-n (BV1) hasonló morfológia alakul ki, mint a NaOH-ot nem tartalmazó bizmut-vanadát (1. ábra-BV0), azonban itt az egyedi lapok összenövése nem figyelhető meg. A pH emelkedésével ez a jól definiált struktúra fokozatosan eltűnik. 5-ös pH-nál (BV5) az egyedi részecskék gömb alakba történő rendeződése figyelhető meg, mely semleges és bázikus szintézis körülmények között ismét megszűnik.



2. ábra SEM felvételek

Felvettük a minták diffúz reflexiós spektrumait, ami során azt tapasztaltuk, hogy a derivált spektrumok elnyelési maximuma a pH változtatásával fokozatosan az UV fény tartományába tolódik el („blue-shift”), ám ez a tendencia a semleges és bázikus pH közelében megfordul. Ez korrelál a felvett porröntgen diffraktogramokkal, ahol megfigyelhető, hogy a (040)-ás kristályoldalhoz tartozó reflexió aránya drasztikusan lecsökken, pH=9 esetén már a (200)-ás és a (002)-es kristályoldal aránya a domináns. Mindemellett egy további reflexió jelenik meg, melyet eddig még nem sikerült beazonosítani.

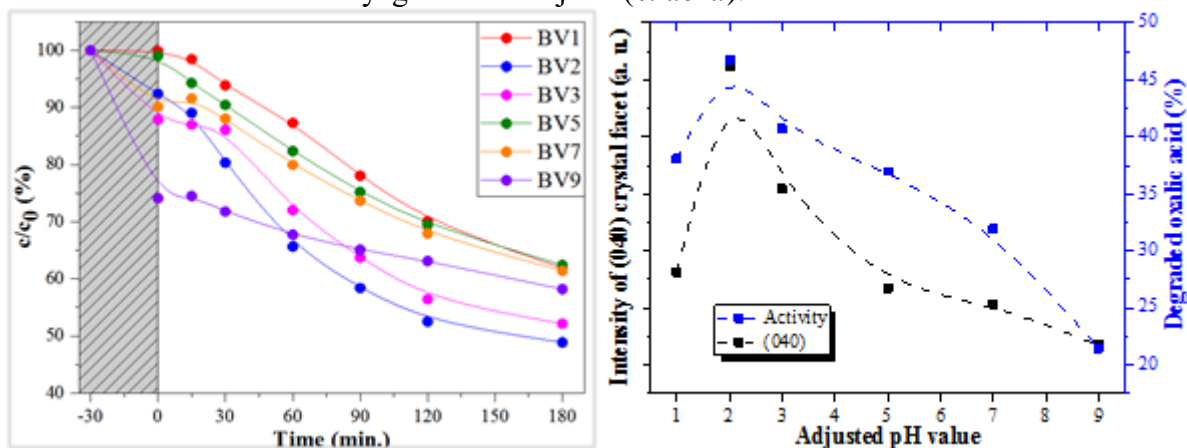


3. ábra Jobbról: derivált DRS spektrumok; balról: röntgen diffraktogramok

Ezt követően megvizsgáltuk a minták fotokatalitikus aktivitását két modellszennyező esetben. Jól látszik, hogy a szintéziselegy pH-ja nagyban befolyásolja a keletkező anyag

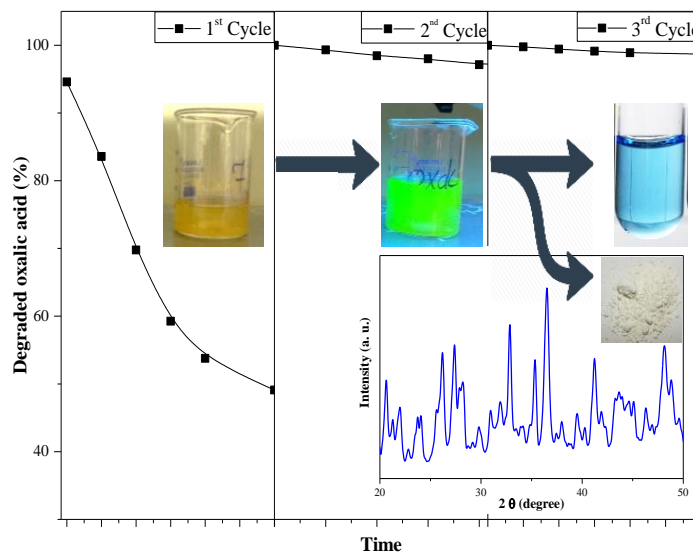


fotokatalitikus aktivitását, mely összefügg a (040)-ás kristályoldal intenzitásával, ugyanis ez az oldal felelős a szerves anyagok oxidációjáért (4. ábra).



4. ábra Jobbról: Rhodami B bomlásgörbe; balról: (040)-ás reflexiójának intenzitása és az elbontott oxálsav mennyiségének viszonya

Ugyanakkor észrevehető volt, hogy az oxálsavval végzett kísérletek esetében a szintelen oxálsav oldat megkékül, s a katalizátor kifehéredik, mely UV megvilágítás és töményebb oxálsav oldat esetében még intenzívebb volt (5. ábra). A kékülés arra utalt, hogy vanadil ionok ( $\text{VO}^{2+}$ ) kerülnek az oldat fázisba, melyet kálium-permanganátos titrálással be is bizonyítottunk. Ezzel egyidőben az átalakult fehér szilárd anyagot porröntgennel vizsgáltuk meg, s adatbázis segítségével sikerült beazonosítani, hogy bizmut-oxalát keletkezett. Érdekes módon a rhodamin B-vel végzett kísérleteknél a katalizátor mindvégig stabil maradt, amit az újrafelhasználhatósági kísérletek is bizonyítottak.



5. ábra  $\text{BiVO}_4$  stabilitásának vizsgálata oxálsav oldatban

### Következtetés

Munkám során sikeresen állítottam elő azonos kristályfázisú, de eltérő hierarchikus szerkezetű és tulajdonságú bizmut-vanadát kristályokat. A keletkező részecskék alakjának és a (040)-ás kristályoldal arányának változtatását kizárólag a szintéziselegy pH-jának beállításával

értem el. Az eredmények alapján elmondható, hogy a fotokatalitikus aktivitás szorosan összefügg a (040)-ás kristályoldal arányával. Ugyanakkor bebizonyosodott, hogy a részecskék nem minden szerves anyaggal szemben ellenállóak. Oxálsav jelenlétében a besugárzott UV fény energiája nem az oxálsav fotokatalitikus degradációra, hanem a bizmut-vanadát átalakulására fordítódik, mely során a vanadil ionok kijutnak az oldatba. Ez bizonyítja, hogy a fotokatalizátor stabilitása anyagfüggő.

### **Köszönetnyilvánítás**

Köszönöm a támogatást a Campus Mundi Programnak (EFOP-3.4.2-VEKOP/15-2015-00001) a Svájci Hozzájárulásnak (SH/7/2/20), az indiai TÉT pályázatnak (TÉT\_15\_IN-1-2016-0013) és a GINOP pályázatnak (GINOP-2.3.2-15-2016-00013). Pap Zsolt köszönetet mond a Magyar Tudományos Akadémia Prémium Posztdoktori pályázatának az anyagi támogatásért.

### **Hivatkozások**

- [1] S. Malato, J. Blanco, A.R. Fernandez-Alba, A. Aguera, *Chemos.* 2000, **40** p. 403
- [2] L. Järup, *Brit. Med. Bull.* 2003, **68** p. 167.
- [3] K. Pirkanniemi, M. Sillanpää, *Chemos.* 2002, **48**. p. 1047.
- [4] G. Zhao, W. Liu, M. Dong, W. Li, L. Chang, *D. 'n Pig.*, 2016, **134**, p. 91.
- [5] T. Das, X. Rocquefelte, R. Laskowski, L. Lajaunie, S. Jobic, P. Blaha, K. Schwarz, *Mat., Chem. of Mat.*, 2017, **29** p. 3380..

**A VÍZMÁTRIX SZERVES- ÉS SZERVETLEN ÖSSZETEVŐINEK HATÁSAI  
KŐOLAJJAL SZENNYEZETT VIZEK ÓZONKEZELÉssel ÉS  
MEMBRÁNSZŰRÉssel TÖRTÉNŐ KOMBINÁLT KEZELÉSÉRE**

**EFFECTS OF ORGANIC- AND INORGANIC COMPOUNDS OF THE WATER  
MATRIX ON OZONATION/MEMBRANE SEPARATION COMBINED  
TREATMENT**

**Gábor Veréb<sup>\*</sup>, Norbert Csizmadia, Szabolcs Kertész, Sándor Beszédes, Cecilia Hodúr,  
Zsuzsanna László**

*Szegedi Tudományegyetem, Mérnöki Kar, Folyamatmérnöki Intézet, Magyarország, HU-6725  
Szeged, Moszkvai krt. 9.; \*e-mail: verebg@mk.u-szeged.hu*

**Abstract**

Oily pollutions can be efficiently eliminated from waters by membrane filtration and by advanced oxidation processes as well, and the advantageous of the combination of these methods have also been reported [1,2]. Humic pollutions naturally can appear in oily contaminated waters (either in surface- or ground waters [3]), which may affect both ozonation and membrane filtration due to their amphiphilic- and antioxidant properties. In the present study the advantages of the combination of pre-ozonation with membrane filtration was investigated in case of humic-acid containing oil in water emulsions. Fluxes, resistances, membrane foulings and purification efficiencies were investigated in case of different durations of pre-ozonation, and applying different water matrixes (low- and high salt concentrations). In summary, a short (2 minute) pre-ozonation (~ 20 mg/L<sup>1</sup> absorbed ozone) increases the available flux and reduces the membrane resistance also in the presence of humic acid.

**Keywords:** ozonation, membrane filtration, humic acid, oil contaminated waters, water matrix

**1. Bevezetés**

A membránszűrés, és a nagyhatékonyságú oxidációs eljárások („AOPs”) egyaránt intenzíven vizsgált módszerei az innovatív vízkezelési eljárásoknak. Korábbi eredményeink alapján (megfelelő paraméterek alkalmazása esetén) az ózonkezelés eredményesen kombinálható membránszűréssel az olajeredetű szennyezések eltávolítására. Az elérhető előnyök közé sorolható a nagyobb fluxus, a kisebb ellenállás, kisebb mértékű eltömődés és a könnyebb membrántisztítás [1,2]. A vizek olajszennyezései mellett természetes módon jelen lehetnek huminanyagok is (mind a felszíni, mind a felszín alatti vizekben [3]), melyek amfifil jellegükből adódóan, illetve közismert antioxidáns hatásuk révén jelentősen befolyásolhatják mind a membránszűrést, mind a nagyhatékonyságú oxidációs eljárások hatékonyságát. Jelen tanulmányban azt vizsgáltuk, hogy az ózonos előkezelés membránszűréssel történő kombinálásának előnyei miként érvényesülnek, ha az olajszennyezések mellett huminanyagokat is tartalmaznak a kezelendő vizek. Vizsgáltuk a különböző mértékben előkezelt vizek szűrése során elérhető fluxusokat, a membráneltömődések mértékét és jellegét, valamint az elérhető tisztítási hatékonyságokat különböző vízmátrixok esetében.



## 2. Alkalmazott anyagok és módszerek

Kísérleteinkben desztillált vizes és modell termálvizes mátrixban elkészített 20 ppm huminsavat is tartalmazó 100 ppm koncentrációjú kőolaj emulziókat vizsgáltunk (*MOL Zrt.* algyői nyers kezeletlen ásványi olaja). Az emulziók ( $d_{\text{olajcsepp}} < 2,0 \mu\text{m}$ ) előállítását két lépésben, nagy fordulatszámú keverő (35000 rpm), illetve ultrahangos homogenizáló (*Hielscher UP200S*) alkalmazásával történt. A modelltermálvíz egy kisteleki kútból származó termálvíz összetételéhez hasonló oldat, melynek előállításához  $\text{NaHCO}_3$ -ot (2,259 g/L),  $\text{NH}_4\text{Cl}$ -ot (53,449 mg/L),  $\text{CaCl}_2$ -ot (19,11 mg/L),  $\text{KCl}$ -ot (20,88 mg/L),  $\text{NaCl}$ -ot (93,5 mg/L),  $\text{FeCl}_3$ -ot (4,49 mg/L) valamint  $\text{MgSO}_4$ -ot (35,31 mg/L) használtunk fel.

Az emulziók ( $V = 500 \text{ ml}$ ) ózonos előkezeléséhez (0, 1, 2, 5, 10 perc) egy *BMT 802X* típusú ózongenerátort, (*Messer 3.5* tisztaságú) oxigént és egy teflon fedéllel szerelt üvegreaktort alkalmaztunk. A gázbevezetés ( $1,0 \text{ dm}^3/\text{perc}$ ) egy üvegdiffúzoron keresztül történt. A bemeneti és a kimeneti ózonkoncentrációt átfolyós küveták ( $l = 1 \text{ cm}$ ) segítségével egy *WPA Biowave II* spektrofotométerrel határoztuk meg 254 nm-en. A térfogatáram ( $q_v = 1,0 \text{ dm}^3/\text{perc}$ ) és az ózonkoncentrációk ismeretében számítottuk az elnyelt ózon mennyiségét.

A membránszűrésekhez egy 6,7 cm átmérőjű membránnal szerelhető, *Millipore* gyártmányú, szakaszos szűrést biztosító, kevertetett cellás membránszűrőt használtunk, 350 rpm (5,83 1/s) kevertetési sebesség és 0,1 Mpa transzmembrán nyomás alkalmazása mellett. A méréseink során 250 ml mennyiségű emulziókat szűrtünk,  $0,2 \mu\text{m}$  pórusátmérőjű poliéterszulfon (PES) mikroszűrő membrán (*New Logic Research Inc.*) segítségével 200 mL permeátum keletkezéséig (5-szörös térfogatsűrítési arány – *volume reduction ratio*:  $\text{VRR} = 5$ ).

A szűrésre jellemző visszatartási értéket (tisztítási hatékonyságot) a szűrendő fluidum kémiai oxigénigényéből ( $\text{KOI}_0$ ) és a szűretet kémiai oxigénigényéből ( $\text{KOI}_{\text{sz}}$ ) számítottuk:

$$R = ((\text{KOI}_0 - \text{KOI}_{\text{sz}}) / \text{KOI}_0) \cdot 100 [\%] \quad (1)$$

A kémiai oxigénigény (kálium-dikromátos) tesztsövekkel határoztuk meg (*Hanna Instruments*), *Lovibond ET 108* roncsoló készülékkel ( $150^\circ\text{C}$ -on, 120 perc roncsolás), és *Lovibond COD Vario* spektrofotométerrel. A vezetőképesség és a pH méréséhez egy *Consort C535 SK10B* multimétert használtunk (*Denver Instruments*). A cseppméreteloszlást és a zeta-potenciál értékeket egy *ZetaSizer4* készülékkel (*Malvern Instruments*) mértük.

A membránszűrés során mérhető teljes szűrési ellenállás ( $R_{\text{teljes}}$ ) három ellenállástípusból adódik össze (számításuk részletei: [1,2]): a membrán saját ellenállásából ( $R_{\text{membrán}}$ ), a reverzibilis ellenállásból ( $R_{\text{reverzibilis}}$  – a lemosható iszaplepleny és a koncentráció polarizációs réteg okozza) és az irreverzibilis ellenállásból ( $R_{\text{irreverzibilis}}$  – a pórusos- és a pórusok közötti eltömődés, illetve a membránhoz tartósan hozzátapadó szennyeződés okozza).

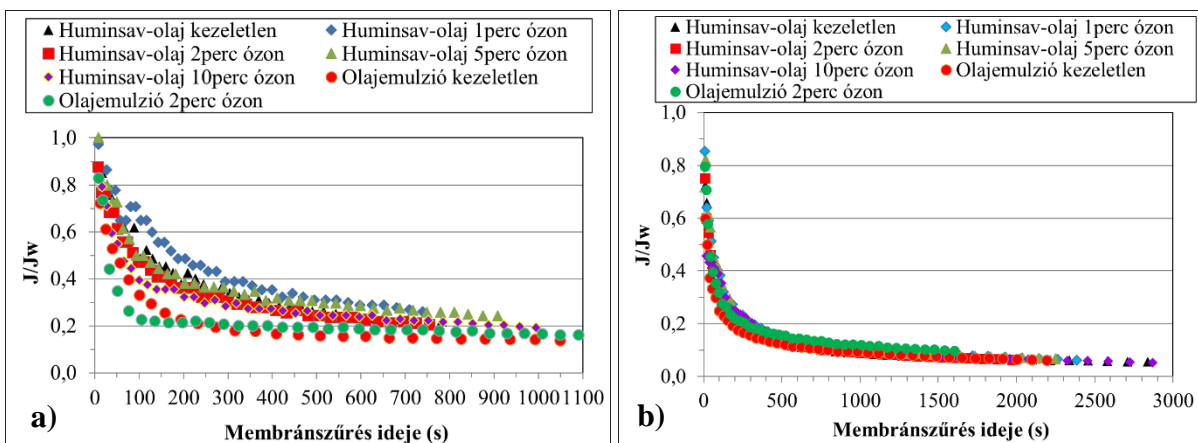
$$R_{\text{teljes}} = R_{\text{membrán}} + R_{\text{reverzibilis}} + R_{\text{irreverzibilis}} [1/\text{m}] \quad (2)$$

## 3. Eredmények és kiértékelésük

Vizsgáltuk, hogy miként befolyásolja a különböző ideig (0, 1, 2, 5, 10 percig) végzett ózonos előkezelés ( $\sim 10\text{-}100 \text{ mg/L}$  elnyelt ózon) a 20 ppm huminsavat és 100 ppm kőolajat tartalmazó emulziók membránszűrhetőségét a fluxus, a szűrési ellenállás illetve tisztítási hatékonyság vonatkozásában (desztillált vizes és modell termálvizes közegben egyaránt). A legkedvezőbb szűrési paramétereket eredményező előkezelési időket alkalmazva, kontrollként vizsgáltuk a huminsavat nem tartalmazó 100 ppm-es olajemulziók szűrhetőségét is annak jellemzésére, hogy a kombinált kezelést miként befolyásolja a huminsav jelenléte.

### 3.1. Membránszűrés során mérhető fluxus

Az **1. ábra** a szűrések során mért relatív fluxusokat ábrázolja a szűrés idő függvényében. Desztillált vizes közegben a huminsavat is tartalmazó emulziók esetében a rövid ideig (1-2 perces) tartó ózonkezelés (kis mértékben) növelte az elérhető fluxust, míg a hosszabb (5-10 perces) előkezelések hatására fluxuscsökkenést figyeltünk meg. Megjegyzendő, hogy a huminsav jelenlétében kevésbé érvényesül a rövid idejű ózonos előkezelés fluxusnövelő hatása, mint a korábbi tanulmányban [2] vizsgált, kizárólag olajat tartalmazó emulzió esetében. Az **1. ábra** alapján ugyanakkor a huminsav jelenléte önmagában is fluxusnövekedést eredményezett, mely összefüggésbe hozható a huminsavak amfifil jellegével, ami azt eredményezheti, hogy az olajcseppek felületén megtapadt huminsavak hatására a membránfelületen kialakuló szennyezőréteg kevésbé lesz hidrofób, ezáltal könnyebben áthaladhat rajta a szűrendő víz.



**1. ábra** Ózonkezelés hatása a fluxusra (a) desztillált vizes és (b) modell termálvizes mátrix esetén

A membránfelületeken kialakuló szennyezőréteg az előkezelés idejének növelésével egyre világosabb lett, ami a huminsav bomlását jelzi. A zeta-potenciál mérések eredményei (**1. táblázat**) alapján már az 1 perces ózonkezelés is jelentős mértékben növelte az olajcseppek negatív felületi töltését, ami azt eredményezi, hogy a cseppek jobban taszítják egymást (illetve a negatív töltésű membránt is), ezáltal kevésbé kompakt szennyezőréteg tud kialakulni a membrán felületén, ami ugyancsak hozzájárulhatott a (mért) nagyobb fluxusok eléréséhez.

**1. Táblázat** Zeta-potenciál és átlagos cseppméret változása az ózonkezelés során

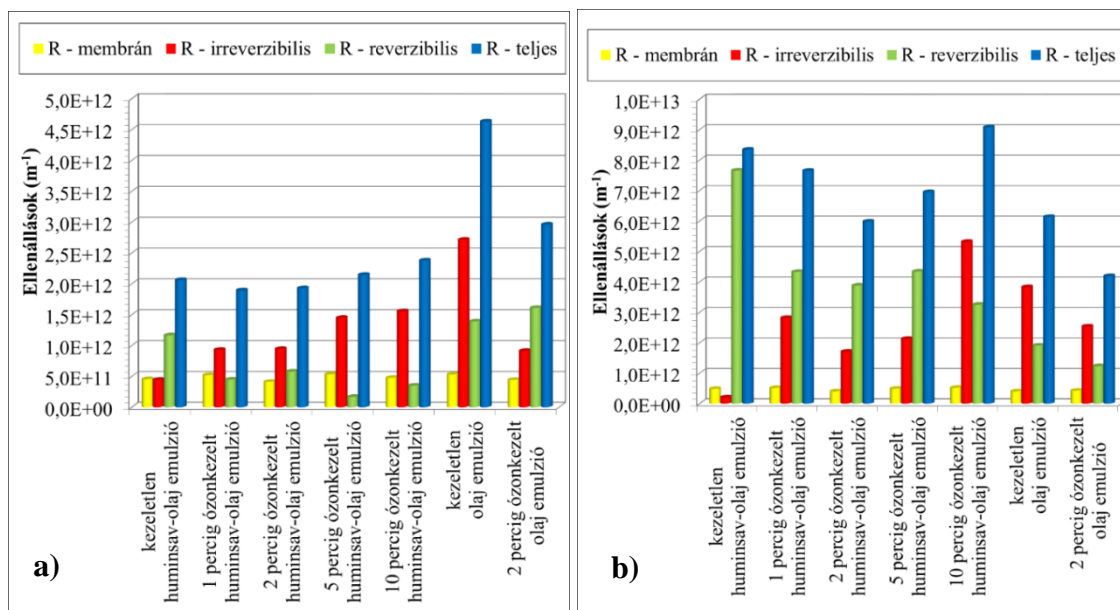
Ózonkezelés ideje (perc)	Desztillált vizes közeg		modell termálvizes közeg	
	Zeta-potenciál (mV)	Átlagos cseppméret (nm)	Zeta-potenciál (mV)	Átlagos cseppméret (nm)
0	-26.4	244.5	-56.4	287
1	-44.2	247.6	-57.1	283
2	-44.6	240.5	-57.6	277
5	-47.7	243.2	-57.8	275
10	-49.3	240.7	-62.3	261

Az ózonkezelés idejét növelve a zeta-potenciál érték már nem csökkennek számottevően, ugyanakkor az átlagos cseppméret (**1. táblázat**) csökkent, ami növelheti a pórusok eltömődésének mértékét. Ezen felül a permeátumok enyhén sárgás színének eltűnése (és a membránfelületek világosodása is) jelzi a huminanyagok bomlását, aminek következtében csökken azok korábban mért fluxusnövelő hatása.

A modell termálvizes közeg esetében jelentősen kisebbek a fluxusértékek, mint a desztillált vizes közeg esetén (**1. ábra**), a membránfelületen felhalmozódó szennyezőanyag is jelentősen több volt ebben az esetben és sokkal intenzívebb volt a membránok sárgás-barnás színe, ami elsősorban a vas-oxid-hidroxidoknak tulajdonítható. A zeta-potenciál értékek (**1. táblázat**) jelen esetben csak csekély csökkenést mutattak és jelentősen nagyobb negatív értékeket vettek fel, mint a desztillált vizes közegben, ezért a modelltermálvizes közeg esetén mért jelentősen kisebb fluxusértékek nem hozhatók összefüggésbe a cseppek felületi töltésével, illetve az olajcseppek méretével sem (**1. táblázat**). Lehetséges magyarázat lehet a vas-hidroxidok jelenléte, melyek könnyedén megtapadhatnak a membrán felületén. A modelltermálvizes közegben mért jelentősen kisebb fluxusok ellenére megállapítható, hogy az 1 és a 2 perces ózonkezelés hatására csökkent az ötszörös sűrítési arány eléréséig szükséges szűrési idő (8 illetve 15 perccel) a nem előkezelt emulzió szűréséhez viszonyítva (~47 perc), vagyis a rövid ideig tartó ózonkezelés ebben az esetben is pozitívan befolyásolta az elérhető fluxust.

### 3.2. Szűrési ellenállások

A membránszűrések során meghatároztuk, a membrán saját ellenállását ( $R_{\text{membrán}}$ ), a reverzibilis ellenállást ( $R_{\text{reverzibilis}}$ ), az irreverzibilis ellenállást ( $R_{\text{irreverzibilis}}$ ) és az ezek összegeként számolható teljes ellenállást ( $R_{\text{teljes}}$ ) is (**2. ábra**). Megfigyelhető, hogy a huminsavat is tartalmazó emulziók esetében a teljes ellenállások az ózonkezelés idejétől függetlenül nagyobbak a modelltermálvizes közegben, mint a desztillált vizes közegben. Az is megfigyelhető, hogy az ózonnal nem kezelt, huminsavat is tartalmazó olajemulziók teljes ellenállásértékei nagyrészt a reverzibilis ellenállásból adódnak mindkét vízmátrix esetében, míg a huminsavat nem tartalmazó kezeletlen emulziók szűrése során az irreverzibilis ellenállás a jelentősebb. A huminsavak jelenléte tehát nem csak a teljes ellenállásértékek vonatkozásában, de az ellenállás reverzibilitásának vonatkozásában is kedvező.



2. ábra Ózonkezelés hatása az ellenállásokra (a) desztillált vizes és (b) modell termálvizes mátrix esetén

Az ózonkezelés hatására a teljes ellenállás mindkét közeg esetében először csökken (1,2 perces ózonkezelések), majd (az ózonkezelés idejét növelve) növekszik. A reverzibilis ellenállás csökkenő, míg az irreverzibilis ellenállás növekvő tendenciát mutat. Utóbbi növekedése első sorban az aprózódó olajcseppekkel magyarázható. A 2 ábrán az is jól látható, hogy a desztillált vizes közeg esetében a kezeletlen emulzió teljes ellenállása jelentősen kisebb a huminsav jelenlétében (a huminsavak korábban is említett amfifil tulajdonsága miatt).

### 3.3. Tisztítási hatékonyság

A kezeletlen emulziók kémiai oxigénigénye 249 - 291 mg/L között voltak. A permeátumok KOI értékeiből számított tisztítási hatékonyságok (94-99%) kis mértékű csökkenést mutattak az előkezelés idejének növelésével, ami az ózonkezelés hatására bekövetkező cseppaprózódásnak, illetve a nagy molekulák vízoldható oldott szervesanyagokká (a pH csökkenését eredményező szerves savakká) való bomlásának az eredménye.

A membránszűrések során a koncentrátumok kémiai oxigénigényét is mértük. A csak olajat tartalmazó, desztillált vizes emulziók koncentrátumai (kezeletlen és 2 perces ózonkezelte emulziók) magas KOI értékeket mutattak (1500 mg/L illetve 1270 mg/L). Ugyanakkor a modelltermálvizes emulziók esetén hasonló KOI értékeket mértünk a koncentrátumra, mint a kiindulási emulziókra (~250 mg/L), ami annak a következménye, hogy a vas-oxid-hidroxidok és az olajcseppek alkotta szennyeződések vastag rétegben megtapadtak a membrán felületén.

A huminsavat is tartalmazó olajemulziók szűrésére használt membránok sötétebbek voltak (vízmátrixtól függetlenül), mint a csak olajat tartalmazó emulziók szűrésére használt membránok. Ehhez hozzájárult a huminsav sárgás barnás színe, illetve a huminsav amfifil tulajdonsága, mely elősegíthette az olajcseppek megtapadását a hidrofil membránon. Ezt igazolja, hogy a desztillált vizes közeg esetén is a koncentrátumok legmagasabb KOI értéke mindösszesen 850 mg/L volt (a várható ~1200-1500 mg/L helyett). Megjegyzendő azonban, hogy a jobb megtapadás ellenére a huminsav jelenléte megnövelte az elérhető fluxust a kezeletlen olajemulziók esetében, ami azt jelzi, hogy a kialakuló szennyezőanyag réteg a víz számára könnyebben átjárható. Továbbá a huminsavat is tartalmazó olajemulziók esetében is

megfigyelhető, hogy a desztillált vizes emulziók koncentrátumainak magasabbak a KOI értékei (420-850), mint a hasonló ideig kezelt modell termálvizes emulziók esetén (320-480). Vagyis a huminsav jelenlétében is a magasabb sókoncentráció és/vagy a vas-oxid-hidroxidok jelenléte elősegítette az olaj megtapadását a membrán felületén.

### **Összefoglalás**

A huminsav tartalmú olajemulziók szűrésekor a membrán elszíneződik, a huminsav- illetve olajszenyezések megtapadnak a membrán felületén. Feltételezhető, hogy a huminanyagok amfifil jellegük miatt jól kötődhetnek mind az olajcseppekhez, mind a membránhoz, így csökkentve a koncentrátum szervesanyag tartalmát; ugyanakkor desztillált vizes közeg esetében a huminsav jelenléte megnövelte az elérhető fluxust a kezeletlen olajemulziók szűrése során, jelezve, hogy a víz számára könnyebben átjárható réteg alakult ki.

A huminsav jelenléte esetén a teljes ellenállások az ózonkezelés idejétől függetlenül nagyobbak a modelltermálvizes közegben, mint a desztillált vizes közegben. Az ózonnal nem kezelt, huminsavat is tartalmazó olajemulziók esetén jelentős a reverzibilis ellenállás mindkét vízmátrix esetében, míg a huminsavat nem tartalmazó kezeletlen emulziók szűrése során az irreverzibilis ellenállás a jelentős.

Összességében megállapítható, hogy egy rövid idejű ózonos előkezelés (~20 mg/L elnyelt ózon) a huminsav jelenlétében is növeli az elérhető fluxust és csökkenti a kialakuló membránellenállást. A 2 perces ózonkezelést követően a tisztítási hatékonyság 96-98 %-os, ugyanakkor a teljes ellenállás értéke 28-36 %-kal csökkenthető, bár huminsav jelenlétében kevésbé érvényesül a rövid idejű ózonos előkezelés fluxusnövelő hatása, mint a kizárólag olajat tartalmazó emulzió [2] esetében.

### **Köszönetnyilvánítás**

A munka a Bolyai János Kutatási Ösztöndíj támogatásával készült. A szerzők hálásak továbbá a Nemzeti Kutatási, Fejlesztési és Innovációs Hivatal által biztosított anyagi támogatásért (NKFI témaszám: K112096) is.

### **Irodalomjegyzék**

- [1] Kiss, Z.L., Kocsis, L., Keszthelyi-Szabó, G., Hodúr, C. and László, Z. (2014) Treatment of oily wastewater by combining ozonation and microfiltration, *Desalination and Water Treatment*, 55(13), 3662-3669.
- [2] G. Veréb, M. Zakar, I. Kovács, K. P. Sziládi, Sz. Kertész, C. Hodúr, Zs. László (2017) Effects of pre-ozonation in case of microfiltration of oil contaminated waters using polyethersulfone membrane at various filtration conditions, *Desalination and Water Treatment*, 73, 409-414.
- [3] Kovács K. É. (2010): Dél-kelet alföldi termálvizekből kinyert humuszanyagok jellemzése, Doktori (Ph.D.) értekezés, Szegedi Tudományegyetem

PHOTOCATALYTIC MEMBRANE REACTORS: COMPARISON OF THE  
APPLICABILITY OF UV-C AND UV-A EXCITATIONS

FOTOKATALITIKUS MEMBRÁNREAKTOROK: UV-C ÉS UV-A FÉNNYEL  
TÖRTÉNŐ GERJESZTÉSEK ALKALMAZHATÓSÁGÁNAK ÖSSZEHASONLÍTÁSA

Tünde Dobó<sup>1</sup>, Gábor Veréb<sup>1\*</sup>, Ildikó Kovács<sup>1</sup>, Szabolcs Kertész<sup>1</sup>, Mónika Vörös<sup>2</sup>, László  
Manczinger<sup>2</sup>, Cecília Hodúr<sup>1</sup>, Zsuzsanna László<sup>1</sup>

<sup>1</sup> Department of Process Engineering, Faculty of Engineering, University of Szeged, H-6724  
Szeged, Moszkvai krt. 9.

<sup>2</sup> Department of Microbiology, Faculty of Sciences and Informatics, University of Szeged, H-  
6701, P.O. Box 533, Szeged, Hungary  
e-mail: \*verebg@mk.u-szeged.hu, dobotundi@gmail.com

**Abstract**

In the present study photocatalytic membranes were prepared and applied in water purification. Titanium dioxide was immobilized onto polyacrylonitrile ultrafilter membrane (by physical deposition method), and the photocatalytic purification efficiencies were compared in case of different contaminations, using two different types of UV light sources (to excite the catalyst) with different emission spectra (intensity maximums were at 254 nm and at 365 nm). As model contaminants dissolved organic compounds (dyes like Acid Red 1 and Rhodamine B), dispersed crude oil, and bacterial contamination (*E.coli*) were applied.

In case of oil contaminated water, the COD value and the extractable oil content were measured, in case of dye contaminated waters the concentrations were measured by a spectrophotometer, meanwhile in case of *E.coli* infected water, the colony forming unit was determined by counting the growing colonies (on agar gel) from a given volume of the samples.

On one hand, UV-C irradiation was preferable in the aspect of disinfection, and therefore UV-C irradiation can be more efficient in the suppression of biofilm formation on membrane surfaces. On the other hand, UV-A irradiation was more effective in the decomposition of either water soluble and dispersed organic contaminants.

**Keywords:** Photocatalytic membranes, Crude oil, Dyes, *E.coli*, UV-A, UV-C

**1. Bevezetés**

Napjaink egyik igen fontos feladata a növekvő népesség megfelelő mennyiségű- és minőségű ivóvízzel történő ellátása, melynek megoldásához nélkülözhetetlen a meglévő vízkezelési technológiák folyamatos fejlesztése. Az utóbbi évtizedek intenzíven vizsgált módszerei közé tartoznak a membránszeparációs és a nagyhatékonyságú oxidációs eljárások (AOPs – *advanced oxidation processes*) egyaránt. Az utóbb említett csoportba sorolható a heterogén fotokatalízis is, mely félvezető nanorészecskéket alkalmaz, amelyeket megfelelő hullámhosszúságú fényel gerjesztve (oxidációs/redukációs folyamatokon keresztül) a szerves szennyezők széles köre lebontható.

A fotokatalizátorok membránfelületeken történő rögzítése számos előnnyel járhat. UV fényel megvilágítva a felületet a szűrés során a szennyező anyagok oxidálhatók illetve a mikrobiológiai szennyezések inaktíválhatók, aminek következtében a fluxuscsökkenés és a



biofilmképződés visszaszorítható. Ezen felül a fotokatalitikus membránfelületek eltömődésük után (fotokatalitikus úton) UV fényel tisztíthatók és újra felhasználhatók. A fotokatalitikus membránreaktorok (PMRs – photocatalytic membrane reactors) egyes tanulmányokban [1] akár VUV fényforrással vannak szerelve ( $\lambda \sim 185$  nm), de sokkal elterjedtebb mind az UV-C ( $\lambda \sim 254$  nm) [1-4], mind az UV-A ( $\lambda \sim 360$  nm) [2, 5] fényforrások alkalmazása a katalizátorok gerjesztésére. Ugyanakkor a szakirodalomban nincs részletes tanulmány arra vonatkozóan, hogy az UV-A és UV-C fényforrások alkalmazása milyen előnyökkel illetve hátrányokkal jellemezhető különböző szerves szennyezőanyagok esetén.

Jelen tanulmányban oldott- és diszpergált szerves szennyezőanyagok, illetve bakteriális szennyezés esetén vizsgáltuk a fotokatalitikus membránfelületek hatékonyságát UV-A és UV-C fényforrással történő gerjesztések esetében.

### Alkalmazott anyagok és módszerek

A fotokatalitikusan aktív membránfelület előállításához „Aeroxide P25” (Evonik industries) titán-dioxidot ( $\text{TiO}_2$ ), valamint poliakrilnitril anyagú, 50 kDa vágásértékű ultraszűrő membránt (VSEP, New Logic Research Inc.) használtunk. Az immobilizálás fizikai rögzítéssel történt: 50 mg  $\text{TiO}_2$ -t szuszpendáltunk el 100 mL desztillált vízben, melyet 1 percre ultrahanggal (Hielscher UP200S) homogenizáltunk. Az előállított  $\text{TiO}_2$  szuszpenzió 0,3 Mpa transzmembrán nyomás alkalmazásával lett rászűrve a membránra egy szakaszos szűrést biztosító, kevertetett cellás membránszűrővel (Millipore, XFUF04701). Ezt követően a membránt levegőn, szobahőmérsékleten szárítottuk (a membrán  $1,5 \text{ mg/cm}^2$   $\text{TiO}_2$ -ot tartalmazott a felületen).

A kőolajjal szennyezett víz (olaj a vízben emulzió) előállítása három lépésben történt (az adalékmentes, természetes ásványi kőolajat a MOL Zrt. biztosította). Először egy 1 m/m%-os emulziót készítettünk nagyfordulatszámú diszpergálással (35000 rpm), majd a diszperziót hígítva ultrahangos homogenizálással (Hielscher UP200S;  $t=10$  perc;  $T=25^\circ\text{C}$ ) 100ppm-es olaj a vízben emulziót állítottunk elő, melynek ötszörös hígításával állítottuk be a végső 20ppm-es koncentrációt (átlagos cseppméret:  $\sim 500\text{nm}$  [6]). A kísérletek során az olajszennyezés fotokatalitikus oxidációját kémiai oxigénigény (KOI) és extrahálható olajtartalom mérésével követtük. A KOI-t kálium-dikromátos módszerrel alapuló tesztszövegekkel határoztuk meg (Hanna Instruments), Lovibond ET 108 roncsoló ( $150^\circ\text{C}$ , 120 perc), és Lovibond COD Vario spektrofotométer használatával. Az extrahálható olajtartalmat egy WILKS gyártmányú, InfraCal TOG/TPH típusú mérőműszerrel mértük, hexánal végzett extrakció után.

Oldott szervesanyagként két különböző festéket alkalmaztunk: „Rhodamine B”-t és „Acid Red 1”-et. A Rhodamine B kiindulási koncentrációja 0,01 mmol volt, fotokatalitikus bomlását egy spektrofotométer (WPA Biowave II+) segítségével követtük nyomon a fényelnyelést  $\lambda=554$  nm-en mérve. Az Acid Red 1 kiindulási koncentrációja 0,032 mmol volt, melynek bomlását ugyancsak spektrofotométer használatával követtük  $\lambda=532$  nm-en.

Az *Escherichia coli*t tartalmazó szuszpenzió elkészítéséhez a baktériumokat 0,9 m/m%-os NaCl oldatban, tápanyagok jelenlétében (1 m/m% Tripton és 0,5 m/m% élesztőkivonat) 24 óra alatt szaporítottuk fel ( $37^\circ\text{C}$ -on), majd a szuszpenzióból centrifugálásos mosással távolítottuk el a tápanyagokat. Ezt követően a szuszpenzió megfelelő hígításával  $10^5$  CFU/mL kezdeti élő sejtszámot (CFU – colony forming unit) állítottunk be. A fotokatalitikus kísérletek során, meghatározott időközönként 50  $\mu\text{l}$  mintát szélesztettünk agar táptalajra. A minták élő sejtszámát a 24 óra alatt  $37^\circ\text{C}$ -on kifejlődő telepek számlálásával határoztuk meg.

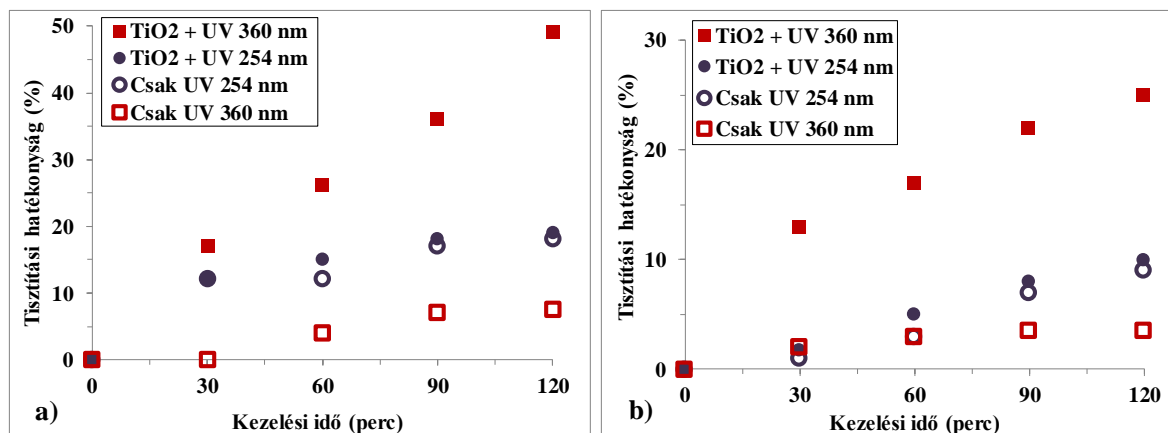


A membránszűrésre is alkalmas fotoreaktor alsó részében helyezkedett el a fotokatalizátorral bevont membrán, míg a reaktor tetején került bevezetésre a katalizátor gerjesztését szolgáló UV fénycsövek valamelyike ( $\lambda_{\max}=254$  ill. 360 nm; *Lighttech*; 10W). A fénycső mellett egy üvegcsövön keresztül levegőt is vezettünk a kezelendő vízbe ( $q_v=0,5$  L/perc), illetve egy a reaktor közepén felfüggesztett mágneses keverővel a rendszer folyamatosan kevertetve volt.

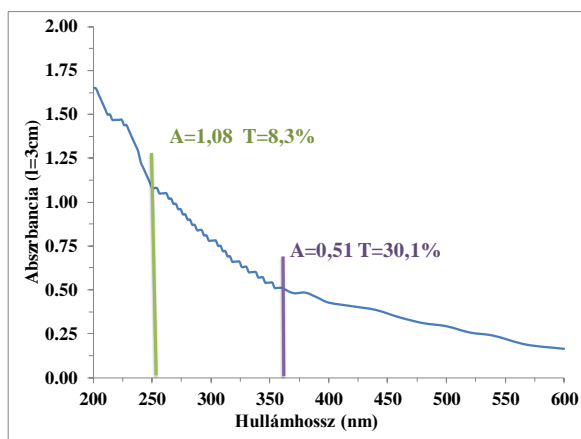
### Eredmények és értékelésük

Az olajos szennyezés fotokatalitikus kezelése esetén extrahálható olajtartalmat és kémiai oxigénigényt is mértünk a 254 nm-es és a 360 nm-es UV fényforrásokkal végzett kísérletek során. Az extrahálható olajtartalomra vonatkoztatott tisztítási hatékonyságok az **1/a ábrán** láthatók. A 254 nm-es UV fény önmagában történő alkalmazása (UV fotolízis) 18%-kal csökkentette az extrahálható olajtartalmat. A fotokatalitikus membránt megvilágítva a tisztítási hatékonyság nagyon hasonló (19%-os csökkenés). A 360 nm-es fénycső önmagában történő alkalmazásakor csekély 7%-kal csökkent az extrahálható olajtartalom, ugyanakkor a TiO<sub>2</sub>-dal bevont membrán esetében 49%-os csökkenést mértünk. Nagyon hasonló arányokat mutattak a KOI mérések eredményei is (**1/b ábra**). A 254 nm-es fény önmagában és TiO<sub>2</sub> jelenlétében is csekély (8, 9%-os) tisztítási hatékonyságot eredményezett, míg a 360 nm-es UV fényel történő gerjesztés sokkal hatékonyabbnak bizonyult (25%-os KOI csökkenés).

Az extrahálható olajtartalom vonatkozásában 49%-os, míg a kémiai oxigénigény vonatkozásában csupán 25%-os volt a tisztítási hatékonyság, ami azzal magyarázható, hogy az olajszennyezés oxidációja olyan vízzeloldható szervesanyagok képződését eredményezheti, melyek nem extrahálhatók hexánnal, de a kémiai oxigénigény mérésekor ezen anyagok is hozzájárulnak a minták KOI értékeihez. Az eredmények értelmezhetők az olajemulzió fényelnyelési spektruma (**2. ábra**) alapján.



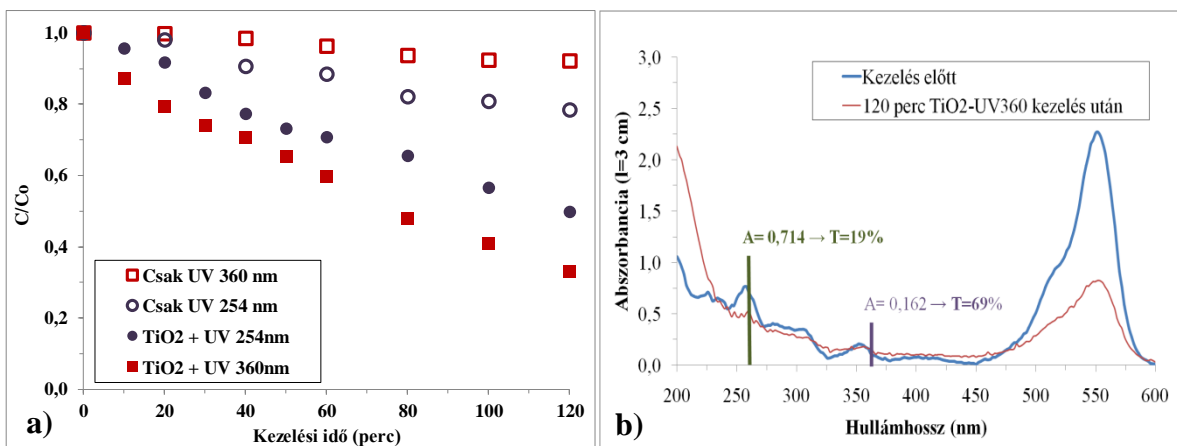
**1. ábra:** (a) Extrahálható olajtartalomtól- és (b) kémiai oxigénigényből számított tisztítási hatékonyságok a kezelési idő függvényében



2. ábra: Az olajszenyvezett modellszennyvíz abszorpciós spektruma

A fényforrások és a membránfelület közötti 3 cm-es fenyúthosszra számított transzmittancia értékek alapján ugyanis a 254 nm-es fotonoknak mindösszesen 8%-a, míg a 360 nm-es fotonok 30%-a jut el a fotokatalizátorig. Az alacsony fényáteresztő képesség magyarázatot ad arra, hogy miért nem látható számottevő különbség az UV-C fény önmagában történő alkalmazása, illetve a  $\text{TiO}_2$ /UV-C alkalmazása között. A 360 nm-en mért jelentősen nagyobb transzmittancia értékkel az UV-A fényel elérhető nagyobb tisztítási hatékonyság is magyarázható.

A *Rhodamine B* festék esetében a 360 nm-es fénynek ugyancsak jelentősen nagyobb hányada (69%-a) jut el a katalizátorig (3/b ábra), mint a 254 nm-es fénynek (19%-a), amivel megmagyarázható a kiemelkedő tisztítási hatékonyság (73%), amelyet a membránnak az ezen fényforrással történő gerjesztése eredményezett (3/a ábra). A 254 nm-es fény ugyanakkor ezt a festéket fotolitikus úton is képes bontani, ahogyan azt jól szemlélteti a 22%-os koncentráció csökkenés (3/a ábra). A  $\text{TiO}_2$  254 nm-es fényel történő besugárzásakor mért 51%-os tisztítási hatékonyság tehát részben fotokatalitikus, részben pedig fotolitikus folyamatok eredménye.

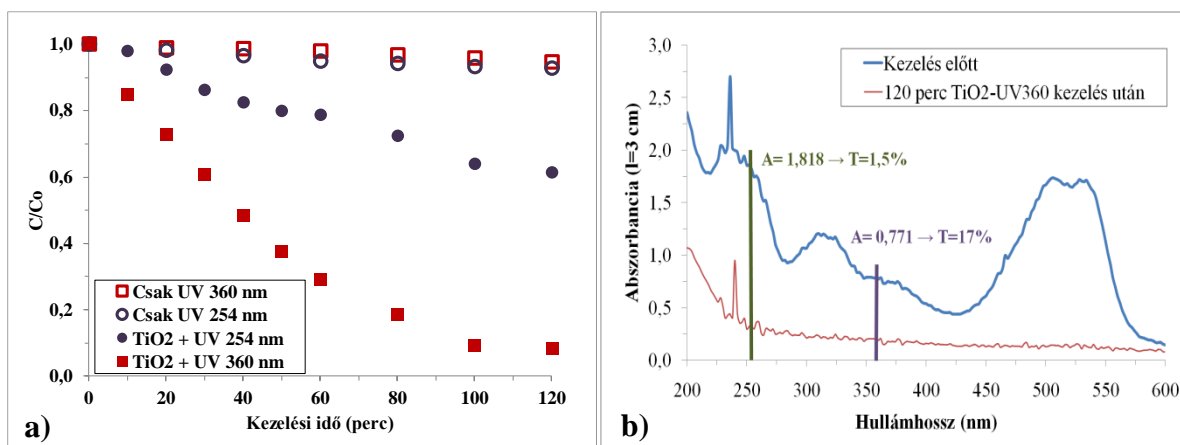


3/a ábra: A *Rhodamine B* festék koncentrációjának csökkenése a kezelési idő függvényében;

3/b ábra: A *Rhodamine B* festék fényelnyelési spektruma

Az *Acid Red 1* festék nem bontható hatékonyan fotolitikus úton (ahogyan az a 4/a ábrán is látható). A fotokatalitikus membránfelület megvilágításakor a 254 nm-es UV fény

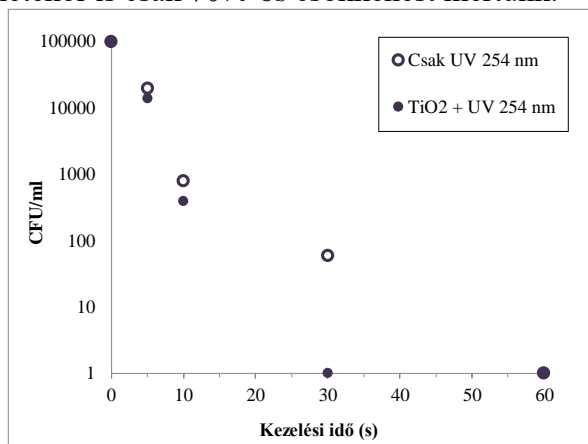
alkalmazásakor 39%-os, míg a 360 nm-es UV fény esetén 92%-os tisztítási hatékonyságot mértünk. Az eredmény jól magyarázható a 254 nm-es megvilágítás esetén számított, egy nagyságrenddel kisebb fényáterestéssel (4/b ábra) és a festék 254 nm-es UV fényvel szembeni ellenálló képességével.



4/a ábra: Az *Acid Red 1* festék bomlása a kezelési idő függvényében;

4/b ábra: Az *Acid Red 1* festék fényelnyelési spektruma

Az *E.coli* baktériummal fertőzött víz esetén a 254 nm-es ultraibolya fény 60 másodperc alatt teljesen fertőtlenítette a vizet, ugyanakkor a fotokatalizátorral bevont membrán jelenlétében már fél perc után sem volt kimutatható mennyiségű élő baktérium a kezelt vízben (5. ábra). A 360 nm-es UV fény önmagában 10 perc után sem csökkentette az élő sejtek számát, sőt a  $\text{TiO}_2$  jelenlétekor is csak 70%-os csökkenést mértünk.



5. ábra: Az élő sejtek számának változása a kezelési idő függvényében

### Következtetések

A kőolajjal szennyezett vizek UV-fotolízissel ( $\lambda=254$  nm) csak igen kis hatékonysággal tisztíthatók. Heterogén fotokatalízis alkalmazásával nagyobb hatékonyság érhető el, és célszerű 360 nm-es fényforrást alkalmazni a katalizátor gerjesztéséhez.

A festékekkel végzett kísérletek eredményei alapján, vízdoldható szerves szennyeződések esetén a kezelés hatékonyságát jelentősen befolyásolja az adott szennyező fotolitikus bonthatósága, illetve az adott szennyező fényelnyelési spektruma. A jelen tanulmányban vizsgált festékek esetén a 360 nm-es UV fény eredményezett nagyobb tisztítási hatékonyságot.

A 254 nm-es UV fény önmagában is alkalmas az *E.coli* sejtek eredményes inaktiválására, de a fotokatalitikusan aktív membránfelülettel a fertőtlenítő hatás tovább fokozható, míg 360 nm-es fényforrás alkalmazásakor jelentősen kisebb mértékű a fertőtlenítő hatás.

Az eredmények alapján a fotokatalitikus membránreaktorokban 254 nm-en illetve 360 nm-en sugárzó fényforrások egyidejű alkalmazása javasolt, mivel előbbi a fertőtlenítésben (ebből adódóan a biofilmképződés gátlásában) jelentősen hatékonyabb, ugyanakkor a szervesanyagok fotokatalitikus úton nagyobb hatékonysággal bonthatók 360 nm-es fényforrás alkalmazásakor.

### **Köszönetnyilvánítás**

A munka a Bolyai János Kutatási Ösztöndíj támogatásával készült. A szerzők hálásak a Nemzeti Kutatási, Fejlesztési és Innovációs Hivatal által biztosított anyagi támogatásért (NKFI témaszám: K112096). A kutatást az Emberi Erőforrások Minisztériuma az „Új Nemzeti Kiválóság Program”-ban a „Nemzeti Felsőoktatási Kiválóság Ösztöndíj – Felsőoktatási Mesterképzés Hallgatói Kutatói Ösztöndíj” (UNKP-17-2) keretében támogatta.

### **Irodalomjegyzék**

- [1] K. Azrague, S. W. Osterhus, Desalination and Water Treatment, 54 (2014) 2648.
- [2] R. Molinari, C. Lavorato, P. Argurio, Catal. Today, 281 (2017) 144.
- [3] G. Rao, K. S. Brastad, Q. Zhang, R. Robinson, Z. He, Y. Li, Frontiers of Environmental Science & Engineering, 10 (2016) 1.
- [4] S. Kertész, J. Cakl, H. Jiráňková, Desalination, 343 (2014) 106.
- [5] C. P. Athanasekou, N. G. Moustakas, S. Morales-Torres, L. M. Pastrana-Martínez, J. L. Figueiredo, J. L. Faria, A. M. T. Silva, J. M. Dona-Rodríguez, G. E. Romanos, P. Falaras, Appl. Catal., B, 178 (2015) 12.
- [6] G. Veréb, M. Zakar, I. Kovács, K. P. Sziládi, Sz. Kertész, C. Hodúr, Zs. László (2017) Effects of pre-ozonation in case of microfiltration of oil contaminated waters using polyethersulfone membrane at various filtration conditions, Desalination and Water Treatment, 73, 409-414.